November 2018 Volume 77 Issue 11

Impact Factor 12.350

Annals of the Rheumatic Diseases

The EULAR Journal

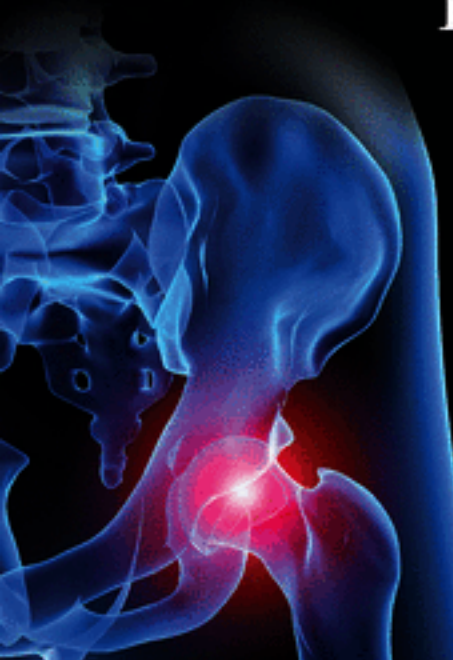

ard.bmj.com

eular BMJ

ARD
The EULAR Journal

Guidelines for Authors and Reviewers

Full instructions are available online at http://ard.bmj.com/pages/authors. Articles must be submitted electronically at http://mc.manuscriptcentral.com/ard. Authors retain copyright but are required to grant ARD an exclusive licence to publish. (http://authors.bmj.com/policies/copyright-and-authors-rights).

Annals of the Rheumatic Diseases publishes original work on all aspects of rheumatology and disorders of connective tissue. Laboratory and clinical studies are equally welcome

Contact Details

Editorial Office
Annals of the Rheumatic Diseases
BMJ Journals, BMA House, Tavistock Square
London WCIH 9JR,UK
E: **ard@bmj.com**

Production Editor
Teresa Jobson
E: **production.ard@bmj.com**

EULAR
EULAR Executive Secretariat
Seestrasse 240, 8802 Kilchberg, Switzerland
E: **eular@eular.org**
www.eular.org

Customer support
For general queries and support with existing and new subscriptions:
W: **support.bmj.com**
T: **+44 (0)20 7111 1105**
E: **support@bmj.com**

Self-archiving and permissions
W: **bmj.com/company/products-services/rights-and-licensing/**
E: **bmj.permissions@bmj.com**

Advertising
W: **bmj.com/company/for-advertisers-and-sponsor/**

Display Advertising ROW
Sophie Fitzsimmons
T: **+44 (0)20 3655 5612**
E: **sfitzsimmons@bmj.com**

Online Advertising ROW
Marc Clifford
T: **+44 (0) 20 3655 5610**
E: **mclifford@bmj.com**

Display & Online Advertising Americas
American Medical Communications (AMC)
T: **+1 973 214 4374**
E: **rgordon@americanmedicalcomm.com**

Reprints

Author Reprints
BMJ Reprints Team
E: **admin.reprints@bmj.com**

Commercial Reprints ROW
Nadia Gurney-Randall
M: **+44 07866 262344**
E: **ngurneyrandall@bmj.com**

Commercial Reprints Americas
Ray Thibodeau
T: **+1 267 895 1758**
M: **+1 215 933 8484**
E: **ray.thibodeau@contentednet.com**

For all other journal contacts
ard.bmj.com/contact-us

Subscription Information

ARD is published monthly; subscribers receive all supplements
ISSN 0003-4967 (print); 1468-2060 (online)

Institutional Rates 2018

Print
£986

Online
Site licences are priced on FTE basis and allow access by the whole institution. Details available online at http://journals.bmj.com/content/subscribers or contact the Subscription Manager in the UK (see above right)

Personal Rates 2018

Print (includes online access at no additional cost)
£407

Online only
£173

EULAR congress delegates
Delegates receive a Continuous Professional Development package that includes a 12 month complimentary subscription to *ARD* in print and/or online

Personal print or online only and institutional print subscriptions may be purchased online at http://journals.bmj.com/content/subscribers (payment by Visa/Mastercard only)

Residents of some EC countries must pay VAT; for details, call us or visit http://journals.bmj.com/content/subscribers

For more information on subscription rates or to subscribe online please visit ard/bmj.com/pages/contact-us/

ARD
The Eular Journal

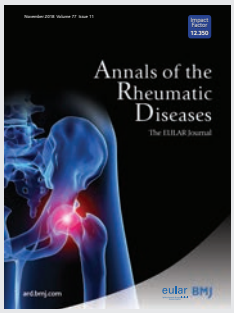

Editorial office
Annals of the Rheumatic Diseases
BMJ Publishing Group Ltd
BMA House
Tavistock Square
London WCIH 9JR,UK
T: **+44 (0)20 3655 5889**
E: **ard@bmj.com**
Twitter: **@ARD_BMJ**
ISSN: 0003-4967 (print)
ISSN: 1468-2060 (online)
Impact Factor: 12.350

ARD is published by BMJ Publishing Group Ltd typeset by Exeter Premedia Services Private Ltd, Chennai, India and printed in the UK on acid-free paper.

Annals of the Rheumatic Diseases (ISSN No: 0003-4967) is published monthly by BMJ Publishing Group and distributed in the USA by Air Business Ltd. Periodicals postage paid at Jamaica NY 11431 POSTMASTER: send address changes to *Annals of the Rheumatic Diseases*, Air Business Ltd, c/o Worldnet Shipping Inc., 156-15, 146th Avenue, 2nd Floor, Jamaica, NY 11434, USA.

Editorial

Recommendation

Criteria

Clinical and epidemiological research

MORE CONTENTS ▶

Basic and translational research

Letters

Electronic pages

2008–2018: a decade of recommendations for systemic lupus erythematosus

Dimitrios T Boumpas,[1,2] George K Bertsias,[3] Antonis Fanouriakis[1]

Recommendations represent a popular way of integrating evidence-based medicine to clinical practice. These systematically developed statements can assist practitioner and patient decisions about appropriate healthcare, facilitate teaching of students and physicians, and educate patients. In 2008, the first European League Against Rheumatism (EULAR) recommendations for the management of general systemic lupus erythematosus (SLE) were published in the *Annals of the Rheumatic Diseases* (ARD).[1] These were based on a combination of evidence and expert opinion, and followed the standard EULAR operating procedures. The effort involved experts on SLE, skilled methodologists and meticulous fellows who undertook an exhaustive systematic literature research (SLR). In this EULAR-endorsed project, a panel of European lupus experts was first updated on current literature and issues on SLE, and then developed and voted on the questions to be included in the SLR in an open and rigorous process. During the second phase, the results of the SLR were presented to the panel which then formulated, graded and voted on the recommendations. Recommendations covered the diagnosis, monitoring and management of general SLE with a few statements on neuropsychiatric and renal disease. Other EULAR panels also prepared recommendations for clinical trials in SLE,[2 3] as well as more specific recommendations on the diagnosis and management of neuropsychiatric SLE[4] and lupus nephritis,[5] the latter in collaboration with the European Renal Association–European Dialysis Transplantation Association.

Subsequently, in 2012, the American College of Rheumatology developed guidelines for screening, treatment and management of lupus nephritis.[6] In the same year, the Kidney Disease Improving Global Outcomes—an international organisation—developed guidelines for the management of lupus nephritis.[7] All three sets of lupus nephritis guidelines were published in the same year and were based on the same body of evidence. As expected, their main statements agreed, but there were also notable differences reflecting the focus and composition of each group (reviewed in Wilhelmus *et al*[8]).

More recently, the British Society for Rheumatology (BSR) also published guidelines for the diagnosis, monitoring and management of SLE in adults.[9] Notably, in the BSR guidelines, lupus is divided into mild, moderate and severe disease with treatment recommendations adjusted accordingly. EULAR has also recently updated its recommendations, and these are currently under review.

This '*flurry*' of recommendations clearly demonstrates a perceived need in the community to avoid fragmentation and optimise the management of SLE, a complex disease where multiple medical specialties are often involved in the care of patients, by establishing an integrated approach based on widely accepted principles and evidence-based recommendations. Crucial elements in developing credible recommendations include (1) a clear understanding of the target group to be following these recommendations (ie, generalists vs specialists vs lupus experts), (2) the quality of expertise and the inclusiveness of experts with differing views, (3) the inclusion of health professionals and patients, and (4) the rigorousness of the SLR methodology and its assessment. It is crucial that all interested parties and stakeholders such as physicians, patients, government bodies, insurance agencies and third payers realise that recommendations are developed for '*group of patients*' to improve homogeneity of care, and they cannot limit physicians' freedom or substitute for their clinical judgement in treating '*individual*' patients. In simple terms, recommendations '*are not the law*' rather an effort to provide general guidance to physicians treating patients. To use the airplane analogue, recommendations are the '*manual of procedures*' not to substitute for the pilot's experience and judgement. An important measure of success for each set of recommendations is reaching the target group of physicians and their compliance. Accordingly, a limited number of simple, crystal clear, concise and unequivocal statements in an eye-friendly and user-friendly format (eg, using diagrams and algorithms) are of paramount importance.

In ARD, a group of leading lupus experts from the Latin American Group for the Study of Lupus (Grupo Latinoamericano De Estudio del Lupus)–Pan-American League of Associations of Rheumatology presents their own recommendations for the management of SLE.[10] The authors argue that although guidelines for SLE treatment do exist, there is scarce evidence to support specific therapies for Latin American patients. Accordingly, in their work, the authors have also considered the impact of racial/ethnic background and socioeconomic status on lupus outcomes and treatment response. Medication variables such as cost and availability were also considered since they may affect adherence and are relevant in decision-making. The recommendations are presented by organ involved with the following format: (1) interventions considered for evaluation; (2) benefits and harms of treatments; (3) recommendation statement with grading of evidence. Although SLE manifestations tend to occur simultaneously in more than one organ, in most cases, treatment directed to the more severe manifestation(s) is also effective for the less severe disease manifestations.

Undoubtedly, regional efforts to develop treatment recommendations could facilitate the dissemination and implementation in local communities. Yet, there is little evidence to support Latin American–specific lupus therapies and interventions. In our opinion, these recommendations represent a regional effort to develop guidelines with the potential of improved penetration to the community. The presented evidence (found in *online supplementary material*) is—in our judgement—biased towards (the few) randomised controlled trials—as opposed to observational studies—in SLE, which is a limitation since valuable real-life data might have been ignored. Experience has shown that physicians using recommendations also seek for practical information such as working definitions for treatment response (or failure), or guidance on the dosage of drugs (eg, corticosteroids), or

[1]Medical School, National and Kapodestrian University of Athens, Athens, Greece
[2]University of Cyprus, Medical School, Nicosia, Cyprus
[3]Rheumatology, Clinical Immunology and Allergy, University of Crete, Medical School, Heraklion, Greece

Correspondence to Dr Dimitrios T Boumpas, Medical School, National and Kapodestrian University of Athens, Athens 124 62, Greece; boumpasd@uoc.gr

the duration of their use. Inclusion of such information in the subsequent updates could increase the usefulness of these recommendations.

Notwithstanding these limitations, the rheumatological community welcomes the efforts of this active group of SLE experts from Latin America and eagerly awaits to see the dissemination and usage of the recommendations in their community, accompanied by studies measuring their impact on improving the quality of care for patients with lupus.

Handling editor Josef S Smolen

Funding The authors have not declared a specific grant for this research from any funding agency in the public, commercial or not-for-profit sectors.

Competing interests None declared.

Patient consent Not required.

Provenance and peer review Commissioned; externally peer reviewed.

To cite Boumpas DT, Bertsias GK, Fanouriakis A. *Ann Rheum Dis* 2018;**77**:1547–1548.

► http://dx.doi.org/10.1136/annrheumdis-2018-213512

Ann Rheum Dis 2018;**77**:1547–1548. doi:10.1136/annrheumdis-2018-214014

REFERENCES

1 Bertsias G, Ioannidis JP, Boletis J, *et al*. EULAR recommendations for the management of systemic lupus erythematosus. Report of a task force of the EULAR standing committee for international clinical studies including therapeutics. *Ann Rheum Dis* 2008;67:195–205.
2 Bertsias GK, Ioannidis JP, Boletis J, *et al*. EULAR points to consider for conducting clinical trials in systemic lupus erythematosus: literature based evidence for the selection of endpoints. *Ann Rheum Dis* 2009;68:477–83.
3 Gordon C, Bertsias G, Ioannidis JP, *et al*. EULAR points to consider for conducting clinical trials in systemic lupus erythematosus. *Ann Rheum Dis* 2009;68:470–6.
4 Bertsias GK, Ioannidis JP, Aringer M, *et al*. EULAR recommendations for the management of systemic lupus erythematosus with neuropsychiatric manifestations: report of a task force of the EULAR standing committee for clinical affairs. *Ann Rheum Dis* 2010;69:2074–82.
5 Bertsias GK, Tektonidou M, Amoura Z, *et al*. Joint European League Against Rheumatism and European Renal Association-European Dialysis and Transplant Association (EULAR/ERA-EDTA) recommendations for the management of adult and paediatric lupus nephritis. *Ann Rheum Dis* 2012;71:1771–82.
6 Hahn BH, McMahon MA, Wilkinson A, *et al*. American College of Rheumatology guidelines for screening, treatment, and management of lupus nephritis. *Arthritis Care Res* 2012;64:797–808.
7 Radhakrishnan J, Cattran DC. The KDIGO practice guideline on glomerulonephritis: reading between the (guide)lines—application to the individual patient. *Kidney Int* 2012;82:840–56.
8 Wilhelmus S, Bajema IM, Bertsias GK, *et al*. Lupus nephritis management guidelines compared. *Nephrol Dial Transplant* 2016;31:904–13.
9 Gordon C, Amissah-Arthur MB, Gayed M, *et al*. The British Society for Rheumatology guideline for the management of systemic lupus erythematosus in adults: executive summary. *Rheumatology* 2018;57:14–18.
10 Pons-Estel BA, Bonfa E, Soriano ER, *et al*. First Latin American clinical practice guidelines for the treatment of systemic lupus erythematosus: Latin American Group for the Study of Lupus (GLADEL, *Grupo Latino Americano de Estudio del Lupus*)–Pan-American League of Associations of Rheumatology (PANLAR). *Ann Rheum Dis* 2018:doi: 10.1136/annrheumdis-2018-213512.

First Latin American clinical practice guidelines for the treatment of systemic lupus erythematosus: Latin American Group for the Study of Lupus (GLADEL, Grupo Latino Americano de Estudio del Lupus)–Pan-American League of Associations of Rheumatology (PANLAR)

Bernardo A Pons-Estel,[1] Eloisa Bonfa,[2] Enrique R Soriano,[3] Mario H Cardiel,[4] Ariel Izcovich,[5] Federico Popoff,[5] Juan M Criniti,[5] Gloria Vásquez,[6] Loreto Massardo,[7] Margarita Duarte,[8] Leonor A Barile-Fabris,[9] Mercedes A García,[10] Mary-Carmen Amigo,[11] Graciela Espada,[12] Luis J Catoggio,[3] Emilia Inoue Sato,[13] Roger A Levy,[14] Eduardo M Acevedo Vásquez,[15] Rosa Chacón-Díaz,[16] Claudio M Galarza-Maldonado,[17] Antonio J Iglesias Gamarra,[18] José Fernando Molina,[19] Oscar Neira,[20] Clóvis A Silva,[21] Andrea Vargas Peña,[22] José A Gómez-Puerta,[23] Marina Scolnik,[3] Guillermo J Pons-Estel,[1,24] Michelle R Ugolini-Lopes,[2] Verónica Savio,[25] Cristina Drenkard,[26] Alejandro J Alvarellos,[27] Manuel F Ugarte-Gil,[28,29] Alejandra Babini,[25] André Cavalcanti,[30] Fernanda Athayde Cardoso Linhares,[22] Maria Jezabel Haye Salinas,[27] Yurilis J Fuentes-Silva,[31] Ana Carolina Montandon de Oliveira e Silva,[32] Ruth M Eraso Garnica,[33] Sebastián Herrera Uribe,[34] Diana Gómez-Martín,[35] Ricardo Robaina Sevrini,[36] Rosana M Quintana,[1,24] Sergio Gordon,[37] Hilda Fragoso-Loyo,[35] Violeta Rosario,[38] Verónica Saurit,[27] Simone Appenzeller,[39] Edgard Torres dos Reis Neto,[13] Jorge Cieza,[40] Luis A González Naranjo,[6] Yelitza C González Bello,[41] María Victoria Collado,[42] Judith Sarano,[42] Soledad Retamozo,[27] María E Sattler,[43] Rocio V Gamboa-Cárdenas,[28] Ernesto Cairoli,[36] Silvana M Conti,[24] Luis M Amezcua-Guerra,[44] Luis H Silveira,[45] Eduardo F Borba,[2] Mariana A Pera,[10] Paula B Alba Moreyra,[46] Valeria Arturi,[10] Guillermo A Berbotto,[43] Cristian Gerling,[37] Carla A Gobbi,[46] Viviana L Gervasoni,[24] Hugo R Scherbarth,[37] João C Tavares Brenol,[47] Fernando Cavalcanti,[30] Lilian T Lavras Costallat,[39] Nilzio A Da Silva,[32] Odirlei A Monticielo,[47] Luciana Parente Costa Seguro,[2] Ricardo M Xavier,[47] Carolina Llanos,[48] Rubén A Montúfar Guardado,[49] Ignacio Garcia de la Torre,[50] Carlos Pineda,[51] Margarita Portela Hernández,[52] Alvaro Danza,[53] Marlene Guibert-Toledano,[54] Gil Llerena Reyes,[54] Maria Isabel Acosta Colman,[8] Alicia M Aquino,[8] Claudia S Mora-Trujillo,[40] Roberto Muñoz-Louis,[38] Ignacio García Valladares,[41] María Celeste Orozco,[55] Paula I Burgos,[48] Graciela V Betancur,[55] Graciela S Alarcón,[56,57] on behalf of the Grupo Latino Americano de Estudio del Lupus (GLADEL) and Pan-American League of Associations of Rheumatology (PANLAR)

Handling editor Josef S Smolen

For numbered affiliations see end of article.

Correspondence to
Dr Mario H Cardiel, Centro de Investigación Clínica de Morelia SC. Morelia, México; mhcardiel@hotmail.com

BAP-E, EB, ERS and MHC contributed equally.

Received 2 April 2018
Revised 26 June 2018
Accepted 28 June 2018
Published Online First 25 July 2018

Linked

► http://dx.doi.org/10.1136/annrheumdis-2018-214014

Check for updates

To cite: Pons-Estel BA, Bonfa E, Soriano ER, *et al*. *Ann Rheum Dis* 2018;**77**:1549–1557.

ABSTRACT

Systemic lupus erythematosus (SLE), a complex and heterogeneous autoimmune disease, represents a significant challenge for both diagnosis and treatment. Patients with SLE in Latin America face special problems that should be considered when therapeutic guidelines are developed. The objective of the study is to develop clinical practice guidelines for Latin American patients with lupus. Two independent teams (rheumatologists with experience in lupus management and methodologists) had an initial meeting in Panama City, Panama, in April 2016. They selected a list of questions for the clinical problems most commonly seen in Latin American patients with SLE. These were addressed with the best available evidence and summarised in a

standardised format following the Grading of Recommendations Assessment, Development and Evaluation approach. All preliminary findings were discussed in a second face-to-face meeting in Washington, DC, in November 2016. As a result, nine organ/system sections are presented with the main findings; an 'overarching' treatment approach was added. Special emphasis was made on regional implementation issues. Best pharmacologic options were examined for musculoskeletal, mucocutaneous, kidney, cardiac, pulmonary, neuropsychiatric, haematological manifestations and the antiphospholipid syndrome. The roles of main therapeutic options (ie, glucocorticoids, antimalarials, immunosuppressant agents, therapeutic plasma exchange, belimumab, rituximab, abatacept, low-dose aspirin and anticoagulants) were summarised in each section. In all cases, benefits and harms, certainty of the evidence, values and preferences, feasibility, acceptability and equity issues were considered to produce a recommendation with special focus on ethnic and socioeconomic aspects. Guidelines for Latin American patients with lupus have been developed and could be used in similar settings.

INTRODUCTION

Systemic lupus erythematosus (SLE) is a complex multisystemic autoimmune disease resulting, oftentimes, in irreversible damage, diminished quality of life and reduced life expectancy.[1–3] Genetic and environmental factors play important roles in its pathogenesis.[4–8] Disease manifestations and severity vary according to the patients' racial/ethnic background and socioeconomic status (SES).[1 9 10] Data from *Grupo Latino Americano de Estudio del Lupus* (GLADEL), Lupus in Minorities: Nature vs Nurture (LUMINA) and the Lupus Family Registry and Repository cohorts have demonstrated that Latin American and North American Mestizo patients (mixed Amerindian and European ancestry), African descendants and Native Americans develop lupus earlier[11 12] although diagnostic delays may occur.[1] They also experience more severe disease, have higher disease activity levels,[1] accrue more organ damage[2] and have higher mortality rates,[1] succumbing mainly to disease activity and/or infections.[1 3 13–15]

Although guidelines for SLE treatment do exist and there is scarce evidence to support specific therapies for Latin American patients with lupus,[16–21] this regional effort has considered the impact of racial/ethnic background[1 10 22–28] and SES[3 9] on lupus outcomes and treatment response.[25 26] Other medication variables such as cost and availability were also taken into account since they affect adherence and are relevant in decision-making.[27 28] GLADEL and the Pan-American League of Associations of Rheumatology have joined efforts to produce these guidelines,[29] which are presented by organ systems, although manifestations usually occur in more than one. Nevertheless, treatment is usually tailored to the more severe manifestation(s), which usually benefits the less severe.

METHODS

Two working teams on logistics and methodological issues constituted by experienced Latin American rheumatologists and experts in the Grading of Recommendations Assessment, Development and Evaluation (GRADE) guideline system developed a framework for these guidelines. Nine organ/system sections were prepared with the main findings. Special emphasis was placed on reviewing local problems and regional publications.

The GRADE approach was followed in the process (http://www.gradeworkinggroup.org) answering the clinical questions voted most relevant by the panel. The description of the methodology followed to develop these guidelines has already been published.[29] All authors listed in this manuscript have participated in planning, drafting, reviewing, final approval and are accountable for all aspects of the manuscript. No ethical approval was required by institutions. We present the final recommendations and their supporting information. Comments from three patients with SLE were also considered.

Box 1 GLADEL–PANLAR Latin American guidelines for the treatment of systemic lupus erythematosus

Overarching principles

a. Treatment should be individualised, specialists and generalists should work together and the active involvement of patients and their family members on the overall therapeutic plan should be emphasised.
b. The therapeutic goal should be to reach and maintain remission or low-disease activity as soon as the diagnosis is made and for as long as possible.
c. Treatment should include photo-protection, osteoporosis, cardiovascular, metabolic syndrome and infection prevention, psychological support and pregnancy counselling.
d. All patients with lupus should receive AMs, except those who refuse them or who have absolute contraindications to take them.
e. GCs, if clinically needed, regardless of patient's disease manifestations, should be prescribed at the lowest possible dose and for the shortest period of time.

AM, antimalarials; GC, glucocorticoid; GLADEL, Grupo Latino Americano de Estudio del Lupus; PANLAR, Pan-American League of Associations of Rheumatology.

RESULTS

For each of the subheadings listed below, the panel considered interventions based on experience, availability, affordability and a stepwise therapeutic approach of the different alternatives. Standard of care (SOC) was defined as the use of hydroxychloroquine (HCQ) and, if clinically indicated, low-dose glucocorticoids (GC) (prednisone ≤7.5 mg or equivalent for the shortest time).[24] Chloroquine remains an alternative for some of the Latin American countries where HCQ is not available and careful monitoring of eye side effect is recommended. Overarching principles are shown in box 1. Tables summarising the evidence that was considered in the process are shown in online supplementary tables in https://doi.org/10.5061/dryad.bg8452h.

Musculoskeletal manifestations

a. Which is the best treatment for adult patients with SLE and musculoskeletal (MSK) manifestations?

Interventions considered

(1) SOC; (2) SOC plus methotrexate (MTX); (3) SOC plus leflunomide (LFN); (4) SOC plus belimumab; (5) SOC plus abatacept (ABT); (6) other options: azathioprine (AZA), mycophenolate mofetil (MMF), cyclosporine A (CsA) or rituximab (RTX) (online supplementary tables S2.1.1, S2.1.4, S2.1.6, S2.1.7, S2.2.11, S2.1.11, S2.1.12, S2.1.14, S2.1.15, S2.1.17, S2.2.1, S2.2.2, S2.2.4, S3.1.1, S3.1.3–S3.1.6, S3.2.1, S3.2.2, S12.2–S12.5, S12.8–S12.10).

Table 1 GLADEL–PANLAR recommendations for musculoskeletal and cutaneous manifestations in patients with systemic lupus erythematosus

Treatment recommendations	Quality of the evidence	Strength of recommendation
Musculoskeletal (MSK) manifestations		
In adult patients with SLE and MSK manifestations		
First line: Use SOC (GCs and AMs) alone over adding other IS.	Low	Weak
If disease remains active after SOC, add either MTX or LFN or belimumab or ABT over other IS.	Low to moderate	Weak
Cutaneous manifestations		
In adult patients with different manifestations of cutaneous lupus		
First line: Use SOC alone over adding other IS.	Low	Weak
If disease remains active after SOC, add MTX, AZA, MMF, CsA, CYC or belimumab over other IS.	Low to moderate	Weak

ABT, abatacept; AM, antimalarials; AZA, azathioprine; CsA, cyclosporine A; CYC, cyclophosphamide; GC, glucocorticoid; GLADEL, *Grupo Latino Americano de Estudio del Lupus*; IS, immunosuppressant; LFN, leflunomide; MMF, mycophenolate mofetil; MTX, methotrexate; PANLAR, Pan-American League of Associations of Rheumatology; SLE, systemic lupus erythematosus; SOC, standard of care.

Benefits and harms

Although the panel judged that compared with SOC alone, adding MTX, LFN, belimumab or ABT is possibly associated with beneficial effects, a significant proportion of patients will achieve adequate symptom control with SOC and could be spared the adverse effects/excess costs associated to those other options.

Recommendation

The panel suggests SOC alone over adding other immunosuppressant (IS) in adult patients with SLE with MSK manifestations (weak recommendation based on low certainty of the evidence). It suggests also adding either MTX, LFN, belimumab or ABT to those failing to respond to SOC (weak recommendation based on low to moderate certainty of the evidence). Cost and availability may favour MTX (table 1).

Cutaneous manifestations

a. Which is the best treatment for adult patients with different manifestations of cutaneous lupus?

Interventions considered

(1) SOC; (2) SOC plus MTX; (3) SOC plus AZA; (4) SOC plus MMF; (5) SOC plus CsA; (6) SOC plus belimumab; (7) SOC plus ABT; (8) SOC plus acitretin; (9) SOC plus atacicept; (10) SOC plus cyclophosphamide (CYC) (online supplementary tables S4.1.1–S4.1.7, S4.2.1–S4.2.5, S4.3.1, S4.4.1, S4.4.2, S4.5.1–S4.5.13).

Benefits and harms

The panel judged that a significant proportion of patients will achieve adequate symptom control with SOC and could be spared the adverse effects/costs of the other therapies.

Recommendation

The panel suggests SOC alone over adding other IS in adult patients with SLE with cutaneous manifestations (weak recommendation based on low certainty of the evidence). It also suggests adding MTX, AZA, MMF, CsA, CYC or belimumab to patients failing to respond to SOC (weak recommendation based on low to moderate certainty of the evidence). Cost and availability may favour MTX and AZA (table 1).

Adult kidney manifestations

a. Which is the best induction treatment for adult patients with lupus nephritis?

Interventions considered

(1) GCs; (2) GCs plus high-dose CYC; (3) GCs plus low-dose CYC; (4) GCs plus MMF; (5) GCs plus RTX plus MMF; (6) GCs plus tacrolimus (TAC); (7) GCs plus AZA (online supplementary tables S1.1.1.2, S1.1.1.7, S1.1.1.8, S1.1.1.10, S1.1.2.2, S1.1.2.5, S1.1.2.7, S1.1.3.2, S1.1.4.1, S1.2.6).

Benefits and harms

Based on the identified evidence the panel concluded that compared with GCs alone, the addition of other IS (CYC, MMF or TAC) is associated with significant benefits, higher remission rates and lower progression rates to end-stage renal disease (ESRD). Head-to-head comparisons between MMF, TAC and high-dose CYC showed that MMF and TAC are associated with less adverse effects than high-dose CYC. Between low and high-dose CYC the balance favours the former because of better safety profile and comparable efficacy, although this conclusion is based on one trial that included predominantly Caucasians. RTX did not provide additional benefits when combined with MMF.

Recommendation

The panel recommends SOC (GCs and antimalarials (AM)) in addition to an IS (CYC in high or low doses, MMF or TAC) over GCs alone, for induction in patients with SLE-related kidney disease (strong recommendation based on moderate certainty of the evidence). Although more African-American descendants and Hispanic patients responded to MMF than CYC (25), limited access to MMF and TAC in several Latin American countries, due primarily to cost issues, makes CYC the best alternative for induction (high or low dose) in these regions (table 2).

b. Which is the best maintenance treatment for adult patients with lupus nephritis?

Interventions considered

Recommendations are applicable to patients showing partial or total remission after induction therapy aiming at sustaining renal remission, preventing relapses and achieving the best long-term outcome. The following interventions were considered: (1) AZA; (2) MMF; (3) CYC; (4) TAC; and (5) CsA (online supplementary tables S1.1.1.7, S1.1.2.1, S1.1.2.2, S1.2.1, S1.2.3, S1.2.4, S1.2.5, S1.2.6, S1.2.7).

Benefits and harms

The panel concluded that long-term IS agents during maintenance therapy prolong stable renal function, reduce proteinuria, extend renal survival and minimise the toxicity of GCs. AZA, CYC, MMF and CsA seem to be equivalent regarding efficacy but MMF and AZA have a better safety profile, particularly regarding gonadal toxicity and blood pressure control. We found very low certainty of the evidence for TAC as maintenance therapy, with studies mostly restricted to Asian populations.

Table 2 GLADEL–PANLAR recommendations for adult and childhood-onset lupus nephritis

Lupus nephritis		
Treatment recommendations	**Quality of the evidence**	**Strength of recommendation**
Induction therapy for adult patients with lupus-related nephritis		
Use SOC (GCs and AMs) plus another IS agent (CYC, MMF or TAC) over GCs alone.	Moderate	Strong
Maintenance therapy for adult patients with lupus-related nephritis		
Use MMF or AZA over CYC.	Low	Strong*
Induction therapy for childhood patient with lupus-related nephritis		
Use high-dose GCs (prednisone 1–2 mg/kg/day, maximum 60 mg/day) plus another IS agent (MMF or CYC) over high-dose GCs alone.	Low	Weak
Maintenance therapy for childhood patient with lupus-related nephritis		
Use MMF or AZA over CYC.	Low	Weak

*Strong recommendation supported on high certainty in less adverse events with MMF or AZA than with CYC.
AM, antimalarials; AZA, azathioprine; CYC, cyclophosphamide; GC, glucocorticoid; GLADEL, *Grupo Latino Americano de Estudio del Lupus*; IS, immunosuppressant; MMF, mycophenolate mofetil; PANLAR, Pan-American League of Associations of Rheumatology; SOC, standard of care; TAC, tacrolimus.

Recommendation

The panel recommends AZA or MMF over CYC for maintenance in patients with SLE-related nephritis (strong recommendation based on low certainty of the evidence, since certainty in better efficacy of MMF or AZA over CYC is low but certainty of fewer adverse effects is high). Cost and availability issues may favour AZA (table 2).

Childhood-onset lupus nephritis

a. Which is the best induction treatment for childhood-onset lupus nephritis (cLN)?

Interventions considered

(1) MMF plus GCs; (2) CYC plus GCs; (3) GCs (online supplementary table S9.2.3).

Benefits and harms

The panel concluded that both MMF plus high-dose GCs (prednisone 1–2 mg/kg/day, maximum 60 mg/day) and CYC plus high-dose GCs are associated with significant benefits in comparison to GCs alone. No significant differences between these two alternatives were noted. The panel pointed that differential pharmacokinetic effects of MMF in cLN may exist, which could require dosing increase.[30] Risk of reduction of ovarian reserve and sperm abnormalities should be considered in patients with cLN treated with CYC.

Recommendation

The panel suggests high-dose GCs plus MMF or CYC over high-dose GCs alone in patients with cLN as induction therapy (weak recommendation based on low certainty of the evidence). Cost and availability may favour CYC despite the risk of gonadal toxicity (table 2).

b. Which is the best maintenance treatment for cLN?

Interventions considered

(1) SOC plus MMF; (2) SOC plus AZA (online supplementary table S9.2.3).

Benefits and harms

The panel concluded that MMF or AZA decreases the occurrence of ESRD without significant adverse events, as maintenance therapy for cLN. The panel pointed that differential pharmacokinetic effects of MMF in cLN may exist, which may require dosing increase.[30]

Recommendation

The panel suggests MMF or AZA over CYC for patients with cLN who responded, partially or completely, to induction therapy (weak recommendation based on low certainty of the evidence). Cost and availability may favour AZA (table 2).

Cardiac manifestations

a. Which is the best treatment for adult patients with lupus-related acute pericarditis?

Interventions considered

(1) SOC plus colchicine; (2) SOC plus non-steroidal anti-inflammatory drugs (NSAID); (3) SOC plus belimumab; (4) low to moderate dose of GCs for 4 weeks and slow tapering (online supplementary tables S6.2.1 and S6.3.1).

Benefits and harms

Based on the identified evidence the panel concluded that the use of SOC combined with colchicine is associated with significant benefits (decrease in pericarditis recurrence rate) compared with SOC alone. Belimumab probably made little or no difference in pericarditis-related symptom improvement.

Recommendation

The panel suggests SOC plus colchicine over SOC plus NSAIDs or belimumab for patients with acute SLE-related pericarditis (weak recommendation based on low certainty of the evidence) (table 3).

Pulmonary manifestations

a. Which is the best treatment for lupus-related diffuse alveolar haemorrhage (DAH)?

Table 3 GLADEL–PANLAR recommendations for cardiac and pulmonary manifestations

Treatment recommendations	Quality of the evidence	Strength of recommendation
Cardiac manifestations		
In adult patients with lupus-related acute pericarditis		
Use SOC plus colchicine over SOC plus NSAIDs or belimumab.	Low	Weak
Pulmonary manifestations		
In adult patient with lupus-related diffuse alveolar haemorrhage		
Use intravenous GCs plus CYC and/or intravenous Ig and/or TPE and/or RTX over GCs alone.	Very low	Strong*

*Strong recommendation supported on possible benefits in the context of a life-threatening situation.
CYC, cyclophosphamide; GC, glucocorticoid; GLADEL, *Grupo Latino Americano de Estudio del Lupus*; Ig, immunoglobulin; NSAID, non-steroidal anti-inflammatory drug; PANLAR, Pan-American League of Associations of Rheumatology; RTX, rituximab; SOC, standard of care; TPE, therapeutic plasma exchange.

Interventions considered

(1) High-dose GCs plus CYC; (2) high-dose GCs plus intravenous immunoglobulins (Ig); (3) high-dose GCs plus therapeutic plasma exchange (TPE); (4) high-dose GCs plus RTX (online supplementary tables S6.1.1 and S6.1.2).

Benefits and harms

In the absence of trustworthy evidence regarding the effects of the different interventions in this scenario and considering DAH's high mortality rate, the panel decided that intense and early approach is mandatory without prioritising one intervention over another.

Recommendation

The panel recommends that patients with SLE-related DAH be treated with intravenous GCs plus CYC and/or intravenous Ig and/or TPE and/or RTX over GCs alone (strong recommendation based on very low certainty of the evidence, since possible benefits exist in a life-threatening situation). Cost and availability may favour GC plus CYC (table 3).

Neuropsychiatric manifestations

a. Which is the best treatment for adult patients with lupus-related severe, acute neuropsychiatric manifestations?

Interventions considered

(1) High-dose GCs; (2) high-dose GCs plus CYC; and (3) high-dose GCs plus RTX (online supplementary tables S5.1.1, S5.1.2, S5.1.3, S5.1.6, S5.2.1, S5.2.3, S5.3.3, S5.4.1, S5.4.3, S5.5.1, S5.5.2, S5.6.1).

Benefits and harms

The panel concluded that both options (GCs plus CYC and GCs plus RTX) were associated with large benefits and moderate harms in comparison to GCs plus placebo in patients with acute neurological manifestations. No studies comparing these two options were identified. In terms of SLE and severe neurological manifestations, clinical trials with GCs plus CYC focused on both general neurologic manifestations, and on seizures, psychosis, myelitis, peripheral neuropathy, brain stem disease and optic neuritis, specifically. No data were found regarding other neuropsychiatric manifestations. The panel significantly weighted the fact that the certainty of the evidence was better for CYC than RTX and that RTX was only evaluated in refractory patients.

Recommendation

The panel suggests using GCs plus CYC over GCs alone or GCs plus RTX for the treatment of severe neurologic manifestations in patients with SLE (weak recommendation based on low certainty of the evidence). Cost and availability may favour CYC (table 4).

Haematological manifestations

a. Which are the best interventions for patients with severe acute lupus-related haemolytic anaemia (haemoglobin ≤8 g/dL)?

Interventions considered

(1) High-dose GCs; (2) GCs plus RTX (online supplementary tables S7.1.12 and S7.1.13).

Table 4 GLADEL–PANLAR recommendations for neuropsychiatric and haematological manifestations

Treatment recommendations	Quality of the evidence	Strength of recommendation
Neuropsychiatric manifestations		
In adult patients with lupus-related severe, acute neuropsychiatric manifestations		
Use GCs plus CYC over GCs alone or GCs plus RTX.	Low	Weak
Haematological manifestations		
In patients with severe acute lupus-related haemolytic anaemia (haemoglobin ≤8 g/dL)		
Use high-dose GCs.	Low	Weak
If life-threatening or haemolytic anaemia remains active use RTX. Cost and availability may prompt the use of IS over RTX.	Low	Weak
In patients with severe lupus-related thrombocytopenia (platelet count ≤30 x10^9/L)		
Use high-dose GCs.	Moderate	Weak
If first line failure, or life-threatening bleeding, urgent surgery or patients with current and ongoing infections: Use intravenous Ig with/without GCs or RTX plus GCs. Cost and availability may prompt the use of IS over RTX.	Moderate	Strong

CYC, cyclophosphamide; GC, glucocorticoid; GLADEL, *Grupo Latino Americano de Estudio del Lupus*; Ig, immunoglobulin; IS, immunosuppressant; PANLAR, Pan-American League of Associations of Rheumatology; RTX, rituximab.

Benefits and harms

The panel concluded that compared with GCs as the first-line therapy, the addition of RTX provided moderate beneficial effects (reducing the risk of flare) and moderate harms (increasing the risk of infections). However, the panel significantly weighted the risks associated with RTX as well as availability and cost issues.

Recommendation

The panel suggests using high-dose GCs for patients with severe haemolytic anaemia (weak recommendation based on low certainty of the evidence).

It also suggests RTX for patients with life-threatening haemolytic anaemia and/or for those in whom high-dose GC treatment fails (weak recommendation based on low certainty of the evidence). Cost and availability, however, may prompt the use of IS instead of RTX although no data support this assertion (table 4).

a. Which are the best interventions for patients with severe lupus-related thrombocytopenia (platelet count ≤ 30 x10^9/L)?

Interventions considered

(1) High-dose GCs; (2) high-dose GCs plus RTX; (3) high-dose GCs plus intravenous Ig (online supplementary tables S7.1.12, S7.1.13, S7.1.15).

Benefits and harms

The panel concluded that compared with GCs as the first-line therapy, RTX and intravenous Ig provided moderate beneficial effects (increasing the platelet count). The harmful effects were judged as moderate for RTX (increase in infections) and small for intravenous Ig (infusion reactions).

The panel significantly weighted the risks associated with RTX as well as availability and cost issues. In life-threatening situations, the panel significantly weighted intravenous Ig's and RTX's beneficial effect on platelet count.

Recommendations

The panel suggests using high-dose GCs in patients with lupus with severe lupus thrombocytopenia (weak recommendation based on moderate certainty of the evidence).

It also recommends intravenous Ig with/without GCs or RTX plus GCs for patients who are refractory to high-dose GCs, those with life-threatening bleeding, those requiring urgent surgery and those with infections (strong recommendation based on moderate certainty of the evidence). Cost and availability, however, may prompt the use of IS instead of RTX although there are no data to support this assertion (table 4).

Antiphospholipid syndrome

a. Which is the best treatment for adult patients with SLE with antiphospholipid syndrome (APS) and venous thromboembolic disease (VTD)?

Interventions considered

(1) Extended anticoagulation (AC) with vitamin K antagonist (compared with not-extended AC); (2) high-intensity AC (international normalised ratio (INR) 3–4.5) compared with moderate-intensity AC (INR 2–3) (online supplementary tables S10.2.1 and S10.2.2).

Benefits and harms

The panel judged the effect of extended AC as a large benefit, reducing VTD with increase in bleeding risk as a moderate harm. For the comparisons of different AC intensities, the panel decided to use the evidence from observational studies because it judged that it probably better reflects reality given that the randomised controlled trials (RCT) are severely flawed (indirectness of intervention as most patients did not reach the INR >3 goal). They judged the reduction in VTD as a large benefit and the bleeding increase as a large harm. Hence, the panel considered that the balance could favour the intervention only when the risk of VTD recurrence is particularly high.

Recommendation

The panel recommends extended AC with vitamin K antagonist therapy for patients with APS with VTD (strong recommendation based on moderate certainty of evidence).

The panel recommends standard (INR 2.0–3.0) over high-intensity (INR 3.0–4.0) AC for patients with APS with VTD (strong recommendation based on very low certainty of the evidence, since certainty of the effect on VTD recurrence is very low but certainty in bleeding risk is high (significant increase in major bleeding with INR 3.0–4.0)).

b. Which is the best treatment for adult patients with SLE with APS and stroke?

Interventions considered

Extended antithrombotic therapy with: (1) vitamin K antagonist; (2) low-dose aspirin (LDA: 81–100 mg/day); (3) vitamin K antagonist plus LDA; (4) high-intensity AC (INR 3–4.5) (online supplementary tables S10.3.1 and S10.3.2).

Benefits and harms

The panel decided to use the body of evidence provided by observational studies because it probably better reflects reality as the RCTs are severely flawed (indirectness of population as most patients were inadequately diagnosed with APS). The panel judged the observed reduction in arterial thrombosis with high-intensity AC as a large benefit, and the bleeding increase as a large harm. Also, it was noted that the observed basal risk (risk with LDA) of thromboembolic recurrence in patients with APS and arterial events was particularly high, compared with the risk of recurrence in patients with VTD.

Recommendation

The panel suggests extended high-intensity (INR 3.0–4.0) over standard-intensity AC (INR 2.0–3.0) or LDA alone for patients with SLE with APS and stroke (weak recommendation based on very low certainty of the evidence).

c. Which is the best treatment for pregnant SLE women with antiphospholipid antibodies and recurrent pregnancy loss?

Interventions considered

(1) HCQ plus LDA; (2) HCQ plus LDA plus heparin; (3) HCQ plus intravenous Ig (online supplementary tables S10.5.1, S10.5.2, S10.5.3, S10.5.4, S10.5.5, S10.5.6, S10.5.7, S10.5.8).

Benefits and harms

The panel judged the observed reduction in pregnancy loss with the addition of heparin to LDA as a large benefit. This intervention was not associated with significant harms. The addition of GCs or intravenous Ig to heparin plus LDA was associated with large harms (significant increase in premature delivery) without relevant benefits. Regarding heparin administration, the panel considered the reduction in pregnancy loss with low molecular weight heparin (LMWH) in comparison with unfractionated heparin (UFH) as a large benefit without significant adverse effects. No additional benefits were observed with LMWH-enoxaparin 80 mg compared with 40 mg.

Recommendation

The panel recommends HCQ plus LMWH plus LDA over HCQ plus LDA or adding GCs or intravenous Ig for pregnant patients with SLE with antiphospholipid antibodies and recurrent pregnancy loss (strong recommendation based on moderate certainty of the evidence (LMWH plus LDA vs other alternatives) and very low certainty of the evidence (GCs and intravenous Ig vs other alternatives), since high certainty of harms related to GCs (increased premature delivery) and intravenous Ig (costs increase, burden related to drug administration) exists).

It also suggests LMWH at a dose of 40 mg/day over UFH or higher doses of LMWH (weak recommendation based on low certainty of the evidence) (table 5).

DISCUSSION

Treatment of SLE in Latin America remains a challenge despite several guidelines published on the management of this disease.[16–21] The distinct epidemiology, healthcare resources, socioeconomic issues and priorities were considered to develop these guidelines.

Although these guidelines consider region limitations, the inclusion of alternative approaches for tailoring treatment did not exclude the task of providing physicians with the state-of-the-art findings in the field. This was a major advantage of the present work since highlighting these advances provides valuable basis for future requirement of government authorisation of new drugs in these countries.

Of note, problems faced by Latin American countries are shared by several developing nations. Therefore, it is expected that these guidelines will also be very useful for them. Furthermore, due to ever increasing globalisation and the increase

Table 5 GLADEL–PANLAR recommendations for adult patients with SLE with antiphospholipid antibodies or antiphospholipid syndrome

Antiphospholipid syndrome		
Treatment recommendations	**Quality of the evidence**	**Strength of recommendation**
In adult patients with lupus with APS and venous thromboembolic disease		
Use extended over time-limited anticoagulation.	Moderate	Strong
Use standard-intensity anticoagulation (INR 2.0–3.0) over high-intensity anticoagulation (INR 3.0–4.0).	Very low	Strong*
In adult patients with SLE with APS and stroke		
Use high-intensity anticoagulation (INR 3.0–4.0) over standard-intensity anticoagulation (INR 2.0– 3.0) or LDA.	Very low	Weak
In pregnant lupus women with obstetric APS and recurrent pregnancy losses		
Use HCQ plus LMWH plus LDA over HCQ plus LDA, or adding GCs or intravenous Ig.	Moderate	Strong

*Strong recommendation supported on high certainty in significant bleeding risk increase with high-intensity anticoagulation.
APS, antiphospholipid syndrome; GC, glucocorticoid; GLADEL, *Grupo Latino Americano del Estudio de Lupus*; HCQ, hydroxychloroquine; Ig, immunoglobulin; INR, international normalised ratio; LDA, low-dose aspirin; LMWH, low molecular weight heparin; PANLAR, Pan-American League of Associations of Rheumatology; SLE, systemic lupus erythematosus.

of migratory movements of people from countries with more susceptible SLE groups in terms of frequency and disease severity both in terms of race/ethnicity (Mestizos, Asians, Africans) and low SES to countries with better life opportunities, we consider that these guidelines may be used by physicians anywhere in the world, even in developed countries, where such individuals may migrate to and seek care for their lupus.

We acknowledge as a limitation that certainty of the evidence was not as high as desirable for most recommendations and probably biased by few randomised clinical trials. Although regional information was published on several topics[1 4 10 11 23 24 31–49] we recognise that these guidelines should be updated as research-based changes in our understanding of SLE emerge. Regardless, the publication of these guidelines must be followed by health system engagement and implementation by specialists, major steps towards improvement of lupus treatment in Latin America and low/middle-income countries.

Author affiliations
[1]Departamento de Medicina Interna, Grupo Oroño-Centro Regional de Enfermedades Autoinmunes y Reumáticas (GO-CREAR), Rosario, Argentina
[2]Rheumatology Division, Faculdade de Medicina, Hospital das Clinicas HCFMUSP, Universidade de São Paulo, São Paulo, Brazil
[3]Sección de Reumatología, Servicio de Clínica Médica, Instituto Universitario, Escuela de Medicina, and Fundación Dr Pedro M Catoggio para el Progreso de la Reumatología, Hospital Italiano de Buenos Aires, Buenos Aires, Argentina
[4]Centro de Investigación Clínica de Morelia, SC, Morelia, México
[5]Servicio de Clínica Médica del Hospital Alemán de Buenos Aires, Hospital Alemán de Buenos Aires, Ciudad Autónoma de Buenos Aires, Argentina
[6]Grupo de Inmunología Celular e Inmunogenética, Universidad de Antioquia, Hospital Universitario, Fundación San Vicente, Medellín, Colombia
[7]Centro de Biología Celular y Biomedicina, Facultad de Medicina y Ciencia. Universidad San Sebastián, Santiago, Chile
[8]Departamento de Reumatología, Hospital de Clínicas, Facultad de Ciencias Médicas, Universidad Nacional de Asunción, Asunción, Paraguay
[9]Hospital Angeles del Pedregal, Ciudad de México, México
[10]Servicio de Reumatología, HIGA General San Martín, La Plata, Argentina
[11]Servicio de Reumatología, Centro Médico ABC, Ciudad de México, México
[12]Servicio de Reumatología Infantil, Hospital de Niños Dr Ricardo Gutiérrez, Buenos Aires, Argentina
[13]Escola Paulista de Medicina, Universidade Federal de São Paulo, São Paul, Brazil
[14]Discipline of Rheumatology, University of the State of Rio de Janeiro, Rio de Janeiro, Brasil
[15]Facultad de Medicina., Universidad Nacional Mayor de San Marcos. Servicio de Reumatología. Clínica San Felipe, J. María., Lima, Perú.
[16]Servicio de Reumatología, Policlínica Méndez Gimón, Caracas, Venezuela
[17]Unidad de Enfermedades Reumáticas y Autoinmunes (UNERA), Corporación Médica Monte Sinaí., Cuenca, Ecuador
[18]Universidad Nacional de Colombia, Bogotá, Colombia
[19]Centro Integral de Reumatología, Reumalab, Medellín, Colombia
[20]Sección de Reumatología, Hospital del Salvador. Universidad de Chile. Unidad de Reumatología. Clínica Alemana de Santiago, Facultad de Medicina Clínica Alemana, Universidad del Desarrollo., Santiago, Chile
[21]Pediatric Department, Faculdade de Medicina, Children's Institute, Hospital das Clinicas HCFMUSP, Universidade de São Paulo, São Paulo, Brazil
[22]Clínica Reumatológica, Universidad de la República, and Unidad Docente Asistencial, Hospital Pasteur, Instituto Nacional de Reumatología., Montevideo, Uruguay
[23]Servicio de Reumatología, Hospital Clinic, Barcelona, Spain
[24]Servicio de Reumatología, Hospital Provincial de Rosario, Rosario, Argentina
[25]Servicio de Reumatología, Hospital Italiano de Córdoba, Córdoba, Argentina
[26]Division of Rheumatology, Department of Medicine, Emory School of Medicine, Atlanta, Georgia, USA
[27]Servicio de Reumatología, Hospital Privado Universitario de Córdoba, Córdoba, Argentina
[28]Servicio de Reumatología, Hospital General Guillermo Almenara Irigoyen, EsSalud., Lima, Perú
[29]Universidad Científica del Sur, Lima, Perú
[30]Serviço de Reumatologia do Hospital das Clínicas da Universidade Federal de Pernambuco (HC-UFPE), Recife, Brazil
[31]Unidad de Reumatología, Departamento de Medicina, Universidad de Oriente, Complejo Hospitalario Universitario Ruiz y Páez, Ciudad Bolívar, Venezuela
[32]Serviço de Reumatologia, Departamento de Clinica Medica, Faculdade de Medicina, Hospital das Clínicas, Universidade Federal de Goiás, Goiânia, Brazil
[33]Departamento de Pediatría, Facultad de Medicina, Universidad de Antioquia, Hospital Pablo Tobón Uribe, Medellín, Colombia
[34]Servicio de Reumatología, Hospital General de Medellín 'Luz Castro de Gutierrez' ESE, ARTMEDICA, Medellín, Colombia
[35]Departamento de Inmunología y Reumatología, Instituto Nacional de Ciencias Médicas y Nutrición, Salvador Zubirán, Ciudad de México, Mexico
[36]Unidad de Enfermedades Autoinmunes Sistémicas, Facultad de Medicina, Clínica Médica 'C', Hospital de Clínicas, Universidad de la República, Montevideo, Uruguay
[37]Unidad de Reumatología y Enfermedades Autoinmunes Sistémicas, HIGA Dr Oscar Alende, Mar del Plata, Argentina
[38]Servicio de Reumatología, Enfermedades Reumatológicas e Investigación Clínica (ERIC), Hospital Docente Padre Billini, Santo Domingo, Dominican Republic
[39]Departamento de Clínica Médica, Disciplina de Reumatologia, Faculdade de Ciências Medicas da UNICAMP, Universidade Estadual de Campinas, Campinas, Brazil
[40]Servicio de Reumatología, Departamento de Especialidades Médicas, Hospital Nacional Edgardo Rebagliati Martins, EsSalud., Lima, Perú
[41]Servicio de Reumatología, CEIBAC, SC, Guadalajara, México
[42]Servicio de Inmunología, Instituto de Investigaciones Médicas "Alfredo "Lanari", Ciudad Autónoma de Buenos Aires, Argentina
[43]Servicio de Reumatología, Hospital Escuela "Eva Perón", Granadero Baigorria, Argentina
[44]Departamento de Inmunología, Instituto Nacional de Cardiología Ignacio Chávez, Ciudad de México, Mexico
[45]Departamento de Reumatología, Instituto Nacional de Cardiología "Ignacio Chávez", Ciudad de México, México
[46]Unidad de Reumatología, Cátedra de Clínica Médica I, Hospital Córdoba. Cátedra de Semiología, Facultad de Ciencias Médicas, Universidad Nacional de Córdoba., Córdoba, Argentina
[47]Rheumatology Division, Department of Internal Medicine, Hospital de Clínicas de Porto Alegre, Universidade Federal do Rio Grande do Sul, Porto Alegre, Brazil
[48]Departamento de Inmunología Clínica y Reumatología, Escuela de Medicina, Pontificia Universidad Católica de Chile, Santiago, Chile
[49]Departamento de Reumatología, Consultorio de Especialidades del Instituto Salvadoreño de la Seguridad Social, San Salvador, El Salvador
[50]Departamento de Inmunología y Reumatología, Hospital General de Occidente., Zapopan, Jalisco, México.
[51]Instituto Nacional de Rehabilitación Luis Guillermo Ibarra Ibarra, Ciudad de México, Mexico
[52]Departamento de Reumatología, Hospital de Especialidades CMN SXXI, IMSS, Ciudad de México, Mexico
[53]Grupo de Trabajo en Enfermedades Autoinmunes Sistémicas, Servicio de Clínica Médica, Facultad de Medicina, Universidad de la Republica, Hospital Pasteur, Administración de Servicios de Salud del Estado, Montevideo, Uruguay
[54]Servicio Nacional de Reumatología, Centro de Investigaciones Médico Quirúrgicas (CIMEQ)., La Habana, Cuba

[55]Servicio de Reumatología, Instituto de Rehabilitación Psicofísica (IREP), Ciudad Autónoma de Buenos Aires, Argentina
[56]Division of Clinical Immunology and Rheumatology, Department of Medicine, School of Medicine, The University of Alabama at Birmingham, Birmingham, Alabama, USA
[57]Department of Medicine, School of Medicine, Universidad Peruana Cayetano Heredia, Lima, Peru

Correction notice This article has been corrected since it published Online First. The author affiliations have been updated.

Acknowledgements The authors are deeply grateful to Miss Teresa Cattoni (Buenos Aires, Argentina), Laura Athie (Mexico City, Mexico) and Kim Schofield (Atlanta, USA), the three patients with SLE who carefully reviewed this manuscript and provided very useful comments and suggestions.

Contributors All authors listed in this manuscript have participated in planning, drafting, reviewing, final approval and are accountable for all aspects of the manuscript.

Funding PANLAR financed the development of these guidelines. PANLAR received unrestricted funds from GlaxoSmithKline (GSK) and UCB Pharma for this endeavour.

Disclaimer None of the entities influenced the content of the guidelines.

Competing interests LBF, BAPE and OAM have been speakers for GlaxoSmithKline (GSK). JCTB has received research grants from GSK. RMX, ON and JFM have received support grants for meetings from GSK. JAGP has been a lecturer for Roche. ERS has received research grants and has been a lecturer for Roche. JFM has been a clinical researcher for Anthera. MHC has received research grants from Roche and is an advisor for Eli Lilly.

Patient consent Not required.

Provenance and peer review Not commissioned; externally peer reviewed.

REFERENCES

1 Pons-Estel BA, Catoggio LJ, Cardiel MH, *et al*. The GLADEL multinational Latin American prospective inception cohort of 1,214 patients with systemic lupus erythematosus: ethnic and disease heterogeneity among "Hispanics". *Medicine* 2004;83:1–17.
2 Alarcón GS, McGwin G, Bartolucci AA, *et al*. Systemic lupus erythematosus in three ethnic groups. IX. Differences in damage accrual. *Arthritis Rheum* 2001;44:2797–806.
3 Alarcón GS, McGwin G, Bastian HM, *et al*. Systemic lupus erythematosus in three ethnic groups. VII [correction of VIII]. Predictors of early mortality in the LUMINA cohort. LUMINA Study Group. *Arthritis Rheum* 2001;45:191–202.
4 Alarcón-Segovia D, Alarcón-Riquelme ME, Cardiel MH, *et al*. Familial aggregation of systemic lupus erythematosus, rheumatoid arthritis, and other autoimmune diseases in 1,177 lupus patients from the GLADEL cohort. *Arthritis Rheum* 2005;52:1138–47.
5 Pons-Estel GJ, Alarcón GS, Scofield L, *et al*. Understanding the epidemiology and progression of systemic lupus erythematosus. *Semin Arthritis Rheum* 2010;39:257–68.
6 Sánchez E, Rasmussen A, Riba L, *et al*. Impact of genetic ancestry and sociodemographic status on the clinical expression of systemic lupus erythematosus in American Indian-European populations. *Arthritis Rheum* 2012;64:3687–94.
7 Alarcón-Riquelme ME, Ziegler JT, Molineros J, *et al*. Genome-Wide association study in an amerindian ancestry population reveals novel systemic lupus erythematosus risk loci and the role of european admixture. *Arthritis Rheumatol* 2016;68:932–43.
8 Guarnizo-Zuccardi P, Lopez Y, Giraldo M, *et al*. Cytokine gene polymorphisms in Colombian patients with systemic lupus erythematosus. *Tissue Antigens* 2007;70:376–82.
9. Durán S, Apte M, Alarcón GS. LUMINA Study Group. Poverty, not ethnicity, accounts for the differential mortality rates among lupus patients of various ethnic groups. *J Natl Med Assoc* 2007;99:1196–8.
10 Ugarte-Gil MF, Pons-Estel GJ, Molineros J, *et al*. Disease features and outcomes in United States lupus patients of Hispanic origin and their Mestizo counterparts in Latin America: a commentary. *Rheumatology* 2016;55:436–40.
11. Ramírez Gómez LA, Uribe Uribe O, Osio Uribe O, *et al*. Childhood systemic lupus erythematosus in Latin America. The GLADEL experience in 230 children. *Lupus* 2008;17:596–604.
12 Kheir JM, Guthridge CJ, Johnston JR, *et al*. Unique clinical characteristics, autoantibodies and medication use in Native American patients with systemic lupus erythematosus. *Lupus Sci Med* 2018;5:e000247.
13 Bernatsky S, Boivin JF, Joseph L, *et al*. Mortality in systemic lupus erythematosus. *Arthritis Rheum* 2006;54:2550–7.
14 Teixeira RCA, Borba Neto EF, Christopoulos GB, *et al*. The Influence of Income and Formal Education on Damage in Brazilian Patients With Systemic Lupus Erythematosus. *J Clin Rheumatol* 2017;23:246–51.
15 Souza DC, Santo AH, Sato EI. Mortality profile related to systemic lupus erythematosus: a multiple cause-of-death analysis. *J Rheumatol* 2012;39:496–503.
16 Ruiz Irastorza G, Espinosa G, Frutos MA, *et al*. Diagnosis and treatment of lupus nephritis. Consensus document from the systemic auto-immune disease group (GEAS) of the Spanish Society of Internal Medicine (SEMI) and Spanish Society of Nephrology (S.E.N.). *Nefrologia* 2012;32(Suppl 1):1–35.
17 Bertsias G, Ioannidis JP, Boletis J, *et al*. EULAR recommendations for the management of systemic lupus erythematosus. Report of a Task Force of the EULAR Standing Committee for International Clinical Studies Including Therapeutics. *Ann Rheum Dis* 2008;67:195–205.
18 Hahn BH, McMahon MA, Wilkinson A, *et al*. American College of Rheumatology guidelines for screening, treatment, and management of lupus nephritis. *Arthritis Care Res* 2012;64:797–808.
19 Aguirre V, Alvo M, Ardiles L, *et al*. [A consensus of the Chilean Nephrology and Rheumatology Societies on renal involvement in systemic lupus erythematosus]. *Rev Med Chil* 2015;143:1569–78.
20 Klumb EM, Silva CA, Lanna CC, *et al*. [Consensus of the Brazilian Society of Rheumatology for the diagnosis, management and treatment of lupus nephritis]. *Rev Bras Reumatol* 2015;55:1–21.
21 Gordon C, Amissah-Arthur MB, Gayed M, *et al*. The British Society for Rheumatology guideline for the management of systemic lupus erythematosus in adults. *Rheumatology* 2017.
22 Burgos PI, McGwin G, Pons-Estel GJ, *et al*. US patients of Hispanic and African ancestry develop lupus nephritis early in the disease course: data from LUMINA, a multiethnic US cohort (LUMINA LXXIV). *Ann Rheum Dis* 2011;70:393–4.
23 Pons-Estel GJ, Alarcón GS, Burgos PI, *et al*. Mestizos with systemic lupus erythematosus develop renal disease early while antimalarials retard its appearance: data from a Latin American cohort. *Lupus* 2013;22:899–907.
24 Pons-Estel GJ, Alarcón GS, Hachuel L, *et al*. Anti-malarials exert a protective effect while Mestizo patients are at increased risk of developing SLE renal disease: data from a Latin-American cohort. *Rheumatology* 2012;51:1293–8.
25 Isenberg D, Appel GB, Contreras G, *et al*. Influence of race/ethnicity on response to lupus nephritis treatment: the ALMS study. *Rheumatology* 2010;49:128–40.
26 Ginzler EM, Dooley MA, Aranow C, *et al*. Mycophenolate mofetil or intravenous cyclophosphamide for lupus nephritis. *N Engl J Med* 2005;353:2219–28.
27 Mehat P, Atiquzzaman M, Esdaile JM, *et al*. Medication Nonadherence in Systemic Lupus Erythematosus: A Systematic Review. *Arthritis Care Res* 2017;69:1706–13.
28 Prudente LR, Diniz JS, Ferreira TX, *et al*. Medication adherence in patients in treatment for rheumatoid arthritis and systemic lupus erythematosus in a university hospital in Brazil. *Patient Prefer Adherence* 2016;10:863–70.
29 Cardiel MH, Soriano ER, Bonfá E, *et al*. Therapeutic Guidelines for Latin American Lupus Patients: Methodology. *J Clin Rheumatol* 2018;24:1.
30 Sagcal-Gironella AC, Fukuda T, Wiers K, *et al*. Pharmacokinetics and pharmacodynamics of mycophenolic acid and their relation to response to therapy of childhood-onset systemic lupus erythematosus. *Semin Arthritis Rheum* 2011;40:307–13.
31 Ugolini-Lopes MR, Seguro LPC, Castro MXF, *et al*. Early proteinuria response: a valid real-life situation predictor of long-term lupus renal outcome in an ethnically diverse group with severe biopsy-proven nephritis? *Lupus Sci Med* 2017;4:e000213.
32 Barile-Fabris L, Ariza-Andraca R, Olguín-Ortega L, *et al*. Controlled clinical trial of IV cyclophosphamide versus IV methylprednisolone in severe neurological manifestations in systemic lupus erythematosus. *Ann Rheum Dis* 2005;64:620–5.
33 Shinjo SK, Bonfá E, Wojdyla D, *et al*. Antimalarial treatment may have a time-dependent effect on lupus survival: data from a multinational Latin American inception cohort. *Arthritis Rheum* 2010;62:855–62.
34 Alarcón GS, McGwin G, Bertoli AM, *et al*. Effect of hydroxychloroquine on the survival of patients with systemic lupus erythematosus: data from LUMINA, a multiethnic US cohort (LUMINA L). *Ann Rheum Dis* 2007;66:1168–72.
35 Fessler BJ, Alarcón GS, McGwin G, *et al*. Systemic lupus erythematosus in three ethnic groups: XVI. Association of hydroxychloroquine use with reduced risk of damage accrual. *Arthritis Rheum* 2005;52:1473–80.
36 Pons-Estel GJ, Alarcón GS, McGwin G, *et al*. Protective effect of hydroxychloroquine on renal damage in patients with lupus nephritis: LXV, data from a multiethnic US cohort. *Arthritis Rheum* 2009;61:830–9.
37 Pons-Estel GJ, Alarcón GS, González LA, *et al*. Possible protective effect of hydroxychloroquine on delaying the occurrence of integument damage in lupus: LXXI, data from a multiethnic cohort. *Arthritis Care Res* 2010;62:393–400.
38 García MA, Alarcón GS, Boggio G, *et al*. Primary cardiac disease in systemic lupus erythematosus patients: protective and risk factors–data from a multi-ethnic Latin American cohort. *Rheumatology* 2014;53:1431–8.
39 González-Naranjo LA, Betancur OM, Alarcón GS, *et al*. Features associated with hematologic abnormalities and their impact in patients with systemic lupus erythematosus: Data from a multiethnic Latin American cohort. *Semin Arthritis Rheum* 2016;45:675–83.

40 Pimentel-Quiroz VR, Ugarte-Gil MF, Pons-Estel GJ, *et al*. Factors predictive of high disease activity early in the course of SLE in patients from a Latin-American cohort. *Semin Arthritis Rheum* 2017;47:199–203.
41 Ugarte-Gil MF, Wojdyla D, Pastor-Asurza CA, *et al*. Predictive factors of flares in systemic lupus erythematosus patients: data from a multiethnic Latin American cohort. *Lupus* 2018;27.
42 Garcia MA, Marcos JC, Marcos AI, *et al*. Male systemic lupus erythematosus in a Latin-American inception cohort of 1214 patients. *Lupus* 2005;14:938–46.
43 Pons-Estel GJ, Saurit V, Alarcón GS, *et al*. The impact of rural residency on the expression and outcome of systemic lupus erythematosus: data from a multiethnic Latin American cohort. *Lupus* 2012;21:1397–404.
44 Pons-Estel GJ, Wojdyla D, McGwin G, *et al*. The American College of Rheumatology and the Systemic Lupus International Collaborating Clinics classification criteria for systemic lupus erythematosus in two multiethnic cohorts: a commentary. *Lupus* 2014;23:3–9.
45 Catoggio LJ, Soriano ER, Imamura PM, *et al*. Late-onset systemic lupus erythematosus in Latin Americans: a distinct subgroup? *Lupus* 2015;24:788–95.
46 Ugarte-Gil MF, Acevedo-Vásquez E, Alarcón GS, *et al*. The number of flares patients experience impacts on damage accrual in systemic lupus erythematosus: data from a multiethnic Latin American cohort. *Ann Rheum Dis* 2015;74:1019–23.
47 Haye Salinas MJ, Caeiro F, Saurit V, *et al*. Pleuropulmonary involvement in patients with systemic lupus erythematosus from a Latin American inception cohort (GLADEL). *Lupus* 2017;26:1368–77.
48 Pons-Estel GJ, Aspey LD, Bao G, *et al*. Early discoid lupus erythematosus protects against renal disease in patients with systemic lupus erythematosus: longitudinal data from a large Latin American cohort. *Lupus* 2017;26:73–83.
49 Ugarte-Gil MF, Wojdyla D, Pons-Estel GJ, *et al*. Remission and Low Disease Activity Status (LDAS) protect lupus patients from damage occurrence: data from a multiethnic, multinational Latin American Lupus Cohort (GLADEL). *Ann Rheum Dis* 2017;76:2071–4.

Consensus proposal for taxonomy and definition of the autoinflammatory diseases (AIDs): a Delphi study

Eldad Ben-Chetrit,[1] Marco Gattorno,[2] Ahmet Gul,[3] Daniel L Kastner,[4] Helen J Lachmann,[5] Isabelle Touitou,[6] Nicolino Ruperto,[7] On behalf of the Paediatric Rheumatology International Trials Organisation (PRINTO) and the AIDs Delphi study participants

Handling editor Josef S Smolen

► Additional material is published online only. To view please visit the journal online (http://dx.doi.org/10.1136/annrheumdis-2017-212515).

For numbered affiliations see end of article.

Correspondence to
Eldad Ben-Chetrit, Rheumatology Unit, Hadassah Hebrew University Medical Center, Jerusalem, Israel; eldad@hadassah.org.il

Received 13 October 2017
Revised 10 July 2018
Accepted 12 July 2018
Published Online First 12 August 2018

To cite: Ben-Chetrit E, Gattorno M, Gul A, *et al*. *Ann Rheum Dis* 2018;**77**:1558–1565.

ABSTRACT

Autoinflammatory diseases (AIDs) are a relatively new family of disorders, defined about 19 years ago. Some of them are hereditary and some are not. The names given to these diseases do not follow any systematic guidelines, and sometimes the same disorder carries several names. The aim of this study is to refine the definition of AIDs and to provide some conventions for their naming. We focused mainly on monogenetic AIDs. Delphi technique, which enables consensus among a group of experts through internet and mail communication and questionnaires, was employed. After achieving 100% consensus among six members of a steering committee, the questionnaire containing AID definitions and the agreed-upon conventions were sent to 26 physicians and researchers working in the field of AIDs in order to gain broader support for the committee's proposals. The committee proposed the following definition for AIDs: "Autoinflammatory diseases are clinical disorders caused by defect(s) or dysregulation of the innate immune system, characterized by recurrent or continuous inflammation (elevated acute phase reactants-APR) and the lack of a primary pathogenic role for the adaptive immune system (autoreactive T-cells or autoantibody production)." Several rules were defined for guiding the naming of these diseases among which are: abandoning eponyms and preferring the name of the gene over its encoded protein. The new definition for AIDs allows inclusion of clinical disorders mainly associated with defects in the innate immune system. The new conventions propose names with clinical meaning and in some cases even clues for treatment.

Taxonomy is the science of naming. It is relevant to all fields of biology in which we name plants, animals, objects and diseases. In medicine, naming of diseases or syndromes has a special importance since it can give some clue about the nature of the clinical condition, its clinical features, pathogenesis and sometimes even an approach to treatment. Naming is also important for accurate and effective communication among different health disciplines. However, medical disorders have not been named in a standard way.[1] Physicians, who treat patients with a particular disorder or face a new clinical condition, are often the first to propose a name for the disease. Expert working groups may later revise the names to improve their usefulness.

Names of medical disorders are often derived from one or a combination of the following sources: genetic basis or biochemical defect; geographic spread or by eponyms. The main drawback of many names is the lack of a clinical meaning that could help the novice to understand the origin of the disease or recognise its clinical characteristics.

The autoinflammatory diseases (AIDs) are a group of medical disorders, derived from defects or dysregulation of the innate immune system.[2] This family of diseases was established in 1999 following the identification of the genes underlying two recurrent fever syndromes: familial Mediterranean fever (FMF)[3 4] and TNF-receptor-associated periodic syndrome (TRAPS).[5] Over the last 19 years, more and more diseases have been classified among this group of disorders, some of which may not fit well with the classical definition of the AIDs. Moreover, many of them were given names with no systematic guidelines or rules. In some cases, the same disease carries several names (table 1).[6–48] This has led to a chaotic situation in naming these clinical disorders and has called for a better standardisation of this field. This need is accentuated by recent progress in next generation sequencing techniques, which have led to an increasing capability to identify new genes and new syndromes, expanding the spectrum of AIDs.

Indeed, following the International Society for Systemic Autoinflammatory Diseases (ISSAID) meeting in Lausanne, in 2013, a mandate was given to one of us (E B-C) to undertake a preliminary consensus-based exercise for the following aims: (1) to refine the definition of the 'autoinflammatory diseases'; (2) to provide some rules and new proposals for naming this current group of clinical conditions and those that will be identified in the future.

METHODS

In order to find the different definitions proposed for AIDs over the years, we searched the MEDLINE/PubMed Central (PMC) from 1998 to January 2016, using the MESH search term: 'autoinflammatory diseases' (online supplementary figure S1). In order to find the names used for each AID, we took one of their current names as depicted in table 1 and searched for papers where they were first reported. Then, we searched for reviews on these items to find additional synonymous names. Table 1 is based on a list of AIDs published by one of the authors (IT),[49] properly integrated and updated during the consensus process and finally approved by all the steering committee members. It focused—mainly—on monogenic disorders.

Table 1 Current name of the disorder (in bold) and additional names (normal characters) derived from the literature

Current name of the disorder and additional names	Proposed nomenclature
CAPS—Cryopyrin-associated periodic fever syndrome[22]	***NLRP3*-associated autoinflammatory disease (*NLRP3*-AID)**
CINCA—Chronic infantile neurological, cutaneous and articular syndrome,[19] NOMID—Neonatal onset multisystem inflammatory disease	Severe
MWS—Muckle-Wells syndrome[20]	Moderate
FCAS—Familial cold autoinflammatory syndrome[21]	Mild
***CARD14*-associated disease**	***CARD14*-associated psoriasis**
PRP—Familial pityriasis rubra pilaris[32]	
CAMPS—*CARD14*-mediated pustular psoriasis[33]	
Cherubism[45]	***SH3BP2* deficiency with multilocular cystic disease of the mandibles (SDCM)**
Familial multilocular cystic disease of the jaws[46]	
Cherubism—familial fibrous dysplasia of the jaws[47]	
CGCL—Central giant cell lesion[48]	
CRMO—Chronic recurrent multifocal osteomyelitis[31]	**Chronic non-bacterial osteomyelitis (CNO)**—(when the gene is known it should be added)
Majeed syndrome,[28] congenital dyserythropoietic anaemia and chronic recurrent multifocal osteomyelitis[30]	
LIPIN2-associated disease [29]	***LPIN2-CNO***
DIRA—Deficiency of the IL-1 receptor antagonist[26]	**(No change)**
DITRA—Deficiency of the IL-3 6receptor antagonist[27]	**(No change)**
FCAS2—Familial cold autoinflammatory syndrome 2[36]	***NLRP12*-associated autoinflammatory disease (*NLRP12*-AID)**
Guadeloupe fever, NALP12 periodic fever syndrome[36]	
	Pyrin-associated autoinflammatory disease (PAAD)
FMF—Familial Mediterranean fever[9]	**(No change)**
Benign paroxysmal peritonitis,[6] periodic disease,[7] Armenian disease, periodic disease 'Maladie periodique',[8] FMF,[9] recurrent polyserositis,[10] familial paroxysmal polyserositis[11]	
PAAND—Pyrin-associated autoinflammation with neutrophilic dermatosis[12]	**(No change)**
JMP	**Proteasome-associated autoinflammatory syndrome (PRAAS)**
Joint contractures, muscle atrophy, microcytic anaemia and panniculitis-induced lipodystrophy,[40]	***PSMB8*-PRAAS, *PSMB4*/*PSMB9*-PRAAS, *PSMB4*/*PSMB9*-PRAAS, *PSMA3*/*PSMB8*-PRAAS**
Chronic atypical neutrophilic dermatosis with lipodystrophy and elevated temperature (CANDLE) syndrome, [39] Nakajo-Nishimura syndrome (NNS)[41]	
Mevalonate kinase disease (deficiency)[15 16]	**Mevalonate kinase deficiency (MKD)**
HIDS—Hyper IgD syndrome[17] **Mevalonic aciduria**	**Mild** **Severe**
Dutch type periodic fever[18]	(Add porokeratosis or retinitis pigmentosa when present)
IL-10 deficiency	**IL-10 deficiency-associated inflammatory bowel disease**
IBD—IL-10R-associated very early[34]	
Infantile colitis[35]	
***NOD2 CARD15*-associated disease**	***NOD2*-associated granulomatous disease** (Optional: add Blau syndrome or IBD according to the main clinical features)
Blau syndrome,[23] early onset sarcoidosis,[24] familial Crohn's disease[25]	
PAPA/Pyogenic arthritis, pyoderma gangrenosum and acne syndrome[37 38]	***PSTPIP1*-associated arthritis, pyoderma gangrenosum and acne (PAPA)**
PFAPA—Periodic fever, aphthous stomatitis, pharyngitis and adenitis	**(No change)**
Periodic fever, aphthous stomatitis, pharyngitis and adenitis or periodic fever aphthous pharyngitis and cervical adenopathy[43]	
Marshall's syndrome[44]	
Schnitzler syndrome[42]	**(No change)**
PUPAP—Periodic fever with urticaria and paraprotein	
TRAPS—TNF receptor-associated periodic fever syndrome[3]	**(No change)**
Familial Hibernian fever[13]	
Familial autosomal-dominant periodic fever[14]	

The last column reports the proposed nomenclature for the AIDs as results of the consensus process.
AIDs, autoinflammatory diseases.

For choosing the best definition for AIDs and the most appropriate name for each AID, we have used the Delphi technique, which enables consensus among a group of experts through mail communication.[50] The Delphi method is essentially a series of questionnaires involving several steps, each of which is based on the results of the previous step. The process stops when consensus of at least 80% of the participants on each item is reached.[51]

An *ad hoc* steering committee of six clinicians and researchers from six different countries who are working in the field of autoinflammation was established.

The first Delphi questionnaire was built through sending broad and open-ended questions in order to elicit different opinions from the panellists about the current definitions and names of AIDs.

Once received, the replies from the panellists were analysed to generate a series of statements that were employed as the basis for follow-up questionnaires that were sent back to the individual participants. In each subsequent questionnaire, the panellists were also provided with the overall results (responses) of the previous questionnaire from all the members. After achieving 100% consensus among the steering committee members, the questionnaire containing the AIDs definitions and the agreed-on names of AIDs were sent to 26 physicians and researchers working in the field of AIDs around the world. They were identified in the Paediatric Rheumatology International Trials Organization (PRINTO) mailing list through their high active participation in the Eurofever registry.[52 53] The aim of this step was to gain broader support for the committee's proposals and to consider changes once a name was rejected by or was not acceptable to more than 80% of the participants of the large group of AIDs experts. Delphi survey implementation was conducted by PRINTO.[54]

RESULTS

AIDs proposed definition

The literature review disclosed 536 papers of which only 7 specifically dealt with the definitions of AIDs[5 49 55–59] (online supplementary figure S1). The first definition for AIDs was proposed by the NIH group in 1999.[5] This definition was as follows: 'The autoinflammatory syndromes are systemic disorders characterised by apparently unprovoked inflammation in the absence of high-titre autoantibodies or antigen-specific T lymphocytes'. This definition was based mainly on the two diseases whose related genes had then been identified: FMF and TRAPS.[3–5] Since in both diseases the flares appeared mostly spontaneous, the definition included the word 'unprovoked'. The definition stresses the lack of involvement of the adaptive immune system in these disorders, since no autoantibodies or autoreactive T-cells were involved.

Seven years later McGonagle and McDermott suggested another definition: 'AIDs are characterised by self-directed inflammation, whereby local factors at sites predisposed to disease lead to activation of innate immune cells, including macrophages and neutrophils, with resultant target tissue damage. For example, disturbed homeostasis of canonical cytokine cascades (as in the periodic fevers), aberrant bacterial sensing (as in Crohn's disease), and tissue microdamage predispose one to site-specific inflammation that is independent of adaptive immune responses'.[55] The authors proposed that immunological diseases ought to be conceived as a continuum with 'pure monogenic autoinflammatory diseases' at one end and 'pure monogenic autoimmune diseases' at the other. This definition is relatively complex, but explicitly invokes innate immunity and widens the spectrum of AIDs.

Later, several other definition or refinement were proposed.[49 56–58] In a recent study, de Jesus *et al* provide an outstanding classification of AIDs strictly based on their pathophysiology.[59] However, the authors do not propose a new definition for the AIDs.

Given the proliferation of AID definitions, with sometimes conflicting concepts, the steering committee agreed to adopt the first and original definition with minor modifications: 'Autoinflammatory diseases are clinical disorders caused by defect(s) or dysregulation of the innate immune system, characterised by recurrent or continuous inflammation (elevated acute phase reactants (APR)) and the lack of a *primary* pathogenic role for the adaptive immune system (autoreactive T-cells or autoantibody production)'.

This definition emphasises the essential fact that the disorders are caused by defects in the innate immune system and are continuous or recurrent. The word 'unprovoked' has been deleted since in many cases there is a trigger for the acute flares.

The steering committee is aware that diseases such as PLCG2-associated antibody deficiency and immune dysregulation (PLAID) or Heme-oxidised IRP2 ubiquitin ligase1 (HOIL-1) deficiency, traditionally included among the AIDs, will not be part of this group, because they may contain components of the adaptive immune system such as autoantibodies.[60] The 'Interferonopathies' include some disorders also manifesting autoantibodies. However, the consensus seemed to be that for disorders like Aicardi-Goutières syndrome in which nucleic acid sensing is primarily intracellular, autoantibodies usually play a minor role in disease pathogenesis, and thus the autoinflammatory designation may still be appropriate. In their recent review, Rodero and Crow propose that 'type I interferonopathies can reasonably be considered as autoinflammatory in origin, with 'spillover' into autoimmunity in some cases'.[61] The group of 'typical' autoimmune diseases includes disorders affecting primarily or only the adaptive system such as systemic lupus erythematosus, Hashimoto thyroiditis, DNAse deficiencies and autoimmune lymphoproliferative syndrome.

AIDs proposed nomenclature

The current names for AIDs bring several problems and issues, which called for a new approach and nomenclature modification; many AIDs possess more than a single name (FMF—seven different names, TRAPS—three and so on) (table 1 and online supplementary table S1); different clinical presentations are associated with similar sequence alterations in the same gene, for example, Muckle-Wells syndrome (MWS), familial cold autoinflammatory syndrome (FCAS) and neonatal onset multisystem inflammatory disease (NOMID) are associated with *NLRP3* gene whereas FMF and pyrin-associated autoinflammation with neutrophilic dermatosis (PAAND) are associated with *MEFV* gene. In addition, discussion arose about several topics briefly summarised herein: In naming AIDs, should we use the name of the gene or that of the encoded protein (*MEFV* or pyrin)? Should we include typical clinical features or just genetic attributes? Should historical names be retained?

Following more than six cycles of Delphi questionnaires and oral discussions among the six members of the steering committee with further involvement of the 26 AIDs experts around the world—a consensus of at least 80% was reached for the nomenclature of the diseases shown in tables 1 and 2.

General conventions

The proposed names for AIDs have been established according to the rules and suggestions outlined in box 1.

In many diseases, the course of the disease is episodic with frequent attacks and attack-free intervals. When the frequency of the attacks is relatively regular (as is the case with Periodic fever, aphthous stomatitis, pharyngitis and adenitis (PFAPA) and sometimes with mevalonate kinase deficiency (MKD), we preferred the term 'periodic'. When the attacks do not have a regular pattern, we suggested the word 'recurrent'.

Table 2 Results from the Delphi questionnaires for consensus on nomenclature

Definition or disease	Group of AIDs experts consensus (n=26)
Definition	
Autoinflammatory diseases are clinical disorders caused by defect(s) or dysregulation of the innate immune system, characterised by recurrent or continuous inflammation (elevated APR) and by the lack of a *primary* pathogenic role of the adaptive immune system (autoreactive T-cells or autoantibody production).	87%
Final names proposed for the AIDs	
CARD14-associated psoriasis	91%
CNO: Chronic non-bacterial osteomyelitis	87%
DIRA: Deficiency of the IL-1 receptor antagonist	96%
DITRA: Deficiency of the IL-36 receptor antagonist	96%
IL-10 deficiency-associated inflammatory bowel diseases	83%
PAAD: Pyrin-associated autoinflammatory disease: FMF, PAAND	88%
MKD: Mevalonate kinase deficiency	87%
NLRP3-AID—*NLRP3*-associated autoinflammatory disease	88%
NLRP12-AID—*NLRP12*-associated autoinflammatory disease	88%
NOD2-associated granulomatous diseases	83%
PAPA: *PSTPIP1*-associated arthritis, pyoderma gangrenosum and acne	87%
PFAPA: Periodic fever, aphthous stomatitis, pharyngitis and adenitis	83%
PRAAS: Proteasome-associated autoinflammatory syndrome	84%
Schnitzler syndrome	87%
SDCM—*SH3BP2* deficiency with multilocular cystic disease of the mandibles	94%
TRAPS—TNF receptor-associated periodic fever syndrome	83%

AIDs, autoinflammatory disease; APR, acute phase reactants; PAAND, pyrin-associated autoinflammation with neutrophilic dermatosis.

Box 1 Recommendations for naming autoinflammatory diseases

1. Try not to change wherever the name is appropriate.
2. Avoid names of persons or geographical spread of disease (eponyms).
3. Include the genetic basis (name of the gene) of the disease where it is known (prefer the name of the gene over the name of the encoded protein unless the name of the gene is not accurate or meaningless).
4. Include key clinical features where appropriate.
5. Shorten the name as much as possible.
6. Choose a name that is as clear as possible.
7. In diseases where our knowledge about the pathogenesis is still limited, leave the previous name (periodic fever, aphthous stomatitis, pharyngitis and adenitis).
8. In diseases with different phenotypes but mutations in the same gene, use a general 'roof' name with subtypes (pyrin-associated autoinflammatory disease, NOD2).
9. When the clinical features seemed to be 'continuous' give a general name ('roof' name) and classify the various presentations according to their phenotypic severity (*NLRP3*-associated autoinflammatory disease, mevalonate kinase deficiency).

In the past, both terms, 'periodic' and 'recurrent', have been used interchangeably but now the term 'periodic' remained in the names of three conditions only: cryopyrin-associated periodic fever syndrome (CAPS), TRAPS and PFAPA. In TRAPS, we decided to keep the original name 'periodic', although its flares are recurrent rather than periodic. In CAPS, we propose a new name (NLRP3-AID) which does not contain the word 'periodic since the attacks are not periodic'. Thus, we strongly suggest using the more appropriate terms in naming disorders in the future.

As a general rule, we tried to use names containing aetiopathological (genetic) features of the disease and where appropriate or possible, to add a significant clinical characteristic of the syndrome. Thus, we left the name TRAPS without change, since it consists of its genetic aetiology (mutations in *TNFRSF1A* gene) and characteristic clinical features (periodic (recurrent) fever). On the other hand, the name hyper IgD syndrome (HIDS) was abandoned since it is an absolutely inaccurate name: serum IgD is not always elevated in these patients while it may be elevated in other AIDs. Therefore, this name was replaced by MKD based on our knowledge of the gene involved, mevalonate kinase (*MVK*). In this way, a physician or researcher who approaches these names for the first time may have immediately a basic understanding of the disorder and sometimes even a clue to the potential treatment.

In cases where the choice was between using the name of the gene associated with the disease or the protein encoded by the gene, we preferred the name of the gene over that of the protein unless the former was meaningless. A typical example is the choice of *NLRP3* gene over cryopyrin despite the tendency of some clinicians to stay with the former term CAPS. Fortunately, in many cases, the name of the gene and the encoded protein are the same (MK, NOD2) making the choice easier. However, this was not the case with the *MEFV* gene and pyrin where the name of the protein was chosen, as will be discussed later.

In our proposals for new taxonomy of AIDs, we tried to avoid the use of names of persons (such as Nakajo Nishimura syndrome) or geographical distribution of the disease (such as Guadeloupe fever) or names with unusual meaning (such as 'Cherubism').

Specific names

In the case of CAPS—which encompasses three clinical entities (FCAS, MWS, NOMID/CINCA), the committee has proposed using a single name; *NLRP3*-associated autoinflammatory disease (*NLRP3*-AID). Since the various disorders reflect different levels of phenotypic severity of the same disease, it was suggested to add the adjectives: mild, moderate and severe phenotypes, instead of using the historical names FCAS, MWS and CINCA/NOMID, respectively (table 1 and online supplementary table S1).

In familial cold autoinflammatory syndrome 2 (FCAS2) (Guadeloupe fever), different families present with different phenotypes.[36] Since the gene associated with the disease (*NLRP12*) is known, the committee decided to name this syndrome *NLRP12*-associated autoinflammatory disease (*NLRP12*-AID).

In the case of *MEFV*-associated diseases, the question raised was as follows: should we use the old name FMF or 'atypical FMF' for all syndromes associated with mutations in the *MEFV* gene even if they have totally different clinical manifestations? Alternatively, should we find a different way to classify these disorders? The committee chose to use a general name (as a 'roof') 'pyrin-associated autoinflammatory diseases' (PAAD)

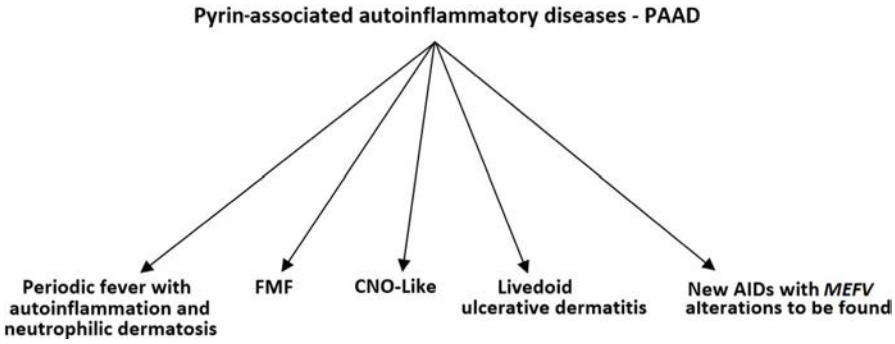

Figure 1 The group of diseases associated with *MEFV* sequence alterations. The 'roof' name is a general name whereas the subtypes are more specific and meaningful. AIDs, autoinflammatory diseases; CNO, chronic non-bacterial osteomyelitis; FMF, familial Mediterranean fever.

which includes all diseases associated with pyrin defects or *MEFV* mutations. Under this general term, there are subtypes of disorders with different names, according to their clinical presentation or genetic features, such as PAAND, FMF and so on[62] (figure 1). Although it is preferred using the name of the gene over the name of the encoded protein, in the case of FMF, the protein pyrin was chosen rather than the *MEFV* gene. One of the reasons was that the name *MEFV,* which was coined to denote its association with FMF, is no longer accurate, since it may lead to totally different AIDs, such as PAAND and CRMO-like disorder. In addition, we did not change the name of FMF, although sometimes it is neither familial nor restricted to the Mediterranean basin and in rare cases, it may even be without a documented fever. Most members of the steering committee thought that FMF is a well known and defined entity and that changing the name would cause discomfort and confusion among the AID clinical community. The name FMF remained under the 'roof' of 'pyrin-associated autoinflammatory diseases' (PAAD) as a clinical entity which is restricted mainly to Middle Eastern patients or to patients elsewhere, whose disease is associated with exon 10 mutations.[63]

Regarding Mevalonate kinase disorders the committee suggested leaving MKD as a general name with the option of adding 'mild' for those with HIDS and 'severe' for those with mevalonic aciduria.[64] In rare cases, where the patient with MKD has also retinitis pigmentosa or porokeratosis, it is suggested to mention these manifestations in addition to MKD (table 1 and online supplementary table S1).

The name *NOD2*-associated granulomatous disease was chosen by the committee for the three phenotypes: Blau syndrome, familial sarcoidosis and familial Crohn's disease. Since all these syndromes are characterised by granulomas, this feature was included in the name. Nevertheless, an option was offered to add inflammatory bowel disease (IBD) in cases where the intestines are the main site of involvement for example, *NOD2*-associated granulomatous IBD (formerly called familial Crohn's disease).

The name for CRMO was replaced by the name chronic non-bacterial osteomyelitis (CNO). The reason for that was the presence of many cases where the disease was neither recurrent nor multifocal. Furthermore, the new name emphasises the main feature of the disease, non-bacterial osteomyelitis. Since this clinical entity may be associated with mutations in various genes, it is optional to add the name of the gene when it is known. For example, in case the gene involved is *LPIN2*, it can be marked as *LPIN2*-CNO (previously known as Majeed's syndrome). In adults, patients with sporadic CNO are usually diagnosed with SAPHO, a symptom complex of synovitis, acne, pustulosis, hyperostosis and osteitis.[65]

Chronic atypical neutrophilic dermatosis with lipodystrophy and elevated temperature syndrome (CANDLE syndrome) gained a new name: *PSMB8*-PRAAS—where *PSMB8* stands for Proteasome Subunit Beta 8 and PRAAS for PRoteasome-Associated Autoinflammatory Syndrome. This name replaces also the eponym Nakajo Nishimura syndrome, and JMP which stands for Joint contractures, Muscle atrophy, microcytic anaemia and Panniculitis-induced lipodystrophy. The name *PSMB8*-PRAAS consists of the genetic aetiopathology of the disorder but does not include any clinical feature of the disease.

CARD14-associated disease is usually characterised by psoriasis with or without pustulosis. Therefore, the name was refined to be *CARD14*-associated psoriasis.

Since the three variants of IL-10 deficiency are always associated with inflammatory bowel disease, the committee proposed a single name as IL-10 deficiency-associated IBD.

The names, deficiency of the interleukin 1 receptor antagonist (DIRA), deficiency of the interleukin 36 receptor antagonist (DITRA), pyogenic arthritis, pyoderma gangrenosum and acne (PAPA) and PFAPA remained unchanged since they already conform to our naming conventions. However, the letter P in the abbreviation 'PAPA' now stands for the name of the gene *PSTPIP1* rather than 'Pyogenic' and, therefore, the new name is '*PSTPIP1*-associated arthritis, pyoderma gangrenosum and acne' (PAPA).

The name 'Cherubism' was derived from the Biblical 'cherub' (plural cherubim) who has four faces of different species and several pairs of wings,. For most physicians, this name does not mean much and therefore, the committee proposed the name *SH3BP2* deficiency with multilocular cystic disease of the mandibles (SDCM). This name gives the aetiopathological basis of the syndrome with the main clinical feature of fibrous dysplasia of the mandibles.

Finally, the name 'Schnitzler syndrome' also remained as an historical one, since its pathogenesis is still obscure and its relationship with *NLRP3* mutations has not been established.[66] A proposal to convert the name of the syndrome to a clinical description: 'late onset gammopathy with recurrent urticaria and fever' did not gain support from most of the committee members.

DISCUSSION

The definition of AIDs has changed over the years in order to accommodate the new diseases discovered since 1999—the year the term was first proposed.[2 5 49 55–58] Widening the scope and

spectrum of definition of AIDs resulted in the inclusion of disorders with additional defects in the adaptive immune system such as PLAID or HOIL-1 deficiency. Most defects in the immune system may affect primarily either the innate or the adaptive arm. However, it is becoming increasingly obvious that the innate immune system almost always has an effect on the adaptive system. This leads to the situation that there are disorders that do not fit neatly into the 'pure' autoinflammatory or autoimmune categories and reside actually in a 'grey zone' between these two groups. In order to include these disorders with the typical AIDs under the same 'rafter', Peckham *et al* offered the term 'autoinflammatory-immune diseases'.[67] We believe that this new name may lead to confusion since all the disorders caused or related to defects in the immune system can be classified under this wide term with no clear categorisation. The interferonopathies are clinical disorders caused by defects in the innate response, leading to inflammation after DNA sensing. The activation of cells of the adaptive immunity is a secondary effect of this condition and seems to play a minor role in their pathogenesis. Therefore, they may create the bridge which fits the concept that the AIDs, and the autoimmune diseases are actually in the same spectrum of immune disorders. This continuum model is further supported by the recent discovery of the innate lymphoid cells. These cells are defined by differential expression of cell-surface markers and are activated by neuropeptides, cytokines and other alarmins.[68] Their specialised distribution in lymphoid and non-lymphoid tissues, coupled with their functional heterogeneity, has provoked a fundamental reassessment of how they integrate innate and adaptive immune responses.

As already mentioned, many of the current names of AIDs were not appropriate, inaccurate or lack any clinical meaning. Therefore, an attempt to establish new conventions for naming them was really needed.

The conventions (box 1), and the ensuing proposals (table 1 and online supplementary table S1), call for using the name of the gene associated with the disease when it is known rather than the encoded protein. In these cases, demonstration of functional significance of the identified sequence alteration is mandatory. The main advantage of using the name of the gene is that such a name gives the physician a clue about the pathogenesis of the disease and sometimes even about a potential treatment. Moreover, it may allow definite diagnosis using genetic testing. However, it should be borne in mind that including the gene in the name of the disease may pose a problem in cases where the clinical features of the patient are compatible with a certain diagnosis while no expected sequence alteration is found. Thus, the main drawback of using the name of the gene is that *definite* diagnosis can be made only by genetic testing.

In cases where the clinical features and the genetic testing results are in accord, the name is appropriate and the diagnosis is correct and definite. When there is a clearly pathogenic mutation but the clinical features are completely incompatible with the expected diagnosis, one should consider a different disease with a different name. This situation is illustrated by the case of the *MEFV* mutation S242R, which causes neutrophilic dermatosis. The name of this disease is not 'FMF' or 'atypical FMF' despite the fact that there are *MEFV* mutations—but 'PAAND'. Similar approach may be applied in the case of *PSTPIP1* with the new mutation and different clinical presentation.[69] We suggest here a 'roof' name: *PSTPIP1*-associated AIDs with two subtypes: PAPA and PAMI (*PSTPIP1*-associated myeloid-related proteinaemia inflammatory syndrome). However, we cannot add this approach to table 1 since it was not discussed in the Delphi questionnaires among the large group of participants.

When the clinical features are typical for a certain disease (eg, FMF) and yet no genetic support for this diagnosis is found, one can denote this medical condition as an FMF-like disease. However, a better choice would be to leave the case as an undefined AID until mutations in other genes are found or additional explanations for the disease are given. The reason is that clinical features typical for one AID may be associated with mutations in different genes. For example, in a recent report, Karacan *et al* described two Turkish families in whom four patients presented with typical clinical features of FMF.[70] Genetic analysis performed in these patients failed to show *MEFV* mutations. However, total exon sequencing revealed that two patients were homozygous for mutations in *MVK* and the two other patients carried mutations in the *TNFRSF1A* gene. These cases illustrate the difficulties in making a diagnosis of AID based on clinical features only and justify the proposal to use the gene in naming AIDs wherever it is known.

The way we proposed naming CAPS and FCAS 2, namely *NLRP3*-AID and *NLRP12*-AID, respectively, may pave the way for naming future disorders to be discovered or identified among the other members of the large family of NOD-like receptors. Similarly, *PSMB8*-PRAAS, the name which was proposed to replace CANDLE syndrome, JMP and NNS, may also serve as an example for naming additional proteasome associated diseases to be discovered, just by changing their number. In fact, Brehm *et al* recently described several cases that carry mutations in *PSMA3* (encodes α7), *PSMB4* (encodes β7), *PSMB9* (encodes β1i) and proteasome maturation protein (*POMP*).[71]

Unfortunately, the current study did not include many other monogenic AIDs such as those associated with *ADA2, NLRC4, NLRP1* genes or X linked inhibitor of apoptosis deficiency and (SLAM)-associated protein deficiency.[72] The reason is that we limited ourselves mainly to the basic list reported by Touitou *et al*.[49] However, we hope that the conventions we propose herein may help modifying names of additional diseases—old and new—when, they do not follow the rules suggested.

For this project, we used the Delphi technique which allowed discussion via an *ad hoc* web-based system developed by the PRINTO staff under the supervision of NR who has an extensive expertise in consensus formation methodologies. The PRINTO system allowed remote interaction between the participants who had the possibility to share written comments with the other participants in a transparent and traceable way. A limitation of the current work was that for lack of funding we could not conduct a formal nominal group technique which is a guided face-to-face discussion and interaction, among small groups of experts. However, the additional discussion of the *ad hoc* steering committee consensus proposal by another group of 26 worldwide experts in the field of AIDs further strengthens these proposals.

In conclusion, the currently proposed rules for nomenclatures of AIDs are expected to allow a better organisation of these groups of immune diseases. However, taxonomy is a dynamic process and some of the proposed names may be changed in the future as we gain a better knowledge about their pathogenesis. The proposed taxonomy may gain a broader consensus following an effective communication with other societies such as the International Union of Immunological Societies Expert Committee.

Author affiliations
[1]Rheumatology Unit, Hadassah Hebrew University Medical Center, Jerusalem, Israel
[2]UOSD Centro Malattie Autoinfiammatorie e Immunodeficienze, Istituto Giannina Gaslini, Genoa, Italy

[3]Division of Rheumatology, Department of Internal Medicine, Istanbul Faculty of Medicine, Istanbul University, Istanbul, Turkey
[4]Inflammatory Disease Section, Metabolic, Cardiovascular and Inflammatory Disease Genomics Branch, National Human Genome Research Institute, Bethesda, Maryland, USA
[5]Division of Medicine, Centre for Amyloidosis & Acute Phase Proteins, University College London Medical School, London, UK
[6]CEREMAIA, CHU Montpellier, INSERM U1183, Université de Montpellier, Montpellier, France
[7]Clinica Pediatrica e Reumatologia–PRINTO, Istituto Giannina Gaslini, Genoa, Italy

Acknowledgements We thank the staff from the PRINTO office (Eugenia Mosci, Luca Villa and Roberto Cavanna).

Collaborators List of additional participants to the Delphi study: Ivona Aksentijevich, Bethesda, USA; Jordi Anton, Barcelona, Spain; Juan I Arostegui, Barcelona, Spain; Karyl S Barron, Bethesda, USA; Luca Cantarini, Siena, Italy; Fatma Dedeoglu, Boston, Massachusetts , USA; Erkan Demirkaya, London, Ontario, Canada; Dirk Foell, Muenster, Germany; Joost Frenkel, Utrecht, Netherlands; Philip J Hashkes, Jerusalem, Israel; Veronique Hentgen, Paris, France; Michael Hofer, Lausanne, Switzerland; Tilmann Kallinich, Berlin, Germany; Isabelle Koné-Paut, Paris, France; Jasmin B Kuemmerle-Deschner, Tuebingen, Germany; Ronald Laxer, Toronto, Ontario, Canada; Avi Livneh, Ramat Gan, Israel; Alberto Martini, Genoa, Italy; Laura Obici, Pavia, Italy; Seza Ozen, Ankara, Turkey; Dorota Rowczenio, London, UK; Ricardo Russo, Buenos Aires, Argentina; Yael Shinar, Tel Hashomer, Israel; Natasa Toplak, Ljubljana, Slovenia; Yosef Uziel, Kfar Saba, Israel; Marielle van Gijn, Utrecht, The Netherlands.

Contributors All authors contributed equally to the planning and conduct of the study. Their placement in the authors' list is dictated by the alphabetic order of their family names. The first version of the present manuscript was written by EB-C, MG and NR and then revised critically by all the remaining coauthors (AG, DLK, HJL, IT).

Funding The development and coordination of the Delphi survey has been funded with the research budgets of Istituto Giannina Gaslini; no external entity such as pharmaceutical companies has been involved at any stage of the project.

Competing interests For EB-C, MG, AG, DLK, HJL, IT: Nothing to disclose for this manuscript. NR received honoraria for consultancy of speaker's bureau from the following pharmaceutical companies since last 5 years: Abbott, AbbVie, Amgen, Biogenidec, Astellas, Alter, AstraZeneca, Baxalta Biosimilars, Boehringer, BMS, CD Pharma, Celgene, CrescendoBio, EMD Serono, Hoffman La Roche, Italfarmaco, Janssen, MedImmune, Medac, Novartis, Novo Nordisk, Pfizer, Rewind Arms, R Pharma, Sanofi Aventis, Servier, Sinergie, Takeda, Vertex, UCB Biosciences GmbH. The Gaslini Hospital, which is the public Hospital where NR works as full time public employee, has received contributions from the following industries: Abbott, BMS, 'Francesco Angelini', GlaxoSmithKline (GSK), Hoffman La Roche, Italfarmaco, Janssen, Novartis, Pfizer, Sanofi Aventis, Schwarz Biosciences, Sobi, Xoma, Wyeth. This money has been reinvested for the research activities of the hospital in a fully independent manner without any commitment with third parties.

Patient consent Not required.

Provenance and peer review Not commissioned; externally peer reviewed.

Data sharing statement There are no data to be shared besides the manuscript.

REFERENCES

1 Ben-Chetrit E, Beil M. Taxonomy of auto-inflammatory diseases: time to consider changing some names. *Clin Exp Rheumatol* 2013;31:3–5.
2 Manthiram K, Zhou Q, Aksentijevich I, *et al*. The monogenic autoinflammatory diseases define new pathways in human innate immunity and inflammation. *Nat Immunol* 2017;18:832–42.
3 International FMF Consortium. Ancient missense mutations in a new member of the RoRet gene family are likely to cause familial Mediterranean fever. The International FMF Consortium. *Cell* 1997;90:797–807.
4 French FMF Consortium. A candidate gene for familial Mediterranean fever. *Nat Genet* 1997;17:25–31.
5 McDermott MF, Aksentijevich I, Galon J, *et al*. Germline mutations in the extracellular domains of the 55 kDa TNF receptor, TNFR1, define a family of dominantly inherited autoinflammatory syndromes. *Cell* 1999;97:133–44.
6 Siegal S. Benign Paroxysmal Peritonitis. *Ann Intern Med* 1945;23:234–47.
7 Reimann HA. Periodic disease; a probable syndrome including periodic fever, benign paroxysmal peritonitis, cyclic neutropenia and intermittent arthralgia. *J Am Med Assoc* 1948;136:239–44.
8 Cattan R, Mamou H. 14 Cases of periodic disease, 8 of which are complicated by kidney diseases. *Bull Mem Soc Med Hop Paris* 1951;67:1104–10.
9 Heller H, Sohar E, Sherf L. Familial Mediterranean fever. *AMA Arch Intern Med* 1958;102:50–71.
10 Ehrenfeld EN, Eliakim M, Rachmilewitz M. Recurrent polyserositis (familial mediterranean fever; Periodic disease): a report of fifty-five cases. *The Am Journal of Med* 1961;3:107–23.
11 Saatci U, Ozen S, Bakkaloglu A, *et al*. Familial Mediterranean fever: a misnomer? *Lancet* 1994;343:485.
12 Masters SL, Lagou V, Jéru I, *et al*. Familial autoinflammation with neutrophilic dermatosis reveals a regulatory mechanism of pyrin activation. *Sci Transl Med* 2016;8:332ra45–45.
13 Williamson LM, Hull D, Mehta R, *et al*. Familial hibernian fever. *Q J Med* 1982;51:469–80.
14 Mulley J, Saar K, Hewitt G, *et al*. Gene localization for an autosomal dominant familial periodic fever to 12p13. *Am J Hum Genet* 1998;62:884–9.
15 Drenth JP, Cuisset L, Grateau G, *et al*. Mutations in the gene encoding mevalonate kinase cause hyper-IgD and periodic fever syndrome. International Hyper-IgD Study Group. *Nat Genet* 1999;22:178–81.
16 Houten SM, Kuis W, Duran M, *et al*. Mutations in MVK, encoding mevalonate kinase, cause hyperimmunoglobulinaemia D and periodic fever syndrome. *Nat Genet* 1999;22:175–7.
17 van der Meer JW, Vossen JM, Radl J, *et al*. Hyperimmunoglobulinaemia D and periodic fever: a new syndrome. *Lancet* 1984;1:1087–90.
18 Frenkel J, Houten SM, Waterham HR, *et al*. Mevalonate kinase deficiency and Dutch type periodic fever. *Clin Exp Rheumatol* 2000;18:525–32.
19 Prieur AM, Griscelli C. Arthropathy with rash, chronic meningitis, eye lesions, and mental retardation. *J Pediatr* 1981;99:79–83.
20 Muckle TJ, Wells M. Urticaria, deafness, and amyloidosis: a new heredo-familial syndrome. *Q J Med* 1962;31:235–48.
21 Kile RL, Rusk HA. A case of cold urticaria with an unusual family history. *J Am Med Assoc* 1940;114:1067–8.
22 Hoffman HM, Mueller JL, Broide DH, *et al*. Mutation of a new gene encoding a putative pyrin-like protein causes familial cold autoinflammatory syndrome and Muckle-Wells syndrome. *Nat Genet* 2001;29:301–5.
23 Blau EB. Familial granulomatous arthritis, iritis, and rash. *J Pediatr* 1985;107:689–93.
24 James DG. A comparison of Blau's syndrome and sarcoidosis. *Sarcoidosis* 1994;11:100–1.
25 McGovern DP, van Heel DA, Ahmad T, *et al*. NOD2 (CARD15), the first susceptibility gene for Crohn's disease. *Gut* 2001;49:752–4.
26 Aksentijevich I, Masters SL, Ferguson PJ, *et al*. An autoinflammatory disease with deficiency of the interleukin-1-receptor antagonist. *N Engl J Med* 2009;360:2426–37.
27 Marrakchi S, Guigue P, Renshaw BR, *et al*. Interleukin-36-receptor antagonist deficiency and generalized pustular psoriasis. *N Engl J Med* 2011;365:620–8.
28 Majeed HA, Kalaawi M, Mohanty D, *et al*. Congenital dyserythropoietic anemia and chronic recurrent multifocal osteomyelitis in three related children and the association with Sweet syndrome in two siblings. *J Pediatr* 1989;115:730–4.
29 Ferguson PJ, Chen S, Tayeh MK, *et al*. Homozygous mutations in *LPIN2* are responsible for the syndrome of chronic recurrent multifocal osteomyelitis and congenital dyserythropoietic anaemia (Majeed syndrome). *J Med Genet* 2005;42:551–7.
30 Keipert JA, Campbell PE. Recurrent hyperostosis of the clavicles: an undiagnostic syndrome. *Aust Paediatr J* 1970;6:97–104.
31 Giedion A, Holthusen W, Masel LF, *et al*. [Subacute and chronic "symmetrical" osteomyelitis]. *Ann Radiol* 1972;15:329–42.
32 Fuchs-Telem D, Sarig O, van Steensel MA, *et al*. Familial pityriasis rubra pilaris is caused by mutations in *CARD14*. *Am J Hum Genet* 2012;91:163–70.
33 Jordan CT, Cao L, Roberson ED, *et al*. PSORS2 is due to mutations in CARD14. *Am J Hum Genet* 2012;90:784–95.
34 Glocker EO, Kotlarz D, Boztug K, *et al*. Inflammatory bowel disease and mutations affecting the interleukin-10 receptor. *N Engl J Med* 2009;361:2033–45.
35 Glocker EO, Frede N, Perro M, *et al*. Infant colitis–it' s in the genes. *Lancet* 2010;376:1272.
36 Jéru I, Duquesnoy P, Fernandes-Alnemri T, *et al*. Mutations in NALP12 cause hereditary periodic fever syndromes. *Proc Natl Acad Sci U S A* 2008;105:1614–9.
37 Lindor NM, Arsenault TM, Solomon H, *et al*. A new autosomal dominant disorder of pyogenic sterile arthritis, pyoderma gangrenosum, and acne: PAPA syndrome. *Mayo Clin Proc* 1997;72:611–5.
38 Wise CA, Gillum JD, Seidman CE, *et al*. Mutations in *CD2BP1* disrupt binding to PTP PEST and are responsible for PAPA syndrome, an autoinflammatory disorder. *Hum Mol Genet* 2002;11:961–9.
39 Liu Y, Ramot Y, Torrelo A, *et al*. Mutations in proteasome subunit β type 8 cause chronic atypical neutrophilic dermatosis with lipodystrophy and elevated temperature with evidence of genetic and phenotypic heterogeneity. *Arthritis Rheum* 2012;64:895–907.
40 Agarwal AK, Xing C, DeMartino GN, *et al*. PSMB8 encoding the β5i proteasome subunit is mutated in joint contractures, muscle atrophy, microcytic anemia, and panniculitis-induced lipodystrophy syndrome. *Am J Hum Genet* 2010;87:866–72.
41 Arima K, Kinoshita A, Mishima H, *et al*. Proteasome assembly defect due to a proteasome subunit beta type 8 (PSMB8) mutation causes the autoinflammatory disorder, Nakajo-Nishimura syndrome. *Proc Natl Acad Sci U S A* 2011;108:14914–9.
42 Schnitzler L. Lésions urticariennes chroniques permanentes (érythème pétaloïde?) Cas cliniques No 46 B. *J Dermatol Angers* 1972. Abstract 46.
43 Thomas KT, Feder HM, Lawton AR, *et al*. Periodic fever syndrome in children. *J Pediatr* 1999;135:15–21.

44 Marshall GS, Edwards KM, Butler J, *et al*. Syndrome of periodic fever, pharyngitis, and aphthous stomatitis. *J Pediatr* 1987;110:43–6.
45 Ueki Y, Tiziani V, Santanna C, *et al*. Mutations in the gene encoding c-Abl-binding protein SH3BP2 cause cherubism. *Nat Genet* 2001;28:125–6.
46 Choremis K, Papadatos C, Caterellos C. Familial multilocular cystic disease of the jaws. *Helv Paediatr Acta* 1959;14:946–50.
47 Jones WA, Gerrie J, Pritchard J. Cherubism–familial fibrous dysplasia of the jaws. *J Bone Joint Surg Br* 1950;32-B:334–47.
48 Jaffe HL. Giant-cell reparative granuloma, traumatic bone cyst, and fibrous (fibro-oseous) dysplasia of the jawbones. *Oral Surg Oral Med Oral Pathol* 1953;6:159–75.
49 Touitou I. Inheritance of autoinflammatory diseases: shifting paradigms and nomenclature. *J Med Genet* 2013;50:349–59.
50 Ruperto N, Meiorin S, Iusan SM, *et al*. Consensus procedures and their role in pediatric rheumatology. *Curr Rheumatol Rep* 2008;10:142–6.
51 Pill J. The Delphi method: Substance, context, a critique and an annotated bibliography. *Socioecon Plann Sci* 1971;5:57–71.
52 Toplak N, Frenkel J, Ozen S, *et al*. An international registry on autoinflammatory diseases: the Eurofever experience. *Ann Rheum Dis* 2012;71:1177–82.
53 Federici S, Sormani MP, Ozen S, *et al*. Evidence-based provisional clinical classification criteria for autoinflammatory periodic fevers. *Ann Rheum Dis* 2015;74:799–805.
54 Ruperto N, Martini A. Networking in paediatrics: the example of the paediatric rheumatology international trials organisation (PRINTO). *Arch Dis Child* 2011;96:596–601.
55 McGonagle D, McDermott MF. A proposed classification of the immunological diseases. *PLoS Med* 2006;3:e297–1248. e297.
56 Kastner DL, Aksentijevich I, Goldbach-Mansky R. Autoinflammatory disease reloaded: a clinical perspective. *Cell* 2010;140:784–90.
57 Grateau G, Hentgen V, Stojanovic KS, *et al*. How should we approach classification of autoinflammatory diseases? *Nat Rev Rheumatol* 2013;9:624–9.
58 Wekell P, Berg S, Karlsson A, *et al*. Toward an inclusive, congruent, and precise definition of autoinflammatory diseases. *Front Immunol* 2017;8:Article 497.
59 de Jesus AA, Canna SW, Liu Y, *et al*. Molecular mechanisms in genetically defined autoinflammatory diseases: disorders of amplified danger signaling. *Annu Rev Immunol* 2015;33:823–74.
60 Milner JD. PLAID: a syndrome of complex patterns of disease and unique phenotypes. *J Clin Immunol* 2015;35:527–30.
61 Rodero MP, Crow YJ. Type I interferon-mediated monogenic autoinflammation: The type I interferonopathies, a conceptual overview. *J Exp Med* 2016;213:2527–38. 3.
62 Shimizu M, Tone Y, Toga A, *et al*. Colchicine-responsive chronic recurrent multifocal osteomyelitis with MEFV mutations: a variant of familial Mediterranean fever? *Rheumatology* 2010;49:2221–3.
63 Ben-Chetrit E, Ozdogan H. Can we make a diagnosis of autoinflammatory diseases based upon clinical features only? *Clin Exp Rheumatol* 2017;108:16–18.
64 Prietsch V, Mayatepek E, Krastel H, *et al*. Mevalonate kinase deficiency: enlarging the clinical and biochemical spectrum. *Pediatrics* 2003;111:258–61.
65 Hofmann SR, Kapplusch F, Girschick HJ, *et al*. Chronic recurrent multifocal osteomyelitis (crmo): presentation, pathogenesis, and treatment. *Curr Osteoporos Rep* 2017;15:542–54.
66 de Koning HD, van Gijn ME, Stoffels M, *et al*. Myeloid lineage-restricted somatic mosaicism of *NLRP3* mutations in patients with variant Schnitzler syndrome. *J Allergy Clin Immunol* 2015;135:561–4.
67 Peckham D, Scambler T, Savic S, *et al*. The burgeoning field of innate immune-mediated disease and autoinflammation. *J Pathol* 2017;241:123–39.
68 Artis D, Spits H. The biology of innate lymphoid cells. *Nature* 2015;517:293–301.
69 Holzinger D, Fassl SK, de Jager W, *et al*. Single amino acid charge switch defines clinically distinct proline-serine-threonine phosphatase-interacting protein 1 (PSTPIP1)–associated inflammatory diseases. *J Allergy Clin Immunol* 2015;136:1337–45.
70 Karacan I, Uğurlu S, Tolun A, *et al*. Other autoinflammatory disease genes in an FMF-prevalent population: a homozygous MVK mutation and a novel heterozygous TNFRSF1A mutation in two different Turkish families with clinical FMF. *Clin Exp Rheumatol* 2017;108:75–81.
71 Brehm A, Liu Y, Sheikh A, *et al*. Additive loss-of-function proteasome subunit mutations in CANDLE/PRAAS patients promote type I IFN production. *J Clin Invest* 2015;125:4196–211.
72 Rigaud S, Fondanèche MC, Lambert N, *et al*. XIAP deficiency in humans causes an X-linked lymphoproliferative syndrome. *Nature* 2006;444:110–4.

EXTENDED REPORT

Predictors of disease activity and structural progression after treatment with adalimumab plus methotrexate or continued methotrexate monotherapy in patients with early rheumatoid arthritis and suboptimal response to methotrexate

Josef S Smolen,[1] Ronald F van Vollenhoven,[2] Stefan Florentinus,[3] Su Chen,[4] Jessica L Suboticki,[5] Arthur Kavanaugh[6]

Handling editor Dimitrios T Boumpas

► Additional material is published online only. To view please visit the journal online (http://dx.doi.org/10.1136/annrheumdis-2018-213502).

[1]Division of Rheumatology, Department of Medicine 3, Medical University of Vienna, Vienna, Austria
[2]Department of Rheumatology, Amsterdam Rheumatology and Immunology Center (ARC), Amsterdam, The Netherlands
[3]Global Medical Affairs, AbbVie Inc., North Chicago, Illinois, USA
[4]Data and Statistical Sciences, AbbVie Inc., North Chicago, Illinois, USA
[5]Global Medical Affairs, AbbVie Inc., North Chicago, Illinois, USA
[6]Division of Rheumatology, Allergy and Immunology, University of California San Diego, La Jolla, California, USA

Correspondence to
Professor Josef S Smolen, Medical University of Vienna, Waehringer Guertel 18-20, Vienna A-1090, Austria ; josef.smolen@wienkav.at

Received 29 March 2018
Revised 3 July 2018
Accepted 5 July 2018
Published Online First 3 August 2018

To cite: Smolen JS, van Vollenhoven RF, Florentinus S, *et al*. *Ann Rheum Dis* 2018;**77**:1566–1572.

ABSTRACT

Objectives Methotrexate is considered to be first-line therapy for rheumatoid arthritis (RA). However, a substantial proportion of treated patients do not achieve the desired goals of therapy. This analysis aimed to identify predictors of insufficient response to methotrexate in patients with early RA.

Methods The Optimal Protocol for Treatment Initiation with Methotrexate and Adalimumab (OPTIMA) and PREMIER studies in patients with RA for <1 and <3 years, respectively, examined the efficacy of methotrexate and adalimumab in methotrexate-naive patients. This post hoc analysis included patients for whom initial methotrexate monotherapy was not successful after 6 months. Candidate predictors of insufficient response and clinically relevant radiographic progression (CRRP) included demographics, baseline disease characteristics and time-averaged disease variables over a 12-week interval. In OPTIMA, adalimumab was added to therapy after insufficient treatment response; in PREMIER, initial methotrexate therapy was continued; clinical, functional and radiologic outcomes were assessed after 1 year.

Results Baseline 28-joint Disease Activity Score based on C-reactive protein (DAS28(CRP)) and time-averaged DAS28(CRP) over 4, 8 and 12 weeks were the strongest predictors of insufficient response to methotrexate and CRRP. Addition of adalimumab to methotrexate therapy was associated with better clinical, functional and radiographic outcomes after 1 year compared with continuing on methotrexate monotherapy.

Conclusions In patients with early RA, baseline disease characteristics and early disease activity can predict response to methotrexate treatment and radiographic progression at 6 months. The addition of adalimumab at 6 months after methotrexate failure is associated with improved outcomes. These results support treatment-to-target strategies and timely adaptation of therapy in patients with early RA.

Trial registration number NCT00420927, NCT00195663; Post-results.

INTRODUCTION

Disease-modifying antirheumatic drugs (DMARDs) such as methotrexate are currently recommended as first-line therapy for the treatment of rheumatoid arthritis (RA).[1 2] However, if patients do not attain the desired goal of therapy (eg, remission or at least low disease activity (LDA)) after 6 months of an initial treatment strategy, consideration must be given for adjustment of therapy.[1] Furthermore, joint damage, one of the hallmarks of RA, develops in many patients during the early stages of the disease and can continue despite conventional synthetic DMARD therapy, leading to bone and cartilage loss.[3–7] Adding a biologic DMARD could be considered in patients with an insufficient response to methotrexate when risk factors are present.[1]

The Optimal Protocol for Treatment Initiation with Methotrexate and Adalimumab (OPTIMA) and PREMIER studies examined the efficacy of methotrexate and adalimumab in methotrexate-naive patients with early RA.[6 8] The studies used different protocols when patients did not achieve response to methotrexate after 6 months: in OPTIMA, adalimumab was added to therapy from week 26 onward for patients with insufficient response to methotrexate, whereas in PREMIER, initial methotrexate therapy was maintained for up to 2 years.

The objective of this post hoc analysis of data from the randomised, double-blind OPTIMA and PREMIER studies in patients with early RA was to identify predictors of insufficient response to methotrexate and clinically relevant radiographic progression (CRRP) after 6 months of methotrexate monotherapy, as well as to evaluate the subsequent benefits of treatment adjustment (OPTIMA) versus no treatment adjustment (PREMIER).

METHODS

Study patients, designs and treatments

The methods and results of the trials have been described previously (see also online supplementary table 1).[6 8 9] Briefly, OPTIMA was a 78-week, randomised, double-blind, double-period, phase 4 trial conducted between December 2006 and July 2010.[8 9] In period 1, methotrexate-naive patients were randomised 1:1 to receive adalimumab 40 mg every other week plus methotrexate weekly (titrated to 20 mg/week by week 8) or placebo every other week plus methotrexate weekly for 26 weeks. In period 2, patients who did not achieve the stable LDA target during period 1 continued or initiated adalimumab 40 mg every other week

plus methotrexate weekly. PREMIER was a 2-year, randomised, double-blind, placebo-controlled phase 3 trial conducted between December 2000 and April 2004.[6] Patients were randomised 1:1:1 to receive adalimumab 40 mg every other week plus methotrexate weekly (titrated to 20 mg/week by week 9), adalimumab 40 mg every other week plus placebo weekly, or placebo every other week plus methotrexate weekly for 2 years. This post hoc analysis included only patients who received initial methotrexate monotherapy in OPTIMA or PREMIER and did not achieve stable LDA. Stable LDA was defined as achieving 28-joint Disease Activity Score based on C-reactive protein (DAS28(CRP)) <3.2 at two consecutive assessments (weeks 22 and 26 in OPTIMA and weeks 20 and 24 in PREMIER).

Assessments

Predictors were assessed for insufficient response to methotrexate, defined as not achieving stable LDA at 6 months, or experiencing CRRP, defined as an increase in modified total Sharp score (mTSS) of >1.5 from baseline to 6 months based on a prior definition of increase >3 in 1 year.[10] Stable DAS28(CRP) <3.2 was chosen as the definition of insufficient response because it was the primary endpoint at the 6-month time point in the OPTIMA trial[8] and was the decisive outcome for subsequent randomisation for the phase 2 portion of that trial.[9]

Assessments after 6 months (week 26 in OPTIMA and week 24 in PREMIER) included clinical outcomes at week 78 for OPTIMA and week 76 for PREMIER: the proportion of patients achieving LDA (DAS28(CRP)<3.2), DAS28(CRP) <2.6, Simplified Disease Activity Index (SDAI) ≤3.3 and Clinical Disease Activity Index (CDAI) ≤2.8. Physical function was evaluated using the Health Assessment Questionnaire Disability Index (HAQ-DI) and reported as the mean score at week 78/76 and the proportion of patients achieving clinically meaningful improvement in HAQ-DI (change of ≥0.22)[11] from week 26 to 78 (OPTIMA) or week 24 to 76 (PREMIER). Radiologic outcomes were assessed using the mTSS and reported as the mean score at week 78/76 and the proportion of patients achieving change in mTSS (ΔmTSS) of ≤0.5 from week 26 to 52 or 78 (OPTIMA) or week 24 to 52 or 76 (PREMIER; value at week 76 estimated from linear extrapolation between actual assessments at weeks 52 and 104).

Statistical analyses

Backward logistic regression was used to identify potential predictors of insufficient response to methotrexate therapy and CRRP during the first 6 months of therapy in a pooled analysis of patients with available data in OPTIMA and PREMIER. Two models were used. The first model included demographic and disease factors (including DAS28(CRP), SDAI or CDAI) at baseline only. The second model included baseline factors and postbaseline, time-averaged disease parameters for three time intervals (through 4, 8 and 12 weeks of methotrexate exposure; three separate models fitted). Time-averaged variables were calculated as area under the curve standardised for length of time interval. Factors were removed from the models if their significance level rose to 0.1.

The percentage of patients achieving DAS28(CRP) <3.2, DAS28(CRP) <2.6, SDAI ≤3.3 and CDAI ≤2.8 at 1 year after the 6-month assessment was analysed using non-responder imputation and X^2 test (or Fisher's exact test if ≥20% of the cells had expected counts ≤5). Differences in mean outcomes between patients who switched to adalimumab rescue therapy in OPTIMA and patients who continued to receive methotrexate monotherapy in PREMIER were assessed using a t-test. A multivariate logistic regression adjusted for study (OPTIMA or PREMIER) and baseline characteristics (age, sex, RA duration, rheumatoid factor status, previous

Table 1 Baseline demographics, disease characteristics and prior therapies of the pooled predictors analysis populations

	Pooled for prediction of insufficient response to methotrexate (n=687)		Pooled for prediction of CRRP (n=670)	
Characteristic	Insufficient responders (n=525)	Responders (n=162)	CRRP (n=171)	No CRRP (n=499)
Demographic characteristics				
Women, n (%)	398 (76)	113 (70)	126 (74)	372 (75)
White, n (%)	483 (92)	148 (91)	158 (92)	456 (91)
Age (years)	51.3 (13.7)	48.8 (13.2)	50.9 (14.9)	50.7 (13.3)
RA duration (years)	0.5 (0.6)	0.5 (0.6)	0.5 (0.6)	0.5 (0.6)
Disease characteristics				
CRP (mg/L)	35.7 (36.5)	26.4 (28.2)	50.7 (45.7)	27.6 (28.1)
TJC68	30.1 (14.8)	23.9 (12.7)	30.7 (13.7)	28.0 (14.8)
SJC66	20.4 (11.4)	15.6 (9.1)	22.3 (11.5)	18.3 (10.8)
DAS28(CRP)	6.2 (0.9)	5.6 (1.0)	6.4 (0.9)	6.0 (1.0)
SDAI	46.7 (13.8)	38.0 (13.9)	49.4 (14.4)	43.1 (14.0)
CDAI	43.3 (12.6)	35.4 (12.3)	44.4 (12.4)	40.4 (13.0)
HAQ-DI (range, 0–3)	1.6 (0.6)	1.3 (0.7)	1.6 (0.6)	1.5 (0.7)
mTSS	15.5 (20.6)	12.2 (17.9)	20.7 (22.1)	12.4 (18.6)
CRRP, n (%)	146 (28)	25 (15)	NA	NA
Insufficient responders, n (%)	NA	NA	146 (85)	364 (73)
Prior therapies, n (%)				
Systemic glucocorticoids	216 (41)	79 (49)	61 (36)	225 (45)
≥1 DMARD	88 (17)	28 (17)	34 (20)	78 (16)

Values are mean (SD), unless otherwise indicated.
Insufficient response to methotrexate was defined as not achieving DAS28(CRP) <3.2 at week 24/26 for OPTIMA or week 20/24 for PREMIER.
CRRP was defined as an increase in mTSS of >1.5 from baseline to week 26 for OPTIMA or week 24 for PREMIER.
CDAI, Clinical Disease Activity Index; CRP, C-reactive protein; CRRP, clinically relevant radiographic progression; DAS28(CRP), 28-joint Disease Activity Score based on CRP; DMARD, disease-modifying antirheumatic drug; HAQ-DI, Health Assessment Questionnaire Disability Index; mTSS, modified total Sharp score; NA, not available; OPTIMA, Optimal Protocol for Treatment Initiation with Methotrexate and Adalimumab; RA, rheumatoid arthritis; SDAI, Simplified Disease Activity Index; SJC66, swollen joint count based on 66 joints; TJC68, tender joint count based on 68 joints.

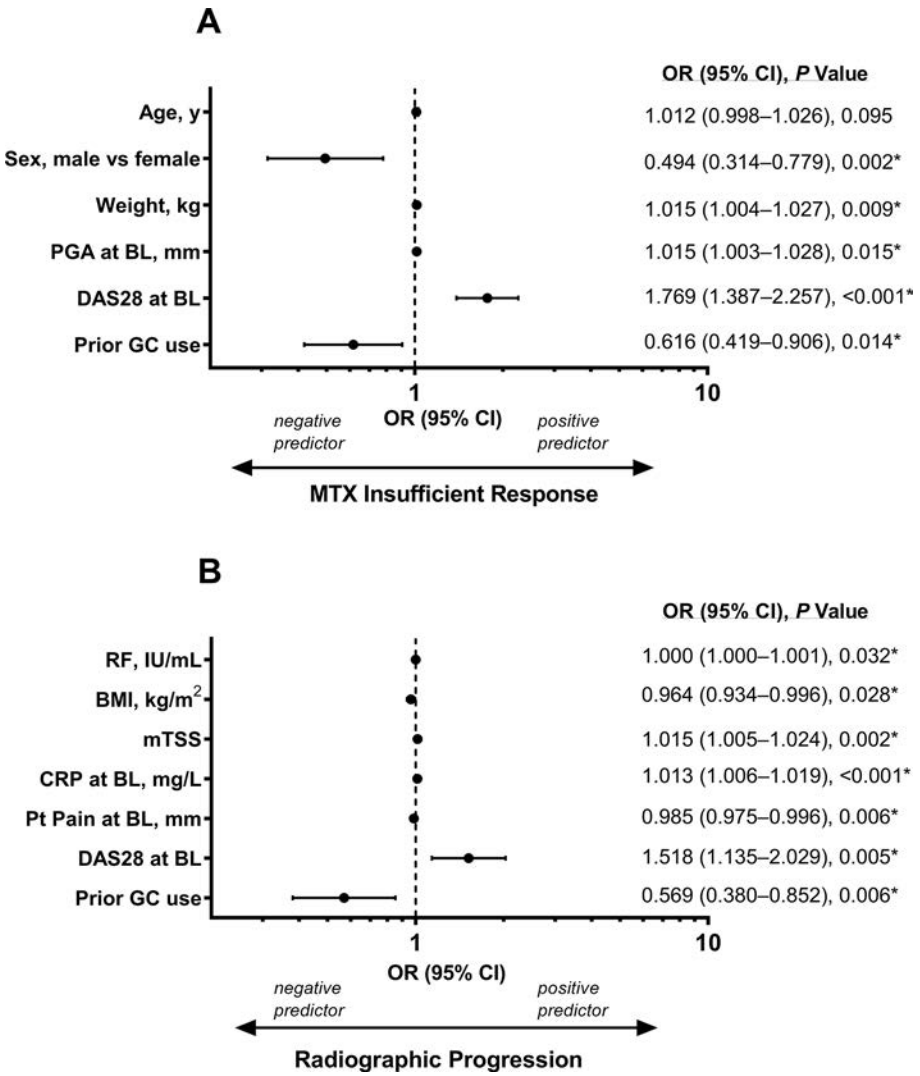

Figure 1 Backward logistic regression analysis of baseline predictors, including DAS28(CRP), of insufficient response to methotrexate at 6 months (A) and CRRP at 6 months (B) in patients with early RA receiving methotrexate monotherapy. Insufficient response to methotrexate was defined as not achieving DAS28(CRP) <3.2 at weeks 22 and 26 (OPTIMA study) or weeks 20 and 24 (PREMIER study). CRRP was defined as increase in mTSS of >1.5 from baseline to week 26 (OPTIMA study) or week 24 (PREMIER study). Predictors analysis considered 500 methotrexate insufficient responders and 156 methotrexate responders; CRRP analysis considered 481 patients without CRRP and 163 patients with CRRP. The OR for each continuous variable (age, BMI, CRP at BL, DAS28 at BL, mTSS, PGA at BL, Pt Pain at BL, RF and weight) reflects the effect of a 1-unit change in that variable; thus, the ORs differ partly because of the different relative meaning of a 1-unit change, such as for DAS28 (scale, about 1–10) compared with SDAI (scale, 0 to about 86). The full regression models, before elimination of factors with p≥0.1, included age, race (white vs non-white), sex (male vs female), weight, RA duration, RF, BMI and mTSS; BL values for CRP, tender joint count based on 68 joints, swollen joint count based on 66 joints, Health Assessment Questionnaire Disability Index, Pt Pain, Pt Global Assessment of Disease Activity on a 100 mm visual analogue scale, PGA and DAS28; and prior use of DMARDs (yes vs no), number of prior DMARDs and prior use of GCs (yes vs no). *P<0.05; statistically significant difference. BL, baseline; BMI, body mass index; CRP, C-reactive protein; CRRP, clinically relevant radiographic progression; DAS28, 28-joint Disease Activity Score; DMARD, disease-modifying antirheumatic drug; GC, glucocorticoid; mTSS, modified total Sharp score; MTX, methotrexate; OPTIMA, Optimal Protocol for Treatment Initiation with Methotrexate and Adalimumab; OR, odds ratio; PGA, Physician Global Assessment of Disease Activity on a 100 mm visual analogue scale; Pt, patient; RA, rheumatoid arthritis; RF, rheumatoid factor; SDAI, Simplified Disease Activity Index.

DMARD use, tender joint count, swollen joint count, CRP, DAS28, HAQ-DI, mTSS and erosion score) was used to determine the odds ratios (ORs) of achieving categorical clinical, functional and radiographic outcomes between the OPTIMA and PREMIER patients.

RESULTS

Predictors of insufficient response to methotrexate and CRRP at 6 months

Patients

The pooled analysis (PREMIER and OPTIMA) of predictors of insufficient response to methotrexate included 525 insufficient responders and 162 responders who had data for all independent variables. The pooled CRRP analysis included 171 patients with CRRP and 499 without CRRP. More patients with an insufficient response to methotrexate were women and had significantly higher baseline mean values for age, CRP, tender and swollen joint counts, DAS28(CRP), SDAI, CDAI, HAQ-DI and mTSS compared with patients achieving stable LDA with methotrexate (table 1). Similarly, patients with CRRP had significantly higher mean CRP, tender and swollen joint counts, DAS28(CRP), SDAI, CDAI and mTSS values at baseline versus patients without CRRP (table 1).

Model with baseline factors

In the baseline model, DAS28(CRP) was the most statistically significant predictor that was positively associated with insufficient response to methotrexate and CRRP at 6 months (figure 1A,B). In separate analyses, SDAI and CDAI also predicted insufficient response to methotrexate at 6 months, similar to the primary analysis with DAS28(CRP), but did not predict CRRP (online supplementary figures 1 and 3). Male sex and prior use of systemic glucocorticoids were the strongest negative predictors of insufficient response to methotrexate (figure 1A; online supplementary figures 1A and 3A); prior systemic glucocorticoid use was also a negative predictor of CRRP (figure 1B; online supplementary figures 1B and 3B).

Model with baseline and postbaseline factors

In the baseline and postbaseline (time-averaged) predictors model, higher time-averaged DAS28(CRP) through week 12 was the strongest positive predictor of insufficient response to methotrexate and CRRP at 6 months ($p<0.001$ for both; figure 2). Additionally, high values of time-averaged DAS28(CRP) through weeks 4 and 8 ($p<0.001$ for all) were also positive predictors of insufficient

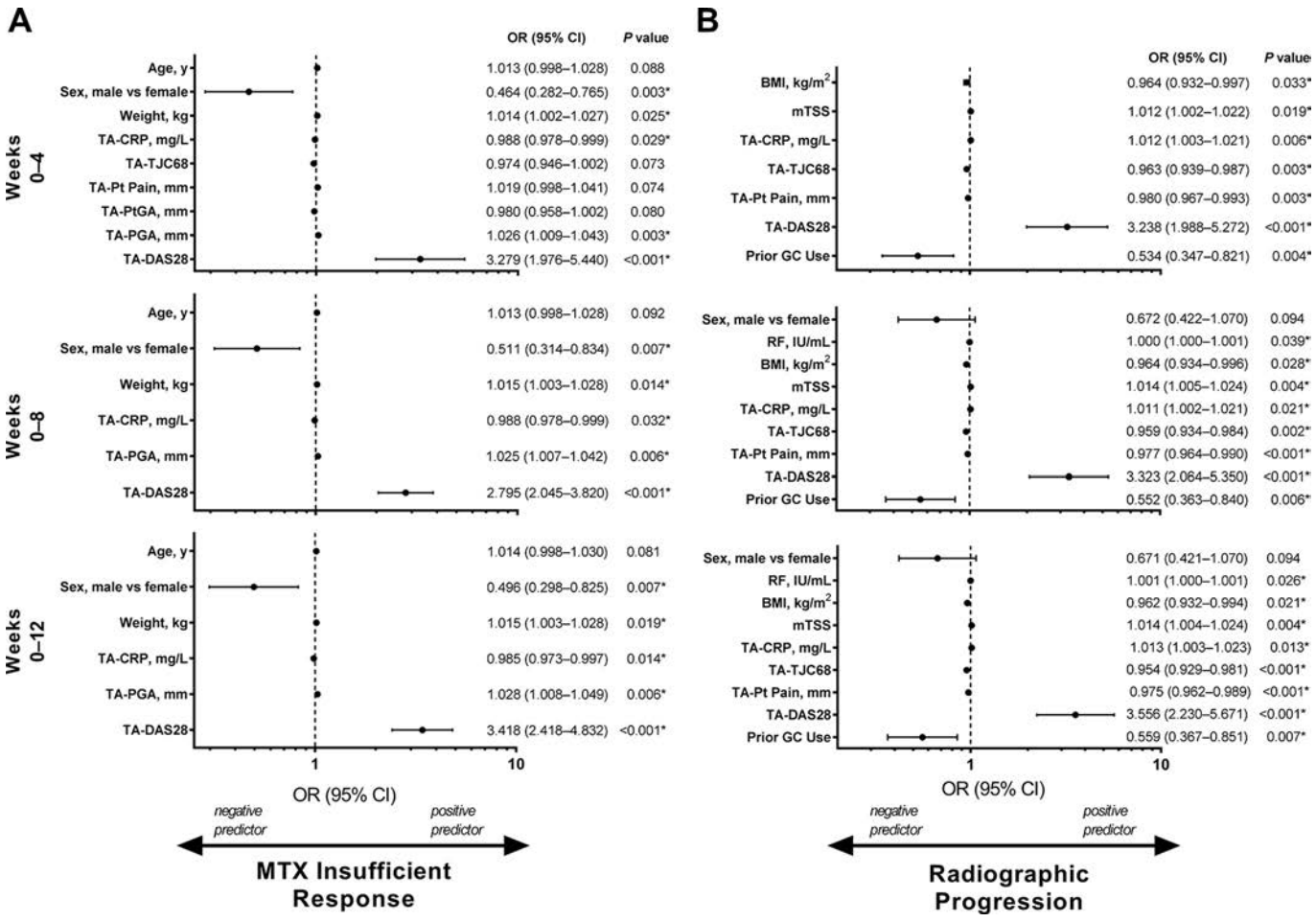

Figure 2 Backward logistic regression analysis of baseline and postbaseline predictors, including DAS28(CRP), of insufficient response to methotrexate at 6 months (A) and CRRP at 6 months (B) based on data from weeks 0–4, weeks 0–8 and weeks 0–12 in patients with early RA receiving methotrexate monotherapy. Week 4 analysis considered 485 methotrexate insufficient responders and 151 methotrexate responders, week 8 analysis considered 507 methotrexate insufficient responders and 160 methotrexate responders and week 12 analysis considered 500 methotrexate insufficient responders and 156 methotrexate responders. Week 4 analysis considered 471 patients without CRRP and 153 patients with CRRP, week 8 analysis considered 491 patients without CRRP and 163 patients with CRRP and week 12 analysis considered 481 patients without CRRP and 163 patients with CRRP. Insufficient response to methotrexate was defined as not achieving DAS28(CRP) <3.2 at weeks 22 and 26 (OPTIMA study) or weeks 20 and 24 (PREMIER study). CRRP was defined as an increase in modified total Sharp score of >1.5 from baseline to week 26 (OPTIMA study) or week 24 (PREMIER study). The OR for each continuous variable (age, BMI, mTSS, RF, TA-CRP, TA-DAS28, TA-PGA, TA-Pt Pain, TA-PtGA, TA-TJC68, weight) reflects the effect of a 1-unit change in that variable; thus, the ORs differ partly because of the different relative meaning of a 1-unit change, such as for DAS28 (scale, about 1–10) compared with SDAI (scale, 0 to about 86). The full regression models, before elimination of factors with $p\geq0.1$, included age, race (white vs non-white), sex (male vs female), weight, RA duration, RF, BMI and mTSS; TA values for CRP, TJC68, swollen joint count based on 66 joints, HAQ-DI, Pt Pain, PtGA, PGA and DAS28; and prior use of DMARDs (yes vs no), number of prior DMARDs and prior use of GCs (yes vs no). *P<0.05; statistically significant difference. BMI, body mass index; CRP, C-reactive protein; CRRP, clinically relevant radiographic progression; DAS28, 28-joint Disease Activity Score; DMARD, disease-modifying antirheumatic drug; GC, glucocorticoid; HAQ-DI, Health Assessment Questionnaire Disability Index; mTSS, modified total Sharp score; MTX, methotrexate; OPTIMA, Optimal Protocol for Treatment Initiation with Methotrexate and Adalimumab; OR, odds ratio; PGA, Physician Global Assessment of Disease Activity on a 100 mm visual analogue scale; Pt, patient; PtGA, Patient Global Assessment of Disease Activity on a 100 mm visual analogue scale; RA, rheumatoid arthritis; RF, rheumatoid factor; SDAI, Simplified Disease Activity Index; TA, time averaged; TJC68, tender joint count based on 68 joints.

methotrexate response and CRRP. As in the model with only baseline factors, time-averaged SDAI and CDAI were also predictors of these outcomes (online supplementary figures 2 and 4). Male sex was again the strongest negative predictor of insufficient response to methotrexate (figure 2A; online supplementary figures 2A and 4A), and prior glucocorticoid was the strongest negative predictor of CRRP in the time-averaged model (figure 2B; online supplementary figures 2B and 4B).

Efficacy at 6 months and onward among patients with an insufficient response to methotrexate

Patients

In OPTIMA, 348 patients who did not achieve the stable LDA target of DAS28(CRP) <3.2 after 26 weeks of methotrexate monotherapy (ie, had an insufficient response to methotrexate) and who advanced to adalimumab plus methotrexate rescue therapy were included in this analysis. In PREMIER, 177 patients who did not achieve the stable LDA target of DAS28(CRP) <3.2 after 24 weeks of methotrexate monotherapy and continued that regimen were included in this analysis. Most demographics and baseline disease characteristics were different between patients who had an insufficient response to methotrexate in OPTIMA and PREMIER (table 2). Mean baseline disease duration was 0.3 and 0.8 years, respectively. The mean mTSS was lower among patients who had an insufficient response to methotrexate in OPTIMA than in PREMIER (11.7 vs 23.0), and a lower percentage of patients in OPTIMA than in PREMIER (63% vs 89%) had >1 erosion at baseline.

Table 2 Baseline demographics, disease characteristics and prior and concomitant therapies of patients who had an insufficient response to methotrexate

Characteristic	Patients with an insufficient response to methotrexate at 6 months (n=525)*	
	OPTIMA Adalimumab Rescue (n=348)	PREMIER Methotrexate Monotherapy (n=177)
Demographic characteristics		
Women, n (%)	266 (76)	132 (75)
White, n (%)	313 (90)	170 (96)
Age (years)	50.7 (13.9)	52.5 (13.3)
RA duration (years)	0.3 (0.3)	0.8 (0.9)
Weight (kg)	77.5 (20.8)	76.5 (18.6)
BMI (kg/m^2)	28.4 (6.8)†	27.6 (6.6)
Disease characteristics		
RF+, n (%)	302 (88)‡	147 (83)
CRP (mg/L)	32.6 (33.3)	41.8 (41.6)
TJC68	28.6 (14.7)	33.3 (14.7)
SJC66	19.1 (10.7)	22.9 (12.3)
DAS28(CRP)	6.1 (0.9)§	6.4 (0.8)¶
SDAI	45.2 (13.7)§	49.7 (13.5)**
HAQ-DI (range, 0–3)	1.7 (0.6)†	1.5 (0.7)¶
mTSS	11.7 (18.5)†	23.0 (22.5)**
>1 erosion, n (%)	217 (63)†	155 (89)**
Prior therapies		
Systemic glucocorticoids, n (%)	133 (38)	83 (47)
≥1 DMARD, n (%)	34 (10)	54 (31)

Values are mean (SD), unless otherwise indicated.
*n consists of patients treated with placebo+methotrexate who did not achieve DAS28(CRP) <3.2 at week 24/26 for OPTIMA or week 20/24 for PREMIER.
†n=347 non-missing values.
‡n=344 non-missing values.
§n=341 non-missing values.
¶n=176 non-missing values.
**n=174 non-missing values.
BMI, body mass index; CRP, C-reactive protein; DAS28(CRP), 28-joint Disease Activity Score based on CRP; DMARD, disease-modifying antirheumatic drug; HAQ-DI, Health Assessment Questionnaire Disability Index; mTSS, modified total Sharp score; NA, not available; OPTIMA, Optimal Protocol for Treatment Initiation with Methotrexate and Adalimumab; RA, rheumatoid arthritis; RF, rheumatoid factor; SDAI, Simplified Disease Activity Index; SJC66, swollen joint count based on 66 joints; TJC68, tender joint count based on 68 joints.

Disease activity

Although by definition none of the patients evaluated here had achieved stable LDA (ie, on at least two assessments) by 6 months, a small and similar percentage of patients achieved LDA (10% vs 12%) in OPTIMA and PREMIER at 6 months (week 26 or 24, respectively). The mean (SD) DAS28(CRP) scores also were similar at the same time points (4.5 (1.2) vs 4.4 (1.1); p=0.144). After 1 year of additional treatment (ie, at week 78 in OPTIMA or week 76 in PREMIER), a significantly higher percentage of patients who received adalimumab rescue therapy at week 26 in OPTIMA, versus patients who continued to receive methotrexate monotherapy in PREMIER, achieved LDA (64% vs 41%, respectively; p<0.001), and their mean DAS28(CRP) score was significantly lower (2.9 vs 3.6; p<0.001). Similar patterns of improvement were also observed in the proportion of patients achieving DAS28(CRP) <2.6 (48% vs 19%), SDAI ≤3.3 (32% vs 10%) and CDAI ≤2.8 (32% vs 10%) at week 78 (OPTIMA) or week 76 (PREMIER), respectively (all p<0.001), as well as in mean SDAI (10.3 vs 16.0; p<0.001) and mean CDAI (9.5 vs 14.9; p<0.001). In multivariate regression analyses, switching to adalimumab rescue therapy was associated with significantly greater odds of achieving LDA (ie, DAS28(CRP) <3.2) versus continuing on methotrexate (OR 3.25 (95% CI 1.83 to 5.74); p<0.001). Similar results were observed for DAS28(CRP) <2.6 (OR 3.27 (95% CI 1.74 to 6.14); p<0.001), SDAI ≤3.3 (OR 3.30 (95% CI 1.52 to 7.15); p=0.002) and CDAI ≤2.8 (OR 3.43 (95% CI 1.58 to 7.44); p=0.002).

Functional and radiographic outcomes

Functional and radiographic outcomes demonstrated similar patterns as disease activity outcomes. At week 78 (OPTIMA) or week 76 (PREMIER), significantly greater proportions of patients who switched to adalimumab rescue therapy achieved improvement in HAQ-DI of ≥0.22 (54% vs 30%; p<0.001), and these patients also had significantly greater mean changes in HAQ-DI from week 26/24 to week 78/76 (−0.3 vs −0.1; p<0.001) versus those who continued on methotrexate monotherapy. However, there was no difference in the mean HAQ-DI scores between groups at week 78/76 (0.7 vs 0.8; p=0.236), although baseline HAQ-DI scores were higher in insufficient methotrexate responders in OPTIMA versus PREMIER (1.7 vs 1.5; table 2), and therefore overall reduction from baseline was also much larger in OPTIMA. At week 52, 88% of patients who switched to adalimumab rescue therapy achieved ΔmTSS of ≤0.5 vs 57% of patients who continued on methotrexate (p<0.001); the mean changes from week 26 were 0.0 and 2.2 (p<0.001) in the two groups, respectively. Similarly, at week 78/76, patients who switched to adalimumab rescue therapy achieved ΔmTSS of ≤0.5 with significantly greater frequency (88% vs 41%; p<0.001) and had significantly less mean progression in mTSS from week 26/24 (0.1 vs 4.7; p<0.001) versus those who continued on methotrexate monotherapy. Furthermore, switching to adalimumab rescue therapy was associated with greater odds of achieving improvement in HAQ-DI of ≥0.22 at week 78/76 (OR

2.27 (95% CI 1.26 to 4.11); p=0.006), ΔmTSS of ≤0.5 at week 52 (OR 4.71 (95% CI 2.56 to 8.65); p<0.001) and ΔmTSS of ≤0.5 at week 78/76 (OR 8.96 (95% CI 4.94 to 16.27); p<0.001) versus continuing on methotrexate monotherapy.

DISCUSSION

Although methotrexate remains the first-line treatment strategy in patients with RA,[1] only 28%–44% of patients with early RA exhibit sufficient clinical response to methotrexate monotherapy within 6 months,[4 12 13] and another treatment strategy must be considered in those for whom the treatment is insufficient. Because radiographic damage occurs early in the course of RA,[3] timely adaptation of therapy after failure of the initial treatment strategy may be necessary to prevent irreversible damage. Current recommendations suggest adjusting therapy when patients have no improvement by 3 months or have not reached the therapeutic target by 6 months.[1] Consequently, identifying patients who are at risk of methotrexate failure would facilitate a more targeted therapy strategy and allow earlier adjustment of treatment.

In our post hoc analysis of two randomised, double-blind, placebo-controlled trials in patients with early RA receiving initial methotrexate monotherapy, baseline disease activity by composite measures was the strongest positive predictor of insufficient response to the starting therapy at 6 months. Although methotrexate was the starting treatment in our analysis, prior research suggests that the predictive value of early disease activity on later outcomes is independent of the particular regimen, as correlations in a previous report were observed whether patients received methotrexate monotherapy or methotrexate plus a tumour necrosis factor (TNF) inhibitor.[14] Furthermore, in our analysis, early clinical activity (ie, time-averaged DAS28(CRP), SDAI and CDAI over 4, 8 and 12 weeks) was a significant predictor of insufficient response to methotrexate, suggesting that changes in clinical disease activity as early as 4 weeks can predict response to methotrexate treatment at 6 months. Similarly, various predictors for response to methotrexate therapy in patients with RA have been identified in previous studies, including high disease activity (measured by DAS, SDAI or CDAI) and HAQ score at baseline[14 15] and disease activity (measured by DAS28, SDAI or CDAI) at 3 months.[14] Early disease activity has been previously found to predict later disease activity in patients with RA treated with the TNF inhibitor certolizumab pegol.[16 17] An analysis of seven pivotal, randomised trials in early and established RA demonstrated that disease activity response reached at 3 months is significantly associated with reaching target at 6 months; interestingly, the type of treatment did not significantly influence the accuracy of the analysis.[18] More studies are warranted to confirm these results.

Besides being predictors of insufficient response to methotrexate, baseline and time-averaged disease activity were also significant predictors of CRRP in the present analysis. Baseline DAS28 and mTSS were also identified as predictors of radiographic progression in early RA in a previous study.[19] This is in line with other studies that have long found that markers of disease activity (eg, CRP, erythrocyte sedimentation rate and swollen joint count) are predictors of radiographic progression, aside from autoantibody positivity and presence of early damage.[7 20–26] Our findings also showed that glucocorticoid treatment at baseline was a negative predictor of CRRP in the baseline and time-averaged models (and also of insufficient response to methotrexate in the baseline models), similar to established understanding.[27] Overall, these results are in line with the treatment-to-target strategy and support timely adaptation of therapy with TNF inhibitors in patients who have insufficient response to methotrexate.[1 2]

When assessing response to methotrexate, more consistent results have been obtained in other studies when using sex as a predictor. Men respond better to methotrexate therapy than women, and studies in early RA have identified female sex as a predictor of poor response to methotrexate.[12 28 29] Greater body mass index also has been shown previously to negatively predict radiographic progression.[30 31] Our findings were consistent with these patterns. Overall, these data suggest that women with early RA who receive methotrexate may benefit from frequent early monitoring of disease activity, allowing for the opportunity to adjust treatment within the first 3–6 months for those with insufficient response. Indeed, it is currently recommended to change treatment regimen if disease activity has not improved by at least 50% within 3 months after treatment start.[1 18]

When assessed for long-term outcomes, patients who received adalimumab rescue therapy at week 26 (OPTIMA) had significantly greater improvements and odds of achieving LDA at week 78 compared with patients who received methotrexate monotherapy (PREMIER) for 76 weeks. Nonetheless, 41% of patients who received methotrexate monotherapy achieved LDA at week 76. A previous study demonstrated delayed response to methotrexate monotherapy versus methotrexate combined with adalimumab.[32] Taken together, these results suggest that, although more patients receiving combination therapy achieve LDA earlier, some patients receiving methotrexate monotherapy will achieve treatment response later. Future analyses should explore what factors predict successful long-term methotrexate treatment in some patients, despite an insufficient response at 6 months, to identify who might not require adaptation of therapy.

In this post hoc analysis, integration of the populations randomised to receive methotrexate in the OPTIMA and PREMIER trials allowed identification of outcomes and predictors of insufficient response to methotrexate and CRRP. However, because population differences can impact treatment response,[33] the possible heterogeneity between pooled study populations is a limitation of this analysis. Other limiting factors included possible patient selection bias and multiple comparisons and the fact that the analyses compared the results of two separate trials that were not conducted head to head, were done in different calendar years and had non-identical designs and baseline characteristics. Also, smoking status, citrullinated peptide positivity and erosions (except as part of mTSS) were not included in the predictor regression models. Furthermore, addition of glucocorticoids when methotrexate treatment failed was not part of the study protocols. However, because (based on recent insights) conducting a 2-year methotrexate monotherapy study in patients with an insufficient response to methotrexate is not in line with current ethical considerations, this analysis provides data not attainable in future studies.

In patients with early RA, baseline disease characteristics and patient demographics as well as early disease activity can predict response to methotrexate treatment and radiographic progression at 6 months. In patients who did not achieve LDA after 6 months of initial methotrexate monotherapy, the addition of adalimumab to the treatment regimen was associated with better clinical, functional and radiographic outcomes. These results support, and indirectly confirm, treatment-to-target strategies and timely adaptation of therapy with TNF inhibitors in patients with early RA and identify risk factors of patients who are not responding sufficiently to methotrexate.

Acknowledgements AbbVie funded the studies, contributed to their designs and was involved in the collection, analysis, and interpretation of the data and in the writing, review and approval of the publication. AbbVie and the authors thank the patients who participated in the clinical trial and all study investigators for their contributions.

Contributors All authors made contributions to the planning, conduct and/or reporting of the work. Medical writing assistance was provided by Michael J Theisen, PhD, and Maria Hovenden, PhD, of Complete Publication Solutions (North Wales, PA), a CHC Group company, and was supported by AbbVie.

Funding The OPTIMA and PREMIER studies and this post hoc analysis were funded by AbbVie (NCT00420927, NCT00195663).

Competing interests JSS and AK provided remunerated expert advice to and received grant/research support for his institution from AbbVie. RFvV has received grants and research support from AbbVie, Amgen, Bristol-Myers Squibb, GlaxoSmithKline, Pfizer, Roche and UCB; and consulting fees and honoraria from AbbVie, AstraZeneca, Biotest, Bristol-Myers Squibb, Celgene, Crescendo, GlaxoSmithKline, Janssen, Lilly, Merck, Novartis, Pfizer, Roche, UCB and Vertex. SF, SC and JLS are employees of AbbVie and may hold stock or stock options.

Patient consent Not required.

Ethics approval The original clinical studies were approved by a central institutional review board or independent ethics committee at each participating site. This post hoc analysis of data from those studies did not require additional approval.

Provenance and peer review Not commissioned; externally peer reviewed.

Data sharing statement AbbVie is committed to responsible data sharing regarding the clinical trials we sponsor. This includes access to anonymised, individual and trial-level data (analysis data sets), as well as other information (eg, protocols and Clinical Study Reports), as long as the trials are not part of an ongoing or planned regulatory submission. This includes requests for clinical trial data for unlicensed products and indications. These clinical trial data can be requested by any qualified researchers who engage in rigorous, independent scientific research, and will be provided following review and approval of a research proposal and Statistical Analysis Plan (SAP) and execution of a Data Sharing Agreement (DSA). Data requests can be submitted at any time and the data will be accessible for 12 months, with possible extensions considered. For more information on the process, or to submit a request, visit the following link: https://www.abbvie.com/our-science/clinical-trials/clinical-trials-data-and-information-sharing/data-and-information-sharing-with-qualified-researchers.html.

REFERENCES

1 Smolen JS, Landewé R, Bijlsma J, *et al*. EULAR recommendations for the management of rheumatoid arthritis with synthetic and biological disease-modifying antirheumatic drugs: 2016 update. *Ann Rheum Dis* 2017;76:960–77.
2 Singh JA, Saag KG, Bridges SL, *et al*. 2015 American college of rheumatology guideline for the treatment of rheumatoid arthritis. *Arthritis Rheumatol* 2016;68:1–26.
3 Lindqvist E, Jonsson K, Saxne T, *et al*. Course of radiographic damage over 10 years in a cohort with early rheumatoid arthritis. *Ann Rheum Dis* 2003;62:611–6.
4 Rezaei H, Saevarsdottir S, Forslind K, *et al*. In early rheumatoid arthritis, patients with a good initial response to methotrexate have excellent 2-year clinical outcomes, but radiological progression is not fully prevented: data from the methotrexate responders population in the SWEFOT trial. *Ann Rheum Dis* 2012;71:186–91.
5 van der Heijde D, Klareskog L, Rodriguez-Valverde V, *et al*. Comparison of etanercept and methotrexate, alone and combined, in the treatment of rheumatoid arthritis: two-year clinical and radiographic results from the TEMPO study, a double-blind, randomized trial. *Arthritis Rheum* 2006;54:1063–74.
6 Breedveld FC, Weisman MH, Kavanaugh AF, *et al*. The PREMIER study: a multicenter, randomized, double-blind clinical trial of combination therapy with adalimumab plus methotrexate versus methotrexate alone or adalimumab alone in patients with early, aggressive rheumatoid arthritis who had not had previous methotrexate treatment. *Arthritis Rheum* 2006;54:26–37.
7 Vastesaeger N, Xu S, Aletaha D, *et al*. A pilot risk model for the prediction of rapid radiographic progression in rheumatoid arthritis. *Rheumatology* 2009;48:1114–21.
8 Kavanaugh A, Fleischmann RM, Emery P, *et al*. Clinical, functional and radiographic consequences of achieving stable low disease activity and remission with adalimumab plus methotrexate or methotrexate alone in early rheumatoid arthritis: 26-week results from the randomised, controlled OPTIMA study. *Ann Rheum Dis* 2013;72:64–71.
9 Smolen JS, Emery P, Fleischmann R, *et al*. Adjustment of therapy in rheumatoid arthritis on the basis of achievement of stable low disease activity with adalimumab plus methotrexate or methotrexate alone: the randomised controlled OPTIMA trial. *Lancet* 2014;383:321–32.
10 Keystone EC, Breedveld FC, van der Heijde D, *et al*. Longterm effect of delaying combination therapy with tumor necrosis factor inhibitor in patients with aggressive early rheumatoid arthritis: 10-year efficacy and safety of adalimumab from the randomized controlled PREMIER trial with open-label extension. *J Rheumatol* 2014;41:5–14.
11 Wells GA, Tugwell P, Kraag GR, *et al*. Minimum important difference between patients with rheumatoid arthritis: the patient's perspective. *J Rheumatol* 1993;20:557–60.
12 van der Kooij SM, de Vries-Bouwstra JK, Goekoop-Ruiterman YP, *et al*. Limited efficacy of conventional DMARDs after initial methotrexate failure in patients with recent onset rheumatoid arthritis treated according to the disease activity score. *Ann Rheum Dis* 2007;66:1356–62.
13 Moreland LW, O'Dell JR, Paulus HE, *et al*. A randomized comparative effectiveness study of oral triple therapy versus etanercept plus methotrexate in early aggressive rheumatoid arthritis: the treatment of Early Aggressive Rheumatoid Arthritis Trial. *Arthritis Rheum* 2012;64:2824–35.
14 Aletaha D, Funovits J, Keystone EC, *et al*. Disease activity early in the course of treatment predicts response to therapy after one year in rheumatoid arthritis patients. *Arthritis Rheum* 2007;56:3226–35.
15 Romão VC, Canhão H, Fonseca JE. Old drugs, old problems: where do we stand in prediction of rheumatoid arthritis responsiveness to methotrexate and other synthetic DMARDs? *BMC Med* 2013;11:17.
16 Curtis JR, Luijtens K, Kavanaugh A. Predicting future response to certolizumab pegol in rheumatoid arthritis patients: features at 12 weeks associated with low disease activity at 1 year. *Arthritis Care Res* 2012;64:658–67.
17 van der Heijde D, Keystone EC, Curtis JR, *et al*. Timing and magnitude of initial change in disease activity score 28 predicts the likelihood of achieving low disease activity at 1 year in rheumatoid arthritis patients treated with certolizumab pegol: a post-hoc analysis of the RAPID 1 trial. *J Rheumatol* 2012;39:1326–33.
18 Aletaha D, Alasti F, Smolen JS. Optimisation of a treat-to-target approach in rheumatoid arthritis: strategies for the 3-month time point. *Ann Rheum Dis* 2016;75:1479–85.
19 Bombardier C, Chen M, Li X, *et al*. A risk model for the prediction of radiographic progression: results from SONORA study. *J Rheumatol* 2010;61:1281.
20 Fautrel B, Granger B, Combe B, *et al*. Matrix to predict rapid radiographic progression of early rheumatoid arthritis patients from the community treated with methotrexate or leflunomide: results from the ESPOIR cohort. *Arthritis Res Ther* 2012;14:R249.
21 Visser K, Goekoop-Ruiterman YP, de Vries-Bouwstra JK, *et al*. A matrix risk model for the prediction of rapid radiographic progression in patients with rheumatoid arthritis receiving different dynamic treatment strategies: post hoc analyses from the BeSt study. *Ann Rheum Dis* 2010;69:1333–7.
22 Smolen JS, Van Der Heijde DM, St Clair EW, *et al*. Predictors of joint damage in patients with early rheumatoid arthritis treated with high-dose methotrexate with or without concomitant infliximab: results from the ASPIRE trial. *Arthritis Rheum* 2006;54:702–10.
23 Amos RS, Constable TJ, Crockson RA, *et al*. Rheumatoid arthritis: relation of serum C-reactive protein and erythrocyte sedimentation rates to radiographic changes. *Br Med J* 1977;1:195–7.
24 Sharp JT, Lidsky MD, Duffy J. Clinical responses during gold therapy for rheumatoid arthritis. Changes in synovitis, radiologically detectable erosive lesions, serum proteins, and serologic abnormalities. *Arthritis Rheum* 1982;25:540–9.
25 Möttönen TT. Prediction of erosiveness and rate of development of new erosions in early rheumatoid arthritis. *Ann Rheum Dis* 1988;47:648–53.
26 van Leeuwen MA, van der Heijde DM, van Rijswijk MH, *et al*. Interrelationship of outcome measures and process variables in early rheumatoid arthritis. A comparison of radiologic damage, physical disability, joint counts, and acute phase reactants. *J Rheumatol* 1994;21:425–9.
27 Kavanaugh A, Wells AF. Benefits and risks of low-dose glucocorticoid treatment in the patient with rheumatoid arthritis. *Rheumatology* 2014;53:1742–51.
28 Saevarsdottir S, Wallin H, Seddighzadeh M, *et al*. Predictors of response to methotrexate in early DMARD naive rheumatoid arthritis: results from the initial open-label phase of the SWEFOT trial. *Ann Rheum Dis* 2011;70:469–75.
29 Wessels JA, van der Kooij SM, le Cessie S, *et al*. A clinical pharmacogenetic model to predict the efficacy of methotrexate monotherapy in recent-onset rheumatoid arthritis. *Arthritis Rheum* 2007;56:1765–75.
30 Joo YB, Bang SY, Ryu JA, *et al*. Predictors of severe radiographic progression in patients with early rheumatoid arthritis: A prospective observational cohort study. *Int J Rheum Dis* 2017;20:1437–46.
31 Baker JF, Ostergaard M, George M, *et al*. Greater body mass independently predicts less radiographic progression on X-ray and MRI over 1-2 years. *Ann Rheum Dis* 2014;73:1923–8.
32 Smolen JS, Bu X, Wang X, *et al*. Characteristics of patients with early rheumatoid arthritis who have a delayed response to treatment with methotrexate in monotherapy or in combination with adalimumab [abstract]. *Arthritis Rheumatol* 2017;69(suppl 10 abstr 1419).
33 Griffiths B, Situnayake RD, Clark B, *et al*. Racial origin and its effect on disease expression and HLA-DRB1 types in patients with rheumatoid arthritis: a matched cross-sectional study. *Rheumatology* 2000;39:857–64.

EXTENDED REPORT

Back pain in psoriatic arthritis: defining prevalence, characteristics and performance of inflammatory back pain criteria in psoriatic arthritis

Kristy S Yap,[1,2] Justine Y Ye,[1] Suzanne Li,[1] Dafna D Gladman,[1,2,3] Vinod Chandran[1,2,3,4]

Handling editor Josef S Smolen

[1]University of Toronto Psoriatic Arthritis Clinic, Centre for Prognostic Studies in the Rheumatic Diseases, Krembil Research Institute, Toronto Western Hospital, Toronto, Ontario, Canada
[2]Division of Rheumatology, Department of Medicine, University of Toronto, Toronto, Ontario, Canada
[3]Institute of Medical Science, University of Toronto, Toronto, Ontario, Canada
[4]Department of Laboratory Medicine and Pathobiology, University of Toronto, Toronto, Ontario, Canada

Correspondence to
Dr Vinod Chandran, Department of Medicine, Division of Rheumatology, Toronto Western Hospital, Toronto, ON M5T 2S8, Canada;
vinod.chandran@uhnres.utoronto.ca

This paper is based on work previously presented at the 2016 ACR/ARHP Annual Meeting and was published as a conference abstract.

Received 1 March 2018
Revised 18 July 2018
Accepted 19 July 2018
Published Online First
4 August 2018

To cite: Yap KS, Ye JY, Li S, *et al*. *Ann Rheum Dis* 2018;**77**:1573–1577.

ABSTRACT

Objective We aimed to determine the agreement between rheumatologist-judged inflammatory back pain (IBP) and criteria defining IBP in patients with psoriatic arthritis (PsA) and predictive value of IBP in identifying axial involvement in PsA.

Methods Using prospectively collected data, we investigated the agreement between rheumatologist judgement of IBP and IBP criteria (Calin, Rudwaleit and Assessment of Spondyloarthritis International Society) using the kappa coefficient. We also determined the sensitivity, specificity and likelihood ratios of the presence of back pain, rheumatologist-judged IBP and the three IBP criteria for detecting axial PsA (AxPsA). Finally, we compared the clinical and genetic markers in patients with PsA with axial radiological changes with and without back pain.

Results 171 patients (52% male, mean age 46.6 years) were identified. Ninety-six (56.13%) patients reported chronic back pain. Sixty-five (38.01%) had IBP. 54 (32%) patients had evidence of radiological change in the spine. The agreement between rheumatologist judgement of IBP and IBP criteria was highest for the Calin criteria (0.70). Positive likelihood ratio for the presence of radiological axial involvement was highest for Rudwaleit criteria (2.17). No differences between patients with AxPsA with or without back pain were found, except for higher Bath Ankylosing Spondylitis Disease Activity Index and lower prevalence of human leucocyte antigen-B*38 in those with back pain.

Conclusion Rheumatologist-judged IBP or the criteria for IBP developed for ankylosing spondylitis may not perform well when ascertaining axial involvement in PsA.

INTRODUCTION

Psoriatic arthritis (PsA) is an inflammatory arthritis associated with psoriasis. PsA has a broad spectrum of features that manifests as peripheral arthritis, enthesitis, dactylitis or axial arthritis. The presence of axial involvement is a marker of PsA severity, since patients with axial arthritis have more severe peripheral arthritis, compared with those without.[1] Therefore, recognising axial involvement may help in stratifying patients for more aggressive therapy.

However, recognising axial involvement in PsA may be difficult. There is no widely accepted definition of axial involvement in PsA and estimates vary from 25% to 70%.[2–4] Definitions of axial disease in PsA have varied and have included the presence of isolated radiographic unilateral at least grade 2 sacroiliitis scored according to the New York (NY) criteria, bilateral grade 2 or unilateral grade 3 or 4 radiographic sacroiliitis, syndesmophytes or bone marrow oedema on MRI.[5] In patients with PsA with predominantly axial disease, based on data extrapolated from ankylosing spondylitis (AS), it is recommended that tumour necrosis factor inhibitors be considered for treating active axial arthritis despite non-steroidal anti-inflammatory drug (NSAID) therapy.[6]

Thus, an important question when evaluating a patient with PsA is to determine if axial PsA (AxPsA) is present. Patients with AxPsA do not report as much pain as patients with AS. In fact, studies found that between 45% and 55% of patients with AxPsA do not have inflammatory back pain (IBP) symptoms.[7–9] On the other hand, patients with PsA are older and tend to be overweight or obese; thus, they might have non-specific back pain (nsBP). Moreover, many patients with PsA and chronic back pain have peripheral arthritis, enthesitis, dactylitis, psoriasis and elevated C-reactive protein (CRP); therefore, the likelihood of having axial involvement is high compared with subjects without PsA presenting with chronic back pain.

Three sets of criteria exist for defining IBP: Calin,[10] Rudwaleit[11] and Assessment of Spondyloarthritis International Society (ASAS) criteria.[12] These criteria have been validated in subsequent studies to have sensitivities and specificities of over 70% for detecting IBP as judged by rheumatologists who were experts in SpA. However, it is not clear whether these criteria are useful for screening for axial involvement in PsA. We therefore aimed to determine the predictive value of IBP criteria for identifying AxPsA. Subsequently, in an exploratory analysis, we also aimed to determine differences in the demographic and disease characteristics between patients with AxPsA with and without back pain.

METHODS

At the University of Toronto PsA clinic, patients with PsA are followed prospectively at intervals of 6–12 month according to a standard protocol. Radiographs of peripheral joints and spine are performed at baseline and 2-year intervals. MRI is done only if there is a suspicion of axial involvement, and the X-rays are unremarkable or suspicious. All data are tracked in a computerised database. At each protocol visit, a rheumatologist expert in PsA records the presence of back pain,

as well as the individual criteria used to determine if the back pain is inflammatory or not including age at onset, duration, insidious onset, the presence of morning stiffness and its duration, improvement with exercise and with rest, alternating buttock pain, pain at second half of the night with improvement on getting out of bed and responsiveness to NSAIDs. From these data, it was electronically determined if the patient satisfied each of the criteria for IBP (Calin, Rudwaleit and ASAS criteria); the rheumatologist did not explicitly determine if any of the above criteria were fulfilled. In addition, the expert rheumatologist also records whether a patient has back pain, and whether it is inflammatory or non-specific or both based on clinical judgement. Clinical judgement of the type of back pain is left to the discretion of the expert who makes the judgement after considering the patient's history and physical examination but not imaging and is likely but not necessarily to consider features of IBP mentioned above. Other information collected includes the presence of peripheral arthritis, enthesitis, dactylitis, psoriasis and comorbidities including cardiovascular comorbidities such as body mass index (BMI), diabetes mellitus (DM), hypertension and hypercholesterolaemia. The components of the Bath Ankylosing Spondylitis Metrology Index (BASMI) are also measured by the clinician, and the patients complete the Bath Ankylosing Spondylitis Disease Activity Index (BASDAI) and Bath Ankylosing Spondylitis Functional Index (BASFI). Routine laboratory assessments include erythrocyte sedimentation rate and CRP. Radiographs of the pelvis, cervical thoracic and lumbar spine as well as hands and feet are evaluated by two rheumatologists by consensus; sacroiliitis is scored according to the NY scoring method from grades 0 to 4, and the presence and site of syndesmophytes (marginal or paramarginal) are recorded. The X-rays were read by at least two expert rheumatologists by consensus. The assessments of axial involvement have previously shown to be reliable.[13] MRI of the sacroiliac joints (SIJs) and spine is conducted if there is clinical suspicion of axial involvement and the radiographs are normal. The readers were aware of the diagnosis of PsA but not about axial symptoms or signs when reading the images. Typing of the human leucocyte antigen (HLA)-A, HLA-C, HLA-B, HLA-DR and DQ loci are done using sequence-specific oligonucleotide (SSO) probes with the reverse line blot technique (RELI SSO HLA typing kits, Invitrogen, Burlington, Ontario, Canada).

For this study, the inclusion criteria included patients with PsA satisfying Classification of Psoriatic Arthritis (CASPAR) criteria, with or without back pain, and whose first clinic visit was between January 2010 and May 2015. The patients also had to have had baseline radiographs of their SIJ and spine. From the clinical research database, the information required for this study was extracted from data collected at the first clinic visit. Patients with axial involvement were also classified into two mutually exclusive groups based on the presence of back pain and radiographical changes as follows:

1. Those with axial radiological (X-ray or MRI) abnormalities with back pain. X-ray abnormalities included at least unilateral grade 2 radiographic sacroiliitis or syndesmophytes. MRI abnormalities included inflammatory (bone marrow oedema on short tau inversion recovery (STIR) images) or structural changes (bone erosion, fat infiltration, bone spur or ankylosis on T1-weighted images) in SIJs or spine as reported by an experienced musculoskeletal radiologist. No formal definition (ASAS/Spondyloarthritis Research Consortium of Canada) was utilised. Back pain was either inflammatory or non-specific according to the judgement by expert rheumatologist.
2. Those with axial radiological (X-ray or MRI) abnormalities without back pain. Patients with radiological involvement described in group 1 above but without back pain.

The results of HLA typing for the markers (HLA-B*27, HLA-B*08, HLA-B*38, HLA-B*39, and HLA-C*06) were extracted from the research laboratory database.

Statistical analyses

We first investigated the agreement between rheumatologist judgement of the presence or absence of IBP and the presence of IBP according to the three IBP criteria using the kappa coefficient. Subsequently, we calculated the sensitivity and specificity of the presence of back pain, rheumatologist-judged IBP, and the three IBP criteria for detecting AxPsA defined by X-ray (at least grade 2 sacroiliitis or syndesmophytes) or MRI (inflammatory or structural changes in SIJs or spine) abnormality. Positive and negative likelihood ratios (LRs) were calculated. Finally, the demographic, clinical features and genetic marker information were compared between the two groups described above—AxPsA with or without back pain using t-test, Wilcoxon test or X^2 test, as appropriate. P value <0.05 was set as the threshold of rejecting a null hypothesis. SAS (V.9.3) was used for all statistical analyses.

RESULTS

One hundred and seventy-one patients who satisfied inclusion criteria were identified from the database.

Demographics

The demographics of the patients are summarised in table 1. Majority of the patients were male (52%) and had a mean (SD) age of onset of PsA of 43.34 (13.6) years and mean (SD) age at

Table 1 Demographics and disease characteristics of study subjects (n=171)

Variable	Mean (SD) or proportion
Sex, male/female	52%/48%
Age at onset of PsA in years	43.34 (13.6)
Age at first PsA clinic visit in years	46.72 (13.0)
Prevalence of back pain*	
IBP (by rheumatologist)	65 (38.01%)
nsBP (by rheumatologist)	31 (18.12%)
No back pain (by rheumatologist)	75 (43.8%)
Psoriasis duration in years	16.86 (14.5)
PsA duration in years	3.38 (5.1)
Swollen joint count (ACR 66)	2.85 (4.0)
Tender joint count (ACR 68)	5.64 (7.5)
Clinically damaged joint count (ACR 68)	1.09 (3.9)
Psoriasis area and severity index	3.84 (5.4)
Radiological damage in peripheral joints, n (%)	65 (38.01%)
Radiological change in spine, n (%)	54 (31.68%)
Satisfying New York radiographic criteria for AS, n (%)	27 (15.79%)
Any axial radiographic change (sacroiliitis grade 2± syndesmophytes), n (%)	45 (26.32%)
Any axial disease on MRI†, n (%)	9/31 (29.03%)
Axial involvement without back pain, n (%)	18/54 (33.33%)

*As judged by expert rheumatologist.
†Among 31 patients who had MRI done.
AS, ankylosing spondylitis; ACR, American College of Rheumatology; IBP, inflammatory back pain; nsBP, non-specific back pain; PsA, psoriatic arthritis.

Table 2 Agreement between rheumatologist judgement of inflammatory back pain (IBP) and IBP criteria

Criteria	Patients with back pain=96, Kappa coefficient, 95% CI
Calin	0.70 (0.56 to 0.85)
Rudwaleit	0.59 (0.44 to 0.74)
Assessment of Spondyloarthritis International Society	0.61 (0.46 to 0.76)

first PsA clinic visit of 46.72 (13.0) years. Ninety-six (56.13%) patients reported chronic back pain. Sixty-five (38.01%) had IBP and 31 (18.12%) had nsBP.

Radiology data

Table 1 shows that 27 out of 171 (15.79%) patients with baseline X-rays fulfilled the NY radiographic criteria for AS, and 45 out of 171 (26.32%) patients had radiographic sacroiliitis not satisfying NY criteria (excluding grade 1) and/or syndesmophytes. Nine out of 31 (29.03%) patients with no axial disease on X-ray had evidence of axial disease on MRI. Eighteen out of 54 (33.33%) patients had axial involvement without back pain.

Agreement between rheumatologist

The agreement (kappa coefficient) between rheumatologist judgement of IBP and IBP criteria in patients with back pain was moderate and was highest for the Calin criteria (0.70, 95% CI 0.56 to 0.85), followed by the ASAS criteria (0.61, 95% CI 0.46 to 0.76) and the Rudwaleit criteria (0.59, 95% CI 0.44 to 0.74) (table 2).

Sensitivity, specificity and LRs of the various criteria in detecting axial disease

Using any X-ray or MRI change as the 'gold standard' for axial involvement in all 171 patients, the specificity was high for rheumatologist judgement of IBP, Calin, Rudwaleit and ASAS criteria; however, sensitivity was low. Table 3 summarises the sensitivity, specificity and LRs. By comparing the positive LRs, the Rudwaleit criteria (2.17) performed the best to rule in axial disease. By comparing the negative LRs, rheumatologist-reported back pain (0.68) performed the best for ruling out axial disease.

Clinical features, comorbidities and key genetic markers in patients with PsA with axial involvement with and without back pain

In an exploratory analysis within patients with PsA with back involvement as defined by X-rays or MRI, we compared those with (n=36) or without (n=18) back pain. We combined those with IBP and nsBP together since the nsBP group was small (only seven patients). There were largely no statistically significant differences in the demographic and disease characteristics between the two groups as shown in table 4. As expected the BASDAI was significantly higher and there was a trend towards a higher BASFI in patients with back pain. The prevalence of HLA-B*38 was significantly higher in patients without back pain. There were no significant differences in the prevalence of HLA-B*27, -B*08, -B*39 and -C*06 between patients with and without back pain (table 4).

Table 3 Sensitivity, specificity and likelihood ratios (LRs) of the various criteria in detecting axial disease

	Any X-ray or MRI change as gold standard (n=171)			
Criteria	Specificity	Sensitivity	LR+	LR−
Rheumatologist-reported back pain	48.72	66.67	1.3	0.68
Rheumatologist judgement of inflammatory back pain	75.21	46.3	1.87	0.71
Calin	73.5	46.3	1.75	0.73
Rudwaleit	82.91	37.04	2.17	0.76
Assessment of Spondyloarthritis International Society	82.05	33.33	1.86	0.81

Table 4 Comparison between patients having axial involvement with and without back pain

	With back pain, n=36	Without back pain, n=18	P values
Demographics and disease characteristics			
Age (years)*	44.29 (11.3)	50.12 (14.7)	0.11
Male (%)	20 (55.56)	11 (61.11)	0.70
Psoriasis duration (years)*	15.20 (14.1)	16.6 (13.8)	0.73
Psoriatic arthritis duration (years)*	2.34 (4.3)	2.23 (2.9)	0.41
Number of tender/swollen joints*	8.37 (9.2)	6.44 (8.5)	0.54
Number of swollen joints*	3.03 (5.8)	3.28 (5.0)	0.42
Radiographic damage n (%)	13 (36.11)	11 (61.11)	0.08
PASI*	4.36 (8.6)	3.44 (5.1)	0.68
BASMI*	2.34 (1.2)	2.21 (0.7)	0.89
BASDAI*	5.72 (1.9)	4.27 (1.9)	0.046
BASFI*	4.94 (2.7)	3.03 (2.5)	0.06
Genetic markers (%)			
HLA-B*27	9 (25)	2 (11.11)	0.23
HLA-B*08	5 (13.89)	2 (11.11)	0.77
HLA-B*38	1 (2.78)	5 (27.78)	0.006
HLA-B*39	2 (5.56)	0	0.31
HLA-C*06	5 (13.89)	3 (16.67)	0.79

*Mean (SD).
BASMI, Bath Ankylosing Spondylitis Metrology Index; BASDAI, Bath Ankylosing Spondylitis Disease Activity Index; BASFI, Bath Ankylosing Spondylitis Functional Index; HLA, human leucocyte antigen; PASI, Psoriasis Area and Severity Index.

DISCUSSION

Detection of axial arthritis in patients with PsA is important but difficult. We therefore aimed to investigate the performance of the methods used to identify AxPsA in patients with PsA. We show that although there is a very good agreement between the IBP criteria and rheumatologist-judged IBP in PsA, the positive LR of IBP (either by rheumatologist judgement or by IBP criteria) for AxPsA is quite low. The Rudwaleit criteria had the highest LR+ to detect any radiological change, whereas rheumatologist-reported back pain had the lowest LR−. On comparing the demographic and disease-related actors and HLA alleles associated with psoriatic disease, there were no striking differences between with axial involvement with and without back pain, except that patients with back pain has a higher BASDAI and those without back pain had higher prevalence of HLA-B*38.

One of the reasons that it may be important to identify patients with PsA who have axial disease is that the natural history of the disease may be different. Axial involvement in PsA is a marker of severity and those with axial disease often have worse outcomes compared with peripheral arthritis alone.[1] Although radiographic severity appears to be worse in AS than in AxPsA as measured by the Bath AS Radiology Index[14] and number of syndesmophytes,[15] measures of disease activity, disability and metrology were high in both AxPsA and AS, with no statistically significant difference between groups.[16] As well, the response to

treatment may be different; axial and peripheral articular manifestations of spondyloarthritis respond differently to treatment with sulfasalazine.[17]

There are five specific features which make up the Calin criteria for IBP—back pain that is insidious in onset, in a patient younger than 40 years, persisting for at least 3 months, and associated with morning stiffness and improving with exercise.[10] The Rudwaleit criteria apply to those patients with chronic back pain for >3 months, age younger than 50 years of age and two out of four of the following had to be met—morning stiffness of >30 min duration, improvement in back pain with activity but not with rest, awakening because of back pain during the second half of the night only and alternating buttock pain.[11] The ASAS criteria include domains such as insidious onset, age less than 40 years, nocturnal pain, no improvement with rest but improvement with exercise.[12]

Patients with PsA are not as tender as patients with rheumatoid arthritis[18] and report less back pain than patients with AS.[15] Our study found that 18 out of 54 (33.33%) patients with axial involvement on imaging had no back pain. Battisone *et al* also found that sacroiliitis can occur in the absence of spinal symptoms in PsA.[3] On the other hand, IBP can be found in patients with PsA without axial involvement. A series from Oxford, UK, found that clinical features of sacroiliitis were present in 33% with normal MRI scans and 38% with abnormal scans.[19] Therefore, the symptoms and signs of lower back pain often do not correlate well with radiological evidence of sacroiliitis or spondylitis. The low positive LRs of the Calin, Rudwaleit and ASAS criteria as well as that of rheumatologist report of back pain or judgement of IBP for AxPsA defined as any axial radiological change found in our study suggests that none of these criteria performed well in detecting axial disease in patients with PsA. Poor associations between spinal MRI changes and IBP characteristics and criteria in patients with chronic back pain have been previously recognised.[20] In AS, IBP is reported to have a positive LR of 3.1. The relatively high negative LRs also suggest that these criteria do not perform well in ruling out AxPsA.

The reasons for the poor performance of tests developed for AS in AxPsA are of interest. There are different radiological characteristics between AxPsA and AS. Sacroiliitis is more commonly bilateral in AS but may be either unilateral or bilateral in AxPsA.[21] However, Jadon *et al* did not find unilateral or asymmetrical grade sacroiliitis to be characteristic of AxPsA.[16] As well, syndesmophytes progress caudal to cranial in AS compared with syndesmophytes in AxPsA which progress randomly.[22] It has also been reported that radiographic spondylitis can occur without sacroiliitis in PsA. It is therefore important to evaluate spinal radiographs in addition to SIJ radiographs and clinical signs and symptoms. Taylor *et al* evaluated 343 patients with PsA, 94 of them had both spinal and SIJ radiographs. Seven of 22 patients with radiographic spondylitis did not have radiographic sacroiliitis and 15 of 30 with radiographic sacroiliitis did not have radiographic spondylitis.[4] The patients in our study had both spinal and SIJ radiographs done. Nearly 16% fulfilled the NY radiologic criteria for AS, and 26.32% had evidence of axial involvement not satisfying the NY criteria. Moreover, patients with PsA at diagnosis are generally older than those with AS. Patients with PsA also have higher BMI. Being overweight increases the likelihood in having nsBP.

A third of patients with radiological changes in the spine reported no back pain. Our exploratory analyses show that except for a significantly higher BASDAI, patients who have spinal radiological change and back pain have similar demographic, genetic and disease characteristics. The higher BASDAI score is expected given the BASDAI is a patient reported measure of disease activity and is strongly influenced by back pain. The BASMI was similar between the two groups, and there was a trend towards worse BASFI in those with back pain. The lower prevalence of HLA-B*38 is interesting; however, the number of patients was small and this observation would need replication in future studies. The prevalence of HLA-*27, HLA-B*08 and HLA-C*06 was, however, similar between the two groups. These results indicate that the two groups are largely similar, and hence for the purpose of defining axial disease in PsA, symptoms (back pain) may not be important.

The strengths of this study are that we were able to study a relatively large number of patients with PsA not selected on the basis of axial disease who had complete information on clinical and radiological features, comorbidities and genetic markers. However, spinal MRI was not performed in all patients. A parallel comparison to a group of patients with axial SpA without psoriasis was also not done. Moreover, the number of patients in subgroup analyses were small. Therefore, these preliminary results would need to be confirmed in a larger study.

In conclusion, the findings of this study suggest that rheumatologist-judged IBP or the criteria for IBP developed for AS may not perform well when ascertaining axial involvement in PsA. Moreover, patients with axial radiological changes without back pain were similar to those with back pain. Thus, in order to stratify patients with poorer prognosis, rheumatologists should consider conducting axial imaging in all patients with PsA regardless of the presence or the nature of back pain.

Contributors All authors were involved in drafting the article or revising it critically for important intellectual content, and all authors approved the final version to be published. All authors were likewise involved in the study conception and design, acquisition of data as well as analysis and interpretation of data. VC had full access to all of the data in the study and takes responsibility for the integrity of the data and the accuracy of the data analysis.

Funding The Psoriatic Arthritis Program is supported by the Krembil Foundation.

Competing interests KSY was supported by a Ken Muirden Scholarship from Arthritis Australia.

Patient consent Not required.

Ethics approval University Health Network Research Ethics Board.

Provenance and peer review Not commissioned; externally peer reviewed.

REFERENCES

1 Chandran V, Tolusso DC, Cook RJ, *et al*. Risk factors for axial inflammatory arthritis in patients with psoriatic arthritis. *J Rheumatol* 2010;37:809–15.
2 Hanly JG, Russell ML, Gladman DD. Psoriatic spondyloarthropathy: a long term prospective study. *Ann Rheum Dis* 1988;47:386–93.
3 Battistone MJ, Manaster BJ, Reda DJ, *et al*. The prevalence of sacroilitis in psoriatic arthritis: new perspectives from a large, multicenter cohort. A Department of Veterans Affairs Cooperative Study. *Skeletal Radiol* 1999;28:196–201.
4 Taylor WJ, Zmierczak HG, Helliwell PS. Problems with the definition of axial and peripheral disease patterns in psoriatic arthritis. *J Rheumatol* 2005;32:974–7.
5 Haroon M, Ahmad M, Baig MN, *et al*. Inflammatory back pain in psoriatic arthritis is significantly more responsive to corticosteroids compared to back pain in ankylosing spondylitis: a prospective, open-labelled, controlled pilot study. *Arthritis Res Ther* 2018;20:73.
6 Gossec L, Smolen JS, Gaujoux-Viala C, *et al*. European League Against Rheumatism recommendations for the management of psoriatic arthritis with pharmacological therapies. *Ann Rheum Dis* 2012;71:4–12.
7 Leung YY, Ho KW, Tam LS, *et al*. Evaluation of spinal mobility measurements in predicting axial psoriatic arthritis. *Clin Rheumatol* 2011;30:1157–62.
8 Queiro R, Belzunegui J, González C, *et al*. Clinically asymptomatic axial disease in psoriatic spondyloarthropathy. A retrospective study. *Clin Rheumatol* 2002;21:10–13.
9 Chandran V, Barrett J, Schentag CT, *et al*. Axial psoriatic arthritis: update on a longterm prospective study. *J Rheumatol* 2009;36:2744–50.
10 Calin A, Porta J, Fries JF, *et al*. Clinical history as a screening test for ankylosing spondylitis. *JAMA* 1977;237:2613–4.

11 Rudwaleit M, Metter A, Listing J, *et al*. Inflammatory back pain in ankylosing spondylitis: a reassessment of the clinical history for application as classification and diagnostic criteria. *Arthritis Rheum* 2006;54:569–78.
12 Sieper J, van der Heijde D, Landewé R, *et al*. New criteria for inflammatory back pain in patients with chronic back pain: a real patient exercise by experts from the Assessment of SpondyloArthritis international Society (ASAS). *Ann Rheum Dis* 2009;68:784–8.
13 Biagioni BJ, Gladman DD, Cook RJ, *et al*. Reliability of radiographic scoring methods in axial psoriatic arthritis. *Arthritis Care Res* 2014;66:1417–22.
14 Pérez Alamino R, Maldonado Cocco JA, Citera G, *et al*. Differential features between primary ankylosing spondylitis and spondylitis associated with psoriasis and inflammatory bowel disease. *J Rheumatol* 2011;38:1656–60.
15 Gladman DD, Brubacher B, Buskila D, *et al*. Differences in the expression of spondyloarthropathy: a comparison between ankylosing spondylitis and psoriatic arthritis. *Clin Invest Med* 1993;16:1–7.
16 Jadon DR, Sengupta R, Nightingale A, *et al*. Axial Disease in Psoriatic Arthritis study: defining the clinical and radiographic phenotype of psoriatic spondyloarthritis. *Ann Rheum Dis* 2017;76:701–7.
17 Clegg DO, Reda DJ, Abdellatif M. Comparison of sulfasalazine and placebo for the treatment of axial and peripheral articular manifestations of the seronegative spondylarthropathies: a Department of Veterans Affairs cooperative study. *Arthritis Rheum* 1999;42:2325–9.
18 Buskila D, Langevitz P, Gladman DD, *et al*. Patients with rheumatoid arthritis are more tender than those with psoriatic arthritis. *J Rheumatol* 1992;19:1115–9.
19 Williamson L, Dockerty JL, Dalbeth N, *et al*. Clinical assessment of sacroiliitis and HLA-B27 are poor predictors of sacroiliitis diagnosed by magnetic resonance imaging in psoriatic arthritis. *Rheumatology* 2004;43:85–8.
20 Arnbak B, Jurik AG, Jensen TS, *et al*. Association between inflammatory back pain characteristics and magnetic resonance imaging findings in the spine and sacroiliac joints. *Arthritis Care Res* 2018;70:244–51.
21 McEwen C, DiTata D, Lingg C, *et al*. Ankylosing spondylitis and spondylitis accompanying ulcerative colitis, regional enteritis, psoriasis and Reiter's disease. A comparative study. *Arthritis Rheum* 1971;14:291–318.
22 Helliwell PS, Hickling P, Wright V. Do the radiological changes of classic ankylosing spondylitis differ from the changes found in the spondylitis associated with inflammatory bowel disease, psoriasis, and reactive arthritis? *Ann Rheum Dis* 1998;57:135–40.

EXTENDED REPORT

Impact of biological therapy on work outcomes in patients with axial spondyloarthritis: results from the British Society for Rheumatology Biologics Register (BSRBR-AS) and meta-analysis

Joanna Shim,[1,2,3] Gareth T Jones,[1,2,3] Ejaz M I Pathan,[4] Gary J Macfarlane[1,2,3]

Handling editor Josef S Smolen

► Additional material is published online only. To view please visit the journal online (http://dx.doi.org/10.1136/annrheumdis-2018-213590).

[1]Epidemiology Group, School of Medicine, Medical Sciences and Nutrition, University of Aberdeen, Aberdeen, UK
[2]Arthritis Research UK/Medical Research Council Centre for Musculoskeletal Health and Work, Aberdeen, UK
[3]Aberdeen Centre for Arthritis and Musculoskeletal Health, University of Aberdeen, Aberdeen, UK
[4]Spondylitis Program, Department of Rheumatology, Toronto Western Hospital, University Health Network, Toronto, Ontario, Canada

Correspondence to
Professor Gary J Macfarlane, Epidemiology Group, School of Medicine, Medical Science and Nutrition, University of Aberdeen, Aberdeen AB25 2ZD, UK; g.j.macfarlane@abdn.ac.uk

Received 16 April 2018
Revised 9 July 2018
Accepted 18 July 2018
Published Online First 3 August 2018

To cite: Shim J, Jones GT, Pathan EMI, *et al*. *Ann Rheum Dis* 2018;**77**:1578–1584.

ABSTRACT

Objectives To quantify, among patients with axial spondyloarthritis (axSpA), the benefit on work outcomes associated with commencing biologic therapy.

Methods The British Society for Rheumatology Biologics Register in Axial Spondyloarthritis (BSRBRAS) recruited patients meeting Assessment of SpondyloArthritis International Society criteria for axSpA naïve to biological therapy across 83 centres in Great Britain. Work outcomes (measured using the Work Productivity and Activity Impairment Index) were compared between those starting biological therapy at the time of recruitment and those not. Differences between treatment groups were adjusted using propensity score matching. Results from BSRBR-AS were combined with other studies in a meta-analysis to calculate pooled estimates.

Results Of the 577 participants in this analysis who were in employment, 27.9% were starting biological therapy at the time of recruitment. After propensity score adjustment, patients undergoing biological therapy, at 12-month follow-up, experienced significantly greater improvements (relative to non-biological therapy) in presenteeism (−9.4%, 95% CI −15.3% to −3.5%), overall work impairment (−13.9%, 95% CI −21.1% to −6.7%) and overall activity impairment (−19.2%, 95% CI −26.3% to −12.2%). There was no difference in absenteeism (−1.5%, 95% CI −8.0 to 4.9). Despite these improvements, impact on work was still greater in the biological treated cohort at follow-up. In the meta-analysis including 1109 subjects across observational studies and trials, treatment with biological therapy was associated with significantly greater improvements in presenteeism, work impairment and activity impairment, but there was no difference in absenteeism.

Conclusions There is consistent evidence that treatment with biological therapy significantly improves work productivity and activity impairment in people with axSpA. However, there remain substantial unmet needs in relation to work.

INTRODUCTION

For working age adults, the ability to participate in working life is important from an economic standpoint and for social and psychological health.[1] In a comprehensive review, Waddell and Burton[2] provided a clear evidence base for the positive impact work has on health and well-being. When these benefits are disrupted by unemployment, they found subsequent poorer mental and physical health, increased morbidity and higher consultation rates.[2] People living with axial spondyloarthritis (axSpA) have identified the ability to stay at work as a priority.[3 4]

AxSpA can lead to significant functional limitations and reduced work productivity.[4 5] Work disability affects up to 30% of patients with ankylosing spondylitis (AS).[6–8] Compared with the general population, patients with AS report lower employment rates and more absenteeism.[6 9 10] Boonen and van der Linden[11] reported that withdrawal from work was three times higher among patients with AS than observed in the general population, especially in those with physically demanding jobs.

Biological therapy leads to short-term and long-term improvements in disease activity and health-related quality of life.[12–14] However, evidence is equivocal on whether work outcomes are improved. In a systematic review, van der Burg *et al*[15] demonstrated significant improvements in presenteeism on biological therapy, but results were inconsistent on whether they improved absenteeism and allowed patients to stay in work.[15]

This study therefore aimed to determine, using a national disease register in Great Britain whether, among patients with axSpA, biological therapy was associated with better work outcomes in comparison with those not on such therapy, and to combine the results with other studies in a meta-analysis.

METHODS

The protocol of the British Society of Rheumatology Biologics register in Axial Spondyloarthritis (BSRBR-AS) has previously been published.[16] Briefly, patients were required to meet the Assessment of SpondyloArthritis International Society criteria for radiographic or non-radiographic axSpA at the time of recruitment and were required to be naïve to biological therapies. Eligible patients commencing on biological therapy were recruited to the 'biological' cohort, the remainder to the 'non-biological' cohort; this was based on clinical decision rather than study protocol. The biological cohort comprised patients commencing adalimumab, etanercept or certolizumab pegol. Clinical data collected by site clinicians and research nurses at routine clinical appointments were entered into electronic case report forms at recruitment (baseline) and at 12-month follow-up. Patients were invited to self-complete a questionnaire at the same time-points, which included demographic

information, smoking status, alcohol consumption, disease activity, AS-related measures and quality of life.

The impact of axSpA on work outcomes was measured using the Work Productivity and Activity Impairment: Specific Health Problem questionnaire.[17] The questionnaire has been psychometrically validated in AS[18] and measures absenteeism (absence from paid work), presenteeism (at-work productivity loss), overall work impairment (combination of absenteeism and presenteeism, ie, reduced overall productivity) and overall activity impairment (reduced leisure activities), in relation to their disease. Higher scores, expressed as percentages, represent a worse state. Participants who were in paid employment at baseline and completed both a baseline and 12-month follow-up questionnaire were eligible for this analysis. Analysis was conducted on the June 2017 download of data. Appropriate National Health Service (NHS) Research and Development approvals were obtained for each site. All patients provided written informed consent.

BSRBR-AS analysis

The principal outcomes of interest for this analysis were changes in self-reported absenteeism, presenteeism, overall work impairment and overall activity impairment in the biological cohort in comparison with the non-biological cohort. In clinical practice, the decision to initiate biological therapy is strongly influenced by disease activity,[19] and therefore, the biological and non-biological cohorts represent distinct clinical populations and direct comparison would lead to confounding by indication. This was addressed by propensity matching. There is currently no strong consensus on the approach to variable selection for propensity score models,[20] but most relevant confounders were considered in our study, and where there were issues of collinearity, variables were omitted from the model based on the variance inflation factor. Propensity scores were developed based on age, gender, smoking status and disease duration in a logistic regression model. For each individual commencing biological therapy, nearest-neighbour propensity score was used to identify an individual for matching, not starting biological therapy, by accounting for covariates that predict treatment assignment. Density distributions of the propensity scores of the two treatment groups were plotted and visually compared with ensure that the common support condition was met as per Caliendo and Kopeinig.[21] The standardised differences and variance ratios for raw and matched observations for presenteeism, work impairment, activity impairment and absenteeism indicated that matching on the propensity score balanced the covariates: differences were close to zero and variance ratios close to one. After propensity score matching, the differences in work outcomes for the biological therapy and non-biological therapy groups were analysed. Independent-sample Student's t-test was used for group comparisons of the changes in work outcomes. A sensitivity analyses was conducted to explore the degree to which unmeasured confounding could alter study results, using the method proposed by Rosenbaum.[22]

Data analysis was performed using STATA V.14.0.

Systematic review and meta-analysis

The conduct and reporting of this meta-analysis was guided by the Preferred Reporting Items for Systematic Reviews and Meta-Analyses statement.[23]

Studies were eligible for inclusion based on the following criteria:

- Population: AxSpA by recognised criteria or clinical diagnosis.
- Study design: observational studies (prospective and retrospective cohort studies), randomised controlled trials (RCTs) and quasi-RCTs.
- Outcomes: outcomes reported included changes in work measures (eg, work status, WPAI, AS-Work Instability Scale (AS-WIS) and sick leave) for a biological treatment group versus a placebo/non-biological treatment group. Studies must have provided data in relation to this comparison or provided sufficient data to allow its calculation.

If more than one publication was identified based on the same cohort or population, a single report was selected based on the relevance of work measures reported and the largest number of subjects.

Studies were identified by searching electronic databases: Ovid MEDLINE, Embase, Evidence Based Medicine and Cochrane Library up to March 2018. Reference lists of articles were also screened for inclusion. The search strategy can be found in online supplementary appendix 1. Potentially eligible abstracts were screened by two reviewers, and any disagreements were resolved by discussion. Ten per cent of the articles excluded at full-text screening were independently reviewed by a third reviewer. One reviewer extracted relevant data from included studies, and a second reviewer cross-checked the extracted data. Disagreements were resolved by discussion among all three reviewers. Where it was considered that a study was potentially eligible but the way that the quantitative results were presented did not meet inclusion criteria, the corresponding author was contacted to determine whether the relevant data, to make the study eligible, could be provided.

For continuous outcome variables, the mean difference of change in work parameters, comparing biological and non-biological therapy groups, was calculated with 95% CIs. Heterogeneity was assessed using the χ^2 statistic and quantified by I^2; $0\% \leq I^2 \leq 40\%$ is considered to indicate minimal heterogeneity and $I^2 > 40\%$ moderate to high heterogeneity.[24] In cases where there was no evidence of moderate to high heterogeneity, a fixed-effects model with inverse variance weighting was used to obtain an overall mean difference or effect estimate. If moderate to high heterogeneity was evident between studies, a random-effects model was adopted, and a sensitivity analysis was conducted by sequentially omitting individual studies to identify the influence of the study on the pooled outcome.

The meta-analysis was conducted using STATA V.14.0.

RESULTS

Within the BSRBR-AS, 972 participants completed and returned both the baseline and 12-month follow-up questionnaire, of whom 577 (59.4%) were employed at the time of recruitment. Of these, 161 (27.9%) patients started biological therapy, while 416 did not, and these two cohorts form the study population for the current analysis (table 1). Persons starting biological therapy were younger (42.4 years vs 47.0 years), more likely to be smokers (21.3% vs 11.0%) with greater disease activity (Bath Ankylosing Spondylitis Disease Activity Index 5.8 vs 3.3 and Ankylosing Spondylitis Disease Activity Scale 3.4 vs 2.3), poorer function (Bath Ankylosing Spondylitis Functional Index 5.4 vs 2.7) and Bath Ankylosing Spondylitis Global Disease Status 6.7 vs 3.2) (table 1). Persons starting biological therapy also reported higher work impairments at the time of recruitment. They were more likely, during the previous week, to be absent from work (10.9% vs 2.8%), experience greater at-work productivity loss (41.0% vs 20.6%), overall productivity loss (42.3% vs 21.4%) and activity impairment (51.0% vs 24.0%) (table 1). Among those who had not reached normal retirement age at the time of follow-up, there was no significant difference in the proportion who were no longer in employment at follow-up (biological group 5.2% vs non-biological group 4.3%).

Table 1 BSRBR-AS study: baseline characteristics of biological and non-biological cohorts

	Biological cohort (n=161)	Non-biological cohort (n=416)	Difference*	95% CI
Age, mean years	42.4	47.0	−4.6	−6.6 to 2.5
Male, %	64.6	67.3	−2.7	−11.3 to 5.9
Disease duration, mean years	7.7	12.3	−4.6	−6.5 to 2.7
Current smokers, %	21.3	11.0	10.2	3.9 to 16.5
BASDAI	5.8	3.3	2.6	2.2 to 2.9
BASFI	5.4	2.7	2.7	2.3 to 3.2
BAS-G§	6.7	3.2	3.4	3.0 to 3.9
CRP (mg/dL)	2.8	2.4	0.4	−0.8 to 1.6
ASDAS	3.4	2.3	1.1	0.9 to 1.3
Physical job, %	44.8	51.0	−6.2	−3.1 to 15.5
WPAI measures (in the last 7 days)				
Absenteeism, %	10.9	2.8	8.1	4.7 to 11.4
Presenteeism, %	41.0	20.6	20.4	15.9 to 24.9
Overall work impairment, %	42.3	21.4	20.9	16.2 to 25.7
Overall activity impairment, %	51.0	24.0	27.0	22.5 to 31.4

*Difference=biological – non-biologic cohort.
ASDAS, Ankylosing Spondylitis Disease Activity Scale; BAS-FI, Bath Ankylosing Spondylitis Functional Index; BAS-G, Bath Ankylosing Spondylitis Global Disease Status; BASDAI, Bath Ankylosing Spondylitis Disease Activity Index; BSRBR-AS, British Society of Rheumatology Biologics register in Axial Spondyloarthritis; CRP, C reactive protein; WPAI, Work Productivity and Activity Impairment.

Persons receiving treatment with biological therapy experienced greater improvement in all work outcomes except absenteeism, at 12-month follow-up, compared with persons not receiving biological therapy (figure 1). These improvements remained after propensity score adjustments for differences between the cohorts. Patients on biological therapy demonstrated a significantly greater improvement in presenteeism (−9.4%, 95%CI −15.3% to −3.5%), overall work impairment (−13.9%, 95%CI −21.1% to −6.7%) and overall activity impairment (−19.2%, 95%CI −26.3% to −12.2%). These figures translate into a benefit of over half a day in terms of full productivity per week, 12 months after starting biological therapy. For absenteeism, there was only a small improvement noted in the biological cohort and no significant difference compared with the non-biological cohort (−1.5%, 95%CI −8.0% to 4.9%) (table 2). Nevertheless, despite the greater improvement in these work indices the impact on work was still greater in the biological-treated compared with the non-biological-treated cohort at follow-up (presenteeism biological cohort – non-biological cohort adjusted for factors used in propensity matching: 11.5%, 95%CI 5.5% to 17.5%; overall work impairment: 9.7%, 95%CI 3.6% to 15.9%; overall activity impairment: 9.2%, 95%CI 2.5% to 16.1%).

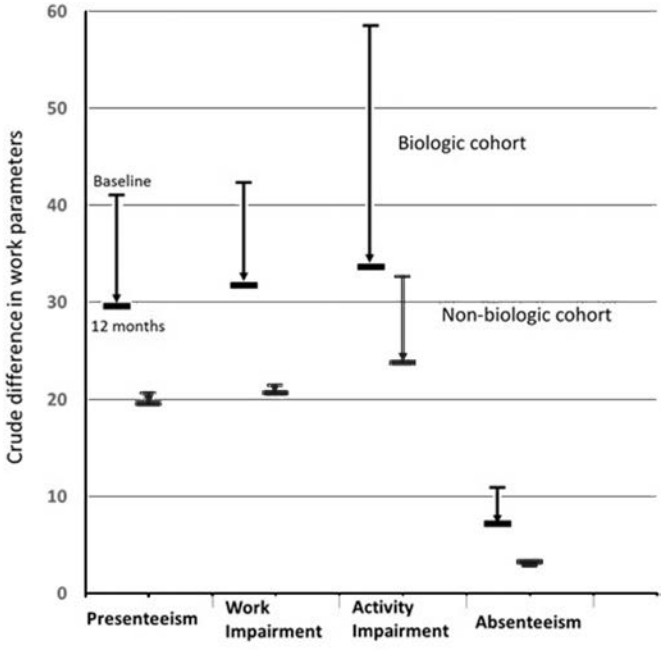

Figure 1 Crude changes in work outcomes after 1 year: BSRBR-AS study. BSRBR-AS, British Society of Rheumatology Biologics register in Axial Spondyloarthritis.

Table 2 BSRBR-AS study: changes in work outcomes between biological and non-biological cohort

WPAI measures (in the last 7 days)	Biological cohort	Non-biological cohort	Mean difference in change*	95% CI
Absenteeism, %	−1.0	0.5	−1.5	−8.0 to 4.9
Presenteeism, %	−11.9	−2.5	−9.4	−15.3 to – 3.5
Overall work impairment, %	−11.9	2.0	−13.9	−21.1 to – 6.7
Overall activity impairment, %	−17.6	1.6	−19.2	−26.3 to – 12.2

+, deterioration; −, improvement.
*Difference=biological – non-biological cohort (adjusted for differences using propensity score matching).
WPAI, Work Productivity and Activity Impairment.

The sensitivity analysis conducted showed that the results were insensitive to an unmeasured factor, which would increase the log odds of biological treatment by approximately 1.9 (presenteeism) and 2.0 (overall work impairment and activity impairment).

Meta-analysis

There were 686 publications identified, of which 547 were excluded because they were duplicates, conference abstracts, case reports or not relevant based on title and abstract screening. The remaining 139 publications were retrieved for full-text review. Of the six publications that were identified as potentially eligible, four were included in the meta-analysis; the remaining two were reporting studies already included[25 26] (figure 2). Results of five studies (four identified in review and the current study) with a total of 1109 participants were therefore included in the meta-analysis. A summary of the characteristics of the studies included is shown in table 3. All of the studies (apart from BSRBR-AS) were RCTs. Three were multinational studies conducted in Europe, Asia and America,[27–29] and the other was a study conducted within the UK[30] (table 3). Follow-up ranged from 3 months to 12 months, and the biological drugs used in the trials were infliximab, etanercept and secukinumab. Statistical heterogeneity tests showed minimal to moderate heterogeneity across studies and outcomes (I^2=0%–66%), and therefore, random effect models were used.

Three studies, with a total of 947 participants (346 biological therapy; 601 non-biological therapy), reported work measures using WPAI. There was a statistically significant difference (in favour of biological therapy groups) for improvement in presenteeism (mean difference (MD)=−5.35, 95%CI −10.68 to −0.02) and overall work impairment (MD=−11.20, 95%CI −16.31 to–6.10), that is, overall at-work productivity improved by 11% more among patients who received biological therapy compared with those on other therapies (figure 3). Furthermore, improvement in self-reported ability to perform daily activities was

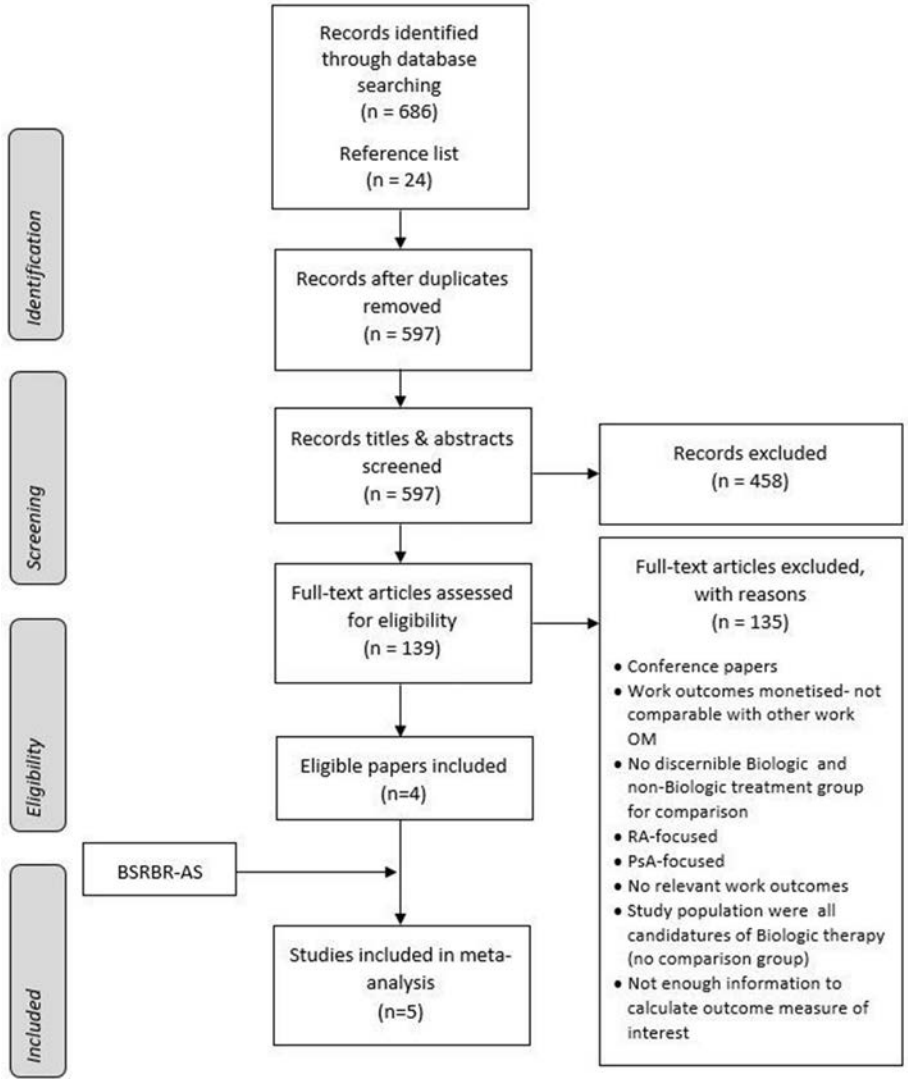

Figure 2 PRISMA flow chart of study selection and inclusion (modified from Moher *et al*[23]). BSRBR-AS, British Society for Rheumatology Biologics Register in Axial Spondyloarthritis; OM, outcome measure; PRISMA, Preferred Reporting Items for Systematic Reviews and Meta-Analyses; PsA, psoriatic arthritis; RA, rheumatoid arthritis.

on average, 12% higher in patients treated with biological therapy (MD=−12.13, 95%CI −18.22 to −6.03) (figure 3). In contrast, there was little improvement in absenteeism in either treatment group; absolute change in biological therapy and non-biologic therapy groups across studies were −2.2% and −6.3%, respectively, and the pooled change in absenteeism was similar in both groups (MD=0.84, 95%CI −3.54 to 5.22) (figure 3).

Only two studies measured work instability that included 163 participants (80 biological; 83 non-biological therapy). On a standardised scale, treatment with biologic therapy was associated with a small improvement on the AS-WIS compared with the non-biological therapy group. However, this difference was not statistically significant (MD=−1.16, 95%CI −2.56 to 0.26) (online supplementary appendix 2).

DISCUSSION

Patients with axSpA recruited to a national disease register, who started biological therapy showed, on average, significantly greater improvements in work outcomes compared with those not commencing such therapy. Furthermore, pooled data across five cohorts with a total of 1109 patients with axSpA quantified that treatment with biological therapy leads to greater improvements in both work productivity (presenteeism (5%), overall work impairment (11%)) and activity impairment (12%)). There was however no benefit across all studies in relation to absenteeism.

The main strength of the BSRBR-AS study is the large sample size, national coverage and prospective study design. It provides a sample of patients with axSpA recruited from 83 outpatient clinics, including both specialist and non-specialist centres across Great Britain. Participants starting biological therapy have been shown to be similar in characteristics to patients with axSpA recruited to the trials of biological therapies.[31] Although the effects on work outcomes could be estimated using an RCT, work outcomes are not routinely collected in such trials and they are rarely long enough for change to occur. As this was an observational study, propensity score matching techniques were used to estimate the effect of treatment; this statistical technique addresses 'confounding by indication' due to treatment group differences. However, propensity score analysis can only take into account measured factors [32]. It is of note that measures of disease activity were not part of the propensity score. However, being highly discriminatory in terms of treatment assignment, this is to be expected, due to the lack of overlap between groups.

Table 3 Characteristics and results of studies eligible for meta-analysis reporting the impact of biological therapy on work participation in patients with axSpA

Authors	Year	Study location	Sampling frame*	Study design	Analysis sample	Sample size†	Biological therapy (N)	Control (N)	Work measure	Reference period of work outcomes	Follow-up
van der Heijde *et al*[27] (ASSERT)	2006	USA, Canada, and Europe	33 centres; adult patients with active AS according to mNYc. Age: mean 39.8 (SD 10.2).	Phase 3, double blind, placebo controlled RCT	Employed patients only	122	94	28	Productivity VAS¶	6 weeks	12 months
Dougados *et al*[28] (EMBARK)	2015	Latin America, Central Europe and Asia	Multicentre; adult patients (≥18 years), satisfied ASAS criteria with non-radiographic sacroiliitis defined as those who did not meet 1984 mNYc. Age: 32.0 (7.8).	Phase 3, double blind, two-period RCT	Employed patients only	123	60	63	WPAI: SHP AS-WIS	1 week	3 months
Deodhar *et al*[29] (MEASURE-1)	2016	Americas, Europe and Asia	65 centres; adult patients (≥18 years) who meet the mNYc for AS and BASDAI ≥4. Age-biological: 40.1 (11.6). Age-placebo: 43.1 (12.4).	Phase 3, double-blind, placebo-controlled RCT.	Employed patients for WPAI (i)–(iii); full population for WPAI (iv).	247	125	122	WPAI: GH	1 week	4 months
Barkham *et al*[30]	2010	UK	Adult patients with AS according to mNYc, BASDAI 2/3, VAS ≥40, early morning stiffness ≥45. Age-biologic: 40.8 (9.7). Age-placebo: 39.4 (10.1).	Double-blind, placebo-controlled RCT	Employed patients only	40	20	20	AS-WIS	–	3 months
BSRBR-AS study	2017	UK	Multicentre; adult patients who are biological naïve; meet ASAS criteria for radiographic and non-radiographic axSpA. Age-biological: 47.2 (13.9). Age-non-biological: 53.9 (13.8).	Prospective, register-based data	Employed patients only	577	161	416	WPAI: SHP	1 week	12 months

*Age: mean years (SD).
†Sample size of analysis.
‡WPAI: (i) absenteeism; (ii) presenteeism; (iii) overall work impairment; and (iv) overall activity impairment.
Work Productivity and Activity Impairment: General Health.
AS, ankylosing spondylitis; ASAS, Assessment of SpondyloArthritis International Society; ASSERT, AS Study for the Evaluation of Recombinant Infliximab Therapy; AS-WIS, AS-Work Instability Scale; axSpA, axial spondyloarthritis; BASDAI, Bath Ankylosing Spondylitis Disease Activity Index; BSRBR-AS, British Society of Rheumatology Biologics register in Axial Spondyloarthritis; EMBARK, Study Comparing Etanercept (ETN) Against a Placebo for Etanercept on a Background Nonsteroidal Anti Inflammatory Drug (NSAIDs) in the Treatment of Early Spondyloarthritis (SpA) Patients Who do Not Have X-ray Structural Changes (based on study title registered in NCT); MEASURE 1, Effect of Secukinumab in Patients With Active Anklylosing Spondylitis; mNYc, Modified New York criteria; RCT, randomised controlled trial; VAS, visual analogue scale; WPAI: GH, Work Productivity and Activity Impairment: General Health; WPAI: SHP, Work Productivity and Activity Index: Specific Health Problem.

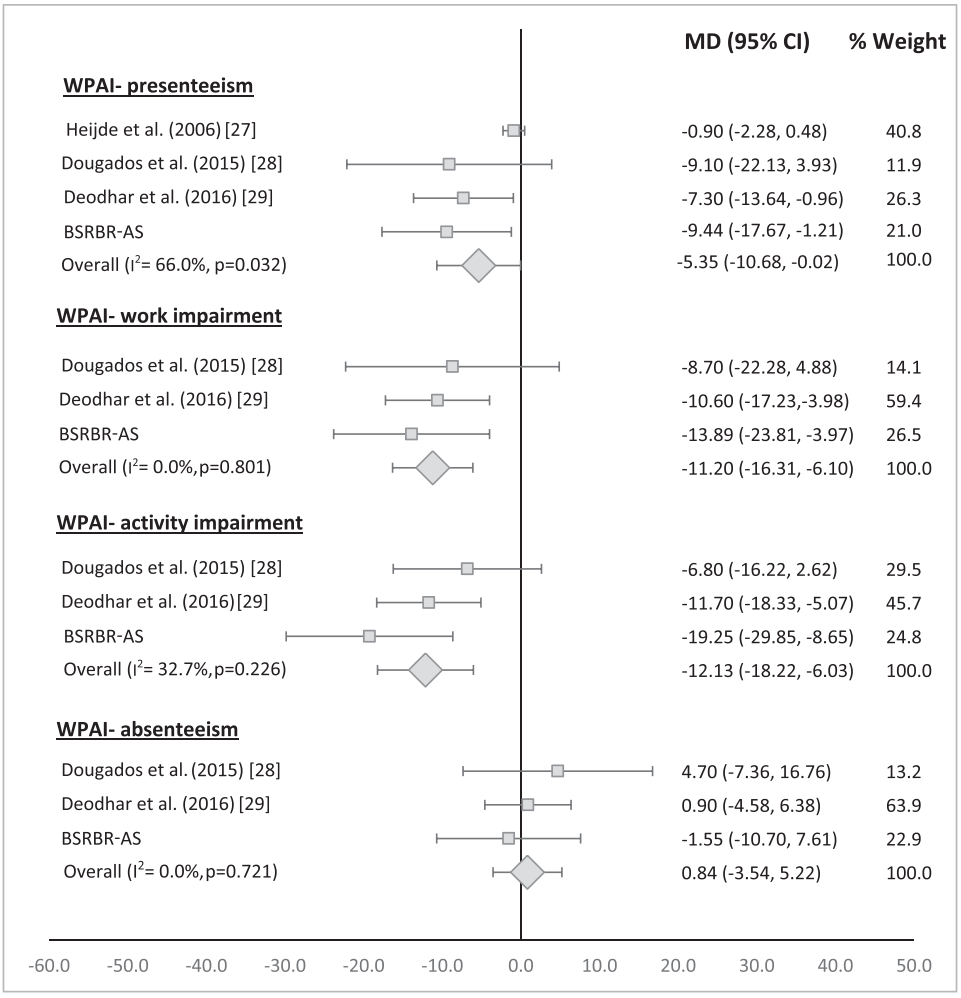

Figure 3 Forest plot comparing changes in WPAI outcomes between patients in the biological and non-biological treatment groups. BSRBR-AS, British Society of Rheumatology Biologics register in Axial Spondyloarthritis; WPAI, Work Productivity and Activity Impairment.

Sensitivity analyses suggested only a strong unmeasured confounder could explain the differences observed. Furthermore, it is of note that the results from the observational study (BSRBR-AS) were very similar to the results from the RCTs included in the meta-analysis (with little heterogeneity noted) suggesting that residual confounding has not been a major issue.

To our knowledge, this is the first meta-analysis to quantify the impact of biological therapy on work participation. One earlier systematic review included nine trials and examined the effect of biological treatment on three work outcomes: work status, absenteeism and presenteeism.[15] It showed that presenteeism decreased by 17%–29% and absenteeism decreased by 8.7–22.3 days over a period of 12 months after commencement of biological therapy. However, these results were based on single group, pre-therapy and post-therapy analysis.[15]

Nevertheless, our review found few studies that investigated the impact of biological therapy on work-related outcomes and relatively small sample sizes in the included trials. Although a substantial improvement in presenteeism and overall work impairment was achieved in the biological cohort, our study shows a persisting gap relative to the non-biological cohort patients with axSpA. This suggests that pharmacological intervention alone is not enough to improve work participation. Overall, the BSRBR-AS study did not demonstrate improvements in absenteeism, and the meta-analysis did not demonstrate any significant differences in the improvements on absenteeism between the biological and non-biological treatment groups. The group who experience presenteeism represent a large proportion of patients with axSpA, and while they are at high risk of absenteeism, this outcome is considerably less common.[33 34] While we have shown that biological therapy improves presenteeism (relative to not receiving biological therapy), it does not necessarily mean therefore that this leads to an improvement in absenteeism. Our data are consistent with the hypothesis that absenteeism is a late stage in terms of work impairment that is not reversed by biological therapy alone but likely also to be influenced by contextual factors. Zhang *et al*[35] assessed the construct validity of the WPAI questionnaire among patients with rheumatoid arthritis and found absenteeism to correlate the least with health-related outcomes compared with other WPAI domains.[35] Saidane *et al*[36] also demonstrated that disease severity and disease activity were not associated with absenteeism among people with AS in a cohort study.[36] We have shown in a previous analysis from BSRBR-AS that presenteeism predicts future absenteeism, which predicts future work loss. Taken together, these results emphasise that biological therapy may be less effective at improving work outcome when given late in the natural history of the condition.[37] Cost-effectiveness analysis often consider costs from a payer's perspective (in the UK, the NHS) rather than considering the wider societal costs (and benefits) associated with treatment. Although presenteeism is an important outcome, it would be interesting to extend existing cost-effectiveness estimates to take important work outcomes into account. However, these

data were not available and is therefore beyond the scope of the current study.

We conclude that there is consistent evidence, across different study designs, that treatment with biological therapy significantly and meaningfully improves work productivity and activity impairment in people with axSpA. However, even with the improvements observed with biological therapy, there is still a substantial impact on work. Future studies in axSpA should include assessment of work outcomes as standard, ensuring a greater evidence base around pharmacological and non-pharmacological approaches to improving work outcomes in patients with axSpA.

Correction notice This article has been corrected since it published Online First. Figure 3 has been updated.

Acknowledgements We are grateful to the staff of the British Society for Rheumatology Biologics Register in Axial Spondyloarthritis register who are currently Claudia Zabke, Maureen Heddle, Nafeesa Nazlee and Barry Morris, and to the recruiting staff at the clinical centres, details of which are available at: https://www.abdn.ac.uk/iahs/research/epidemiology/spondyloarthritis.php#panel1011. We would like to thank Dr Atul Deodhar, Benjamin Hsu and Chenglong Han for providing additional data relating to one of the studies, to allow it be included in the meta-analysis.

Contributors GJM and GTJ conceived the idea for the study, and GJM wrote the analysis plan, which was undertaken by JS. JS led the systematic review and meta-analysis with input from GTJ and GJM. The manuscript was written by JS together with GJM. All authors reviewed the data and critically reviewed the manuscript for important intellectual content.

Funding The BSRBR-AS is funded by the British Society for Rheumatology who have received funding for this from Pfizer, AbbVie and UCB. These companies receive advance copies of manuscripts for comments. This work was conducted within the Arthritis Research UK/Medical Research Council Centre for Musculoskeletal Work and Health (Grant No: 20665)

Disclaimer Pfizer, AbbVie and UCB have no input in determining the topics for analysis or work involved in undertaking it.

Competing interests None declared.

Patient consent Not required.

Ethics approval The study was approved by the National Research Ethics Service Committee North East-County Durham and Tees Valley (Research Ethics Committee reference 11/NE/0374).

Provenance and peer review Not commissioned; externally peer reviewed.

REFERENCES

1 Bryngelson A. Long-term sickness absence and social exclusion. *Scand J Public Health* 2009;37:839–45.
2. Waddell G, Burton AK. Great Britain: Department for Work. *Is work good for your health and well-being?* London: Stationery Office, 2006.
3 Boonen A, Brinkhuizen T, Landewé R, *et al*. Impact of ankylosing spondylitis on sick leave, presenteeism and unpaid productivity, and estimation of the societal cost. *Ann Rheum Dis* 2010;69:1123–8.
4 Cakar E, Taskaynatan MA, Dincer U, *et al*. Work disability in ankylosing spondylitis: differences among working and work-disabled patients. *Clin Rheumatol* 2009;28:1309–14.
5 Ramos-Remus C, Hernandez-Rios G, Duran-Barragan S, *et al*. Fifteen-year trends of long-term disability and sick leaves in ankylosing spondylitis. *Clin Rheumatol* 2011;30:361–7.
6 Boonen A. A review of work-participation, cost-of-illness and cost-effectiveness studies in ankylosing spondylitis. *Nat Clin Pract Rheumatol* 2006;2:546–53.
7 Barlow JH, Wright CC, Williams B, *et al*. Work disability among people with ankylosing spondylitis. *Arthritis Rheum* 2001;45:424–9.
8 Ariza-Ariza R, Hernández-Cruz B, Collantes E, *et al*. Work disability in patients with ankylosing spondylitis. *J Rheumatol* 2009;36:2512–6.
9 Ward MM, Reveille JD, Learch TJ, *et al*. Impact of ankylosing spondylitis on work and family life: comparisons with the US population. *Arthritis Rheum* 2008;59:497–503.
10 Ramonda R, Marchesoni A, Carletto A, *et al*. Patient-reported impact of spondyloarthritis on work disability and working life: the ATLANTIS survey. *Arthritis Res Ther* 2016;18:18.
11 Boonen A, Van Der Linden SM. The burden of ankylosing spondylitis. *J Rheumatol* 2006;33:4–11.
12. Callhoff J, Sieper J, Weiß A, *et al*. Efficacy of TNFα blockers in patients with ankylosing spondylitis and non-radiographic axial spondyloarthritis: a meta-analysis. *Ann Rheum Dis* 2015;74:1241–8.
13. Gorman JD, Sack KE, Davis JC. Treatment of ankylosing spondylitis by inhibition of tumor necrosis factor alpha. *N Engl J Med* 2002;346:1349–56.
14 Maruotti N, Cantatore FP. Impact of biological therapy on spondyloarthritis. *Eur J Clin Pharmacol* 2014;70:1021–7.
15 van der Burg LR, Ter Wee MM, Boonen A. Effect of biological therapy on work participation in patients with ankylosing spondylitis: a systematic review. *Ann Rheum Dis* 2012;71:1924–33.
16. Macfarlane GJ, Barnish MS, Jones EA, *et al*. The British Society for Rheumatology Biologics Registers in Ankylosing Spondylitis (BSRBR-AS) study: Protocol for a prospective cohort study of the long-term safety and quality of life outcomes of biologic treatment. *BMC Musculoskelet Disord* 2015;16:347.
17 Reilly MC, Zbrozek AS, Dukes EM. The validity and reproducibility of a work productivity and activity impairment instrument. *Pharmacoeconomics* 1993;4:353–65.
18 Reilly MC, Gooch KL, Wong RL, *et al*. Validity, reliability and responsiveness of the Work Productivity and Activity Impairment Questionnaire in ankylosing spondylitis. *Rheumatology* 2010;49:812–9.
19. Kalkan A, Roback K, Hallert E, *et al*. Factors influencing rheumatologists' prescription of biological treatment in rheumatoid arthritis: an interview study. *Implement Sci* 2014;9:153.
20. Austin PC. An Introduction to Propensity Score Methods for Reducing the Effects of Confounding in Observational Studies. *Multivariate Behav Res* 2011;46:399–424.
21. Caliendo M, Kopeinig S. Some practical guidance for the implementation of propensity score matching. *J Econ Surv* 2008;22:31–72.
22. Rosenbaum PR. Observational Study. In: Everitt BS, Howell DC, eds. *Encyclopedia of statistics in behavioral science*. Chichester: John Wiley and Sons, Ltd, 2005:1809–14.
23 Moher D, Liberati A, Tetzlaff J, *et al*. Preferred reporting items for systematic reviews and meta-analyses: the PRISMA statement. *J Clin Epidemiol* 2009;62:1006–12.
24 Higgins JP, Thompson SG. Quantifying heterogeneity in a meta-analysis. *Stat Med* 2002;21:1539–58.
25 Maksymowych WP, Dougados M, van der Heijde D, *et al*. Clinical and MRI responses to etanercept in early non-radiographic axial spondyloarthritis: 48-week results from the EMBARK study. *Ann Rheum Dis* 2016;75:1328–35.
26. Wei JC, Tsai WC, Citera G, *et al*. Efficacy and safety of etanercept in patients from Latin America, Central Europe and Asia with early non-radiographic axial spondyloarthritis. *Int J Rheum Dis* 2018;21:1443–51.
27 van der Heijde D, Han C, DeVlam K, *et al*. Infliximab improves productivity and reduces workday loss in patients with ankylosing spondylitis: results from a randomized, placebo-controlled trial. *Arthritis Rheum* 2006;55:569–74.
28. Dougados M, Tsai WC, Saaibi DL, *et al*. Evaluation of Health Outcomes with Etanercept Treatment in Patients with Early Nonradiographic Axial Spondyloarthritis. *J Rheumatol* 2015;42:1835–41.
29. Deodhar AA, Dougados M, Baeten DL, *et al*. Effect of Secukinumab on Patient-Reported Outcomes in Patients With Active Ankylosing Spondylitis: A Phase III Randomized Trial (MEASURE 1). *Arthritis Rheumatol* 2016;68:2901–10.
30 Barkham N, Coates LC, Keen H, *et al*. Double-blind placebo-controlled trial of etanercept in the prevention of work disability in ankylosing spondylitis. *Ann Rheum Dis* 2010;69:1926–8.
31. Jones GT, Keat A, Pathan E, *et al*. Real-world effectiveness of TNF inhibition in spondyloarthritis: data from a large nationwide prospective cohort – the British Society for Rheumatology biologics Register for Ankylosing Spondylitis [abstract]. *Arthritis Rheumatol* 2017;69(suppl 10).
32 Guo S, Fraser WM. *Propensity Score Analysis: Statistical Methods and Applications*. Second edition. Thousand Oaks, CA: Sage Publications, 2014.
33 de Hooge M, Ramonda R, Lorenzin M, *et al*. Work productivity is associated with disease activity and functional ability in Italian patients with early axial spondyloarthritis: an observational study from the SPACE cohort. *Arthritis Res Ther* 2016;18:18.
34 Nadin TG, Wallis D, Holroyd C, *et al*. 100. High levels of employment but persisting work impairment in patients with severe axial spondyloarthritis using biologic therapies. *Rheumatology* 2017;56:ke062.
35 Zhang W, Bansback N, Boonen A, *et al*. Validity of the work productivity and activity impairment questionnaire--general health version in patients with rheumatoid arthritis. *Arthritis Res Ther* 2010;12:R177.
36 Saidane O, Mahmoud I, Gafsi L, *et al*. Factors leading to work absenteeism in Tunisian ankylosing spondylitis patients. *The Egyptian Rheumatologist* 2018;40:183–5.
37 Macfarlane GJ, Jones GT, Shim J. Are Work Outcomes Improved in Axial Spondyloarthritis (axSpA) Patients with biologic Therapy? Results from the British Society for Rheumatology Register [abstract]. *Arthritis Rheumatol* 2017;69(suppl 10).

CONCISE REPORT

Improved detection of erosions in the sacroiliac joints on MRI with volumetric interpolated breath-hold examination (VIBE): results from the SIMACT study

Torsten Diekhoff,[1] Juliane Greese,[1] Joachim Sieper,[2] Denis Poddubnyy,[2] Bernd Hamm,[1] Kay-Geert A Hermann[1]

Handling editor Josef S Smolen

► Additional material is published online only. To view please visit the journal online (http://dx.doi.org/10.1136/annrheumdis-2018-213393).

[1]Department of Radiology, Charité – Universitätsmedizin Berlin, Campus Mitte, Humboldt-Universität zu Berlin, Freie Universität Berlin, Berlin, Germany
[2]Clinic of Rheumatology, Medical Department I, Charité – Universitätsmedizin Berlin, Campus Benjamin Franklin, Humboldt-Universität zu Berlin, Freie Universität Berlin, Berlin, Germany

Correspondence to
Dr Kay-Geert A Hermann, Department of Radiology (CCM), Charité – Universitätsmedizin Berlin, Berlin, 10117, Germany; kgh@charite.de

Received 10 March 2018
Revised 10 July 2018
Accepted 21 July 2018
Published Online First 10 August 2018

To cite: Diekhoff T, Greese J, Sieper J, *et al*. *Ann Rheum Dis* 2018;**77**:1585–1589.

ABSTRACT

Objective To compare the performance of a new three-dimensional MRI sequence (volumetric interpolated breath-hold examination; MR-VIBE) with a conventional T1-weighted sequence (MR-T1) for the detection of erosions in the sacroiliac joints (SIJs) using low-dose CT (ldCT) as reference.

Methods ldCT and T1-MRI and MR-VIBE of 110 prospectively included patients with low back pain and suspected axial spondyloarthritis (axSpA) were scored for erosions by two readers. The presence of erosions on the patients' level, the erosion sum score, sensitivity and specificity of both MRI sequences using ldCT as a reference as well as agreement between the readers were assessed.

Results MR-VIBE had a higher sensitivity than MR-T1 (95% vs 79%, respectively) without a decrease in specificity (93% each). MR-VIBE compared with MR-T1 identified 16% more patients with erosions (36 vs 30 of 38 patients with positive ldCT findings). The erosion sum score was also higher for MR-VIBE (8.1±9.3) than MR-T1 (6.7±8.4), p=0.003. The agreement on erosion detection was also higher for MR-VIBE (κ=0.71) compared with MRI-T1 (κ=0.56).

Conclusion VIBE detected erosions in the SIJs with higher sensitivity without a loss of specificity and superior reliability compared with a standard T1-weighted sequence. Its value for the diagnosis of axSpA has still to be determined.

INTRODUCTION

Lesions of the sacroiliac joints (SIJs) are key findings in axial spondyloarthritis (axSpA).[1 2] Typical imaging findings include structural changes such as erosions or ankylosis in radiographs and signs of active inflammation such as osteitis in water-sensitive, fat-suppressed sequences in MRI. Structural MRI changes remain to be standardised for the diagnosis and classification of patients with axSpA and are not yet part of a positive MRI definition of sacroiliitis according to the Assessment of SpondyloArthritis international Society (ASAS).[1] Moreover, it has been argued that bone marrow oedema might be too non-specific for a reliable diagnosis of axSpA in some cases—a limitation that might be overcome by adding structural lesions to the definition of a positive MRI.[3–5] Furthermore, recent studies show that a T1-weighted MRI sequence is at least equally able to depict structural changes compared with radiography[6] or even superior.[7] State-of-the-art MRI techniques that provide a high contrast of joint space and bone and thinner slices may further improve sensitivity for those changes and, therefore, the diagnostic accuracy of MRI.

The aim of our study was to compare a fast 3D spoiled gradient echo sequence (volumetric interpolated breath-hold examination, MR-VIBE) with a standard T1-weighted sequence (MR-T1) for the detection of erosions in the SIJs[8 9] using low-dose CT (ldCT) as standard of reference.

PATIENTS AND METHODS

Subjects

One hundred and ten patients (53 men and 57 women) from the SacroIliac joint MRI and CT (SIMACT) study, a prospective cross-sectional single-centre investigator-initiated study, and 18 healthy age-matched and sex-matched controls were included in this analysis.

The study complies with the declaration of Helsinki and was approved by the local ethics committee. All patients gave written informed consent.

Imaging procedures

All patients, but for ethical reasons (radiation) not the healthy controls, underwent a ldCT scan of the SIJs on a 64-row dual-source scanner (Somatom Definition Flash, Siemens, Erlangen, Germany) as described in detail elsewhere.[7] Directly thereafter, the patients underwent a 3-Tesla pelvic MRI (Magnetom Skyra, Siemens, Erlangen, Germany). Besides a standard STIR-weighted sequence, a standard T1-weighted (repetition time 652.0 ms, echo time 11.0 ms, slice thickness 3 mm, flip angle 156°, spatial resolution 410×512 pixels) and a high-resolution iso-voxel VIBE sequence were acquired with a TE of 5.2 and TR of 11.7 ms, a flip angle of 10° and a matrix of 256×256 pixels with a slice thickness of 0.6 mm. Oblique coronal slices parallel to the axis of the second sacral segment were acquired.

Postprocessing and scoring

The ldCT, MR-T1 and MR-VIBE datasets were anonymised separately using Osirix 6.4 (Pixmeo SARL, Bernex, Switzerland). Two readers were trained and scored 15 test cases in consensus before they separately evaluated the images blinded to clinical data and findings of the other modality.

However, they had access to a T2-weighted fat-suppressed sequence when scoring the MR images.

Each SIJ was divided into 12 regions (4 quadrants in ventral, middle and dorsal position), resulting in 24 regions per patient.[7] The anterior position is defined as ventral to the slices depicting the sacral neuroforamina (<180% circumference of S2). Pelvic organs and fat are seen in the middle of the image. In the middle position, the anterior sacral neuroforamina and the sacral bone is visualised. The posterior position is defined as visualising the entheseal joint compartment that stretches to the posterior-inferior aspect of the joint. Accurate oblique-coronal slice orientation is crucial. For each region, erosions were scored on a four-point scale as described earlier in detail[7]: *0*—no erosions; *1*—small isolated erosions (1–2) or questionable single erosion; *2*—definite erosions (3-5; <3 mm) or larger single erosion (>3 mm); *3*—multiple (>5) or confluent erosions. Therefore, the sum-score ranged from 0 to 72. The total number of erosions was calculated by summing the number in each region.

A patient was considered positive for erosions if any of the 24 regions was assigned a score ≥2. The agreement of both, reader 1 and 2, was considered necessary for a positive finding.

Additionally, the readers were asked to rate their diagnostic confidence using ldCT, MR-T1 and MR-VIBE on a 0-to-10 numerical scale.

Statistical analysis

We performed a contingency table analysis on the patient level to relate the positivity of MR-VIBE and MR-T1 for erosions to ldCT, which served as standard of reference. The inter-rater reliability was evaluated using Cohen's kappa[10] for the presence or absence of erosions on the patients' level, and the intraclass correlation coefficient (ICC) for the total number of erosions and erosions sum score using a two-way mixed model for single measures. Erosion sum-scores, total numbers of erosions and diagnostic confidence related to ldCT, MR-T1 and MR-VIBE were tested for significant differences by a repeated-measurements analysis of variance with pair-by-pair comparison. The p values were corrected for multiple comparisons using Tukey's test with individual variances and considered significant if smaller than 0.05. Missing data, for example, incomplete imaging of a region, were included in the analysis as negative for all modalities. Statistics were performed using GraphPad Prism (V.6.0 for MacOS, GraphPad Software, La Jolla, California, USA).

RESULTS

The patients had a mean age of 36.1 years (range, 19–57 years) with a mean duration of chronic back pain of 6 years and 10 months (range, 2 months to 32 years; median: 4 years). Eighty-seven patients had inflammatory back pain (79.1%), 71 (64.5%) were HLA-B27 positive. Fifty-eight patients were diagnosed with axSpA (63% male, 81% HLA-B27 positive) by the expert rheumatologist (axSpA group: 23 with radiographic and 35 with non-radiographic axSpA) and 52 had other diagnoses (non-axSpA group; 34.6% male, 46% HLA-B27 positive).

All regions were assessable in T1 and ldCT, in VIBE only 0.3% (10/3072) regions were not fully depicted by the sequence. Results and overview of statistics are presented in a flow chart (figure 1). Using ldCT positivity (score of ≥2) as standard of reference the sensitivity of VIBE (93%) was higher than of T1 (79%) with a similar specificity of 93%. The mean sum score of both readers for erosions was 7.1±9.0 in ldCT, 6.7±8.4 in MR-T1 and 8.1±9.3 in MR-VIBE with a total number of erosions of 11.4±16.5 in ldCT, 9.2±12.1 in MR-T1 and 15.5±21.8 MR-VIBE (see figure 2A and B). For MR-VIBE, the erosion score was higher in patients positive for erosions in ldCT (figure 2C). Examples in figure 3 illustrate that erosions are better visible by ldCT and MR-VIBE than by MR-T1, but also that MR-VIBE is sometimes even more sensitive for erosions than ldCT (figure 3G and I). None of the 18 healthy controls was scored positive for erosions by either reader in MR-T1 or MR-VIBE. When using the clinician's diagnosis of axial SpA and an erosion score of ≥2 as a cut-off (online supplementary figure S1B) MR-VIBE showed a better sensitivity than MR-T1 (65% vs 53%, respectively) and a better specificity for a cut-off of a ≥1 erosion score (68 vs 53%, respectively) while there was no difference for an erosion score of ≥3 (see online supplementary figure S1).

The agreement on erosion detection on the patients' level was good for ldCT and MR-VIBE (Cohen's κ=0.77, 95% CI 0.65 to 0.89 and 0.71, 95% CI 0.57 to 0.84, respectively) and only moderate for MR-T1 (κ=0.56, 95% CI 0.4 to 0.71). The ICC of the total erosion score was comparable for all three imaging modalities (online supplementary table S1).

The diagnostic confidence was highest for MR-VIBE (6.9±2.6), followed by ldCT (6.3±2.7) and MR-T1 (5.6±2.9). These differences were statistically significant for all modalities: MR-VIBE vs ldCT, p=0.006; ldCT vs MR-T1, p=0.002; MR-VIBE vs MR-T1, p<0.0001.

DISCUSSION

This is the first study comparing a modern three-dimensional MR technique (VIBE) with a standard-of-care T1-weighted sequence using ldCT as standard of reference for the detection of erosions in the SIJs. We found that MR-VIBE had a higher sensitivity for erosions than MR-T1 without a decrease in specificity. MR-VIBE identified 16% more patients with erosions compared with MR-T1 (figure 1). MR-VIBE detected significantly more erosions (sum score and total number) than MR-T1 but also than seen on ldCT. When erosion counts were analysed in ldCT-negative patients only, the use of MR-VIBE did not increase the number of false positive findings compared with MR-T1. MR-VIBE performed also better than MR-T1 in terms of inter-rater reliability. Similarly, readers' overall diagnostic confidence for detecting erosions was significantly higher using MR-VIBE than MR-T1 or ldCT. It has to be shown how much a better and more reliable detection of erosions in the SI-joint can contribute to a better diagnosis of axSpA where all clinical, laboratory and imaging aspects, and not only erosions, are taken into account.

We believe that the higher sensitivity of MR-VIBE vs ldCT can be explained by the high contrast of cartilage and bone in VIBE images and by the image noise in the ldCT scan, which might obscure small lesions. This assumption is also supported by the absence of erosions in MR-VIBE in the healthy controls. The search for sensitive and specific imaging technique for detecting structural lesions of the SIJs has become of high relevance[6 11 12] because interpretation of radiographs has repeatedly been shown to be unreliable.[13 14]

Regarding other studies addressing this topic, Algin *et al* tested different sequences in a small cohort of 30 patients with SpA and 9 controls and found that 3D-FLASH with fat saturation (VIBE is such a sequence) is the most useful technique to detect cartilage and bone abnormalities.[15] In other anatomical locations (eg, hands or knee), similar high-resolution techniques are already standard of care.[16 17]

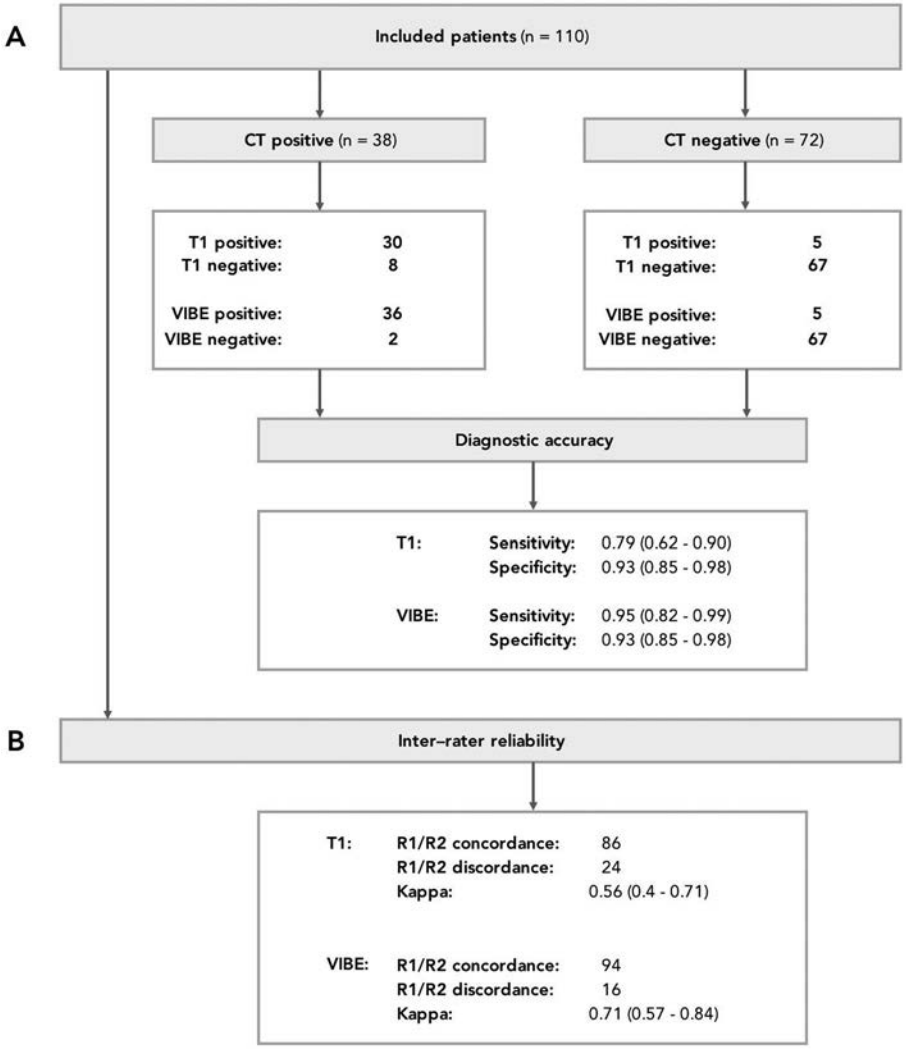

Figure 1 Findings in a flowchart. (A) Positivity for erosions in MR-T1 and MR-VIBE is reported separately for patients positive and negative in ldCT. MR-VIBE detected more erosions in patients with erosions in ldCT, while there was no difference in patients who were ldCT-negative. This increases sensitivity without a loss of specificity. (B) For the assessment of inter-reader reliability, we analysed the number of concordant and discordant ratings for MR-T1 and MR-VIBE. Sensitivity, specificity and kappa values are given with the 95% CI in brackets. ldCT, low-dose CT; VIBE, volumetric interpolated breath-hold examination.

The investment of another 3 min for acquiring an MR-VIBE sequence to supplement the standard T1 and STIR MR protocol can increase the sensitivity for erosions and improve diagnostic confidence. That our results obtained with 3-Tesla MRI can also be achieved at lower field strengths is likely but has to be proven. Also, due to the limitations of this single-centre study, the application and interpretation of MR-VIBE should be tested in a larger multicentre trial. The availability of T2 fat-suppressed images during reading might have influenced the result, however, is more close to clinical practice.

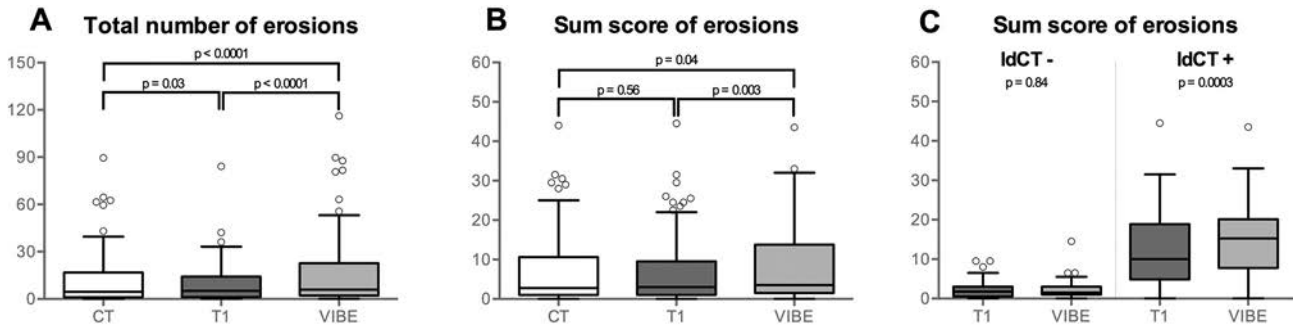

Figure 2 Comparison of results in terms of the total number of detected erosions (A), the erosion sum score (B) and erosion sum score in patients positive and negative for erosions in ldCT (C) for ldCT (CT), MR-T1 (T1) and MR-VIBE (VIBE). MR-VIBE detects significantly more erosions (total number and sum score, A and B) than the other modalities, however, only in patients positive in ldCT (C). The total number of erosions is also significantly lower for MR-T1 compared with ldCT (A). ldCT, low-dose CT; VIBE, volumetric interpolated breath-hold examination.

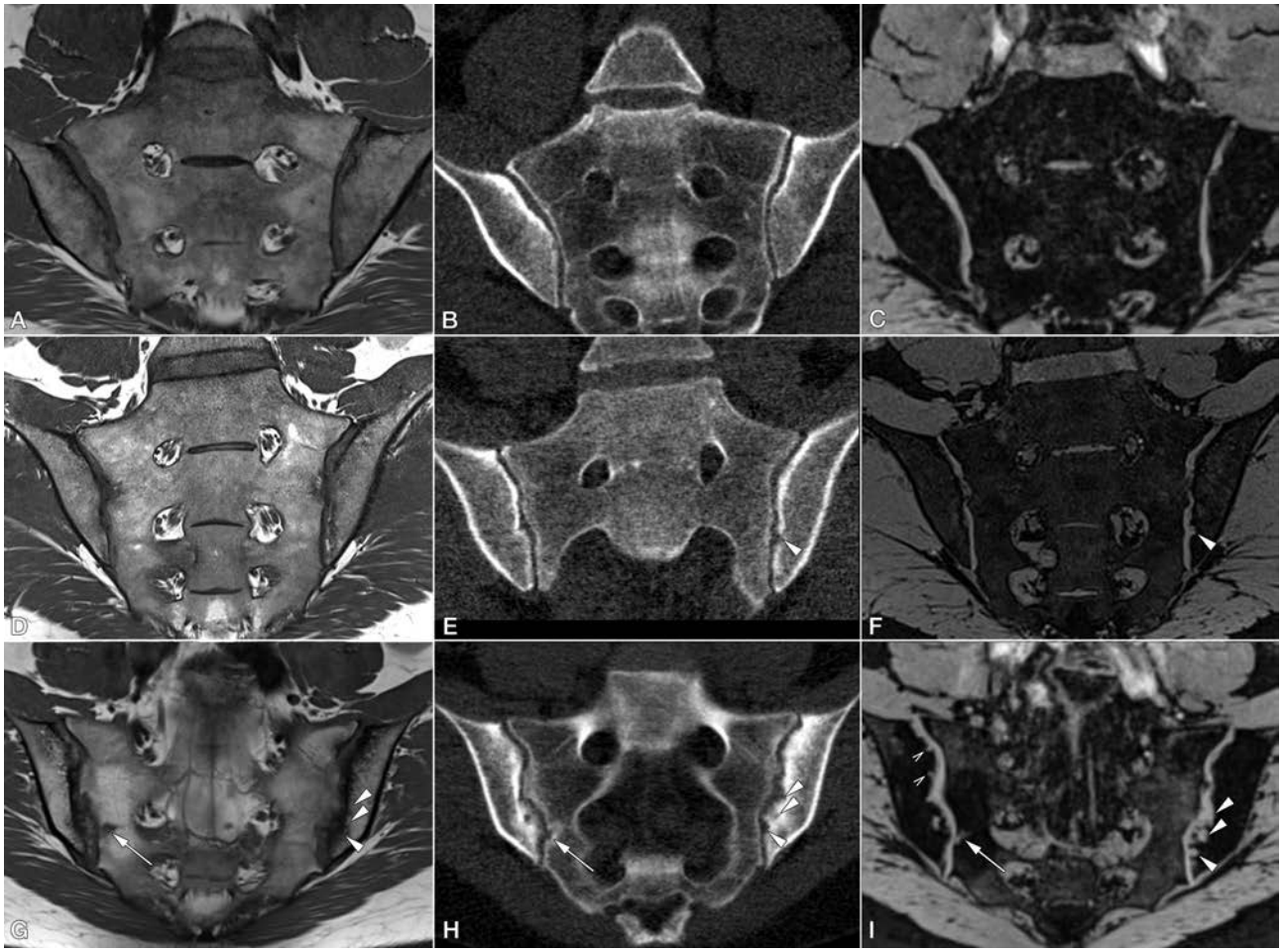

Figure 3 Imaging examples. (A, D and G) Oblique coronal MR-T1 sequence; (B, E and H) ldCT images in oblique coronal reconstruction; (C, F and I) oblique coronal MR-VIBE sequence. Slice positions and orientation are identical for T1 and VIBE. ldCT was reconstructed to match orientation and position. (A–C) normal findings in the SIJ without erosions (erosion sum score 0 for both readers). (D–F) Patient with axial spondyloarthritis with a single but prominent erosion of the left iliac surface that is shown by ldCT and MR-VIBE (arrowheads) but not by MR-T1. (G–I) Patient with axial spondyloarthritis and multiple erosions. Some erosions (arrow) are depicted by all modalities. However, some larger erosions are hardly seen with MR-T1 due to sclerosis, while they are more conspicuous using ldCT and MR-VIBE (arrowheads). The smallest erosions are only depicted with MR-VIBE (open arrowheads). ldCT, low-dose CT; VIBE, volumetric interpolated breath-hold examination.

In summary, MR-VIBE detected SIJ erosions with higher sensitivity and reliability and in more patients compared with standard T1 MRI in a patient population with low back pain. Thus, the MR-VIBE sequence seems to be a valuable supplement to standard MR protocols for axSpA and its differential diagnosis; however, its value for the diagnosis of axSpA still has to be determined.

Acknowledgements The authors thank Bettina Herwig for language editing.

Contributors TD: conception and design of the study, design of scoring system, image scoring, data evaluation, statistical calculations, article draft, critical revision of the manuscript for important intellectual content. JG: patient acquisition, data management, image scoring, critical revision of the manuscript for important intellectual content. JS: patient acquisition, conception and design of the study with critical revision of the manuscript for important intellectual content. DP: patient acquisition, critical revision of the manuscript for important intellectual content. BH: conception of the study, critical revision of the manuscript for important intellectual content. K-GAH: conception and design of the study, design of scoring system, image scoring, data evaluation, with critical revision of the manuscript for important intellectual content and final approval of the version to be published.

Funding This work was supported by a research grant to TD from the Assessment of Spondyloarthritis international Society (ASAS).

Competing interests None declared.

Patient consent Obtained.

Ethics approval Institutional Review Board of Charité Medical School, Berlin, Germany.

Provenance and peer review Not commissioned; externally peer reviewed.

REFERENCES

1 Lambert RG, Bakker PA, van der Heijde D, *et al*. Defining active sacroiliitis on MRI for classification of axial spondyloarthritis: update by the ASAS MRI working group. *Ann Rheum Dis* 2016;75:1958–63.
2 Mandl P, Navarro-Compán V, Terslev L, *et al*. EULAR recommendations for the use of imaging in the diagnosis and management of spondyloarthritis in clinical practice. *Ann Rheum Dis* 2015;74:1327–39.
3 Berthelot JM, le Goff B, Maugars Y, *et al*. Sacroiliac joint edema by MRI: far more often mechanical than inflammatory? *Joint Bone Spine* 2016;83:3–5.
4 Arnbak B, Grethe Jurik A, Hørslev-Petersen K, *et al*. Associations between spondyloarthritis features and magnetic resonance imaging findings: a cross-sectional analysis of 1,020 patients with persistent low back pain. *Arthritis Rheumatol* 2016;68:892–900.
5 Dubreuil M, Deodhar AA. Axial spondyloarthritis classification criteria: the debate continues. *Curr Opin Rheumatol* 2017;29:317-322.
6 Bakker PA, van den Berg R, Lenczner G, *et al*. Can we use structural lesions seen on MRI of the sacroiliac joints reliably for the classification of patients according to the ASAS axial spondyloarthritis criteria? Data from the DESIR cohort. *Ann Rheum Dis* 2017;76:392–8.
7 Diekhoff T, Hermann KG, Greese J, *et al*. Comparison of MRI with radiography for detecting structural lesions of the sacroiliac joint using CT as standard of reference: results from the SIMACT study. *Ann Rheum Dis* 2017;76:1502–8.

8 Abdulaal OM, Rainford L, MacMahon P, *et al*. 3T MRI of the knee with optimised isotropic 3D sequences: Accurate delineation of intra-articular pathology without prolonged acquisition times. *Eur Radiol* 2017;27:4563–70.
9 Gholipour A, Afacan O, Aganj I, *et al*. Super-resolution reconstruction in frequency, image, and wavelet domains to reduce through-plane partial voluming in MRI. *Med Phys* 2015;42:6919–32.
10 Landis JR, Koch GG. The measurement of observer agreement for categorical data. *Biometrics* 1977;33:159–74.
11 Weber U, Zubler V, Zhao Z, *et al*. Does spinal MRI add incremental diagnostic value to MRI of the sacroiliac joints alone in patients with non-radiographic axial spondyloarthritis? *Ann Rheum Dis* 2015;74:985–92.
12 Akkoc N, Khan MA. ASAS classification criteria for axial spondyloarthritis: time to modify. *Clin Rheumatol* 2016;35:1415–23.
13 Omar A, Sari I, Bedaiwi M, *et al*. Analysis of dedicated sacroiliac views to improve reliability of conventional pelvic radiographs. *Rheumatology* 2017;56:1740–5.
14 Christiansen AA, Hendricks O, Kuettel D, *et al*. Limited reliability of radiographic assessment of sacroiliac joints in patients with suspected early spondyloarthritis. *J Rheumatol* 2017;44:70–7.
15 Algin O, Gokalp G, Ocakoglu G. Evaluation of bone cortex and cartilage of spondyloarthropathic sacroiliac joint: efficiency of different fat-saturated MRI sequences (T1-weighted, 3D-FLASH, and 3D-DESS). *Acad Radiol* 2010;17:1292–8.
16 Siddle HJ, Hensor EM, Hodgson RJ, *et al*. Anatomical location of erosions at the metatarsophalangeal joints in patients with rheumatoid arthritis. *Rheumatology* 2014;53:932–6.
17 Braum LS, McGonagle D, Bruns A, *et al*. Characterisation of hand small joints arthropathy using high-resolution MRI--limited discrimination between osteoarthritis and psoriatic arthritis. *Eur Radiol* 2013;23:1686–93.

EXTENDED REPORT

High-sensitive troponin is associated with subclinical imaging biosignature of inflammatory cardiovascular involvement in systemic lupus erythematosus

Lea Winau,[1] Rocio Hinojar Baydes,[1,2] Axel Braner,[3] Ulrich Drott,[3] Harald Burkhardt,[3] Shirish Sangle,[4] David P D'Cruz,[4] Gerry Carr-White,[5] Mike Marber,[6] Katrin Schnoes,[1,7] Christophe Arendt,[8] Karin Klingel,[9] Thomas J Vogl,[8] Andreas M Zeiher,[1] Eike Nagel,[1] Valentina O Puntmann[1,5,7]

Handling editor Josef S Smolen

For numbered affiliations see end of article.

Correspondence to
Dr Valentina O Puntmann, Institute for Experimental and Translational Cardiovascular Imaging, DZHK Centre for Cardiovascular Imaging, Goethe University Frankfurt, University Hospital Frankfurt am Main, Germany; vppapers@icloud.com

Received 26 April 2018
Revised 14 July 2018
Accepted 17 July 2018
Published Online First
4 August 2018

To cite: Winau L, Hinojar Baydes R, Braner A, *et al*. *Ann Rheum Dis* 2018;**77**:1590–1598.

ABSTRACT

Background Cardiovascular (CV) involvement in patients with systemic lupus erythematosus (SLE) is presumably subclinical for the major part of its evolution. We evaluated the associations between high-sensitive troponin T (hs-TropT), a sensitive marker of myocardial injury, and CV involvement using cardiac magnetic resonance (CMR).

Methods and results This is a two-centre (London and Frankfurt) CMR imaging study at 3.0 Tesla of consecutive 92 patients with SLE free of cardiac symptoms, undergoing screening for cardiac involvement. Venous samples were drawn and analysed post-hoc for cardiac biomarkers, including hs-TropT, high-sensitive C reactive protein and N-terminal pro brain natriuretic peptide. Compared with age-matched/gender-matched non-SLE controls (n=78), patients had significantly raised cardiac biomarker levels, native T1 and T2, aortic and ventricular stiffness, and reduced global longitudinal strain (p<0.01). In SLE, hs-TropT was significantly and independently associated with native T2, followed by the models including native T1 and aortic stiffness (X^2 0.462, p<0.01). There were no relationships between hs-TropT and age, gender, CV risk factors, duration of systemic disease, cardiac structure or function, or late gadolinium enhancement.

Conclusions Patients with SLE have a high prevalence of subclinical myocardial injury as demonstrated by raised high-sensitive troponin levels. CMR with T2 mapping reveals myocardial oedema as the strongest predictor of hs-TropT release, underscoring the inflammatory interstitial remodelling as the main mechanism of injury. Patients without active myocardial inflammation demonstrate diffuse interstitial remodelling and increased vascular stiffness. These findings substantiate the role of CMR in screening of subclinical cardiac involvement.

Trial registration numer NCT02407197; Results.

INTRODUCTION

Systemic lupus erythematosus (SLE) is a chronic systemic inflammatory condition associated with complex cardiovascular (CV) involvement with high morbidity and CV mortality.[1–3] It is recognised that the first decade since the diagnosis of systemic disease represents a period of intense systemic disease activity. This includes CV involvement, which in contrast to systemic disease progresses silently for the major part of its evolution. Only a small proportion of patients eventually proceed into manifest cardiac disease, most commonly congestive heart failure, which is poorly reversible and difficult to treat.[4–8] Underscored by the pathophysiological pathways of inflammation and remodelling, CV involvement is phenotypically characterised by non-ischaemic cardiomyopathy, and coronary and aortic vasculitis.[2 9–14] A number of previous studies using cardiovascular magnetic resonance (CMR) reported significantly elevated non-invasive quantifiable myocardial tissue measures of remodelling and inflammation T1 and T2 mapping, and myocardial scar by late gadolinium enhancement (LGE), respectively (reviewed in refs [9 10 15–21]). Studies further demonstrated considerable vascular involvement in SLE, including carotid, aortic and coronary vessel wall vasculitis, and high frequency of myocardial microvascular disease and myocardial fibrosis.[2 6 7 11 22–29] Despite the above knowledge, the relationship with the biomarkers of myocardial injury (high-sensitive troponin, hs-TropT[26 27]), inflammation (high-sensitive C reactive protein, hs-CRP) and remodelling (N-terminal pro brain natriuretic peptide, NT-proBNP) remains unclear.[28] Furthermore, the pathophysiological relationship between these markers and changes observed in subclinical CV involvement is not ascertained.

METHODS

Consecutive 92 patients with an established diagnosis of SLE as per the American College of Rheumatology revised classification criteria,[29] without previously known or symptomatic cardiac disease, were referred for screening with CMR for CV involvement from the local rheumatology departments (London, n=56; Frankfurt, n=36). Seventy-eight (non-SLE) subjects, matched for age, gender and CV risk factor profile, with low-pretest likelihood for left ventricular (LV) cardiomyopathy, no clinical or serological evidence for systemic inflammation, taking no anti-inflammatory medication, and no history of cardiac events or known coronary artery disease (CAD), served as controls. The general contraindication to contrast-enhanced CMR was observed as per local rules (known allergy to contrast agents, pregnancy, cochlear implants,

Table 1 Subjects' characteristics, including the characteristics of the disease and medication of patients with SLE

Variable	Controls (n=78)	Patients with SLE (n=92)	Significance (P values)
Age (years)	42±13	43±14	0.632
Male, n (%)	9 (12)	12 (13)	0.845
BMI, kg/m^2	26±3	25±5	0.523
Heart rate, bpm	62±12	65±14	0.139
BP systolic, mm Hg	115±13	119±17	0.413
BP diastolic, mm Hg	72±12	73±13	0.575
Hypertension, n (%)	15 (19)	23 (34)	0.054
Diabetes mellitus (type 2), n (%)	2 (3)	5 (7)	0.240
Hypercholesterolaemia, n (%)	13 (17)	20 (22)	0.509
Smoking, current or previous, n (%)	10 (13)	12 (16)	0.581
Time since SLE diagnosis (years)	–	7 (5)	–
History of nephritis, n (%)	–	45 (49)	–
CNS involvement, n (%)	–	11 (12)	–
Antiphospholipid syndrome, n (%)	–	28 (30)	–
SLEDAI	–	6 (8)	–
Cardiac medication			
Aspirin, n (%)	2 (3)	8 (8)	0.161
Anticoagulation, n (%)	0 (0)	29 (32)	<0.001
Beta-blockers, n (%)	3 (4)	6 (7)	0.401
RAS inhibitors, n (%)	35 (46)	51 (55)	0.242
Statin, n (%)	16 (21)	19 (21)	0.99
DMARDs			
None, n (%)	–	6 (9)	–
Prednisolone, n (%)	–	69 (75)	–
HCQ, n (%)	–	37 (40)	–
Mycophenolate, n (%)	–	25 (27)	–
Other, n (%)	–	11 (12)	–
Blood markers			
eGFR, mL/min/1.73 m^2	89±11	72±15	<0.001
hs-CRP, mg/L	2.2±1.4	4.2±4.0	<0.001
hs-TropT, ng/L	2.2±1.9	21.4±15.3	<0.001
Abnormal hs-TropT (>13.9 ng/L, n (%))	0 (0)	50 (54)	<0.001
NT-proBNP (pg/L)	74 (42)	142 (274)	<0.001
Complement C3 (mg/L)	–	103±25	–
Complement C4 (mg/L)	–	21±9	–
CMR measures of function and structure			
LV-EDV (index), mL/m²	76±12	80±20	0.124
LV-ESV (index), mL/m²	29±10	34±15	0.013
LV-EF, %	63±5	59±10	0.007
LVmass (index), g/m²	49±12	54±17	0.048
RV-EF, %	58±8	61±9	0.029
LA area, cm²	18±4	20±4	0.015
Global longitudinal strain, %	26±3	18±7	<0.001
Global circumferential strain, %	28±5	27±7	0.262
PWV, m/s	5.4±1.7	7.1±3.2	<0.001
E/e'	7.6±1.2	9.1±2.7	<0.001
CMR tissue characterisation			
Native T1 (ms)	1062±23	1156±51	<0.001
Native T2 (ms, GraSE, n=46/56)	44±4	51±9	<0.001
Native T2 (ms, FLASH, n=32/36)	35±4	42±7	<0.001
Myocardial LGE			
Present, n (%)	0 (0)	28 (30)	<0.001
Ischaemic, n (%)	–	6 (7)	
Non-ischaemic, n (%)	–	22 (24)	
Pericardial enhancement	0 (0)	9 (13)	0.001
Pericardial effusion	0 (0)	7 (10)	0.004
Microvascular disease, n (%)	0 (0)	24(26)	<0.001

BMI, body mass index; BP, blood pressure; bpm, beats per minute; CMR, cardiovascular magnetic resonance; CNS, central nervous system; DMARDs, disease-modifying antirheumatic drugs; EDV, end-diastolic volume; EF, ejection fraction; eGFR, estimated glomerular filtration rate; ESV, end-systolic volume; GraSE, gradient and spin echo; HCQ, hydroxychloroquine; hs-CRP, high-sensitive C reactive protein; LA, left atrium; LGE, late gadolinium enhancement; LV, left ventricular; NT-proBNP, N-terminal pro brain natriuretic peptide (expressed as median (IQR)); PWV, pulse wave velocity; RAS, renin angiotensin system; RV, right ventricular; SLE, systemic lupus erythematosus; SLEDAI, SLE Disease Activity Score Index.

cerebral aneurysm clips, non-CMR compatible pacemakers; no subject was excluded due to these contraindications in the present study). Patient characteristics were recorded using a standardised questionnaire for all subjects, including symptoms, age, gender, body mass index, renal function, CV risk factors and immunosuppressive therapy (table 1).

Cardiovascular magnetic resonance

All subjects underwent a routine clinical scan protocol using a 3 Tesla clinical scanner (Achieva, Philips Healthcare, Best, The Netherlands, and Skyra, Siemens Healthineers, Erlangen), CMR protocol (figure 1). After standardised patient-specific planning, myocardial T1 and T2 mapping was performed in a single mid-ventricular short-axis (SAX) slice. T1 mapping was performed using modified Look-Locker imaging.[30 31] For T2 mapping, a hybrid gradient and spin echo (GraSE) sequence was used at the London site,[32] whereas in Frankfurt T2 mapping fast low angle shot (FLASH) sequence was employed.[33 34] All sequence types and parameters have been validated and reported previously.[12 18 20] Sequence-specific normal ranges were employed (native T1: 3.0 T; mean of the normal range 1052±23 ms; ie, upper limit of normal range: 1098 ms at 3.0 T[35]; native T2: GraSE sequence: 45±4 ms[32 36]; T2-FLASH sequence 35±4 ms[33 34 36]). Myocardial perfusion imaging with adenosine infusion (140 μg/kg/min) and administration of 0.1 mmol/kg body weight gadobutrol (Gadovist, Bayer AG, Leverkusen, Germany) was performed,[37 38] followed by volumetric cavity assessment by whole-heart coverage of SAX slices. Central aortic pulse wave velocity (PWV), a measure of aortic stiffness, was obtained with an inplane sagittal oblique acquisition of the ascending and descending aorta, using a retrospectively gated, free-breathing, phase-contrast gradient echo sequence, as reported previously.[39 40] Representative acquisitions are included in figure 1.

Cardiac volume and function were quantified using commercially available software (Medis, Leiden) following standardised postprocessing recommendations.[41] LGE was characterised as present or absent, and ischaemic or non-ischaemic in type, based on the predominant pattern.[38 41] Quantitative tissue characterisation and myocardial deformation analysis were performed by the core-lab (Goethe CVI, Frankfurt), blind to the underlying subject group allocation and the time-point of the examination. The rates of T1 and T2 relaxation were measured in the septal myocardium of the mid-ventricular SAX using the ConSept approach, as previously described.[31 42] Areas of

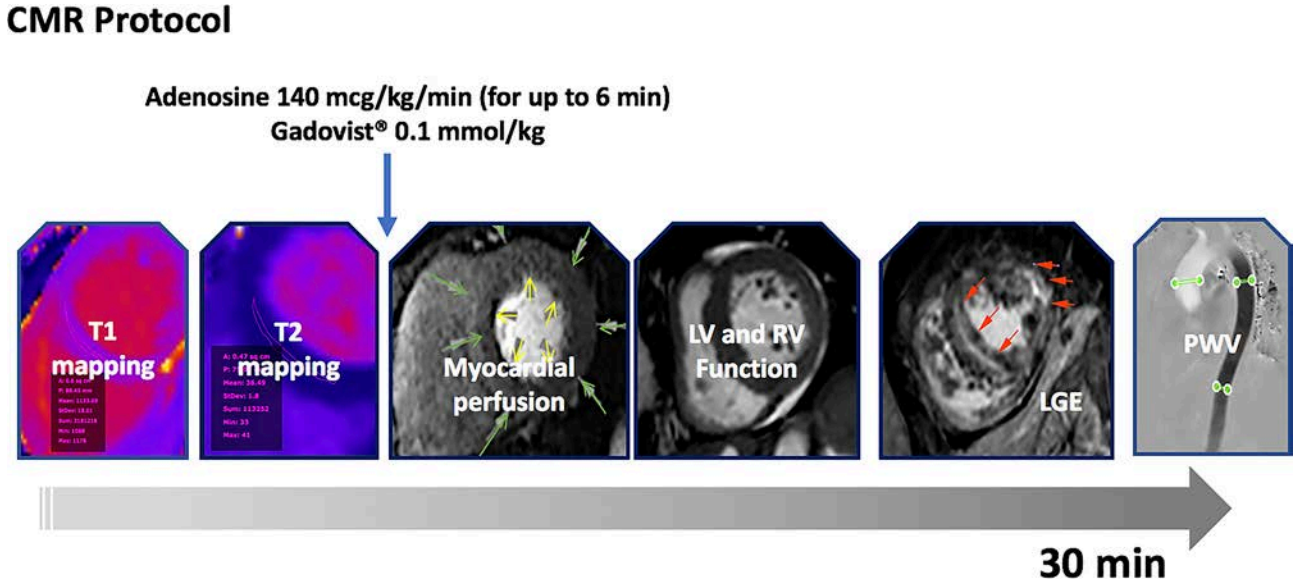

Figure 1 CMR protocol for screening of subclinical cardiovascular involvement in SLE with representative images of acquisitions and findings in a patient with SLE. CMR, cardiovascular magnetic resonance; LGE, late gadolinium enhancement; LV, left ventricular; PWV, pulse wave velocity; RV, right ventricular; SLE, systemic lupus erythematosus.

LGE were excluded from mapping the region of interest (ROIs) to allow T1 and T2 measurements to avoid areas of replacement scar.[42 43] Global longitudinal and circumferential strain was measured within a feature tracking application using feature tracking two-dimensional prototype software (TomTec, Munich, Germany), as previously described.[44] Longitudinal deformation was obtained in three long-axis views, whereas circumferential included three SAX slices. Both are expressed as an absolute global peak systolic strain per direction.[9] All patients underwent venous blood sampling at the time of the CMR study. Plasma samples were frozen at −80°C and analysed subsequently using standardised commercially available test kit analysis for hs-TropT, hs-CRP and NT-proBNP (Elecsys 2010, Roche, Basel, Switzerland). Analytical validation and limits of detection of the hs-TropT test were used to define normal/abnormal (using a cut-off value of 99th percentile of 13.9 ng/L, as previously reported).[45]

Statistics

Statistical analysis was performed using SPSS V.24. Normality of distributions was tested using Shapiro-Wilk test. Categorical data are expressed as counts (percentages), and continuous variables as mean±SD or median (range), as appropriate. Comparisons between groups were performed using Student's t-test or one-way analysis of variance for normally distributed variables, and χ^2 and Mann-Whitney test for non-normally distributed variables. Fisher's exact tests were conducted for proportions. The associations were analysed by univariate and multivariate linear regression analyses. Collinearity diagnostics was used to examine the variance inflation factor analysis. Interobserver and intraobserver reproducibility and agreement of postprocessing approaches have been reported previously.[36 42 46] All tests were two-tailed and p values <0.05 were considered statistically significant.

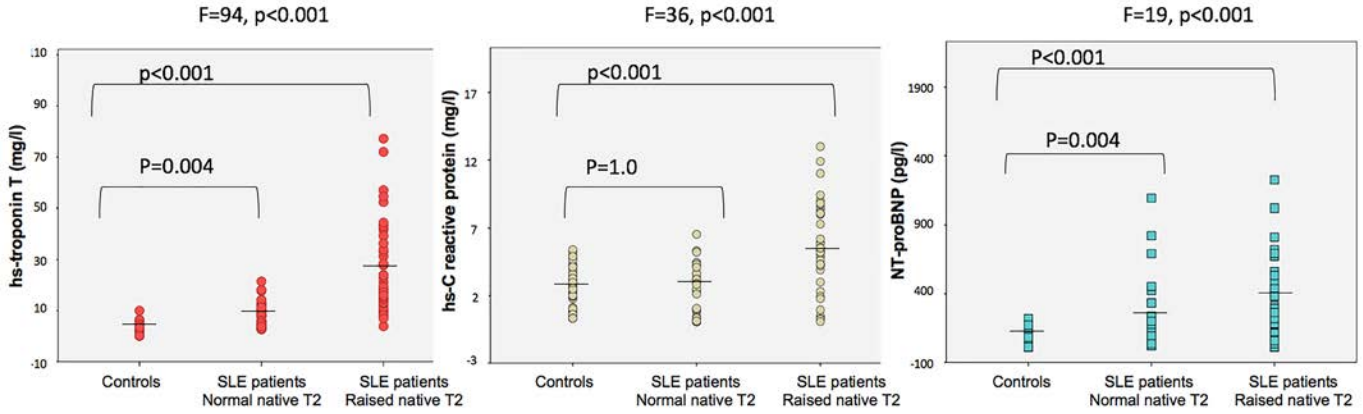

Figure 2 Serological biomarkers in controls and patients outlining the patient subgroups with evidence of myocardial oedema based on T2 mapping (defined as >2 SD above the mean of the sequence-specific normal range).[32 33 45] hs, high-sensitive; NT-proBNP, N-terminal pro brain natriuretic peptide; SLE, systemic lupus erythematosus.

Table 2 Associations of variables with hs-troponin T levels in controls and patients with SLE

hs-Troponin T	Controls		Patients with SLE	
Variables				
Correlations	**Pearson's r**	**Significance (P values)**	**Pearson's r**	**Significance (P values)**
Age (years)	0.12	0.31	0.11	0.28
Gender* (male)	0.15	0.20	0.17	0.10
hs-CRP (mg/L)	0.05	0.69	0.42	<0.001
NT-proBNP (pg/L)	0.07	0.53	0.29	0.005
eGFR (mL/min/1.73 m^2)	0.11	0.33	0.02	0.89
BMI (kg/m^2)	0.06	0.62	0.04	0.73
Heart rate (bpm)	0.04	0.72	0.18	0.08
Systolic BP (mm Hg)	0.01	0.93	0.13	0.12
Diastolic BP (mm Hg)	0.02	0.85	0.24	0.02
Native T1 (ms)	0.302	0.007	0.54	<0.001
Native T2 (ms)	–0.2	0.08	0.60	<0.001
GLS (%)	0.16	0.18	–0.29	0.005
GCS (%)	–0.14	0.24	0.01	0.91
LV-EDV (index), mL/m^2	0.01	0.96	–0.05	0.62
LV-EF (%)	0.03	0.82	–0.11	0.32
LVmass (index), g/m^2	0.24	0.04	0.1	0.37
RV-EF (%)	0.10	0.38	0.14	0.18
LA area, cm^2	0.07	0.57	0.07	0.57
LGE present*	–	–	0.13	0.22
E/e′	0.03	0.78	0.21	0.045
PWV (m/s)	–0.1	0.24	0.48	<0.001
SLEDAI			0.21	0.08
Linear regression (stepwise)	**r^2**	**Variable**	**B (95% CI)**	**Significance (P values)**
Controls				
Model 1	0.100	Native T1 (10 ms)	0.2 (0.1 to 0.4)	0.007
Model 2	0.138	Native T1 (10 ms)	0.2 (0.1 to 0.0)	0.009
		LVmass (index)	0.03 (0.01 to 0.08)	0.048
Patients with SLE				
Model 1	0.391	Native T2 (1 ms)	1.2 (0.9 to 1.5)	<0.001
Model 2	0.462	Native T2 (1 ms)	0.9 (0.5 to 1.2)	<0.001
		Native T1 (10 ms)	0.9 (0.4 to 1.5)	0.001
Model 3	0.494	Native T2 (1 ms)	0.9 (0.6 to 1.2)	<0.001
		Native T1 (10 ms)	0.9 (0.3 to 1.5)	0.002
		PWV (1 m/s)	3.2 (1.7 to 4.7)	0.004

Adjusted for age, gender, cardiovascular risk profile, SLEDAI, hs-CRP, NT-proBNP, eGFR, BMI, heart rate, systolic and diastolic BP, GLS, GCS, LV-EDV, LV-EF, LVmass (index), RVEF, LA area, LGE and E/e′.
*Bivariate correlations are expressed with Pearson's (or Spearman's for categorical variables) coefficient, as suitable for the type of data. Abbreviations as per table 1.
GCS, global circumferential strain; GLS, global longitudinal strain.

RESULTS

Subject characteristics, results of blood markers and CMR measurements are summarised in table 1. Patients were well matched to controls for age, gender, blood pressure, heart rate and CV risk profile. The average duration of systemic disease was 7±5 years. Patients with SLE took a variety of disease-modifying antirheumatic medication, including prednisolone (39, 42%), hydroxychloroquine (37, 40%), mycophenolate (25, 27%) or others (11, 12%). Twenty-nine patients with SLE (32%) were taking anticoagulation treatment in the context of antiphospholipid syndrome.

Compared with controls, LV end-systolic volume (LV-ESV) and mass were increased and LV ejection fraction reduced in patients with SLE ($p<0.05$ for all), although the means remained within the normal range.[47 48] Myocardial native T1 and T2 and central aortic PWV were significantly higher in patients with SLE, whereas the global longitudinal strain (GLS) was reduced ($p<0.001$ for all). LGE was present in 28 (30%) patients with SLE, of whom a minority (6, 7%) were ischaemic in type.[41] Pericardial enhancement and effusion were present in 9 (13%) and 7 (10%) patients (figure 1). Myocardial perfusion imaging in patients with SLE revealed no subjects with regional hypoperfusion due to obstructive epicardial CAD,[40] whereas microvascular disease pattern was observed in 24 (31%).[11]

Hs-TropT levels were detectable in 81% (n=139) of all subjects. A total of 50 (64%) patients with SLE had hs-TropT above the 99th percentile,[45 49] although only 4 (8%) above the clinically relevant threshold >30 ng/L.[49] Compared with controls, patients with SLE had mildly but significantly raised hs-CRP and NT-proBNP and reduced estimated glomerular filtration rate levels ($p<0.01$; table 1). In patients with evidence of myocardial oedema defined as raised native T2 (defined as >2 SD above the mean of the sequence-specific normal range,

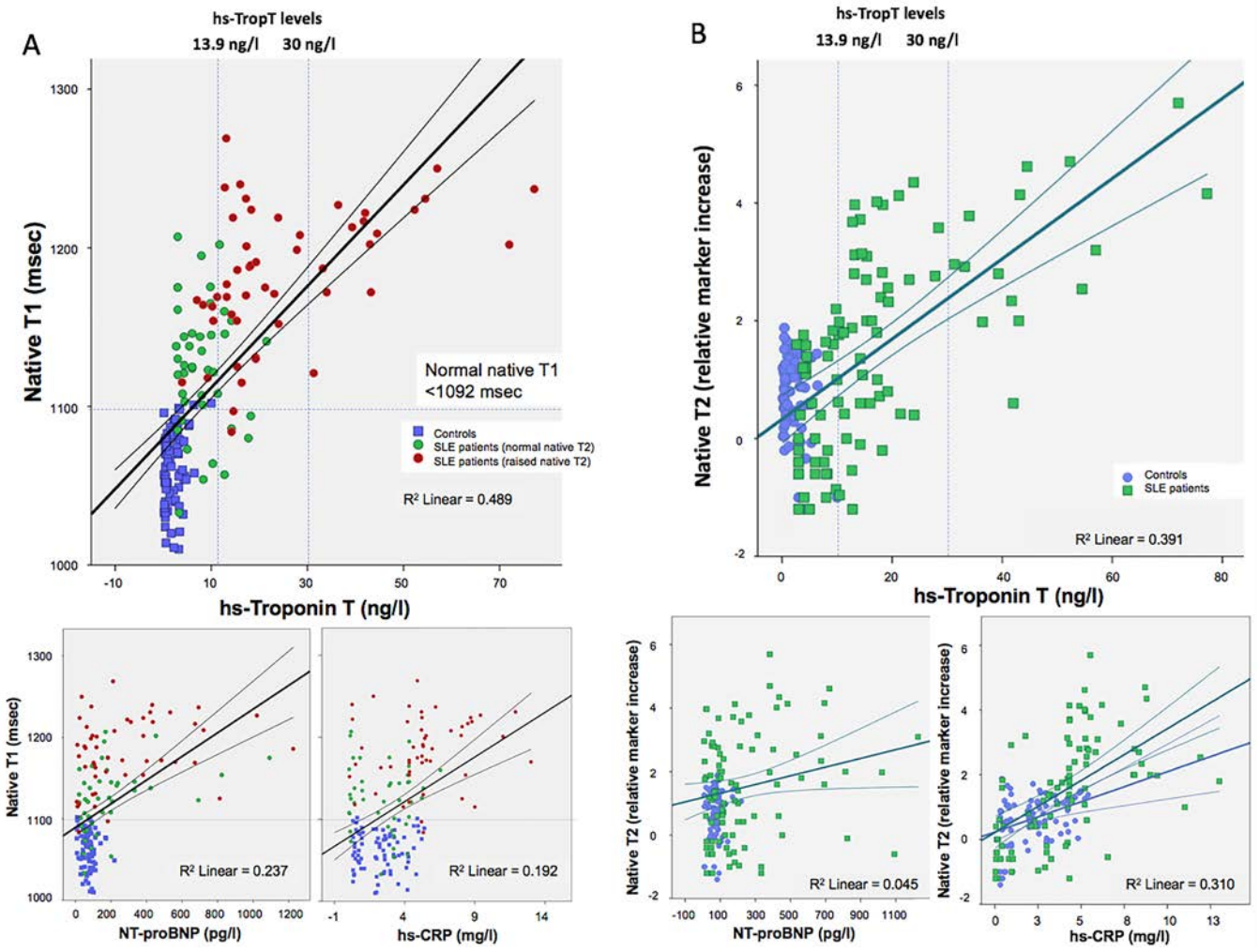

Figure 3 Associations between native T1 (A) and native T2 (B) serological biomarkers. Analytical LoD (13.9 ng/L[45]) and of clinically relevant range in the context of an acute coronary syndrome (30 ng/L[27 49 50]) are marked, as well as the upper limit of LoD (>2 SD above the normal range) for native T1[35] and a relative (sequence-specific) increase in T2, as a proportion of SD of the normal range (SD=2 ms). hs-CRP, high-sensitive C reactive protein; hs-TropT, high-sensitive troponin T; LoD, limits of detection; NT-proBNP, N-terminal pro brain natriuretic peptide; SLE, systemic lupus erythematosus.

n=48 (61%)),[32 33 45] there was also a significant rise in hs-TropT, hs-CRP and NT-proBNP (figure 2).

Analyses of the relationships between hs-TropT, serological markers and CMR measures of CV involvement are presented in table 2 and figures 3 and 4. In controls, hs-TropT levels were mildly associated with native T1 and LVmass (<0.05). In patients with SLE, hs-TropT was associated with native T1 and T2, GLS, E/e', PWV, hs-CRP and NT-proBNP (p<0.01 for all).

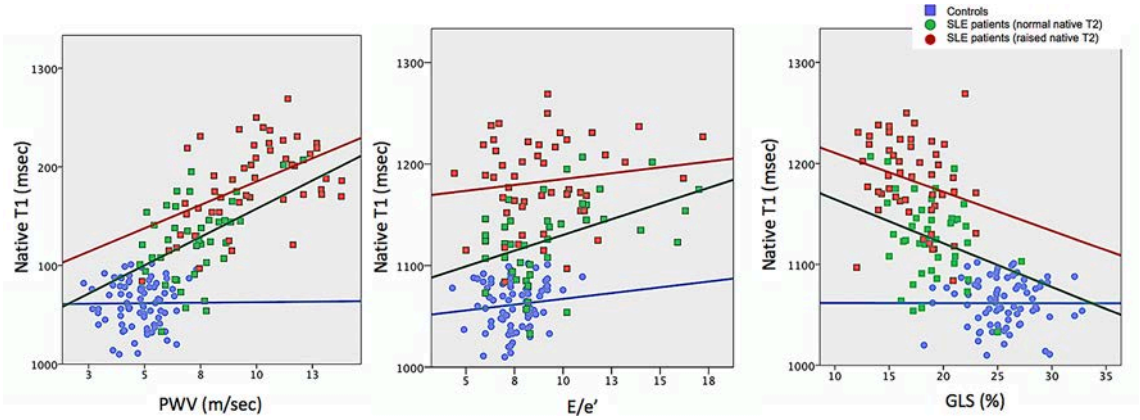

Figure 4 Associations between native T1 and aortic (PWV) and ventricular stiffness (E/e') and global longitudinal strain (GLS) outlining the patient subgroups with evidence of myocardial oedema based on T2 mapping (defined as >2 SD above the mean of the sequence-specific normal range).[32 33 45] PWV, pulse wave velocity; SLE, systemic lupus erythematosus.

Table 3 Histopathological and immunohistochemical (IHC) and results of patients who underwent endomyocardial biopsy following CMR study

Endomyocardial biopsy findings	Case 1	Case 2	Case 3
RV biopsy		+	+
LV biopsy	+		
Cardiomyocytolysis	+	++	+
SM-Aktin+myofibroblasts			
Endomyocardial	+	–	–
Perivascular	+	+	+
Interstitial	+	++	++
Cell infiltration			
Neutrophil	–	–	–
Eosinophil	–	–	–
Giant cell	–	–	–
Lymphocyte B (CD20+)	–	–	+
Lymphocyte T (CD3+)	+	+	+
Macrophage (CD68+, MHC-II+)	++	++	++
Vasculitis (CD34+)	–	–	+
Amyloid (Congo Red staining)	–	–	–
Viral presence (PCR)	–	–	–
Desmin (IHC)	–	–	–
Iron loading (Berlin blue)	–	–	–
Comparative individual results			
Native T1 (ms)	1265	1250	1288
Native T2 (ms)	42	56	46
hs-TropT (pg/mL)	62	76	85

- none, + present-mild, ++ present strong .
CMR, cardiovascular magnetic resonance; hs-TropT, high-sensitive troponin T; LV, left ventricular; RV, right ventricular; SM, smooth muscle.

Furthermore, hs-CRP was associated with PWV (r=0.46), native T1 (r=0.39) and T2 (r=0.56) (p<0.01 for all), but not E/e'. NT-proBNP was moderately associated with PWV (r=0.35), native T1 (r=0.34), native T2 (0.29) and strongly associated with E/e' (r=0.79) and left atrium (LA) area (r=0.60) (p<0.01 for all). In patients with SLE, there was no association with LVmass, left ventricular ejection fraction or left ventricular end-diastolic volume for any of the serological markers. The results of multivariate linear regression analysis (stepwise) of the relationships with hs-TropT are presented in table 2. On the contrary, in patients with SLE, hs-TropT was independently associated with native T2 (χ^2 0.391, p<0.01), followed by the models which also included native T1 and PWV (χ^2 0.462, p<0.01). The relationships between diffuse myocardial remodelling by native T1 and markers of aortic and ventricular stiffness and deformation were significant and accentuated in the subgroups of patients with evidence of myocardial inflammation (figure 3). The results of patients (n=3) who underwent endomyocardial biopsy (EMB) following CMR findings are included in table 3 and figure 5.

DISCUSSION

Patients with SLE and no known or symptomatic cardiac disease have a high prevalence of subclinical myocardial injury, as evidenced by detectable hs-TropT release. The extent of subclinical myocardial injury is independently associated with the relevant components of CV involvement, including myocardial inflammation (by native T2), interstitial remodelling (by native T1), aortic (by PWV) and ventricular stiffness (by E/e'), respectively. There are no relationships between hs-TropT and changes of cardiac function or structure. The role of inflammation as the pathophysiological driver of myocardial injury is further reiterated by a considerably greater rise of hs-TropT (as well as hs-CRP and NT-proBNP) in the subgroup of patients with significantly raised native T2, indicating the presence of oedema (33,34). These findings substantiate the role of CMR with native T1 and T2 mapping and PWV in screening for the presence of subclinical cardiac involvement.

The present observations importantly complement the insights of previous studies in deciphering the natural course of inflammatory cardiomyopathy in patients with SLE.[15 18] The significantly and prevalently raised troponin levels in patients with SLE provide a sensitive validation of the subclinical myocardial injury.[26] We and others have previously shown raised troponin levels in clinically manifest lupus myocarditis (10,16,52-54). In the present study, the post-hoc analysis of systematically collected research blood samples in patients with no known CV involvement reveals detectable troponin release in a majority of patients with SLE, which are on average significantly higher than in non-SLE controls.[28 50] Different from the presentation of an acute coronary syndrome, troponin levels in most patients with SLE remain below the acute coronary syndrome (ACS) threshold (>30 ng/L),[45 49] indicating a much smaller amount of the total myocardial necrosis in SLE myocardial injury, compared with an acute atherosclerotic coronary artery occlusion. This important difference in the underlying pathophysiology—the non-coronary mechanism of myocardial injury in SLE—is further apparent through the absence of a typical ischaemic pattern of LGE, corresponding to a coronary vascular territory. On the contrary, the pattern of myocardial scar (if observed) is non-ischaemic and intramyocardial (41,43) (figure 1). Furthermore, tissue characterisation with native T2 mapping, a sensitive marker of myocardial oedema, is the strongest predictor of hs-TropT release, demonstrating the underlying myocardial inflammation as the main mechanism of injury. hs-TropT levels and native T1 both remain significantly elevated (compared with controls) in patients without significant myocardial oedema (normal native T2), although commonly beyond the abnormal threshold (hs-TropT—13.9 ng/L; native T1—1098 ms; please see the Methods section), indicating the sustained diffuse process of interstitial remodelling and fibrosis.[43 46] These observations correspond with the finding of hs-CRP rise in the group with oedema (raised native T2) but not without, despite it being commonly subdued in SLE.[51–53] A number of previous observations on NT-proBNP levels in patients with SLE, such as associations with echocardiographic LA diameter and aortic stiffness,[54] but not LV structure or function, were also replicated in our study.[55] We expand these observations by demonstrating systematic associations between NT-proBNP with aortic and ventricular stiffness (by PWV and E/e'), and interstitial and inflammatory remodelling (by native T1 and T2). In non-ischaemic cardiomyopathy, myocardial native T1 correlates with the degree of aortic and ventricular stiffness[38 56 57]; similar associations in the present cohort of patients with SLE relate the communality of vascular and myocardial remodelling processes. Our findings also revealed detectable structural LV enlargement (LV-ESV and LVmass) and reduction in global LV and RV function, although not reaching the clinically relevant thresholds nor showing significant association with hs-TropT. Thus, the absence of significant associations between hs-TropT and markers of cardiac structure and function exposes the limited value of methods, such as echocardiography, in detecting early abnormalities or assessment of the subclinical disease. Our observations first communicate the

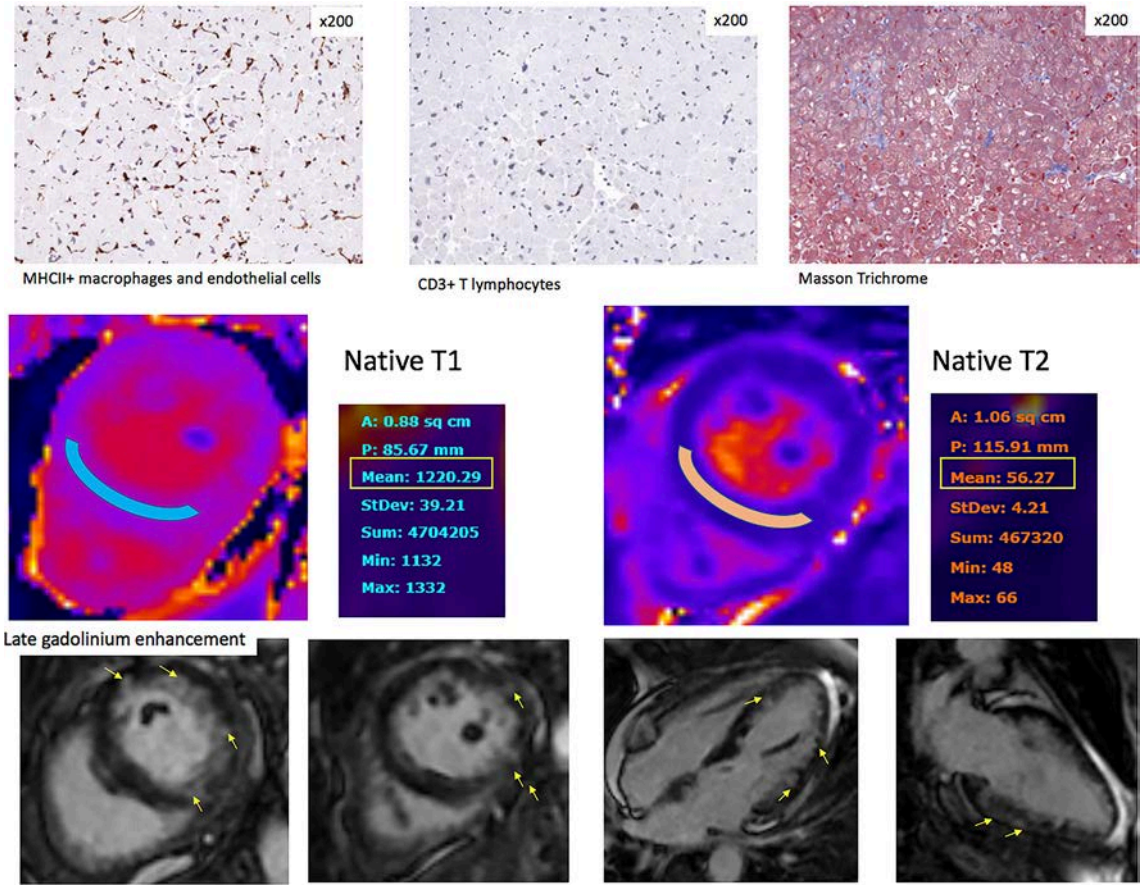

Figure 5 Endomyocardial biopsy findings following CMR involvement (case 1, table 3) showing diffuse macrophage-rich infiltration (CD68+ with expressed MHC II) and interstitial and perivascular fibrosis. No evidence of myocardial infiltration with giant cells, eosinophils or CD20+ B lymphocytes. Histological findings are consistent with active chronic myocarditis. Corresponding CMR images with native T1 and T2 measurements and late gadolinium enhancement. CMR, cardiovascular magnetic resonance; MHC, major histocompatibility complex.

link between the pathophysiological mechanism of myocardial inflammation and CV involvement based on the common direction of change in the serological and imaging measures. Second, native T1 and T2 are quantitative measures of tissue abnormalities, allowing to stratify the degree of inflammatory and interstitial myocardial involvement. Third, whereas significant hs-TropT levels correspond well with the presence of myocardial oedema, 'biochemically low-grade' troponin release (<13.9 ng/L) in patients with diffuse fibrosis but no active inflammation may lead to falsely misclassify this subgroup as having no CV involvement. Native T1 can unravel myocardial abnormalities that develop beyond the analytical limits of detection by the hs-TropT assay (45). Whereas it might be possible to adjust the troponin thresholds to the context of inflammatory injury, further studies are required to establish the sensitivity/specificity ranges, prognostic associations and its ability to change treatment. Troponin identifies patients with sufficiently active inflammation leading to cell necrosis and its release. Also, raised troponin levels may frequently persist over several weeks, obscuring the insight into changes in disease activity or recovery. On the contrary, imaging measures respond rapidly to altered disease dynamics and/or to anti-inflammatory treatment, providing an objective and immediate clinical assessment.[10 56] While not used routinely to support the diagnosis of myocardial involvement in SLE, the results from the few patients who underwent EMB following CMR results corroborate our findings with histological evidence of chronic autoimmune macrophage-rich diffuse interstitial myocardial inflammation and interstitial and perivascular fibrosis.[4]

A few limitations apply. This is a two-centre multivendor observational study with patients on stable treatment, as guided by their systemic and not cardiac disease. Whereas an effect of reduced inflammation due to treatment could not have been fully avoided, we strived for consecutive broad inclusion of subjects with SLE, allowing a balanced and realistic representation of a typical cohort. Standardisation of data acquisition and postprocessing for application of T1 and T2 mapping methods were achieved by unifying the T1 mapping imaging parameters, performing the on-the-fly image quality control and by using centralised postprocessing.[35] Whereas the T2 mapping sequence was different at the two sites, the acquisitions show similar precision and accuracy (ie, sensitivity to inflammatory substrate).[57]

In summary, patients with SLE without known or symptomatic cardiac disease have a high prevalence of subclinical myocardial injury as evidenced by a significant hs-TropT elevation. This is paralleled by a significant rise in hs-CRP and NT-proBNP, as well as of the non-invasive imaging measures of CV inflammatory involvement. We demonstrate a strong and predictive relationship between hs-TropT and non-invasive tissue measures of diffuse myocardial fibrosis and inflammation by native T1 and T2, aortic by PWV, and ventricular stiffness by E/e', respectively, but not changes in cardiac function or structure. Taken together, these findings reveal a significant subclinical CV involvement in patients with SLE, which

is amenable to detection with non-invasive tissue characterisation measures and is directly related to CV inflammatory injury.

Author affiliations
[1]Institute of Experimental and Translational Cardiac Imaging, DZHK Centre for Cardiovascular Imaging, Goethe University Hospital Frankfurt, Frankfurt am Main, Germany
[2]Department of Cardiology, University Hospital Ramon y Cajal de Madrid, Madrid, Spain
[3]Department of Rheumatology, Goethe University Hospital Frankfurt, Frankfurt am Main, Germany
[4]The Louise Coote Lupus Unit, St Thomas' Hospital, London, UK
[5]Department of Cardiology, St Thomas' Hospital, London, UK
[6]Cardiovascular Sciences, King's College London, London, UK
[7]Department of Cardiology, Goethe University Hospital Frankfurt, Frankfurt am Main, Germany
[8]Department of Radiology, Goethe University Hospital Frankfurt, Frankfurt am Main, Germany
[9]Institute for Pathology and Neuropathology, University Hospital Tübingen, Tübingen, Germany

Acknowledgements We would like to acknowledge the support of cardiac radiographers, local cardiology and rheumatology departments at participating centres, and MR clinical scientists, Dr Christian Stehning (Philips), Dr Andreas Greiser (Siemens) and Dr Ralph Strecker (Siemens). We would also like to acknowledge Banher Sandhu (London), Catia Canepa and Franziska Weiss (Frankfurt) for their contribution to clinical data collection.

Contributors All authors have made relevant contributions to this manuscript as outlined by the International Committee of Medical Journal Editors. Substantial contributions to the conception or design of the work; or the acquisition, analysis or interpretation of data for the work: LW, RH, AB, UD, HB, SS, DPD'C, GC-W, MM, KS, CA, KK, TJV, AMZ, EN, VOP. Drafting the work or revising it critically for important intellectual content: LW, RH, AB, UD, HB, EN, VOP. Final approval of the version to be published: LW, RH, AB, UD, HB, SS, DPD'C, GC-W, MM, KS, CA, KK, TJV, AMZ, EN, VOP. Agreement to be accountable for all aspects of the work in ensuring that questions related to the accuracy or integrity of any part of the work are appropriately investigated and resolved: LW, EN, VOP.

Funding Department of Health via the National Institute for Health Research (NIHR) comprehensive Biomedical Research Centre (BRC) award to Guy's and St Thomas' NHS Foundation Trust in partnership with King's College London and King's College Hospital NHS Foundation Trust. Spanish Cardiology Society Fellowship to RH. German Ministry of Education and Research via the German Centre for Cardiovascular Research (DZHK) to VOP, AMZ and EN.

Competing interests None declared.

Patient consent Obtained.

Ethics approval The study protocol was reviewed and approved by the respective local ethics committee (Guy's and St Thomas' Ethics Committee (London site), and Ethikkommission, Goethe University Frankfurt, Germany). All procedures were carried out in accordance with the Declaration of Helsinki.

Provenance and peer review Not commissioned; externally peer reviewed.

REFERENCES

1 Bengtsson C, Ohman ML, Nived O, *et al*. Cardiovascular event in systemic lupus erythematosus in northern Sweden: incidence and predictors in a 7-year follow-up study. *Lupus* 2012;21:452–9.
2 Palmieri V, Migliaresi P, Orefice M, *et al*. High prevalence of subclinical cardiovascular abnormalities in patients with systemic lupus erythematosus in spite of a very low clinical damage index. *Nutr Metab Cardiovasc Dis* 2009;19:234–40.
3 Manzi S, Meilahn EN, Rairie JE, *et al*. Age-specific incidence rates of myocardial infarction and angina in women with systemic lupus erythematosus: comparison with the Framingham Study. *Am J Epidemiol* 1997;145:408–15.
4 Caforio ALP, Adler Y, Agostini C, *et al*. Diagnosis and management of myocardial involvement in systemic immune-mediated diseases: a position statement of the European Society of cardiology working group on myocardial and pericardial disease. *Eur Heart J* 2017;38:2649–62.
5 Winau L, Nagel E, Herrmann E, *et al*. Towards the clinical management of cardiac involvement in systemic inflammatory conditions—a central role for CMR. *Current Cardiovascular Imaging Reports* 2018;11.
6 Mavrogeni S, Karabela G, Stavropoulos E, *et al*. Heart failure imaging patterns in systemic lupus erythematosus. Evaluation using cardiovascular magnetic resonance. *Int J Cardiol* 2014;176:559–61.
7 Maradit-Kremers H, Crowson CS, Nicola PJ, *et al*. Increased unrecognized coronary heart disease and sudden deaths in rheumatoid arthritis: a population-based cohort study. *Arthritis Rheum* 2005;52:402–11.
8 Nicola PJ, Maradit-Kremers H, Roger VL, *et al*. The risk of congestive heart failure in rheumatoid arthritis: a population-based study over 46 years. *Arthritis Rheum* 2005;52:412–20.
9 Puntmann VO, D'Cruz D, Smith Z, *et al*. Native myocardial T1 mapping by cardiovascular magnetic resonance imaging in subclinical cardiomyopathy in patients with systemic lupus erythematosus. *Circ Cardiovasc Imaging* 2013;6:295–301.
10 Hinojar R, Foote L, Sangle S, *et al*. Native T1 and T2 mapping by CMR in lupus myocarditis: Disease recognition and response to treatment. *Int J Cardiol* 2016;222:717–26.
11 Varma N, Hinojar R, D'Cruz D, *et al*. Coronary vessel wall contrast enhancement imaging as a potential direct marker of coronary involvement. *JACC Cardiovasc Imaging* 2014;7:762–70.
12 Selzer F, Sutton-Tyrrell K, Fitzgerald S, *et al*. Vascular stiffness in women with systemic lupus erythematosus. *Hypertension* 2001;37:1075–82.
13 Bessant R, Duncan R, Ambler G, *et al*. Prevalence of conventional and lupus-specific risk factors for cardiovascular disease in patients with systemic lupus erythematosus: a case-control study. *Arthritis Rheum* 2006;55:892–9.
14 Selzer F, Sutton-Tyrrell K, Fitzgerald SG, *et al*. Comparison of risk factors for vascular disease in the carotid artery and aorta in women with systemic lupus erythematosus. *Arthritis Rheum* 2004;50:151–9.
15 Gerster M, Peker E, Nagel E, *et al*. Deciphering cardiac involvement in systemic inflammatory diseases: noninvasive tissue characterisation using cardiac magnetic resonance is key to improved patients' care. *Expert Rev Cardiovasc Ther* 2016;14:1283–95.
16 Zhang Y, Corona-Villalobos CP, Kiani AN, *et al*. Myocardial T2 mapping by cardiovascular magnetic resonance reveals subclinical myocardial inflammation in patients with systemic lupus erythematosus. *Int J Cardiovasc Imaging* 2015;31:389–97.
17 Ntusi NAB, Piechnik SK, Francis JM, *et al*. Diffuse myocardial fibrosis and inflammation in rheumatoid arthritis. *JACC Cardiovasc Imaging* 2015;8:526–36.
18 Mavrogeni S, Spargias C, Bratis C, *et al*. Myocarditis as a precipitating factor for heart failure: evaluation and 1-year follow-up using cardiovascular magnetic resonance and endomyocardial biopsy. *Eur J Heart Fail* 2011;13:830–7.
19 Patel MR, Cawley PJ, Heitner JF, *et al*. Detection of myocardial damage in patients with sarcoidosis. *Circulation* 2009;120:1969–77.
20 Greulich S, Deluigi CC, Gloekler S, *et al*. CMR imaging predicts death and other adverse events in suspected cardiac sarcoidosis. *JACC Cardiovasc Imaging* 2013;6:501–11.
21 Puntmann VO, Isted A, Hinojar R, *et al*. T1 and T2 Mapping in recognition of early cardiac involvement in systemic sarcoidosis. *Radiology* 2017;285:162732.
22 Puntmann VO, D'Cruz D, Taylor PC, *et al*. Contrast enhancement imaging in coronary arteries in SLE. *JACC Cardiovasc Imaging* 2012;5:962–4.
23 Mavrogeni S, Manoussakis MN, Karagiorga TC, *et al*. Detection of coronary artery lesions and myocardial necrosis by magnetic resonance in systemic necrotizing vasculitides. *Arthritis Rheum* 2009;61:1121–9.
24 Ishimori ML, Anderson L, Weisman MH, *et al*. Microvascular angina: an underappreciated cause of SLE chest pain. *J Rheumatol* 2013;40:746–7.
25 Recio-Mayoral A, Mason JC, Kaski JC, *et al*. Chronic inflammation and coronary microvascular dysfunction in patients without risk factors for coronary artery disease. *Eur Heart J* 2009;30:1837–43.
26 Seliger SL, Hong SN, Christenson RH, *et al*. High-sensitive cardiac troponin t as an early biochemical signature for clinical and subclinical heart failure: MESA (Multi-Ethnic Study of Atherosclerosis). *Circulation* 2017;135:1494–505.
27 Thygesen K, Alpert JS, Jaffe AS, *et al*. Third universal definition of myocardial infarction. *J Am Coll Cardiol* 2012;60:1581–98.
28 Liebetrau C, Nef HM, Hamm CW. Troponin: more lessons to learn. *Eur Heart J* 2014;35:338–40.
29 Gladman D, Ginzler E, Goldsmith C, *et al*. The development and initial validation of the systemic lupus international collaborating clinics/American college of rheumatology damage index for systemic lupus erythematosus. *Arthritis Rheum* 1996;39:363–9.
30 Messroghli DR, Radjenovic A, Kozerke S, *et al*. Modified Look-Locker inversion recovery (MOLLI) for high-resolution T1 mapping of the heart. *Magn Reson Med* 2004;52:141–6.
31 Puntmann VO, Voigt T, Chen Z, *et al*. Native T1 mapping in differentiation of normal myocardium from diffuse disease in hypertrophic and dilated cardiomyopathy. *JACC Cardiovasc Imaging* 2013;6:475–84.
32 Bönner F, Janzarik N, Jacoby C, *et al*. Myocardial T2 mapping reveals age- and sex-related differences in volunteers. *J Cardiovasc Magn Reson* 2015;17:9.
33 Giri S, Chung YC, Merchant A, *et al*. T2 quantification for improved detection of myocardial edema. *J Cardiovasc Magn Reson* 2009;11:56.
34 Verhaert D, Thavendiranathan P, Giri S, *et al*. Direct T2 quantification of myocardial edema in acute ischemic injury. *JACC Cardiovasc Imaging* 2011;4:269–78.
35 Dabir D, Child N, Kalra A, *et al*. Reference values for healthy human myocardium using a T1 mapping methodology: results from the International T1 Multicenter cardiovascular magnetic resonance study. *J Cardiovasc Magn Reson* 2014;16:34.

36 Hinojar R, Foote L, Cummins C, *et al*. Standardised postprocessing of native T2 in detection and discrimination of myocarditis - comparison with native T1 mapping. *J Cardiovasc Magn Reson* 2016;18:O14.
37 Hussain ST, Paul M, Plein S, *et al*. Design and rationale of the MR-INFORM study: stress perfusion cardiovascular magnetic resonance imaging to guide the management of patients with stable coronary artery disease. *J Cardiovasc Magn Reson* 2012;14:65.
38 Schulz-Menger J, Bluemke DA, Bremerich J, *et al*. Standardized image interpretation and post processing in cardiovascular magnetic resonance: Society for Cardiovascular Magnetic Resonance (SCMR) board of trustees task force on standardized post processing. *J Cardiovasc Magn Reson* 2013;15:35.
39 Westenberg JJ, de Roos A, Grotenhuis HB, *et al*. Improved aortic pulse wave velocity assessment from multislice two-directional in-plane velocity-encoded magnetic resonance imaging. *J Magn Reson Imaging* 2010;32:1086–94.
40 Puntmann VO, Arroyo Ucar E, Hinojar Baydes R, *et al*. Aortic stiffness and interstitial myocardial fibrosis by native T1 are independently associated with left ventricular remodeling in patients with dilated cardiomyopathy. *Hypertension* 2014;64:762–8.
41 Valbuena-López S, Hinojar R, Puntmann VO. Cardiovascular magnetic resonance in cardiology practice: a concise guide to image acquisition and clinical interpretation. *Rev Esp Cardiol* 2016;69:202–10.
42 Rogers T, Dabir D, Mahmoud I, *et al*. Standardization of T1 measurements with MOLLI in differentiation between health and disease--the ConSept study. *J Cardiovasc Magn Reson* 2013;15:78.
43 Puntmann VO, Carr-White G, Jabbour A, *et al*. T1-Mapping and outcome in nonischemic cardiomyopathy. *JACC Cardiovasc Imaging* 2016;9:40–50.
44 Hor KN, Gottliebson WM, Carson C, *et al*. Comparison of magnetic resonance feature tracking for strain calculation with harmonic phase imaging analysis. *JACC Cardiovasc Imaging* 2010;3:144–51.
45 Giannitsis E, Kurz K, Hallermayer K, *et al*. Analytical validation of a high-sensitivity cardiac troponin T assay. *Clin Chem* 2010;56:254–61.
46 Child N, Suna G, Dabir D, *et al*. Comparison of MOLLI, shMOLLLI, and SASHA in discrimination between health and disease and relationship with histologically derived collagen volume fraction. *Eur Heart J Cardiovasc Imaging* 2018;19:768-776.
47 Kawel-Boehm N, Maceira A, Valsangiacomo-Buechel ER, *et al*. Normal values for cardiovascular magnetic resonance in adults and children. *J Cardiovasc Magn Reson* 2015;17:3.
48 Natori S, Lai S, Finn JP, *et al*. Cardiovascular function in multi-ethnic study of atherosclerosis: normal values by age, sex, and ethnicity. *AJR Am J Roentgenol* 2006;186:S357–S365.
49 Roffi M, Patrono C, Collet J-P, *et al*. ESC Guidelines for the management of acute coronary syndromes in patients presenting without persistent ST-segment elevation. *European Heart Journal* 2015;4:267–315.
50 Heeschen C, Deu A, Langenbrink L, *et al*. Analytical and diagnostic performance of troponin assays in patients suspicious for acute coronary syndromes. *Clin Biochem* 2000;33:359–68.
51 ter Borg EJ, Horst G, Limburg PC, *et al*. C-reactive protein levels during disease exacerbations and infections in systemic lupus erythematosus: a prospective longitudinal study. *J Rheumatol* 1990;17:1642–8.
52 Mok CC, Birmingham DJ, Ho LY, *et al*. High-sensitivity C-reactive protein, disease activity, and cardiovascular risk factors in systemic lupus erythematosus. *Arthritis Care Res* 2013;65:441–7.
53 Firooz N, Albert DA, Wallace DJ, *et al*. High-sensitivity C-reactive protein and erythrocyte sedimentation rate in systemic lupus erythematosus. *Lupus* 2011;20:588–97.
54 Goldenberg D, Miller E, Perna M, *et al*. Association of N-terminal pro-brain natriuretic peptide with cardiac disease, but not with vascular disease, in systemic lupus erythematosus. *Arthritis Rheum* 2012;64:316–7.
55 Chung CP, Solus JF, Oeser A, *et al*. N-terminal pro-brain natriuretic peptide in systemic lupus erythematosus: relationship with inflammation, augmentation index, and coronary calcification. *J Rheumatol* 2008;35:1314–9.
56 Hinojar R, Foote L, Arroyo Ucar E, *et al*. Native T1 in discrimination of acute and convalescent stages in patients with clinical diagnosis of myocarditis. *JACC Cardiovasc Imaging* 2015;8:37–46.
57 Spieker M, Katsianos E, Gastl M, *et al*. T2 mapping cardiovascular magnetic resonance identifies the presence of myocardial inflammation in patients with dilated cardiomyopathy as compared to endomyocardial biopsy. *Eur Heart J Cardiovasc Imaging* 2018;19:574-582.

EXTENDED REPORT

In silico validation of the Autoinflammatory Disease Damage Index

Nienke M ter Haar,[1,2] Amber Laetitia Justine van Delft,[3] Kim Valerie Annink,[3] Henk van Stel,[3] Sulaiman M Al-Mayouf,[4] Gayane Amaryan,[5] Jordi Anton,[6] Karyl S Barron,[7] Susanne Benseler,[8] Paul A Brogan,[9] Luca Cantarini,[10] Marco Cattalini,[11] Alexis-Virgil Cochino,[12] Fabrizio de Benedetti,[13] Fatma Dedeoglu,[14] Adriana Almeida de Jesus,[15] Erkan Demirkaya,[16] Pavla Dolezalova,[17] Karen L Durrant,[18] Giovanna Fabio,[19] Romina Gallizzi,[20] Raphaela Goldbach-Mansky,[15] Eric Hachulla,[21] Veronique Hentgen,[22] Troels Herlin,[23] Michaël Hofer,[24,25] Hal M Hoffman,[26] Antonella Insalaco,[27] Annette F Jansson,[28,29] Tilmann Kallinich,[28] Isabelle Kone-Paut,[30] Anna Kozlova,[31] Jasmin Beate Kuemmerle-Deschner,[32] Helen J Lachmann,[33] Ronald M Laxer,[34] Alberto Martini,[35] Susan Nielsen,[36] Irina Nikishina,[37] Amanda K Ombrello,[38] Seza Özen,[39] Efimia Papadopoulou-Alataki,[40] Pierre Quartier,[41] Donato Rigante,[42] Ricardo Russo,[43] Anna Simon,[44] Maria Trachana,[45] Yosef Uziel,[46] Angelo Ravelli,[47] Grant Schulert,[48,49] Marco Gattorno,[47] Joost Frenkel[3]

Handling editor Josef S Smolen

► Additional material is published online only. To view please visit the journal online (http://dx.doi.org/10.1136/annrheumdis-2018-213725).

For numbered affiliations see end of article.

Correspondence to
Dr Joost Frenkel, Wilhelmina Children's Hospital, University Medical Center Utrecht, Utrecht 3508 AB, The Netherlands; j.frenkel@umcutrecht.nl

Received 7 May 2018
Revised 22 June 2018
Accepted 12 July 2018
Published Online First 4 August 2018

To cite: ter Haar NM, van Delft ALJ, Annink KV, *et al*. *Ann Rheum Dis* 2018;**77**:1599–1605.

ABSTRACT

Introduction Autoinflammatory diseases can cause irreversible tissue damage due to systemic inflammation. Recently, the Autoinflammatory Disease Damage Index (ADDI) was developed. The ADDI is the first instrument to quantify damage in familial Mediterranean fever, cryopyrin-associated periodic syndromes, mevalonate kinase deficiency and tumour necrosis factor receptor-associated periodic syndrome. The aim of this study was to validate this tool for its intended use in a clinical/research setting.

Methods The ADDI was scored on paper clinical cases by at least three physicians per case, independently of each other. Face and content validity were assessed by requesting comments on the ADDI. Reliability was tested by calculating the intraclass correlation coefficient (ICC) using an 'observer-nested-within-subject' design. Construct validity was determined by correlating the ADDI score to the Physician Global Assessment (PGA) of damage and disease activity. Redundancy of individual items was determined with Cronbach's alpha.

Results The ADDI was validated on a total of 110 paper clinical cases by 37 experts in autoinflammatory diseases. This yielded an ICC of 0.84 (95% CI 0.78 to 0.89). The ADDI score correlated strongly with PGA-damage (r=0.92, 95% CI 0.88 to 0.95) and was not strongly influenced by disease activity (r=0.395, 95% CI 0.21 to 0.55). After comments from disease experts, some item definitions were refined. The interitem correlation in all different categories was lower than 0.7, indicating that there was no redundancy between individual damage items.

Conclusion The ADDI is a reliable and valid instrument to quantify damage in individual patients and can be used to compare disease outcomes in clinical studies.

INTRODUCTION

Autoinflammatory diseases (AID) are characterised by seemingly unprovoked, recurrent episodes of inflammation caused by activation of the innate immune system. The four most common monogenic AIDs are cryopyrin-associated periodic syndromes (CAPS), tumour necrosis factor receptor-associated periodic syndrome (TRAPS), mevalonate kinase deficiency (MKD) and familial Mediterranean fever (FMF).[1 2] Chronic inflammation in AIDs may cause irreversible damage in multiple organ systems, such as visual loss, deafness, joint restriction and amyloidosis.[3]

Even though targeted therapy for these AIDs has become available,[4–6] permanent damage may still accumulate before diagnosis or start of therapy. Furthermore, the majority of studies on new biological therapies for AIDs are recently initiated, with limited follow-up, hence the potency of these drugs to prevent or stop the development of damage is not yet known.[3 7 8] The Autoinflammatory Disease Damage Index (ADDI) has been developed to enable assessment of the long-term burden of AIDs in a standardised manner, as a comprehensive tool measuring damage in patients with AIDs.[5] Although developed for the four main monogenic AIDs, the ADDI may potentially also be useful in other diseases with autoinflammatory features.[9 10]

To properly validate a damage index such as the ADDI, several aspects are important: reliability, content validity, face validity, criterion validity and construct validity.[11] A reliable index means that for a given patient, different observers will give the same score; this can be assessed by calculating the interobserver variability (intraclass correlation coefficient, ICC). Content validity tests whether the content of the index truthfully reflects the subject the index applies to. Face validity is the subjective

impression whether a test measures the intended phenomenon. Criterion validity tests whether an index is as good as the gold standard. Construct validity consists of convergent and discriminant validity: convergent validity determines whether an index correlates to a similar index (eg, whether the ADDI correlates to other indices of damage or impairments in daily living), whereas discriminant validity determines whether the index is different from a dissimilar index (eg, the ADDI should not correlate with indices of disease activity).

Continuously during development and validation of the ADDI, content validity, face validity and adherence to the OMERACT principles (truth, discrimination and feasibility) were assessed.[12–14] As a reference standard for disease damage in AIDs is lacking, criterion validity cannot be determined. Physician Global Assessment (PGA) of damage can be considered the best alternative for a gold standard, but it is not a validated measure. Therefore, we decided to use the PGA-damage to assess construct validity rather than criterion validity. Hence, in this study we aimed to investigate the reliability and construct validity, using paper clinical cases of patients with FMF, CAPS, TRAPS and MKD, designed to ensure that all the damage items were adequately covered.

METHODS

Development of the validation plan

Together with an experienced methodologist (HvS), a validation plan was developed. Paper clinical cases were based on real patient data, but modified to protect patient privacy and to ensure that all damage items would be sufficiently represented and different degrees of damage could be tested. Using a pilot with a limited number of cases and expert participants, a preliminary ICC was determined and the final number of cases required for the validation was calculated. All expert physicians who participated in the development of the ADDI (top 40 enrollers in the Eurofever Registry and nine experts from the Americas) were invited to participate in the validation process. One expert involved in the development of paper cases (JF) did not take part in the scoring.

Development of the cases

The cases for validation of the ADDI were derived from anonymised clinical data of patients with confirmed FMF, CAPS, TRAPS and MKD included in the European-based online Eurofever Registry.[15 16] All physicians involved in the Eurofever project (Executive Agency for Health and Consumers, Project No 2007332) were asked to complete follow-up data on patients they had entered in the registry. The registry collects detailed information on all potential organ involvement as well as general features of AIDs. To cover a wide case mix, expert physicians from the Americas were asked to submit their anonymous patient data using a preformed template. The patient information retrieved from the Eurofever Registry and American cases served as a resource for paper clinical case scenarios. Cases were modified to ensure that each ADDI item was represented at least four times. Precautions were made to provide a similar number of cases for each disease and to have cases with different grades of disease activity and damage. All paper cases were checked for comprehensiveness and realistic character by one expert (JF).

Case distribution

The case summaries were distributed via a web-based survey, in which experts completed the ADDI, estimated the degree of disease damage and disease activity using a 10-point PGA-damage and PGA-activity, respectively, and could provide comments. The distribution of cases followed the 'observer-nested-within-subject' design, meaning that a large group of experts all scored a subset of the cases.[11] Each group of four experts scored 10 cases each, a minimum of three doctors was needed per group to calculate the ICC. Additional experts were asked to complete the survey when necessary. An equal proportion of adult and paediatric physicians was ensured in each participant group. Furthermore, each group contained four doctors from different countries and centres.

Definition of damage

Damage is defined as persistent or irreversible change in structure or function, which is present for at least 6 months. Damage items should not be scored if they are attributed to ongoing disease activity. Damage may be the result of prior disease activity, complications of therapy or comorbid conditions that developed after the onset of AID signs and symptoms. If damage has been present for longer than 6 months, but later resolves, it should still be scored in order to capture the damage that was present in the individual for that time period. This definition can be found within in the ADDI in earlier versions of the damage index.[12]

Statistical analysis

Statistical analyses were performed in IBM SPSS Statistics V.21. The total score of the ADDI is the sum of points given for all categories. The ICC was determined to assess the reliability of the damage index as a whole, as well as for the eight categories and all individual items. The ICC determined absolute agreement, for example, whether two different physicians give the exact same score for a given patient, and considered single measures, indicating reliability of a single observer.[11] The ICC was also assessed for the PGA-damage and the PGA-activity, in order to determine whether these measurements would be sufficiently reliable to test construct validity. An ICC of 0.8 or higher was considered indicative for excellent reliability.[11 17] Cronbach's alpha was used to determine possible redundancy of different items (eg, whether two items would score the same damage). An interitem correlation of more than 0.7 was considered to indicate redundancy.[18] A Spearman rank test was used to assess discriminant and convergent validity, correlating the ADDI to PGA-activity and PGA-damage, respectively. A Spearman rank test with r=0.1–0.3 was considered weak, r=0.3–0.5 was considered moderate and r>0.5 was considered strong.[19]

Discussion on the items and definitions

A small team (NMtH, ALJvD, JF) discussed all items with an ICC below 0.7. This discussion encompassed possible explanations for a low score (eg, unclear definition of an item or the lack of a growth chart hampering easy scoring of growth failure). Further, based on experts' comments and suggestions during the scoring, possibilities to improve the item and/or definition were discussed. The initial and refined items were proposed to all experts via a web-based survey and subsequently discussed in an open face-to-face meeting at the Paediatric Rheumatology Congress in Athens (PReS 2017). Consensus was considered achieved if more than 70% of experts agreed.

RESULTS

Pilot

A pilot study with 15 paper cases was completed by four experts. This yielded a preliminary ICC of 0.85 (95% CI 0.70 to 0.94), which implied that a minimum of 90 cases would be needed for

the validation of the ADDI. We therefore decided to assign 110 cases to the experts.

Collection of cases

A total of 120 patients whose follow-up had been documented in the Eurofever Registry were identified, and an additional 20 cases were submitted by non-European experts. By selecting and combining case information, a total of 110 cases were compiled from these 140 cases. The final paper clinical cases included 29 patients with CAPS, 27 with TRAPS, 29 with FMF and 25 with MKD.

Validation

In total, 37 of 44 participants responded. In 10 groups at least three participants responded, which led to 100 cases that could be used for the analyses. Due to insufficient response in one group, these 10 cases could not be used. Each item received a non-zero score (indicating presence of that item) at least 18 times.

Intracluster correlation coefficient

The ICC of the ADDI was 0.84 (95% CI 0.78 to 0.89). This indicates good inter-rater reliability. The ICCs per disease, for different organ systems and the individual damage items are shown in table 1. The highest ICC was found for the item 'hearing loss' (0.86, 95% CI 0.81 to 0.90) exceeding the overall ICC, the lowest ICC was found for the item 'puberty delay' (0.29, 95% CI 0.16 to 0.43).

Construct validity

The ICCs of PGA-damage (0.75, 95% CI 0.67 to 0.81) and PGA-activity (0.62, 95% CI 0.52 to 0.71) were considered sufficiently reliable to determine construct validity. A strong relation was found between the score of the ADDI and PGA-damage (Spearman's r=0.92, 95% CI 0.88 to 0.95, p<0.001, see figure 1). This correlation coefficient indicates that an increase in the ADDI score is strongly associated with an increase in the total estimated damage. The relation between disease activity (PGA-activity) and the ADDI score was much weaker (Spearman's r=0.40, 95% CI 0.21 to 0.55, p<0.001, see figure 2), indicating that the ADDI is not primarily driven by disease activity.

Interitem correlation

In order to assess whether items had too much overlap, interitem correlation was determined using Cronbach's alpha. Of specific interest was the interitem correlation between cognitive impairment (mainly relating to adult patients or adolescents) and developmental delay (mainly relating to paediatric patients), as the experts worried that these might have too much overlap. The interitem correlation between cognitive impairment and developmental delay was 0.66, indicating that there was minimal redundancy. All interitem correlation matrixes can be found in online supplementary table 1a–e.

Comments from the experts

The ADDI was considered a simple and easily applicable tool. The most important feedback during the survey included comments and uncertainties about scoring, for example, due to limited information in the case description (eg, the lack of growth charts to completely assess growth failure), unclear definitions in the ADDI (eg, whether psychiatric comorbidities are part of the item central nervous system (CNS) involvement), or doubts about the severity of organ involvement (eg, severity of visual loss). A full overview of these comments can be found in online supplementary table 2.

Other important comments comprised item scoring (suggesting a higher/lower weighting), or suggestions to refine item definitions. These suggestions were presented to all participants using an online survey. The results of this survey were subsequently discussed in a face-to-face meeting. Following this meeting, the maximum total score of the category 'reproductive' was limited to 2, in order to reduce sex differences in scoring of this category. Furthermore, slight changes were made in the definitions for growth failure, CNS involvement, joint restriction, puberty delay and serosal scarring (online supplementary table 2). The revised ADDI can be found in table 2.

All items were considered truthful, discriminative and feasible; however, doubts were raised about the reliability and feasibility of the scoring of musculoskeletal pain as there is no objective test to assess this. Despite that, it was considered that this particular

Table 1 Intraclass correlation coefficient (ICC) of the total ADDI score in all patients (overall), the ICC of the ADDI in the four different diseases and separate ICCs for each category and damage item. Numbers in brackets indicate the 95% CI

	ICC (95% CI)
Overall	0.84 (0.78 to 0.89)
Per disease	
CAPS	0.82 (0.71 to 0.91)
TRAPS	0.62 (0.39 to 0.80)
FMF	0.84 (0.72 to 0.92)
MKD	0.73 (0.55 to 0.86)
Per category	
Reproductive	0.67 (0.59 to 0.76)
Sub/infertility	0.72 (0.63 to 0.79)
Amenorrhea	0.57 (0.46 to 0.67)
Renal/amyloidosis	0.88 (0.84 to 0.92)
Amyloidosis	0.76 (0.69 to 0.82)
Proteinuria	0.80 (0.73 to 0.85)
Renal insufficiency	0.84 (0.78 to 0.88)
Developmental	0.54 (0.43 to 0.64)
Growth failure	0.57 (0.46 to 0.67)
Puberty delay	0.29 (0.16 to 0.43)
Serosal	0.64 (0.54 to 0.72)
Serosal scarring	0.64 (0.54 to 0.72)
Neurological	0.75 (0.67 to 0.81)
Developmental delay	0.48 (0.37 to 0.60)
Cognitive impairment	0.54 (0.43 to 0.65)
Elevated ICP	0.65 (0.56 to 0.74)
CNS involvement	0.67 (0.58 to 0.75)
Ears	0.86 (0.82 to 0.90)
Hearing loss	0.86 (0.82 to 0.90)
Ocular	0.74 (0.66 to 0.80)
Ocular damage	0.74 (0.66 to 0.80)
Musculoskeletal	0.73 (0.64 to 0.80)
Joint restriction	0.52 (0.41 to 0.63)
Bone deformity	0.74 (0.66 to 0.81)
Osteoporosis	0.86 (0.81 to 0.90)
Musculoskeletal pain	0.47 (0.35 to 0.58)

ADDI, Autoinflammatory Disease Damage Index; CAPS, cryopyrin-associated periodic syndrome; CNS, central nervous system; FMF, familial Mediterranean fever; ICP, intracranial pressure; MKD, mevalonate kinase deficiency; TRAPS, tumour necrosis factor receptor-associated periodic syndrome.

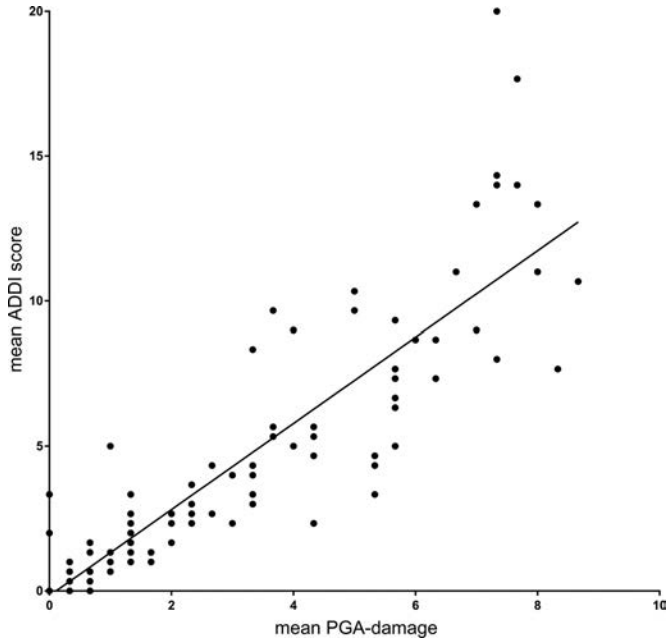

Figure 1 Correlation of the mean ADDI score and the mean score of damage (PGA-damage) per case, assessed by at least three observers. Each dot represents a patient case. The line indicates the correlation. ADDI, Autoinflammatory Disease Damage Index; PGA, Physician Global Assessment.

item was sufficiently valid and very important to patients; therefore it was kept as part of the ADDI.

DISCUSSION

This validation study demonstrates that the ADDI is a reliable tool to measure damage in the four main monogenic AIDs. Most items were considered clearly defined and easy to score.

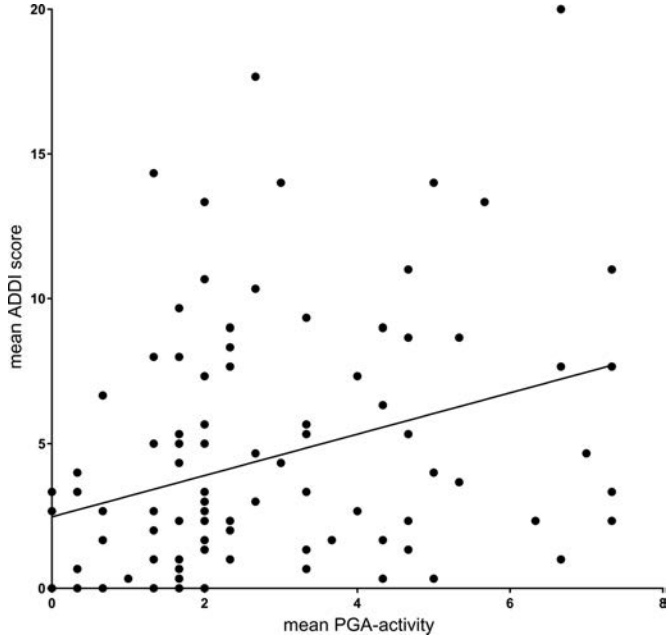

Figure 2 Correlation of the mean ADDI score and the mean score of activity (PGA-activity) per case, assessed by at least three observers. Each dot represents a patient case. The line indicates the correlation. ADDI, Autoinflammatory Disease Damage Index; PGA, Physician Global Assessment.

Further, the ADDI correlated well with the estimated damage and was not strongly influenced by disease activity, indicating good convergent and discriminant validity, respectively. No significant overlap was found between items, therefore all items were included in the final version of the ADDI. Some items were slightly refined, based on comments provided by the clinical experts.

This is the first validation of a disease damage index for AIDs. An ICC of 0.84 is comparable to other damage indices for rheumatic diseases, such as the Juvenile Arthritis Damage Index (ICC 0.85–0.97),[20] Localized Scleroderma Skin Damage Index (ICC 0.99),[21] Cutaneous Lupus Erythematosus Disease Area and Severity Index (ICC 0.86),[22] Vasculitis Damage Index (ICC 0.94)[23] and Combined Damage Assessment (ICC 0.78).[23]

A key strength of this validation study is the participation of adult and paediatric experts worldwide who all provided patient cases and scored the ADDI. This makes it plausible that the ADDI can be used in clinical settings involving paediatric as well as adult patients with FMF, CAPS, TRAPS or MKD. However, the fact that the AID experts scoring the cases were also involved in the development of the ADDI and the collection of patient information might have resulted in a relatively high ICC. Physicians with less knowledge of the tool or AIDs in general might encounter more difficulties interpreting the damage items and scoring the ADDI.

Another strength of this study is the development of cases, which were based on actual patient data while modifications were made to ensure a sufficient representation of all damage items. The total of 110 cases is a large number for validation, given the rarity of these diseases. However, the lack of validation in a real clinical setting is also a drawback of this study. The modification of cases could have resulted in less realistic scenarios. Additionally, scoring paper cases may be easier than applying ADDI in the clinical setting as all the information is summarised and presented in a uniform way. On the other hand, due to the nature of cases (paper clinical instead of real patients) participants may have interpreted data more ambiguously than they would in real life. Scoring anonymous cases, without knowing the patients or being able to ask additional questions, is probably harder than in daily practice. Indeed, comments of the participants reflected some of these difficulties they experienced when assessing the paper cases.

Some important issues could not yet be addressed due to the design of this validation study. The responsiveness to change, that is, whether accrued damage over time is also reflected in an increasing score of the ADDI in an individual patient, could not be determined. A long-term observational study would be needed to measure responsiveness to change and subsequently assess the minimal clinically important difference of the ADDI. Further, convergent validity of the ADDI should preferentially include correlations with scores on quality of life and functional ability, especially because the damage items in the ADDI had been selected for their impact on patients' lives. As the information about quality of life and functional ability was lacking in the Eurofever Registry, this part of the construct validity was impossible to assess. Moreover, ideally the discriminative validity of the ADDI should be assessed by its correlation to a validated activity index, such as the Auto-Inflammatory Disease Activity Index (AIDAI).[24 25] As we could not derive the AIDAI values from the patient data, we used PGA-activity as a surrogate marker. However, the ICC of PGA-activity was low with a broad CI, meaning that this estimate for activity as provided by the experts was not a very reliable measure. This may be explained by the characteristics of these AIDs, for example, episodes of

Table 2 Definitive ADDI including glossary of terms

Damage item	Grading*	Points†
Reproductive		*Max 2*
Sub/infertility		2
Amenorrhea		1
Renal/amyloidosis		*Max 6*
Amyloidosis	Limited/extensive[1]	2/3
Proteinuria		1
Renal insufficiency	Moderate/severe[2]	2/3
Developmental		*Max 3*
Growth failure		2
Puberty delay		1
Serosal		*Max 1*
Serosal scarring		1
Neurological		*Max 6*
Developmental delay		2
Cognitive impairment		3
Elevated intracranial pressure		2
Central nervous system involvement		3
Ears		*Max 2*
Hearing loss	Moderate/severe[3]	1/2
Ocular		*Max 3*
Ocular involvement	Mild/moderate/severe[4]	1/2/3
Musculoskeletal		*Max 4*
Joint restriction		2
Bone deformity		2
Osteoporosis		1
Musculoskeletal pain		1

The total ADDI score is the sum of the eight categories (maximum 27 points).
*Grading: scoring depends on the severity of damage:
[1]Amyloidosis: limited, affecting one organ extensive, affecting more than one organ.
[2]Renal insufficiency: moderate, glomerular filtration rate (GFR) between 15 and 60 mL/min/1.73 m^2; severe, GFR <15 mL/min/1.73 m^2, dialysis or transplantation.
[3]Hearing loss: moderate, hearing impairment without requirement of hearing aids or a cochlear implant; severe, hearing impairment requiring hearing aids or a cochlear implant.
[4]Ocular involvement: mild, ocular damage without visual impairment; moderate, with visual impairment; severe, legal blindness.
†Points are given when the item is present. For items with grading in severity, the lowest score is given for mild involvement and the highest for severe involvement. For each category, the score is limited to a specific maximum.
ADDI, Autoinflammatory Disease Damage Index; Max, maximum.

Glossary of terms

Amenorrhea: Primary amenorrhea: absence of menarche at the age of 16 years or absence of menarche 5 years after the larche in a woman. Secondary amenorrhea: absence of the menses for six consecutive months or more in a woman who previously had menstrual cycles.
Amyloidosis: Symptomatic amyloidosis confirmed by examination of tissue sections by Congo red dye or serum amyloid P component (SAP) scintigraphy.
Bone deformity: Bone deformation or overgrowth on clinical examination and/or imaging studies.
Central nervous system involvement: Focal deficits (gross and/or fine sensorimotor), diffuse deficits (eg, memory, behaviour), seizures and spinal cord symptoms. Neuropsychiatric disorders unrelated to the disease should not be scored.
Cognitive impairment: Requirement of special education because of cognitive impairment or IQ below 70 as defined by neuropsychological assessment (eg, Wechsler Intelligence Scale for Children, WISC) or other age-appropriate equivalents.
Developmental delay$: Failure to reach age-appropriate developmental milestones, including language/speech, motor, social/emotional, and cognitive milestones.
Elevated intracranial pressure: Signs and/or symptoms of elevated intracranial pressure supported by appropriate techniques#.
Growth failure: Defined as the presence of at least two of the three features:

- Lower than the third percentile or −2 SD height for age.
- Growth velocity over 6 months lower than the third percentile or −2 SD for age.
- Crossing at least two centiles (5%, 10%, 25%, 50%, 75%, 90%, 95%) on growth chart.

For patients older than 18 years: Pathological short stature (eg, below third percentile or −2 SD for normal ethnic population).
Hearing loss: Sensorineural hearing impairment of better ear, confirmed by audiometry or another age-appropriate technique, or requirement of hearing aids or a cochlear implant.
Infertility: A disease of the reproductive system defined by the failure to achieve a clinical pregnancy after 12 months or more of regular unprotected sexual intercourse, not due to known disorders in the unaffected partner.
Joint restriction: Fixed limitation in the normal range of motion of joints affecting function, with or without destructive arthropathy or avascular necrosis.
Musculoskeletal pain: Non-inflammatory musculoskeletal pain impairing activities of daily living.
Ocular involvement: Ocular damage (eg, optic nerve atrophy, elevated intraocular pressure or cataract) of better eye, documented by an ophthalmologist, with or without visual impairment.
Osteoporosis: Reduced bone mineral density with vertebral collapse and/or pathological fractures confirmed with imaging, which may include bone densitometry. Requires both evidence of decreased bone density and fracture, 'low bone density' by itself is insufficient.
Proteinuria: Persistent urinary protein-to-creatinine ratio of >20 mg/mmol in the first morning void; and/or a daily protein excretion of >0.3 g/24 hours, or urine albumin-to-creatinine ratio of >15 mg/mmol.
Puberty delay: A Tanner stage below −2 SDs for age or below the third percentile for age or any Tanner stage after pharmacological induction of puberty.
Renal insufficiency: Glomerular filtration rate (GFR) of <60 mL/min/1.73 m^2, dialysis or transplantation.
Serosal scarring: Symptomatic adhesions or fibrosis affecting pericardium, pleura, peritoneum and/or retroperitoneum, supported by imaging techniques, endoscopy or surgery.
$Only for paediatric patients; #such as funduscopy, neuroimaging or lumbar cerebrospinal fluid (CSF) pressure measurement.

febrile attacks with symptom-free periods in-between. Altogether, a long-term prospective study assessing the ADDI, AIDAI and scores of quality of life and functional ability in patients over time is needed to address the above-mentioned issues.

Besides the strong correlation between the ADDI and PGA-damage, the ADDI also moderately correlated to the PGA of disease activity. For a perfect discriminant validity, there would be no correlation between the ADDI and an activity score. However, in this case some degree of correlation is acceptable and probably unavoidable, since patients with more disease activity over the years generally accrue more damage. Furthermore, some items such as hearing loss may (initially) reflect both activity and damage. This overlap is partly prevented by the criterion that an item should be present for at least 6 months to be scored as a damage item. Therefore, disease activity has limited influence on the ADDI score.

Although the overall ICC was >0.8, the ICC of some individual items was less than 0.6. This could be explained by limited information provided in some of the paper cases, less experience of adult rheumatologists with paediatric measures (eg, scoring of pubertal delay) or the more subjective nature of some items (eg, musculoskeletal pain). Indeed, objective items such as hearing loss, renal insufficiency and osteoporosis all had an individual ICC of >0.8. As the overall ICC was good and the nature of the cases may be an important reason for a lower ICC, items scoring less than 0.6 were deemed acceptable, although sometimes with small alterations in the definition. A study testing the ADDI in real-life patients and also by individuals not involved in its development would be needed to overcome the above-mentioned issues.

During the face-to-face meeting, it was suggested to omit musculoskeletal pain from the ADDI, as it seems to be more subjective than the other items. Musculoskeletal pain, and other less objectively scored items such as fatigue and headache, might better be captured by patient-reported outcome measurements (PROM) in addition to the ADDI. A combination with (items from) the juvenile autoinflammatory disease multidimensional assessment report (JAIMAR) is worth considering.[26] However, the JAIMAR is only validated on patients with FMF. Because musculoskeletal pain was emphasised by the patient representatives during the development phase of the ADDI as an important long-term disease burden in their daily activities, it was decided to keep this item in the ADDI, at least until a composite damage assessment including internationally validated PROMs is available.

As we found a relatively high ICC for the PGA-damage among the experts, one could argue that a detailed damage index is not necessary when the PGA is also reliable. However, we would still recommend the use of a damage index, since the physicians scoring the ADDI were considered experts in the area of AIDs, therefore their estimation of damage might be more accurate than that of physicians with less experience. Second, even though the estimates of PGA-damage might be reliable, an estimate of damage on a numerical scale does not give transparent information on why a certain amount of damage was estimated for a patient. The ADDI provides insight to the reasons why a certain level of damage is scored for a patient. Third, the ADDI provides a useful aide memoire and systematic means of collecting and quantifying damage, which is crucial to enable future comparisons between different studies.

Since damage prevention is one of the main purposes in the anti-inflammatory treatment of AIDs, its reliable assessment is an important measure in clinical practice as well as in therapeutic trials. As more information becomes available for the long-term outcomes of AIDs, the ADDI will have to reflect these in a data-driven manner. So far, it can be considered a reliable tool to assess disease damage for the four most commonly encountered monogenic AIDs.

Author affiliations
[1]Laboratory for Translational Immunology, University Medical Centre Utrecht, Utrecht, The Netherlands
[2]Department of Paediatric Immunology and Rheumatology, University Medical Centre Utrecht, Utrecht, The Netherlands
[3]Department of Paediatrics, Universitair Medisch Centrum Utrecht–Locatie Wilhelmina Kinderziekenhuis, Utrecht, The Netherlands
[4]Department of Pediatrics, King Faisal Specialist Hospital and Research Center, Riyadh, Saudi Arabia
[5]National Paediatric Centre for Familial Mediterranean Fever and Gastroenterology Service, Arabkir Medical Centre–Institute of Child and Adolescent Health, Yerevan, Armenia
[6]Paediatric Rheumatology Unit, Hospital Sant Joan de Déu, Barcelona, Spain
[7]Division of Intramural Research and National Institute of Allergy and Infectious Diseases, National Institutes of Health, Bethesda, Maryland, USA
[8]Departments of Paediatrics and Rheumatology, Alberta Children's Hospital, Calgary, Alberta, Canada
[9]Department of Infection, Inflammation and Rheumatology, University College London Institute of Child Health, London, UK
[10]Rheumatology Unit, Department of Medical Sciences, Surgery and Neurosciences, University of Siena, Siena, Italy
[11]Paediatric Clinic, University of Brescia and Spedali Civili di Brescia, Brescia, Italy
[12]Department of Paediatrics, National Institute for Mother and Child Health Alessandrescu-Rusescu, Bucharest, Romania
[13]Division of Rheumatology, Ospedale Pediatrico Bambino Gesù, Rome, Italy
[14]Rheumatology Program, Division of Immunology, Boston Children's Hospital, Harvard Medical School, Boston, Massachusetts, USA
[15]Translational Autoinflammatory Disease Section, NIAMS/NIH, Bethesda, Maryland, USA
[16]Western University Children's Hospital, London Health Sciences Centre, London, UK
[17]Department of Paediatrics and Adolescent Medicine, Charles University, General University Hospital, Praha, Czech Republic
[18]Autoinflammatory Alliance, San Francisco, California, USA
[19]Department of Internal Medicine, Fondazione IRCCS Ca' Granda Ospedale Maggiore Policlinico, Milano, Italy
[20]Department of Paediatric Rheumatology, AOUG Martino, Messina, Italy
[21]Département de Médecine Interne et Immunologie Clinique, Université de Lille, Lille, France
[22]Reference Centre for Autoinflammatory Diseases (CEREMAI), Versailles Hospital, Le Chesnay, France
[23]Departmentof Paediatrics, Aarhus University Hospital, Aarhus, Denmark
[24]Department of Paediatric Rheumatology, University of Lausanne, Lausanne, Switzerland
[25]Departmentof Paediatric Rheumatology, University Hospital of Geneva, Geneva, Switzerland
[26]Department of Paediatrics, University of California, San Diego, California, USA
[27]Dipartimento di Medicina Pediatrica, IRCCS Ospedale Pediatrico Bambino Gesù, Roma, Italy
[28]Paediatric Pneumology and Immunology and Interdisciplinary Centre for Social Paediatrics, Charite University Medicine Berlin, Berlin, Germany
[29]Department of Rheumatology and Immunology, Dr von Hauner Children's Hospital, Ludwig-Maximilians-University, Munich, Germany
[30]Department of Paediatric Rheumatology and CEREMAI, Bicêtre Hospital, APHP, University of Paris Sud, Paris, France
[31]Department of Immunology, Federal Research and Clinical Centre for Paediatric Haematology, Oncology and Immunology, Moscow, Russian Federation
[32]Division of Pediatric Rheumatology, Department of Pediatrics, University Hospital Tübingen, Tübingen, Germany
[33]Division of Medicine, University College London, London, UK
[34]Department of Paediatrics and Medicine, University of Toronto and the Hospital for Sick Children, Toronto, Ontario, Canada
[35]Direzione Scientifica, Istituto Giannina Gaslini, Genova, Liguria, Italy
[36]Paediatric Rheumatology Unit 4272, Rigshospitalet, Copenhagen, Denmark
[37]Department of Paediatric Rheumatic Diseases, VA Nasonova Research Institute of Rheumatology, Moscow, Russian Federation
[38]Inflammatory Disease Section, National Human Genome Research Institute, Bethesda, Maryland, USA
[39]Pediatric Rheumatology, Hacettepe University, Ankara, Turkey
[40]Fourth Department of Pediatrics, Aristotle University of Thessaloniki, Thessaloniki, Greece

[41]Department of Paediatric Immunology–Hematology and Rheumatology Unit and IMAGINE Institute, Institution Necker-Enfants Malades Hospital and Paris Descartes University, Paris, Île-de-France, France
[42]Institute of Paediatrics, Fondazione Policlinico Universitario A Gemelli, Università Cattolica Sacro Cuore, Rome, Italy
[43]Servicio de Inmunología/Reumatología, Hospital de Pediatria Juan P Garrahan, Buenos Aires, Argentina
[44]Department of General Internal Medicine, Radboud Expertise Centre for Immunodeficiency and Autoinflammation, Radboud University Medical Centre, Nijmegen, The Netherlands
[45]Paediatric Immunology and Rheumatology Referral Centre, First Paediatric Clinic, Aristotle University of Thessaloniki, Thessaloniki, Greece
[46]Department of Paediatrics, Meir Medical Centre, Kfar Saba, Israel
[47]Institution Università degli Studi di Genova and G Gaslini Institute, Genova, Italy
[48]Division of Rheumatology, Cincinnati Children's Hospital Medical Center, Cincinnati, Ohio, USA
[49]Department of Pediatrics, University of Cincinnati, Cincinnati, Ohio, USA

Acknowledgements The authors thank Dr Nicolino Ruperto and the PRINTO's staff for their precious collaboration.

Contributors NMtH, ALJvD, KVA and JF designed the study, created the patient cases and wrote the manuscript. HvS contributed to the study design and analysis. KLD represented the patient's perspective. SMAM, GA, JA, KSB, SB, PAB, LC, MC, AVC, FdB, FD, AAdJ, ED, PD, KLD, GF, RG, RGM, EH, VH, TH, MH, HMH, AI, AFJ, TK, IKP, AK, JBKD, HJL, RML, AM, SN, IN, AKO, SO, EPA, PQ, DR, RR, AS, MT, YU, AR, GS, MG and JF provided patient cases and (except for JF) scored the ADDI on the rewritten case scenarios. All authors have read and approved the manuscript.

Funding The project was supported by ERANET-PRIOMEDCHILD RaDiCEA Project No 40-41800-98-007. The Eurofever Registry was funded by the Executive Agency for Health and Consumers (EAHC, Project No 2007332). The consensus meeting was supported by an unrestricted grant by Novartis Pharma.

Disclaimer Novartis Pharma did not have any influence on the selection of participants or on the content of the ADDI/consensus meeting or the reporting of the findings.

Competing interests Novartis Pharma financially supported meetings with the methodologist. PAB: consultancy/speaking fees from Novartis, Roche, SOBI, UCB. FdB: Novartis, Novimmune, Hoffmann-La Roche, SOBI, AbbVie. LC: speaker's fee from Novartis and SOBI. MC: consultancy fees for Novartis, SOBI and Abbvie. KLD: consultancy work for SOBI and Novartis; donations, honorariums and unrestricted grants have been received by the Autoinflammatory Alliance from SOBI, Novartis and Regeneron. RG: consultant for Abbvie. RGM: study support from SOBI, Novartis, Regeneron. VH: honorariums and educational grants from Novartis; honorariums from SOBI. MH: consultant for Novartis. HMH: consultant for Novartis and SOBI; speaker for Novartis. TK: research grant by Novartis; speaker's bureau by Roche, BMS, Novartis and SOBI. JKD: consultant/speaker for Novartis and SOBI, and has received grant support from SOBI and Novartis. RML: ad board and consultant for Abbvie and Novartis. PQ: investigator, consultant and speaker's bureau for Novartis and SOBI. MG: consultant for and unrestricted grants to Eurofever and speaker's fee from SOBI and Novartis. YU: grant/research support from Novartis; consultant for Novartis; speaker's bureau of Abbvie, Neopharm, Novartis, Roche. JF: consultant for Novartis. GS: consulting fees for Novartis. FD: attended to Novartis advisory board meeting.

Patient consent Not required.

Ethics approval Local IRB of each participating centre granted approval to enter patient data in the Eurofever Registry. The present study is a validation of the ADDI; development of the ADDI was approved by the IRB of UMC Utrecht.

Provenance and peer review Not commissioned; externally peer reviewed.

REFERENCES

1 Federici S, Sormani MP, Ozen S, *et al*. Paediatric Rheumatology International Trials Organisation (PRINTO) and Eurofever Project. Evidence-based provisional clinical classification criteria for autoinflammatory periodic fevers. *Ann Rheum Dis* 2015;74:799–805.
2 Masters SL, Simon A, Aksentijevich I, *et al*. Horror autoinflammaticus: the molecular pathophysiology of autoinflammatory disease (*). *Annu Rev Immunol* 2009;27:621–68.
3 Savic S, Dickie LJ, Wittmann M, *et al*. Autoinflammatory syndromes and cellular responses to stress: pathophysiology, diagnosis and new treatment perspectives. *Best Pract Res Clin Rheumatol* 2012;26:505–33.
4 ter Haar NM, Oswald M, Jeyaratnam J, *et al*. Recommendations for the management of autoinflammatory diseases. *Ann Rheum Dis* 2015;74:1636–44.
5 Ter Haar N, Lachmann H, Özen S, *et al*. Treatment of autoinflammatory diseases: results from the Eurofever Registry and a literature review. *Ann Rheum Dis* 2013;72:678–85.
6 Broderick L, Tourangeau LM, Kavanaugh A, *et al*. Biologic modulators in allergic and autoinflammatory diseases. *Curr Opin Allergy Clin Immunol* 2011;11:355–60.
7 Vitale A, Rigante D, Lucherini O, *et al*. Biological treatments: new weapons in the management of monogenic autoinflammatory disorders. *Mediators Inflamm* 2013;2013:939847.
8 Holzinger D, Kessel C, Omenetti A, *et al*. From bench to bedside and back again: translational research in autoinflammation. *Nat Rev Rheumatol* 2015;11:573–85.
9 Damiani G, della Valle V, Iannone M, *et al*. Autoinflammatory Disease Damage Index (ADDI): a possible newborn also in hidradenitis suppurativa daily practice. *Ann Rheum Dis* 2017;76:e25.
10 Annink KV, ter Haar NM, Frenkel J. Response to: 'Autoinflammatory disease damage index (ADDI): a possible newborn also in hidradenitis suppurativa daily practice' by Damiani *et al*. *Ann Rheum Dis* 2017;76:e26.
11 Streiner DL, Norman GR. *Health measurement scales: a practical guide to their development and use*. Oxford University Press: Oxford, 2008.
12 ter Haar NM, Annink KV, Al-Mayouf SM, *et al*. Development of the autoinflammatory disease damage index (ADDI). *Ann Rheum Dis* 2017;76:821–30. BMJ Publishing Group Ltd and European League Against Rheumatism.
13 Boers M, Brooks P, Strand VC, *et al*. The OMERACT filter for outcome measures in rheumatology. *J Rheumatol* 1998;25:198–9.
14 Tugwell P, Boers M, Brooks P, *et al*. OMERACT: An international initiative to improve outcome measurement in rheumatology. *Trials* 2007;8:38.
15 Ozen S, Frenkel J, Ruperto N, *et al*. The Eurofever Project: towards better care for autoinflammatory diseases. *Eur J Pediatr* 2011;170:445–52.
16 Toplak N, Frenkel J, Ozen S, *et al*. An International registry on Autoinflammatory diseases: the Eurofever experience. *Ann Rheum Dis* 2012;71:1177–82.
17 Field AP. *Discovering statistics using IBM SPSS statistics: and sex and drugs and rock 'n' roll*. Los Angeles: SAGE, 2013.
18 Boyle GJ. Does item homogeneity indicate internal consistency or item redundancy in psychometric scales? *Pers Individ Dif* 1991;12:291–4.
19 Cohen J. *Statistical Power Analysis for the Behavioral Sciences*. Hoboken: Taylor and Francis, 1988.
20 Viola S, Felici E, Magni-Manzoni S, *et al*. Development and validation of a clinical index for assessment of long-term damage in juvenile idiopathic arthritis. *Arthritis & Rheumatism* 2005;52:2092–102.
21 Arkachaisri T, Vilaiyuk S, Torok KS, *et al*. Development and initial validation of the Localized Scleroderma Skin Damage Index and Physician Global Assessment of disease Damage: a proof-of-concept study. *Rheumatology* 2010;49:373–81.
22 Albrecht J, Taylor L, Berlin JA, *et al*. The CLASI (Cutaneous Lupus Erythematosus Disease Area and Severity Index): An Outcome Instrument for Cutaneous Lupus Erythematosus. *J Invest Dermatol* 2005;125:889–94.
23 Suppiah R, Flossman O, Mukhtyar C, *et al*. Measurement of damage in systemic vasculitis: a comparison of the Vasculitis Damage Index with the Combined Damage Assessment Index. *Ann Rheum Dis* 2011;70:80–5.
24 Piram M, Frenkel J, Gattorno M, *et al*. A preliminary score for the assessment of disease activity in hereditary recurrent fevers: results from the AIDAI (Auto-Inflammatory Diseases Activity Index) Consensus Conference. *Ann Rheum Dis* 2011;70:309–14.
25 Piram M, Koné-Paut I, Lachmann HJ, *et al*. Validation of the Auto-Inflammatory Diseases Activity Index (AIDAI) for hereditary recurrent fever syndromes. *Ann Rheum Dis* 2014;73:2168–73.
26 Konukbay D, Gattorno M, Yildiz D, *et al*. A novel assessment tool for clinical care of patients with autoinflammatory disease: juvenile autoinflammatory disease multidimensional assessment report. *Clin Exp Rheumatol* 2016;34:129–35.

CONCISE REPORT

Comparing image analysis approaches versus expert readers: the relation of knee radiograph features to knee pain

Luca Minciullo,[1] Matthew J Parkes,[2] David T Felson,[2,3] Timothy F Cootes[1]

Handling editor Josef S Smolen

[1]Division of Informatics, Imaging & Data Sciences, The University of Manchester, Manchester, UK
[2]NIHR Manchester Musculoskeletal Biomedical Research Centre, Manchester University Hospitals NHS Foundation Trust, Manchester Academic Health Science Centre, Manchester, UK
[3]Clinical Epidemiology Research and Training Unit, Boston University School of Medicine, Boston, Massachusetts, USA

Correspondence to
Luca Minciullo, The University of Manchester, Manchester M139PT, UK;
luca.minciullo@manchester.ac.uk

Received 28 March 2018
Revised 12 July 2018
Accepted 14 July 2018
Published Online First 1 August 2018

To cite: Minciullo L, Parkes MJ, Felson DT, *et al*. *Ann Rheum Dis* 2018;**77**:1606–1609.

ABSTRACT

Objectives The relationship between radiographic evidence of osteoarthritis and knee pain has been weak. This may be because features that best discriminate knees with pain have not been included in analyses. We tested the correlation between knee pain and radiographic features taking into account both image analysis features and manual scores.

Methods Using data of the Multicentre Osteoarthritis Study, we tested in a cross-sectional design how well X-ray features discriminated those with frequent knee pain (one question at one time) or consistent frequent knee pain (three questions at three times during the 2 weeks prior to imaging) from those without it. We trained random forest models on features from two radiographic views for classification.

Results X-rays were better at classifying those with pain using three questions compared with one. When we used all manual radiographic features, the area under the curve (AUC) was 73.9%. Using the best model from automated image analyses or a combination of these and manual grades, no improvement over manual grading was found.

Conclusions X-ray changes of OA are more strongly associated with repeated reports of knee pain than pain reported once. In addition, a fully automated system that assessed features not scored on X-ray performed no better than manual grading of features.

INTRODUCTION

Despite considerable effort, the existence of pain has not found to be strongly correlated with radiographic osteoarthritis (OA).[1–5] First, this poor agreement may be because the global measures of radiographic disease that are used in these studies are insensitive to specific features that are better correlated with pain than global scores. Second, these studies have generally been limited to uniplanar radiographs and therefore miss features that are correlated with the presence of pain. Third, some individuals may have knee pain as part of a syndrome of widespread pain and do not have OA. Last, knee pain is often transient and radiographic disease may be more likely in persons in whom it is consistently reported.

Previous studies involve the investigation of correlation between individual structural features such as osteophytes and joint space narrowing (JSN)[2 5 6] and pain. Felson and colleagues[7] gave an alternative definition of OA based on a combination of structural features and showed a modestly improved correlation with pain. Minciullo *et al*[8] used constrained local models (CLMs) to find landmark points for the knee joint in both lateral and PA radiographs and extracted features related to bone shape, texture and their combination to predict onset of knee pain, showing a weak correlation with structural features and suggesting that the lateral view contains features that are significantly more discriminative compared with the PA view. Galvan-Tejada *et al*[1] used radiographs from the osteoarthritis initiative (OAI) to prove that osteophytes are early predictors of joint pain, while joint space reduction is not clearly associated with future joint pain.

The objective of our work was to determine the correlation between knee pain and various sets of radiographic features of OA obtained at the time of the pain report, using both features automatically extracted from knee radiographs and manual grades assigned by clinicians. To do so, we built random forest classifiers using a large collection of features and, unlike most previous works, we used both posteroanterior and lateral radiographs. We also tried combining structural features with image independent features such as age and Body Mass Index (BMI), which are known to increase risk of developing OA.[4] Furthermore, we tried to exclude from the study people who were experiencing widespread pain, under the assumption that such pain may not be due to OA.

METHODS

Images were taken from the Multicentre Osteoarthritis Study (MOST) dataset.[9] Bilateral PA standing flexed and unilateral weight bearing, flexed lateral radiographs were obtained at baseline. At baseline, subjects were asked three times whether they had knee pain, aching or stiffness on most of the last 30 days. First, a telephone screening (TScreen) done roughly 2 weeks before the clinic visit was performed to check eligibility criteria. Second, before the visit, participants filled a Self-Assessed Questionnaire (SAQ) at home. Last, an interview was done as part of the clinical visit (Clinic). We used the TScreen, the Clinic and SAQ variable together to create a measure we called 'Consistent Pain'. By consistent pain, we meant selecting participants who gave the same binary score at all three time points. We used data on right knee pain and right knee imaging findings. We characterised widespread pain as present when the person reported frequent pain above and below the waist and on

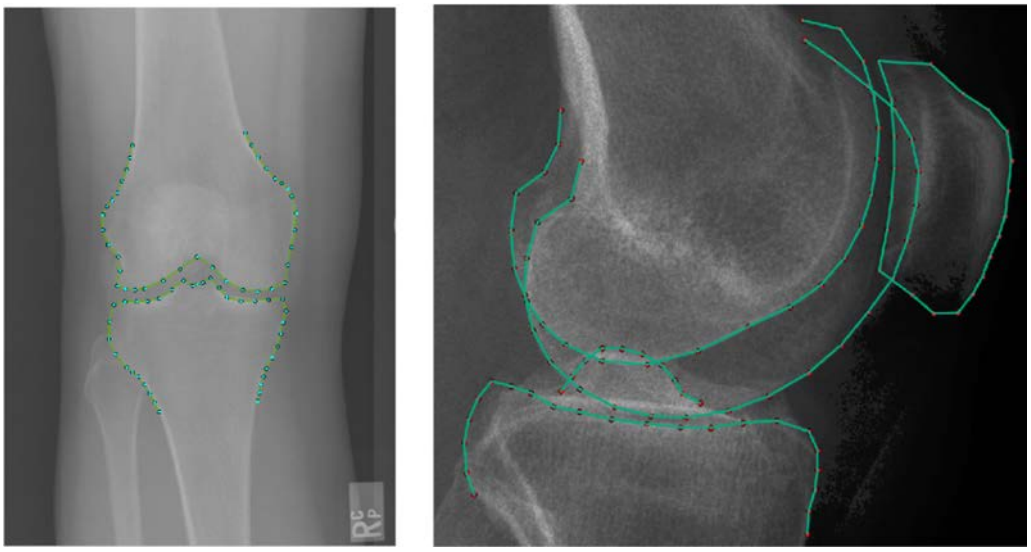

Figure 1 Our model for lateral radiographs (right) was made of four subshapes: the patella (21 points), the lateral femoral condyle (24 points), the medial femoral condyle (25 points) and the tibia (32 points). We considered the femur as the union of the two femoral condyles (49 points). The PA model (left) was made of two shapes: the femur and the tibia (37 points each, a total of 74 points).

both sides of the body and in the axial region. In our experiments, we only considered data from the baseline.

The radiographic grades used in our work were assigned by central readers as part of the MOST study protocol. Two types of features were used in our experiments.

- Manual grades for features of OA assigned by readers during the MOST study. We used scores for all the features that were read on both the PA and lateral views, including Kellgren-Lawrence (KL grades.
- Shape, texture and appearance features automatically extracted using CLMs to find landmark points in radiographs.

CLMs have been successfully applied in medical imaging on a large variety of radiographic images.[8 10 11] Our models for lateral and PA radiographs are shown in figure 1.

Appearance model

We extracted features by building an appearance model. Combined appearance models [12] are an attempt to better use textural information and are based on a statistical model that uses shape as one of its components. Such a model incorporates non-redundant information of the shape and the texture of the object of interest. For full details see Minciullo *et al*.[8]

Object detection and shape model matching

We developed an automatic system to locate the outlines of the bones in both radiographic views. It first finds the position of a bounding box around the joint and then refines this with a shape model matching algorithm—for full details, see Minciullo *et al*, Gall *et al* and Lindner *et al*.[11 13 14]

Analysis approach

First, we tested the relation of individual features and KL grades with the presence of pain. All the experiments were performed training and testing a random forest classifier with 40 trees, running a 5-fold cross validation with five repeats. We used the area under this receiver operator characteristic (ROC)curve to determine the relation of knee pain with radiographic features. We report the SD of the performance evaluated using the AUC over five repetitions.

We compared a single question for frequent knee pain with the same question administered three times in relation to the baseline MOST visit. For the latter approach, we compared people who consistently reported knee pain to those who did not report knee pain at any of the three time points.

The subsequent analyses tested whether automated image analysis generated a higher AUC than did a combination of manually scored features. In addition, we tested whether a combination of information provided by image analysis and manual grading improved on the ROC curve area compared with manual grading alone.

χ^2 tests were used to assess the difference in AUC between the manual scoring (as the gold standard), adding BMI and sex and the best fully automated model. The p value of 0.05 or below was selected to indicate that the ROC curve differed from the gold standard statistically significantly.

RESULTS

We studied 2756 MOST participants at baseline. The mean age was 62.3 years (SD 8) and mean BMI was 30.7 (SD 5.9). Of those studied, 60% were women.

Testing individual radiographic features

There are 36 individual radiographic features (mostly Osteoarthritis Research Society International (OARSI) grades) scored from the PA and lateral radiographs (listed in table 1). For each, we measured the AUC when using the grade as the only feature in a classifier. We observe that KL grade, osteophytes, JSN and sclerosis were the most discriminative with the KL grade achieving the best result. On the other hand, chondrocalcinosis, cyst, attrition and ossification of the patella-tendon performed no better than chance. While some of these results were expected, bone attrition (as MRI feature) was previously found to be associated with OA pain.[5]

Testing combinations of radiographic features

Next we combined all the available manually graded features considering all pain scores defined previously (see table 2). Removing participants with widespread pain made little

Table 1 Testing each radiographic feature individually using the pain score reported during the visit (Clinic)

Variable	AUC (%)
Chondrocalcinosis (OARSI grades 0–1) PF joint on LA view	50±0.3
Osteophytes (OARSI grades 0–3) femur anterior PF joint on LA view	58.3±0.2
Osteophytes (OARSI grades 0–3) femur posterior PF joint on LA view	60±0.5
Joint space narrowing (OARSI grades 0–3) lateral TF compartment on LA view	55.2±0.2
Joint space narrowing (OARSI grades 0–3) medial TF compartment on LAT view	59.1±0.3
Effusion (OARSI grades 0–1) PF joint on LA view	56±0.3
Kellgren & Lawrence (grades 0–4) on PA view	**64.8±0.1**
Chondrocalcinosis (OARSI grades 0–1) lateral TF compartment on PA view	50.4±0.3
Cyst (OARSI grades 0–3) femur lateral TF compartment on PA view	50.6±0.3
Osteophytes (OARSI grades 0–3) femur lateral TF compartment on PA view	60.2±0.2
Sclerosis (OARSI grades 0–3) femur lateral TF compartment on PA view	54.3±0.3
Joint space narrowing (OARSI grades 0–3) lateral TF compartment on PA view	54.9±0.3
Attrition (OARSI grades 0–1) lateral TF compartment on PA view	50.6±0.2
Cyst (OARSI grades 0–3) tibia lateral TF compartment on PA view	50.6±0.2
Osteophytes (OARSI grades 0–3) tibia lateral TF compartment on PA view	60±0.2
Sclerosis (OARSI grades 0–3) tibia lateral TF compartment on PA view	54.2±0.3
Chondrocalcinosis (OARSI grades 0–1) medial TF compartment on PA view	50.7±0.1
Cyst (OARSI grades 0–3) femur medial TF compartment on PA view	50.8±0.3
Osteophytes (OARSI grades 0–3) femur medial TF compartment on PA view	61±0.3
Sclerosis (OARSI grades 0–3) femur medial TF compartment on PA view	57.7±0.2
Joint space narrowing (OARSI grades 0–3) medial TF compartment on PA view	57.7±0.2
Attrition (OARSI grades 0–1) medial TF compartment on PA view	52.1±0.2
Cyst (OARSI grades 0–3) tibia medial TF compartment on PA view	51.5±0.3
Osteophytes (OARSI grades 0–3) tibia medial TF compartment on PA view	59.7±0.2
Sclerosis (OARSI grades 0–3) tibia medial TF compartment on PA view	58.3±0.4
Ossification (OARSI grades 0–3) patella tendon lower PF joint on LA view	49.5±0.1
Ossification (OARSI grades 0–3) patella tendon upper PF joint on LA view	50±0.6
Ossified loose body (OARSI grades 0–1) femur posterior PF joint on LA view	52.2±0.3
Ossification of quadriceps femoris insertion (OARSI grades 0–3) PF joint on LA view	51±0.3
Cyst (OARSI grades 0–3) PF joint on LA view	51±0.2
Joint space narrowing (OARSI grades 0–3) PF joint on LA view	53.2±0.3
Sclerosis (OARSI grades 0–3) PF joint on LA view	53.1±0.4
Osteophytes (OARSI grades 0–3) patella inferior PF joint on LA view	59.5±0.2
Osteophytes (OARSI grades 0–3) patella superior PF joint on LA view	60.1±0.3
Osteophytes (OARSI grades 0–3) tibia anterior PF joint on LA view	55.5±0.1
Osteophytes (OARSI grades 0–3) tibia posterior PF joint on LA view	59.4±0.3

Bold values correspond to the best results.

Table 2 Performance of R classifiers when using all the available clinician grades as features

Features	# Samples	AUC±SD	P value vs Referent
Telephonic screening interview			
Manual grades	2756	62.8±0.4	Referent
Manual Grades+Gender+BMI		66±0.5	**<0.001**
Best automated		63.8±0.2	0.15
Manual+Automated		65.6±0.3	**<0.001**
Removing widespread pain	1374	61±0.2	0.51
Clinic			
Manual grades	2756	66.4±0.2	Referent
Manual Grades+Gender+BMI		68.8±0.2	**<0.001**
Best automated		65.6±0.9	0.29
Manual+Automated		63±0.3	**0.01**
Removing widespread pain	1374	61±0.2	**0.02**
Self-assessed questionnaire (HOME)			
Manual grades	2756	66.7±0.3	Referent
Manual Grades+Gender+BMI		68.9±0.4	**<0.001**
Best automated		67.7±0.3	0.30
Manual+Automated		68±0.2	**0.05**
Removing widespread pain	1374	69±0.2	0.10
Consistent pain (answered yes to pain at all time points)			
Manual grades	1066	73.9±0.5	Referent
Manual Grades+Gender+BMI		**76.1±0.2**	**0.01**
Best automated		73.1±0.7	0.97
Manual+Automated		75.6±0.6	0.14
Removing widespread pain	565	78±1	**0.04**

The p values compare the AUCs with the referent in that pain group. For example, for telephone screening, compared with manual grades, none of the other approaches was significant.* Sometimes these p values show significantly worse AUCs than the referent.
*Comparison eliminating participants with widespread pain was performed using manual grades+Gender+BMI features.
Bold values correspond to the best results.

difference to the manual model, while adding BMI and sex significantly improved the ROC for both Clinic and SAQ pain. The AUCs for consistent pain were higher, especially for manual grades (eg, 73.9 vs 62.8–66.7) and the SD around these estimates were narrow.

When working with each pain score individually, the results show that using the best performing automated model gives results that were not significantly different from those of manual grades.

The combination between manual grades and the appearance features extracted from the model was not more discriminative than manual grades alone.

DISCUSSION

We found that identifying persons with consistent knee pain using manually read radiographic features gave the highest AUC. The best model using features computed automatically from the images could be used to discriminate pain from non-pain, without significant loss in AUC compared with using manual grades. Furthermore, removing participants with widespread pain made the classification better for consistent pain.

The main strengths of this work are (1) the size of the dataset used, one order of magnitude larger than most similar studies, (2) we presented the most comprehensive corpus of experiments looking at correlations between radiographs and symptomatic OA, using both PA and lateral view images, therefore including PF joint[15] and posterior compartments and (3) we explored for the first time OARSI grades of the lateral view of the MOST study and their combination with other radiographic features.

Limitations are the absence of skyline view radiographs, which could provide further discriminative information, but were not acquired during the MOST study. We did not have information

on the duration of knee pain and examined only cross-sectional, not prospective, data. The correlations with more chronic or persistent pain and the impact of other risk factors remain to be determined. The extension of this work to MRI features, that have been shown to be more correlated with symptoms, is a promising addition for future work. Another area of interest will be the search for patterns in fMRI related to pain perception in participants with OA or at risk of developing it.

Acknowledgements The authors would like to thank Raja Ebsim, Luke Chaplin and Manuele Reani for their useful comments.

Contributors LM conceived the project, contributed to the study design, analysed and interpreted data, drafted the article and approved the final version for submission. DTF and TFC conceived and oversaw the project, contributed to the study design, analysed and interpreted data, drafted the article and approved the final version for submission. MJP contributed to the statistical analysis and drafting the paper.

Funding The research leading to these results has received funding from EPSRC Centre for Doctoral Training grant 1512584, NIH AR47785 and AG18820. The study was also funded by an NIHR Biomedical Research Centre Grant to the University of Manchester.

Competing interests None declared.

Patient consent Not required.

Ethics approval This study was conducted in accordance with the declaration of Helsinki, Good Clinical practices and applicable regulatory requirements.

Provenance and peer review Not commissioned; externally peer reviewed.

REFERENCES

1 Galvan-Tejada J I, Trevino V, Celaya-Padilla JM, *et al*. Knee Osteoarthritis pain prediction from X-ray imaging: Data from Osteoarthritis Initiative. *2014 International Conference on Electronics, Communications and Computers (CONIELECOMP)*: IEEE, 2014:194–9.
2 Hannan MT, Felson DT, Pincus T. Analysis of the discordance between radiographic changes and knee pain in osteoarthritis of the knee. *J Rheumatol* 2000;27:1513 7.
3 Silverwood V, Blagojevic-Bucknall M, Jinks C, *et al*. Current evidence on risk factors for knee osteoarthritis in older adults: a systematic review and meta-analysis. *Osteoarthritis Cartilage* 2015;23:507–15.
4 Szebenyi B, Hollander AP, Dieppe P, *et al*. Associations between pain, function, and radiographic features in osteoarthritis of the knee. *Arthritis Rheum* 2006;54:230–5.
5 Lanyon P, O'Reilly S, Jones A, *et al*. Radiographic assessment of symptomatic knee osteoarthritis in the community: definitions and normal joint space. *Ann Rheum Dis* 1998;57:595–601.
6 Bedson J, Croft PR. The discordance between clinical and radiographic knee osteoarthritis: a systematic search and summary of the literature. *BMC Musculoskelet Disord* 2008;9:116.
7 Felson DT, McAlindon TE, Anderson JJ, *et al*. Defining radiographic osteoarthritis for the whole knee. *Osteoarthritis Cartilage* 1997;5:241–50.
8 Minciullo L, Thomson J, Cootes TF. Combination of lateral and PA view radiographs to study development of knee OA and associated pain. *Inter Soc Opt Photonics* 2017.
9 Felson DT, Niu J, Neogi T, *et al*. *Synovitis and the risk of knee osteoarthritis: the MOST Study*: Osteoarthritis and Cartilage, 2015.
10 Lindner C, Thiagarajah S, Wilkinson JM, *et al*. Accurate bone segmentation in 2d radiographs using fully automatic shape model matching based on regression-voting. In: *International conference on medical image computing and computer-assisted intervention*: Springer, 2013b:181–9.
11 Minciullo, Luca and Cootes, Tim. Fully automated shape analysis for detection of Osteoarthritis from lateral knee radiographs. In: *2016 23rd International Conference on Pattern Recognition (ICPR)*: IEEE, 2016:3787–91.
12 Cootes TF, Taylor CJ, *et al*. Statistical models of appearance for computer vision. 2004.
13 Gall, Juergen and Lempitsky, Victor. Class-specific hough forests for object detection. In: *Decision forests for computer vision and medical image anal ysis*: Springer, 2013:143–57.
14 Lindner C, *et al*. "Robust and accurate shape model matching using random forest regression-voting." IEEE transactions on pattern analysis and machine intelligence. 2015;37:1862–74.
15 McAlindon TE, Snow S, Cooper C, *et al*. Radiographic patterns of osteoarthritis of the knee joint in the community: the importance of the patellofemoral joint. *Ann Rheum Dis* 1992;51:844–9.

EXTENDED REPORT

Glucocorticoid receptor in stromal cells is essential for glucocorticoid-mediated suppression of inflammation in arthritis

Mascha Koenen,[1] Stephan Culemann,[2,3] Sabine Vettorazzi,[1,2] Giorgio Caratti,[1] Lucien Frappart,[2,4] Wolfgang Baum,[3] Gerhard Krönke,[3] Ulrike Baschant,[2,5] Jan P Tuckermann[1,2]

Handling editor Josef S Smolen

► Additional material is published online only. To view please visit the journal online (http://dx.doi.org/10.1136/annrheumdis-2017-212762).

For numbered affiliations see end of article.

Correspondence to
Dr Ulrike Baschant; Ulrike.Baschant@uniklinikum-dresden.de and Professor Jan P Tuckermann, Institute for Comparative Molecular Endocrinology, University of Ulm, Ulm 89081, Germany; jan.tuckermann@uni-ulm.de

UB and JPT contributed equally.

For Presented at statement see end of article.

Received 28 November 2017
Revised 31 May 2018
Accepted 19 June 2018
Published Online First
11 July 2018

To cite: Koenen M, Culemann S, Vettorazzi S, *et al*. *Ann Rheum Dis* 2018;**77**:1610–1618.

ABSTRACT

Background Glucocorticoid (GC) therapy is frequently used to treat rheumatoid arthritis due to potent anti-inflammatory actions of GCs. Direct actions of GCs on immune cells were suggested to suppress inflammation.

Objectives Define the role of the glucocorticoid receptor (GR) in stromal cells for suppression of inflammatory arthritis.

Methods Bone marrow chimeric mice lacking the GR in the hematopoietic or stromal compartment, respectively, and mice with impaired GR dimerisation (GR^{dim}) were analysed for their response to dexamethasone (DEX, 1 mg/kg) treatment in serum transfer-induced arthritis (STIA). Joint swelling, cell infiltration (histology), cytokines, cell composition (flow cytometry) and gene expression were analysed and RNASeq of wild type and GR^{dim} primary murine fibroblast-like synoviocytes (FLS) was performed.

Results GR deficiency in immune cells did not impair GC-mediated suppression of STIA. In contrast, mice with GR-deficient or GR dimerisation-impaired stromal cells were resistant to GC treatment, despite efficient suppression of cytokines. Intriguingly, in mice with impaired GR function in the stromal compartment, GCs failed to stimulate non-classical, non-activated macrophages ($Ly6C^{neg}$, $MHCII^{neg}$) and associated anti-inflammatory markers CD163, CD36, AnxA1, MerTK and Axl. Mice with GR deficiency in FLS were partially resistant to GC-induced suppression of STIA. Accordingly, RNASeq analysis of DEX-treated GR^{dim} FLS revealed a distinct gene signature indicating enhanced activity and a failure to reduce macrophage inflammatory protein (Mip)-1α and Mip-1β.

Conclusion We report a novel anti-inflammatory mechanism of GC action that involves GR dimerisation-dependent gene regulation in non-immune stromal cells, presumably FLS. FLS control non-classical, anti-inflammatory polarisation of macrophages that contributes to suppression of inflammation in arthritis.

INTRODUCTION

Rheumatoid arthritis (RA) is characterised by severe infiltration of various immune cells into the joints and a tight interplay of these immune cells with non-immune stromal cells, like fibroblast-like synoviocytes (FLS).[1 2] Pro-inflammatory cytokines secreted by immune cells result in the activation, hyperproliferation and cytokine secretion of FLS. RA is mainly medicated with glucocorticoids (GC)[3 4] due to their strong immune suppressive effects, however, long-term usage is compromised by severe side effects such as osteoporosis, insulin resistance and GC resistance.[5 6] A better understanding of the cell type-specific actions of GCs will provide rationales for specialised treatment strategies to overcome these negative side effects.

GCs act via the glucocorticoid receptor (GR), a nuclear receptor that operates as ligand-induced transcription factor acting as a homodimer or monomer. The dimeric GR directly interacts with GC-response elements on the DNA, mainly inducing gene expression, a mechanism called transactivation. GR dimers are strong inducers of metabolic genes and were considered to be mainly responsible for side effects.[7] The monomeric GR binds either directly to DNA[8 9] or indirectly via transcription factors (eg, NF-κB and AP-1) leading in the latter case to transrepression of gene activity. Previously, transrepression in immune cells was considered to mediate the anti-inflammatory effects of GCs.[7] This view, however, was challenged by recent studies with mice harbouring an impaired GR dimerisation (GR^{dim}),[10] which fail to suppress inflammation in response to GCs in lethal inflammation[11 12] acute lung injury[13] and antigen-induced arthritis (AIA).[14]

Non-immune cells, in particular FLS, were reported to exhibit a strong decrease of inflammatory mediators on GC treatment *in vitro*.[15 16] Whether direct GC actions on these stromal cells contribute to the suppression of inflammation *in vivo* is still unknown. Thus, we addressed this question in a T cell independent model of arthritis, the serum transfer-induced arthritis (STIA) model.

Herein, we show that direct actions of GCs on immune cells are not sufficient to reduce inflammation in STIA, whereas intact GR dimerisation in stromal cells such as FLS is required to increase proportion of non-classical $Ly6C^{neg}$, $MHCII^{neg}$ macrophages, and to suppress STIA.

METHODS

Methods are available in the online supplementary methods.

Statistics

Results are presented as mean±SEM and statistical analysis was performed with two-way

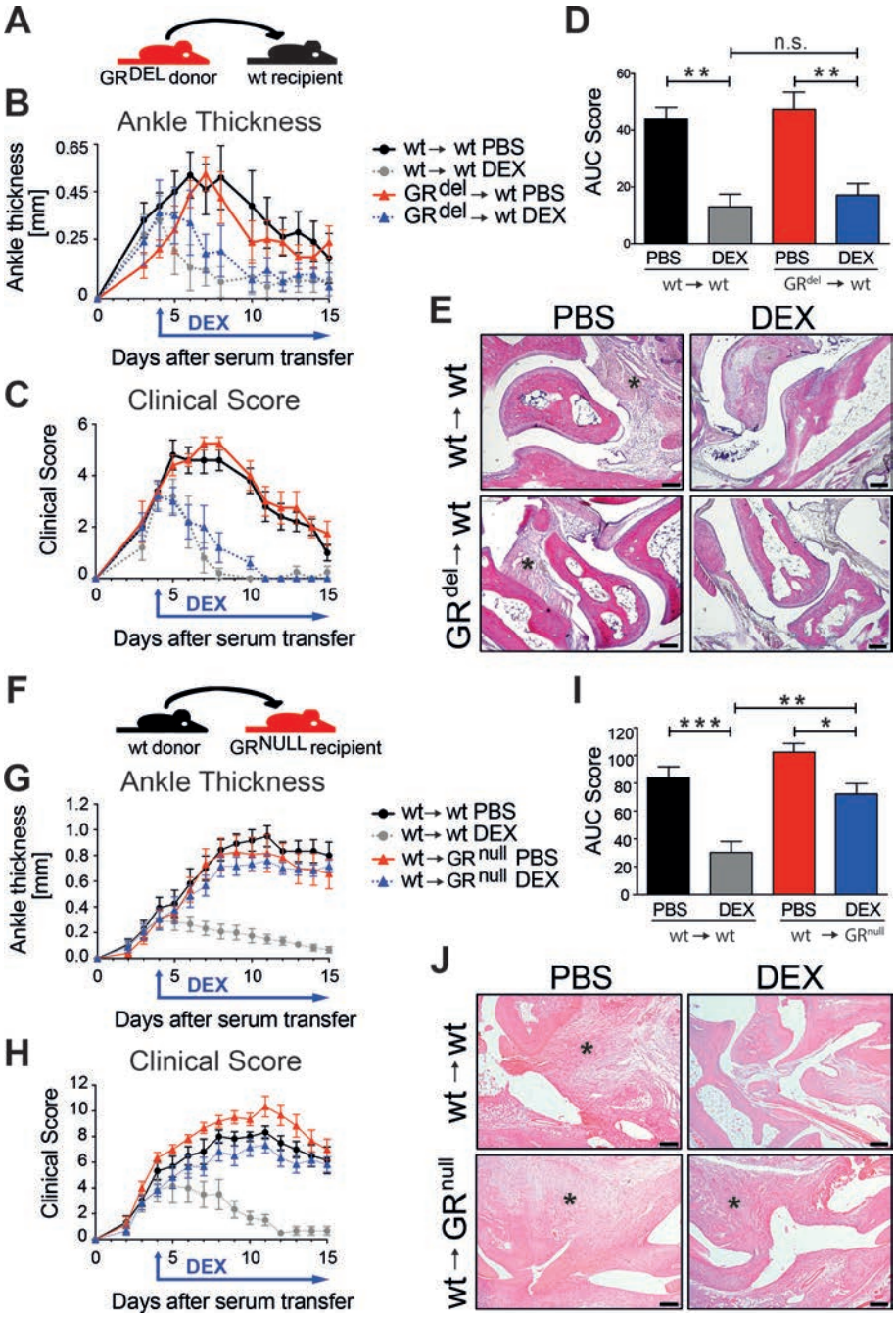

Figure 1 GR deficiency in stromal cells abrogates anti-inflammatory effects of glucocorticoid (GC) treatment in serum transfer-induced arthritis (STIA). (A) Scheme of fetal liver cell transfer into irradiated wt recipient mice. Mice were either reconstituted with wt donor fetal liver cells (wt→wt) or with GR-deficient donor fetal liver cells (GR^{del}→wt). (B) Ankle thickness and (C) clinical score of mice treated with PBS (black and red) or DEX (grey and blue). (D) AUC of the clinical score of mice treated with PBS (black and red) or DEX (grey and blue). (E) H&E staining of paraffin sections of hind paws of wt→wt and GR^{del}→wt mice (scale bar=200 µm); asterisks show the area of inflammation. Group size n=5 mice per group. (F) Scheme of bone marrow transplantation of irradiated wt and GR-deficient recipients with wt donor bone marrow cells (wt→wt and wt→GR^{null}). (G) Ankle thickness and (H) clinical score of mice treated with PBS (black and red) or DEX (grey and blue). (I) AUC of the clinical score of mice treated with PBS (black and red) or DEX (grey and blue). (J) H&E staining of paraffin sections of hind paws of wt→wt and wt→GR^{null} mice (scale bar=200 µm); asterisks show area of inflammation. Group size n=5 mice per group. AUC, area under the curve; DEX, dexamethasone; GR, glucocorticoid receptor; ns, not significant; PBS, phosphate buffered saline; wt, wild type.

analysis of variance (ANOVA), followed by Tukey's post hoc test (multiple comparisons for qRT-PCR, flow cytometry and area under the curve), with one-way ANOVA (ankle swelling) and a two-tailed Student's t-test (cytokine analysis, efferocytosis measurements and cartilage and bone destruction).

RESULTS

Functional GR in stromal cells is crucial to mediate the anti-inflammatory effects of GC treatment

First, we tested whether GCs act directly on immune cells to suppress inflammation by using the STIA model. To eliminate

radiosensitive immune cells, we irradiated wild-type (wt) recipient mice and reconstituted them with fetal liver cells of GR-deficient donor mice (GR^{del}→wt) and as control with cells of wt donor mice (wt →wt) (figure 1A). GR^{del}→wt mice were deficient for the GR in the haematopoietic compartment (online supplementary figure 1A). The absence of GR in radiosensitive immune cells did not lead to differences in the onset or progression of STIA in wt→wt and GR^{del}→wt mice (figure 1B–D). Surprisingly, daily GC treatment starting at day 4 efficiently reduced ankle thickness (figure 1B) and clinical score (figure 1C,D), as well as infiltrating immune cells (figure 1E) in wt→wt and GR^{del}→wt mice. Thus, deletion of the GR in radiosensitive immune cells had no influence on GC therapy of STIA. Next, we generated mice with GR deletion in the radioresistant compartment by using irradiated tamoxifen-inducible GR^{flox}; Rosa-26-Cre ERT ('GR^{null}') mice as recipients and reconstituted them with wt bone marrow (wt→GR^{null} and wt→wt, figure 1F) (online supplementary figure 1B). GR-deficient mice with a GR competent haematopoietic system (wt→GR^{null}) had a strongly attenuated response to dexamethasone (DEX) treatment compared with DEX-treated wt→wt controls assessed by ankle thickness (figure 1G), clinical score (figure 1H,I) and cellular infiltration (figure 1J). Cartilage and bone injury was strongly reduced by DEX in wt→wt mice, and to a lesser extent in wt→GR^{null} mice (online supplementary figure 2). In conclusion, GR expression in stromal cells is crucial for anti-inflammatory action of GCs.

The anti-inflammatory actions of GC treatment require intact GR dimerisation in stromal cells

To test the impact of intact GR dimerisation on exogenous GC exposure in STIA, we analysed mice with an impaired GR dimerisation (GR^{dim}). In contrast to wt mice, GR^{dim} mice were resistant to DEX treatment in STIA reflected by sustained inflammation (figure 2A–D). Cartilage and bone injury was less reduced in DEX-treated GR^{dim} mice as compared with wt mice (online supplementary figure 3).

To address whether the necessity of GR dimerisation for suppression of inflammation is restricted to stromal cells, we analysed lethal irradiated GR^{dim} mice that received wt bone marrow (figure 2E, online supplementary figure 1C). In contrast to control mice (wt→wt), GR^{dim} mice with a wt haematopoietic compartment (wt→GR^{dim}) did not respond to DEX treatment in STIA (figure 2F–I). Thus, GR dimerisation in stromal cells is essential to suppress inflammation in arthritis.

Loss of GR dimerisation in stromal cells has no effect on cytokine suppression

Since suppression of cytokines is a hallmark of the anti-inflammatory activities of GCs, we determined serum cytokine levels after 72 hours of DEX treatment in wt→wt and wt→GR^{dim} chimeric mice. Despite the fact that wt→GR^{dim} mice were resistant to GC therapy (figure 3A, online supplementary figure 1D), we observed a reduction of interleukin (IL)-1β, tumour necrosis factor (TNF)α and interferon-γ in both wt→wt and wt→GR^{dim} mice (figure 3B). Thus, GC-mediated suppression of cytokines is insufficient to fully suppress STIA.

GR dimers in stromal cells induce non-classical, non-activated macrophages

Flow cytometry analysis of joints of wt→wt and wt→GR^{dim} mice after DEX treatment (figure 4 and online supplementary figure 5) revealed a significant reduction of the fraction of infiltrating leucocytes ($CD45^{pos}$) and myeloid cells ($CD11b^{pos}$) in DEX-treated wt→wt mice, but not in wt→GR^{dim} mice (figure 4A). Neutrophils ($CD45^{pos}$, $CD11b^{pos}$, $Ly6G^{pos}$) and T cells ($CD45^{pos}$, $CD3^{pos}$) were not changed in wt→wt or wt→GR^{dim} mice (figure 4A). In addition, the fraction of classical activated macrophages ($Ly6C^{pos}$, $F4/80^{pos}$ and $F4/80^{pos}$, $MHCII^{pos}$) of $CD11b^{pos}$ cells (figure 4B) was also unchanged. Strikingly, we detected a strong and significant induced fraction of non-classical ($CD11b^{pos}$, $Ly6C^{neg}$, $F4/80^{pos}$) and non-activated macrophages ($CD11b^{pos}$, $F4/80^{pos}$, $MHCII^{neg}$) (figure 4B). This was supported by an increased ratio of non-activated macrophages to activated macrophages ($MHCII^{neg}/MHCII^{pos}$) in DEX-treated wt→wt mice, but not in wt→GR^{dim} mice (figure 4C).

Accordingly, anti-inflammatory macrophage marker gene expression (CD163, CD36, AnxA1, Axl and MerTK) was induced in DEX-treated wt→wt mice but not in wt→GR^{dim} mice (figure 5A,B). Of note, complete GR^{dim} mice treated with DEX showed a comparable lack of upregulation of CD163, CD36 and Axl mRNA expression (online supplementary figure 6). Thus, in STIA DEX treatment increases the fraction of non-classical, non-activated anti-inflammatory macrophages dependent on GR dimerisation in stromal cells.

GR deficiency in FLS delays GC-induced suppression of STIA

Next, we addressed to which extent the GR in FLS mediates the GC-induced suppression of inflammation in STIA. We therefore crossed GR^{flox} mice to Col1a2CreERT mice[17] to generate tamoxifen-inducible GR^{flox}; Col1a2-$CreERT^{tg/+}$ mice ($GR^{Col1a2\text{-}CreERT}$). We observed a strong reduction of GR mRNA expression in FLS isolated from the joints (online supplementary figure 7A) and reduced GR protein expression in cadherin-11 positive cells (online supplementary figure 7B). Subsequently, we subjected these mice to STIA and started DEX treatment after STIA induction when an ankle thickness of 0.93±0.12 and 0.89±0.11 mm was reached in mutant and control mice. Strikingly, DEX treatment of $GR^{Col1a2\text{-}CreERT}$ mice resulted in a delayed and reduced reduction of the ankle thickness and clinical score compared with GR^{flox} littermates (figure 6A,B). Histological analysis revealed ongoing infiltration of immune cells in the joints of DEX-treated $GR^{Col1a2\text{-}CreERT}$ mice, where inflammatory infiltration was resolved in DEX-treated GR^{flox} mice (figure 6C). Thus, deletion of the GR in FLS reduces the anti-inflammatory responsiveness towards DEX treatment in STIA.

As FLS sustain inflammation in arthritis in tight interplay with macrophages, we subsequently analysed to which extent impaired GR dimerisation in FLS changes the effects of GCs on macrophage function. We therefore cultured wt and GR^{dim} FLS with GR-deficient macrophages treated with IL1β and DEX and determined their capacity of efferocytosis of labelled apoptotic T lymphocytes. DEX-treated cocultures of wt FLS and macrophages showed a small, but significant increase of efferocytosis that was absent in cultures of macrophages with GR^{dim} FLS (online supplementary figure 8). Next we analysed the transcriptome of wt and GR^{dim} FLS treated with IL-1β and DEX by RNASeq. We found 346 genes upregulated and 212 genes downregulated in GR^{dim} FLS compared with wt FLS. Among these genes, classically known GR-target genes such as Gilz, Metallothionein-1 and 2 and Fkbp5 were strongly induced in wt FLS treated with IL-1β and DEX, whereas in GR^{dim} FLS these genes were significantly less induced (online supplementary figure 9A). Enriched KEGG pathways included cell cycle, cell adhesion, extracellular matrix (ECM)-receptor interaction and others, indicating a higher activity of GR^{dim}

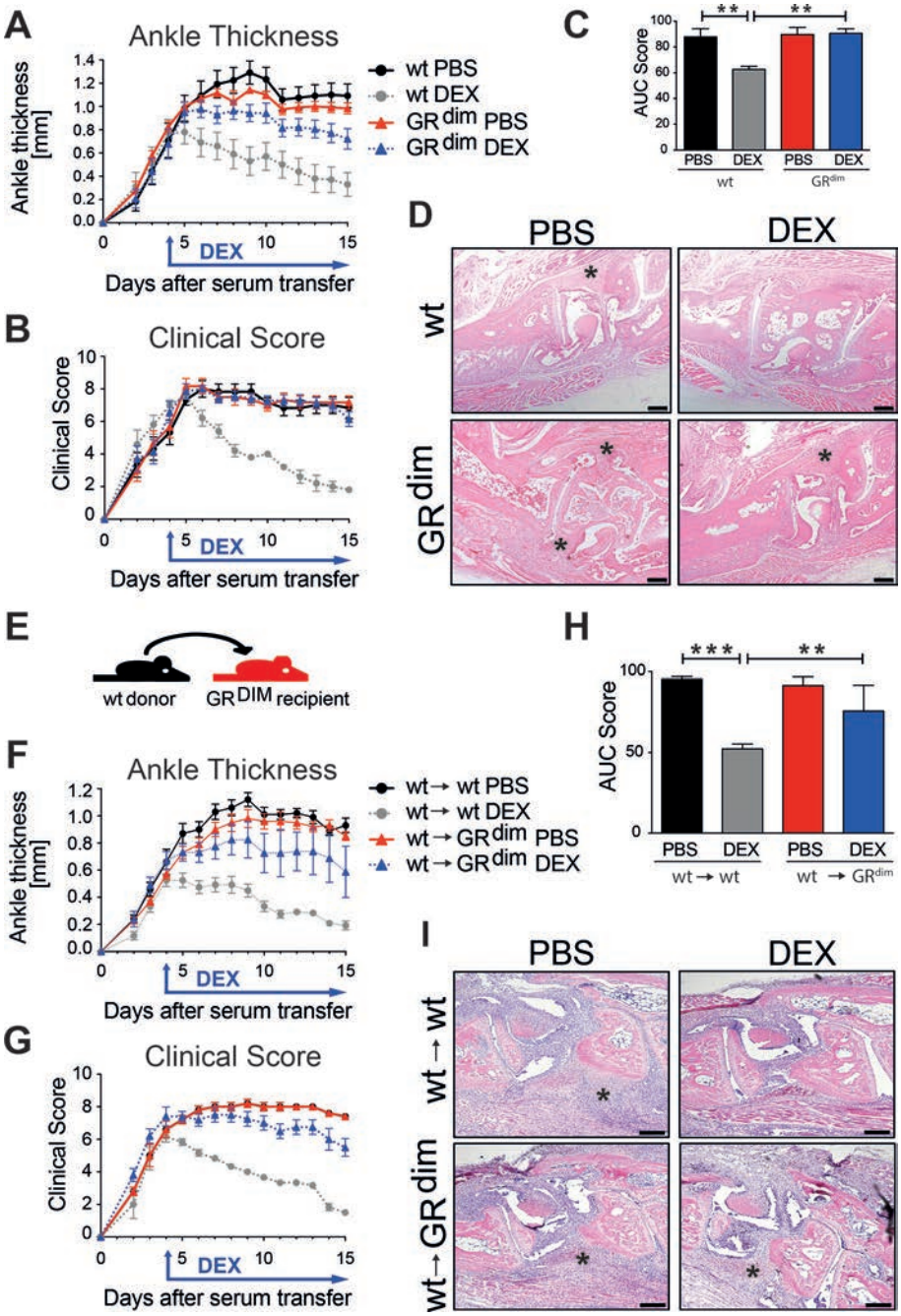

Figure 2 Intact GR dimerisation in stromal cells is crucial for proper anti-inflammatory glucocorticoid (GC) actions in serum transfer-induced arthritis (STIA). (A) Ankle thickness and (B) clinical score of wt mice and mice with an impaired GR dimerisation (GR^{dim}) treated with PBS (black and red) or DEX (grey and blue). (C) AUC for the clinical score of wt and GR^{dim} mice treated with PBS (black and red) or DEX (grey and blue). (D) H&E staining of paraffin sections of hind paws of wt and GR^{dim} mice (scale bar=200 µm); asterisks show area of inflammation. Group size n=5–7 mice per group. (E) Scheme of bone marrow transplantation of irradiated wt and GR^{dim} recipient mice that were reconstituted with wt bone marrow cells (wt→wt and wt→GR^{dim}). (F) Ankle thickness and (G) clinical score of mice treated with PBS (black and red) or DEX (grey and blue). (H) AUC of the clinical score of mice treated with PBS (black and red) or DEX (grey and blue). (I) H&E staining of paraffin sections of hind paws of wt→wt and wt→GR^{dim} mice (scale bar=200 µm); asterisks show area of inflammation. Group size n=4–6 mice per group. AUC, area under the curve; DEX, dexamethasone; GR, glucocorticoid receptor; ns, not significant; PBS, phosphate buffered saline; wt, wild type.

FLS exposed to DEX (online supplementary figure 9C). Interestingly, we found macrophage-associated chemokines "macrophage inflammatory protein -1α and -β" (Mip-1α and Mip-1β) strongly downregulated in wt but not in GR^{dim} FLS (online supplementary figure 9B). These results were confirmed by a multiplex analysis of wt and GR^{dim} FLS supernatants (figure 6E). However, classical inflammatory cytokines, like IL-6 and TNFα, were sufficiently suppressed by DEX in both wt and GR^{dim} FLS (figure 6E).

Taken together FLS with compromised GR dimerisation are less efficient to induce macrophage efferocytosis, have a distinct gene signature including enriched KEGG pathway for cell cycle and cell adhesion, and are impaired in DEX-mediated chemokine regulation.

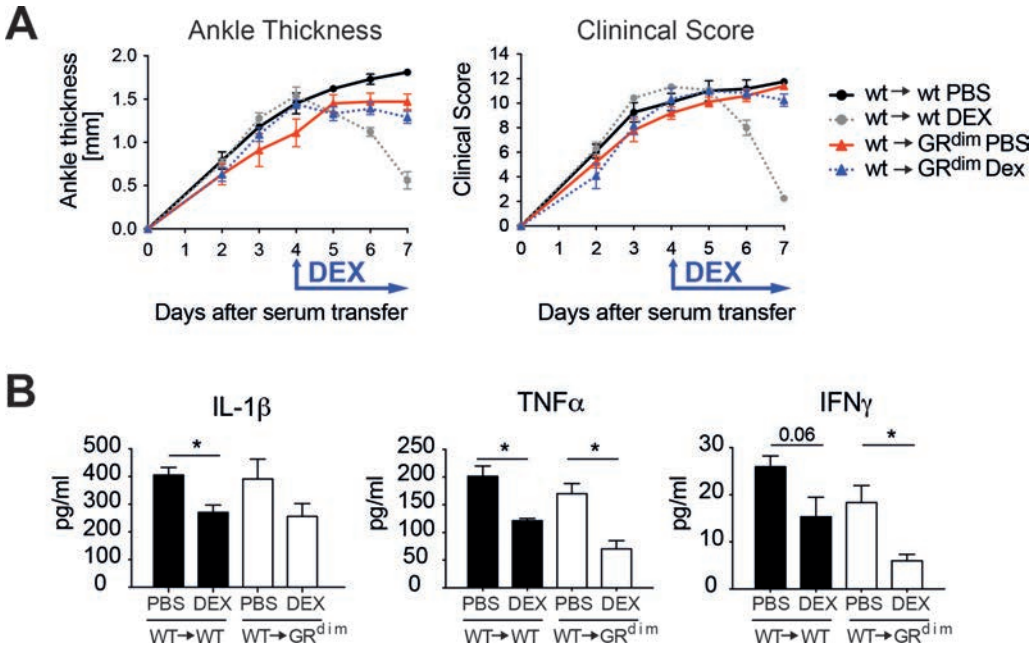

Figure 3 Impaired GR dimerisation in stromal cells abrogates suppression of serum transfer-induced arthritis (STIA) but does not affect cytokine suppression by glucocorticoids (GC). (A) Ankle thickness and clinical score of irradiated wt and GR^{dim} recipient mice reconstituted with wt bone marrow (wt→wt and wt→GR^{dim}) treated for 72 hours with PBS (black and red) or DEX (grey and blue). (B) Serum cytokine levels of IL-1β, TNFα and IFNγ are suppressed in both wt→wt and wt→GR^{dim} mice after DEX treatment. *p<0.05, group size n=5–6 mice per group. DEX, dexamethasone; GR, glucocorticoid receptor; IFN, interferon; IL, interleukin; PBS, phosphate buffered saline; TNF, tumour necrosis factor; wt, wild type.

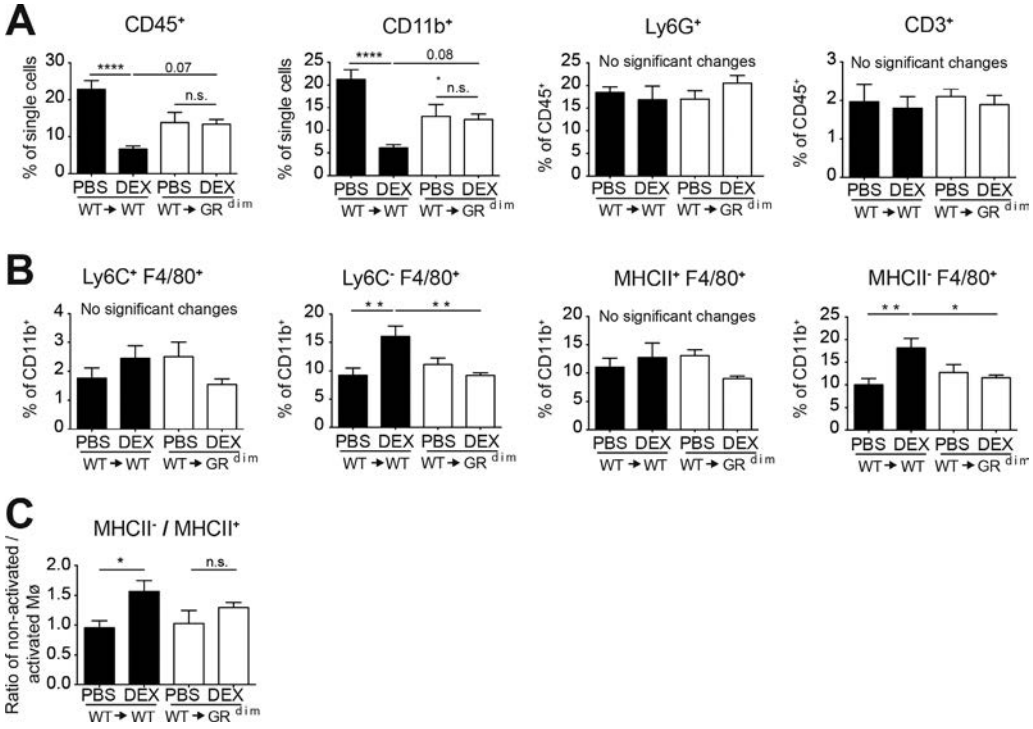

Figure 4 Glucocorticoids (GC) reduce the percentage of $CD45^{pos}$ and $CD11b^{pos}$ cells and increase the fraction of non-classical, non-activated macrophages after 72 hours ofDEX treatment during serum transfer-induced arthritis (STIA) by a GR dimer-dependent mechanism in stromal cells. (A) Haematopoietic cells ($CD45^{pos}$) and myeloid cells ($CD11b^{pos}$) presented as percentage of single cells, and neutrophils ($Ly6G^{pos}$) and T cells ($CD3^{pos}$) presented as percentage of $CD45^{pos}$ cells in the ankles of irradiated wt and GR^{dim} mice reconstituted with wt bone marrow (wt→wt (black) and wt→GR^{dim} (white)) treated with PBS or DEX for 72 hours. (B) Classical macrophages ($Ly6C^{pos}$, $F4/80^{pos}$), non-classical macrophages ($Ly6C^{neg}$, $F4/80^{pos}$), activated macrophages ($MHCII^{pos}$, $F4/80^{pos}$) and non-activated macrophages ($MHCII^{neg}$, $F4/80^{pos}$) in wt→wt (black) and wt→GR^{dim} (white) mice after PBS or DEX treatment for 72 hours presented as percentage of $CD11b^{pos}$ cells and (C) the ratio of non-activated macrophages versus activated macrophages. *p<0.05; **p<0.01; ***p<0.001 by two-way analysis of variance (ANOVA) followed Tukey's multiple comparison correction, group size n=5–6 mice per group. DEX, dexamethasone; GR, glucocorticoid receptor; Mø, macrophages; PBS, phosphate buffered saline.

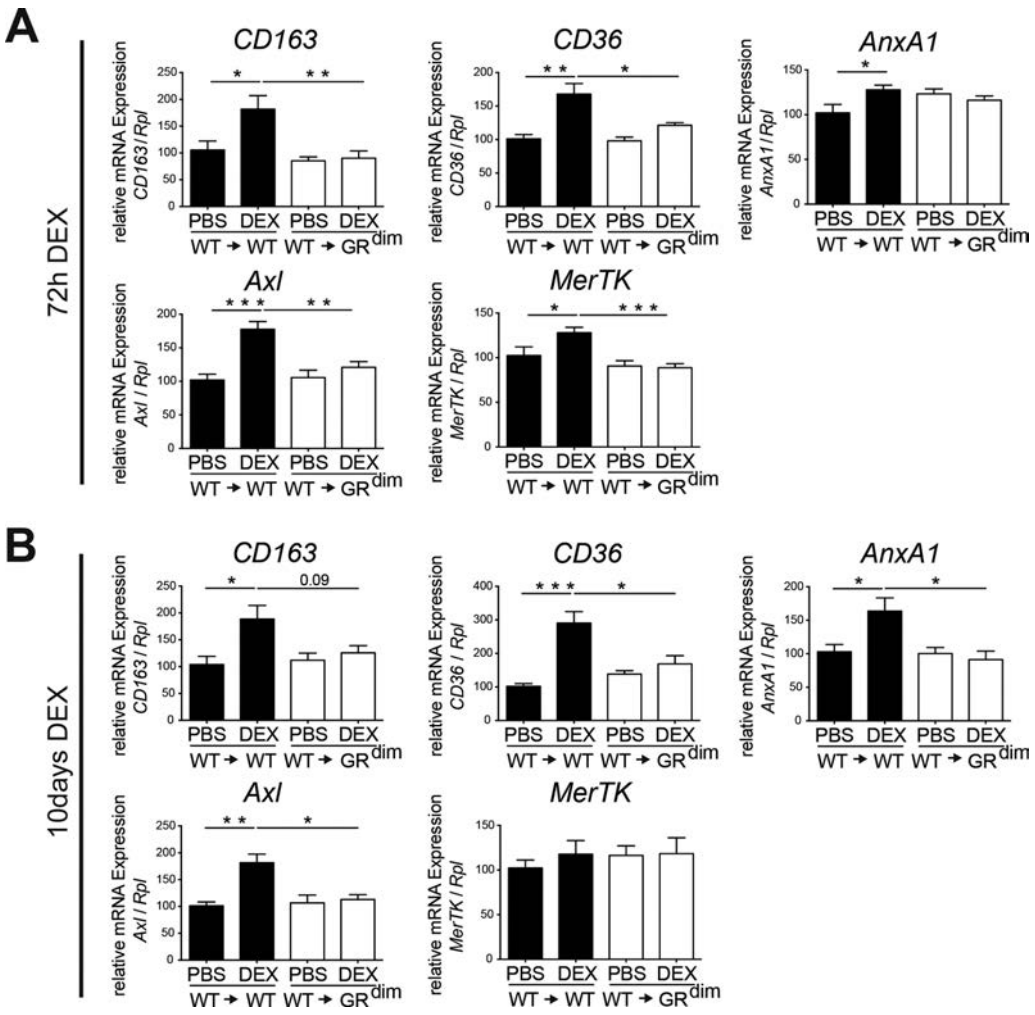

Figure 5 The GR dimer in stromal cells mediates the induction of genes of anti-inflammatory macrophages after DEX treatment in serum transfer-induced arthritis (STIA). (A) Quantitative RT-PCR of isolated ankle mRNA extracts showing the regulation of CD163, CD36, AnxA1, Axl and MerTK after 72 hours of DEX treatment in wt→wt and wt→GR^{dim} mice. Group size n=5–6 mice per group. (B) Quantitative RT-PCR of isolated ankle mRNA extracts showing the regulation of CD163, CD36, AnxA1, Axl and MerTK after 10 days of DEX treatment in wt→wt and wt→GR^{dim} mice. Group size n=4–6 mice per group. *P<0.05; **P<0.01; ***P<0.001 by two-way analysis of variance (ANOVA) followed Tukey's multiple comparison correction. DEX, dexamethasone; GR, glucocorticoid receptor; PBS, phosphate buffered saline.

DISCUSSION

Here we show for the first time that stromal cells, presumably FLS, are essential for suppression of inflammation by GCs in an arthritis mouse model that closely resembles the pathology of the human disease. In STIA, GR deficiency in immune cells is dispensable for anti-inflammatory effects of GCs. These findings challenge the general assumption that the GR mediates anti-inflammatory actions mainly by direct actions on immune cells. We could further show that functional GR dimerisation in stromal cells is crucial to mediate the anti-inflammatory effects, emphasising the importance of GR dimerisation for mediating GC actions in multiple models of arthritis such as AIA, G6PI arthritis[14] and STIA. The spontaneous resolution of STIA in the absence of DEX, however, is not affected by an impaired GR dimerisation (data not shown).

Intriguingly, repression of inflammatory cytokines by GCs in a therapeutic setting was not affected by impaired GR dimerisation in stromal cells, despite an ongoing joint inflammation. In addition, we could show that DEX treatment from day 0 onwards does not prevent initiation of STIA, but strongly impairs progression of disease comparable to therapeutic conditions (online supplementary figure 4). Thus, although cytokines like IL-1β and TNFα are shown to be important for the induction of STIA[18] their decline alone is not enough to inhibit progression of inflammation. This finding is important considering the increasing focus on cytokine inhibitors as treatment for patients with arthritis. Recombinant IL1 receptor antagonist treatment in patients with RA shows only weak effects.[19] Also, TNFα inhibitors failed to exert effective disease remission and 20%–40% of patients are not responding at all to the therapy.[20] However, cytokine blockade, achieved with different functional antibody treatments, can result in positive outcomes,[20] and cytokine suppression has shown to affect bone and cartilage destruction in arthritis.[21] Here we observed a strong attenuation of DEX-mediated reduction in bone and cartilage damage, when GR in stromal cells was compromised, indicating that reduction of cytokines alone is not sufficient to reduce STIA-induced damage.

Since the immune cells in the bone marrow chimeric wt→GR^{dim} mice are still expressing the functional GR we hypothesise that the suppression of these cytokines is mediated by a direct effect of DEX on immune cells. This is supported by findings that mice with a macrophage-specific GR deletion or a complete impaired GR dimerisation are not able to suppress lipopolysaccharide-induced cytokine expression after DEX treatment *in vitro*.[22 23] Of

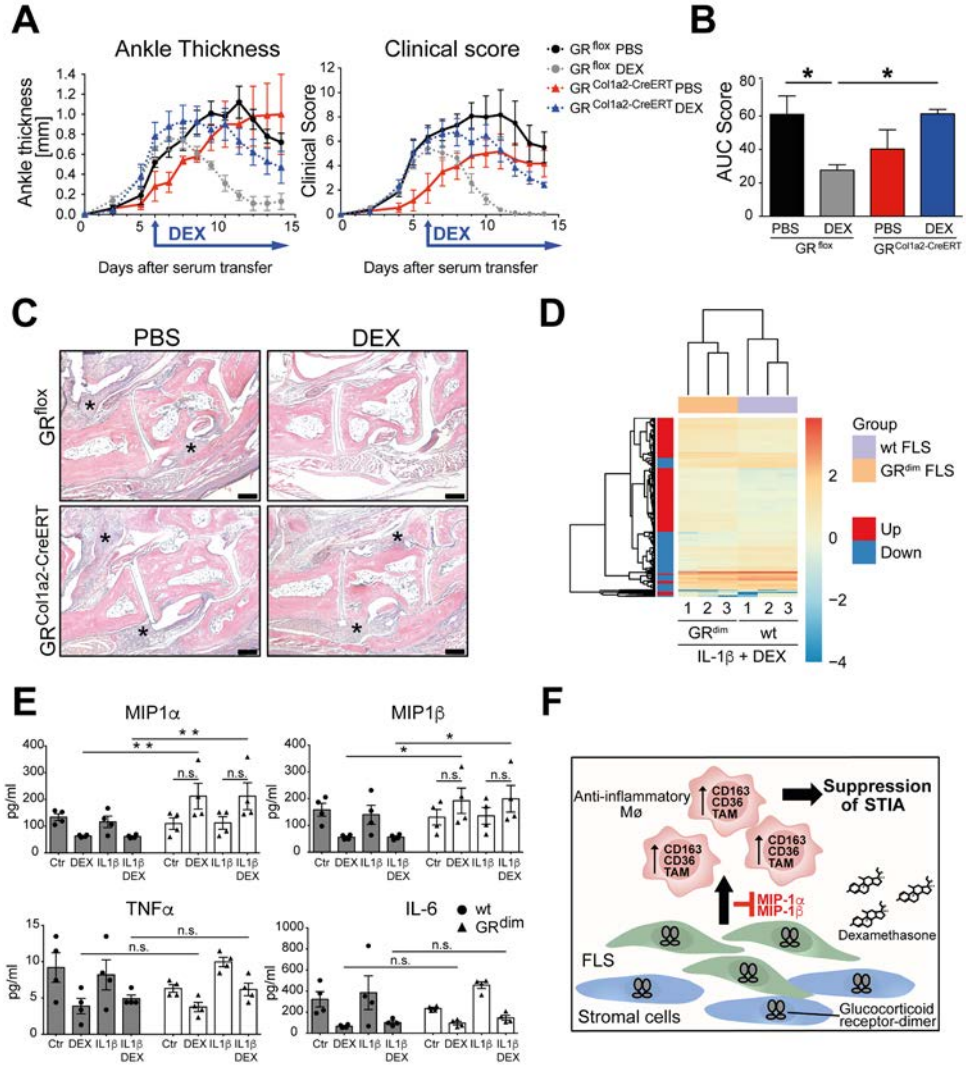

Figure 6 GR deficiency in FLS results in delayed suppression of STIA after DEX treatment and impaired GR dimerisation in FLS leads to a distinct gene expression pattern after DEX treatment. (A) Ankle thickness and clinical score of tamoxifen-inducible $GR^{Col1a2\text{-}CreERT}$ and GR^{flox} control mice treated with PBS (black and red) or DEX (grey and blue). (B) AUC of the clinical score of tamoxifen-inducible $GR^{Col1a2\text{-}CreERT}$ and GR^{flox} control mice treated with PBS (black and red) or DEX (grey and blue). (C) H&E staining of paraffin sections of hind paws of $GR^{Col1a2\text{-}CreERT}$ and GR^{flox} control mice. Original magnification: 5× (scale bar=200 µm), asterisks show the area of inflammation. Group size n=5–7 mice. *P<0.05 by two-way analysis of variance (ANOVA) followed Tukey's multiple comparison correction. (D) Differentially expressed genes of wt and GR^{dim} FLS treated with interleukin (IL)-1β and DEX by RNASeq analysis. n=3. (E) Cytokine multiplex analysis of supernatants of wt and GR^{dim} FLS treated with control medium, DEX, IL-1β or in combination with DEX and IL-1β. n=4. *p<0.05 and **p<0.01 by two-way ANOVA followed Tukey's multiple comparison correction. (F) Scheme of glucocorticoid (GC)-induced suppression of STIA. AUC, area under the curve; DEX, dexamethasone; FLS, fibroblast-like synoviocytes; GR, glucocorticoid receptor; ns, not significant; PBS, phosphate buffered saline; STIA, serum transfer-induced arthritis; TNF, tumour necrosis factor; wt, wild type.

note, GCs did not alter the percentage of classical activated macrophages ($F4/80^{pos}$, $Ly6C^{pos}$ and $F4/80^{pos}$, $MHCII^{pos}$), but reduced the fraction of $CD45^{pos}$ and $CD11b^{pos}$ cells. Thus, they might be the targets of cytokine suppression. However, we could show that GCs increased the relative abundance of non-classical, non-activated macrophages ($F4/80^{pos}$, $Ly6C^{neg}$ and $F4/80^{pos}$, $MHCII^{neg}$).

These anti-inflammatory acting macrophages were previously shown to be essential for the resolution of STIA and collagen-induced arthritis.[24 25] In line with the induction of the percentage of anti-inflammatory macrophages we detected only in wt mice an increased expression of several anti-inflammatory markers known to be associated with increased phagocytosis and efferocytosis activity (*CD163*, *CD36*, *AnxA1*, *Axl* and *MerTK*). For instance, AnxA1-deficient mice have decreased levels of phagocyting cells.[26] CD36 silencing attenuates efferocytosis[27] and loss of MerTK and Axl results in a lack of apoptotic cell clearance, induction of autoimmunity[28] and aggravated STIA.[29] Accordingly, cocultures of FLS with macrophages failed to increase efferocytosis in the presence of GR^{dim} FLS. Taken together, the failure of wt→GR^{dim} mice to increase these factors upon DEX treatment suggests an impaired clearance of apoptotic cells after DEX treatment, resulting in an ongoing inflammation. This emphasises the possibility to improve therapeutic strategies by inducing the generation of non-classical, non-inflammatory macrophages.

We suggest that the induction of therapeutically important anti-inflammatory macrophages can be indirectly stimulated by actions of stromal cells, in particular FLS. So far, FLS were mainly characterised as drivers of chronic inflammation in RA due to their hyperproliferation and secretion of multiple inflammatory mediators such as cytokines, matrix metalloproteinases and other factors.[30] It is also well known that FLS contribute substantially to the TNF response of macrophages[31] and support monocyte survival and integrity in the lining structure.[32] We also could show a slightly increased efferocytosis efficiency of Mø cocultured with wt FLS compared with those that were cocultured with GR^{dim} FLS, when treated with IL-1β and DEX. GR^{dim} FLS show a specific gene signature induced by DEX exposure. Cell cycle-associated factors and their regulators, but also cell adhesion molecules are in general higher expressed, suggesting a higher proliferative and migratory activity of FLS. Whether this is the reason for failing to trigger anti-inflammatory macrophages in vivo in GR^{dim} mice requires further investigation. In addition, GR^{dim} FLS are resistant to DEX-mediated suppression of macrophage-recruiting cytokines Mip-1α and Mip-1β. Interestingly, Mip-1α-deficient mice are protected from collagen induced arthritis (CIA), which was independent of serum TNFα levels that were equal in wt and Mip-1α-deficient mice.[33] This is supported by anti-Mip-1α antibody treatment of CIA mice resulting in the attenuation of CIA.[34] Taken together, these data imply an important crosstalk between FLS and macrophages in GC-induced suppression of STIA.

So far, GC actions on FLS were considered as anti-inflammatory due to the attenuation of expression of inflammatory mediators[15 16] mediated by the monomeric GR. Challenging this view, we provide here the concept that FLS can mediate anti-inflammatory effects evoked by GCs and their dimerised receptor by increasing anti-inflammatory macrophage populations (figure 6F).

The action of GR in FLS and stromal cells is essential; the action of GR in macrophages themselves does not suffice to reduce inflammation. Accordingly, liposomal-packed prednisolone only reduced inflammatory gene expression but did not induce non-classical, anti-inflammatory macrophages.[35] Supporting our conclusion, prednisolone-carrying liposomes targeting synovial lining cells strongly increase therapeutic benefits in collagen-induced arthritis[36] and adjuvant arthritis in rats.[37]

In summary, our data revealed a major role of stromal cells such as FLS in GC-mediated suppression of arthritis to induce anti-inflammatory acting macrophages. Exploiting the GC-induced anti-inflammatory crosstalk between stromal cells and the immune system will provide novel rationales for therapies with higher efficiency and may avoid side effects of steroid therapy.

Author affiliations
[1]Institute for Comparative Molecular Endocrinology, University of Ulm, Ulm, Germany
[2]Tuckermann Lab, Leibniz Institute for Age Research–Fritz-Lipmann-Institute, Jena, Germany
[3]Department of Internal Medicine 3 and Institute for Clinical Immunology, University Hospital Erlangen, Erlangen, Germany
[4]INSERM, Oncogenèse et Progression Tumorale, Universitè Claude Bernard Lyon I, Lyon, France
[5]Division of Endocrinology, Diabetes and Bone Diseases, Department of Medicine III, Technische Universität Dresden, Dresden, Germany

Presented at
Parts of this manuscript were orally presented at the 2016 ACR/ARHP Annual Meeting and as such the abstract was published in an online supplementary of Arthritis & Rheumatology: Koenen M, Baschant U, Culemann S, Kockmann T, Kaltenbach HM, Vettorazzi S, Nanni P, Roschitzki B, Auf dem Keller U, Tuckermann JP. Glucocorticoid receptor dimerization in stromal cells modulates macrophage polarization during serum transfer-induced arthritis [abstract]. Arthritis Rheumatol. 2016;68 (suppl 10).

Acknowledgements We are grateful to the staff of the animal facilities of the University of Ulm, our animal welfare officer Dr Sibylle Ott and in particular to Birgit Widmann. We thank Sandra Förtsch of the Institute for Molecular Psychosomatics for providing IHC reagents.

Contributors MK performed experiments, processed the data and wrote the manuscript. SC performed experiments and processed the data. SV and GC performed experiments. LF analysed the data. WB provided materials. GK provided materials and revised the manuscript. UB designed the study, performed experiments, processed the data and wrote the manuscript. JPT designed the study and wrote the manuscript. UB and JPT contributed equally to the study and share correspondence.

Funding This study was funded by the Boehringer Ingelheim Foundation (to JPT), Deutsche Forschungsgemeinschaft (DFG, Priority Program Immunobone 1468, Tu 220/6-1, 6-2, Collaborative Research Centre 1149, C02/INST 40/492-1, Trilateral Consortium Tu 220/12-1 to JPT).

Competing interests None declared.

Patient consent Not required.

Provenance and peer review Not commissioned; externally peer reviewed.

Data sharing statement All data are in the manuscript and supplementary figures, except the raw data of the RNASeq study. These data will be made available upon publication.

REFERENCES

1 McInnes IB, Schett G. The pathogenesis of rheumatoid arthritis. *N Engl J Med* 2011;365:2205–19.
2 Bartok B, Firestein GS. Fibroblast-like synoviocytes: key effector cells in rheumatoid arthritis. *Immunol Rev* 2010;233:233–55.
3 Hench PS. *The reversibility of certain rheumatic and non-rheumatic conditions by the use of cortisone or of the pituitary adrenocorticotropic hormone*, 1950.
4 van Everdingen AA, Jacobs JW, Siewertsz Van Reesema DR, *et al*. Low-dose prednisone therapy for patients with early active rheumatoid arthritis: clinical efficacy, disease-modifying properties, and side effects: a randomized, double-blind, placebo-controlled clinical trial. *Ann Intern Med* 2002;136:1–12.
5 Hartmann K, Koenen M, Schauer S, *et al*. Molecular actions of glucocorticoids in cartilage and bone during health, disease, and steroid therapy. *Physiol Rev* 2016;96:409–47.
6 Ogawa A, Johnson JH, Ohneda M, *et al*. Roles of insulin resistance and beta-cell dysfunction in dexamethasone-induced diabetes. *J Clin Invest* 1992;90:497–504.
7 Schäcke H, Berger M, Rehwinkel H, *et al*. Selective glucocorticoid receptor agonists (SEGRAs): novel ligands with an improved therapeutic index. *Mol Cell Endocrinol* 2007;275:109–17.
8 Lim HW, Uhlenhaut NH, Rauch A, *et al*. Genomic redistribution of GR monomers and dimers mediates transcriptional response to exogenous glucocorticoid in vivo. *Genome Res* 2015;25:836–44.
9 Schiller BJ, Chodankar R, Watson LC, *et al*. Glucocorticoid receptor binds half sites as a monomer and regulates specific target genes. *Genome Biol* 2014;15:418.
10 Reichardt HM, Kaestner KH, Tuckermann J, *et al*. DNA binding of the glucocorticoid receptor is not essential for survival. *Cell* 1998;93:531–41.
11 Vandevyver S, Dejager L, Van Bogaert T, *et al*. Glucocorticoid receptor dimerization induces MKP1 to protect against TNF-induced inflammation. *J Clin Invest* 2012;122:2130–40.
12 Kleiman A, Hübner S, Rodriguez Parkitna JM, *et al*. Glucocorticoid receptor dimerization is required for survival in septic shock via suppression of interleukin-1 in macrophages. *Faseb J* 2012;26:722–9.
13 Vettorazzi S, Bode C, Dejager L, *et al*. Glucocorticoids limit acute lung inflammation in concert with inflammatory stimuli by induction of SphK1. *Nat Commun* 2015;6:7796.
14 Baschant U, Frappart L, Rauchhaus U, *et al*. Glucocorticoid therapy of antigen-induced arthritis depends on the dimerized glucocorticoid receptor in T cells. *Proc Natl Acad Sci U S A* 2011;108:19317–22.
15 Hardy RS, Hülso C, Liu Y, *et al*. Characterisation of fibroblast-like synoviocytes from a murine model of joint inflammation. *Arthritis Res Ther* 2013;15:R24.
16 Gossye V, Elewaut D, Bougarne N, *et al*. Differential mechanism of NF-kappaB inhibition by two glucocorticoid receptor modulators in rheumatoid arthritis synovial fibroblasts. *Arthritis Rheum* 2009;60:3241–50.
17 Singh K, Maity P, Krug L, *et al*. Superoxide anion radicals induce IGF-1 resistance through concomitant activation of PTP1B and PTEN. *EMBO Mol Med* 2015;7:59–77.

18 Ji H, Pettit A, Ohmura K, *et al*. Critical roles for interleukin 1 and tumor necrosis factor alpha in antibody-induced arthritis. *J Exp Med* 2002;196:77–85.
19 Burger D, Dayer JM, Palmer G, *et al*. Is IL-1 a good therapeutic target in the treatment of arthritis? *Best Pract Res Clin Rheumatol* 2006;20:879–96.
20 Mikuls TR, Weaver AL. Lessons learned in the use of tumor necrosis factor-alpha inhibitors in the treatment of rheumatoid arthritis. *Curr Rheumatol Rep* 2003;5:270–7.
21 Jung SM, Kim KW, Yang CW, *et al*. Cytokine-mediated bone destruction in rheumatoid arthritis. *J Immunol Res* 2014;2014:1–15.
22 Tuckermann JP, Kleiman A, Moriggl R, *et al*. Macrophages and neutrophils are the targets for immune suppression by glucocorticoids in contact allergy. *J Clin Invest* 2007;117:1381–90.
23 Bhattacharyya S, Brown DE, Brewer JA, *et al*. Macrophage glucocorticoid receptors regulate Toll-like receptor 4-mediated inflammatory responses by selective inhibition of p38 MAP kinase. *Blood* 2007;109:4313–9.
24 Park SY, Lee SW, Lee SY, *et al*. SIRT1/adenosine monophosphate-activated protein kinase α signaling enhances macrophage polarization to an anti-inflammatory phenotype in rheumatoid arthritis. *Front Immunol* 2017;8.
25 Misharin AV, Cuda CM, Saber R, *et al*. Nonclassical Ly6C(-) monocytes drive the development of inflammatory arthritis in mice. *Cell Rep* 2014;9:591–604.
26 Hannon R, Croxtall JD, Getting SJ, *et al*. Aberrant inflammation and resistance to glucocorticoids in annexin $1^{-/-}$ mouse. *Faseb J* 2003;17:253–5.
27 Kim W, Lee HN, Jang JH, *et al*. 15-Deoxy-$\Delta^{12,14}$-prostaglandin J_2 exerts proresolving effects through nuclear factor E_2-related factor $_2$-induced expression of CD36 and heme oxygenase-1. *Antioxid Redox Signal* 2017;27:1412–31.
28 Seitz HM, Camenisch TD, Lemke G, *et al*. Macrophages and dendritic cells use different Axl/Mertk/Tyro3 receptors in clearance of apoptotic cells. *J Immunol* 2007;178:5635–42.
29 Waterborg CEJ, Través PG, Beermann S, *et al*. 03.05 The tam receptors axl and mer play a protective role in a temporal and spatial manner in inflammatory arthritis. *Ann Rheum Dis* 2017;76:A31.
30 Bottini N, Firestein GS. Duality of fibroblast-like synoviocytes in RA: passive responders and imprinted aggressors. *Nat Rev Rheumatol* 2013;9:24–33.
31 Donlin LT, Jayatilleke A, Giannopoulou EG, *et al*. Modulation of TNF-induced macrophage polarization by synovial fibroblasts. *J Immunol* 2014;193:2373–83.
32 Kiener HP, Watts GF, Cui Y, *et al*. Synovial fibroblasts self-direct multicellular lining architecture and synthetic function in three-dimensional organ culture. *Arthritis Rheum* 2010;62:742–52.
33 Chintalacharuvu SR, Wang JX, Giaconia JM, *et al*. An essential role for CCL3 in the development of collagen antibody-induced arthritis. *Immunol Lett* 2005;100:202–4.
34 Kasama T, Strieter RM, Lukacs NW, *et al*. Interleukin-10 expression and chemokine regulation during the evolution of murine type II collagen-induced arthritis. *J Clin Invest* 1995;95:2868–76.
35 Hofkens W, Schelbergen R, Storm G, *et al*. Liposomal targeting of prednisolone phosphate to synovial lining macrophages during experimental arthritis inhibits M1 activation but does not favor M2 differentiation. *PLoS One* 2013;8:e54016.
36 Metselaar JM, van den Berg WB, Holthuysen AE, *et al*. Liposomal targeting of glucocorticoids to synovial lining cells strongly increases therapeutic benefit in collagen type II arthritis. *Ann Rheum Dis* 2004;63:348–53.
37 Vanniasinghe AS, Manolios N, Schibeci S, *et al*. Targeting fibroblast-like synovial cells at sites of inflammation with peptide targeted liposomes results in inhibition of experimental arthritis. *Clin Immunol* 2014;151:43–54.

EXTENDED REPORT

Tetraspanin CD82 affects migration, attachment and invasion of rheumatoid arthritis synovial fibroblasts

Elena Neumann,[1] Maria C Schwarz,[1] Rebecca Hasseli,[1] Marie-Lisa Hülser,[1] Simon Classen,[2] Michael Sauerbier,[3] Stefan Rehart,[4] Ulf Mueller-Ladner[1]

Handling editor Josef S Smolen

► Additional material is published online only. To view please visit the journal online (http://dx.doi.org/10.1136/annrheumdis-2018-212954).

[1]Department of Rheumatology and Clinical Immunology, Campus Kerckhoff, Justus-Liebig University Giessen, Bad Nauheim, Germany
[2]Division of Vascular Surgery, Harvey-Vascular-Healthcare Center, Kerckhoff-Klinik GmbH, Bad Nauheim, Germany
[3]Department of Plastic, Hand and reconstructive Surgery, BGU Frankfurt, Frankfurt, Germany
[4]Department of Orthopaedics and Trauma Surgery, Agaplesion Markus Hospital, Frankfurt, Germany

Correspondence to
Dr Elena Neumann, Internal Medicine and Rheumatology, Justus-Liebig-University Gießen, Bad Nauheim 61231, Germany; e.neumann@kerckhoff-klinik.de

Received 4 January 2018
Revised 18 June 2018
Accepted 19 June 2018
Published Online First 6 July 2018

To cite: Neumann E, Schwarz MC, Hasseli R, *et al*. *Ann Rheum Dis* 2018;**77**:1619–1626.

ABSTRACT

Tetraspanins function as membrane adaptors altering cell-cell fusion, antigen presentation, receptor-mediated signal transduction and cell motility via interaction with membrane proteins including other tetraspanins and adhesion molecules such as integrins. CD82 is expressed in several malignant cells and well described as tumour metastasis suppressor. Rheumatoid arthritis (RA) is based on persistent synovial inflammation and joint destruction driven to a large extent by transformed-appearing activated synovial fibroblasts (SF) with an increased migratory potential.

Objective CD82 is upregulated in RA synovial fibroblasts (RASF) compared with osteoarthritis (OA) SF as well as within RA compared with OA synovial lining layer (LL) and the role of CD82 in RASF was evaluated.

Methods CD82 and integrin immunofluorescence was performed. Lentiviral CD82 overexpression and siRNA-mediated knockdown was confirmed (realtime-PCR, Western blot, immunocytochemistry). RASF migration (Boyden chamber, scrape assay), attachment towards plastic/Matrigel, RASF-binding to endothelial cells (EC) and CD82 expression during long-term invasion in the SCID-mouse-model were evaluated.

Results CD82 was induced by proinflammatory stimuli in SF. In RA-synovium, CD82 was expressed in RASF close to blood vessels, LL, sites of cartilage invasion and colocalised with distinct integrins involved in tumour metastasis suppression but also in RA-synovium by RASF. CD82 overexpression led to reduced RASF migration, cell-matrix and RASF-EC adhesion. Reduced CD82 expression (observed in the sublining) increased RASF migration and matrix adhesion whereas RASF-EC-interaction was reduced. In SCID mice, the presence of CD82 on cartilage-invading RASF was confirmed.

Conclusion CD82 could contribute to RASF migration to sites of inflammation and tissue damage, where CD82 keeps aggressive RASF on site.

INTRODUCTION

The proteins of the tetraspanin superfamily function as membrane adaptors facilitating protein interactions.[1 2] There are 34 known tetraspanins in mammals and of those 33 are expressed in humans. Tetraspanins alter processes including antigen presentation, receptor-mediated signalling and cell motility. The effects are mediated by forming multimeric complexes consisting of tetraspanins and other proteins including kinases, adhesion molecules and adaptor proteins.[2] Tetraspanins form interlinked networks of functional hubs, called tetraspanin-enriched microdomains regulating the clustering of associated receptors on the cell.[1]

Structure and splicing variants of the tetraspanin CD82 are well described[3 4] with varying glycosylation.[5 6] Although CD82 is expressed in different tissues including bone marrow as well as hematopoietic cells,[5] its function in inflammatory diseases is unclear. CD82 is a well characterised metastasis suppressor of different solid malignant tumours without affecting primary tumour growth[4 7] and a recognised biomarker to predict metastatic potential.[5] CD82 inhibits multiple steps of the metastatic cascade including cell motility, invasion, cell-cell-interaction, proliferation, apoptosis and senescence.[2] Regarding cell-cell-adhesion, CD82 overexpression enhances homophilic aggregation of different cells including tumour cells and leucocytes[2 4] and mediates hematopoietic progenitor cell/osteoblast and tumour cell/endothelial cell (EC) interactions.[8 9] In cell-matrix-adhesion, CD82 is negatively correlated with solid tumour cell adhesiveness onto matrices,[3] whereas in leukaemia cells CD82 had opposite effects.[7]

CD82 regulates the signalling of membrane molecules by altering their distribution, thus inhibiting migration and invasiveness of solid tumour cells.[2 4] CD82 interacts with cell surface molecules such as integrins via its extracellular loops and mediates rearrangement and clustering of these molecules on the cell surface. Trafficking of cell adhesion proteins, for example, integrins and CD44, is modified by CD82 thus altering their initiated outside-in signalling and their cell surface presence.[3 10 11] CD82 is partially localised in lipid rafts.[12] DARC, a CD82 binding partner, is a cell surface protein expressed in endothelium.[8] DARC/CD82 engagement inhibits tumour cell proliferation and induces senescence. However, experimental CD82 overexpression did not inhibit proliferation of cancer cells.[3]

CD82 expression in melanoma cells reduced IL-8 secretion facilitating adherens junction disassembly and tumour cell extravasation.[13 14] In turn, silencing CD82 in leukaemia stem cells reduced IL-10 and MMP9[15] while overexpression induced IL-10 in melanoma.[16] CD82 serves as negative regulator of epidermal growth factor receptor (EGFR) signalling via association with the EGFR[17 18] and suppresses the TGF-β1 pathway, which in turn affects CD82-mediated migration inhibition.[19] Interestingly, CD82 expression is induced by proinflammatory cytokines such as IL-6, TNFα, IL-1β, growth factors and hypoxia.[2 4]

Rheumatoid arthritis (RA) is a chronic autoinflammatory joint disease and with key therapeutic targets being TNFα, IL-6, IL-1β.[20] CD82 was increased in RA synovial fibroblasts (RASF) compared with primarily non-inflammatory osteoarthritis (OA)SF[21] as well as in the hyperplastic synovial lining layer (LL) of patients with RA.[22] RASF are permanently activated cells showing increased migration towards and invasiveness into cartilage of affected joints, thereby being a key cell promoting joint inflammation and destruction but also carrying the disease to non-affected areas.[23 24] Due to the increased presence of CD82 in the RA synovial LL and close to the microvasculature, the effects of CD82 on RASF were evaluated with focus on RASF adhesion, migration and proliferation.

METHODS

For detailed methods, see online supplementary file 1.

Tissues and cells

Synovium and cartilage were obtained during knee replacement surgeries (Agaplesion Markus-Hospital Frankfurt/Main). Patients fulfilled the ACR classification criteria.[25–27] Non-arthritic synovial fibroblasts (NSF) served as control. The study was approved by the local ethics committee. All patients gave written informed consent. Synovium was snap frozen or digested for cell isolation. SF were cultured in DMEM (GE Healthcare, Germany) containing 10% fetal calf serum (FCS) (Sigma-Aldrich, Germany), 100 U/mL penicillin/streptomycin (Applichem, Germany), 10 mM HEPES (GE Healthcare).[28] Proteins for 16 hours stimulation: 50 ng/mL TNFα, 10 ng/mL IL-1β, 2 ng/mL TGF-β (R&D-Systems, Germany), 25 µg/mL adiponectin, 100 ng/mL visfatin (Biovendor, Heidelberg, Germany), 10 ng/mL lipopolysaccheride (LPS) (Sigma-Aldrich).

CD82 overexpression/knockdown

For lentiviral *Cd82* transduction, Precision LentiORF individual clone and Precision LentiORF red fluorescent protein *(RFP) were used (MOI=5, GE Healthcare). After 48 hours, blasticidin-S-hydrochloride was added resulting in stable CD82 overexpression (>90%). Mock treated cells served as control.

The Amaxa Nucleofector II (program U23) and Basic Nucleofector Kit (primary mammalian fibroblasts, Lonza, Germany) were used. siRNA: ON-TARGETplus SMART pool CD82 siRNA; non-targeting-pool (NTP) siRNA (PerbioScience, Germany). At day 5–6 after nucleofection, maximum CD82 protein reduction was confirmed by Western blot.

Western blot

Cells were lysed (1% Nonidet P-40, Sigma-Aldrich) with 0.05M Tris-HCl pH6.7 containing complete protease inhibitor mix (Roche). Antibodies: anti-human CD82 (ab59509, Abcam, Cambridge, UK); anti-mouse horseradish peroxidase(HRP)-conjugated secondary (Agilent Technologies). Loading control: Cyclophilin B (Abcam). Band intensity was quantified using the ImageJ software.

Immunohistochemistry/immunofluorescence

Acetone-fixed sections or chamber slides were blocked in 2% BSA. Antibodies: anti-human CD82 (ab109529), isotype control (ab125938, Abcam). Secondary antibodies: biotinylated goat anti-rabbit (550338, BD Biosciences) and HRP-conjugated streptavidin (016-030-084, Dianova, Germany). Peroxidase substrate kit (AEC, Vector-Laboratories, Germany) detection was used.

Fluorescent double-staining: Blocking: FCS, chicken serum and BSA (10%). First antibodies: anti-human Integrin α6 (MAB1350, R&D), αV (MAB-1980, Merck Millipore), β1 (CP26, Merck Millipore), CD82 (PA5-20356, Thermo Fisher). Secondary antibodies: anti-mouse (Alexa-Fluor 488, A-11001), anti-rabbit (Alexa Fluor 546, A11071, Thermo Fisher). Nuclei were DAPI stained (Sigma Aldrich). Staining was evaluated as indicated in the online supplementary method.

SCID-mouse-model

Female immunodeficient Crl-scidBR mice (Charles River, Germany) were kept pathogen-free with water and food ad libitum. Animals underwent inverse-wrap implantation[29] with subcutaneous implantation of human RASF together with human cartilage (intact areas from OA cartilage) in a Gelfoam matrix (Pfizer, USA) at the ipsilateral side. Contralaterally, cartilage without RASF was implanted.[23 30] Implants removed after 60 days were snap frozen, 5 µm sections H/E-stained and scored.[23 29 30]

Laser-mediated microdissection (LMM)

Eight µm cryosections on PEN-membrane coated slides (P.A.L.M., Germany) were fixed, nuclei haematoxylin-stained and dehydrated. LMM was performed using a Robot-MicroBeam laser microscope (P.A.L.M. Microlaser Technologies). Dissected areas (3000 cells) from different tissues/implants were collected in RLT-lysis buffer (RNA from different tissues was pooled before isolation).

Real-time PCR

For RNA isolation of LMM samples, the RNeasy Micro Kit, otherwise Mini Kits (Qiagen) were used. RNA was transcribed using AMV reverse transcriptase (Promega, Madison, USA) and random hexamer primers (Roche Diagnostics). Real-time PCR followed by melting curve analysis was performed using a LightCycler (Roche).[5 6] Primers: human CD82 forward 5′-ggtgtggatcctggccgacaagagc-3′/reverse 5′-atgcagcccaggaagcccatgagc-3′. Results were normalised to 18S rRNA and analysed using the LightCycler software.[31]

Migration assay

The lower compartment of a Boyden chamber containing a 8 µm pore membrane (GE Water and Process Technologies, Germany) coated with fibronectin was filled with DMEM containing 10% FCS (as chemoattractant) and RASF (harvested with Accutase) in DMEM with 2% FCS placed on top (three replicates each). After 16 hours, migrated cells on membranes were fixed, haematoxylin-stained and nuclei counted. 6.5 mm polycarbonate filters were used in the transwell assay (Corning, USA) under the same conditions. Migrated cells at the lower filter sides were detached and counted. For statistics, means per biological sample were used.

Cell motility assay

Fibroblasts (100% confluency) on uncoated plates were wounded with micropipette tips (scratch). Supernatants were replaced, cells incubated for 17 hours, then photographed. Gap closure was evaluated in five experimental replicates. The number of nuclei moved into the scratch was counted (mean per biological sample used for statistics).

Adhesion assay

SF detached with Accutase were added to 24-well plates coated with/without Matrigel (BD Biosciences) and incubated for 1 hour. The plate was shaken 5 min full speed thrice. Cells were stained with 0.1% crystal-violet dye in methanol and counted (three wells per population, means used for statistics).

Cell-to-cell binding assay

HUVEC or primary EC from human varicose veins (for details, see online supplementary file 1) were cultured on rat tail collagen-I-coated plates (Life Technologies) until confluency. RASF were Calcein-AM (Thermo Fisher) stained and detached using Accutase. RASF added to confluent EC-layers were incubated 30 min. Plates were shaken 5 min at full speed. Attached fibroblasts were counted (three different wells, mean per population used for statistics).

Proliferation assay

RASF were BrdU (proliferation 5-bromo-2′-deoxyuridine) labelled for 24 hours using a colorimetric BrdU-ELISA assay

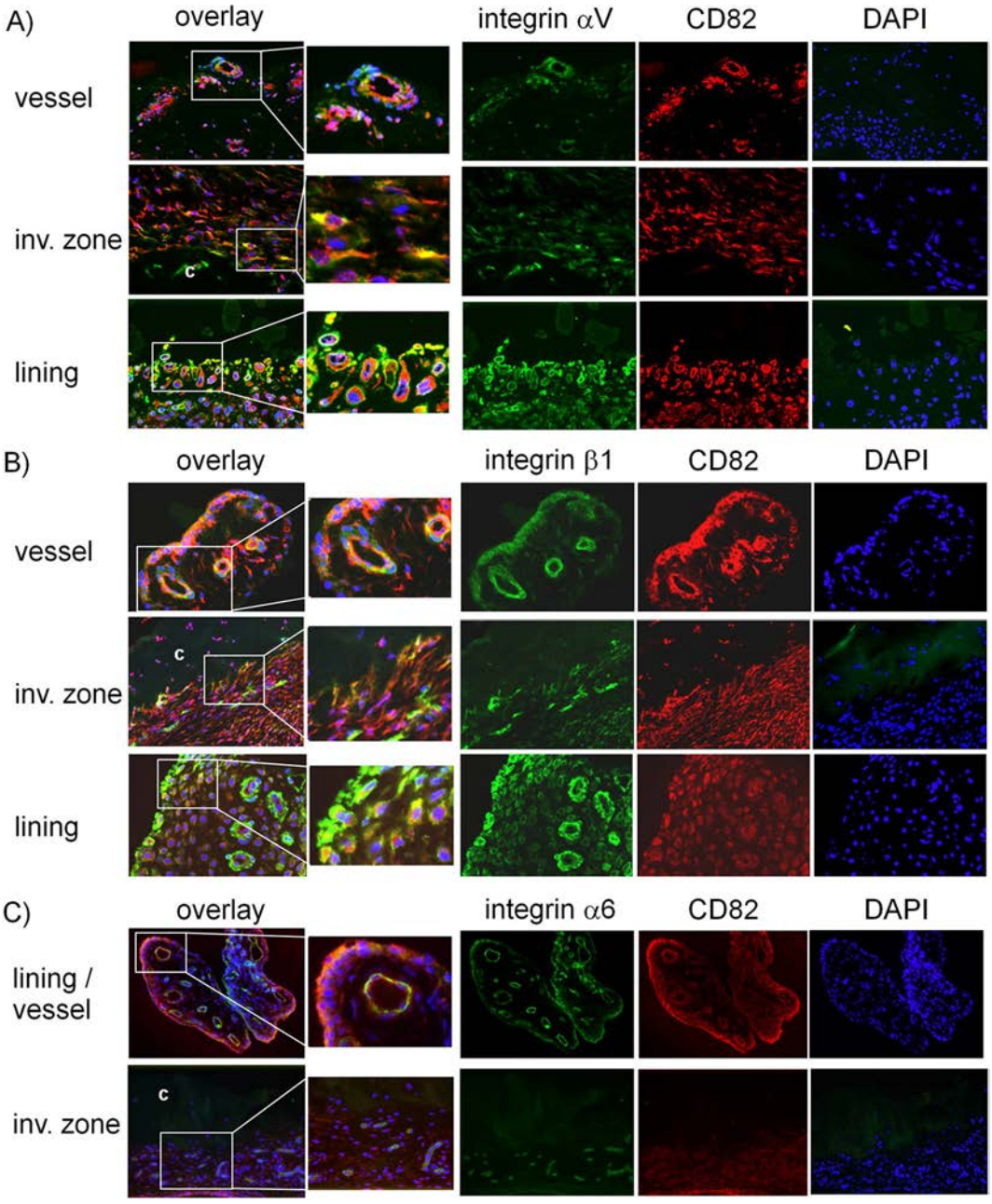

Figure 1 Localisation of CD82 and integrins. Immunofluorescence for CD82 (red) and integrins (green) was performed, nuclei were stained blue (DAPI). Synovial tissues from seven different patients with RA were evaluated and the presence of CD82 and integrins evaluated for each tissue, representative tissues are shown. (A) Integrin alpha V was localised close to and in vessel walls (upper panel) and at the cartilage invasion zone. Colocalisation shows double-stained cells especially in the lining layer and invasion zone (yellow). (B) Integrin beta 1 was localised at the vessel wall, the lining layer and to a limited extent at the cartilage invasion zone. CD82-overlay showed a strong signal at the inner vessel layer as well as sublining cells and some double positive cells at the invasion zone. (C) Integrin alpha 6 was expressed in the inner layer of vessels and weakly in the sublining, invasion zone and lining layer. Overlay with CD82 was most prominent within the lining layer and vessels. C, cartilage; Inv, invasion zone; RA, rheumatoid arthritis.

(Merck Millipore) according to the manufacturer and quantified using a TECAN reader.

Statistics

GraphPad Prism 6.0 was used. Data were analysed parametrically using RM one-way ANOVA with Geissner-Greenhouse correction followed by Tukey's multiple comparisons test with individual variances computed for each comparison. Figure 2A shows the parametric paired two-tailed t-test. Figure 2B,C were calculated with Mann-Whitney test. Data in figures are shown as box-whisker plots with median, 25th/75th percentile (box) and lowest/highest value (whiskers) per data set. P values less than 0.05 were considered significant (*p<0.05/**p<0.005/***p<0.001/n.s.=not significant).

RESULTS

Cellular and compartmental CD82 localisation

The increased CD82 expression in cultured RASF compared with OASF and in the RA synovial LL and close to blood vessels versus OA synovial tissue has previously been described[21 22] and could be confirmed (figure 1) by immunofluorescence showing an increased presence of CD82 also in the invasion zone into cartilage. LMM out of the LL and sublining from n=6 different synovial tissues was performed, RNA from 12 tissues (different patients) was pooled (one pool of 6, two pools of 3 tissues) and subsequent real-time PCR performed. Comparison showed that tissue mRNA expression of CD82 was significantly stronger in the RA LL compared with sublining cells (figure 2A).

The percentage of positive tissues (12 in total) was calculated in LL, outer LL, vessel wall, EC layer, lymphocyte infiltrates and cartilage invasion zone of immunofluorescence stainings. One hundred per cent (12/12) RA tissues were CD82-positive in the outer LL and total LL. Lymphocyte infiltrates were CD82-negative. Several cells showed CD82 signals in sublining and vessel walls (100% of tissues). Cartilage invading cells were CD82-positive (100% of tissues).

αV-integrin was positive in 80% of outer LL, 100% were positive in the deeper LL. Several double stained cells were located in the outer LL (figure 1A). Single sublining cells were αV-positive (100%), but double-stained cells were detectable in only 50% of tissues. αV-positive vessel walls were detectable in 100% of tissues. CD82 and αV-double-positive cells were limited to the vessel wall (figure 1A). Cartilage invading cells showed weaker αV-integrin signals compared with CD82, not all cells being αV-positive.

β1-integrin was present in outer and deeper LL areas of all tissues (100%). In sublining, single cells were β1-positive. CD82/ß1-positive cells were mainly detectable in the outer LL (figure 1B). All tissues displayed β1-integrin positive vessel walls. Deeper areas but not EC showed a CD82/β1-overlay. CD82/β1-positive cartilage invading cells were detectable in all tissues (figure 1B).

α6-integrin was positive in the outer LL (100%) whereas deeper areas were negative or contained single positive cells (figure 1C). An overlay was only observed at the outer LL. In vessels, EC were α6-positive (100%) and double-positive for CD82. At the invasion zone, none of the tissues showed α6 signals.

CD82 induction in RASF by proinflammatory factors

To evaluate the factors responsible for the increased presence of CD82 in RA-synovium, proinflammatory factors increased in RA were used for SF stimulation and CD82 expression was measured. RASF/OASF were stimulated with proinflammatory factors (TNFα, IL-1β, LPS), TGF-β or adipokines (visfatin, adiponectin). All stimuli influenced CD82 expression on RASF (figure 2B). Although cultured SF already produce CD82 on RNA and protein level, CD82 was significantly induced by TNFα, IL-1β and LPS in RASF and OASF (figure 2B,C). Adipokines induced CD82

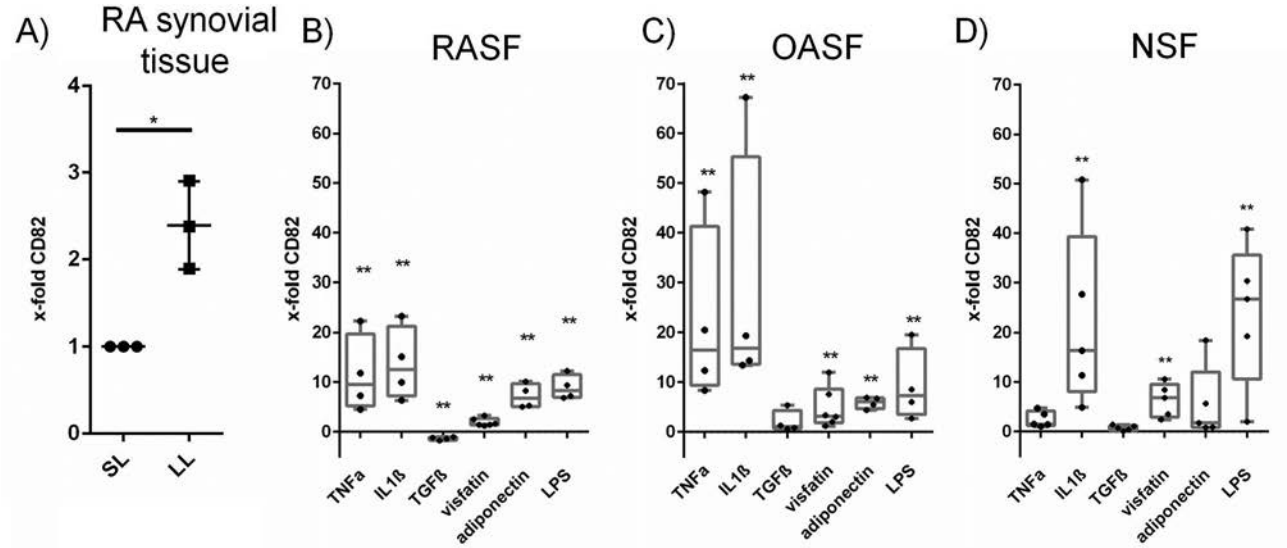

Figure 2 CD82 in RA synovial tissue and RASF. (A) mRNA after LMM of SL and LL was isolated from different RA synovial tissues in three different RNA pools (6, 3, 3 with a total of 12 tissues analysed). Pooled RNA was used for real-time PCR (normalised to 18S and sublining set to 1) revealing a significantly stronger expression within the RA LL compared with the sublining (parametric paired two-tailed t-test). (B) TNFα, IL-1β and LPS significantly induced CD82 in RASF as well as (C) OASF vs unstimulated control (p>0.005 each, Mann-Whitney test; n=4 each). (D) NSF showed similar results except for TNFα showing a weak CD82-induction. Visfatin and adiponectin induced CD82 in RASF and OASF to a lower extent compared with unstimulated control (RASF: Visfatin p=0.002, n=6, adiponectin p=0.005, n=4; OASF: Visfatin p=0.002, n=6, adiponectin p=0.005, n=4; Mann-Whitney test). TGF-β reduced CD82 expression in RASF (p=0.005) but not OASF (p=0.999) compared with unstimulated control. Of note, unstimulated OASF had lower CD82 levels than RASF in the unstimulated control. n=4 each, except n=6 for visfatin (Mann-Whitney test). Values are presented as x-fold versus unstimulated control (set to 1). LL, lining layer; LMM, laser-mediated microdissection; NSF, non-arthritic synovial fibroblasts; OASF, osteoarthritis synovial fibroblasts; RA, rheumatoid arthritis; RASF, RA synovial fibroblasts; SL, sublining layer.

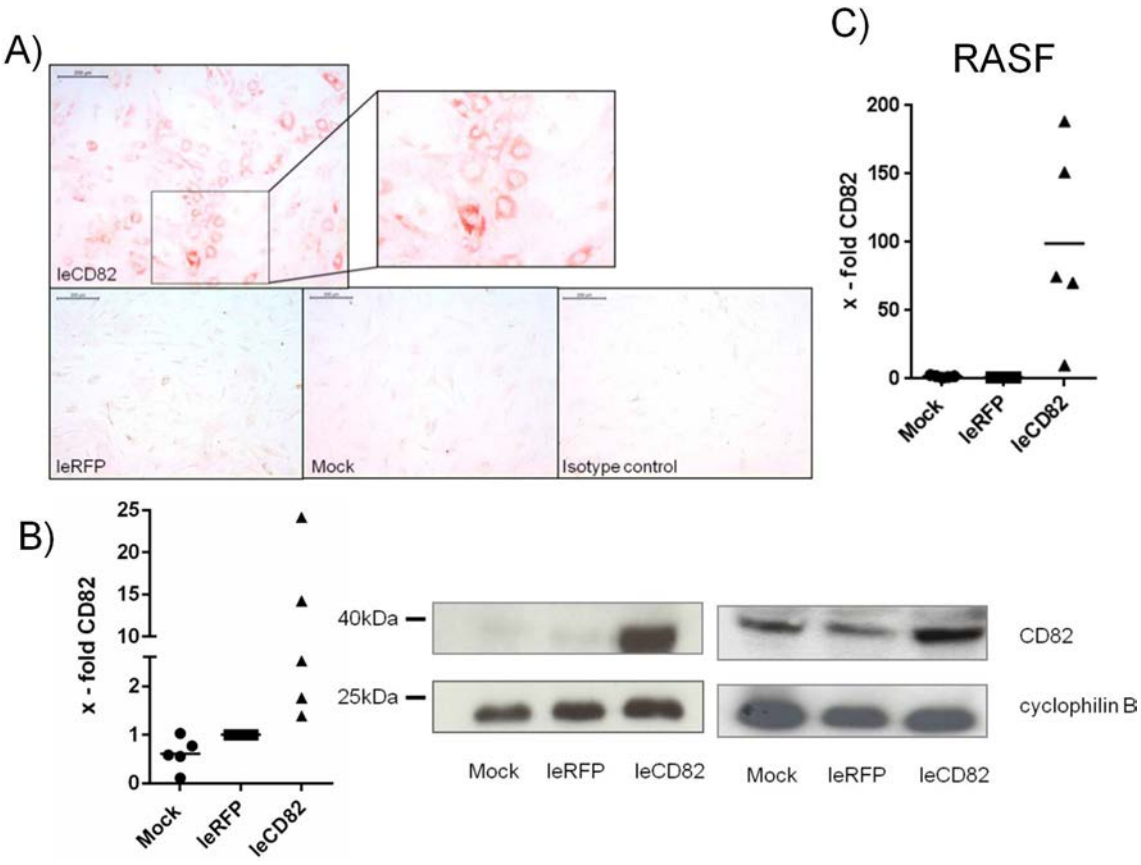

Figure 3 CD82 overexpression in synovial fibroblasts. (A) Immunocytochemistry showed the induction of CD82 in RASF in comparison to mock-treated as well as leRFP-treated cells in contrast to the isotype control. Magnification: 10×. (B) Quantification of Western blots was performed using the ImageJ software showing CD82 protein induction compared with leRFP (set to 1) and mock-treated cells. CD82 could be overexpressed in primary human synovial fibroblasts by lentiviral gene transfer in patients with weak CD82 expression (left) as well as moderate CD82 expression (right panel) as shown in exemplary Western blots. (C) Real-time PCR confirmed the CD82 upregulation after transduction in comparison to mock treated or RFP control (n=5 RASF from different patients) with 10-fold to 189-fold upregulation for the respective transduced cells (each population was significant in replicate measurements. Test: one-way ANOVA). LeCD82: lentiviral CD82 overexpression. leRFP: lentiviral red fluorescent protein overexpression. Mock: treatment control without virus. ANOVA, analysis of variance; RA, rheumatoid arthritis; RASF, RA synovial fibroblasts.

expression significantly but to a lower extent in both RASF and OASF (figure 2B, C).

For OASF, the baseline expression of CD82 was lower, similar to previously published results.[21 22] Therefore, the relative CD82 inducibility was higher in OASF due to the lower CD82 baseline levels. NSF showed comparable results to OASF except for TNF showing weaker CD82-induction (figure 2D). Although TGF-β significantly reduced the CD82 expression in RASF (figure 2A), the grade of regulation was low and not detectable for OASF (figure 2B).

CD82 overexpression in RASF

CD82 expression level in RASF from different patients varied. For lentiviral overexpression, RASF with moderate to intermediate CD82 expression were used. In comparison to mock and RFP-transduced cells, overexpression of CD82 in RASF resulted in an induction of CD82 on protein (figure 3A,B) and RNA level (n=5, figure 3C).

CD82 overexpression: fibroblast motility, migration, adhesion, proliferation

Lentiviral CD82 overexpression significantly reduced RASF migration (Boyden chamber) compared with RFP and to mock (figure 4A). In the cell motility assay, a significant reduction of RASF migration into the gap was observed for CD82-transduced RASF compared with mock (figure 4B). Apoptosis was not altered by CD82 (not shown) and RASF proliferation was non-significantly reduced after CD82 overexpression compared with controls (figure 4C). Cell-to-cell binding of RASF to confluent EC-layers showed reduced RASF-EC-interaction in CD82-overexpressing cells (figure 4D) and adhesion to culture plates was significantly reduced (figure 4E).

Confirmation of CD82-expression of RASF under in vivo conditions

To evaluate whether cultured RASF express similar CD82 levels compared with sites of cartilage invasion in vivo, the SCID-mouse-model was used. Human RASF (one population with intermediate CD82 expression) were implanted together with human cartilage subcutaneously at the ipsilateral site. Contralaterally, human cartilage was implanted without RASF. As shown previously, human RASF invade the coimplanted and contralateral cartilage.[23] Using LMM, cells at the implant cartilage invasion zone were isolated (n=6 animals). Pooled RNA was evaluated for CD82 expression compared with cultured RASF used for implantation. The presence of human CD82 at sites of

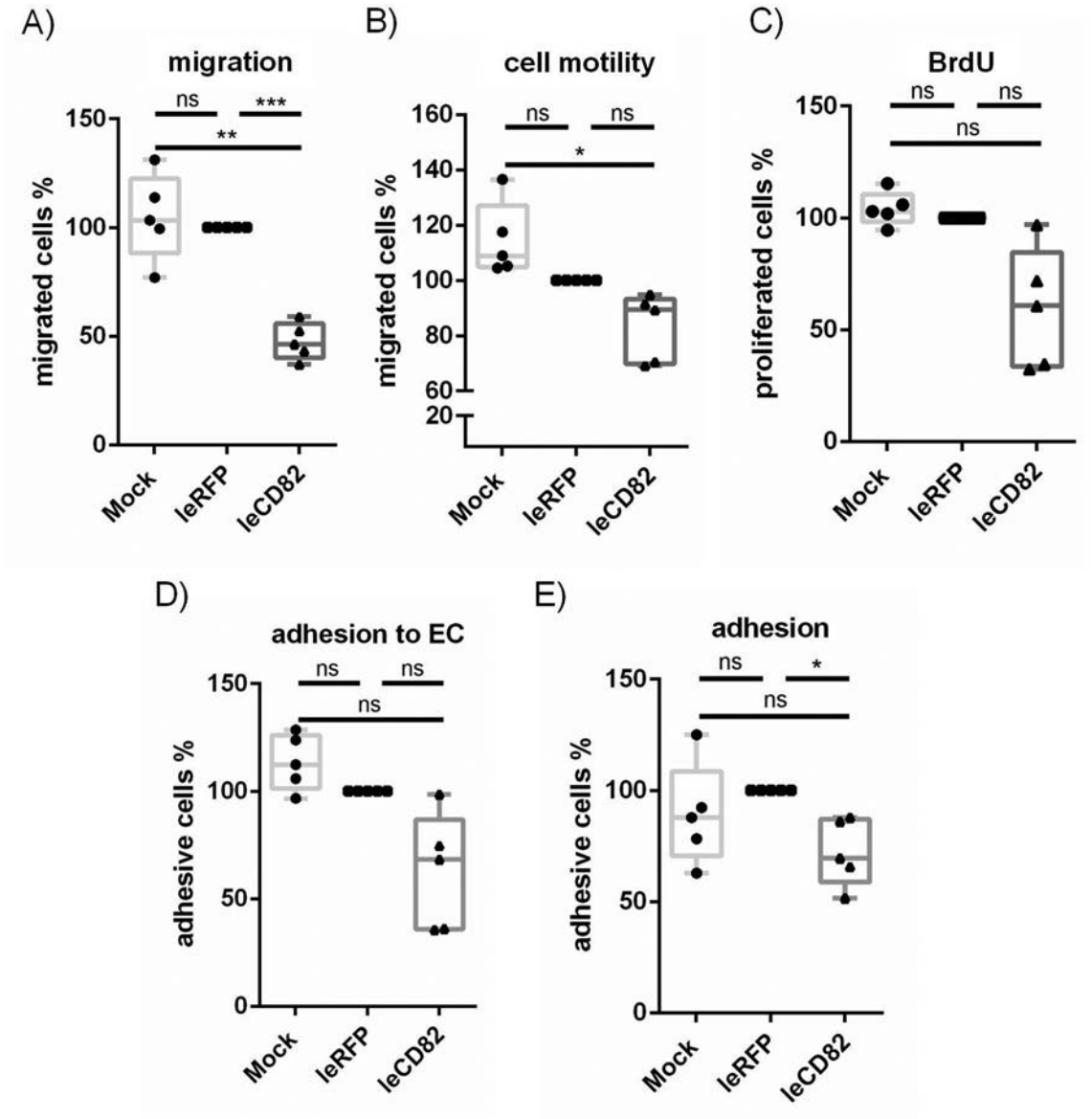

Figure 4 Effect of CD82 overexpression on cell migration, adhesion and proliferation. (A) CD82 significantly reduced RASF migration in the Boyden chamber assay towards a higher FCS gradient after 16 hours compared with mock-treated as well as RFP overexpressing cells (RFP set to 100% vs CD82 p=0.0004 and to mock p=0.0029; n=5, one-way ANOVA with Geissner-Greenhouse correction and Tukey's multiple comparisons test). (B) Cell motility was also significantly reduced by CD82 overexpression in the cell motility assay (scratch assay) without chemoattractant after 17 hours in comparison to mock control (leRFP set to 100% vs CD82 p=0.0771 and to mock p=0.0197; n=5, one-way ANOVA with Geissner-Greenhouse correction and Tukey's multiple comparisons test). (C) Proliferation of CD82 overexpressing cells was not significantly reduced after 24 hours compared with RFP or mock (CD82 vs RFP, p=0.0594; vs mock p=0.0600; n=5, one-way ANOVA with Geissner-Greenhouse correction and Tukey's multiple comparisons test). (D) CD82 overexpression reduced RASF adhesion to EC compared with RFP (leRFP set to 100%, p=0.0765; n=5) without reaching significance (one-way ANOVA with Geissner-Greenhouse correction and Tukey's multiple comparisons test). (E) Adhesion of RASF to culture surfaces was significantly reduced compared with RFP overexpressing RASF (leRFP set to 100%, p=0.0314; n=5, one-way ANOVA with Geissner-Greenhouse correction and Tukey's multiple comparisons test). Mock: Treatment control without virus. leRFP: lentiviral red fluorescent protein overexpression. LeCD82: lentiviral CD82 overexpression. ANOVA, analysis of variance; EC, endothelial cells; RA, rheumatoid arthritis; RASF, RA synovial fibroblasts.

cartilage invasion (online supplementary file 2) was comparable to cultured RASF used for implantation with similar levels of *human* (not mouse) CD82 mRNA (online supplementary file 2). Of note, human CD82 expression was comparable in the invasion zone of both sites (data not shown).

CD82 knockdown in RASF

To evaluate whether CD82 downregulation has opposite effects, siRNA-mediated CD82 knockdown was confirmed by Western blot (figure 5A). RASF adhesion was induced by CD82 knockdown in contrast to RASF cell-to-cell binding to EC, which was reduced versus NTP and mock (figure 5B). CD82 knockdown significantly increased RASF migration towards a higher FCS gradient as chemoattractant (figure 5C). Similarly, cell motility assays without chemoattractant showed increased RASF migration compared with NTP or mock (figure 5D).

DISCUSSION

In RA-synovium, CD82 expression was mainly detectable in the hyperplastic LL and vessels.[21 22] We observed a CD82 induction

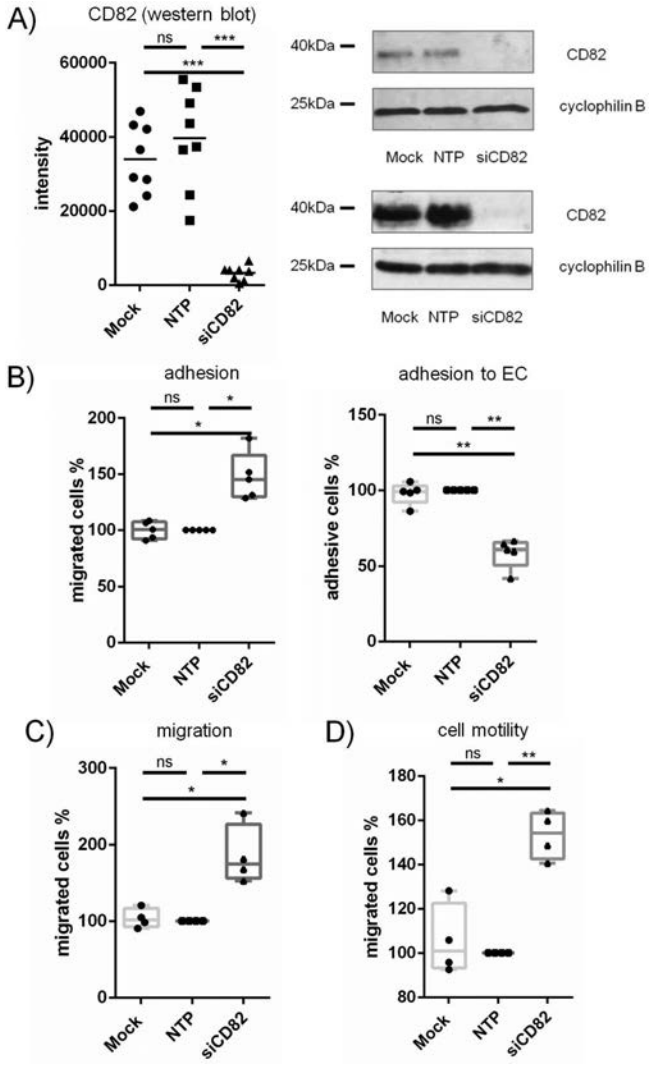

Figure 5 Effect of CD82 knockdown on RASF. (A) Knockdown efficiency of siRNA-mediated CD82 knockdown was confirmed by Western blot and signal intensity quantified (ImageJ software) showing a significant CD82 reduction compared with NTP siRNAs and mock controls (vs NTP, p=0.0002, vs mock p=0.0001, one-way ANOVA with Geissner-Greenhouse correction and Tukey's multiple comparisons test was used). (B) siRNA-mediated knockdown of CD82 significantly induced cell-matrix adhesion of RASF (left; NTP set to 100% vs CD82 p=0.0166) and to mock (p=0.0230; n=5) in contrast to reduced cell-to-cell binding capacity of RASF to EC (right; NTP set to 100% vs CD82 p=0.0015) and to mock (p=0.0064; n=5, RM one-way ANOVA test as described in methods). (C) Migration of RASF towards a higher FCS gradient was significantly increased in comparison to controls (CD82 vs NTP p=0.0437; vs mock p=0.0199; n=4) as well as cell motility (D) without chemoattractant shown in the scratch motility assay (CD82 vs NTP p=0.0045; vs mock p=0.0420; n=4, RM one-way ANOVA test as described in methods). ANOVA, analysis of variance; EC, endothelial cells; NTP, non-targeting-pool; RA, rheumatoid arthritis; RASF, RA synovial fibroblasts.

in RASF by proinflammatory factors, which could explain the increased CD82 expression in inflamed RA tissue similar to the situation in cancer.[2 4] Interestingly, the proinflammatory stimuli were also able to induce CD82 in OASF. However, due to chronic inflammation in RA, the exposure of SF to these factors is increased in RA. Aside of the LL, we found increased CD82 levels in RASF at the cartilage invasion zone, which was also confirmed in the SCID-mouse-model. In contrast, the main localisation of CD82 in the sublining was around vessels. Therefore, CD82 expression in RASF appears dependent on the localisation within the tissue and on local factors.

SF, especially activated fibroblasts in the LL, express increased amounts of different integrins, including the collagen receptor α1β1, the fibronectin receptor α5β1, the laminin receptors α3β1 and α6β1, the vitronectin receptor αvβ3.[32] CD82 has been described to attenuate β1-integrin activation in prostate cancer cells[33] but also to downregulate the level, activity and signalling of integrins,[34] the latter correlating with decreases in focal adhesions, stress fibres[34 35] and maturation of β1-integrin.[34] In our study, β1-integrin was colocalised with CD82, especially in deeper areas of the LL but also in invading RASF. We observed a reduced migration after CD82-overexpression, likely contributing to RASF accumulation at sites of cartilage invasion, a process that could be increased by inflammation.[24 36] CD82 colocalised with αVβ3-integrin on experimental overexpression in ovarian cancer cells.[37] The expressions of CD82 and αV-integrin, however, was inversely correlated in cancer[4] and EC.[10] We observed the colocalisation of CD82 with αV-integrin mainly in single cells of the invasion zone and LL. Association of CD82 with α6-integrin decreased adhesion and migration of prostate cancer cells.[38] In our study, α6-integrin was not detectable close to cartilage invasion and colocalisation with CD82 was limited to the LL. The strongest colocalisation with CD82 was present in the endothelium, supporting the role of endothelium in RASF recruitment and mobility. The RASF recruitment and the increased integrin expression at the site of cartilage invasion is well known.[39] However, the CD82-induction at sites of cartilage erosion may contribute to hold activated RASF on-site.

CD82-overexpression significantly reduced RASF motility similar to the observations in tumour cells.[4 7] Interestingly, cell-matrix adhesion and binding to EC were reduced by CD82 overexpression, suggesting a reduced potential for RASF-attachment to EC in local vessels. The increased expression of CD82 in the vascular wall and its close proximity[22] suggests a role of CD82 in vascular activation including synovial neoangiogenesis.[40]

Due to lower CD82 expression in RASF in the sublining, a CD82 knockdown was performed showing that the migratory capability of RASF was significantly increased. However, cell-to-cell binding of RASF to EC was reduced in contrast to cell-matrix adhesion, which was increased in contrast to CD82 overexpression. Therefore, RASF in the sublining expressing less CD82 may be able to migrate but their capacity to attach to EC is not increased. Potentially, at sites of inflammation and matrix destruction CD82-induction takes place, contributing to RASF accumulation. A similar observation has been made for podoplanin (PDPN) and CD248 with a high expression of PDPN in the LL, whereas CD248 expression was restricted to sublining cells.[41] In this study, TNF or IL-1β also increased PDPN expression whereas TGF-ß induced CD248. Local RASF-proliferation may also contribute to increased RASF numbers at the site of erosion. In our study, CD82-overexpression had only limited effects on RASF-proliferation.

CD82 appears to play a role in cell adhesion and motility in the inflamed rheumatoid synovium. Our data show that CD82 is induced by inflammation, both in RASF close to vessels and at sites of cartilage damage. On cellular level, this may be mediated by interaction of CD82 with surface integrins, expressed at the sites of cartilage invasion and LL. Reduced CD82 in the sublining may facilitate RASF migration to sites of inflammation and tissue damage.

Acknowledgements We would like to thank Dirk Schröder for technical contributions as well as Simone Benninghoff, Carina Schreiyäck. We thank Mona Arnold for her help during the revision.

Contributors Project conception and design: EN, MSc, UM-L. Acquisition of data: MSc, RH, M-LH, MSa, SR. Analysis and interpretation of data: EN, MSc, M-LH, SC. Drafting and/or revision of article: EN, MSc, M-LH, UM-L.

Funding This project was funded by the Kerckhoff-Stiftung, the DFG excellence cluster for cardiopulmonary research (ECCPS) and the BMBF (IMPAM, project 01EC1008G).

Competing interests None declared.

Patient consent Not required.

Ethics approval Local ethics committee.

Provenance and peer review Not commissioned; externally peer reviewed.

Data sharing statement There are no shared additional unpublished data from the study available.

REFERENCES

1 Berditchevski F, Odintsova E. ErbB receptors and tetraspanins: Casting the net wider. *Int J Biochem Cell Biol* 2016;77(Pt A):68–71.
2 Tsai YC, Weissman AM. Dissecting the diverse functions of the metastasis suppressor CD82/KAI1. *FEBS Lett* 2011;585:3166–73.
3 Liu WM, Zhang XA. KAI1/CD82, a tumor metastasis suppressor. *Cancer Lett* 2006;240:183–94.
4 Feng J, Huang C, Wren JD, *et al*. Tetraspanin CD82: a suppressor of solid tumors and a modulator of membrane heterogeneity. *Cancer Metastasis Rev* 2015;34:619–33.
5 Zöller M. Tetraspanins: push and pull in suppressing and promoting metastasis. *Nat Rev Cancer* 2009;9:40–55.
6 Malik FA, Sanders AJ, Jiang WG. KAI-1/CD82, the molecule and clinical implication in cancer and cancer metastasis. *Histol Histopathol* 2009;24:519–30.
7 Dong JT, Lamb PW, Rinker-Schaeffer CW, *et al*. KAI1, a metastasis suppressor gene for prostate cancer on human chromosome 11p11.2. *Science* 1995;268:884–6.
8 Bandyopadhyay S, Zhan R, Chaudhuri A, *et al*. Interaction of KAI1 on tumor cells with DARC on vascular endothelium leads to metastasis suppression. *Nat Med* 2006;12:933–8.
9 Larochelle A, Gillette JM, Desmond R, *et al*. Bone marrow homing and engraftment of human hematopoietic stem and progenitor cells is mediated by a polarized membrane domain. *Blood* 2012;119:1848–55.
10 Wei Q, Zhang F, Richardson MM, *et al*. CD82 restrains pathological angiogenesis by altering lipid raft clustering and CD44 trafficking in endothelial cells. *Circulation* 2014;130:1493–504.
11 Xu C, Zhang YH, Thangavel M, *et al*. CD82 endocytosis and cholesterol-dependent reorganization of tetraspanin webs and lipid rafts. *Faseb J* 2009;23:3273–88.
12 Delaguillaumie A, Harriague J, Kohanna S, *et al*. Tetraspanin CD82 controls the association of cholesterol-dependent microdomains with the actin cytoskeleton in T lymphocytes: relevance to co-stimulation. *J Cell Sci* 2004;117(Pt 22):5269–82.
13 Khanna P, Chung CY, Neves RI, *et al*. CD82/KAI expression prevents IL-8-mediated endothelial gap formation in late-stage melanomas. *Oncogene* 2014;33:2898–908.
14 Gabellini C, Trisciuoglio D, Desideri M, *et al*. Functional activity of CXCL8 receptors, CXCR1 and CXCR2, on human malignant melanoma progression. *Eur J Cancer* 2009;45:2618–27.
15 Nishioka C, Ikezoe T, Furihata M, *et al*. $CD34^{+}/CD38^{-}$ acute myelogenous leukemia cells aberrantly express CD82 which regulates adhesion and survival of leukemia stem cells. *Int J Cancer* 2013;132:2006–19.
16 Nishioka C, Ikezoe T, Yang J, *et al*. CD82 regulates STAT5/IL-10 and supports survival of acute myelogenous leukemia cells. *Int J Cancer* 2014;134:55–64.
17 Odintsova E, van Niel G, Conjeaud H, *et al*. Metastasis suppressor tetraspanin CD82/KAI1 regulates ubiquitylation of epidermal growth factor receptor. *J Biol Chem* 2013;288:26323–34.
18 Danglot L, Chaineau M, Dahan M, *et al*. Role of TI-VAMP and CD82 in EGFR cell-surface dynamics and signaling. *J Cell Sci* 2010;123(Pt 5):723–35.
19 Zhu J, Liang C, Hua Y, *et al*. The metastasis suppressor CD82/KAI1 regulates cell migration and invasion via inhibiting TGF-β 1/Smad signaling in renal cell carcinoma. *Oncotarget* 2017;8:51559–68.
20 Smolen JS, Landewé R, Bijlsma J, *et al*. EULAR recommendations for the management of rheumatoid arthritis with synthetic and biological disease-modifying antirheumatic drugs: 2016 update. *Ann Rheum Dis* 2017;76:960–77.
21 Neumann E, Kullmann F, Judex M, *et al*. Identification of differentially expressed genes in rheumatoid arthritis by a combination of complementary DNA array and RNA arbitrarily primed-polymerase chain reaction. *Arthritis Rheum* 2002;46:52–63.
22 Hashimoto A, Tarner IH, Bohle RM, *et al*. Analysis of vascular gene expression in arthritic synovium by laser-mediated microdissection. *Arthritis Rheum* 2007;56:1094–105.
23 Lefèvre S, Knedla A, Tennie C, *et al*. Synovial fibroblasts spread rheumatoid arthritis to unaffected joints. *Nat Med* 2009;15:1414–20.
24 Neumann E, Lefèvre S, Zimmermann B, *et al*. Rheumatoid arthritis progression mediated by activated synovial fibroblasts. *Trends Mol Med* 2010;16:458–68.
25 Altman R, Asch E, Bloch D, *et al*. Development of criteria for the classification and reporting of osteoarthritis. Classification of osteoarthritis of the knee. Diagnostic and Therapeutic Criteria Committee of the American Rheumatism Association. *Arthritis Rheum* 1986;29:1039–49.
26 Arnett FC, Edworthy SM, Bloch DA, *et al*. The American Rheumatism Association 1987 revised criteria for the classification of rheumatoid arthritis. *Arthritis Rheum* 1988;31:315–24.
27 Taylor W, Gladman D, Helliwell P, *et al*. Classification criteria for psoriatic arthritis: development of new criteria from a large international study. *Arthritis Rheum* 2006;54:2665–73.
28 Neumann E, Judex M, Kullmann F, *et al*. Inhibition of cartilage destruction by double gene transfer of IL-1Ra and IL-10 involves the activin pathway. *Gene Ther* 2002;9:1508–19.
29 Judex M, Neumann E, Fleck M, *et al*. "Inverse wrap": an improved implantation technique for virus-transduced synovial fibroblasts in the SCID mouse model for rheumatoid arthritis. *Mod Rheumatol* 2001;11:145–50.
30 Neumann E, Lefèvre S, Zimmermann B, *et al*. Migratory potential of rheumatoid arthritis synovial fibroblasts: additional perspectives. *Cell Cycle* 2010;9:2286–91.
31 Frommer KW, Schäffler A, Büchler C, *et al*. Adiponectin isoforms: a potential therapeutic target in rheumatoid arthritis? *Ann Rheum Dis* 2012;71:1724.1–32.
32 Lowin T, Straub RH. Integrins and their ligands in rheumatoid arthritis. *Arthritis Res Ther* 2011;13:244.
33 Lee HA, Park I, Byun HJ, *et al*. Metastasis suppressor KAI1/CD82 attenuates the matrix adhesion of human prostate cancer cells by suppressing fibronectin expression and β1 integrin activation. *Cell Physiol Biochem* 2011;27:575–86.
34 Jee BK, Lee JY, Lim Y, *et al*. Effect of KAI1/CD82 on the beta1 integrin maturation in highly migratory carcinoma cells. *Biochem Biophys Res Commun* 2007;359:703–8.
35 Liu WM, Zhang F, Moshiach S, *et al*. Tetraspanin CD82 inhibits protrusion and retraction in cell movement by attenuating the plasma membrane-dependent actin organization. *PLoS One* 2012;7:e51797.
36 Angelotti F, Parma A, Cafaro G, *et al*. One year in review 2017: pathogenesis of rheumatoid arthritis. *Clin Exp Rheumatol* 2017;35:368–78.
37 Ruseva Z, Geiger PX, Hutzler P, *et al*. Tumor suppressor KAI1 affects integrin alphavbeta3-mediated ovarian cancer cell adhesion, motility, and proliferation. *Exp Cell Res* 2009;315:1759–71.
38 He B, Liu L, Cook GA, *et al*. Tetraspanin CD82 attenuates cellular morphogenesis through down-regulating integrin alpha6-mediated cell adhesion. *J Biol Chem* 2005;280:3346–54.
39 Lowin T, Straub RH, Neumann E, *et al*. Glucocorticoids increase alpha5 integrin expression and adhesion of synovial fibroblasts but inhibit ERK signaling, migration, and cartilage invasion. *Arthritis Rheum* 2009;60:3623–32.
40 Leblond A, Allanore Y, Avouac J. Targeting synovial neoangiogenesis in rheumatoid arthritis. *Autoimmun Rev* 2017;16:594–601.
41 Croft AP, Naylor AJ, Marshall JL, *et al*. Rheumatoid synovial fibroblasts differentiate into distinct subsets in the presence of cytokines and cartilage. *Arthritis Res Ther* 2016;18:270.

EXTENDED REPORT

Huntingtin-interacting protein 1 (HIP1) regulates arthritis severity and synovial fibroblast invasiveness by altering PDGFR and Rac1 signalling

Teresina Laragione,[1] Max Brenner,[2] Amit Lahiri,[1] Erjing Gao,[1] Carolyn Harris,[1] Percio S Gulko[1]

Handling editor Josef S Smolen

► Additional material is published online only. To view please visit the journal online (http://dx.doi.org/10.1136/annrheumdis-2018-213498).

[1]Division of Rheumatology, Department of Medicine, Icahn School of Medicine at Mount Sinai, New York City, New York, USA
[2]Center of Immunology and Inflammation, Feinstein Institute for Medical Research, Manhasset, New York, USA

Correspondence to
Dr Percio S Gulko, Division of Rheumatology, Icahn School of Medicine at Mount Sinai, New York, NY 10029, USA; percio.gulko@mssm.edu

Received 29 March 2018
Revised 18 June 2018
Accepted 19 June 2018
Published Online First 26 July 2018

To cite: Laragione T, Brenner M, Lahiri A, *et al*. *Ann Rheum Dis* 2018;**77**:1627–1635.

ABSTRACT

Objectives While new treatments for rheumatoid arthritis (RA) have markedly improved disease control by targeting immune/inflammatory pathways, current treatments rarely induce remission, underscoring the need for therapies that target other aspects of the disease. Little is known about the regulation of disease severity and joint damage, which are major predictors of disease outcome, and might be better or complementary targets for therapy. In this study, we aimed to discover and characterise a new arthritis severity gene.

Methods An unbiased and phenotype-driven strategy including studies of unique congenic rat strains was used to identify new arthritis severity and joint damage genes. Fibroblast-like synoviocytes (FLS) from rats and patients with RA expressing or not Huntingtin-interacting protein 1 (HIP1) were studied for invasiveness, morphology and cell signalling. HIP1 knockout mice were used in in vivo confirmatory studies. Paired t-test was used.

Results DNA sequencing and subcongenic strains studied in pristane-induced arthritis identified a new amino acid changing functional variant in HIP1. HIP1 was required for the increased invasiveness of FLS from arthritic rats and from patients with RA. Knocking down HIP1 expression reduced receptor tyrosine kinase-mediated responses in RA FLS, including RAC1 activation, affecting actin cytoskeleton and cell morphology and interfering with the formation of lamellipodia, consistent with reduced invasiveness. HIP1 knockout mice were protected in KRN serum-induced arthritis and developed milder disease.

Conclusion HIP1 is a new arthritis severity gene and a potential novel prognostic biomarker and target for therapy in RA.

INTRODUCTION

Rheumatoid arthritis (RA) is one of the most common autoimmune diseases affecting nearly 1% of the population and is associated with reduced quality of life and increased risk for disability and reduced survival.[1–3] New and more effective therapies developed over the past two decades targeting the inflammatory mediators such as TNFα, costimulatory molecules and immune cells[4–7] have significantly improved quality of life and disease control. However, disease remission remains uncommon underscoring the residual need for better treatments for RA. Current therapies targeting different aspects of the immune response render patients more susceptible to infections, suggesting that greater inhibition of immunity or inflammation would not be helpful.[8] However, there are other approaches to target pathogenic mechanisms that should not increase the risk for infections. Currently, little is known about the regulation of disease severity and joint damage, which are major predictors of disease outcome and the risk for disability. Therefore, identifying severity and joint damage genes might yield promising novel targets for therapy. To our knowledge, few and small RA cohorts have prospectively studied the genetics of disease severity and joint damage,[9] and therefore very few discoveries have emerged from those studies.[10 11]

We used an unbiased strategy including unique congenic strains in rat models of RA varying in disease phenotype, and here report that Huntingtin-interacting protein 1 (HIP1) is a mediator of arthritis severity and joint damage. Fibroblast-like synoviocytes (FLS) from arthritis-protected congenic rats carrying ACI alleles at the Cia25/Pia42 locus had reduced invasiveness, a property known to strongly correlate with joint damage in rodent models of arthritis[12] and also in RA.[13] HIP1 was required for increased invasiveness of FLS from both arthritic rats and patients with RA, and thus is a promising therapeutic target. The mechanism of HIP1 regulation of invasiveness was analysed.

MATERIAL AND METHODS

Congenic and subcongenic breeding

DA.ACI(Cia25/Pia42) congenic breeding was previously reported.[14] We used a genotype-guided strategy to backcross congenics with DA/HsdNsi (DA) to generate partially overlapping subcongenics. Subcongenics sharing ACI alleles in the same recombinant interval were intercrossed to generate homozygous subcongenics, which were expanded and then used in arthritis studies. Rats and mice were kept in SPF conditions. Breeding and in vivo experiments were conducted under an Institutional Animal Care and Use Committee-approved protocol at the Feinstein Institute for Medical Research.

Induction of arthritis and disease severity scoring in rats

Pristane-induced arthritis (PIA) was induced by intradermal injection of 150 µL of pristane (Sigma, St. Louis, Missouri, USA)[15 16] and CIA by injection of rat type II collagen (RII) with incomplete Freud's adjuvant as previously described.[14] A well-established and reproducible arthritis scoring system

was used to evaluate rat joints including a functional parameter (weight bearing; score 0–80 per rat per time point).[17] The arthritis severity index (ASI; disease severity over time) provides a comprehensive evaluation of disease severity and correlates with histological damage.[16]

Arthritis studies in HIP1$^{-/-}$ (knockout) mice

HIP1$^{+/-}$ mice (C57BL/6 background) (gift from T. Ross, UT Southwestern Medical Center, Dallas, Texas, USA) were bred to homozygosity. The C57BL/6 background is susceptible to KRN serum-induced arthritis[18] but resistant to CIA or PIA. KRN arthritogenic serum was generated by breeding KRN TCR transgenic mice (gift from C. Benoist, Harvard, Boston, Massachusetts, USA) with NOD (KRNxNOD F1) and serum collected from arthritic mice. The serum was administered at 150 µL IP on day 0 and day 2.[18] HIP1$^{-/-}$ mice and HIP1 wild-type littermate controls were scored daily using a previously reported system[19] without knowledge of genotype (blindly) for 16 days.

Histology

Ankles were collected at the end of the in vivo studies, fixed in 1% formalin, decalcified, embedded in paraffin, sectioned, stained with H&E and assessed as previously described.[16]

Isolation and culture of FLS

FLS (human and rodent) were obtained as previously described.[19] Briefly, freshly obtained synovial tissues were minced and incubated with a solution containing DNase (0.15 mg/mL), hyaluronidase type I-S (0.15 mg/mL) and collagenase type IA (1 mg/mL) (Sigma) in DMEM (Invitrogen, Carlsbad, California, USA) for 1 hour at 37°C. Cells were washed and resuspended in complete media containing DMEM supplemented with 10% FBS (Invitrogen), glutamine (300 ng/mL), amphotericin B (250 µg/mL) (Sigma) and gentamicin (20 µg/mL) (Invitrogen). After overnight culture, non-adherent cells were removed and adherent cells cultured. All experiments were performed with FLS after passage four (>95% FLS purity).

Invasion assay

The in vitro invasiveness of FLS was assayed in a transwell system using Matrigel-coated inserts (BD Biosciences, Franklin Lakes, New Jersey, USA), as previously described.[12 19] Briefly, 70%–80% confluent cells were harvested by trypsin-EDTA digestion and resuspended in 500 µl of serum-free DMEM. 2×10^4 cells were placed in the upper compartment of each Matrigel-coated inserts. The lower compartment was filled with media containing 10% FBS or RTK ligands and the plates were incubated at 37°C for 24 hours. After 24 hours, the upper surface of the insert was wiped with cotton-swabs to remove non-invading cells and the Matrigel layer. The opposite side of the insert was stained with Crystal Violet (Sigma) and the total number of cells that invaded through Matrigel counted at 25× magnification. Experiments were done in duplicate.

siRNA knockdown

Dharmacon SMARTpool siRNA targeting either HIP1, GAPDH or a non-coding control was purchased from GE Lifesciences (Lafayette, Colorado, USA) and transfected into DA or RA FLS according to the manufacturer's instructions. Cells were then incubated at 37°C for 24–48 hours prior to initiating the invasion assays. Knockdown was confirmed with qPCR and western blot.

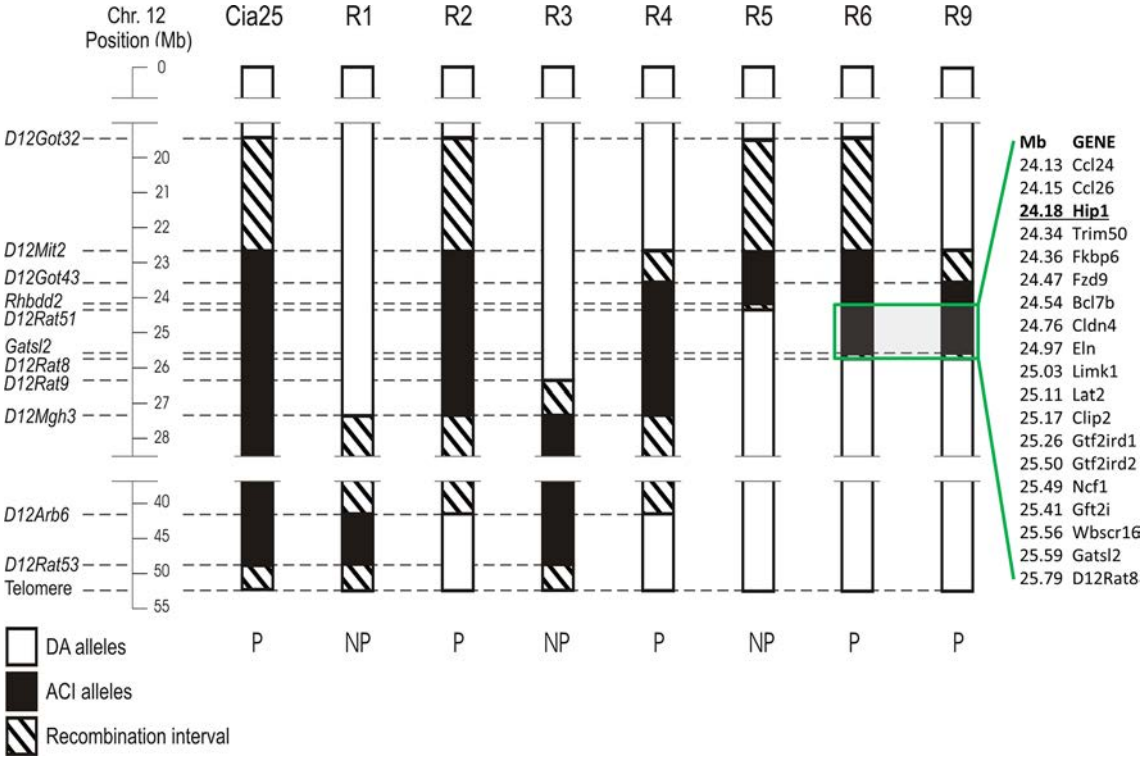

Figure 1 Physical map of the DA.ACI(Cia25/Pia42) congenic and recombinant (R) subcongenic strains. SSLP and SNP markers and their physical location (Mb) are shown on the left. The right side of the figure shows the refined Cia25/Pia42 1.7 Mb interval defined by *Rhbdd2* and *D12Rat8* (green box) and selected genes in the interval. (P=protected; NP=not protected; white segments=homozygous DA alleles; black segments=homozygous ACI alleles; striped segments=recombination intervals).

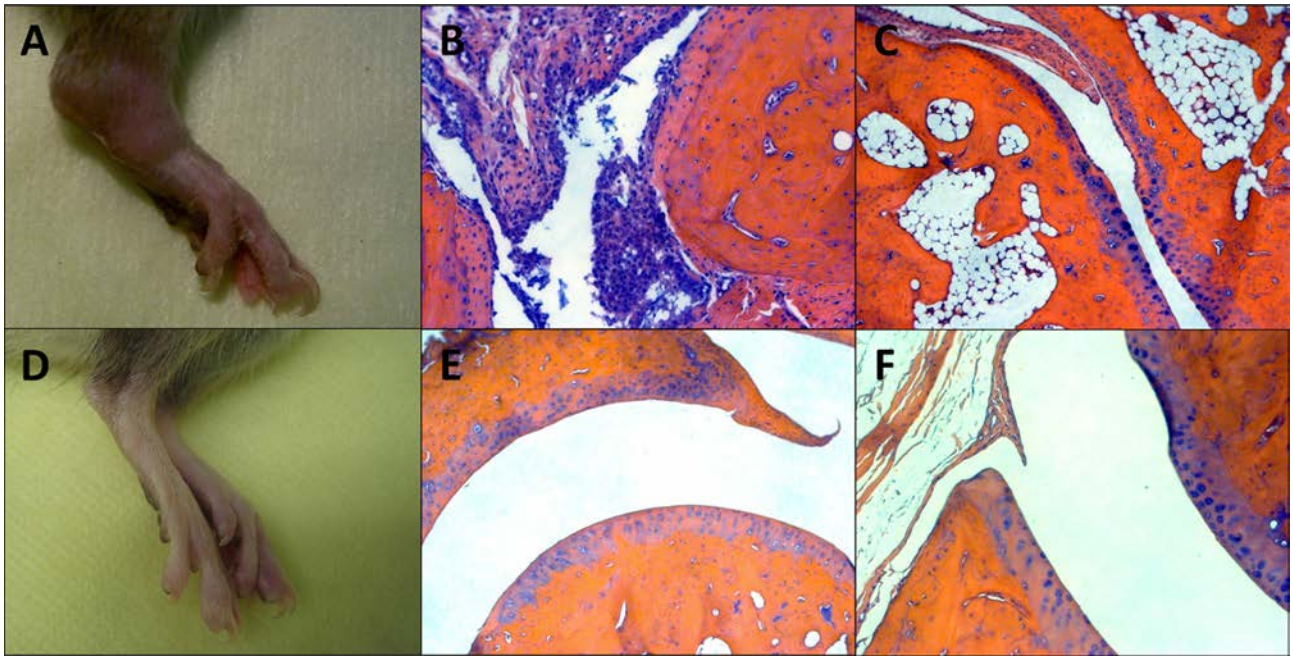

Figure 2 Decreased arthritis severity and joint damage in rats carrying ACI alleles at the R6 interval. (A) DA rat joints had pronounced ankle swelling, and (B,C) synovial hyperplasia, cartilage and bone erosions and inflammatory cell infiltration detectable as early as day 21 after the induction of disease. (D) Joints from DA.ACI(Cia25/Pia42-R6) subcongenics developed minimal arthritis on a few interphalangeal joint (joint swelling) but (E,F) retained a normal joint architecture with no damage. H&E staining; 100× magnification.

Immunofluorescence microscopy

Immunofluorescence was performed as previously reported.[19] Cells were treated with siRNA and then stimulated with either vehicle, FBS 10% or PDGFβ 50 ng/mL (Gemini Bioproduct, Sacramento, California, USA) for 15 min, fixed with 4% formaldehyde, permeabilised with PBS-Triton 0.01% and stained with phalloidin (Thermo Scientific) and anti-phospho-FAK (Abcam, Cambridge, Massachusetts, USA). Cells were visualised and scored using a LEICA DMi8 microscope (Leica, Buffalo Grove, Illinois, USA) and analysed with LASX software (Leica).

Confocal microscopy

RA FLS were cultured and treated with siRNA and PDGFβ 50 ng/mL as described above, then fixed, permeabilised and stained with anti-GM130 (Golgi) (Abcam, Cambridge, Massachusetts, USA), anti-clathrin heavy chain Alex-Fluo488 (Thermo Scientific, Rockford, Illinois, USA) or anti-PDGFRβ (Cell Signaling, Danvers, Massachusetts, USA). Cells were visualised and scored using a LEICA SP5 DM microscope and analysed with LASX software (Leica).

Sequencing candidate genes within the refined 1.7 Mb Cia25/Pia42-R6 interval

Genes in the refined interval were identified from the Rat Genome Database, Ensembl and NCBI[20–22] and the conservation of gene number and order was confirmed in the most updated versions of syntenic intervals in the mouse and human genomes. The sequencing analyses focused on coding regions of each gene, using cDNA generated from splenic RNA. All genes were expressed in the spleen and those also expressed in FLS were sequenced. PCR products were sequenced bidirectionally by a

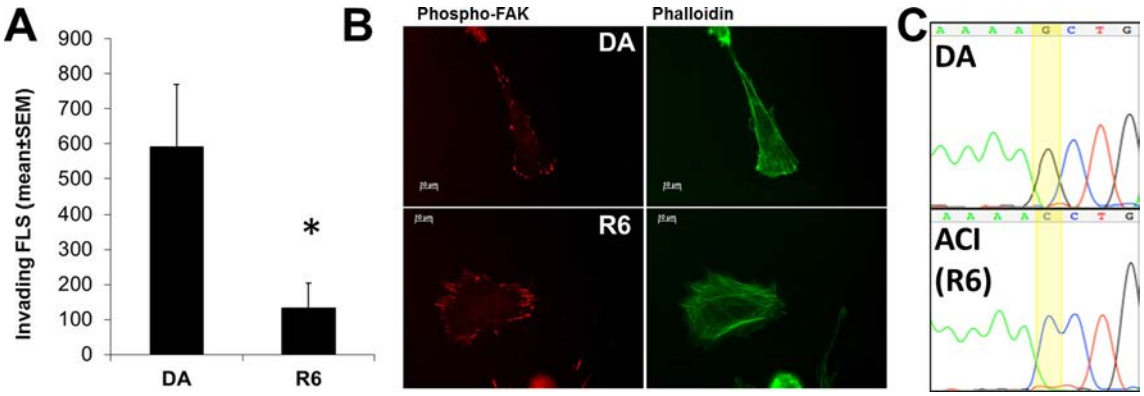

Figure 3 Decreased invasiveness and morphological changes in FLS from DA.ACI(Cia25/Pia42-R6) subcongenics. (A) FLS derived from Cia25/Pia42-R6 subcongenics were 78% less invasive than DA. *P=0.026, Mann-Whitney test; n=6 (per strain). (B) DA FLS had an elongated shape with linearised actin filaments and polarised formation of lamellipodia stained positive for p-FAK (top panels), while FLS from R6 subcongenics had a round morphology with disorganised actin filaments and p-FAK positive lamellipodia-like structures all around the cell periphery (bottom panels). (C) Sequencing data showing the amino acid changing G to C SNP in DA and ACI (R6 subcongenic). FLS, fibroblast-like synoviocytes.

service contractor (Genewiz) using BigDye Terminator reagents (ABI) and data analysed with DNASTAR/Lasergene package (Madison, Wisconsin, USA).

Cloning and expression of DA and R6 (ACI) HIP1 alleles

cDNA from DA and the R6 (ACI) HIP1 were subcloned into PCDNA3.1 as an N-terminal GFP fusion protein using TOPO-TA expression kit (Invitrogen). The clones were confirmed by sequencing. DA and R6 FLS cells were transiently transfected with the other strain's HIP1 allele by TransIT2020 (Mirus Bio, Madison, Wisconsin, USA) with 500 ng of HIP1-GFP constructs (from the other strain) or empty vector (PCDNA3.1-GFP). Twenty-four hours after transfection, FLS were trypsinised, counted and used in the in vitro invasion assay. After 24 hours, non-invading cells were wiped from the upper surface of the insert and total GFP positive cells that invaded through the Matrigel were counted at 10× magnification in a fluorescence microscope. Cell viability was assessed 48 hours after transfection (time required for transfection and invasion) by CellTitre One Solution (Promega). Similarly, Western blot was performed 48 hours post-transfection to confirm HIP1-GFP allele overexpression (140 KDa) using anti-HIP1 antibody (Sigma, diluted 1:5000). Endogenous HIP1 protein (115 KDa) served as the loading control.

RAC1 activity

RAC1 activity was measured in cell lysates using the RAC1 G-ELISA Activation kit (Cytoskeleton, Denver, Colorado, USA), according to the manufacturer's instructions.

RESULTS

Refining the chromosomal interval containing the *Cia25/Pia42* gene

We have previously studied an F2 intercross between the arthritis-susceptible and erosive rat strain DA (DA/HsdNsi) and MHC-identical but arthritis-resistant and non-erosive strain ACI (ACI/HsdNsi) in collagen-induced arthritis (CIA). One of the major arthritis severity quantitative trait loci (QTL) we identified in this intercross was *Cia25/Pia42* on rat chromosome 12.[23] DA.ACI(Cia25/Pia42) congenics were generated containing a 22.3 Mb interval derived from the ACI strain and introgressed into DA. These congenics were protected in both CIA and even more significantly in the also erosive model PIA.[14]

Using a genotype-guided breeding strategy, partially overlapping congenics were generated and studied in PIA leading to the reduction of the gene-containing interval from 22.7 Mb to a 1.7 Mb region on rat chromosome 12 contained within the DA.ACI(Cia25/Pia42-R6) (R6) subcongenic line (figure 1 and online supplementary figures 1 and 2). The defined region contained 41 genes (online supplementary table 1). While DA rats developed severe disease with early erosive changes (figure 2A–C) protected R6 congenics had minimal disease with no significant joint damage (figure 2D–F and online supplementary table 2), suggesting that the gene in this interval might regulate FLS invasiveness and destruction.

The *Cia25/Pia42* locus regulates FLS invasiveness

Primary FLS cell lines generated from R6 subcongenics (which carry ACI alleles at the protective 1.7 Mb interval) were 78% less invasive than FLS from DA rats (p=0.026; figure 3A), suggesting that the arthritis severity gene acted at least in part via FLS. DA FLS cultured with FBS developed a predominantly elongated shape with polarised formation of lamellipodia and thick linearised actin filaments, while R6 subcongenic-derived FLS had a round shape with non-polarised formation of lamellipodia and disorganised actin filaments, characteristics of non-invading cells (figure 3B).

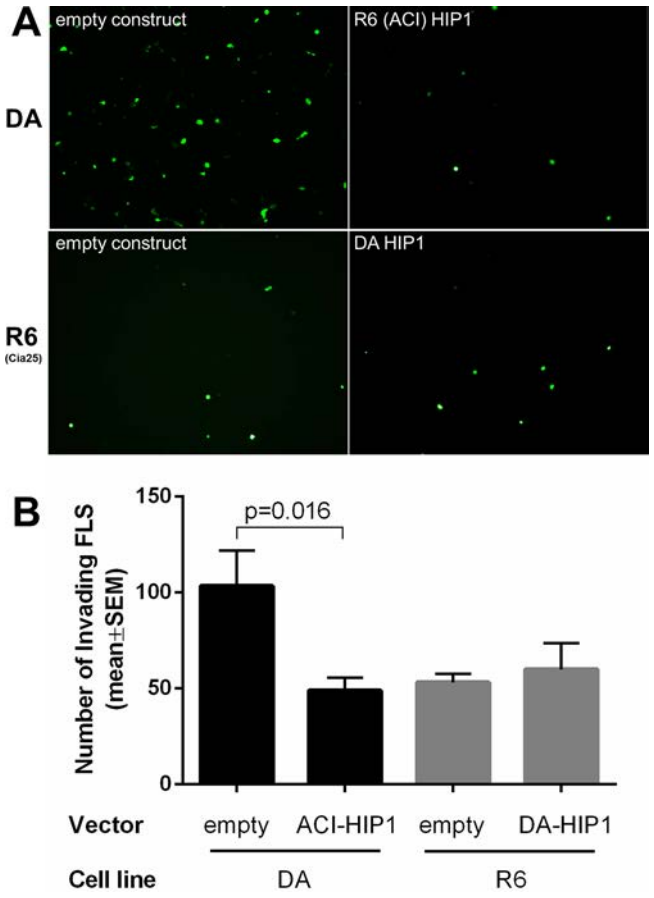

Figure 4 DA FLS transfected with HIP1 alleles derived from R6 (ACI) have reduced invasiveness. (A) The number of invading GFP-positive DA FLS was markedly reduced after transfection with the R6 (ACI) HIP1 allele (top panels), but the number of invading DA.ACI(Cia25/Pia42-R6) (R6) FLS was not affected by transfection with HIP1 alleles from DA (bottom panels). (Matrigel invasion assay; 25× magnification). (B) Transfection with the HIP1 allele from R6 (ACI) reduced the invasiveness of DA FLS by 50%, while transfection with HIP1 alleles from DA did not increase the invasiveness of R6 FLS. (P=0.016, paired t-test; n=4 per treatment in duplicates). FLS, fibroblast-like synoviocytes; HIP1, Huntingtin-interacting protein 1.

Identification of HIP1 as a new arthritis severity and FLS invasion gene

As the arthritis gene contained within the Cia25/Pia42 interval regulated FLS invasion we devised an integrated approach to determine the specific gene(s) involved. Specifically, we sequenced the genes in the 1.7 Mb interval, analysed the potential functional consequences of amino acid coding region changes using SIFT[24] and PolyPhen2,[25] and determined their expression in FLS (rat and human). Using this strategy, we identified three genes expressed in FLS and with amino acid changing SNPs predicted to have functional consequences. One of these three genes, HIP1, was expressed in synovial tissues, with higher protein levels in DA compared with R6 subcongenics, correlating with cell invasiveness (online supplementary figure 3). HIP1 protein was also abundantly expressed in human RA FLS.

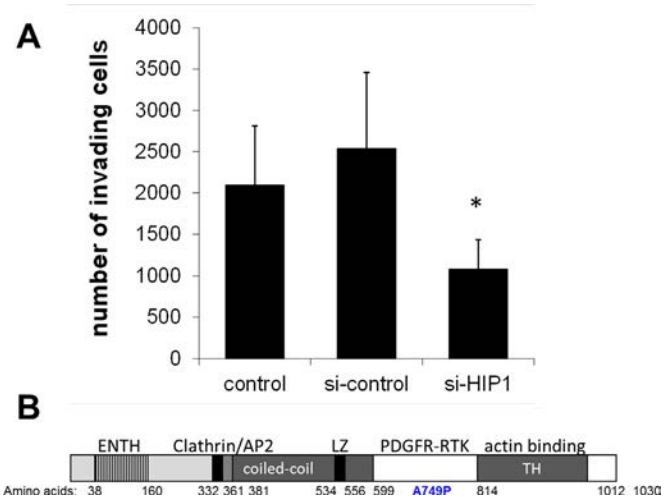

Figure 5 Reduction of DA FLS invasion by HIP1 siRNA knockdown and location of HIP1 non-synonymous SNP. (A) siRNA knockdown of HIP1 reduced the number of invading FLS by 42% compared with the siRNA control group. Mean±SEM; n=7; p=0.046, paired t-test. (B) Schematic depiction of HIP1 and the location of the A749P SNP in the RTK-binding region. FLS, fibroblast-like synoviocytes; HIP1, Huntingtin-interacting protein 1.

Six SNPs were identified in HIP1 coding regions. These included four synonymous changes, one amino acid changing SNP predicted to be non-functional (non-polar to non-polar) and only one non-synonymous C2245G SNP that caused an A749P (non-polar to polar) amino acid change (figure 3C) in its receptor tyrosine kinase (RTK) binding region. HIP1 is a 35-exon, 1038-amino acid protein in the rat and 1037-amino acid protein in humans expressed in increased levels in several cancers[26 27] and capable of transforming cells and increasing accumulation of RTK such as EGFR.[28]

HIP1 alleles from DA and R6 (ACI) strains differentially affect FLS invasion

To determine whether HIP1 alleles from DA and R6 (ACI) directly modified and accounted for the difference in FLS invasiveness the two different alleles were cloned into a PCDNA3.1 construct as an N-terminal GFP fusion protein and reciprocally transfected into FLS cells of R6 (ACI) and DA rats, followed by invasion studies in the Matrigel transwell system. DA FLS transfected with the R6 (ACI) HIP1 allele had a significant 50% reduction in the number of invading cells (p=0.016, paired t-test; figure 4A) without affecting cell survival, suggesting a dominant negative effect of the R6 (ACI) HIP1 allele on invasiveness. Transfection of the DA HIP1 allele into R6 FLS had no detectable effect on invasiness (figure 4B).

HIP1 is required for increased invasiveness of DA FLS

To examine whether HIP1 is required for FLS invasiveness siRNA was used to knock down HIP1 in DA cell lines. siRNA HIP1 reduced the mRNA and protein levels of HIP1 by more than 60% (online supplementary figure 4) and reduced invasiness by 42% compared with control siRNA (p=0.046, paired t-test; figure 5). The reduction in FLS invasiveness seen in HIP1 knocked down cells was similar to that seen in congenics compared with DA and as well as in the DA FLS transfected with R6 alleles, suggesting that HIP1 accounted for most of the differences in FLS invasiveness.

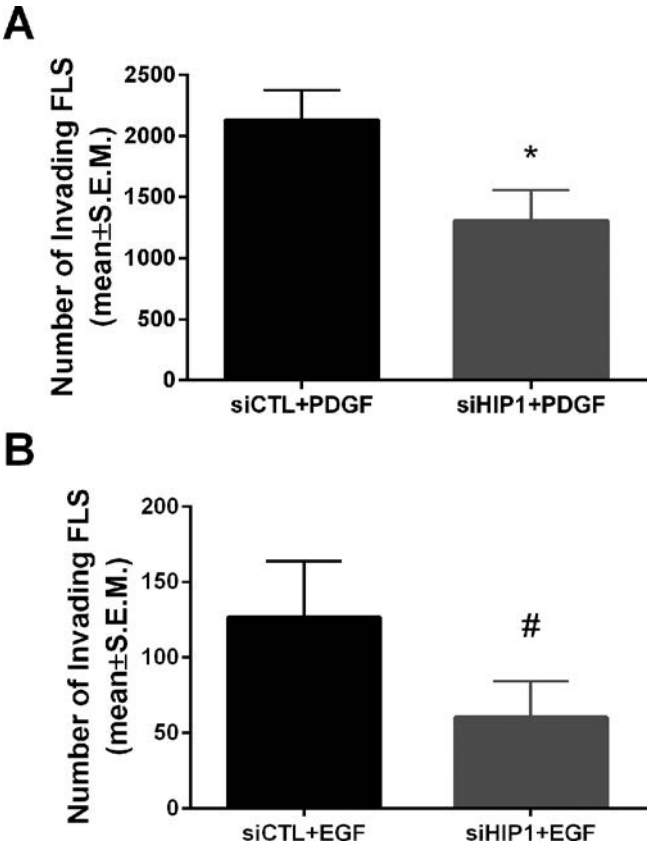

Figure 6 Knockdown of HIP1 in RA FLS reduces RTK ligand-induced invasion. RA FLS subjected to HIP1 siRNA knockdown showed (A) a 40% reduction in cell invasion induced with 50 ng/mL PDGFβ (*p=0.01; n=8) and (B) a 57% reduction in the invasion induced with 1 µg/mL EGF (#p=0.06; n=7). Mean±SEM; paired t-test. FLS, fibroblast-like synoviocytes; HIP1, Huntingtin-interacting protein 1.

HIP1 regulates invasiveness of human RA FLS

HIP1 was also expressed in RA FLS. To examine whether HIP1 was required and critical for RA FLS invasiveness siRNA was used to knock down HIP1. Similarly to DA FLS, knockdown of HIP1 in RA FLS reduced cell invasiveness by nearly 44% compared with control siRNA (p=0.057, paired t-test; online supplementary figure 5).

HIP1 mediates RA and rodent FLS invasion induced by RTK ligands

Given the known interaction between the region containing the A749P amino acid changing SNP and RTKs (figure 5B), it was considered that HIP1 might be regulating invasion mediated by these receptors or RTK-induced HIP1 interaction with actin to modify the cell morphology. In the presence of PDGFβ DA FLS were highly invasive while FLS from congenics remained minimally invasive (online supplementary figure 6). Next, the role of HIP1 in RTK-mediated invasion was examined in cells from patients with RA. siRNA knockdown of HIP1 significantly reduced PDGFβ-induced (50 ng/mL) invasion by 40% (p=0.01, paired t-test; figure 6A) and EGF-induced (1 µg/mL) invasion by 57% (figure 6B).

HIP1 is required for PDGF-induced cell morphological and cytoskeleton changes in RA FLS

RA FLS transfected with siRNA control and stimulated with PDGFβ developed the typical elongated FLS morphology

with thick actin filaments (figure 7A) and polarised formation of lammelipodia with colocalisation of p-FAK (figure 7B,C). However, knockdown of HIP1 induced an atypical stellate morphology, with thin and disorganised actin filaments, few thick actin fibres and non-polarised formation of small lamellipodia-like structures (figure 7D-F). These lamellipodia-like structures were seen around the cell periphery and did not have the characteristic colocalisation with p-FAK, suggesting a non-invading and non-mobile cell.

HIP1 regulates RTK cell signalling in RA FLS, regulating RAC1 activity

In order to characterise specific RTK intracellular signalling proteins regulated by HIP1, RA FLS treated with siRNA control or siRNA HIP1 were stimulated with vehicle or PDGFβ (50 ng/mL). Knockdown of HIP1 significantly reduced RAC1 activity by 50% (p=0.0018, paired t-test; figure 7G) compared with control siRNA. There was also a trend towards reduction in levels of p-ERK (data not shown).

The phosphorylation of each of five different tyrosines in PDGFR (tyr740, tyr1021, tyr751, tyr771, tyr1009) in RA FLS was not consistently affected by HIP1 siRNA. Moreover, no significant differences were detected in levels of other intracellular phosphorylated signalling proteins including those implicated in RTK signalling such as p-CREB, p-JNK, p-NFkB, p-p38, pAkt, p-p70S6K p-STAT3, p-STAT5 and p-FAK. mRNA levels of MMP1, MMP2, MMP3, MMP8, MMP9, MMP10, MMP12 and MMP13 as well as levels of proinflammatory mediators IL-1β, IL-6 and TNFα were also not significantly affected by HIP1 knockdown (data not shown).

Stable expression of RTK on the cell surface of FLS requires HIP1

Total protein levels of PDGF receptors were not affected by HIP1 knockdown in RA FLS. However, HIP1 knockdown was associated with a 17% reduction in cell surface levels of PDGFR compared with control siRNA (flow cytometry mean 3440.68 vs 4146.48 MFI; p=0.0289, paired t-test; n=4 different cell lines; figure 7H). The levels of PDGFR on the cell surface remained lower in HIP1 knockdown cells at most time-points except for at 5 min poststimulation with PDGFβ when levels were also reduced in control siRNA. Those observations suggested an effect of HIP1 on PDGFR endocytosis. Confocal microscopy revealed that HIP1 knockdown reduced PDGFR and clathrin localisation at the plasma membrane with increased diffuse cytoplasmic distribution (figure 7I–O). These results suggest that while HIP1 stabilises clathrin vesicles as previously known, it is also required for the stable expression of PDGFR in the plasma membrane.

HIP1 knockout mice are protected and develop milder arthritis

To determine whether HIP1 was a critical regulator of arthritis severity in vivo, we used a HIP1 functional knockout mouse. HIP1 knockout mice were significantly protected developing lower arthritis severity scores compared with littermate wild-type HIP1 in KRN serum-induced arthritis (p=0.001, Mann-Whitney test; figure 8).

DISCUSSION

While biologics and small molecules that target the immune response in RA have significantly improved disease control, disease outcomes and quality of life, most patients achieve only a moderate improvement and disease remission remains uncommon. Better understanding of disease pathogenesis including the unexplored topic of regulation of disease severity and joint damage might generate better targets for treatment, in isolation or combined with existing therapies. Currently, very little is known about the genes implicated in the regulation of these processes.[29 30]

In the present study, we report the discovery of a previously unsuspected arthritis severity gene, HIP1. We started with an unbiased strategy using unique congenic and subcongenics studied in well-established rat models of RA. HIP1 regulates FLS invasiveness which strongly correlates with histological and radiographic damage in rodent models of arthritis[12] and in RA.[13] HIP1 is a 35-exon gene encoding a 1037-amino acid protein expressed in most tissues, including brain, lungs and urinary tract, characterised by four main domains implicated in its different cellular functions: (1) the N-terminal domain binds phospholipids; (2) a coiled-coil domain binds clathrin, Huntington protein, the androgen receptor and is required for dimerisation; (3) an RTK-binding domain and (4) the C-terminal domain has a nuclear localisation signal and binds actin[31] (figure 5C). The A749P HIP1 SNP was localised in the RTK binding region and regulates RTK signalling. Confirming these effects in rats, knockdown of HIP1 similarly affected RTK signalling in FLS from patients with RA.

We demonstrate that HIP1 regulates disease severity, joint damage and invasiveness of FLS derived from patients with RA and from rats with arthritis. The effect of HIP1 in FLS invasiveness was confirmed using independent experimental strategies. We also demonstrate that HIP1 is required for the morphological and cytoskeletal characteristics of invading FLS, such as thick and organised actin filaments and the polarised formation of lamellipodia. In the absence of HIP1, RA FLS developed morphological and cytoskeletal characteristics of a cell that is unable to migrate or invade.

We further demonstrate that HIP1 is required for the stable expression of RTK in the FLS cell surface and for RTK-mediated FLS invasion and intracellular signalling. We describe that HIP1 regulates RAC1 activation. RAC1 has been documented to be of major importance in actin cytoskeleton rearrangements and hence in cell invasion.[32 33] Given that no significant differences in tyrosine phosphorylation were detected in PDGFR itself, HIP1 might increase PDGF-induced invasion by regulating both the cell surface expression of PDGFR and signalling events downstream from the receptor to modulate RAC1 activation.

RA FLS have characteristics that resemble those of cancer cells, including increased cell numbers (hyperplasia), increased in vitro longevity, increased invasiveness beyond tissue boundaries and increased expression of oncogenes, proteases and other mediators of invasion.[34–36] RA FLS can move from one joint to another, like a cancer potentially 'spreading' disease.[37] HIP1 is expressed in increased levels in several cancers and its levels correlate with poor prognosis in prostate cancer and glioblastoma.[26 27 38] Interestingly, both prostate cancer and glioblastomas are known to have increased levels of activated RAC1 and increased RAC1-mediated invasion,[39 40] raising the possibility that HIP1 may be an important contributor to RAC1 activation in those and other cancer cells. While in vitro overexpression of HIP1 transforms benign cells and affects receptor trafficking,[41] its role in cancer remains incompletely understood. Our discoveries raise the possibility that the association of increased HIP1 levels with worse outcome in certain cancers might be related to increased local or metastatic cancer invasiveness.

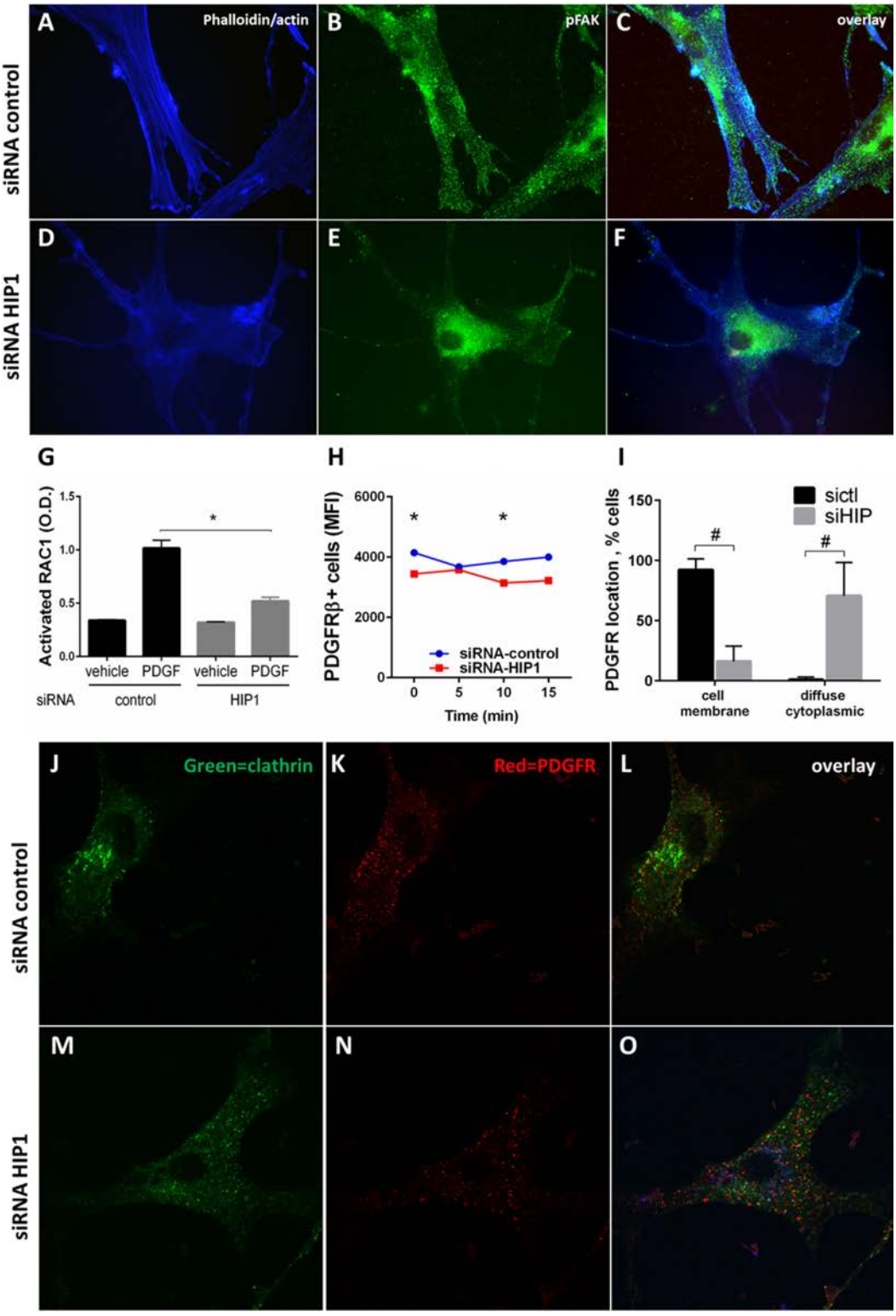

Figure 7 HIP1 effects on RA FLS morphology, actin filaments, RAC1 and PDGFRβ localisation. (A) RA FLS transfected with control siRNA and stimulated with PDGFβ (50 ng/mL) retained a typical elongated morphology with thick actin filaments, polarised formation of lamellipodia with (B and C) colocalisation with phospho-FAK. (D) siRNA knockdown of HIP1 induced a stellate and atypical morphology in RA FLS, with mostly thin and disorganised actin filaments (E) with small and non-polarised lamellipodia-like structures that had (F) reduced colocalisation with p-FAK. Knockdown of HIP1 significantly reduced PDGFβ-induced (5 min) (G) RAC1 activation by 50% (p=0.0018; n=4). (H) Levels of PDGFRβ were reduced by 17% in the cell surface of RA FLS knockdown for HIP1 before stimulation with PDGFβ 50 ng/mL (*p<0.05; paired t-test) and remained similarly lower at all time-points except 5 min poststimulation (n=4; flow cytometry). (I) Confocal microscopy scoring of PDGFR location in the cell revealed increased cell membrane localisation in RA FLS treated with siRNA control, while siRNA HIP1 treated cells had a predominantly cytoplasmic distribution ($^{\#}$p<0.01, t-test). (J–L) Increased localisation of clathrin (green) and PDGFR (red) near or at the plasma membrane in RA FLS treated with siRNA control. (M–O) RA FLS knockdown for HIP1 had reduced cell membrane and a more diffuse cytoplasmic localisation of clathrin and PDGFR. FLS, fibroblast-like synoviocytes; HIP1, Huntingtin-interacting protein 1.

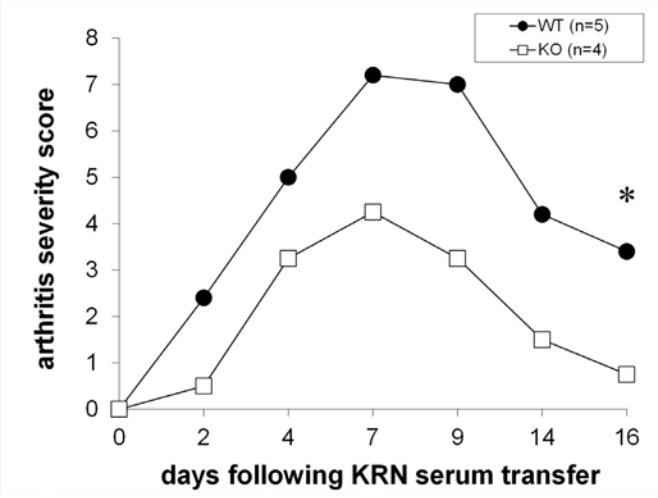

Figure 8 Reduced arthritis severity in homozygous HIP1 knockout mice. Homozygous HIP1 knockout mice developed a milder form of KRN serum transfer-induced arthritis compared with littermate controls. *P=0.032 (day 16), Mann-Whitney test. HIP1, Huntingtin-interacting protein 1.

The central role for HIP1 in arthritis severity was further demonstrated in in vivo studies in KRN serum induced arthritis. HIP1 homozygous knockout mice were protected and developed a milder form of arthritis. The KRN model is short-lived and joint erosive changes are not typically observed and therefore could not be examined. HIP1 knockout mice had reduced joint swelling, which suggests that HIP1 also affects components of the inflammatory response in the joints.

HIP1 has not been associated with susceptibility to RA in genome-wide association studies. However, our results demonstrate that HIP1 is a severity and joint damage regulatory gene and not a susceptibility gene. Until now, very few and small cohorts have prospectively followed patients with RA to assess the genetic regulation of disease severity and joint damage,[9] and therefore only few discoveries have emerged from those studies.[10 11] As such, it will be interesting to see whether HIP1 is also associated with genetic risk for disease severity and joint damage.

This is the first time that HIP1 has been implicated in arthritis severity and in the regulation of cell invasion. This new discovery suggests that HIP1 has the potential to become a new target for therapy in RA that, like IL-6 and TNFα, is not associated with genetic susceptibility to disease.

We acknowledge that the 1.7 MB rat chromosomal interval containing HIP1 contained a total of 41 genes (online supplementary table 1), and therefore we do not exclude the possibility that one or more of those genes might also regulate arthritis and/or arthritis-related phenotypes. Once we detected DNA sequencing differences in HIP1 from arthritis-susceptible and protected congenic strains, and evidence that HIP1 alleles regulated rat FLS behaviour, we focused our work on HIP1. We then demonstrated that HIP1 regulates the behaviour and cell signalling of FLS obtained from patients with RA. Additional evidence implicating HIP1 in arthritis was provided in studies with HIP1 homozygous knockout mice with KRN serum induced arthritis. While the arthritis studies in HIP1 knockout mice were conducted with a small number of mice (HIP1 homozygous knockout are known to be poor breeders), they were still able to provide important supportive evidence implicating HIP1 in the regulation of disease in vivo. These new findings and the discovery of a new gene regulating disease severity are of major interest to rheumatologists and open the possibilities for novel pathogenic aspects and novel targets for treatment.

A major limiting and concerning factor associated with most of the available treatments for RA is immunosuppression and increased risk of infections. HIP1 knockout mice did not develop any systemic or spontaneous severe infection suggesting that they were not immunocompromised. These observations raise the possibility that targeting this gene with a small molecule could be a promising future therapy to use alone or in combination with existing biologics that might not increase the risk of infections.

In conclusion, we have identified HIP1 as a new arthritis severity and joint damage gene. HIP1 inhibition might be a feasible future option to treat RA as a monotherapy or in combination with a well-established agent such as anti-TNFα or others to target the FLS to reduce joint damage. HIP1 also has the potential to become a prognostic biomarker in RA.

Acknowledgements The authors wish to thank Sir Marc Feldmann for insightful and critical review of this manuscript.

Contributors TL: concepts and design, experiments, interpretation or results and manuscript writing. MB: designed and conducted some in vivo experiments, interpretation of results and reviewed final manuscript. AL: conducted and designed, conducted and interpreted in vitro experiments with FLS and reviewed final manuscript. EG: assisted with animal breeding and tissue culture and reviewed final manuscript. CH: assisted with animal breeding, tissue culture and conducted invasion, WB and qPCRs, and reviewed final manuscript; PSG: conceptualised and oversaw this project, conducted in vivo experiments, interpreted all data, prepared figures and wrote the manuscript.

Funding Institutional funds.

Competing interests None declared.

Patient consent Not required.

Ethics approval All the experiments with animals were conducted according to a protocol approved by the Feinstein Institute's animal care and use committee. All RA synovial cell lines were developed from deidentified tissues obtained by the Feinstein Institute Tissue Donation programme under and IRB-approved protocol.

Provenance and peer review Not commissioned; externally peer reviewed.

Data sharing statement All sequencing data are available on request or via the Rat Genome Database.

REFERENCES

1 van Zeben D, Breedveld FC. Prognostic factors in rheumatoid arthritis. *J Rheumatol Suppl* 1996;44:31–3.
2 Gossec L, Dougados M, Goupille P, *et al*. Prognostic factors for remission in early rheumatoid arthritis: a multiparameter prospective study. *Ann Rheum Dis* 2004;63:675–80.
3 Wolfe F, Mitchell DM, Sibley JT, *et al*. The mortality of rheumatoid arthritis. *Arthritis Rheum* 1994;37:481–94.
4 Feldmann M, Maini RN. Lasker Clinical Medical Research Award. TNF defined as a therapeutic target for rheumatoid arthritis and other autoimmune diseases. *Nat Med* 2003;9:1245–50.
5 Nishimoto N, Hashimoto J, Miyasaka N, *et al*. Study of active controlled monotherapy used for rheumatoid arthritis, an IL-6 inhibitor (SAMURAI): evidence of clinical and radiographic benefit from an x ray reader-blinded randomised controlled trial of tocilizumab. *Ann Rheum Dis* 2007;66:1162–7.
6 Edwards JC, Szczepanski L, Szechinski J, *et al*. Efficacy of B-cell-targeted therapy with rituximab in patients with rheumatoid arthritis. *N Engl J Med* 2004;350:2572–81.
7 Genovese MC, Becker JC, Schiff M, *et al*. Abatacept for rheumatoid arthritis refractory to tumor necrosis factor alpha inhibition. *N Engl J Med* 2005;353:1114–23.
8 Feldmann M, Maini RN. Perspectives From Masters in Rheumatology and Autoimmunity: Can We Get Closer to a Cure for Rheumatoid Arthritis? *Arthritis Rheumatol* 2015;67:2283–91.
9 Bridges SL, Hughes LB, Mikuls TR, *et al*. Early rheumatoid arthritis in African-Americans: the CLEAR Registry. *Clin Exp Rheumatol* 2003;21(5 Suppl 31):S138–45.
10 Danila MI, Laufer VA, Reynolds RJ, *et al*. Dense Genotyping of Immune-Related Regions Identifies Loci for Rheumatoid Arthritis Risk and Damage in African Americans. *Mol Med* 2017;23:1.
11 van der Linden MP, Feitsma AL, le Cessie S, *et al*. Association of a single-nucleotide polymorphism in CD40 with the rate of joint destruction in rheumatoid arthritis. *Arthritis Rheum* 2009;60:2242–7.

12 Laragione T, Brenner M, Mello A, *et al*. The arthritis severity locus Cia5d is a novel genetic regulator of the invasive properties of synovial fibroblasts. *Arthritis Rheum* 2008;58:2296–306.
13 Tolboom TC, van der Helm-Van Mil AH, Nelissen RG, *et al*. Invasiveness of fibroblast-like synoviocytes is an individual patient characteristic associated with the rate of joint destruction in patients with rheumatoid arthritis. *Arthritis Rheum* 2005;52:1999–2002.
14 Brenner M, Laragione T, Mello A, *et al*. Cia25 on rat chromosome 12 regulates severity of autoimmune arthritis induced with pristane and with collagen. *Ann Rheum Dis* 2007;66:952–7.
15 Vingsbo C, Sahlstrand P, Brun JG, *et al*. Pristane-induced arthritis in rats: a new model for rheumatoid arthritis with a chronic disease course influenced by both major histocompatibility complex and non-major histocompatibility complex genes. *Am J Pathol* 1996;149:1675–83.
16 Brenner M, Meng HC, Yarlett NC, *et al*. The non-major histocompatibility complex quantitative trait locus Cia10 contains a major arthritis gene and regulates disease severity, pannus formation, and joint damage. *Arthritis Rheum* 2005;52:322–32.
17 Gulko PS, Kawahito Y, Remmers EF, *et al*. Identification of a new non-major histocompatibility complex genetic locus on chromosome 2 that controls disease severity in collagen-induced arthritis in rats. *Arthritis Rheum* 1998;41:2122–31.
18 Ji H, Gauguier D, Ohmura K, *et al*. Genetic influences on the end-stage effector phase of arthritis. *J Exp Med* 2001;194:321–30.
19 Laragione T, Cheng KF, Tanner MR, *et al*. The cation channel Trpv2 is a new suppressor of arthritis severity, joint damage, and synovial fibroblast invasion. *Clin Immunol* 2015;158:183–92.
20 Shimoyama M, De Pons J, Hayman GT, *et al*. The Rat Genome Database 2015: genomic, phenotypic and environmental variations and disease. *Nucleic Acids Res* 2015;43:D743–50.
21 National Center for Biotechnology Information N, NIH. Rat Genome Resources. 2004. http://www.ncbi.nlm.nih.gov/genome/guide/rat/index.html
22 Birney E, Andrews TD, Bevan P, *et al*. An overview of Ensembl. *Genome Res* 2004;14:925–8.
23 Meng HC, Griffiths MM, Remmers EF, *et al*. Identification of two novel female-specific non-major histocompatibility complex loci regulating collagen-induced arthritis severity and chronicity, and evidence of epistasis. *Arthritis Rheum* 2004;50:2695–705.
24 Ng PC, Henikoff S. Predicting deleterious amino acid substitutions. *Genome Res* 2001;11:863–74.
25 Adzhubei IA, Schmidt S, Peshkin L, *et al*. A method and server for predicting damaging missense mutations. *Nat Methods* 2010;7:248–9.
26 Bradley SV, Smith MR, Hyun TS, *et al*. Aberrant Huntingtin interacting protein 1 in lymphoid malignancies. *Cancer Res* 2007;67:8923–31.
27 Rao DS, Hyun TS, Kumar PD, *et al*. Huntingtin-interacting protein 1 is overexpressed in prostate and colon cancer and is critical for cellular survival. *J Clin Invest* 2002;110:351–60.
28 Rao DS, Bradley SV, Kumar PD, *et al*. Altered receptor trafficking in Huntingtin Interacting Protein 1-transformed cells. *Cancer Cell* 2003;3:471–82.
29 Drossaers-Bakker KW, Zwinderman AH, Vliet Vlieland TP, *et al*. Long-term outcome in rheumatoid arthritis: a simple algorithm of baseline parameters can predict radiographic damage, disability, and disease course at 12-year followup. *Arthritis Rheum* 2002;47:383–90.
30 Forslind K, Ahlmén M, Eberhardt K, *et al*. Prediction of radiological outcome in early rheumatoid arthritis in clinical practice: role of antibodies to citrullinated peptides (anti-CCP). *Ann Rheum Dis* 2004;63:1090–5.
31 Hyun TS, Ross TS. HIP1: trafficking roles and regulation of tumorigenesis. *Trends Mol Med* 2004;10:194–9.
32 Chan A, Akhtar M, Brenner M, *et al*. The GTPase Rac regulates the proliferation and invasion of fibroblast-like synoviocytes from rheumatoid arthritis patients. *Mol Med* 2007;13(5-6):1–304.
33 Bartok B, Hammaker D, Firestein GS. Phosphoinositide 3-kinase δ regulates migration and invasion of synoviocytes in rheumatoid arthritis. *J Immunol* 2014;192:2063–70.
34 Bartok B, Firestein GS. Fibroblast-like synoviocytes: key effector cells in rheumatoid arthritis. *Immunol Rev* 2010;233:233–55.
35 Neumann E, Lefèvre S, Zimmermann B, *et al*. Rheumatoid arthritis progression mediated by activated synovial fibroblasts. *Trends Mol Med* 2010;16:458–68.
36 Han Z, Boyle DL, Chang L, *et al*. c-Jun N-terminal kinase is required for metalloproteinase expression and joint destruction in inflammatory arthritis. *J Clin Invest* 2001;108:73–81.
37 Lefèvre S, Knedla A, Tennie C, *et al*. Synovial fibroblasts spread rheumatoid arthritis to unaffected joints. *Nat Med* 2009;15:1414–20.
38 Bradley SV, Holland EC, Liu GY, *et al*. Huntingtin interacting protein 1 is a novel brain tumor marker that associates with epidermal growth factor receptor. *Cancer Res* 2007;67:3609–15.
39 Feng H, Hu B, Liu KW, *et al*. Activation of Rac1 by Src-dependent phosphorylation of Dock180(Y1811) mediates PDGFRα-stimulated glioma tumorigenesis in mice and humans. *J Clin Invest* 2011;121:4670–84.
40 Kato T, Kawai K, Egami Y, *et al*. Rac1-dependent lamellipodial motility in prostate cancer PC-3 cells revealed by optogenetic control of Rac1 activity. *PLoS One* 2014;9:e97749.
41 Ross TS, Gilliland DG. Transforming properties of the Huntingtin interacting protein 1/ platelet-derived growth factor beta receptor fusion protein. *J Biol Chem* 1999;274:22328–36.

EXTENDED REPORT

Hexokinase 2 as a novel selective metabolic target for rheumatoid arthritis

Marta F Bustamante,[1] Patricia G Oliveira,[1] Ricard Garcia-Carbonell,[2] Adam P Croft,[3] Jeff M Smith,[2] Ramon L Serrano,[4] Elsa Sanchez-Lopez,[2] Xiao Liu,[1] Tatiana Kisseleva,[1,5] Nissim Hay,[6] Christopher D Buckley,[3] Gary S Firestein,[4] Anne N Murphy,[2] Shigeki Miyamoto,[2] Monica Guma[1,7]

Handling editor Josef S Smolen

► Additional material is published online only. To view please visit the journal online (http://dx.doi.org/10.1136/annrheumdis-2018-213103).

For numbered affiliations see end of article.

Correspondence to
Dr Monica Guma, Division of Rheumatology, Allergy and Immunology, UCSD School of Medicine, Jolla, CA 92093-0656, USA; mguma@ucsd.edu

PGO, RG-C and APC contributed equally.

This manuscript is based on work previously presented at 2016 and 2017 ACR conferences and published as conference abstract.

Received 24 January 2018
Revised 3 July 2018
Accepted 4 July 2018
Published Online First 30 July 2018

ABSTRACT

Objectives Recent studies indicate that glucose metabolism is altered in rheumatoid arthritis (RA) fibroblast-like synoviocytes (FLS). Hexokinases (HKs) catalyse the first step in glucose metabolism, and HK2 constitutes the principal HK inducible isoform. We hypothesise that HK2 contributes to the synovial lining hypertrophy and plays a critical role in bone and cartilage damage.

Methods HK1 and HK2 expression were determined in RA and osteoarthritis (OA) synovial tissue by immunohistochemistry. RA FLS were transfected with either HK1 or HK2 siRNA, or infected with either adenovirus (ad)-GFP, ad-HK1 or ad-HK2. FLS migration and invasion were assessed. To study the role of HK2 in vivo, 10^8 particles of ad-HK2 or ad-GFP were injected into the knee of wild-type mice. K/BxN serum transfer arthritis was induced in $HK2^{F/F}$ mice harbouring Col1a1-Cre ($HK2^{Col1}$), to delete HK2 in non-haematopoietic cells.

Results HK2 is particular of RA histopathology (9/9 RA; 1/8 OA) and colocalises with FLS markers. Silencing HK2 in RA FLS resulted in a less invasive and migratory phenotype. Consistently, overexpression of HK2 resulted in an increased ability to migrate and invade. It also increased extracellular lactate production. Intra-articular injection of ad-HK2 in normal knees dramatically increased synovial lining thickness, FLS activation and proliferation. HK2 was highly expressed in the synovial lining after K/BxN serum transfer arthritis. $HK2^{Col1}$ mice significantly showed decreased arthritis severity, bone and cartilage damage.

Conclusion HK2 is specifically expressed in RA synovial lining and regulates FLS aggressive functions. HK2 might be an attractive selective metabolic target safer than global glycolysis for RA treatment.

INTRODUCTION

Rheumatoid arthritis (RA) is a systemic autoimmune disease that leads to chronic inflammation and progressive joint destruction.[1] One of the apparent histopathological changes of the joint in RA is the hypertrophic synovial lining.[2 3] Fibroblast-like synoviocytes (FLS) are stromal cells that give structure to the synovial lining and are contributing to RA pathology by invading and promoting cartilage destruction, expressing metalloproteases (MMP) and inducing chronic inflammation by secreting pro-inflammatory cytokines and chemokines.[2 4 5] There is an unmet need to target FLS aggressive phenotype in RA in combination with current therapies.

Different approaches have highlighted underlying mechanisms that explain RA FLS behaviour, including activation of signalling pathways[6 7], and epigenetic modifications.[8 9] RA FLS metabolism has gained attention as recent studies have pointed out to modifications in RA FLS cell metabolism.[3 10] Many key signalling pathways that are activated by the inflamed joint microenvironment converge to adapt cell metabolism in order to support FLS activation and aggressive phenotype, suggesting that the study of metabolic changes in RA FLS and key players could potentially lead to the identification of new therapeutic agents.[3 10–12]

Among other metabolic changes, our recent work and others have highlighted a critical role of glucose metabolism in activated FLS.[13 14] The high level of activity in glycolytic inflamed tissues is manifested by the use of positron emission tomography (PET), which can be observed by PET in swollen joints.[15 16] Also, synovial fluid from patients with RA has higher levels of lactate and less glucose levels than osteoarthritis (OA) synovial fluid.[17 18] This dependency of activated cells on accelerated glucose metabolism could render them more vulnerable to the disruption of glucose metabolism and support that targeting glucose metabolism might be a reasonable complementary approach for patients with RA.[11]

Hexokinases (HKs) catalyse the first committed step in glucose metabolism.[19 20] By catalysing the phosphorylation of glucose to G6P, hexokinases promote and sustain a concentration gradient that facilitates glucose entry into cells and the initiation of all major pathways of glucose utilisation. HK1 is constitutively expressed in most mammalian adult tissues. HK2, which also has high affinity for glucose and harbours two catalytic domains, constitutes the principal inducible isoform.[21] The identification of isoform-specific contributors to elevated cell glucose metabolism without compromising systemic homeostasis or normal metabolic functions could make targeting cell metabolic changes an approach more feasible.

Here, we test the hypothesis that HK2 is a specific isoform contributing to elevated cell glucose metabolism in RA FLS and is a key regulator of aggressive FLS phenotype. We show that HK2 expression is elevated in the RA synovial tissue and overexpression of HK2 in the murine synovial lining promotes

To cite: Bustamante MF, Oliveira PG, Garcia-Carbonell R, *et al*. *Ann Rheum Dis* 2018;**77**:1636–1643.

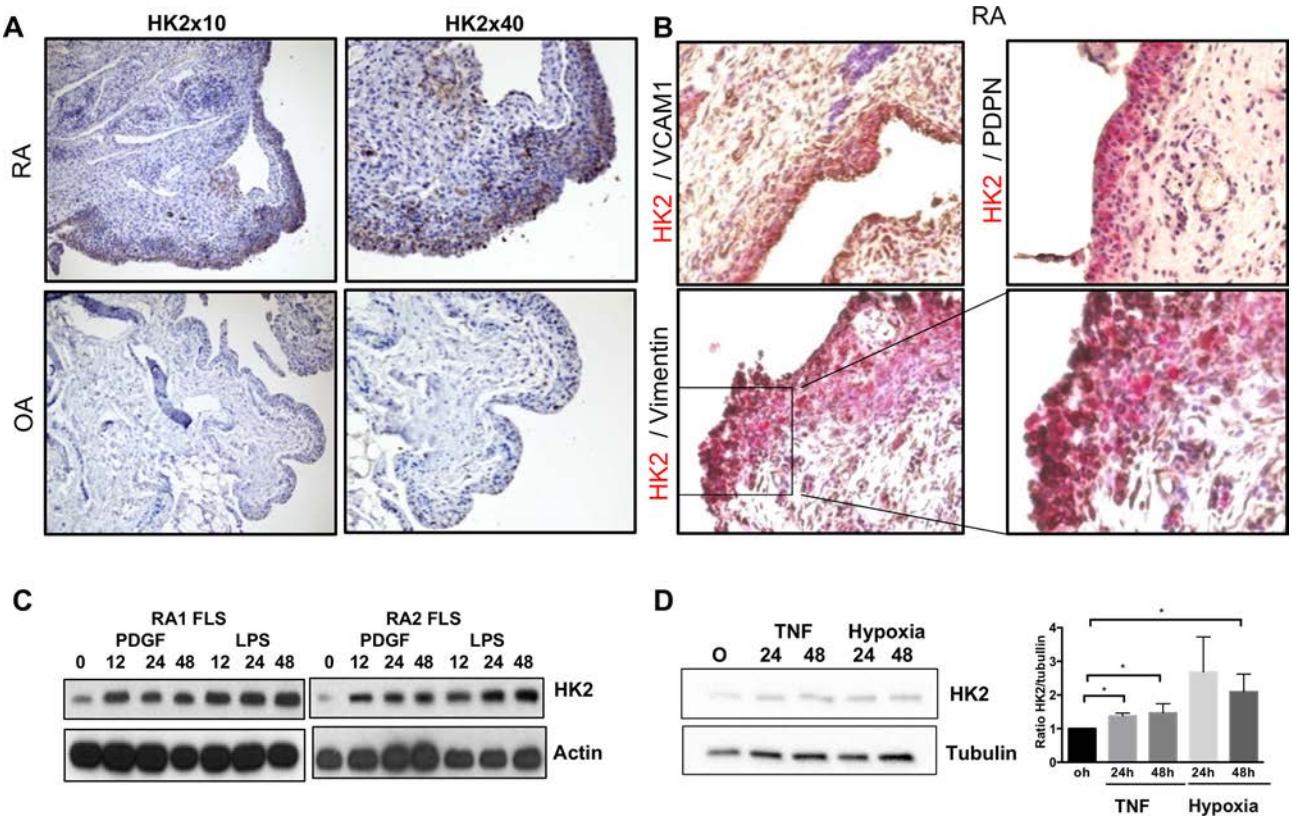

Figure 1 HK2 expression in the inflamed synovial lining of patients with rheumatoid arthritis (RA). (A) Representative immunohistochemistry (IHC) images of HK2 staining in RA and osteoarthritis (OA) synovium. (B) Representative IHC images of double-colour staining of HK2 (red) and vimentin (black), vascular cell adhesion protein 1 (VCAM1) (black) or podoplanin (PDPN) (black) in a RA human synovium. (C) Immunoblot (IB) of the indicated proteins in RA fibroblast-like synoviocytes (FLS) at baseline and after PDGFor LPS stimulation for 24 and 48 hours. (D) IB and quantification of the indicated proteins in RA FLS after tumour necrosis factor (TNF) or hypoxia (1%) stimulation. Results are average of three different RA FLS lines. Values are the mean ±SEM. *p<0.05.

hypertrophy of healthy synovium as well as RA FLS activation. HK2 deletion in FLS decreases its aggressive phenotype, and HK2 deletion in Col1a1-expressing cells ameliorates disease severity of arthritis. Taken together, our data suggest that HK2 is involved in FLS activation and synovial hypertrophy and could play a role in RA.

METHODS

Human synovium and FLS

Human synovium or FLS were extracted from patients with RA or OA undergoing total joint replacement. All patients with RA met the American College of Rheumatology 1987 revised criteria for seropositive RA as previously described.[22 23] FLS were used between p4 and p9 passages.

More detailed methods are provided as online supplementary methods.

RESULTS

HK2 expression is mainly induced in the inflamed synovial lining of patients with RA

We first studied the expression of both HK isoforms in synovium to determine whether or not HK2 is an inducible isoform in synovial tissue. Immunohistochemistry (IHC) analysis of HK2 expression in RA synovium revealed that HK2 was detected in RA synovial tissue, very predominant in the lining but also in sublining (figure 1A). Of interest, while HK2 expression was abundant in all RA synovial samples tested (nine different RA donors), both lining and sublining were negative for HK2 expression in most OA synovial samples (seven out of eight different OA donors) (figure 1A). HK1 expression, as expected, was uniformly present in both OA and RA synovial tissue (online supplementary figure 1A). Of note, when cultured in vitro, both RA and OA FLS cell lines expressed HK2 at basal level, although HK2 expression level was higher in RA than in OA FLS (online supplementary figure 1B).

We then performed a double-colour IHC to determine whether or not FLS expressed HK2 in the RA synovium. We identified FLS as cells positive for vimentin, vascular cell adhesion protein 1 (VCAM1) or podoplanin (PDPN).[2 24] As shown in figure 1B, HK2-positive staining colocalised with all the different FLS markers in the lining. Of interest, other cells in the sublining of some RA samples, which were negative for FLS markers, did expressed HK2, suggesting that other synovial cell types could also upregulate HK2 expression in RA synovial tissue.

Effect of HK2 modulation in aggressive functions of human FLS

In order to investigate the role of HK2 in RA FLS functions, we conducted in vitro studies. We first studied whether inflammatory mediators implicated in FLS inflammatory response upregulated HK2 expression. As shown in figure 1C, D, stimulation of RA FLS with platelet-derived growth factor (PDGF), lipopolysaccharide (LPS), tumour necrosis factor (TNF) or hypoxia increased the expression of HK2 protein. TNF and hypoxia stimulation also increased HK2 protein levels in OA FLS (online supplementary figure 1C).

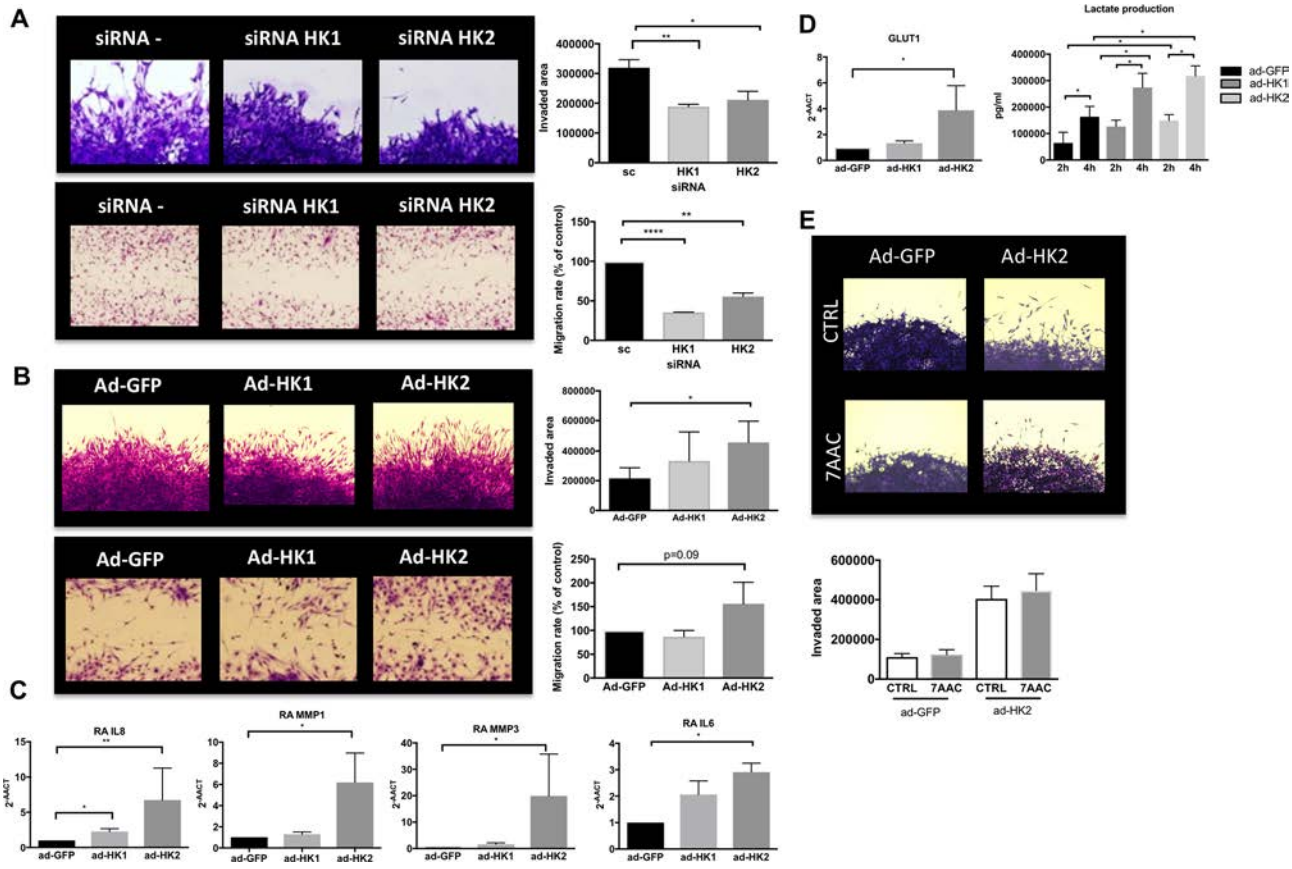

Figure 2 Effect of HK2 modulation in human rheumatoid arthritis (RA) fibroblast-like synoviocytes (FLS) migration and invasion. (A) RA FLS were transfected with either siRNA control, siRNA HK1 or siRNA HK2 as detailed in 'Methods'. Representative images of invasion area (upper panels) and migration (lower panels) are shown. Quantification, as detailed in 'Methods', of area of invasion and migration after PDGF stimulation for 24 hours are shown. Results are average of three different RA FLS lines. Values are the mean ±SEM (B) RA FLS were infected with adenovirus carrying GFP (ad-GFP), adenovirus carrying human HK1 (ad-hHK1) or HK2 (Ad-hHK2) as detailed in 'Methods'. Representative images of invasion area (upper panels) and migration (lower panels) are shown. Quantification, as detailed in 'Methods', of area of invasion and migration after PDGF stimulation for 24 hours are shown. Results are average of three different RA FLS lines. Values are the mean ±SEM (C) qPCR analysis of the indicated genes in RA FLS 72 hours after ad-GFP, ad-HK1 and ad-HK2 infection. Results are average of five different RA FLS lines. Values are shown as mean ±SEM. *p<0.05; **p<0.01. (D) Left: RNA levels of GLUT1 in RA FLS, 72 hours after ad-GFP, ad-HK1 or ad-HK2 infection. Results are average of three different RA FLS lines. Values are the mean ±SEM. Right: RA FLS were infected with ad-GFP, ad-HK1 or ad-HK2. Media was changed 48 hours after infection and lactate was measured in the supernatants at 2 and 4 hours. Data are pooled from thee technical replicates, and three different RA FLS lines. Values are the mean ±SEM. (**E**) RA FLS were infected with ad-GFP or ad-hHK2 as detailed in 'Methods'. Representing images and quantification are shown of area of invasion after PDGF stimulation for 24 hours in the presence or absence of 10 µM 7AAC. Results are average of three different RA FLS lines. Values are the mean ±SEM. *p<0.05, **p<0.01, ***p<0.001.

We then silenced HK1 and HK2 expression in those cell lines. Online supplementary figure 2A, B shows HK1 and HK2 expression by qPCR and immunoblotting (IB) after HK silencing in RA FLS. As glycolysis inhibition was shown to induce cell death in FLS,[25] we confirmed that HK1 or HK2 silencing did not change cell viability or shape (online supplementary figure 2C). As shown in figure 2A, RA FLS after HK silencing were less invasive (HK1: p<0.001; HK2: p<0.05) and migration measured by the length of the scar was also diminished (HK1: p<0.0001; HK2 p<0.001). Yet, HK silencing did not modify interleukin (IL)-6, IL-8 or MMP expression (online supplementary figure 2D).

We also tested the effect of HK2 overexpression in RA FLS by infecting with adenovirus carrying human HK1 or HK2 (ad-huHK1 or ad-huHK2). Online supplementary figure 3A and B shows HK1 and HK2 expression by qPCR and IB after ad-HK infection in RA FLS. After HK2 overexpression, RA FLS were more invasive than after HK1 overexpression (HK2: p=0.01, figure 2B). HK2 overexpression also decreased the length of the scar in the migration assay in FLS although did not reach significance (figure 2B), and increased RNA levels of the pro-inflammatory cytokine IL-6, IL-8 and MMP (figure 2C). Yet, it did not induce any change in proliferation (online supplementary figure 3C) Interestingly, both HK1 and HK2 overexpression increased RA FLS extracellular lactate production but only HK2 overexpression also increased GLUT1 mRNA levels (figure 2D). Yet, inhibition of the extracellular lactate transporters after HK2 overexpression by 7AAC, which specifically inhibits monocarboxylate transporter 1 and 4 (MTC1/4), did not abolish HK2 invasive phenotype in RA FLS (figure 2E).

HKs can bind to mitochondria through their N-terminal hydrophobic regions. Confocal studies were conducted to determine HKs intracellular distribution in FLS. Of interest, these studies showed that the distribution of HKs in non-infected FLS was different between HK1 and HK2. While HK1 was colocalised with or adjacent to mitochondria, HK2 was only partially mitochondria-bounded and it also displayed diffuse cytoplasmic distribution (figure 3A and online supplementary figure 4). Notably, after HK1 overexpression, the intensity of HK1

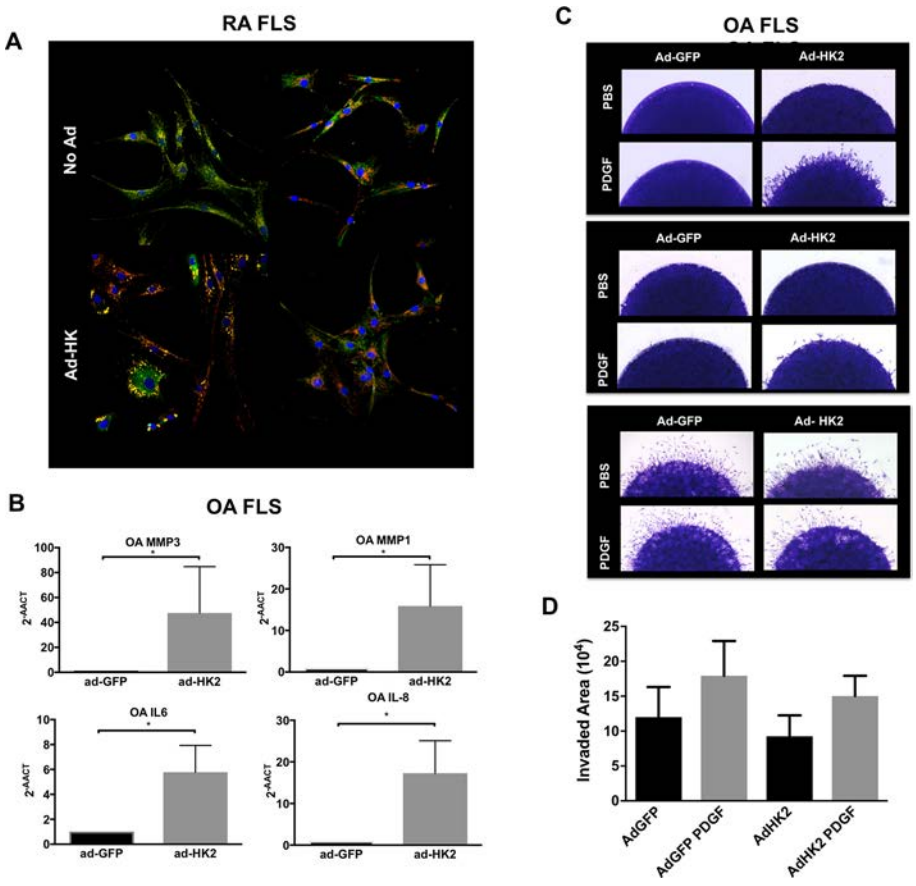

Figure 3 Intracellular distribution of hexokinases (HKs) and osteoarthritis (OA) fibroblast-like synoviocytes (FLS) phenotype after HKs overexpression. (A) Intracellular distribution of HKs (in green) and mitochondria (Tom20; in red) in FLS at baseline (upper panels) and after Ad- infection (lower panels) examined by confocal microscopy. Figure shows overlapping images (yellow, colocalisation of HKs with Tom20). Representative images of three different rheumatoid arthritis (RA) FLS are shown. (B) qPCR analysis of the indicated genes in OA FLS 72 hours after adenovirus carrying GFP (ad-GFP) and adenovirus carrying human HK2 (ad-HK2) infection. Results are average of three different OA FLS lines. Values are shown as mean ±SEM. *p<0.05. (C) OA FLS were infected with ad-GFP or ad-hHK2 as detailed in 'Methods'. Representative images of invasion area of three different OA FLS cell lines are shown. (D) OA FLS were infected with ad-GFP or ad-hHK2 as detailed in 'Methods'. Quantification, as detailed in 'Methods', of area of invasion after PDGF stimulation for 24 hours is shown. Results are average of four different OA FLS lines. Values are the mean ±SEM.

colocalisation with mitochondria and mitochondria distribution differed considerably from HK2 distribution and colocalisation after HK2 overexpression, which may explain the discrepancies observed after HK1 and HK2 overexpression (figure 3A and online supplementary figure 4).

We finally addressed whether HK2 overexpression could induce an inflammatory phenotype in OA FLS. As shown in figure 3B, overexpression of HK2 induced an increase of RNA levels of the pro-inflammatory cytokine IL-6, IL-8 and MMP in OA cell lines. Of interest, the overexpression of HK2 induced an invasive phenotype compared with ad-GFP but not in all OA FLS cell lines tested. As opposed to the homogeneity of the HK2 overexpression effect on RA FLS, the invasive phenotype after HK2 overexpression varied among OA FLS cell lines (figure 3C), and overall quantification (figure 3D) did not show significant differences, suggesting that HK2 expression contributes but is not sufficient to completely recapitulate the aggressive phenotype of RA FLS.

HK2 overexpression leads to a synovial lining hypertrophy in murine healthy joints

In order to assess the effect of HK2 overexpression in synovial tissue in vivo, we intra-articularly injected adenovirus carrying murine HK2 (ad-mHK2) into murine knees, and adenovirus carrying GFP (ad-GFP) as a control in the contralateral knee of wild-type (WT) healthy mice. Overexpression of HK2 in the synovial lining was effective since HK2 expression was increased in ad-mHK2-injected joints compared with ad-GFP-injected joints (figure 4A). Interestingly, we observed that intra-articular injection of ad-mHK2 in normal knees dramatically increased synovial lining thickness (mean±SEM: ad-GFP: 0.54±0.21; ad-HK2: 2.91±0.28; p<0.00001) (figure 4B). We also observed synovial lining from ad-HK2-injected knee migrating towards the cartilage compared with ad-GFP-injected knees (mean±SEM: ad-GFP: 0.75±0.22; ad-HK2: 2.03±0.29; p=0.0015) (figure 4B). Double-colour IHC with vimentin confirmed HK2 expression in FLS after ad-mHK2 injection (figure 4C).

We then tested if HK2 overexpression modified FLS activation and proliferation by staining for anti-alpha smooth muscle actin (α-sma), a myofibroblastic marker, MMP3 and Ki67, a marker of proliferative cells. Figure 4D shows that anti α-sma staining was increased in ad-mHK2-injected knees compared with ad-GFP-injected knees. MMP3 staining was also widely present in the hypertrophic lining in ad-mHK2 synovium (figure 4D). Of interest, intra-articular injection of ad-mHK2 also increased the number of positive Ki67 cells in the synovium (figure 4E)

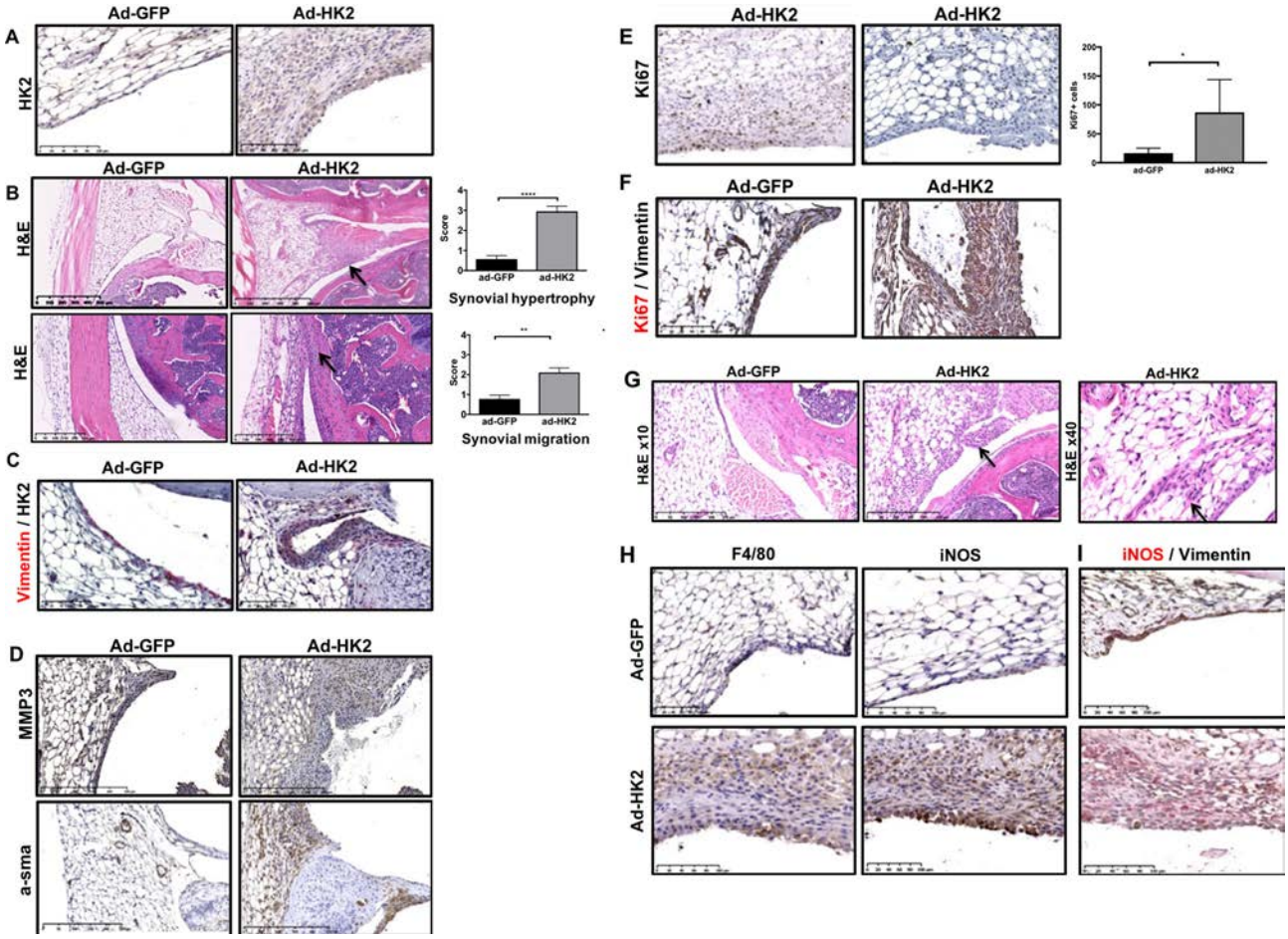

Figure 4 HK2 overexpression leads to a hypertrophic synovia in healthy joints. Control wild-type (WT) mice (n=13) were injected intra-articularly in one knee with 10^8adenovirus carrying murine HK2 (ad-mHK2) and adenovirus carrying GFP (ad-GFP) in contralateral knee. (A) Representative image of HK2 staining of the indicated mice. (B) Upper panels: representative images of H&E showing hypertrophy (arrow indicates synovial hypertrophy), and quantification (mean±SEM: ad-GFP: 0.54±0.21; ad-HK2: 2.91±0.28; p<0.00001) are shown. Lower panels: representative images of H&E showing synovial attachment to cartilage (arrow indicates synovial migration), and quantification (mean±SEM: ad-GFP: 0.75±0.22; ad-HK2: 2.03±0.29; p=0.0015) are shown. (C) Representative immunohistochemistry (IHC) image of double-colour staining of anti-vimentin (red) and anti-HK2 (black) of the indicated mice. (D) Representative IHC image of anti-alpha-sma and MMP3 of the indicated mice. (E) Representative Ki67 staining of the indicated mice and quantification of Ki67-positive cells in the synovium of ad-GFP or ad-HK2-injected knees (mean±SEM: ad-GFP: 16.5±8.7; ad-HK2: 87.14±56.64, p=0.05, n=6 per group). (F) Representative IHC image of double-colour staining of anti-vimentin (black) and anti-Ki67 (red) of the indicated mice. (G) Representative images of H&E showing sublining infiltration (100× magnification in upper images and 400× magnification in lower images) of indicated mice. Quantification: mean±SEM: ad-GFP: 0.08±0.08; ad-HK2: 0.92±0.29; p=0.02. (H) Representative IHC image of F4/80, iNOS and vimentin (black) and iNOS (red) staining of the synovial of the indicated mice.

mean±SEM: ad-GFP: 16.5±8.7; ad-HK2: 87.14±56.64, p=0.05. Double-colour IHC with vimentin showed some Ki67-positive cells in vimentin positive cells, suggesting that HK2 overexpression in FLS-induced FLS proliferation in vivo (figure 4F).

We also determined whether the overexpression of ad-mHK2 in the lining induced the recruitment of infiltrating cells. Although the response was more heterogeneous than the synovial hypertrophy induction by HK2 overexpression, we observed a mild sublining infiltration in 6 out of 13 knees after ad-mHK2 injection compared with none after ad-GFP injection (mean±SEM: ad-GFP: 0.08±0.08; ad-HK2: 0.92±0.29; p=0.02) (figure 4G). When observed at higher magnification, most of the infiltrating cells were mononuclear cells (figure 4G). We then stained for F4/80, a marker of monocyte-macrophage lineage, and for iNOS, which stains activated myeloid cells. We observed that both sublining infiltrating cells were positive for F4/80 and iNOS. Double-colour IHC with vimentin and iNOS confirmed that most of vimentin-positive cells were negative for iNOS, suggesting that the infiltrating cells were indeed activated myelomonocitic cells (figure 4H).

HK2 expression in murine joints is also increased in synovial FLS after arthritis induction

The effect of HK2 on FLS migration and invasion led us to evaluate the role of HK2 in the K/BxN arthritis model. The K/BxN passive serum transfer model is FLS dependent and requires only innate immunity.[26 27] PDPN, glycoprotein highly expressed in activated RA FLS, is also expressed in the arthritic murine lining (figure 5A). As we recently published,[14] several genes related to glucose metabolism were upregulated early in the course of the arthritis, at day 5 after K/BxN serum transfer, in enriched arthritic $CD45^{neg}PDPN^{pos}$ cells. We confirmed that HK2 expression had higher expression in enriched arthritic $CD45^{neg}PDPN^{pos}$ cells (1.04±0.4 in normal joints vs 1.8±0.3 in

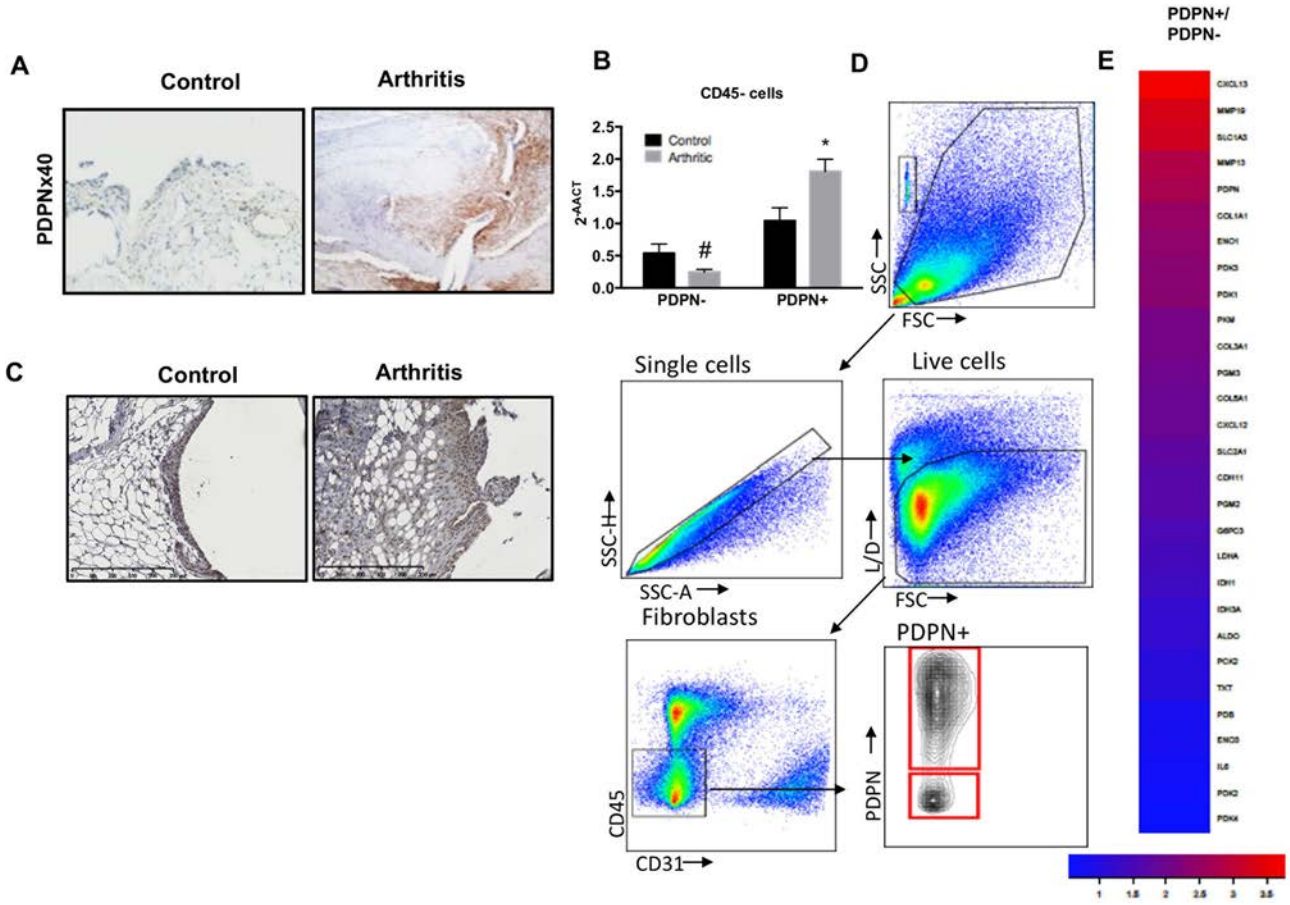

Figure 5 Specific deletion of HK2 in Col1a1 expressing cells ameliorates arthritis in an animal model of inflammatory arthritis. Serum passive K/BxN arthritis was induced after intraperitoneally injection of 150 µL of K/BxN mouse serum on day 0. (A) Representative immunohistochemistry (IHC) images at day 9 after serum injection of PDPN expression in synovial tissue of arthritic wild-type (WT) mice. (B) Gene expression level of HK2 in isolated $CD45^{neg}PDPN^{pos}$ cells from control mice or KRN-induced arthritic mice. HK2 expression is increased in arthritic $CD45^{neg}PDPN^{pos}$ (1.04±0.4 in normal joints vs 1.8±0.3 in arthritic joints; p=0.03). (C) Representative IHC images at day 9 after serum injection of HK2 expression in synovial tissue of arthritic WT mice versus control WT mice. (D) Single cells from arthritic joints were enriched for CD45-PDPN+ as described in 'Methods'. Shown sorted populations for further RNAseq analysis. (E) Heat map of gene expression level of isolated $CD45^{neg}PDPN^{pos}$ cells compared with $CD45^{neg}PDPN^{neg}$ from arthritic joints as described in 'Methods'.

arthritic joints: p=0.03; 1.8±0.3 in arthritic $CD45^{neg}PDPN^{pos}$ cells vs 0.25±0.09 in arthritic $CD45^{neg}PDPN^{neg}$ cells: p<0.01) (figure 5B). HK2 was highly and uniformly expressed in the invasive lining in arthritic joints (figure 5C). Several glucose metabolism related genes together with other markers of activated FLS were also increased at the peak of the arthritis in $CD45^{neg}PDPN^{pos}$ cells compared with $CD45^{neg}PDPN^{neg}$ (figure 5D, E). Specifically, GLUT1, ENO1 but also pyruvate kinase muscle isoenzyme 2, pyruvate dehydrogenase kinase (PDK) 1 and 3 were upregulated in this population.

Conditional knockout of HK2 in Col1a1-expressing cells has an ameliorated arthritic disease

As there is no available Cre-recombinase expressing strain that deletes specifically in FLS, we generated HK2F/F Col1a1-Cre ($HK2^{Col1}$) mice to delete HK2 in collagen type I expressing cells including FLS. As shown in figure 6A, HK2 was deleted in $HK2^{Col1}$ joint FLS. We then conducted the arthritic model of K/BxN serum-transfer arthritis. Deletion of HK2 in Col1a1 expressing cells significantly decreased arthritis severity (clinical score at day 12 was 9±2.5 in WT mice vs. 6.1±3.2 in $HK2^{F/F}$Col1a1-Cre; p=0.02) (figure 6B). Histopathological studies at day 12 showed that bone erosion (p=0.04) and cartilage damage (p=0.05), but not less cellular infiltration was reduced in $HK2^{Col1}$ mice compared with littermate control (figure 6C, D). Of note, MMP3 and Ki67 expression that were upregulated in K/BxN arthritis synovium were decreased in $HK2^{Col1}$ mice compared with littermate control (figure 6E).

DISCUSSION

The concept of metabolic reprogramming to improve immunotherapy slowly is being translated into autoimmune diseases to complement current therapies.[28] Yet, there are little data about targeting metabolic changes in RA. We here showed that targeting the first step in glucose metabolism could be a potential selective metabolic therapy for RA and regulates FLS aggressive behaviour.

Although previous works have demonstrated a role of glucose metabolism in cell activation and function,[29–31] inhibiting general glucose metabolism is not desirable in the overall body. Thus, there is a need of finding specific metabolic targets that are induced in activated cells such as FLS. HKs are the first enzymatic step in glucose metabolism. While HK1 is a ubiquitously expressed enzyme in all living cells, HK2 is an inducible form and only expressed in adulthood in some organs. Our data suggest that HK2 constitutes an attractive potential selective

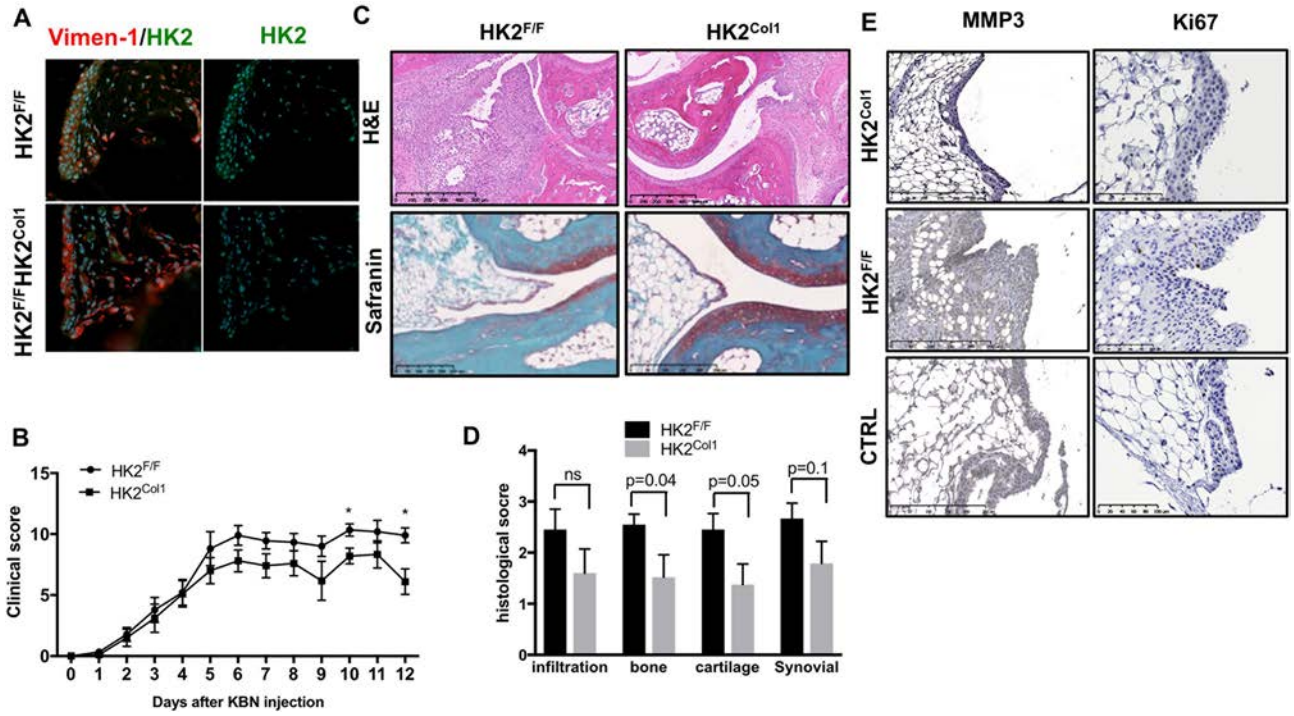

Figure 6 Specific deletion of HK2 in Col1a1 expressing cells ameliorates arthritis in an animal model of inflammatory arthritis. Serum passive K/BxN arthritis was induced after intraperitoneally injection of 150 µL of K/BxN mouse serum on day 0. (A). Immunofluorescence of the murine synovium (vimentin in red; HK2 in green; DAPI blue) in the indicated mice, showing that $HK2^{Col1}$ synovial cells lack HK2 in murine fibroblast-like synoviocytes (FLS) compared with control $HK2^{F/F}$.(B) Clinical arthritis scores were determined in $HK2^{F/F}$ and $HK2^{Col1}$ mice after arthritis induction. Values are the mean±SEM of 10 mice per group. *p<0.05. (C) Sections of the ankle joints of $HK2^{F/F}$ and $HK2^{Col1}$ mice were stained with H&E or Safranin O on day 12 after arthritis induction. (D) Histological scores were determined on day 12 after serum transfer in $HK2^{F/F}$ and $HK2^{Col1}$ mice. (E) Representative immunohistochemistry images of MMP3 and Ki67 of the indicated mice.

target for arthritis therapy. Indirect evidence of HK2 redundancy in adulthood is the fact that global HK2 ablation in adult mice was well tolerated, and HK2-deficient mice were indistinguishable from control mice both morphologically, and in terms of growth, bodyweight and glucose homeostasis.[19] Adult tissues that abundantly express HK2 also express relatively high levels of HK1, which might play a compensatory or redundant role in the absence of HK2.

Here, we have observed that HK2 is not expressed in most of OA patient's synovial tissue. Consistent with the idea of upregulation secondary to synovial inflammation, we observed that its expression was induced by inflammatory and activation signals including LPS, PDGF, TNF and hypoxia. In K/BxN model of mice, its expression is also elevated in inflamed joints but not in healthy joints. Interestingly, HK2 mRNA expression levels are also increased in TNF or IL-1β-stimulated RA FLS as published in Geo Datasets (Array GSE49604, GSE516, GSE2676), together with other glucose metabolism related genes. While both HK1 and HK2 silencing reduced migratory and invasive phenotype of RA FLS, only the overexpression of HK2 contributed to aggressive phenotype of FLS since its overexpression increased the invasiveness of these cells and induced IL-6, MMPs and IL-8 mRNA expression. Other studies performed in cancer cells observed similar effects. When HK2 was silenced, breast cancer cells were less migratory after in vitro TNF stimulation,[32] and pancreatic cells were less metastatic in an in vivo model.[33] Although extracellular lactate was shown to be involved in cancer cell invasive phenotype,[33] in RA FLS, the inhibition of lactate transporters (MTC1 and 4) did not reverse the HK2-dependent invasive phenotype. Interestingly, although both HK2 and HK1 similarly increase extracellular lactate, only HK2 and not HK1 overexpression triggers a FLS aggressive phenotype, suggesting the involvement of glycolysis independent mechanisms. Confocal studies revealed that HK1 and HK2 differ in their intracellular colocalisation, but further mechanistic studies are warranted. Of note, HK2 deletion was not sufficient to modulate IL-6 or TNF expression, which might indicate that targeting HK2 will not change pro-inflammatory cytokine profile and could potentially complement current immunotherapies.

In addition, HK2 overexpression in the synovium of a healthy murine knee transformed the thin lining into a hypertrophic synovium and it also enhanced FLS activation and migration towards cartilage. HK2, therefore, led a healthy normal synovial lining into a hypertrophic and aggressive synovium upregulating α-sma and MMP3 expression, and also stimulating proliferation as shown by the presence of Ki67 cells in vimentin positive cells. Yet, HK2 overexpression did not increase proliferation in vitro, suggesting that other mediators are involved in the proliferation observed in the in vivo experiments. The myofibroblastic marker α-sma might explain the migratory phenotype since α-sma has been associated with higher contractile profile in fibroblasts.[34] Whether or not HK2 also plays a role in synovial macrophage recruitment, activation and differentiation requires further studies. Although double-colour IHC showed that most of HK2-positive cells colocalised with vimentin-positive cells, suggesting FLS HK2 involvement in recruiting and activating synovial macrophages, we cannot rule out a direct activation of macrophages by the ad-HK2.

Partial ablation of HK2 in FLS slightly ameliorated the clinical signs of arthritis animal model. We did not see a significant effect on inflammation, probably because as shown in vitro, deletion of HK2 in FLS was not sufficient to modulate the expression

of inflammatory mediators. Yet, histological scores of bone and cartilage damage were significantly improved in $HK2^{Col1}$ mice, suggesting a predominant role of HK2 in synovial migration and invasion. Col1a1-Cre does not delete only in FLS so the effect of HK2 deletion in other cells including chondrocytes and osteoblasts needs further attention. Although our conditional mice explains the effect of HK2 in non-haematopoietic cells, double-staining IHC suggest that human RA synovial cells other than FLS also expresses HK2, so further experiments are needed to study the effect of HK2 in other synovial cell types.

This is the first study to identify an isoform-specific contributor to metabolism changes in RA synovial tissue that could be selectively targeted without compromising systemic homeostasis or corresponding metabolic functions in normal cells, offering a safer and novel additional approach for combination therapy in RA joint disease independent of systemic immunosuppression. Given HK2 selective overexpression in RA inflamed synovium, and its restricted distribution of expression in normal adult tissues, HK2 constitutes an attractive potential selective target for arthritis therapy and safer than global glycolysis inhibition.

Author affiliations
[1]Department of Medicine, University of California San Diego, San Diego, California, USA
[2]Department of Pharmacology, University of California, San Diego, California, USA
[3]Rheumatology Research Group, Institute of inflammation and Ageing, College of Medical and dental Sciences, University of Birmingham, Queen Elizabeth Hospital, Birmingham, UK
[4]Medicine, VA San Diego Healthcare System/UC, San Diego, California, USA
[5]Department of Surgery, University of California, San Diego, California, USA
[6]Department of Biochemistry and Molecular Genetics, University of California, Chicago, Illinois, USA
[7]Department of Medicine, Autonomous University of Barcelona, Bellaterra, Spain

Acknowledgements The authors thank Tissue Technology Shared Resources (TTSR) and microscope core: NINDS P30 NS047101.

Contributors All authors were involved in drafting the article or revising it critically for important intellectual content, and all authors approved the final version to be published. MG had full access to all of the data in the study and takes responsibility for the integrity of the data and the accuracy of the data analysis. Study conception and design: MFB, ANM, SM and MG. Acquisition of data. MFB, PGO, RGC, APC, JMS, RS and ESL. Analysis and interpretation of data: MFB, ESL,NH, CDB, ANM, SM, GF and MG.

Funding MG was supported by NIH 1K08AR064834, R03AR068094 and Rheumatology Research Foundation. RGC's work was supported by a fellowship from the Boehringer-Ingelheim Foundation. AC was supported by a Wellcome Trust Clinical Career Development Fellowship (WT104551MA). Additional support was provided by grants DK-054441-15 and CA-188652 to ANM, R56 HL097037 to SM; and R01 CA206167 and the VA merit award BX000733 to NH. This work was also supported in part by the Erickson Family.

Competing interests None declared.

Patient consent Not required.

Provenance and peer review Not commissioned; externally peer reviewed.

REFERENCES

1 Firestein GS. Evolving concepts of rheumatoid arthritis. *Nature* 2003;423:356–61.
2 Bartok B, Firestein GS. Fibroblast-like synoviocytes: key effector cells in rheumatoid arthritis. *Immunol Rev* 2010;233:233–55.
3 Bustamante MF, Garcia-Carbonell R, Whisenant KD, *et al*. Fibroblast-like synoviocyte metabolism in the pathogenesis of rheumatoid arthritis. *Arthritis Res Ther* 2017;19:110.
4 Bottini N, Firestein GS. Duality of fibroblast-like synoviocytes in RA: passive responders and imprinted aggressors. *Nat Rev Rheumatol* 2013;9:24–33.
5 Neumann E, Lefèvre S, Zimmermann B, *et al*. Rheumatoid arthritis progression mediated by activated synovial fibroblasts. *Trends Mol Med* 2010;16:458–68.
6 Hammaker D, Firestein GS. "Go upstream, young man": lessons learned from the p38 saga. *Ann Rheum Dis* 2010;69(Suppl 1):i77–82.
7 Hammaker D, Sweeney S, Firestein GS. Signal transduction networks in rheumatoid arthritis. *Ann Rheum Dis* 2003;62(Suppl 2):86ii–9.
8 Araki Y, Tsuzuki Wada T, Aizaki Y, *et al*. Histone Methylation and STAT-3 Differentially Regulate Interleukin-6-Induced Matrix Metalloproteinase Gene Activation in Rheumatoid Arthritis Synovial Fibroblasts. *Arthritis Rheumatol* 2016;68:1111–23.
9 Bottini N, Firestein GS. Epigenetics in rheumatoid arthritis: a primer for rheumatologists. *Curr Rheumatol Rep* 2013;15:372.
10 Falconer J, Murphy AN, Young SP, *et al*. Review: synovial cell metabolism and chronic inflammation in rheumatoid arthritis. *Arthritis Rheumatol* 2018;70:984–99.
11 Semerano L, Roméo PH, Boissier MC. Metabolomics for rheumatic diseases: has the time come? *Ann Rheum Dis* 2015;74:1325–6.
12 Guma M, Sanchez-Lopez E, Lodi A, *et al*. Choline kinase inhibition in rheumatoid arthritis. *Ann Rheum Dis* 2015;74:1399–407.
13 Fearon U, Canavan M, Biniecka M, *et al*. Hypoxia, mitochondrial dysfunction and synovial invasiveness in rheumatoid arthritis. *Nat Rev Rheumatol* 2016;12:385–97.
14 Garcia-Carbonell R, Divakaruni AS, Lodi A, *et al*. Critical Role of Glucose Metabolism in Rheumatoid Arthritis Fibroblast-like Synoviocytes. *Arthritis Rheumatol* 2016;68:1614–26.
15 Vijayant V, Sarma M, Aurangabadkar H, *et al*. Potential of (18)F-FDG-PET as a valuable adjunct to clinical and response assessment in rheumatoid arthritis and seronegative spondyloarthropathies. *World J Radiol* 2012;4:462–8.
16 Vogel WV, van Riel PL, Oyen WJ. FDG-PET/CT can visualise the extent of inflammation in rheumatoid arthritis of the tarsus. *Eur J Nucl Med Mol Imaging* 2007;34:439.
17 Bushinsky DA, Frick KK. The effects of acid on bone. *Curr Opin Nephrol Hypertens* 2000;9:369–79.
18 Treuhaft PS, MCCarty DJ, Mc DJ. Synovial fluid pH, lactate, oxygen and carbon dioxide partial pressure in various joint diseases. *Arthritis Rheum* 1971;14:475–84.
19 Patra KC, Wang Q, Bhaskar PT, *et al*. Hexokinase 2 is required for tumor initiation and maintenance and its systemic deletion is therapeutic in mouse models of cancer. *Cancer Cell* 2013;24:213–28.
20 Wilson JE. Isozymes of mammalian hexokinase: structure, subcellular localization and metabolic function. *J Exp Biol* 2003;206(Pt 12):2049–57.
21 Robey RB, Hay N. Mitochondrial hexokinases, novel mediators of the antiapoptotic effects of growth factors and Akt. *Oncogene* 2006;25:4683–96.
22 Alvaro-Gracia JM, Zvaifler NJ, Brown CB, *et al*. Cytokines in chronic inflammatory arthritis. VI. Analysis of the synovial cells involved in granulocyte-macrophage colony-stimulating factor production and gene expression in rheumatoid arthritis and its regulation by IL-1 and tumor necrosis factor-alpha. *J Immunol* 1991;146:3365–71.
23 Alvaro-Gracia JM, Zvaifler NJ, Firestein GS. Cytokines in chronic inflammatory arthritis. V. Mutual antagonism between interferon-gamma and tumor necrosis factor-alpha on HLA-DR expression, proliferation, collagenase production, and granulocyte macrophage colony-stimulating factor production by rheumatoid arthritis synoviocytes. *J Clin Invest* 1990;86:1790–8.
24 Ekwall AK, Eisler T, Anderberg C, *et al*. The tumour-associated glycoprotein podoplanin is expressed in fibroblast-like synoviocytes of the hyperplastic synovial lining layer in rheumatoid arthritis. *Arthritis Res Ther* 2011;13:R40.
25 Del Rey MJ, Valín Á, Usategui A, *et al*. Hif-1α Knockdown Reduces Glycolytic Metabolism and Induces Cell Death of Human Synovial Fibroblasts Under Normoxic Conditions. *Sci Rep* 2017;7:3644.
26 Kyburz D, Corr M. The KRN mouse model of inflammatory arthritis. *Springer Semin Immunopathol* 2003;25:79–90.
27 Lee DM, Kiener HP, Agarwal SK, *et al*. Cadherin-11 in synovial lining formation and pathology in arthritis. *Science* 2007;315:1006–10.
28 Guma M, Tiziani S, Firestein GS. Metabolomics in rheumatic diseases: desperately seeking biomarkers. *Nat Rev Rheumatol* 2016;12:269–81.
29 Galván-Peña S, O'Neill LA. Metabolic reprograming in macrophage polarization. *Front Immunol* 2014;5:420.
30 Van den Bossche J, O'Neill LA, Menon D. Macrophage Immunometabolism: Where Are We (Going)? *Trends Immunol* 2017;38:395–406.
31 Borregaard N, Herlin T. Energy metabolism of human neutrophils during phagocytosis. *J Clin Invest* 1982;70:550–7.
32 Gao Y, Yang Y, Yuan F, *et al*. TNFα-YAP/p65-HK2 axis mediates breast cancer cell migration. *Oncogenesis* 2017;6:e383.
33 Anderson M, Marayati R, Moffitt R, *et al*. Hexokinase 2 promotes tumor growth and metastasis by regulating lactate production in pancreatic cancer. *Oncotarget* 2017;8:56081–94.
34 Shinde AV, Humeres C, Frangogiannis NG. The role of α-smooth muscle actin in fibroblast-mediated matrix contraction and remodeling. *Biochim Biophys Acta* 2017;1863:298–309.

EXTENDED REPORT

Maresin 1 improves the Treg/Th17 imbalance in rheumatoid arthritis through miR-21

Shengwei Jin,[1] Huaijun Chen,[2] Yongsheng Li,[3,4] Hao Zhong,[2] Weiwei Sun,[2] Jianmin Wang,[5] Tingting Zhang,[2] Jinglan Ma,[2] Songfan Yan,[1] Jiangang Zhang,[3,4] Qingqing Tian,[2] Xinyu Yang,[6] Jianguang Wang[2]

Handling editor Josef S Smolen

► Additional material is published online only. To view please visit the journal online (http://dx.doi.org/10.1136/annrheumdis-2018-213511).

For numbered affiliations see end of article.

Correspondence to
Mr Xinyu Yang, Xinyu Yang, Department of Medicinal Chemistry, School of Pharmaceutical Sciences, Wenzhou Medical University, Wenzhou, 325035, China; cyrillyoung@163.com and Dr Jianguang Wang, Department of Biochemistry, School of Basic Medical Sciences, Wenzhou Medical University, Wenzhou, 325035, China; wz_wjg@163.com

SJ, HC and YL contributed equally.

Received 1 April 2018
Revised 4 July 2018
Accepted 5 July 2018
Published Online First 25 July 2018

To cite: Jin S, Chen H, Li Y, *et al*. *Ann Rheum Dis* 2018;**77**:1644–1652.

ABSTRACT

Objective Treg/Th17 imbalance plays an important role in rheumatoid arthritis (RA). Maresin 1 (MaR1) prompts inflammation resolution and regulates immune responses. We explored the effect of MaR1 on RA progression and investigated the correlation between MaR1 and Treg/Th17 balance.

Methods Both patients with RA and healthy controls were recruited into the study. Collagen-induced arthritis (CIA) model was constructed to detect the clinical score, histopathological changes and Treg/Th17 ratio. Purified naive CD4+ T-cells were used to study the effect of MaR1 on its differentiation process and microRNA microarray studies were performed to investigate MaR1 downstream microRNAs in this process. MicroRNA transfection experiments were conducted by lentivirus to verify the mechanism of MaR1 on Treg/Th17 balance.

Results Compared with controls, the MaR1 concentration was higher in the patients with inactive RA and lower in the patients with active RA. Expression of the Treg transcription factor FoxP3 was the highest in inactive RA and the lowest in active RA, while the Th17 transcription factor RORc showed a reverse trend. An inverse correlation was observed between the FoxP3/RORc ratio and Disease Activity Score 28. Intervention of MaR1 in the CIA model reduced joint inflammation and damage, and improved the imbalanced Treg/Th17 ratio. MaR1 increased Treg cells proportion while reduced Th17 cells proportion under specific differentiation conditions. Furthermore, miR-21 was verified as MaR1 downstream microRNA, which was upregulated by MaR1, modulating the Treg/Th17 balance and thus ameliorating the RA progression.

Conclusions MaR1 is a therapeutic target for RA, likely operating through effects on the imbalanced Treg/Th17 ratio found in the disease.

INTRODUCTION

Rheumatoid arthritis (RA) is a common chronic inflammatory disease characterised by joint destruction and bone erosion, as well as other serious complications.[1 2] Although the aetiology and pathogenesis of RA remains largely unknown, previous studies pointed out that the imbalance of Th17/Treg may play a role in the progression of RA.[3] Th17 cells mainly promote inflammation by secreting interleukin (IL)-17 and thus accelerate the occurrence of autoimmune diseases. IL-17 can induce the production of pro-inflammatory cytokines (such as tumour necrosis factor (TNF)-α, IL-6 and IL-1β), chemokines (such as monocyte chemoattractant protein (MCP)-1 and MCP-2) and matrix metalloproteinases, which lead to tissue invasion and destruction as well as damage of articular cartilage and bone.[4 5] In contrast, Treg cells mediate the anti-inflammatory response by secreting IL-10 and transforming growth factor (TGF)-β and maintain the state of autoimmune tolerance.[6] In RA development, the proportion of Treg cells decreases[7] and their function is inhibited. TNF-α in the synovium of patients with RA can inhibit FoxP3 phosphorylation, restraining Treg cells proliferation and secretion of functional cytokines (IL-10 and TGF-β).[8] The resulting imbalance of Th17/Treg may be responsible for the occurrence and development of RA.[9]

Several recent studies have demonstrated that multiple chemical mediators derived from ω-3 polyunsaturated fatty acids (ω-3 PUFA) can ameliorate the acute inflammatory response. Among these are the so-called specialised pro-resolving lipid mediators, which include lipoxins, resolvins, protectins and maresins (MaRs).[10] Maresin 1 (MaR1) is one of the newly identified mediators, which is produced from docosahexaenoic acid (DHA) in macrophages.[11] MaR1 inhibits neutrophil infiltration,[12] promotes macrophage efferocytosis and enhances tissue regeneration in acute inflammation[13]; however, its effect on chronic inflammation is not clear. Barden reported that MaR1 increased in plasma and synovia from patients with RA treated with ω-3 PUFA.[14] Dawczynski demonstrated that RA disease activity decreased by taking foods enriched with DHA,[15] which is one of ω-3 PUFA metabolised into MaR1 in macrophages. Serhan observed the reduction of MaR1 in joints of K/BxN serum transfer induced arthritis mice, an animal model of RA.[16] These facts indicate a potential relationship between MaR1 and RA, requiring further study to establish and determine the functional mechanisms involved.

MicroRNAs (miRNAs) are small non-coding RNA that regulate various biological processes including immune and inflammatory responses.[17] Li found that MaR1 can inhibit miR-466l expression in zymosan-stimulated macrophages,[18] suggesting that MaR1 can exert its biological functions by regulating miRNA.

In this study, we investigated the effect of MaR1 on RA and the balance of Th17/Treg, and the involvement of miRNA in this process.

METHODS AND MATERIALS

Patients and samples

Samples were obtained from patients with RA and healthy controls at the First Affiliated Hospital of Wenzhou Medical University from May 2016 to December 2017. RA diagnosis was based on the 2010 American College of Rheumatology criteria. The clinical details of the patients are shown in online supplementary tables S1 to S2. Blood was acquired on the first day of clinical admission prior to commencement of any treatment, and synovium was acquired during joint arthroplasty surgery from patients with RA and control subjects with either femoral neck fractures or meniscal injuries. Synovia and blood of active and inactive RA groups was obtained from the same group of people, while synovia and synovium of normal groups were obtained from the same group of people.

UPLC-MS/MS-based MaR1 determination

The concentration of MaR1 (7R, 14S-dihydroxy-4Z, 8E, 10E, 12Z, 16Z, 19Z-docosahexaenoic acid, CAS no. 1268720-28-0) in human serum samples was assessed as described previously.[18 19] Samples (2 mL each) were placed in ice-cold methanol (4 mL). Prior to sample extraction, 500 pg of d4-LTB4 (5S, 12R-dihydroxy-6Z, 8E, 10E, 14Z-eicosatetraenoic-6, 7, 14, 15-d4 acid, CAS no. 124629-74-9) (Cayman Chemical, USA) was added to facilitate quantification. Lipid mediators (LM) were extracted by solid-phase extraction using a C18 column (Waters, USA). The methyl formate fractions were analysed for MaR1 levels by ultra-performance liquid chromatography tandem mass spectrometry (UP LC-MS/MS) using an UPLC I-Class system (Waters, USA) equipped with an Agilent Eclipse Plus C18 column (2.1 mm × 100 mm × 1.7 µm) paired with Sciex 6500 Q-TRAP mass spectrometer (Sciex, USA). Instrument control and data acquisition were performed using AnalystTM 1.6.2 software (Applied Biosystems, California, USA). To monitor and quantify the levels of the various LM, a multiple reaction monitoring (MRM) method was developed with signature ion fragments for MaR1. Identification was conducted using previously published criteria where a minimum of six diagnostic ions were employed. Quantification was performed based on peak area of MRM transitions and the linear calibration curve of MaR1.

Collagen-induced arthritis (CIA) model, clinical evaluation and histological analysis

DBA/1 mice (male, 6–8 weeks, 18–20 g) were purchased from Shanghai SLAC Laboratory Animal. All procedures in the animal experiments were performed in accordance with UK (Home Office) regulation and approved by the Institutional Animal Care and Use Committee of Wenzhou Medical University.

On day 0, mice were injected intradermally at the base of the tail with 100 µL of type II bovine collagen (2 mg/mL) (Chondrex, Washington, USA) emulsified in equal volumes of Freund's complete adjuvant (Chondrex). After 3 weeks, the mice were given a booster immunisation with 100 µL of type II bovine collagen (2 mg/mL) emulsified in equal volumes of Freund's incomplete adjuvant. Mice were then treated with MaR1 (0, 20 and 100 ng) (Cayman Chemical) by tail vein injection every three days until day 48 and sacrificed on day 49. Serum, joint tissues and lymph nodes were harvested for further study (figure 2A).

Histological analysis

The knee joints were fixed in 4% paraformaldehyde, decalcified in 50 nM EDTA and embedded in paraffin. Sections were then deparaffinised, rehydrated and stained with H&E, or toluidine blue stain. Histology scores were assessed as previously described.[20]

ELISA

Cytokine concentration of TNF-α, interferon (IFN)-γ, IL-1β, IL-6, IL-10, IL-17 and TGF-β was detected using ELISA kits (Biolegend, USA). Samples were diluted to 100 µL (1:20), incubated with the specific capture antibody and detection antibody, determined at an optical density of 450 nm.

Flow cytometry

Inguinal and axillary lymph nodes were harvested from anaesthetised CIA mice and gently triturated with a 300 mesh cell strainer. The strained cells were washed twice with phosphate buffered saline and resuspended in RPMI 1640 medium.

For the assessment of Th17 cells, lymphocytes were stimulated for 4 hours with phorbol myristate acetate (25 ng/mL), Ionomycin (1 µg/mL) and brefeldin A (10 µg/mL). Cells were then stained with FITC conjugated anti-CD4 for 30 min in the dark at 4°C. Subsequently, the cells were fixed and permeabilised using Cytofix/Cytoperm for 20 min in the dark at 4°C. The cells were then washed in 0.05% saponin before being labelled intracellularly with APC-Cy7 conjugated anti-IL-17 for 30 min in the dark at 4°C. Similarly, for the assessment of Treg cells, lymphocytes were stained with FITC conjugated anti-CD4 and PE conjugated anti-CD25. Following fixing and permeabilising, cells were washed before being stained with APC-conjugated anti-FoxP3 intracellularly. Lymphocytes were then washed in 0.05% saponin, resuspended in a 300 µL flow cytometry staining buffer and then analysed using cytoflex (BD Biosciences, USA). The cytometric data were analysed with FlowJo software. All the reagents involved in flow cytometry were purchased from BD Biosciences.

MiRNA microarray and qPCR analysis

Total RNA samples in synovium and lymphocytes were isolated using TRIzol reagent (Invitrogen, Carlsbad, California, USA) according to the manufacturer's protocol.

The miRNA expression profiling of naive CD4+ T-cells treated with 10 nM MaR1 was determined by miRNA microarray analysis with human miRNA array probes (Exiqon, Denmark).

The cDNA of mRNA and miRNA were synthesised using the reverse transcription kit (Bio-Rad, USA) and miRNA First Strand cDNA Synthesis kit (Stem-loop Method) (Sangon Biotech, China), respectively. The expression of mRNA and miRNA was detected using SsoFast EvaGreen supermix PCR kit (Bio-Rad) by qPCR (ABI7500, Applied Biosystems). The gene-specific primers used are listed in online supplementary table S3. The relative expression of miRNA normalised to U6 controls, and mRNA normalised to β-actin, was calculated using the $2^{-\Delta\Delta Ct}$ method.

Peripheral blood mononuclear cells (PBMCs) isolation and naive CD4+ T-cell purification

PBMCs were isolated by Ficoll gradient centrifugation (Sigma-Aldrich, USA). The subpopulation of CD4+ T-lymphocytes was purified by immunomagnetic depletion using the human CD4+ T-Cell Isolation Kit II (Miltenyi Biotec, Germany). The purity of naive CD4+ T-cells was >95% confirmed by flow cytometry.

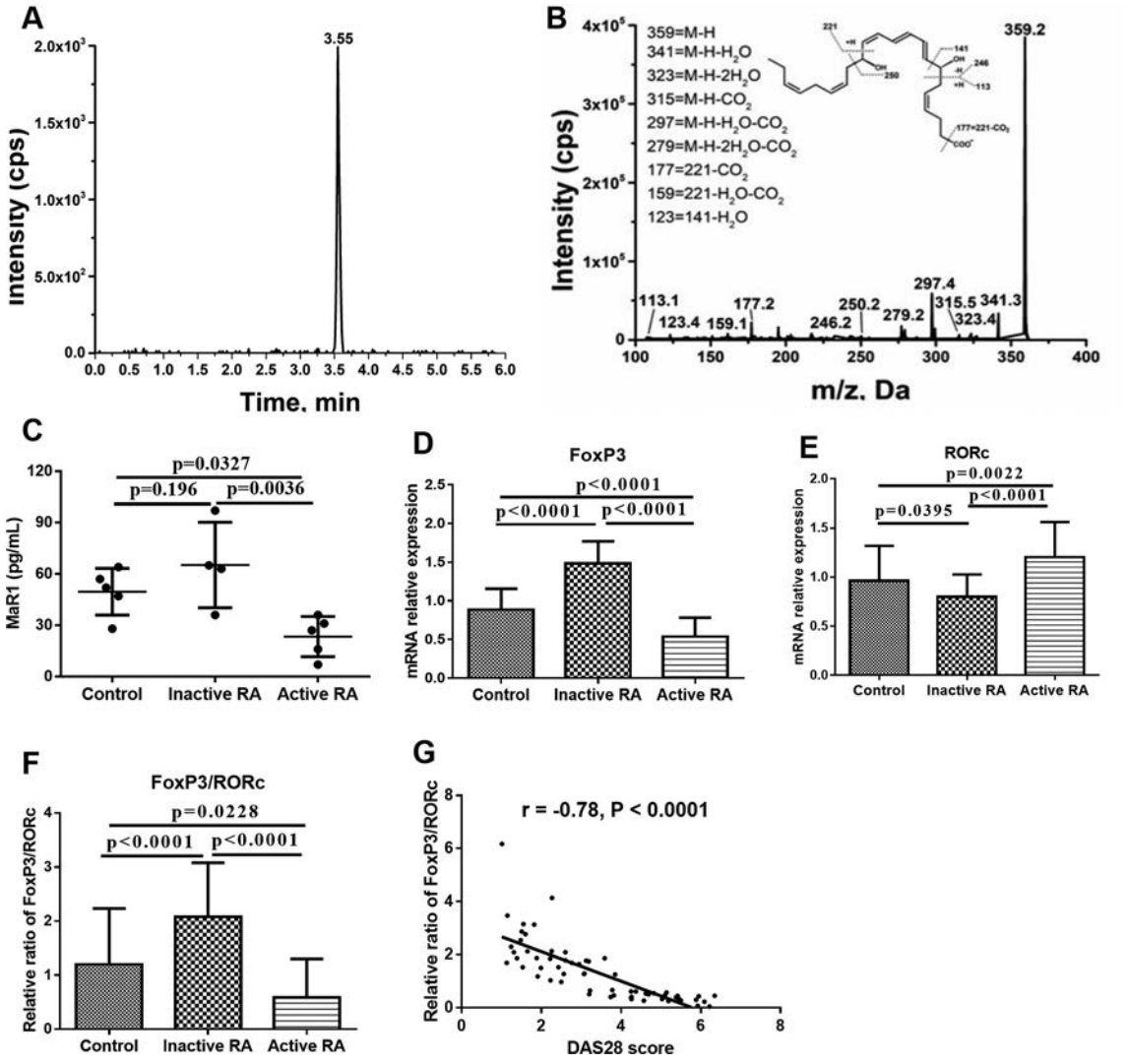

Figure 1 Maresin 1 (MaR1) concentration and levels and Treg/Th17 balance in patients with rheumatoid arthritis (RA) and control. (A) Multiple reaction monitoring chromatogram shows the retention time for MaR1 (m/z 359/177). Q1, M-H (parent ion); and Q3, diagnostic ion in the tandem mass spectrometry (MS/MS) (daughter ion). (B) MS/MS spectrum of MaR1. (C) The levels of MaR1 in serum samples from control patients, patients with inactive and active RA (n=4–5 clinical samples each group) ($F(2, 11)=7.090$). (D, E) The expression of FoxP3 and RORc mRNA was detected in peripheral blood mononuclear cells from control patients (n=39), patients with inactive RA (n=30) and patients with active RA (n=33) by qPCR ($F(2, 99)=99.64$ for FoxP3 and $F(2, 99)=12.53$ for RORc). (F) The ratio of FoxP3/RORc in control patients, patients with inactive RA and patients with active RA ($F(2, 99)=20.26$). (G) Correlation between FoxP3/RORc ratio and Disease Activity Score 28 (DAS28) score. Linear correlation was observed with $r=-0.78$, $p<0.0001$ ($F(1, 61)=96.55$) using the Pearson coefficient analysis. Data were presented with means±SD. The differences among three groups were assessed by one-way analysis of variance and the post hoc tests (Turkey method) was applied to investigate the differences one by one.

Naive CD4+ T-cell differentiation and transfection assay

The GV309 and GV280 lentivirus vector (Genechem, China) were used to upregulate and knock down miR-21 expression in naive CD4+ T-cells. The assays of lentivirus infection were performed according to manufacturer's instructions. Briefly, 50 µL GV309 and GV280 lentivirus vector and 50 µL polybrene (50 µg/mL; Sigma-Aldrich) were added in a 24-well plate containing 500 µL RPMI 1640 and 1×10^5 naive CD4+ T-cells. After 6 hours, the transfection medium was replaced by 500 µL RPMI 1640 containing 10% fetal bovine serum. The cells were then harvested and activated by plate-bound anti-CD3 (5 µg/mL) and anti-CD28 (2 µg/mL) (Biolend, California, USA). IL-1β (10 ng/mL), IL-6 (20 ng/mL), IL-23 (100 ng/mL) and TGF-β (1 ng/mL) were added for Th17 cells polarisation, while TGF-β (2 ng/mL) and IL-2 (20 U/mL) (Miltenyi Biotec, Germany) were added for Treg cells polarisation. At the same time, MaR1 (10 nM) was added once a day for 4 days.

Statistical analysis

Statistical analysis was performed using SPSS software V.19.0. The Shapiro-Wilk method was used to test whether the data were normally distributed. The Levene method was used to test the homogeneity of variance. Two sets of data that met the normal distribution and homogeneity of variance were analysed by Student's t-test. Multigroup comparisons of the means were carried out by one-way analysis of variance test with post hoc contrasts by Turkey test. The Kruskal-Wallis and Mann-Whitney non-parametric tests were used to compare interassay differences in data that did not meet the normal distribution or the homogeneity of variance.

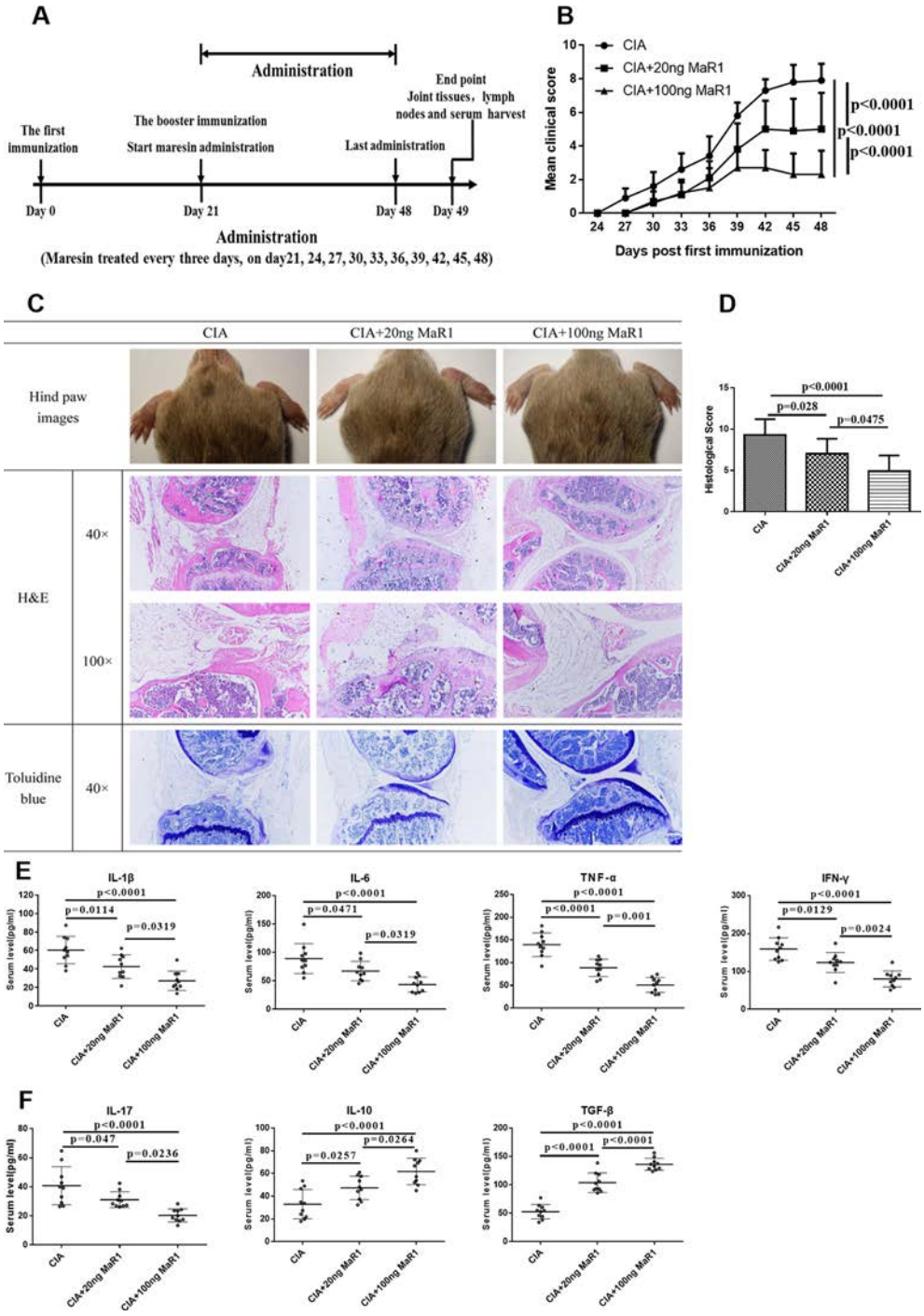

Figure 2 The effect of maresin 1 (MaR1) on joint injury and inflammatory response in the collagen-induced arthritis (CIA) model. (A) Timeline of MaR1 treatment experiment in the CIA model. (B) Clinical scores of CIA mice during the MaR1 treatment. Mice were inspected every three days for severity of arthritis by two independent observers who were not aware of the animal's treatment. Score system was defined as 0=no evidence of erythema and swelling, 1=erythema and mild swelling confined to the tarsals or ankle joint, 2=erythema and mild swelling extending from the ankle to the tarsals, 3=erythema and moderate swelling extending from the ankle to metatarsal joints and 4=erythema and severe swelling encompass the ankle, foot and digits, or ankylosis of the limb. Statistical significance was conducted by analysis of variance (ANOVA) of repeated measurement ($F(16, 144)=12.56$). (C, D) Macroscopic images and histopathological analysis of CIA mice. Macroscopic images of mice were taken on day 49 before being sacrificed. Knee joints of mice were stained by H&E and toluidine blue staining. Semiquantitative scores for inflammatory cell infiltration, synovial hyperplasia and bone destruction were assessed by H&E staining while cartilage damage was assessed by toluidine blue staining, graded on a scale of 0 (normal) to 3 (severe) in 12 totally ($F(2, 27)=13.77$ for histological score). (E, F) Serum cytokines (interleukin (IL)-1β, IL-6, tumour necrosis factor (TNF)-α, interferon (IFN)-γ, IL-17, IL-10 and transforming growth factor (TGF)-β) were detected by ELISA ($F(2, 27)=16.90$ for IL-1β, $F(2, 27)=13.48$ for IL-6, $F(2, 27)=45.79$ for TNF-α, $F(2, 27)=23.33$ for IFN-γ, $F(2, 27)=14.19$ for IL-17, $F(2, 27)=15.38$ for IL-10 and $F(2, 27)=93.77$ for TGF-β). All of the reactions were conducted in triplicate. Data were presented with means±SD. The differences of C–F were assessed by one-way ANOVA and the post hoc tests (Turkey method) was applied to investigate the differences one by one. n=10 per group.

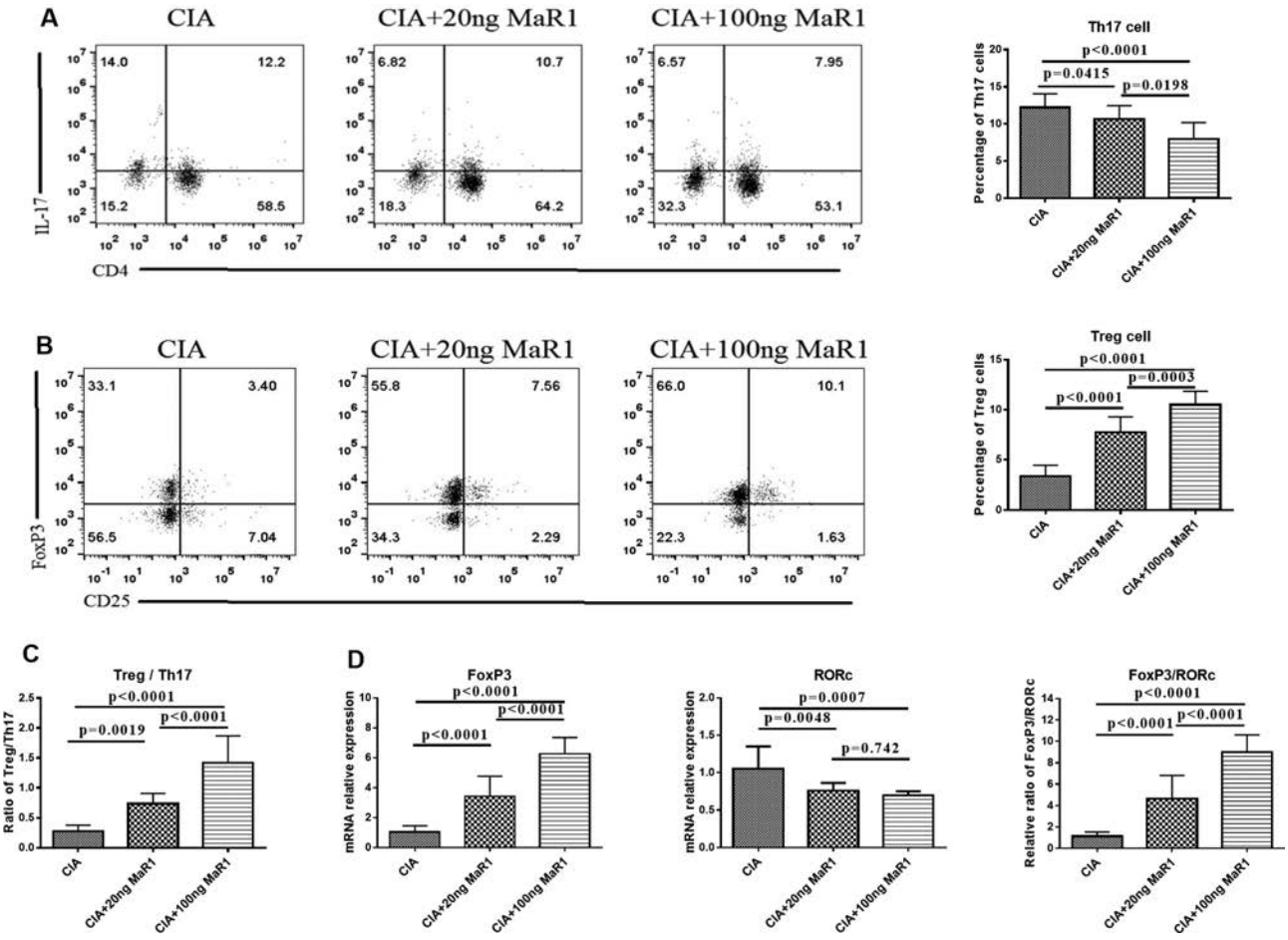

Figure 3 Maresin 1 (MaR1) influenced the Treg/Th17 balance in collagen-induced arthritis (CIA) mice. (A, B) Representative flow cytometric pictures indicated the percentage of Th17 cells and Treg cells in lymph nodes of CIA mice treated with MaR1 ($F(2, 27)=12.15$ for Th17 cells and $F(2, 27)=72.32$ for Treg cells). (C) The ratio of Treg/Th17 in lymph nodes of CIA mice treated with MaR1 ($F(2, 27)=40.89$). (D) The RORc and FoxP3 mRNA expression as well as the ratio of FoxP3/RORc in primarily cultured lymphocytes from lymph nodes of CIA mice treated with MaR1 ($F(2, 27)=10.15$ for RORc, $F(2, 27)=64.94$ for FoxP3 and $F(2, 27)=62.28$ for FoxP3/RORc). Data were presented with means±SD. The differences among three groups were assessed by one-way analysis of variance and the post hoc tests (Turkey method) was applied to investigate the differences one by one. n=10 per group.

RESULT

MaR1 level decreased in patients with active RA and increased in patients with inactive RA

MaR1 levels were quantified by UPLC-MS/MS. The mean value of level was higher in inactive RA, but lower in active RA, than in control subjects (figure 1A–C). However, no significant difference was observed between control and inactive RA. The data of ELISA was similar with the UPLC-MS/MS result (online supplementary figure 1).

FoxP3/RORc ratio inversely correlated with RA disease activity

As Foxp3 and RORc are specific transcription factors of Treg and Th17 cells, respectively, the FoxP3/RORc ratio indirectly reflects the Treg/Th17 ratio cells. The expression of FoxP3 mRNA in PBMCs was higher in inactive RA, but lower in active RA, than in control subjects (figure 1D). The result of RORc mRNA expression showed an inverse trend (figure 1E). Not unexpectedly, the FoxP3/RORc ratio in the inactive RA groups was the highest while that in the active RA groups was the lowest (figure 1F). We used the Disease Activity Score 28 (DAS28) to explore the relationship between disease activity of RA[21] and the FoxP3/RORc ratio. Inverse correlation of the FoxP3/RORc ratio and the DAS28 was observed with $r=-0.78$, $p<0.0001$ (figure 1G). Expression of RORc and FoxP3 in human synovium was also detected. The data seemed different to that of PBMCs possibly because of prior treatment with disease-modifying antirheumatic drugs and/or non-steroidal anti-inflammatory drugs in the RA cases (online supplementary figure S2).

MaR1 ameliorated joint injury and inflammatory response in CIA model

We used CIA model to study the effect of MaR1 on the RA process. After MaR1 treatment, the clinical scores and paw swelling decreased (figure 2B, C). The MaR1 intervention can reduce the histological score of CIA mice which was dose-dependent (figure 2C, D). Furthermore, MaR1 decreased pro-inflammatory cytokines (TNF-α, IFN-γ, IL-1β and IL-6) and a Th17 cell-related cytokine (IL-17), while Treg cell-related cytokines (IL-10 and TGF-β) increased, thus indicating that it inhibits inflammatory responses effectively and may also modulate the Th17/Treg balance (figure 2E, F).

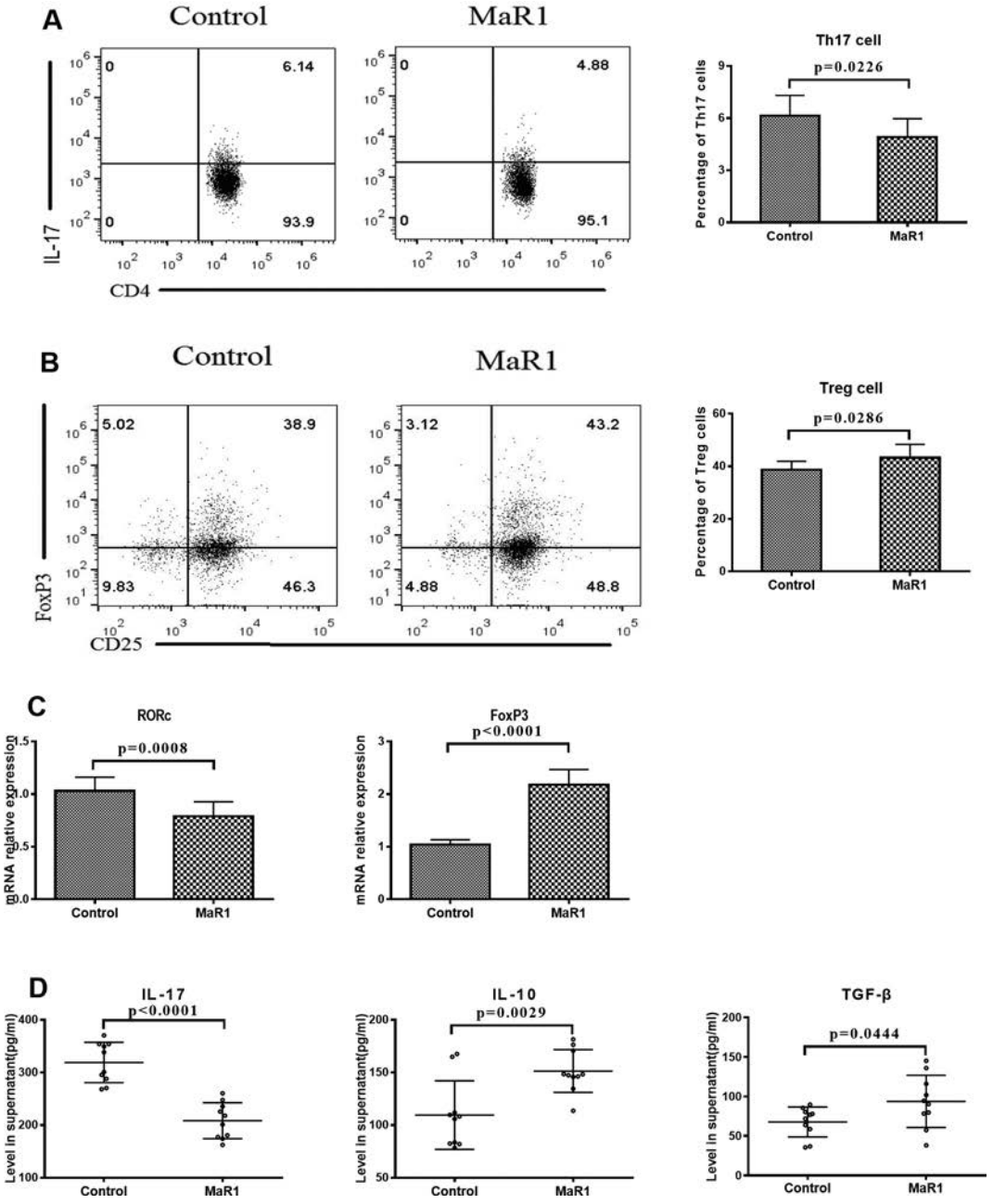

Figure 4 Maresin 1 (MaR1) affected Th17 and Treg cell polarisation from naive CD4+ T-cell. (A, B) The proportion of Th17 and Treg cells was detected after naive CD4+ T-cell-specific polarisation by flow cytometry. The differentiation experiments were conducted in a pairwise manner. Naive CD4+ T-cells from the same patient were polarised into Treg cells and Th17 cells under specific condition, and treated with MaR1 or vehicle at the same time ($F(9, 9)=1.23$ for Th17 cells and $F(9, 9)=2.43$ for Treg cells). (C) The expression of RORc and FoxP3 mRNA was determined by qPCR ($F(9, 9)=1.10$ for RORc and $F(9, 9)=9.93$ for FoxP3). (D) The concentration of interleukin (IL)-17, IL-10 and transforming growth factor (TGF)-β in cell supernatant was detected by ELISA ($F(9, 9)=1.26$ for IL-17, $F(9, 9)=2.59$ for IL-10 and $F(9, 9)=3.02$ for TGF-β). All of the reactions were conducted in triplicate. Naive CD4+ T-cells were isolated from peripheral blood mononuclear cells of patients with rheumatoid arthritis. Data were presented with means±SD and the differences were conducted by Student's t-test. n=5 per group.

MaR1 decreased Th17 cells proportion and increased Treg cells proportion in CIA mice

The proportions of Th17 and Treg cells isolated from lymph nodes were analysed by flow cytometry to evaluate the Th17/Treg balance in MaR1-treated mice. Compared with control mice, MaR1 caused a dose-dependent decrease in the percentage of Th17 cells (figure 3A). By contrast, MaR1 increased the proportion of Treg cells in a dose-dependent manner (figure 3B). Not surprisingly, the ratio of Treg/Th17 cells was elevated in the MaR1-treated group (figure 3C). The expression of FoxP3 mRNA increased while that of RORc mRNA decreased in MaR1-treated mice (figure 3D).

MaR1 promoted Treg cells differentiation while inhibited Th17 cells differentiation

The effect of MaR1 on the differentiation of Treg and Th17 cells was explored using naive CD4+ T-cells isolated from PBMCs of patients with RA. Compared with control, MaR1 treatment decreased the proportion of Th17 cells (figure 4A).

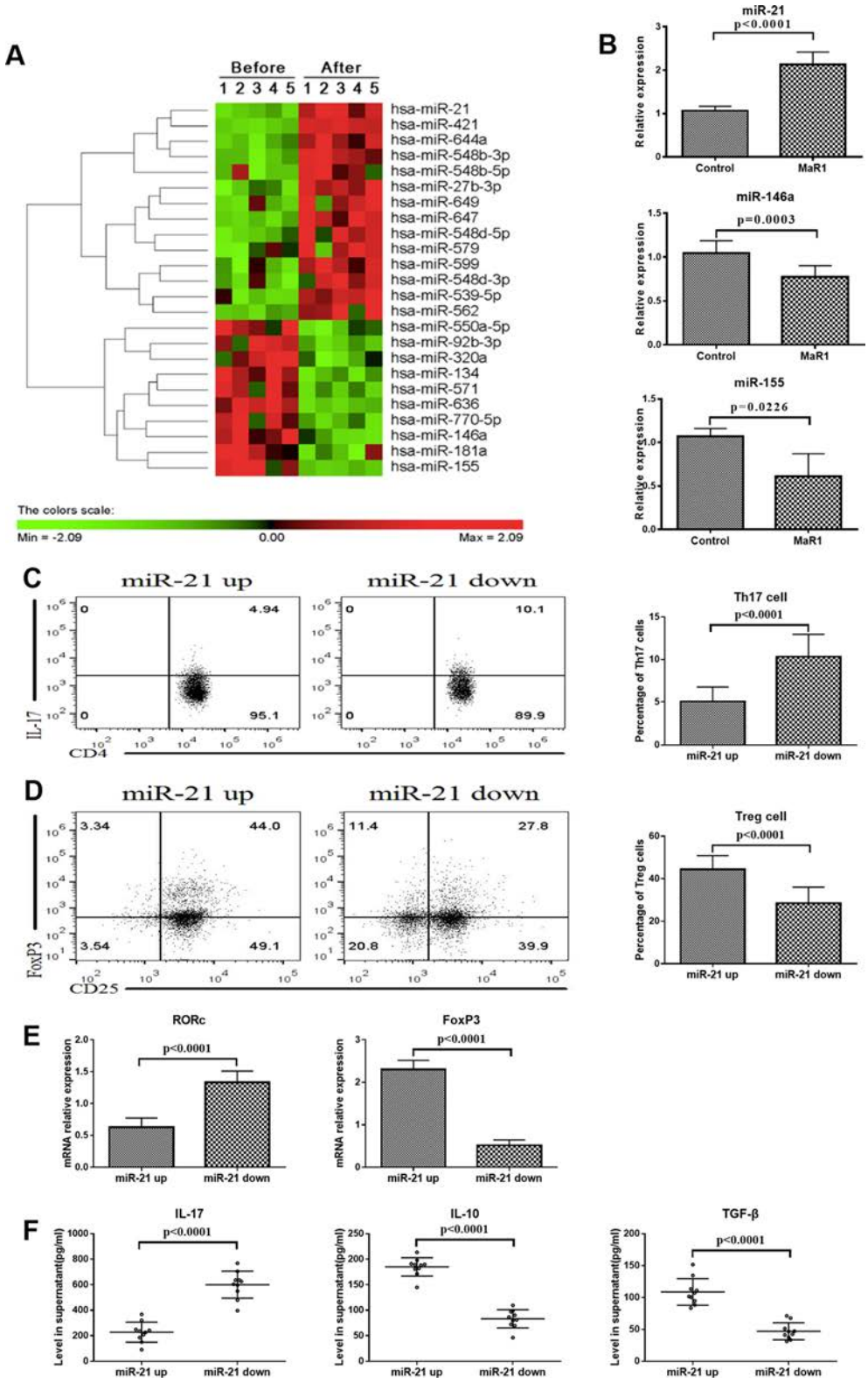

Figure 5 Effect of miR-21 on the differentiation of naive CD4+ T-cells from patients with rheumatoid arthritis. (A) Heatmap analysis of miRNA expression profiles in naive CD4+ T-cells before and after maresin 1 (MaR1) treatment. (B) The expression of miR-146a, miR-155 and miR-21 was verified by qPCR in independent patients (n=10) ($F(9, 9)=1.19$ for miR-146a, $F(9, 9)=8.16$ for miR-155 and $F(9, 9)=7.74$ for miR-21). (C, D) Representative flow cytometric pictures indicated the percentage of Th17 and Treg cells polarised from naive CD4+ T-cells transfected with miR-21 ($F(9, 9)=2.31$ for Th17 cells and $F(9, 9)=1.36$ for Treg cells). (E) The expression of RORc and FoxP3 was determined by qPCR ($F(9, 9)=1.54$ for RORc and $F(9, 9)=2.98$ for FoxP3). (F) The concentration of interleukin (IL)-17, IL-10 and transforming growth factor (TGF)-β in supernatant was detected by ELISA ($F(9, 9)=1.81$ for IL-17, $F(9, 9)=1.00$ for IL-10 and $F(9, 9)=2.45$ for TGF-β). All of the reactions were conducted in triplicate. Data were presented with means±SD and the differences were conducted by Student's t-test. n=5 per group.

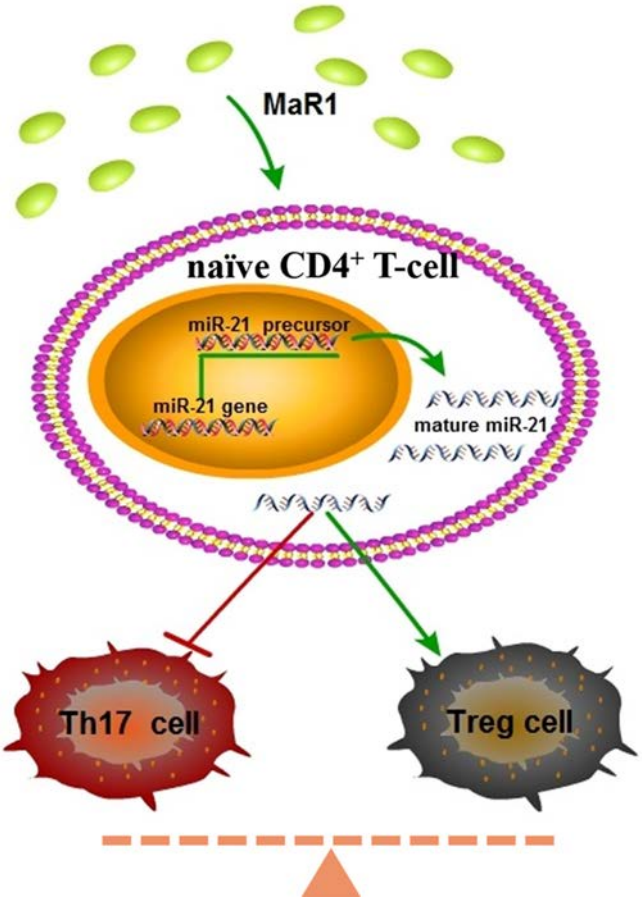

Figure 6 The mechanism of maresin 1 (MaR1) regulating Th17/Treg cells balance through miR-21.

In contrast, the percentage of Treg cells increased significantly compared with control (figure 4B). MaR1 treatment decreased the expression level of RORc while increasing the level of FoxP3 (figure 4C). MaR1 decreased IL-17 but increased the IL-10 and TGF-β levels in the culture supernatant (figure 4D).

MaR1 promoted Treg cells differentiation and inhibited differentiation of Th17 cells by upregulating miR-21

To investigate the mechanism by which MaR1 influences naive CD4+ T-cell differentiation, the expression profile of miRNA was analysed by microarray in naive CD4+ T-cells treated with MaR1 (figure 5A). MiR-146a, miR-155 and miR-21 were selected for further qPCR verification experimentation, based on the relationship between miRNA and RA. The expression of miR-146a and miR-155 was downregulated while the expression of miR-21 was dramatically upregulated after MaR1 treatment (figure 5B). The effect of miR-21 on naive CD4+ T-cell differentiation was investigated. MiR-21 decreased the proportion of Th17 cells while it increased the proportion of Treg cells (figure 5C, D). Also, miR-21 downregulated RORc mRNA and upregulated FoxP3 mRNA (figure 5E). Additionally, miR-21 decreased the level of IL-17 while increasing IL-10 and TGF-β levels in the culture supernatant (figure 5F).

DISCUSSION

The function of MaR1 in acute inflammation has recently been demonstrated, whereas the role of MaR1 in chronic inflammatory conditions such as in RA is still unclear. Giera *et al* identified MaR1 in serum and synovia from patients with RA, suggesting a relationship between MaR1 and RA.[22] However, the difference of MaR1 concentration between normal and patients with RA had not been elucidated. We demonstrate here differences in the levels of MaR1 in healthy controls, and in patients with inactive and active RA. Interestingly, the data showed a decrease of MaR1 in patients with active RA and an increase in patients with inactive RA, suggesting that the disorder of MaR1 is an important factor in the pathogenesis of RA; and the decline of MaR1 in patients with RA may play a vital role in the conversion of the inactive phase into the active phase.

Several studies have confirmed the decreasing proportion of Treg cells and increasing proportion of Th17 cells in patients with RA.[23 24] Our qPCR data also demonstrate an imbalance of Th17/Treg in PBMCs from patients with RA. Consistent with Wang,[7] the expression of RORc was dramatically higher in patients with active RA compared with that in inactive patients and healthy controls while the expression of FoxP3 showed an reverse trend. The inverse correlation between the FoxP3/RORc ratio and DAS28 scores was validated in the RA patient cohort, suggesting a potential clinical significance of the FoxP3/RORc ratio as an indicator of RA disease activity.

Woo reported that ω-3 PUFAs can attenuate arthritis in K/BxN serum transfer induced arthritis mice in terms of clinical scores, ankle thickness and pathological severity.[25] To explore the effect of MaR1 on RA progression, different doses of MaR1 were used for CIA mice treatment. As expected, MaR1 intervention alleviated the progression of arthritis in CIA mice as reflected in the reduction of clinical and histological scores, and remission of inflammatory response. Further, a higher proportion of Treg cells and a lower proportion of Th17 cells in lymph nodes were detected after MaR1 treatment using flow cytometry.

Kim and Serhan demonstrated that ω-3 PUFA and MaR1 can restore the Th17/Treg balance in collagen antibody-induced arthritis models and healthy donors, respectively.[26 27] However, the effect of MaR1 on Th17/Treg balance in patients with RA has not been investigated. Therefore, we conducted the naive CD4+ T-cell differentiation experiments. The results showed that MaR1 could promote Treg cells polarisation while inhibiting Th17 cell polarisation. Recent studies have reported that miRNAs have emerged as key regulators in the process of MaR1 exercising biological function.[18 28] Thus, miRNA microarray studies were performed in naive CD4+ T-cells treated with MaR1. Based on the p value and fold changes, miR-21 was selected for the further study.

MiR-21 was demonstrated to play a role in regulating theTh17/Treg balance. A positive correlation between miR-21 and the Treg/Th17 ratio was observed in hepatocellular carcinoma and patients with RA.[29 30] During Th17 cell differentiation, miR-21 was significantly downregulated compared with controls.[31] However, miR-21 could upregulate FoxP3 expression to promote Treg differentiation.[32] As expected, our results showed that naive CD4+ T-cells transfected with miR-21 tended to polarise into Treg cells rather than Th17 cells, demonstrating that miR-21 is a downstream microRNA mediating the restoration of MaR1 on Th17/Treg balance in patients with RA (figure 6).

Nevertheless, the mechanism of the effect of miR-21 on the balance of Th17/Treg is still unclear. In Th17 cells, STAT3 signalling is essential for their differentiation and function.[33 34] In Treg cells, TGF-β1 influences both its differentiation and function while STAT5 regulates their differentiation.[34 35] Kim and Iliopoulos reported that miR-21 was involved in the regulation of STAT3 and STAT5, respectively.[36 37] An inverse correlation between miR-21 and STAT3 as well as the positive correlation

between miR-21 and STAT5 was observed in PBMCs from patients with RA.[30] In fact, miR-21 could upregulate the expression of TGF-β1 in FLS from patients with RA.[38] These results indicate that the effect of miR-21 on Th17/Treg balance may be mediated by STAT3, STAT5 and TGF-β1, which requires further studies for verification.

In summary, we confirmed that MaR1 can effectively ameliorate RA progression. The mechanism of alleviation is related to Treg/Th17 imbalance which is primarily mediated by miR-21.

Author affiliations
[1]Department of Anesthesia and Critical Care, The Second Affiliated Hospital of Wenzhou Medical University, Wenzhou, China
[2]Department of Biochemistry, School of Basic Medical Sciences, Wenzhou Medical University, Wenzhou, China
[3]Clinical Medicine Research Center, Xinqiao Hospital, Third Military Medical University, Chongqing, China
[4]Institute of Cancer, Xinqiao Hospital, Third Military Medical University, Chongqing, China
[5]Department of Rheumatology, Jiamusi Central Hospital, Jiamusi, China
[6]Department of Medicinal Chemistry, School of Pharmaceutical Sciences, Wenzhou Medical University, Wenzhou, China

Correction notice This article has been corrected since it published Online First. The fourth affiliation has been updated.

Contributors SJ, HC and JW conceived of the study and participated in its design and coordination. XY, HZ, JW, WS, QT, HC and JM collected samples, carried out ELISA assay and induced the CIA model. YL and JZ conducted UPLC-MS/MS experiment and data analysis. QT, JM, TZ and SY carried on the naive CD4+ T-cell differentiation experiment and flow cytometry. XY, WS and JW performed the statistical analysis. HZ, SJ and JW drafted and revised the manuscript. All authors read and approved the final manuscript. SJ, HC and YL made equal contributions to this work. All authors take responsibility for the integrity of the work.

Funding This project was supported by The National Key Research and Development Program of China (grant no. 2017YFC0909000); the Public Technology Applied Research Foundation of Zhejiang Province (grant no. LGF18H060009) and the National Natural Science Foundation (grant nos. 81472055, 81672129 and 81570076).

Competing interests None declared.

Patient consent Obtained.

Ethics approval The study protocol was approved by the Clinical Research Ethics Committees of the First Affiliated Hospital of Wenzhou Medical University (no. 2016157).

Provenance and peer review Not commissioned; externally peer reviewed.

REFERENCES

1 McInnes IB, Schett G. The pathogenesis of rheumatoid arthritis. *N Engl J Med* 2011;365:2205–19.
2 Smolen JS, Aletaha D, McInnes IB. Rheumatoid arthritis. *Lancet* 2016;388:2023–38.
3 Noack M, Miossec P. Th17 and regulatory T cell balance in autoimmune and inflammatory diseases. *Autoimmun Rev* 2014;13:668–77.
4 Miossec P, Kolls JK. Targeting IL-17 and TH17 cells in chronic inflammation. *Nat Rev Drug Discov* 2012;11:763–76.
5 Koenders MI, Joosten LA, van den Berg WB. Potential new targets in arthritis therapy: interleukin (IL)-17 and its relation to tumour necrosis factor and IL-1 in experimental arthritis. *Ann Rheum Dis* 2006;65:iii29–33.
6 Wang Y, Zhou C, Gao H, *et al*. Therapeutic effect of Cryptotanshinone on experimental rheumatoid arthritis through downregulating p300 mediated-STAT3 acetylation. *Biochem Pharmacol* 2017;138:119–29.
7 Wang W, Shao S, Jiao Z, *et al*. The Th17/Treg imbalance and cytokine environment in peripheral blood of patients with rheumatoid arthritis. *Rheumatol Int* 2012;32:887–93.
8 Nie H, Zheng Y, Li R, *et al*. Phosphorylation of FOXP3 controls regulatory T cell function and is inhibited by TNF-α in rheumatoid arthritis. *Nat Med* 2013;19:322–8.
9 Gaafar T, Farid R, *et al*. The TH17/Treg Imbalance in rheumatoid arthritis and relation to disease activity. *J Clin Cell Immunol* 2015;06:381.
10 Serhan CN. Pro-resolving lipid mediators are leads for resolution physiology. *Nature* 2014;510:92–101.
11 Buckley CD, Gilroy DW, Serhan CN. Proresolving lipid mediators and mechanisms in the resolution of acute inflammation. *Immunity* 2014;40:315–27.
12 Gong J, Liu H, Wu J, *et al*. Maresin 1 prevents lipopolysaccharide-induced neutrophil survival and accelerates resolution of acute lung injury. *Shock* 2015;44:371–80.
13 Fullerton JN, Gilroy DW. Resolution of inflammation: a new therapeutic frontier. *Nat Rev Drug Discov* 2016;15:551–67.
14 Barden AE, Moghaddami M, Mas E, *et al*. Specialised pro-resolving mediators of inflammation in inflammatory arthritis. *Prostaglandins Leukot Essent Fatty Acids* 2016;107:24–9.
15 Dawczynski C, Dittrich M, Neumann T, *et al*. Docosahexaenoic acid in the treatment of rheumatoid arthritis: A double-blind, placebo-controlled, randomized cross-over study with microalgae vs. sunflower oil. *Clin Nutr* 2018;37.
16 Norling LV, Headland SE, Dalli J, *et al*. Proresolving and cartilage-protective actions of resolvin D1 in inflammatory arthritis. *JCI Insight* 2016;1:e85922.
17 Chen XM, Huang QC, Yang SL, *et al*. Role of Micro RNAs in the pathogenesis of rheumatoid arthritis: novel perspectives based on review of the literature. *Medicine* 2015;94:e1326.
18 Li Y, Dalli J, Chiang N, *et al*. Plasticity of leukocytic exudates in resolving acute inflammation is regulated by MicroRNA and proresolving mediators. *Immunity* 2013;39:885–98.
19 Zhang Q, Wang X, Yan G, *et al*. Anti- versus pro-inflammatory metabololipidome upon cupping treatment. *Cell Physiol Biochem* 2018;45:1377–89.
20 Zhou C, You Y, Shen W, *et al*. Deficiency of sorting nexin 10 prevents bone erosion in collagen-induced mouse arthritis through promoting NFATc1 degradation. *Ann Rheum Dis* 2016;75:1211–8.
21 Wang JG, Xu WD, Zhai WT, *et al*. Disorders in angiogenesis and redox pathways are main factors contributing to the progression of rheumatoid arthritis: a comparative proteomics study. *Arthritis Rheum* 2012;64:993–1004.
22 Giera M, Ioan-Facsinay A, Toes R, *et al*. Lipid and lipid mediator profiling of human synovial fluid in rheumatoid arthritis patients by means of LC-MS/MS. *Biochim Biophys Acta* 2012;1821:1415–24.
23 Samson M, Audia S, Janikashvili N, *et al*. Brief report: inhibition of interleukin-6 function corrects Th17/Treg cell imbalance in patients with rheumatoid arthritis. *Arthritis Rheum* 2012;64:2499–503.
24 Niu Q, Cai B, Huang ZC, *et al*. Disturbed Th17/Treg balance in patients with rheumatoid arthritis. *Rheumatol Int* 2012;32:2731–6.
25 Woo SJ, Lim K, Park SY, *et al*. Endogenous conversion of n-6 to n-3 polyunsaturated fatty acids attenuates K/BxN serum-transfer arthritis in fat-1 mice. *J Nutr Biochem* 2015;26:713–20.
26 Kim JY, Lim K, Kim KH, *et al*. N-3 polyunsaturated fatty acids restore Th17 and Treg balance in collagen antibody-induced arthritis. *PLoS One* 2018;13:e0194331.
27 Chiurchiù V, Leuti A, Dalli J, *et al*. Proresolving lipid mediators resolvin D1, resolvin D2, and maresin 1 are critical in modulating T cell responses. *Sci Transl Med* 2016;8:353ra111.
28 Rius B, Duran-Güell M, Flores-Costa R, *et al*. The specialized proresolving lipid mediator maresin 1 protects hepatocytes from lipotoxic and hypoxia-induced endoplasmic reticulum stress. *Faseb J* 2017;31:5384–98.
29 Yao SX, Zhang GS, Cao HX, *et al*. Correlation between microRNA-21 and expression of Th17 and Treg cells in microenvironment of rats with hepatocellular carcinoma. *Asian Pac J Trop Med* 2015;8:762–5.
30 Dong L, Wang X, Tan J, *et al*. Decreased expression of microRNA-21 correlates with the imbalance of Th17 and Treg cells in patients with rheumatoid arthritis. *J Cell Mol Med* 2014;18:2213–24.
31 Huang J, Liang Z, Kuang Y, *et al*. 1,25-Dihydroxyvitamin D3 Does Not Affect MicroRNA Expression When Suppressing Human Th17 Differentiation. *Med Sci Monit* 2017;23:535–41.
32 Rouas R, Fayyad-Kazan H, El Zein N, *et al*. Human natural Treg microRNA signature: role of microRNA-31 and microRNA-21 in FOXP3 expression. *Eur J Immunol* 2009;39:1608–18.
33 Wei L, Laurence A, O'Shea JJ. New insights into the roles of Stat5a/b and Stat3 in T cell development and differentiation. *Semin Cell Dev Biol* 2008;19:394–400.
34 Ju JH, Heo YJ, Cho ML, *et al*. Modulation of STAT-3 in rheumatoid synovial T cells suppresses Th17 differentiation and increases the proportion of Treg cells. *Arthritis Rheum* 2012;64:3543–52.
35 Fontenot JD, Rasmussen JP, Gavin MA, *et al*. A function for interleukin 2 in Foxp3-expressing regulatory T cells. *Nat Immunol* 2005;6:1142–51.
36 Kim YJ, Hwang SH, Cho HH, *et al*. MicroRNA 21 regulates the proliferation of human adipose tissue-derived mesenchymal stem cells and high-fat diet-induced obesity alters microRNA 21 expression in white adipose tissues. *J Cell Physiol* 2012;227:183–93.
37 Iliopoulos D, Kavousanaki M, Ioannou M, *et al*. The negative costimulatory molecule PD-1 modulates the balance between immunity and tolerance via miR-21. *Eur J Immunol* 2011;41:1754–63.
38 Xiong G, Huang Z, Jiang H, *et al*. Inhibition of microRNA-21 decreases the invasiveness of fibroblast-like synoviocytes in rheumatoid arthritis via TGFβ/Smads signaling pathway. *Iran J Basic Med Sci* 2016;19:787–93.

EXTENDED REPORT

Photosensitivity and type I IFN responses in cutaneous lupus are driven by epidermal-derived interferon kappa

Mrinal K Sarkar,[1] Grace A Hile,[2] Lam C Tsoi,[1,3,4] Xianying Xing,[1] Jianhua Liu,[2] Yun Liang,[1] Celine C Berthier,[5] William R Swindell,[1] Matthew T Patrick,[1] Shuai Shao,[1] Pei-Suen Tsou,[2] Ranjitha Uppala,[1] Maria A Beamer,[1] Anshika Srivastava,[6] Stephanie L Bielas,[6] Paul W Harms,[1,7] Spiro Getsios,[8] James T Elder,[1] John J Voorhees,[1] Johann E Gudjonsson,[1] J Michelle Kahlenberg[2]

Handling editor Josef S Smolen

► Additional material is published online only. To view please visit the journal online (http://dx.doi.org/10.1136/annrheumdis-2018-213197).

For numbered affiliations see end of article.

Correspondence to
Dr Johann E Gudjonsson, Department of Dermatology, University of Michigan, Ann Arbor, MI 48109, USA; johannng@med.umich.edu and Dr J Michelle Kahlenberg, Department of Internal Medicine, Division of Rheumatology, University ofMichigan, Ann Arbor, MI, 48109, USA ; mkahlenb@med.umich.edu

JEG and JMK contributed equally.

Received 6 February 2018
Revised 1 June 2018
Accepted 3 July 2018
Published Online First 18 July 2018

To cite: Sarkar MK, Hile GA, Tsoi LC, *et al*. *Ann Rheum Dis* 2018;**77**:1653–1664.

ABSTRACT

Objective Skin inflammation and photosensitivity are common in patients with cutaneous lupus erythematosus (CLE) and systemic lupus erythematosus (SLE), yet little is known about the mechanisms that regulate these traits. Here we investigate the role of interferon kappa (IFN-κ) in regulation of type I interferon (IFN) and photosensitive responses and examine its dysregulation in lupus skin.

Methods mRNA expression of type I IFN genes was analysed from microarray data of CLE lesions and healthy control skin. Similar expression in cultured primary keratinocytes, fibroblasts and endothelial cells was analysed via RNA-seq. *IFNK* knock-out (KO) keratinocytes were generated using CRISPR/Cas9. Keratinocytes stably overexpressing IFN-κ were created via G418 selection of transfected cells. IFN responses were assessed via phosphorylation of STAT1 and STAT2 and qRT-PCR for IFN-regulated genes. Ultraviolet B-mediated apoptosis was analysed via TUNEL staining. In vivo protein expression was assessed via immunofluorescent staining of normal and CLE lesional skin.

Results *IFNK* is one of two type I IFNs significantly increased (1.5-fold change, false discovery rate (FDR) q<0.001) in lesional CLE skin. Gene ontology (GO) analysis showed that type I IFN responses were enriched (FDR=6.8×10^{-04}) in keratinocytes not in fibroblast and endothelial cells, and this epithelial-derived IFN-κ is responsible for maintaining baseline type I IFN responses in healthy skin. Increased levels of IFN-κ, such as seen in SLE, amplify and accelerate responsiveness of epithelia to IFN-α and increase keratinocyte sensitivity to UV irradiation. Notably, KO of IFN-κ or inhibition of IFN signalling with baricitinib abrogates UVB-induced apoptosis.

Conclusion Collectively, our data identify IFN-κ as a critical IFN in CLE pathology via promotion of enhanced IFN responses and photosensitivity. IFN-κ is a potential novel target for UVB prophylaxis and CLE-directed therapy.

INTRODUCTION

Cutaneous lupus erythematosus (CLE) affects up to 70% of patients with systemic lupus erythematosus (SLE) and can also exist without the presence of systemic disease. CLE lesions can result in disfiguring scars, permanent hair loss and significant loss of quality of life for patients.[1] There are no Food and Drug Administration (FDA)-approved therapies for CLE, largely related to a lack of pathogenic understanding of this disease.

A hallmark of CLE and SLE is the induction of skin lesions by ultraviolet (UV) light in up to 93% of patients.[2] These lesions are characterised by interface dermatitis and infiltration by both innate and adaptive immune cells. Patients with CLE exhibit increased type I interferon (IFN) signalling in their blood, which correlates with cutaneous disease activity,[3] and increased expression of IFN responsive genes in lesional skin.[4–6] Cutaneous lesions in lupus are characterised by infiltration of plasmacytoid dendritic cells (pDCs),[7] and their production of IFN-α is a suggested source of type I IFN signalling in CLE.[8 9] However, the sources of IFN in cutaneous lupus have not been systematically evaluated.

Interferon kappa (IFN-κ) is a member of the type I IFN family that is expressed primarily by keratinocytes.[10] The chromosomal region encompassing *IFNK* has been suggested as a genetic risk locus for SLE, including some associations with CLE phenotypes.[11] Intriguingly, overexpression of *IFNK* can induce autoimmune phenotypes in mice.[12] *IFNK* expression in keratinocytes is upregulated by UV light exposure,[13] a well-known trigger of CLE,[2] and IFN-κ can prime keratinocytes for inflammatory cytokine production. Importantly, we have shown that IFN-κ is required for overproduction of IL-6 by keratinocytes from patients with SLE.[13] Despite this knowledge, little is known about the function of IFN-κ in the skin and its contribution to CLE and UV sensitivity. We thus hypothesised that epidermal production of IFN-κ is elevated in CLE and that it is an essential contributor to cutaneous type I IFN responses and CLE lesions. Indeed, we found that IFN-κ is upregulated in CLE lesions and in keratinocytes from non-lesional SLE skin. IFN-κ is required for baseline expression of type I IFN-regulated genes in keratinocytes and drives enhanced responses to IFN-α. IFN-κ upregulates type I IFN-regulated gene expression in neighbouring skin cells and stimulates activation of dendritic cells, which are important contributors to CLE pathogenesis.[14] Importantly, IFN-κ regulates the apoptotic response to UVB, and inhibition of

IFN responses in lupus keratinocytes abrogates their enhanced apoptosis to UVB. Thus, we propose IFN-κ as a novel IFN critical for CLE pathology and a potentially important target for photoprophylaxis and specific CLE-directed therapy.

MATERIALS AND METHODS

Human subjects

According to the Declaration of Helsinki, all patients and controls gave written informed consent. The study protocol was approved by the Institutional Review Board of the University of Michigan Medical School. Patients with SLE fulfilled ≥4 ACR criteria,[15] had a documented history of cutaneous lesions and were recruited from the University of Michigan Lupus Cohort. Patients with CLE used for microarray studies had both clinical and pathologic confirmation of diagnosis (online supplementary table S1). Normal controls were recruited by advertisement.

Cell culture

N/TERTs,[16] an immortalised keratinocytes line, was used with the kind permission of Dr James G Rheinwald for generation of knock-out (KO) cell lines using non-homologous end joining (NHEJ) via CRISPR/Cas9. N/TERTs were grown in Keratinocyte-SFM medium (ThermoFisher #17 005–042) supplemented with 30 µg/mL bovine pituitary extract, 0.2 ng/mL epidermal growth factor and 0.3 mM calcium chloride.[17] Primary human keratinocytes were established from healthy adults or lupus patients with a history of CLE as previously described.[13 18] Dermal fibroblasts and endothelial cells were isolated from normal human skin as previously described.[19 20]

Generation of KO keratinocytes by CRISPR/cas9

Guide RNAs were developed using a web interface for CRISPR design (http://crispr.mit.edu). The pSpCas9 (BB)−2A-GFP (PX458) was a gift from Feng Zhang (Addgene plasmid #48138) and used as cloning backbone. We followed the CRISPR/Cas9 protocol as previously discussed[17 21] to generate *TYK2* KO and *IFNK* KO cell lines. In short, for the *TYK2* KO, the following oligonucleotides were used for annealing: TYK2E3G1F: 5′-CACCGGACTCACTGAAAGTGACCCA-3′ and TYK2E3G1R: 5′-AAACTGGGTCACTTTCAGTGAGTCC-3′. For the *IFNK* KO, the following oligonucleotides were used for annealing: IFNKSGRNA1F1: 5′-CACCGGTTCAGTAAGTTACA GTCCA-3′ and IFNKSGRNA1R1: 5′-AAACTGGACTGTAACT TACTGAACC-3′. The annealed oligonucleotides were inserted into the cloning vector Px458 following the Ran *et al*[21] protocol. Ligated plasmids were transformed into competent *Escherichia coli* (ThermoFisher #C737303) and then plated on LB-agar plate overnight. Twelve colonies from each of the groups were selected and cultured in LB medium, and plasmids were purified using Qiagen mini-prep kit (cat #27106), and then the proper insertion of sgRNA target sequences were verified by Sanger sequencing. Purified plasmid was transfected into an immortalised keratinocyte line (N/TERTs) using the TransfeX transfection kit (ATCC #ACS4005). Single cells positive for green fluorescent protein (GFP) were sorted into 96-well plates using a MoFlo Astrios #1 cell sorter and grown up to ∼50% confluence. Cells from 96-well plates were transferred into 12-well plates and grown to 50% confluence. DNA was extracted, and PCR was amplified using specific primers for *TYK2* and *IFNK: TYK2*: TYK2E3PCR-F: GTCTCTGGGCTGAGACTTGG, TYK2E3PCR-R: CCCCAGACTCACCAACTTTA and *IFNK*: IFNK1PCRF1: GTGTTTGTGGCTTGAGATCC, IFNK-1PCRR1: GGTTGGGTGTATTGCAGAAA. Homozygous *TYK2* and *IFNK* mutations were verified by Sanger sequencing of the PCR product. For validation of findings, a total of three independent CRISPR/Cas9 KO mutants were generated for *IFNK* and for *TYK2*.

Generation of IFN-κ overexpressing N/TERTs

N/TERT keratinocytes stably overexpressing IFN-κ were generated using 4D-Nucleofector X Unit (Lonza Cologne, Germany). Cells were prepared using standard protocol for Normal Human Epidermal Keratinocyte X Unit kit (4D Nucleofector Solution, supplement and 100 µL single nucleocuvette) obtained from Lonza. For each electroporation, 3 µg pCMV6-AC-GFP-IFNκ plasmid (Origene, Rockville, Maryland, USA) was used. Unit X program used was DS-138 for stable keratinocytes. Following transfection, keratinocytes were grown in a 48-well plate using fully supplemented Keratinocyte-SFM medium, penicillin streptomycin and 500 µg/mL G418 (Geneticin by Thermo Fisher Scientific (Waltham, Massachusetts, USA)) (for selection) followed by expansion for approximately 60 days. IFNκ-GFP overexpression was validated using western blotting.

Evaluation of IFN response in N/TERT-IFN-κ cells

IFN-κ overexpressing N/TERTs were grown in parallel to wild-type N/TERTs with 2 µg/mL anti-IFN-κ goat polyclonal neutralising antibody (Santa Cruz Biotechnology, Dallas, Texas, USA) or 2 µg/mL isotype normal goat IgG (R&D Systems, Minneapolis, Minnesota, USA) for 3 days followed by stimulation with 5 ng/mL human recombinant IFNα2 (Schering Corporation, Kenilworth, New Jersey, USA) for 1, 4 or 12 hours. Cells were harvested in Tripure (Sigma-Aldrich, St. Louis, Missouri, USA). RNA was isolated following protocol for Direct-zol RNA MiniPrep (Zageno, Berlin, Germany), and cDNA was made. RT-PCR for *MX1* (normalised to *RPLP0*) was performed using ABI PRISM 7900HT (Applied Biosystems) using SYBR Green at the University of Michigan DNA-sequencing core.

Dendritic cell (DC) culture

Human DCs were generated in vitro as previously described.[22] Briefly, monocytes were isolated from PBMC using MACS negative selection beads (Miltenyi) and cultured in RPMI containing 10% FCS supplemented with GM-CSF (100 ng/mL, R&D Systems #215 GM-050) and IL-4 (20 ng/mL, R&D Systems #204-IL-010). Cultures were fed on day 4. On day 8, DCs were seeded into poly (2-hydroxyethyl-methacrylate) coated 12-well culture plates (Fisher Scientific #0720082) at a density of 1 million cells/well and stimulated for 6 hours (PCR) or 2 days (flow cytometry) with conditioned mediated generated from control or SLE KC exposed to 50 mJ/cm^2 UVB. The DCs were treated in the presence/absence of baricitinib. DC phenotype was analysed by flow cytometry using an LSR2 flow cytometer (BD) using antibodies against CD80 (Biolegend #305218) and appropriate isotype control antibodies. Data analysis was performed using FCS Express (V.4) software.

Microarray

Biopsies of CLE cases (n=90) were identified through the University of Michigan Pathology Database using the search terms 'lupus' and 'cutaneous lupus'. Control blocks were obtained from healthy volunteers. Patients who met both clinical and histological criteria for discoid lupus erythematosus (DLE) or subacute cutaneous lupus erythematosus (SCLE) were included in the study. Validation of clinical and pathological CLE diagnosis was made via review of dermatology notes for

each case. Detailed clinical information was obtained for each sample (online supplementary table S1). RNA was isolated from five 10 µm sections of formalin-fixed paraffin embedded blocks of identified skin biopsies. As previously described,[23] RNA was extracted using the E.N.Z.A. FFPE RNA Kit (Omega Bio-tek). Complementary DNA was prepared and biotinylated using the NuGEN Encore Biotin Module (Encore Biotin Module Manual, P/N M01111 V.6). Labelled cDNA was hybridised at 48°C to Affymetrix Human Gene ST 2.1 array plates, which were then washed, stained and scanned using the Affymetrix GeneTitan system (software V.3.2.4.1515) with the assistance of the University of Michigan DNA Sequencing Core. Quality control and RMA (Robust Multi-array Average)[24]normalisation of CEL files were performed in R software V.3.1.3 using custom CDF V.19 and modified Affymetrix_1.44.1 package from BrainArray (http://brainarray.mbni.med.umich.edu/brainarray/default.asp). Log_2 expression values were batch corrected using Combat implemented into GenePattern (http://www.broadinstitute.org/cancer/software/genepattern/). The baseline expression was defined as minimum plus one SD of the median of all genes. A variance filter of 80% was then applied. Of the 25 582 unique genes represented on the Human ST2.1 chip, a total of 20 410 genes passed the defined criteria. The normalised data file was uploaded to the Gene Expression Omnibus (GEO) website (http://www.ncibi.nlm.nih.gov/geo/) under accession number GSE81071 and will be available on acceptance of this manuscript.

RNA extraction, qRT-PCR and RNA-Sequencing

RNAs were isolated from cell cultures using Qiagen RNeasy plus kit (Cat #74136). qRT-PCR was performed on a 7900HT Fast Real-time PCR system (Applied Biosystems) with TaqMan Universal PCR Master Mix (ThermoFisher Scientific). Libraries for RNA-seq were generated from polyadenylated RNA and sequenced at six libraries per lane on the Illumina Genome Analyzer IIx. We used Tophat2[25] to align RNA-seq reads to the human genome, using annotations of GENCODE as gene model.[26] HTSeq was used to quantify gene expression levels[27]; normalisation and differential expression analysis were performed by DESeq2.[28] The RNA-seq data will be made available to the GEO on the acceptance of the manuscript.

Immunostaining

According to our previous protocol,[29] formalin fixed, paraffin-embedded tissue slides obtained from patients with cutaneous lupus were heated for 30 min at 60°C, rehydrated, and epitope retrieved with Tris-EDTA, pH 9. Slides were blocked, incubated with primary antibody (IFN-κ, Abnova #: H00056832-M01; IFN-α, Santa Cruz #sc-80996; IFN-β, Biolegend #514004; MX1, Abcam #ab95926; Cytokeratin 14, Abcam #ab51054; p-STAT1, Cell Signaling #9167; p-STAT2, Cell Signaling #4441; CD11c, Abcam #ab52632; CD80, Life Span Biosciences #LS-C115529; CD3, Dako #A0452; CD123, Sigma-Aldrich #HPA003539; Mouse IgG2a, kappa isotype control (for IFN-κ), ThermoFisher #14-4724-81; Mouse IgG2a Isotype Control (for CD80), ThermoFisher #02–6200; Mouse IgG1, kappa isotype control (for IFN-α and IFN-β), ThermoFisher #14-4714-81; Rabbit IgG Isotype Control (for Mx1, cytokeratin 14, p-STAT1, p-STAT2 and CD11c,), LSBio #LS-C149375) overnight at 4°C. Slides were incubated with biotinylated secondary antibody (biotinylated goat antirabbit IgG Antibody, Vector Laboratories #BA1000; biotinylated horse antimouse IgG Antibody, Vector Laboratories #BA2000) and then incubated with fluorochrome-conjugated streptavidin. Slides were prepared in mounting medium with 4',6-diamidino-2-phenylindole (DAPI). Images were acquired using Zeiss Axioskop 2 microscope and analysed by SPOT software V.5.1. Images presented are representative of three experiments.

Western blot

Total protein was isolated from cultured cells using Pierce RIPA buffer (ThermoFisher #89900) and run on precast gel (Bio-Rad #456–1094S). The membrane was blocked and then probed by a primary antibody (IFN-κ, Abnova, Catalog #: H00056832-M01; Tyk2, Cell Signaling #9312s; STAT1, Cell Signaling #9172; STAT2, Cell Signaling #4594; pSTAT1, Cell Signaling #9167; pSTAT2, Cell Signaling #4441; β-Actin, sigma #A5441), followed by a secondary antibody (antimouse IgG, AP-linked antibody, Cell Signaling #7056S), then washed five times, and substrate added (Fisher Scientific #45-000-947). Membrane was scanned on Molecular Dynamics STORM 860 PhosphorImager (GE Health Care, STORM 860).

UVB irradiation and TUNEL assays

Keratinocyte cultures were grown to 80% confluence and were irradiated in PBS with 50 mJ/cm^2 UVB (310 nm) via a UV-2 irradiator (Tyler Industries, Alberta, Canada). After media replacement, cells were grown for 8 hours followed by staining for TUNEL according to manufacturer's instructions (Sigma) and counterstaining with DAPI. Per cent TUNEL+cells were quantified using CellC (# cells positive for Red (TUNEL) and DAPI staining/# cells DAPI positive). For CLE biopsies, TUNEL staining was performed according to manufacturer protocol (Roche #12156792910). In short, paraffin-embeded CLE and control slides were dewaxed and rehydrated according to stadard protocol and then treated with proteinase K solution. Slides were then treated with TUNEL reaction mixture in a humidified chamber followed by PBS washing. Finally slides were mounted by vectashield mounting medium with DAPI. Images were acquired using Zeiss Axioskop 2 microscope and analysed by SPOT software V.5.1. Images presented are representative of three experiments.

Statistical analysis

Calculations were made using GraphPad Prism V.6. For in vitro studies, comparisons of the means between experimental variables was made via unpaired two-sided Student's t-test for normally distributed variables and via Mann-Whitney for non-normally distributed variables. For both microarray and RNA-seq, false discovery rate (FDR) was used to control for multiple testing.

RESULTS

IFN-κ is increased in lesional and non-lesional lupus skin

Type I IFNs have been purported to play a role in CLE; however, which IFNs are present in CLE are unknown. To address this, we investigated the expression of type I IFN family members in microarray data obtained from CLE lesions (n=90) and healthy control skin (n=13). Ten type I IFN members passed cut-off values for detectible expression, and of those, only *IFNA10* (1.7-fold change, FDR q<0.05) and *IFNK* (1.5-fold change, FDR q<0.001) had significantly increased expression in lesional CLE skin (figure 1A). This finding held true when subtypes of CLE (DLE vs SCLE were considered or whether patients had CLE only or CLE associated with SLE (online supplementary figure S1A). No elevations of IFN-λ, a type III

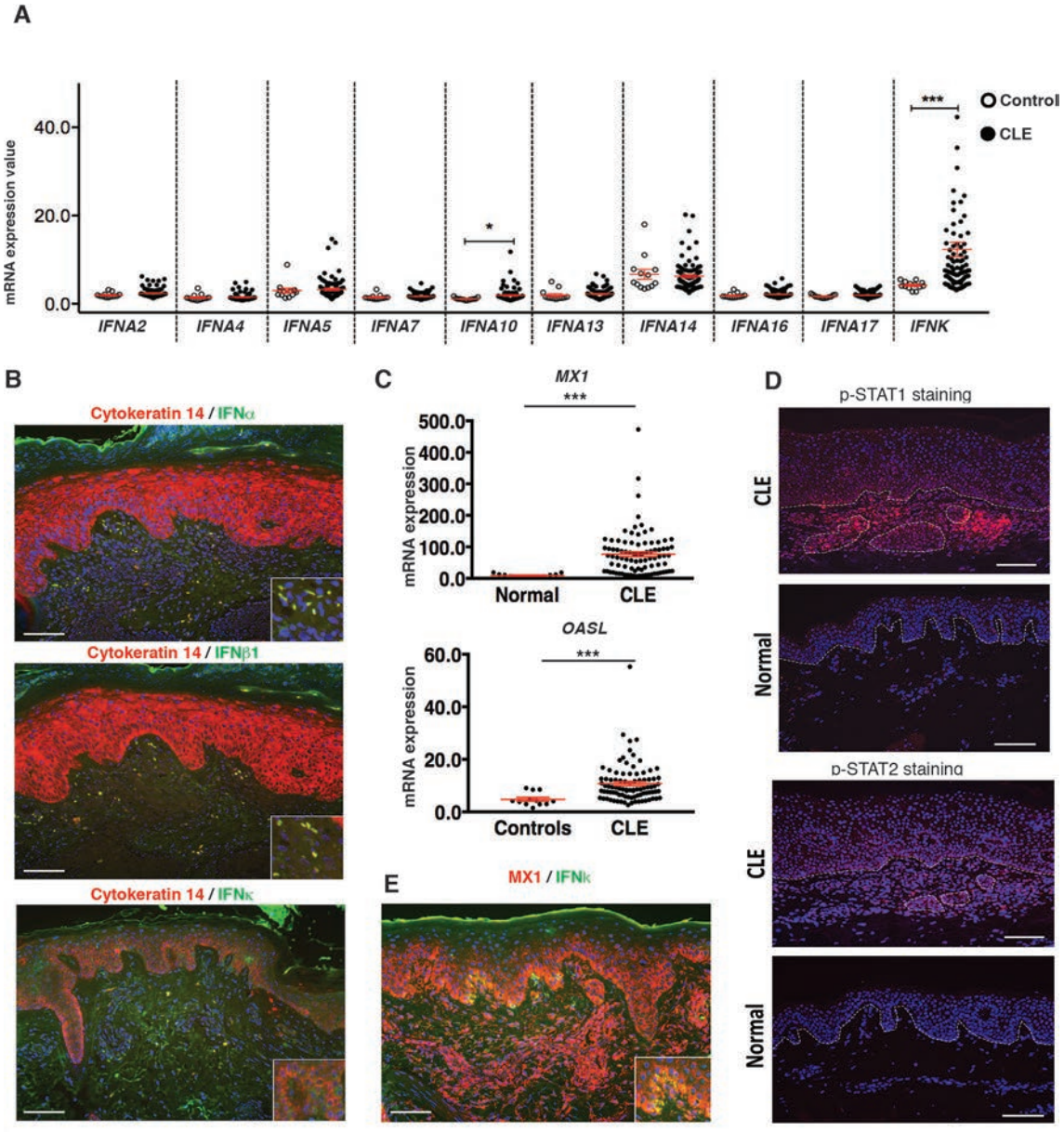

Figure 1 IFN-κ is upregulated in cutaneous lupus erythematosus (CLE) lesions and lupus keratinocytes. (A) mRNA expression of type I interferon genes in cutaneous lupus (n=90 CLE, n=13 control). Of the 10 type I family members that had detectable mRNA expression on Affymetrix ST 2.1 array, only *IFNK* (FDR q<0.001) and *IFNA10* (FDR q<0.05) had significantly increased expression in CLE compared with healthy skin (*IFNB* was not detectable). (B) Immunofluorescence of CLE lesions revealed IFN-α and IFN-β1 staining in the dermis near the inflammatory infiltrate, whereas IFN-κ expression was seen in the epidermis and dermis of CLE lesions (epidermis is indicated by cytokeratin 14 staining). Representative staining of three CLE and three controls are shown. (C) Type I IFN response genes, including *MX1* and *OASL*, are increased in CLE lesional biopsies (FDR q<0.001) (n=90 CLE, n=13 control). (D) In skin lesions of CLE compared with healthy skin, there is increased phosphorylation of both STAT1 (pSTAT1; red) and STAT2 (pSTAT2; red). Representative staining of three CLE and three controls are shown. (E) The IFN response protein MX1 was prominently expressed in CLE skin and exhibited colocalisation with IFN-κ in the epidermis (as evidenced by yellow colour). FDR, false discovery rate; IFN, interferon.

IFN, were detected by microarray (online supplementary figure S1C). To validate the microarray data, we examined expression of IFN-α, IFN-β and IFN-κ in CLE lesions by immunofluorescence. While IFN-α and IFN-β1 were exclusively found to be localised to the dermal inflammatory infiltrate, IFN-κ expression was localised primarily to the epidermis and costained with epidermal cytokeratin 14 (figure 1B and online supplementary figures S2 and S3). Some IFN-κ staining was also noted in the dermis, which may reflect IFN-κ binding to dermal mucin or possible secretion by infiltrative pDCs (online supplementary figure S4) or myeloid dendritic cells (mDCs), which has been reported.[10 30] To confirm increased IFN signalling in CLE, we confirmed expression of *MX1* and *OASL*, two type I IFN regulated genes, to be increased in CLE skin (8.6-fold and 2.4-fold change, respectively, FDR p<0.001) (figure 1C and online supplementary figure S1B), and this was paralleled by increased STAT1 and STAT2 expression (online supplementary figure S1D) and pSTAT1 and pSTAT2 activation in lesional skin (figure 1D). IFN-κ demonstrated colocalisation with MX1 in the epidermis, whereas no costaining between IFN-κ and MX1 was seen in the inflammatory infiltrate (figure 1E and online supplementary figure S3), suggesting epidermal IFN-κ along

with dermal IFN-α and IFN-β likely contribute to the overall type I IFN signalling in CLE.

Keratinocyte-produced IFN-κ is the source of basal type I IFN activity in healthy skin

Little is known about the production of type I IFNs in the skin. To understand this, we started by examining healthy cultured keratinocyte (KC) global gene expression using RNA-seq (n=3), fibroblasts (n=3) and endothelial cells (n=4) from healthy controls. Gene ontology analysis of transcripts differentially expressed uniquely to each cell population demonstrated that 'type I interferon responses' were enriched in KCs (FDR=6.8E-04) but not in fibroblasts or endothelial cells. Consistent with this observation, type I IFN response genes including *MX1*, *OASL and OAS1-3*, and *IRF5-7* were predominantly expressed in keratinocytes (figure 2A). To address the source of the type I IFN response in KCs, we analysed the expression of all type I IFN family members in those three cell types. Of the 17 known type I IFN family members, *IFNK* had higher expression in KCs and was the most elevated IFN when keratinocytes, fibroblasts and endothelial cells were compared (figure 2B). These observations were confirmed by immunofluorescence of healthy control skin, which demonstrated low-level expression of IFN-κ in the epidermis, co-localising with the epidermal marker; cytokeratin 14, but no expression of IFN-α or IFN-β1, was detected in the epidermis (figure 2C and online line supplementary

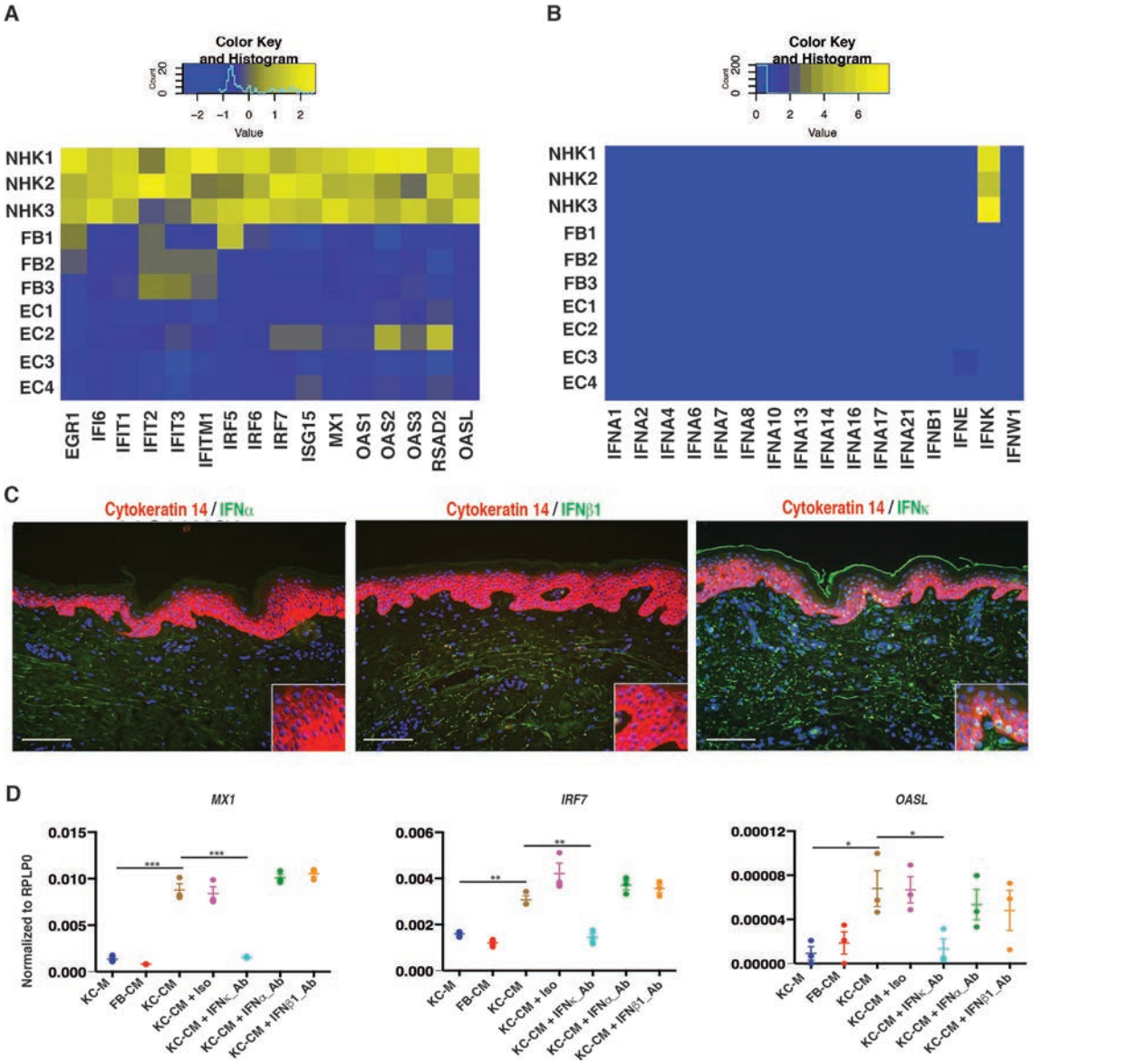

Figure 2 Keratinocytes exhibit baseline type I interferon activity and express IFN-κ. (A) Unstimulated normal human keratinocytes (NHK1-3) exhibit heightened expression of type I IFN target genes compared with dermal fibroblasts (FB1-3) and dermal endothelial cells (EC1-4) as measured by RNA-seq (FDR=6.8E-04). (B) RNA-seq reveals *IFNK* as the only type I IFN detectable in the three skin-derived cell types, and its expression was limited to keratinocytes. (C) Immunofluorescent colocalisation with the epidermal marker cytokeratin 14 showed colocalisation with IFN-κ in healthy epidermis, but no expression of IFN-α or IFN-β1. Representative of three slides is shown. (D) The type I IFN response could be transferred to fibroblasts following exposure to keratinocyte conditioned medium for 24 hours (KC-CM) but not non-conditioned keratinocyte medium (KC-M) or conditioned fibroblast medium (FB-CM), as determined by expression of *MX1*, *IRF7* and *OASL*. This response could be effectively inhibited by addition of neutralising anti-IFN-κ antibody (10 µg/mL) but not with isotype (KC-CM+Iso), anti-IFN-α (KC-CM-IFN-α_Ab) or anti-IFN-β1(KC-CM-IFNβ1_Ab) antibodies (10 µg/mL) (n=3 for all). Data shown with SEM, *p<0.05, **p<0.01, ***p<0.001 (unpaired two-sided Student's t-test). n=3 for each experiment. IFN, interferon.

figures S2 and S3). Similarly, the IFN response protein MX1 was expressed throughout the epidermis and showed patchy colocalisation with IFN-κ, particularly in the basal epidermal layers (online supplementary figure S5). To confirm whether production of IFN-κ from keratinocytes was functional, we collected the conditioned media of cultured human keratinocytes and transferred that to primary human fibroblast cultures. After 6 hours in the conditioned KC medium, fibroblasts had increased mRNA expression of type I IFN response genes including *MX1* ($p<0.001$), *IRF7* ($p<0.01$) and *OASL* ($p<0.05$) ($n=3$ for all), but no increase was seen in fibroblasts treated with non-conditioned keratinocyte medium or conditioned fibroblast medium (figure 2D). This increase in IFN response genes was driven by IFN-κ as *MX1*, *IRF7* and *OASL* expression could be blocked by addition of a neutralising antibody against IFN-κ (10 µg/mL) but not with isotype, anti-IFN-α or IFN-β1 antibodies (10 µg/mL).

To further study the role of IFN-κ in keratinocyte biology, we knocked out *IFNK* using NHEJ repair via CRISPR/Cas9 in a human keratinocyte line. Guide RNA was designed for the *IFNK* gene and homozygous mutation was confirmed by Sanger sequencing (figure 3A). Absence of the IFN-κ protein was confirmed by western blotting of KC lysates (online supplementary figure S6A) and ELISA from conditioned KC medium (figure 3B). KO of *IFNK* in unstimulated KCs reduced basal mRNA expression of type I IFN response genes compared with WT, including *MX1* ($p<0.001$), *IRF7* ($p<0.01$), *IRF9* ($p<0.01$) and *OASL* ($p<0.001$) ($n=3$ for all) (figure 3C and online supplementary figure S6A). Collectively, these data indicate that human keratinocytes express and secrete functionally active IFN-κ that is required to maintain basal expression of IFN response genes in keratinocytes.

Type I IFN activity in keratinocytes is dependent on Tyk2

Type I IFNs signal through the type I IFN receptor (IFNAR1 and IFNAR2) followed by activation of the non-receptor tyrosine kinase 2 (TYK2). To determine if IFN-κ used TYK2 to maintain basal type I IFN activity in keratinocytes, we used CRISPR/Cas9 to knock out the *TYK2* gene in N/TERT KCs (online supplementary figure S6B). Insertion of a frameshift mutation was confirmed by Sanger sequencing (online supplementary figure S6B). KO of *TYK2* in unstimulated KCs led to decreased basal expression of type I IFN response genes including *MX1* ($p<0.001$), *IRF7* ($p<0.001$), *IRF9* ($p<0.001$), *OASL* ($p<0.01$) ($n=3$ for all) (figure 3D). In addition, KO of *TYK2* led to an inability of KCs to respond to exogenous IFN-α (50 ng/mL) or IFN-κ (figure 3D). Notably, IFN-κ was induced by IFN-α or IFN-κ exposure, and this induction was abolished in *TYK2* KO ($p<0.001$ for both, $n=3$) (figure 3D).

IFN-κ is required for rapid triggering of IFN responses in keratinocytes

The ability of cells to generate a rapid IFN response can depend on proper priming of the IFN pathway. For example, in peripheral blood mononuclear cells (PBMCs), basal IFN-β production is required to confer 'IFN readiness' for responses to commensal organisms.[31] Similarly, we hypothesised that IFN-κ may provide a similar 'IFN readiness' in keratinocytes. Consistent with this hypothesis, baseline pSTAT1 and pSTAT2 levels were markedly suppressed in *IFNK* KO KCs compared with wild type (WT) ($p<0.001$, $n=3$ for each) (figure 4A,B). Similar findings were noted in unstimulated *TYK2* cells, which serve as an IFN-signalling KO control. With stimulation by exogenous IFN-α (50 ng/mL), pSTAT1 and pSTAT2 levels in *IFNK* KO displayed a small lag in activation but approached WT levels after 20 min of stimulation. In contrast, pSTAT1 and pSTAT2 in *TYK2* KO remained suppressed at all time points (10, 20 and 30 min) (figure 4A,B), consistent with its role in transmitting all type I IFN signals. Notably, *IFNK* KO KCs had both a decreased and a delayed response to added IFN-α (as measured by mRNA expression of *MX1* and *OASL*), which was most notable at lower doses of IFN-α stimulation (1 ng/mL and 5 ng/mL) and approximated WT levels of expression at higher concentrations (50 ng/mL) ($n=3$ for all) (figure 4C).

Non-lesional lupus keratinocytes express increased IFN-κ, which contributes to dendritic cell activation, rapid IFN-regulated gene transcription and photosensitivity

Patients with lupus have abnormal responses to UV light, which lead to CLE development. In order to determine whether 'normal' appearing keratinocytes from patients with lupus also demonstrated dysregulated IFN-κ expression, we cultured keratinocytes from non-lesional, non-sun-exposed skin biopsies from patients with SLE and a history of CLE lesions or healthy controls. These unstimulated keratinocytes had increased baseline protein expression of IFN-κ and demonstrated constitutively higher baseline pSTAT1 and pSTAT2 activity ($n=3$, two examples shown) (figure 5A). In contrast, keratinocytes from uninvolved and lesional psoriatic skin did not show increased IFN-κ mRNA expression ($n=4$) (online supplementary figure S7). As further validation of the increased basal IFN-κ production in SLE KCs, we were able to induce a greater IFN response in fibroblasts by transfer of conditioned media from SLE KCs than of conditioned media from healthy control KCs (figure 5B). To study the impact of increased IFN-κ in KCs, we generated N/TERT keratinocytes overexpressing IFN-κ at about twice the amount of endogenous IFN-κ (figure 5C). Similar to lupus-derived KCs, these cells had higher baseline expression of type I IFN response genes (figure 5D). IFN-κ overexpressing KCs had accelerated and increased early responses to IFN-α compared with non-overexpressing N/TERTs (as shown by *MX1* mRNA expression at 1 hour; figure 5E). Importantly, the early upregulation of *MX1* was abrogated by addition of neutralising IFN-κ antibody (figure 5E). After 4 hours of IFN-α stimulation, N/TERT control KCs had a robust type I IFN response that was also dependent on IFN-κ as neutralising antibodies also diminished *MX1* expression (figure 5E). These data support a role for IFN-κ in CLE pathogenesis in which chronic elevation of IFN-κ amplifies basal IFN responses and promotes rapid response to other type I IFNs.

UVB induction of keratinocyte apoptosis is thought to be an essential trigger for CLE lesions.[32] Indeed, consistent with reported literature,[33] we detected increased apoptosis in CLE lesions via TUNEL staining (figure 6A). We next examined if increased UVB-mediated apoptosis was a feature of SLE keratinocytes. As shown in figure 6B, non-lesional SLE keratinocytes exhibited increased UVB-mediated apoptosis compared with control keratinocytes ($p=0.0013$). We thus examined the impact of IFN-κ overexpression on UVB-mediated apoptosis in keratinocytes. As shown in figure 6C, overexpression of IFN-κ resulted in enhanced basal and UVB-mediated increases in TUNEL staining, whereas UVB-induced apoptosis was nearly completely abrogated in IFN-κ KO keratinocytes (figure 6D). Similarly, UVB-induced apoptosis could be inhibited by the Jak inhibitor, baricitinib, in both normal and SLE keratinocytes ($p<0.05$ and $p<0.01$, respectively) (figure 6E).

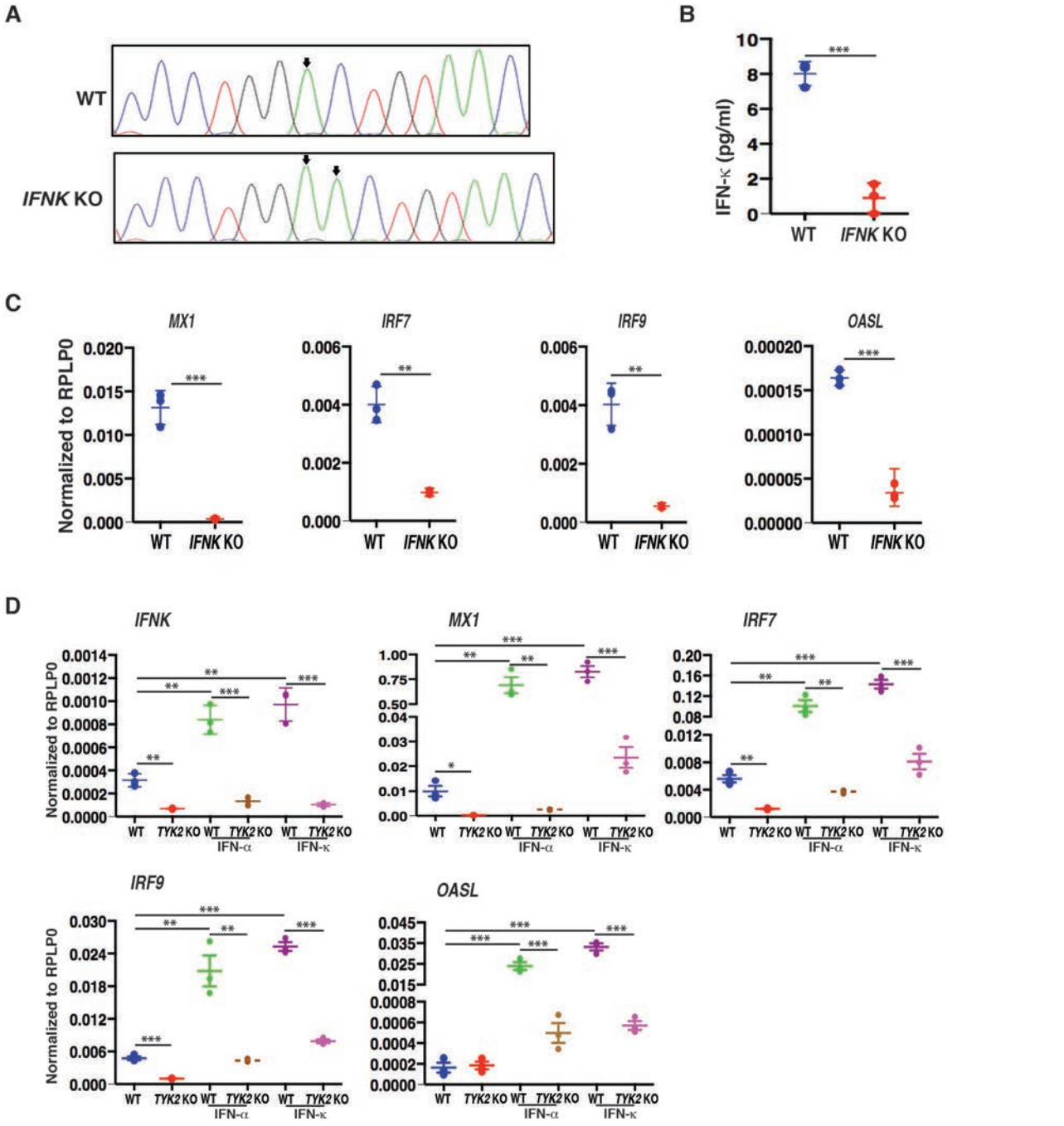

Figure 3 *IFNK* knock-out abolishes type I interferon activity in keratinocytes. (A) A guide RNA targeting a 20nt sequence in exon 1 of the *IFNK* gene was designed, and knock-out was performed via non-homologous end-joining repair (NHEJ) resulting in the insertion of a single nucleotide (A) in the *IFNK* gene. (B) Absence of the secreted IFN-κ protein was confirmed by ELISA. (C) *IFNK* KO suppressed baseline type I IFN activity in unstimulated keratinocytes as determined by expression of *MX1*, *IRF7*, *IRF9* and *OASL*. Data shown with SEM, **p<0.01, ***p<0.001, n=3 for all). (D) Baseline type I IFN activity was measured in unstimulated WT and *TYK2* KO keratinocytes as determined by expression of IFNK, *MX1*, *IRF7*, *IRF9* and *OASL via real-time PCR*. Similar expression changes were measured after treatment with either IFN-α (5 ng/mL) or IFN-κ (5 ng/mL). Data shown with SEM, **p<0.01, ***p<0.001, n=3 for all (unpaired two-sided Student's t-test). IFN, interferon; *IFNK* KO, *IFNK* knock-out keratinocytes; *TYK2* KO, *TYK2* knock-out keratinocytes; WT, N/TERTs (immortalised human keratinocytes).

One mechanism for enhanced immune activation in SLE is type I IFN activation of dendritic cells.[34] Previously, we had identified increased IFN-κ secretion from SLE versus control keratinocytes following UVB stimulation.[13] To determine whether conditioned medium from UV irradiated keratinocytes was sufficient to induce CD80 expression on dendritic cells and elicit a type I IFN response (via *MX1* mRNA expression), SLE and healthy control keratinocytes were treated with UVB, and the supernatants were collected and added to primary dendritic cell cultures. Consistent with heightened type I IFN responses in SLE keratinocytes, all three SLE cultures resulted in induction of MX1 and CD80 after UVB exposure (figure 6F). Notably, the responses from UVB conditioned keratinocyte media were completely inhibited by IFN blockade by baricitinib (p<0.001) (figure 6F). Consistent with these findings, we observed increased expression of CD80 on CD11c+dendritic cells in CLE

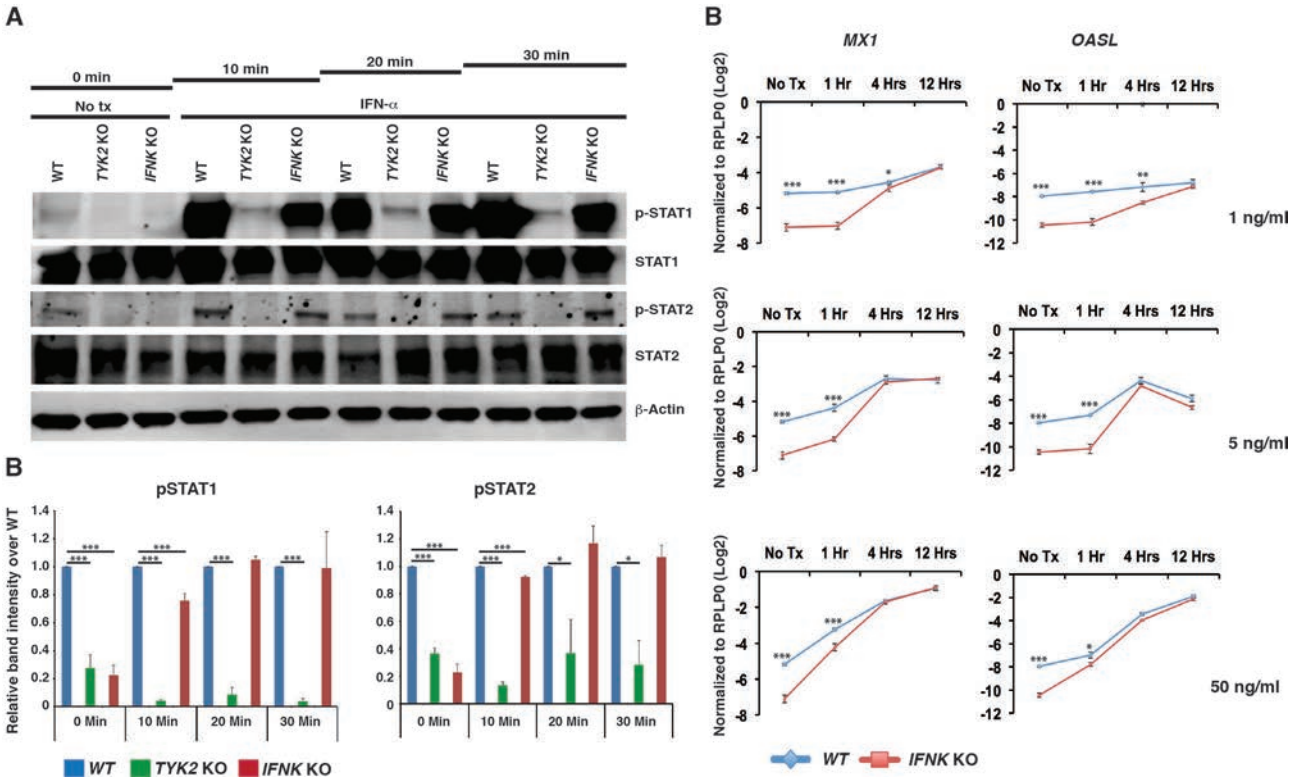

Figure 4 IFN-κ is required for rapid keratinocyte responses to exogenous IFN-α. (A and B) WT, *IFNK* KO or *TYK2* KO KCs were treated with or without IFN-α for the indicated time points followed by western blot for phosphorylated and total STAT1 and STAT2. Quantification of phosphorylation as compared with WT is shown in figure part (B. (C) WT or *IFNK* KO KCs were treated with the indicated concentrations of IFN-α followed by qRT-PCR for the indicated genes. Data shown with SEM, *p<0.05, **p<0.01, ***p<0.001, n=3 for all (unpaired two-sided Student's t-test). IFN, interferon; *IFNK* KO, *IFNK* knock-out keratinocytes; KCs, keratinocytes; *TYK2* KO, *TYK2* knock-out keratinocytes; WT, N/TERTs (immortalised human keratinocytes);

skin lesions (figure 6G). These data support the upregulation of IFN-κ in lupus keratinocytes as a key regulator of heightened inflammatory and apoptotic responses in SLE skin, which leads to a priming of SLE skin for enhanced keratinocyte apoptosis and immune activation following UVB stimulation (figure 6H).

DISCUSSION

In this study, we have identified IFN-κ as the most prominent type I IFN produced by keratinocytes and characterised its role in regulation of basal type I IFN responses in skin. Furthermore, we have shown that this cytokine can amplify exogenous IFN signals and drive enhanced type I IFN responses and photosensitivity in SLE keratinocytes. Importantly, we have identified IFN-κ as one of two type I IFNs significantly increased in lesional CLE and have implicated it in the activation of dendritic cells, an important pathogenic cell population in CLE skin.

Regulation of the type I IFN response in the skin is important for antiviral defences, and consistent with this, IFN-κ has recently been found to be important for protection against human papillomavirus infections.[35] Using high-resolution RNA-seq data, we found baseline type I IFN activity in keratinocytes but minimal activity in dermal fibroblasts or endothelial cells. Others have also identified basal IFN-κ activity in healthy control cultured KCs through multiple methods of detection; however, using chromogenic immunohistochemistry, they were unable to detect IFN-κ in vivo. Our staining, using a different antibody and immunofluorescent technique with high resolution microscopy, was able to show the presence of IFN-κ in basal KC in vivo. While IFN-κ was not one of the most dysregulated genes in healthy control KCs, the unstimulated IFN signature in epithelial cells was prominent. This is consistent with new data that suggest very low levels (attomolar) of type I IFNs are sufficient for generating IFN responses.[36] Importantly, the IFN activity was transferable to fibroblasts and endothelial cells in an IFN-κ-dependent manner. This suggests that IFN-κ has pleotropic functions in healthy skin: protecting keratinocytes against intracellular pathogens and 'sounding the alarm' to other immune and non-immune cell populations in the skin.

The effects of IFN-κ on upregulation of IFN response genes were dependent on the expression of Tyk2 and neutralised by anti-IFN-κ antibody, suggesting that IFN-κ is secreted by keratinocytes and uses classical IFN signalling pathways to activate cellular responses. Both *TYK2* and *IFNK* gene loci have been implicated as susceptibility factors for SLE and cutaneous manifestations of lupus.[11 37] Our data suggest that one mechanism by which *TYK2* might contribute to CLE susceptibility is through regulation of autocrine IFN-κ activity. Further studies will test this hypothesis.

Our data support a role for IFN-κ as a rheostat for IFN responses in keratinocytes. For example, we found that phosphorylation of STAT1 and STAT2 was delayed by the absence of IFN-κ and that transcriptional responses to small amounts of IFN-α were delayed in the absence of IFN-κ. This could be overcome by higher doses of IFN-α. These data suggest that baseline IFN-κ expression primes keratinocytes for responses to low grade signalling through the type I IFN receptor. This is similar to data that support a parallel role for IFN-β, which primes for IFN responses in myeloid cells in response to gut

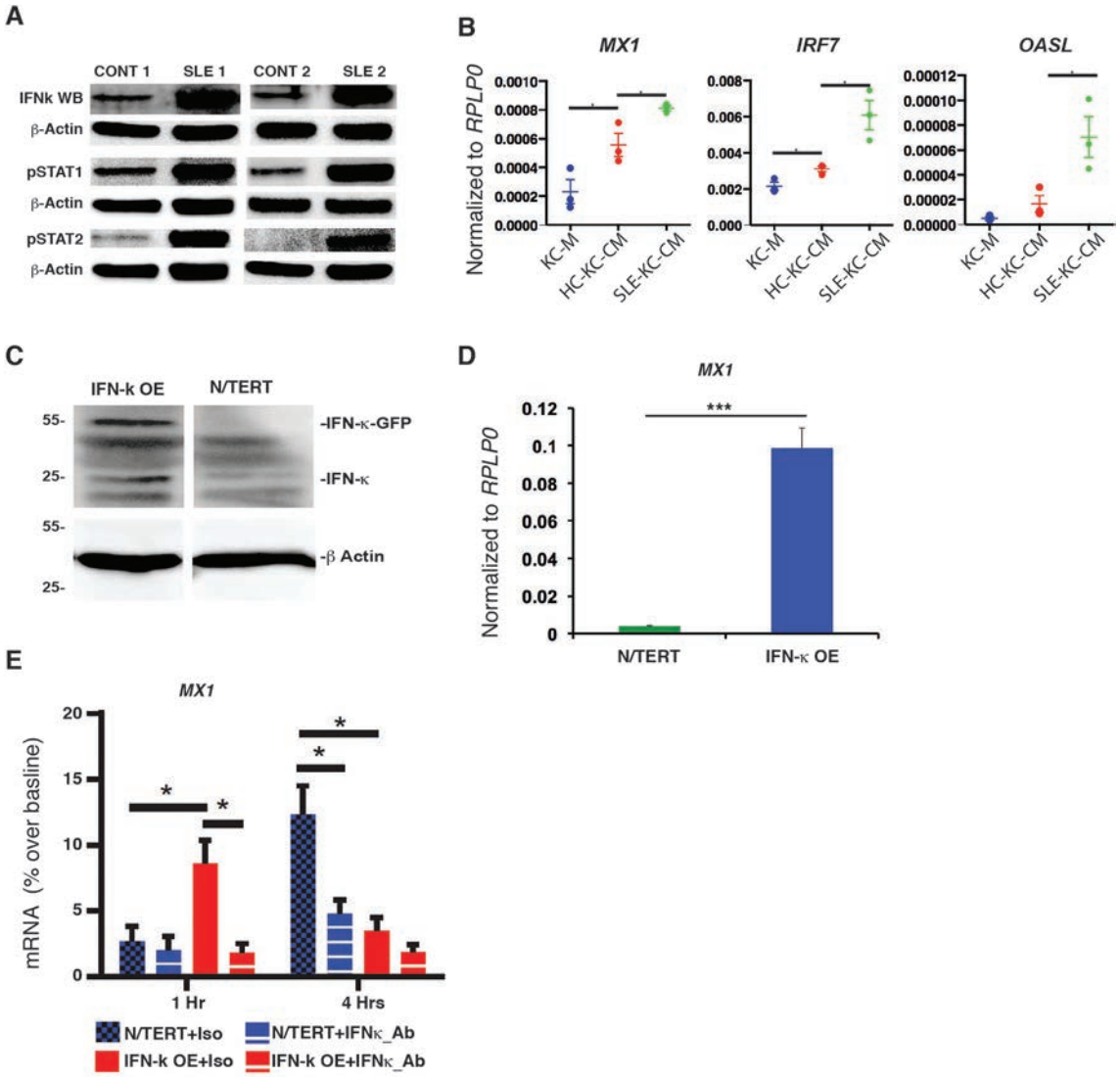

Figure 5 CLE keratinocytes have heightened basal IFN-κ expression and type I IFN activity. (A) Cultured keratinocytes from uninvolved skin of patients with SLE and a history of cutaneous lupus exhibited increased protein expression of IFN-κ along with increased pSTAT1 and pSTAT2 activity (representative data from two (out of three) control and two (out of three) patients with SLE shown). (B) Fibroblasts were treated with KC media (KC-M) alone, conditioned media from healthy control KCs (HC-KC-CM) or conditioned media from SLE-KCs (SLE-KC-CM) (n=3 each in triplicate) for 24 hours followed by qRT-PCR for IFN-regulated genes *MX1*, *IRF7* and *OASL*. (C) KCs stably overexpressing IFN-κ were generated; representative western Blot of IFN-κ overexpressing line (IFN-κ OE) (both native and GFP tagged) is shown. (D) MX1 mRNA expression in IFN-κ OE compared with N/TERTs. (E) IFN-κ OE or N/TERTs were grown in the presence or absence of a neutralising antibody to IFN-κ for 3 days followed by stimulation with 5 ng/mL IFN-α for the indicated time points. *MX1* expression was assessed via real-time PCR, normalised to *RPLP0* expression and expressed as per cent change over unstimulated cells. Data shown with SEM, *p<0.05, **p<0.01, ***p<0.001, n=3 for all (unpaired two-sided Student's t-test). CLE, cutaneous lupus erythematosus; IFN, interferon; IFN-κ_Ab, IFN-κ antibody; Iso, isotype control for IFN-κ antibody; SLE, systemic lupus erythematosus.

flora.[31] In contrast, overexpression of IFN-κ has pathological consequences. Indeed, we found that 'normal' keratinocytes from patients with SLE produce more IFN-κ at baseline and that overexpression of IFN-κ can amplify responses to other type I IFNs in an IFN-κ dependent manner.

The heightened expression of type I IFN response genes in CLE has been known for some time.[7] However, which type I IFNs contribute to cutaneous IFN signatures has not been examined until now. Intriguingly, we find that IFN-κ is one of only two type I IFNs upregulated in CLE lesions. Our data support keratinocytes as a source of this cytokine but does not exclude production by myeloid populations, which have also been cited to produce IFN-κ.[30 38] IFN-α10 is also detected in CLE lesions, and we would surmise that this cytokine stems from recruited pDC populations in CLE skin. Importantly, given our data on the role of IFN-κ in fine-tuning the IFN response, we propose that an important step in CLE pathogenesis is the amplification of IFN signalling as lupus keratinocytes make more IFN-κ at baseline and have skewed IFN responses as a result. Paracrine IFN-α thus can further amplify this loop, priming for inflammatory responses as we have recently shown[13] and upregulating IFN-κ (figure 3D) (summarised in figure 6H). Paracrine IFN-κ produced by pDCs (online supplementary figure 4) may also contribute to this loop. Indeed, our data may also explain the recent clinical trial results in which blockade of IFN-α, which does not block IFN-κ, results in only mild improvements in CLE lesions,[39] whereas blockade of the type I IFN receptor, which blocks IFN-κ signalling as well as IFN-α, appears to result in more robust clinical improvement.[40]

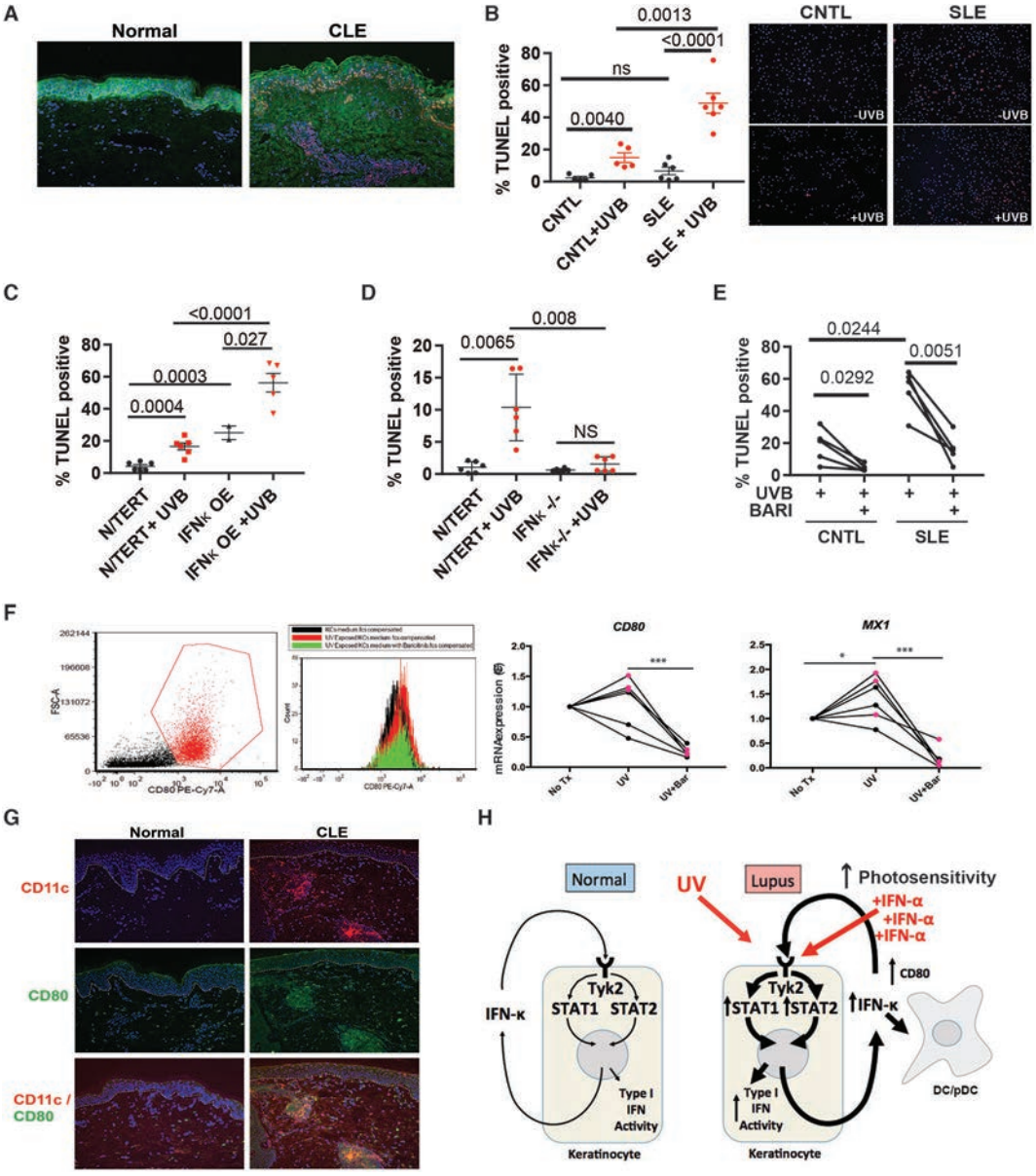

Figure 6 IFN-κ promotes UVB induced apoptosis in CLE. (A) TUNEL staining of normal and CLE skin shows prominent apoptosis in CLE epidermis. Figure is representative of three samples. (B) Healthy control and non-lesional SLE KCs (n=6 each) were treated with or without 50 mJ/cm^2 UVB followed by TUNEL staining after 8 hours of culture. Representative photos are shown on the right. (C) IFNκ-OE KCs or N/TERTs were treated with UVB followed by TUNEL staining as in figure part B (n=5 each). (D) *IFNK* KO or N/TERT KCs were treated with UVB followed by TUNEL staining as in figure part B (n=6 each). (E) Control or SLE KCs (n=5 each) were treated with or without baricitinib (BARI) followed by treatment with 50 mJ/cm^2 UVB followed by TUNEL staining after 8 hours of culture. (F) Condition medium from control or SLE UVB-irradiated KCs was added to monocyte-derived dendritic cell cultures in the presence or absence of baricitinib followed by measurement of CD80 surface expression by flow cytometry and *CD80* and *MX1* mRNA expression via RT-PCR. Red dots: SLE keratinocyte conditioned media (three different patients); black dots: control conditioned media (three different healthy controls). All statistical comparisons made via unpaired two-sided Student's t-test. (G) Immunofluorescent staining denotes increased expression of CD80 on CD11c+dendritic cells in CLE skin lesions. (H) Schematic outline of the role of IFN-κ in SLE. In control KCs, a basal level of IFN-κ maintains tonic low-level IFN signalling and primes for IFN responses. In SLE KCs, increased autocrine IFN-κ expression drives an elevated tonic IFN response and primes for rapid, robust IFN responses and apoptosis to UVB. Secreted IFN-κ can activate DCs to stimulate immune responses in the skin. CLE, cutaneous lupus erythematosus; DCs, dendritic cells; IFN, interferon; KCs, keratinocytes; SLE, systemic lupus erythematosus; UVB, ultraviolet B.

Photosensitivity is a hallmark of patients with SLE and is strong contributor to poor quality of life.[1] Photosensitive lesions are characterised by increased epidermal apoptosis and increased inflammatory infiltrates, including dendritic and pDCs, in the dermis.[41] Until now, we have not understood *why* SLE skin is predisposed to this reaction. Here, we have identified that chronic exposure to IFN-κ is sufficient to increase apoptosis of keratinocytes after UVB exposure and that SLE keratinocytes, which overexpress IFN-κ, display increased sensitivity to UVB in an IFN-signalling-dependent manner. In addition, keratinocyte-produced IFN-κ is able to activate DCs, which further amplifies inflammatory responses after UVB exposure. This identifies regulation of IFN-κ as a key to controlling photosensitivity. Further research will

explore the mechanisms by which IFN-κ predisposes to photosensitivity.

Other groups have identified IFNλ, a type III IFN with importance for antiviral responses as dysregulated in CLE keratinocytes. IFNλ1 levels are increased via immunohistochemistry in the epidermis of DLE and SCLE lesions and were identified as increased in the serum of patients.[42] Serum IFNλ3 levels (IFNλ1 and IFNλ2 levels were undetectable in this study) may be higher in patients with anti-Ro antibodies, which is a common feature of patients with SCLE.[43] Our microarray data did not support increased IFNλ2 or IFNλ3 in CLE biopsies. Unfortunately, IFNλ1 did not meet cut-off thresholds for detection. However, our in vitro data that evaluated the effects of IFNAR or IFNκ neutralisation on baseline IFN gene expression in keratinocytes does not support a role for IFNλ in maintaining basal IFN signatures in keratinocytes. It is possible that elevated IFNλ production may contribute stimulated IFN responses, and this can be addressed in future studies.

In summary, we have identified IFN-κ as a critical regulator of basal type I IFN responses in keratinocytes and as a dysregulated cytokine in non-lesional SLE skin, which contributes to amplification of IFN responses, activation of dendritic cells and photosensitive apoptosis. Further research into the role of IFN-κ in SLE and the targeting of IFN-κ in CLE lesions should be considered.

Author affiliations
[1]Department of Dermatology, University of Michigan, Ann Arbor, Michigan, USA
[2]Division of Rheumatology, Department of Internal Medicine, University of Michigan, Ann Arbor, Michigan, USA
[3]Department of Computational Medicine & Bioinformatics, University of Michigan, Ann Arbor, Michigan, USA
[4]Department of Biostatistics, University of Michigan, Ann Arbor, Michigan, USA
[5]Division of Nephrology, Department of Internal Medicine, University of Michigan, Ann Arbor, Michigan, USA
[6]Department of Human Genetics, University of Michigan, Ann Arbor, Michigan, USA
[7]Department of Pathology, University of Michigan, Ann Arbor, Michigan, USA
[8]Department of Dermatology, Northwestern University, Chicago, Illinois, USA

Acknowledgements The authors would like to thank all of the Michigan Lupus patients who graciously gave of their time and samples to further lupus research.

Contributors MKS, GAH, JEG, JMK and JJV designed the study and wrote the manuscript; MKS, GAH, XX, JL, YL, WRS, MP, SS, EPST, RU, MAB, AS, SLB, PWH, SG and JTE collected and analysed data; and CCB and LCT analysed data. All authors reviewed and commented on the manuscript.

Funding The work was in part supported by the University of Michigan Babcock Endowment Fund (MKS, LCT, JTE, JJV and JEG), the National Institute of Arthritis and Musculoskeletal and Skin Diseases of the National Institutes of Health under Award Numbers R03AR066337 (JMK), K08AR063668 (JMK), K08-AR060802 (JEG), T32AR007080 (supporting EPST), R01-AR071384 (JMK) and R01-AR069071 (JEG), the A. Alfred Taubman Medical Research Institute Parfet Emerging Scholar Award (JMK) and Kenneth and Frances Eisenberg Emerging Scholar Award (JEG), Doris Duke Charitable Foundation Grant #2013106 (JEG) and the Rheumatology Research Foundation Career Development K Supplement Award (JMK). EPST received support from the Scleroderma Foundation. LCT is supported by the Dermatology Foundation, Arthritis National Research Foundation and National Psoriasis Foundation.

Competing interests None declared.

Patient consent Obtained.

Ethics approval Skin.

Provenance and peer review Not commissioned; externally peer reviewed.

REFERENCES

1 Klein R, Moghadam-Kia S, Taylor L, *et al*. Quality of life in cutaneous lupus erythematosus. *J Am Acad Dermatol* 2011;64:849–58.
2 Sanders CJ, Van Weelden H, Kazzaz GA, *et al*. Photosensitivity in patients with lupus erythematosus: a clinical and photobiological study of 100 patients using a prolonged phototest protocol. *Br J Dermatol* 2003;149:131–7.
3 Braunstein I, Klein R, Okawa J, *et al*. The interferon-regulated gene signature is elevated in subacute cutaneous lupus erythematosus and discoid lupus erythematosus and correlates with the cutaneous lupus area and severity index score. *Br J Dermatol* 2012;166:971–5.
4 Meller S, Winterberg F, Gilliet M, *et al*. Ultraviolet radiation-induced injury, chemokines, and leukocyte recruitment: An amplification cycle triggering cutaneous lupus erythematosus. *Arthritis Rheum* 2005;52:1504–16.
5 Wenzel J, Tüting T. Identification of type I interferon-associated inflammation in the pathogenesis of cutaneous lupus erythematosus opens up options for novel therapeutic approaches. *Exp Dermatol* 2007;16:454–63.
6 Wenzel J, Wörenkämper E, Freutel S, *et al*. Enhanced type I interferon signalling promotes Th1-biased inflammation in cutaneous lupus erythematosus. *J Pathol* 2005;205:435–42.
7 Farkas L, Beiske K, Lund-Johansen F, *et al*. Plasmacytoid dendritic cells (natural interferon- alpha/beta-producing cells) accumulate in cutaneous lupus erythematosus lesions. *Am J Pathol* 2001;159:237–43.
8 Jego G, Palucka AK, Blanck JP, *et al*. Plasmacytoid dendritic cells induce plasma cell differentiation through type I interferon and interleukin 6. *Immunity* 2003;19:225–34.
9 Lövgren T, Eloranta ML, Båve U, *et al*. Induction of interferon-alpha production in plasmacytoid dendritic cells by immune complexes containing nucleic acid released by necrotic or late apoptotic cells and lupus IgG. *Arthritis Rheum* 2004;50:1861–72.
10 LaFleur DW, Nardelli B, Tsareva T, *et al*. Interferon-kappa, a novel type I interferon expressed in human keratinocytes. *J Biol Chem* 2001;276:39765–71.
11 Harley IT, Niewold TB, Stormont RM, *et al*. The role of genetic variation near interferon-kappa in systemic lupus erythematosus. *J Biomed Biotechnol* 2010;2010:1–11.
12 Vassileva G, Chen SC, Zeng M, *et al*. Expression of a novel murine type I IFN in the pancreatic islets induces diabetes in mice. *J Immunol* 2003;170:5748–55.
13 Stannard JN, Reed TJ, Myers E, *et al*. Lupus Skin Is Primed for IL-6 Inflammatory Responses through a Keratinocyte-Mediated Autocrine Type I Interferon Loop. *J Invest Dermatol* 2017;137:115–22.
14 Mori M, Pimpinelli N, Romagnoli P, *et al*. Dendritic cells in cutaneous lupus erythematosus: a clue to the pathogenesis of lesions. *Histopathology* 1994;24:311–21.
15 Hochberg MC. Updating the American College of Rheumatology revised criteria for the classification of systemic lupus erythematosus. *Arthritis Rheum* 1997;40:1725–25.
16 Dickson MA, Hahn WC, Ino Y, *et al*. Human keratinocytes that express hTERT and also bypass a p16(INK4a)-enforced mechanism that limits life span become immortal yet retain normal growth and differentiation characteristics. *Mol Cell Biol* 2000;20:1436–47.
17 Swindell WR, Beamer MA, Sarkar MK, *et al*. RNA-Seq Analysis of IL-1B and IL-36 Responses in Epidermal Keratinocytes Identifies a Shared MyD88-Dependent Gene Signature. *Front Immunol* 2018;9:80.
18 Elder JT, Fisher GJ, Zhang QY, *et al*. Retinoic acid receptor gene expression in human skin. *J Invest Dermatol* 1991;96:425–33.
19 Rittié L, Fisher GJ. Isolation and culture of skin fibroblasts. *Methods Mol Med* 2005;117:83–98.
20 Tsou PS, Rabquer BJ, Ohara RA, *et al*. Scleroderma dermal microvascular endothelial cells exhibit defective response to pro-angiogenic chemokines. *Rheumatology* 2016;55:745–54.
21 Ran FA, Hsu PD, Wright J, *et al*. Genome engineering using the CRISPR-Cas9 system. *Nat Protoc* 2013;8:2281–308.
22 Tedder TF, Jansen PJ. Isolation and generation of human dendritic cells. *Curr Protoc Immunol* 2001;Chapter 7:32.
23 Liu J, Berthier CC, Kahlenberg JM. Enhanced Inflammasome Activity in Systemic Lupus Erythematosus Is Mediated via Type I Interferon-Induced Up-Regulation of Interferon Regulatory Factor 1. *Arthritis Rheumatol* 2017;69:1840–9.
24 Irizarry RA, Hobbs B, Collin F, *et al*. Exploration, normalization, and summaries of high density oligonucleotide array probe level data. *Biostatistics* 2003;4:249–64.
25 Trapnell C, Roberts A, Goff L, *et al*. Differential gene and transcript expression analysis of RNA-seq experiments with TopHat and Cufflinks. *Nat Protoc* 2012;7:562–78.
26 Harrow J, Frankish A, Gonzalez JM, *et al*. GENCODE: the reference human genome annotation for The ENCODE Project. *Genome Res* 2012;22:1760–74.
27 Anders S, Pyl PT, Huber W. HTSeq--a Python framework to work with high-throughput sequencing data. *Bioinformatics* 2015;31:166–9.
28 Love MI, Huber W, Anders S. Moderated estimation of fold change and dispersion for RNA-seq data with DESeq2. *Genome Biol* 2014;15:550.
29 Liang Y, Tsoi LC, Xing X, *et al*. A gene network regulated by the transcription factor VGLL3 as a promoter of sex-biased autoimmune diseases. *Nat Immunol* 2017;18:152–60.
30 Nardelli B, Zaritskaya L, Semenuk M, *et al*. Regulatory effect of IFN-kappa, a novel type I IFN, on cytokine production by cells of the innate immune system. *J Immunol* 2002;169:4822–30.
31 Abt MC, Osborne LC, Monticelli LA, *et al*. Commensal bacteria calibrate the activation threshold of innate antiviral immunity. *Immunity* 2012;37:158–70.
32 Gehrke N, Mertens C, Zillinger T, *et al*. Oxidative damage of DNA confers resistance to cytosolic nuclease TREX1 degradation and potentiates STING-dependent immune sensing. *Immunity* 2013;39:482–95.

33 Sáenz-Corral CI, Vega-Memíje ME, Martínez-Luna E, *et al*. Apoptosis in chronic cutaneous lupus erythematosus, discoid lupus, and lupus profundus. *Int J Clin Exp Pathol* 2015;8:7260–5.
34 Sozzani S, Del Prete A, Bosisio D. Dendritic cell recruitment and activation in autoimmunity. *J Autoimmun* 2017;85:126–40.
35 Habiger C, Jäger G, Walter M, *et al*. Interferon Kappa Inhibits Human Papillomavirus 31 Transcription by Inducing Sp100 Proteins. *J Virol* 2016;90:694–704.
36 Rodero MP, Decalf J, Bondet V, *et al*. Detection of interferon alpha protein reveals differential levels and cellular sources in disease. *J Exp Med* 2017;214:1547–55.
37 Cunninghame Graham DS, Morris DL, Bhangale TR, *et al*. Association of NCF2, IKZF1, IRF8, IFIH1, and TYK2 with systemic lupus erythematosus. *PLoS Genet* 2011;7:e1002341.
38 Scarponi C, Nardelli B, Lafleur DW, *et al*. Analysis of IFN-kappa expression in pathologic skin conditions: downregulation in psoriasis and atopic dermatitis. *J Interferon Cytokine Res* 2006;26:133–40.
39 Khamashta M, Merrill JT, Werth VP, *et al*. Sifalimumab, an anti-interferon-α monoclonal antibody, in moderate to severe systemic lupus erythematosus: a randomised, double-blind, placebo-controlled study. *Ann Rheum Dis* 2016;75:1909–16.
40 Furie R, Khamashta M, Merrill JT, *et al*. Anifrolumab, an Anti-Interferon-α Receptor Monoclonal Antibody, in Moderate-to-Severe Systemic Lupus Erythematosus. *Arthritis Rheumatol* 2017;69:376–86.
41 Kim A, Chong BF. Photosensitivity in cutaneous lupus erythematosus. *Photodermatol Photoimmunol Photomed* 2013;29:4–11.
42 Zahn S, Rehkämper C, Kümmerer BM, *et al*. Evidence for a pathophysiological role of keratinocyte-derived type III interferon (IFNλ) in cutaneous lupus erythematosus. *J Invest Dermatol* 2011;131:133–40.
43 Amezcua-Guerra LM, Márquez-Velasco R, Chávez-Rueda AK, *et al*. Type III Interferons in Systemic Lupus Erythematosus: Association Between Interferon λ3, Disease Activity, and Anti-Ro/SSA Antibodies. *J Clin Rheumatol* 2017;23:368-375.

EXTENDED REPORT

Slit2/Robo4 axis may contribute to endothelial cell dysfunction and angiogenesis disturbance in systemic sclerosis

Eloisa Romano,[1] Mirko Manetti,[2] Irene Rosa,[1,2] Bianca Saveria Fioretto,[1] Lidia Ibba-Manneschi,[2] Marco Matucci-Cerinic,[1] Serena Guiducci[1]

Handling editor Josef S Smolen

► Additional material is published online only. To view please visit the journal online (http://dx.doi.org/10.1136/annrheumdis-2018-213239).

[1]Department of Experimental and Clinical Medicine, Division of Rheumatology, University of Florence, Scleroderma Unit, Azienda Ospedaliero-Universitaria Careggi (AOUC), Florence, Italy
[2]Department of Experimental and Clinical Medicine, Section of Anatomy and Histology, University of Florence, Florence, Italy

Correspondence to
Dr Eloisa Romano, Department of Experimental and Clinical Medicine, Division of Rheumatology, University of Florence, Florence, 50139, Italy; eloisaromano@libero.it

ER and MM contributed equally.

Part of this work has been presented at the EULAR 2018 congress and published as a conference abstract: *Ann Rheum Dis* 2018;77(Suppl 2):97–8. doi: 10.1136/annrheumdis-2018-eular.4610.

Received 13 February 2018
Revised 11 June 2018
Accepted 4 July 2018
Published Online First 18 July 2018

To cite: Romano E, Manetti M, Rosa I, *et al*. *Ann Rheum Dis* 2018;**77**:1665–1674.

ABSTRACT

Objective In systemic sclerosis (SSc), early microvascular injury is followed by impaired angiogenesis and peripheral capillary loss. Here, we investigated the possible contribution of the neurovascular guidance molecule Slit2 and its Roundabout (Robo) receptors to SSc-related endothelial cell dysfunction.

Methods Circulating Slit2 levels were measured in patients with SSc and healthy controls. Slit2, Robo1 and Robo4 expression was investigated in SSc and healthy skin biopsies and explanted dermal microvascular endothelial cells (MVECs). Slit2/Robo4 function in MVEC angiogenesis was studied by cell viability, wound healing and capillary-like tube formation assays.

Results Circulating Slit2 was significantly increased in either SSc or patients with a very early diagnosis of SSc (VEDOSS) compared with controls. Interestingly, serum Slit2 levels were raised in patients with VEDOSS with nailfold videocapillaroscopy (NVC) abnormalities, while they were similar in VEDOSS with normal NVC and controls. In SSc, Slit2 and Robo4 expression was upregulated in clinically affected skin and explanted MVECs in respect to controls. The angiogenic performance of healthy MVECs was significantly reduced after challenge with recombinant human Slit2 or SSc sera. These inhibitory effects were significantly attenuated when SSc sera were preincubated with an anti-Slit2 blocking antibody. In vitro angiogenesis was severely compromised in SSc-MVECs and could be significantly ameliorated by Slit2 neutralisation or *ROBO4* gene silencing. Slit2/Robo4 axis interfered with angiogenesis through the inhibition of Src kinase phosphorylation.

Conclusions In SSc, increased circulating levels of Slit2 and activation of the Slit2/Robo4 antiangiogenic axis may contribute to peripheral microangiopathy since the very early phase of the disease.

INTRODUCTION

Systemic sclerosis (SSc) is a chronic multisystem autoimmune disease characterised by vascular injury and tissue fibrosis of the skin and internal organs.[1–3] Despite recent advances in the understanding of SSc pathogenesis, the primary causes of SSc or the molecular mechanisms underlying its clinical onset, progression and outcomes remain unclear.[1–3] Peripheral microvascular abnormalities and dysfunction consistently precede tissue fibrosis,[4–6] suggesting that microvascular endothelial cells (MVECs) are the primary target in this disease, and that the interaction of MVECs with other cells and pathways, such as cells of the immune system, smooth muscle cells and fibroblasts, may drive disease pathogenesis.[5] Raynaud's phenomenon (RP) is the first clinical manifestation of vascular dysfunction,[7] and though its pathophysiology is still not completely understood, it has been suggested that a dysregulation in neuroendothelial control mechanisms may play a key role in RP onset.[3 7]

Compelling evidence indicates that blood vessels and nerves course throughout the body in an orderly pattern and that the mechanisms involved in wiring neural and vascular networks share some deep similarities.[8 9] Axons are guided to their targets by finely tuned codes of attractive and repulsive cues, and recent studies revealed that these cues also help blood vessels to navigate to their targets.[8 9] In fact, many molecules with attractive and repulsive properties, such as members of neuropilin/semaphorin, ephrin/ephrin receptor and Notch/Delta gene families, are able to modulate the guidance of both nerves and blood vessels.[8 9] In this context, another class of neurovascular guidance molecules, Slit/Roundabout (Robo), is increasingly being appreciated.[10–13] Slit/Robo signalling was first identified by studying axonal growth cones. Slits are secreted glycoproteins acting as cognate ligands for transmembrane Robo receptors, which induce repulsive signals during axon guidance. Currently, three members of the Slit family (Slit1, Slit2 and Slit3) and four members of the Robo family (Robo1, Robo2, Robo3 and Robo4) have been described. Robo2 and Robo3 are highly expressed in the nervous system but untraceable in the vascular system, while Robo1 has been shown to be expressed in both systems.[10–13] The latest member of this family, Robo4, also called 'magic roundabout', is a novel endothelial cell protein that was recently identified by using bioinformatic data miming.[14] A number of studies have highlighted important roles for the Slit/Robo signalling during angiogenesis. In particular, some reports have suggested that Slit2 exerts proangiogenic effects by promoting endothelial cell migration and tube formation in a Robo1-dependent manner.[12 15–17] Similarly, Robo1 signalling has been demonstrated to be necessary for vascular endothelial growth factor (VEGF)-induced phosphorylation of VEGF receptor (VEGFR)-2 in endothelial cells, especially in the presence of Slit2.[16 17] On the contrary, the interaction of Slit2 with Robo4

exerts potent antiangiogenic properties by inhibiting VEGF-induced endothelial cell migration, tube formation and vessel permeability in vitro and vascular leak in vivo,[12 18–22] possibly by blocking Src family kinase activation.[18] The in vivo relevance of these findings was confirmed with the generation of *Robo4* knockout mice that express normal levels of Slit2 and Robo1. These mice develop normally, suggesting that Robo4 is dispensable for murine developmental angiogenesis.[18 23] However, in comparison with wild-type littermates, *Robo4* knockout mice exhibit increased basal and VEGF-induced vascular permeability and pathological angiogenesis during experimentally induced ocular neovascularisation.[12 23] These data suggest that Robo4 is required to maintain endothelial cells in a quiescent state by counteracting VEGF and behaving as a negative regulator of angiogenesis in these model systems.

As far as neurovascular trophic factors are concerned, recent studies from our group demonstrated that neuropilin-1 and semaphorin3E are implicated in SSc-related angiogenesis disturbances.[24 25] However, the Slit/Robo axis has never been explored in SSc. Therefore, the aims of the present study were to investigate whether the levels of Slit2, Robo1 and Robo4 could be altered in SSc circulation, skin and explanted endothelial cells and whether Slit/Robo-mediated mechanisms could be functionally implicated in the defective angiogenic process characteristic of this disorder.

METHODS

Methods and any associated references are available in the online supplement.

RESULTS

Circulating levels of the secreted glycoprotein Slit2 are raised in SSc and patients with a very early diagnosis of SSc (VEDOSS)

A total of 78 patients with SSc,[1] 64 patients not fulfilling the 2013 American College of Rheumatology/European League Against Rheumatism classification criteria for SSc (ie, total score <9)[1] and enrolled in the VEDOSS project (ie, patients with RP, puffy fingers and positivity of antinuclear antibodies, together with 'scleroderma type' nailfold capillaroscopic abnormalities or specific SSc antibody positivity)[26] and 74 healthy individuals sorted in a discovery cohort (online supplementary table S1) and a replication cohort (online supplementary table S2) were included in this study.

In the discovery cohort, serum Slit2 levels were significantly higher in both patients with SSc (n=48) and patients with VEDOSS (n=32) in respect to controls (n=40) (p=0.022 and p=0.035, respectively) (figure 1A). No significant differences in circulating Slit2 were detected between patients with SSc and patients with VEDOSS. These results were subsequently validated in the replication cohort, where circulating Slit2 resulted significantly increased in SSc (n=30) and in VEDOSS (n=32) sera compared with control sera (n=34) (p=0.032 and p=0.012, respectively) (figure 1B).

A pooled analysis was performed by combining patients and controls from the discovery and replication cohorts. As displayed in figure 1C, circulating Slit2 levels were significantly higher in both patients with SSc and patients with VEDOSS than in healthy controls (p=0.002 and p=0.001, respectively). We also evaluated the possible correlation of Slit2 levels with the nailfold videocapillaroscopy (NVC) pattern[27] and the presence/absence of digital ulcers in SSc, as measures of peripheral microvascular involvement severity. Either patients with SSc with early/active NVC pattern or those with late NVC pattern had increased Slit2 levels in respect to controls (p=0.009 and p=0.024, respectively) (figure 1D). When compared with controls, circulating Slit2 was also significantly elevated both in patients with SSc with digital ulcers (p=0.016) and in those without digital ulcers (p=0.003) (figure 1E). No significant association was found with other clinicodemographic and laboratory parameters including the SSc cutaneous subset. Interestingly, when we stratified patients with VEDOSS according to NVC changes, we found differences in serum Slit2 levels between patients with VEDOSS with early/active pattern and controls (p<0.0005), while Slit2 concentrations were similar in VEDOSS with normal NVC and controls (figure 1F).

Median and IQR values of circulating Slit2 in the study cohorts are summarised in online supplementary table S3.

Increased expression of Slit2 and its transmembrane receptor Robo4 in SSc endothelial cells ex vivo and in vitro

The protein expression of Slit2 and Robo1 and Robo4 receptors in forearm skin biopsies from patients with SSc and controls was investigated by immunofluorescence (figure 2A–C). The expression of either Slit2 or Robo4 was strongly increased in clinically affected skin from patients with SSc compared with healthy skin, in particular in dermal endothelial cells, perivascular cells and fibroblasts, as well as epidermal keratinocytes (figure 2A, C). No significant differences in skin expression of Slit2 and Robo4 were observed according to disease duration or cutaneous SSc subsets (data not shown). The localisation of Slit2 and Robo4 in vascular endothelial cells was highlighted by double immunofluorescence staining with the pan-endothelial cell marker CD31 (figure 2A, C). Conversely, no difference in Robo1 immunostaining was evident when comparing SSc and control skin sections (figure 2B). Densitometric analysis of immunofluorescent staining intensity confirmed that the protein expression of Slit2 and Robo4, but not of Robo1, was significantly increased in SSc dermal vessels compared with controls (p<0.001 for both) (figure 2D). Moreover, quantitative real-time PCR analysis revealed that *SLIT2* and *ROBO4* gene expression levels were significantly upregulated in MVECs isolated from SSc dermis (SSc-MVECs) compared with healthy dermal MVECs (H-MVECs) (p<0.001) (figure 3A). On the contrary, *ROBO1* gene expression was similar in H-MVECs and SSc-MVECs (data not shown). The upregulation of Slit2 and Robo4 in cultured SSc-MVECs was confirmed at the protein level by either Western blot or immunocytochemistry (figure 3B, C). In addition, Slit2 levels were significantly higher in supernatants collected from SSc-MVECs (mean±SEM, 2.06±0.25 ng/mL) than in those from H-MVECs (mean±SEM, 1.16±0.06 ng/mL) (p<0.005) (figure 3D). As shown in online supplementary figure S1, treatment with SSc sera was able to significantly increase Robo4 protein levels in H-MVECs (p<0.005 vs basal H-MVECs and H-MVECs treated with healthy sera).

Upregulation of Slit2 and Robo4 contributes to disturbed angiogenesis in SSc

It has been widely demonstrated that treatment with SSc sera impairs the angiogenic performance of H-MVECs[24 28–30] and, as we demonstrate herein, SSc sera are strongly enriched in Slit2. Therefore, in order to clarify the regulatory effects of Slit2 on different angiogenesis steps, such as MVEC proliferation, migration and tube formation, we challenged H-MVECs with recombinant human Slit2 or with sera from patients with SSc preincubated or not with an antihuman Slit2 blocking antibody.

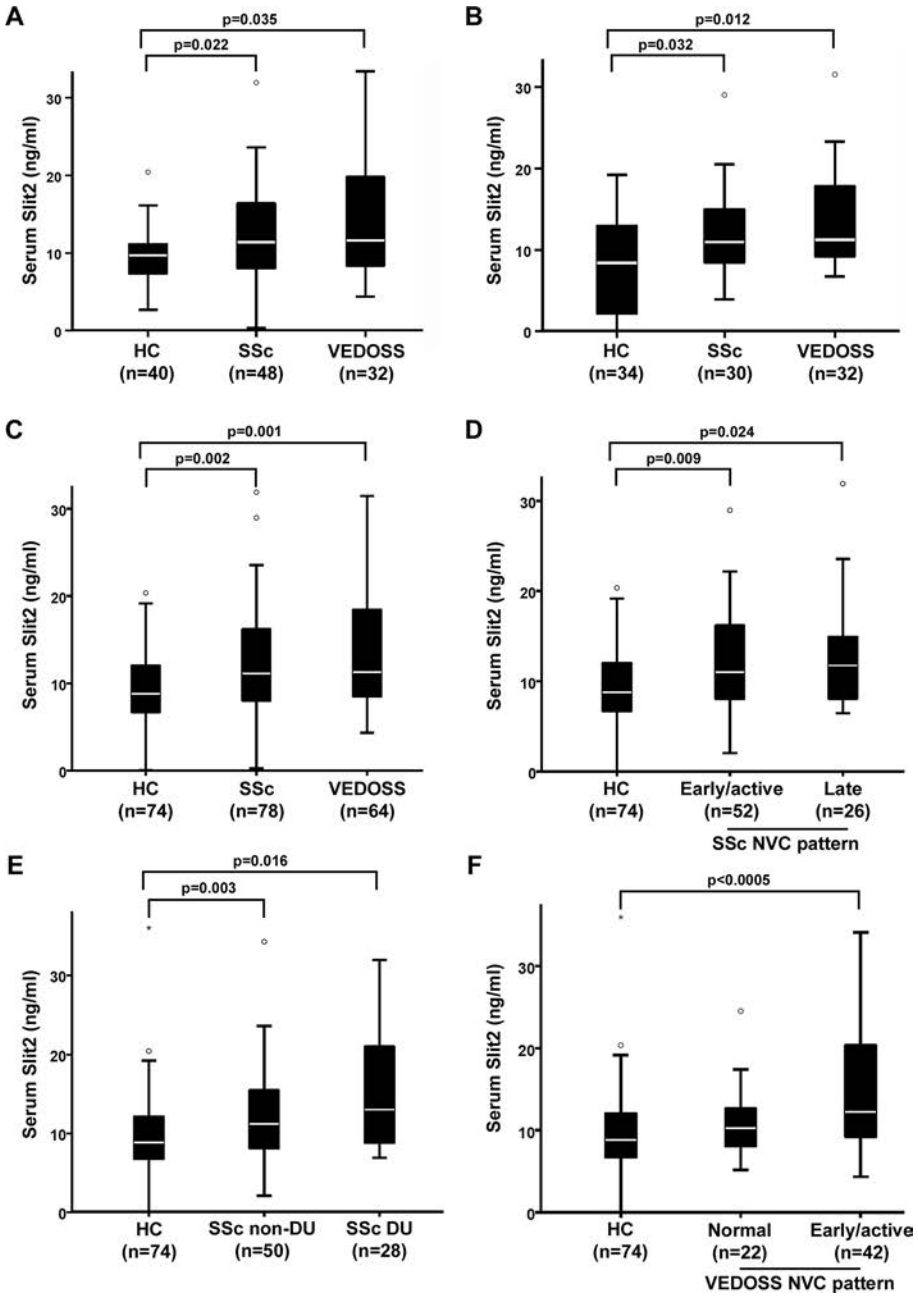

Figure 1 Serum levels of Slit2 determined by colorimetric sandwich ELISA. (A–C) Serum Slit2 levels in healthy controls (HC), patients with systemic sclerosis (SSc) and patients not fulfilling the 2013 American College of Rheumatology/European League Against Rheumatism classification criteria for SSc and enrolled in the very early diagnosis of SSc (VEDOSS) project. Results from the discovery (A), replication (B) and pooled (C) cohorts are shown. (D and E) Serum Slit2 levels in total HC and patients with SSc stratified according to (D) nailfold videocapillaroscopy (NVC) pattern (early/active and late) or (E) the presence/absence of digital ulcers (DU). (F) Circulating Slit2 levels in total HC and patients with VEDOSS stratified according to NVC pattern (normal and early/active). Data are shown as box plots. Each box represents the 25th to 75th percentiles. Lines inside the boxes represent the median. Lines outside the boxes represent the 10th and the 90th percentiles. Circles indicate outliers, and asterisks indicate the extreme values. Mann-Whitney U test was used for statistical analysis.

Moreover, numerous studies suggested that SSc-MVECs have a reduced ability to proliferate, migrate and perform angiogenesis in vitro due to dysregulation of different angiogenic and angiostatic factors.[31–40] Since we found that the angiogenesis regulator Slit2 is abundantly secreted by SSc-MVECs, which also express high levels of the Robo4 cognate receptor, we interfered with Slit2/Robo4 signalling by blocking secreted Slit2 or *ROBO4* gene silencing to clarify its possible contribution to SSc endothelial cell dysfunction.

H-MVECs challenged with recombinant human Slit2 had a significant decrease in cell viability compared with basal condition ($p<0.05$) as assessed by WST-1 assay (figure 4A). Quantification of active caspase-3 levels demonstrated that the aforementioned antiproliferative effects were not due to the induction of apoptosis by Slit2 (online supplementary figure S2). According to previous reports,[24 28–30] treatment of H-MVECs with SSc sera resulted in a significant reduction in proliferation ($p<0.05$ vs untreated cells), an effect that could be significantly

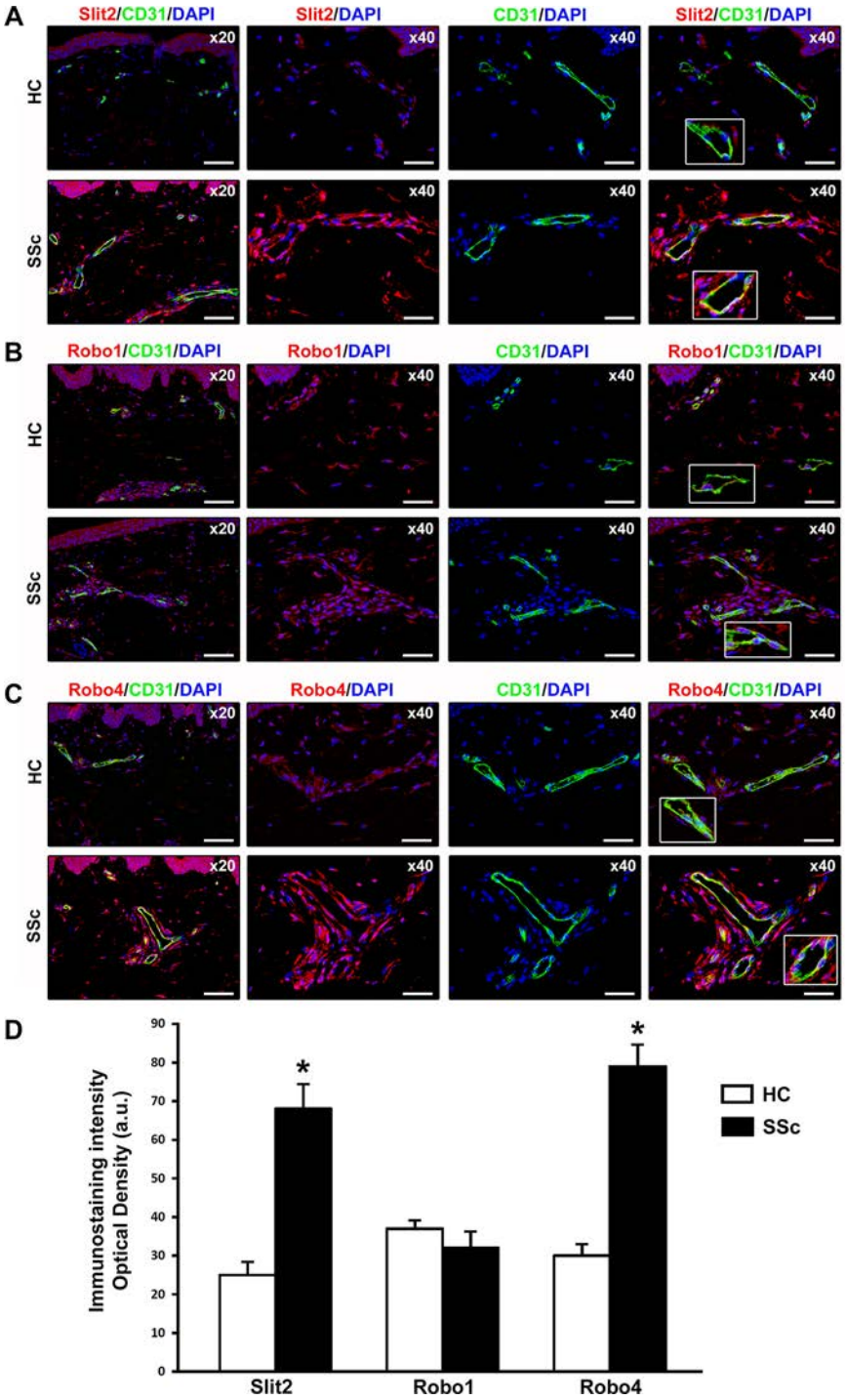

Figure 2 Expression of Slit2 and Robo1 and Robo4 receptors in skin biopsies. (A–C) Representative microphotographs of skin sections from healthy controls (HC) (n=10) and patients with systemic sclerosis (SSc) (n=15) double immunostained for (A) Slit2 (red), (B) Robo1 (red), (C) Robo4 (red) and the pan-endothelial cell marker CD31/platelet-endothelial cell adhesion molecule-1 (green). Nuclei are counterstained with 4′,6-diamidino-2-phenylindole (DAPI; blue). Merged images are shown in the right panels. Insets: higher magnifications of microvessels from the respective panels. Original magnification (×20 or ×40) is indicated in each panel. Scale bar=100 µm (×20 panels) and 50 µm (×40 panels). (D) Densitometric analysis of Slit2, Robo1 and Robo4 immunofluorescent staining in dermal microvessels expressed as optical density in arbitrary units (a.u.). Data are mean±SEM. Student's t-test was used for statistical analysis. *P<0.001 vs HC for both Slit2 and Robo4.

attenuated when cells were challenged with SSc sera preincubated with an anti-Slit2 blocking antibody ($p<0.005$ vs cells treated with non-preincubated SSc sera) (figure 4A). Conversely, elevated Slit2 levels were not involved in the induction of apoptosis by SSc sera (online supplementary figure S2). Viability of SSc-MVECs was significantly promoted either by treatment with anti-Slit2 antibody or *ROBO4* gene silencing with small interfering RNA (siRNA) ($p<0.05$ vs untreated cells for both comparisons) (figure 4A, B).

The in vitro wound healing assay was performed to evaluate the ability of MVECs to repair the injured area in the same experimental conditions used for the cell viability assay

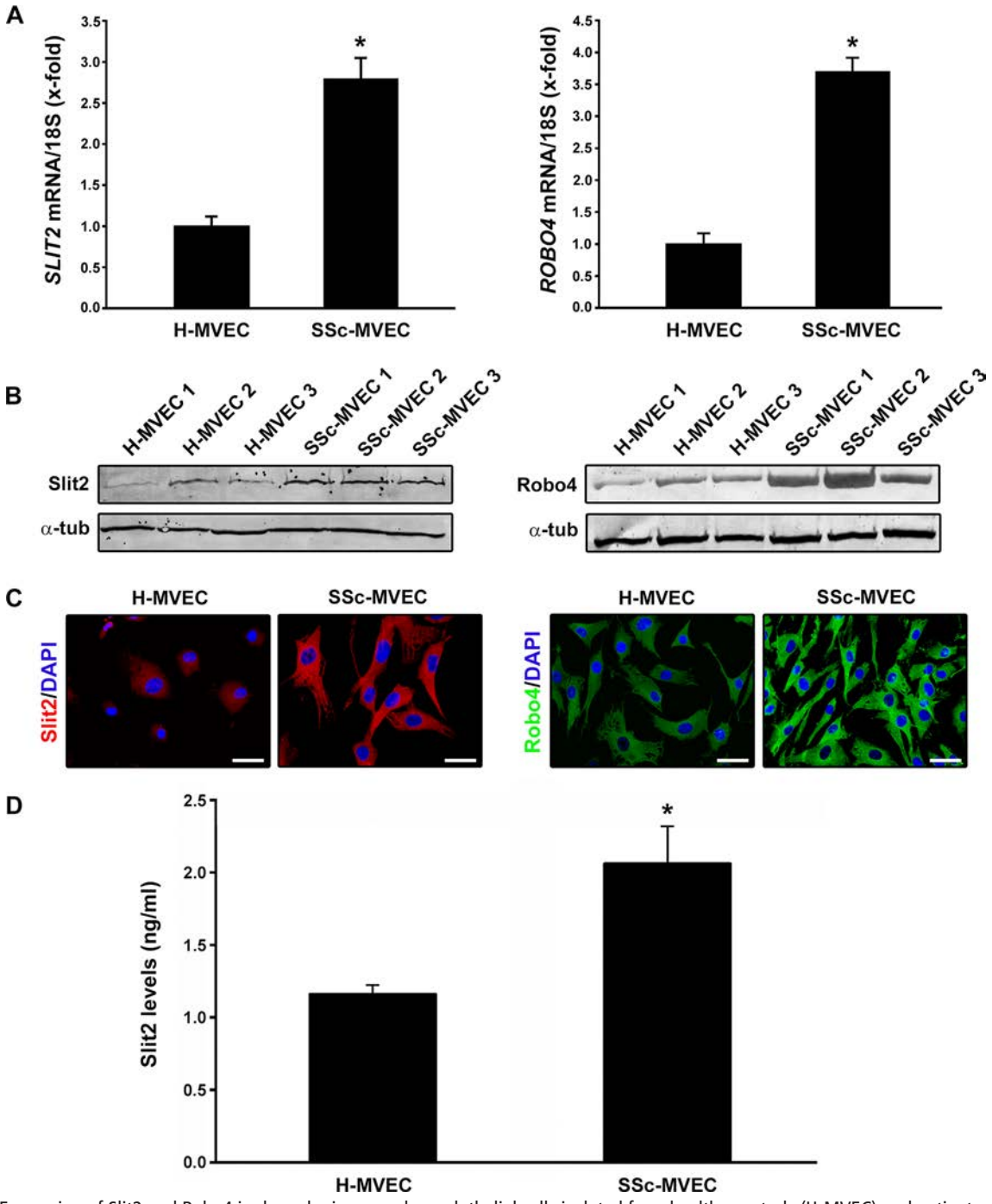

Figure 3 Expression of Slit2 and Robo4 in dermal microvascular endothelial cells isolated from healthy controls (H-MVEC) and patients with systemic sclerosis (SSc-MVEC). (A) Quantification of mRNA expression by real-time reverse transcription PCR. The levels of *SLIT2* (left panel) or *ROBO4* (right panel) gene expression in H-MVEC were set to 1; the other results are normalised to this value. 18S ribosomal RNA was used as reference gene. Bars represent the mean±SEM values of triplicate determinations from five H-MVEC and five SSc-MVEC lines. *P<0.001 vs H-MVEC (Student's t-test). (B) Slit2 and Robo4 protein expression in H-MVEC and SSc-MVEC assessed by Western blot. Representative immunoblots are shown; α-tubulin was measured as a loading control. (C) Representative microphotographs of H-MVEC and SSc-MVEC immunostained for Slit2 (red) or Robo4 (green) and counterstained with 4′,6-diamidino-2-phenylindole (DAPI; blue) for nuclei. Scale bar=50 µm. (D) Slit2 levels in culture supernatants collected from H-MVEC and SSc-MVEC (n=5 each). Bars represent the mean±SEM values of triplicate determinations. *P<0.005 vs H-MVEC.

(figure 5). In unstimulated H-MVECs, the monolayer integrity was almost completely restored at 24 hours after scratching (figure 5A, B). On the contrary, the ability to repair the wounded area was significantly impaired in H-MVECs challenged with recombinant Slit2 or with SSc sera (p<0.001 vs basal H-MVECs) (figure 5A, B). Interestingly, the SSc serum-mediated inhibitory effects on H-MVEC wound healing were significantly reduced by preincubation of sera with an anti-Slit2 antibody (p<0.005 vs cells challenged with non-preincubated SSc sera) (figure 5A, B). As expected, wound healing capacity was compromised in SSc-MVECs respect to H-MVECs, but it could be significantly ameliorated by antibody-mediated neutralisation of Slit2 or *ROBO4* gene silencing (p<0.001 vs basal SSc-MVECs) (figure 5A, B).

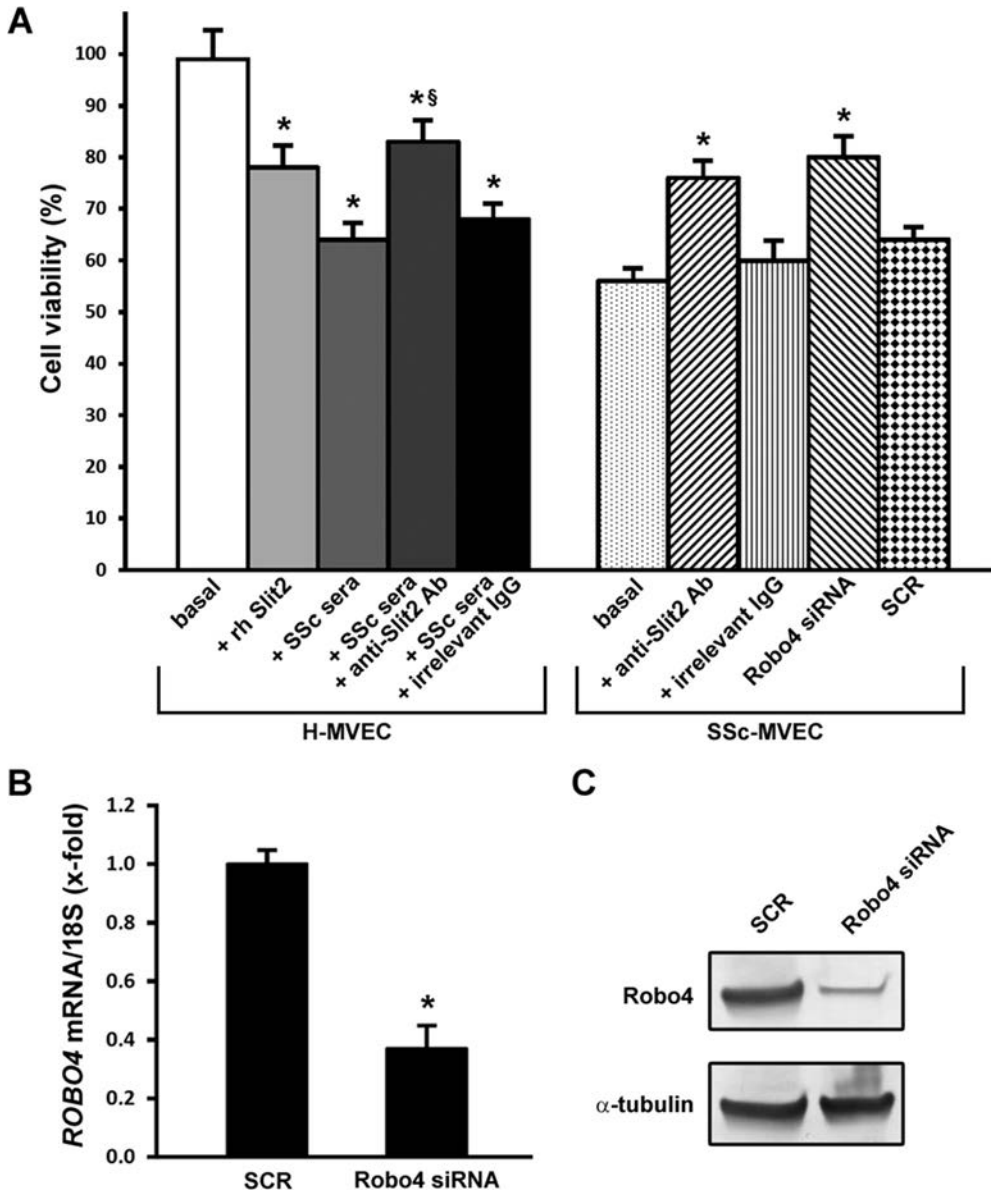

Figure 4 Cell viability of dermal microvascular endothelial cells from healthy controls (H-MVEC) and patients with systemic sclerosis (SSc-MVEC) measured by WST-1 assay. (A) Cell viability was evaluated after 24 hours in H-MVEC at basal condition and after stimulation with recombinant human (rh) Slit2 (100 ng/mL) or 10% sera from patients with SSc (n=6) preincubated or not with an antihuman Slit2 antibody (Ab) (10 µg/mL) or irrelevant isotype-matched and concentration-matched IgG. SSc-MVEC were challenged with an antihuman Slit2 antibody or irrelevant IgG. SSc-MVEC transfected with 10 nM of Robo4 small interfering RNA (siRNA) or non-silencing scrambled RNA (SCR) were also assayed. H-MVEC viability at basal condition was set to 100%; the other results are normalised to this value. Data are the mean±SEM of three independent experiments performed in triplicate with each one of the five H-MVEC and SSc-MVEC lines. Statistical analysis was carried out with Student's t-test. *P<0.05 vs the corresponding basal condition and §p<0.005 vs H-MVEC challenged with SSc sera non-preincubated with anti-Slit2 antibody. (B and C) Verification of the silencing capacity of Robo4 siRNA. (B) *ROBO4* gene expression levels in SSc-MVEC transfected with Robo4 siRNA or SCR were measured by quantitative real-time PCR and normalised to 18S ribosomal RNA gene levels. Values are expressed as mean±SEM of three independent experiments. *P<0.01 vs SCR (Student's t-test). (C) Protein levels of Robo4 in H-MVEC transfected with Robo4 siRNA or SCR were measured by Western blot; α-tubulin was used as a loading control. Representative immunoblots are shown.

To verify whether the endothelial Slit2/Robo4 axis had a role in the modulation of the whole angiogenic process in vitro, we carried out the capillary-like tube formation assay on Geltrex matrix. The stimulation with either exogenous Slit2 or SSc sera significantly decreased the angiogenic response of H-MVECs in respect to cells at basal conditions (p<0.005 for both) (figure 6A, B). The negative effect of SSc sera on H-MVEC angiogenesis was significantly reversed by preincubation with an anti-Slit2 blocking antibody (p<0.005 vs cells stimulated with non-preincubated SSc sera) (figure 6A, B). As reported in previous studies,[29–31] the ability of SSc-MVECs to form capillary-like tubular structures was dramatically impaired compared with H-MVECs (figure 6A, B). However, the angiogenic performance of SSc-MVECs could be effectively improved when targeting the Slit2/Robo4 axis through the addition of an anti-Slit2 antibody or Robo4 siRNA (p<0.005 vs basal SSc-MVECs for both comparisons) (figure 6A, B). In line with these findings, experimental upregulation of Robo4 resulted in a significant decrement in the angiogenic potential of H-MVECs, with the highest antiangiogenic effect being observed after administration of

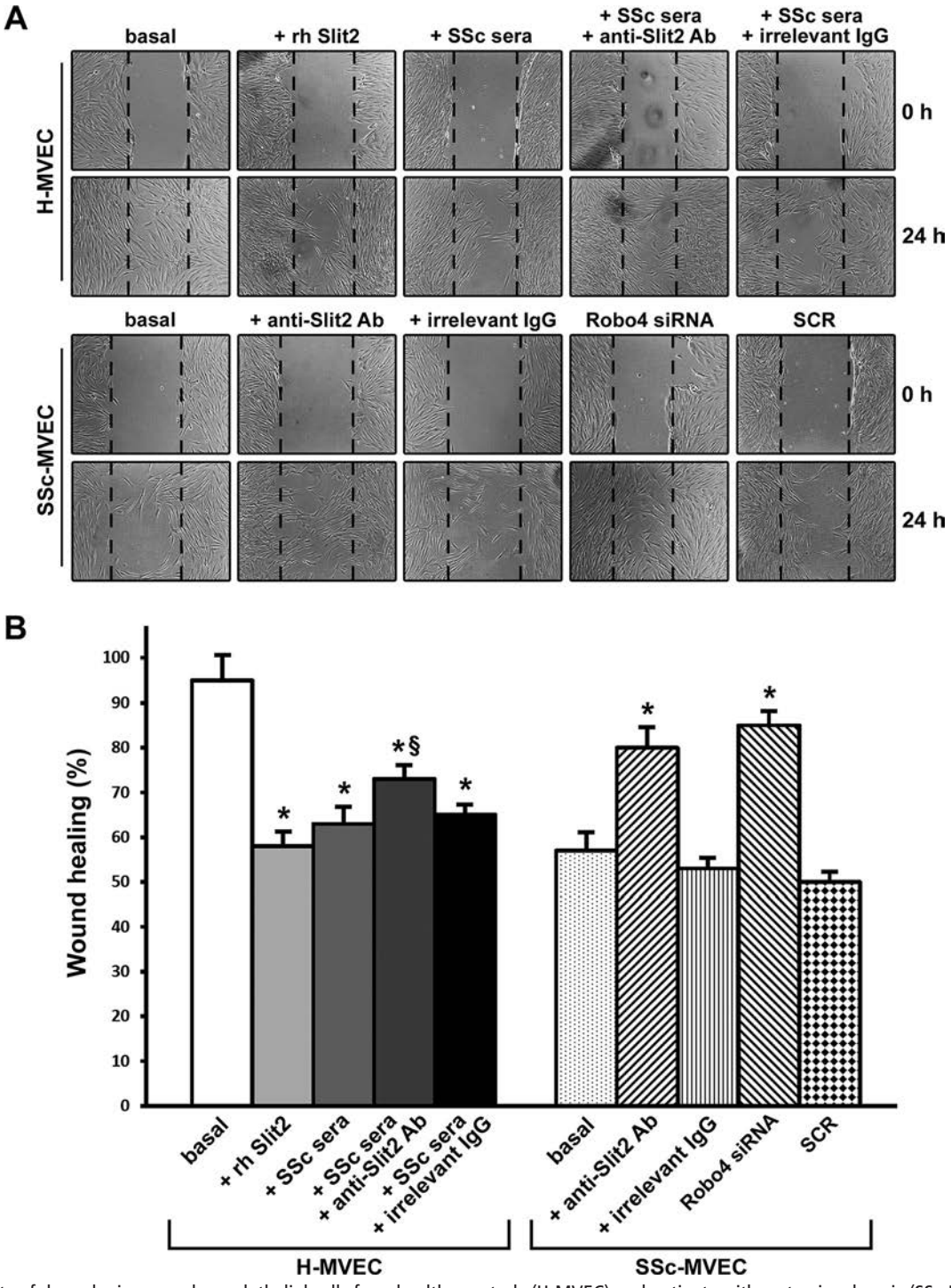

Figure 5 Ability of dermal microvascular endothelial cells from healthy controls (H-MVEC) and patients with systemic sclerosis (SSc-MVEC) to repair the injured area was evaluated by the in vitro wound healing assay. (A) Wound healing capacity was assessed after 24 hours in H-MVEC at basal condition or after challenge with recombinant human (rh) Slit2 (100 ng/mL) or 10% SSc sera (n=6) preincubated or not with an antihuman Slit2 antibody (Ab) (10 µg/mL) or irrelevant isotype-matched and concentration-matched IgG. SSc-MVEC incubated with anti-Slit2 antibody or irrelevant IgG or transfected with 10 nM of Robo4 small interfering RNA (siRNA) or non-silencing scrambled RNA (SCR) were also assayed. A representative image of the wounded area at 0 hours and 24 hours after scratching is shown for each experimental condition (original magnification ×10); dotted lines represent wound margins. (B) Histograms represent results of quantitative analysis of the percentage of wound repair. Data are mean±SEM of three independent experiments performed with each one of the five H-MVEC and five SSc-MVEC lines. Statistical analysis was carried out with Student's t-test; *p<0.001 vs the corresponding basal condition and §p<0.005 vs H-MVEC challenged with SSc sera non-preincubated with anti-Slit2 antibody.

exogenous Slit2 to Robo4 plasmid DNA-transfected cells (online supplementary figure S3).

Since it has been demonstrated that Slit2 may inhibit endothelial cell migration and tube formation by blocking the activation of the proto-oncogene tyrosine-protein kinase Src,[18] we next assessed the phosphorylation of Src at position Y418 in our different experimental conditions. As displayed in figure 6C, treatment of H-MVECs with recombinant human Slit2 reduced

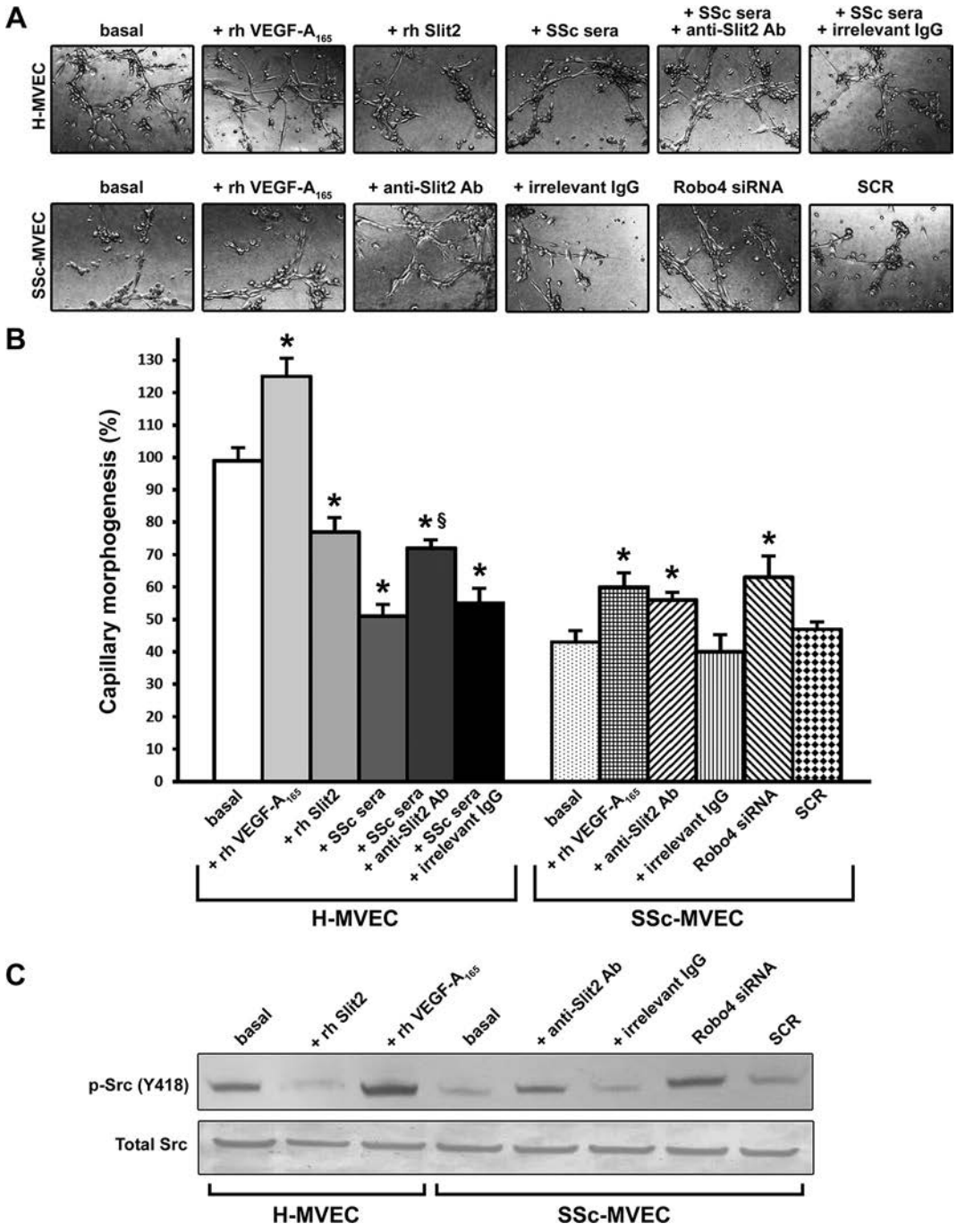

Figure 6 (A and B) In vitro capillary-like tube formation by dermal microvascular endothelial cells from healthy controls (H-MVEC) and patients with systemic sclerosis (SSc-MVEC). Capillary morphogenesis of H-MVEC was evaluated at basal condition and after stimulation with recombinant human (rh) Slit2 (100 ng/mL) or 10% SSc sera (n=6) preincubated or not with an antihuman Slit2 antibody (Ab) (10 µg/mL) or irrelevant isotype-matched and concentration-matched IgG. SSc-MVEC were tested at basal condition and on challenging with anti-Slit2 antibody or irrelevant IgG. SSc-MVEC transfected with 10 nM of Robo4 small interfering RNA (siRNA) or non-silencing scrambled RNA (SCR) were also assayed. Stimulation with rh vascular endothelial growth factor-A_{165} (VEGF-A_{165}) was used as positive control of angiogenesis. (A) Representative images of capillary morphogenesis on Geltrex after 24 hours are shown. (B) In vitro angiogenesis quantified as per cent field occupancy of capillary projections. Capillary morphogenesis of H-MVEC at basal condition was set to 100%; the other results are normalised to this value. Data are the mean±SEM of three independent experiments performed in triplicate with each one of the five H-MVEC and five SSc-MVEC lines. Six to nine photographic fields from three plates were scanned for each experimental point. Student's t-test was used for statistical analysis. *P<0.005 vs the corresponding basal condition and §p<0.005 vs H-MVEC challenged with SSc sera non-preincubated with anti-Slit2 antibody. (C) The protein levels of phosphorylated (p)-Src (Y418) and total Src were evaluated by Western blot in lysates from H-MVEC at basal condition or challenged with rh Slit2 or rh VEGF-A_{165}. SSc-MVEC at basal condition, treated with anti-Slit2 antibody or irrelevant IgG, as well as transfected with Robo4 siRNA or SCR were also assayed. Representative immunoblots are shown. Results are representative of three independent experiments performed with each one of the five H-MVEC and five SSc-MVEC lines.

phosphorylated (p)-Src to levels comparable with those of basal SSc-MVECs. On the other hand, Slit2 neutralisation or silencing of *ROBO4* effectively increased p-Src in SSc-MVECs as compared with unstimulated cells (figure 6C).

DISCUSSION

This is the first study to investigate the possible contribution of neurovascular guidance molecules belonging to the Slit/Robo family to SSc endothelial cell dysfunction. Our data show that serum Slit2 levels are significantly increased in both patients with SSc and patients enrolled in the VEDOSS project[26] and that higher circulating Slit2 levels associate with the presence of microvascular abnormalities in VEDOSS. Moreover, Slit2 and its cognate receptor Robo4 were found to be strongly increased in SSc dermal microvessels when compared with healthy skin, and Slit2/Robo4 upregulation was maintained in vitro in dermal SSc-MVECs. Furthermore, our functional experiments clearly demonstrate that the blockade of Slit2/Robo4 axis may effectively improve angiogenic functions in SSc-MVECs.

Angiogenesis requires the coordinated proliferation and migration of endothelial cells in developing capillaries followed by stabilisation of newly formed vessels.[41] Given the well-documented role of secreted Slit2 as a repellent of migrating neurons during development, numerous recent studies demonstrated that this glycoprotein is also able to regulate critical endothelial processes required for angiogenesis, including proliferation, migration, tube formation and cell permeability.[10–13] Endothelial cells and other resident vascular cells, such as pericytes and vascular smooth muscle cells, constitutively express Slit2 and/or Robo1 and Robo4 receptors, though the specific effects of Slit2 on microvasculature remain unclear, as either proangiogenic or angiostatic activities have been reported for this secreted glycoprotein.[10–13] Our in vitro findings show that the administration of exogenous Slit2 to H-MVECs exerts potent antiangiogenic properties similar to those elicited by Slit2-enriched SSc sera, as testified by the ability to reduce cell viability, wound healing capacity and capillary-like tube formation. This is in agreement with recent reports showing that Slit2 inhibits chemotaxis, migration and invasion of different types of cancer cells[42] and suppresses TNF-α-induced cell proliferation and migration of rat aortic endothelial cells.[43] Strikingly, we observed that blocking elevated Slit2 in SSc sera resulted in significantly attenuated antiangiogenic effects on administration to H-MVECs. Therefore, these data add Slit2 to the considerable list of angiogenesis mediators, which are dysregulated in SSc circulation and appear to be largely responsible for MVEC dysfunction in this disorder.[24 28–30 39]

Of note, a large body of evidence suggests that the effects of Slit2 may be highly cell type and/or context dependent[12] and that this glycoprotein may switch from proangiogenic to angiostatic depending on the binding to Robo1 or Robo4 receptor and consequent differential modulation of VEGF/VEGFR-2 signalling on endothelial cells.[16–19] In particular, activation of Robo4 by Slit2 was found to inhibit vascular migration, tube formation and permeability in vitro even in the presence of proangiogenic VEGF-A_{165}.[18] The Robo4:Robo1 ratio is known to be greater in MVECs than in their macrovascular counterpart, which suggests a predominant antiangiogenic action of Slit2 in the microvasculature.[12] Here, we demonstrate that SSc-MVECs express and release large amounts of Slit2 and also display a strong upregulation of Robo4 compared with H-MVECs. Conversely, no difference in Robo1 expression was detected. Thus, SSc-MVECs seem to present a much higher Robo4:Robo1 ratio than H-MVECs rendering them potentially more responsive to the antiangiogenic and less responsive to the proangiogenic effects of Slit2. This was further corroborated by the evidence that administration of exogenous Slit2 profoundly impaired angiogenesis in H-MVECs subjected to experimental upregulation of Robo4. These data are consistent with previous studies demonstrating that overexpression of Robo4 in endothelial cells may inhibit cell migration mostly by downregulating the VEGFR-2 downstream signalling in the presence of Slit2.[22] Moreover, Slit2 is capable of inhibiting both migration and tube formation of Robo4+/+, but not Robo4−/− endothelial cells expressing normal levels of Robo1.[18] Interestingly, it also appears that Robo4 may inhibit angiogenesis irrespective of Slit2 by acting as a ligand for UNC5B,[23] which might explain our observation that Robo4 plasmid DNA transfection was sufficient to reduce the angiogenic response of H-MVECs even in the absence of exogenous Slit2. In this complex scenario, we cannot exclude that other mechanisms, such as an overexpression of the angiogenesis mediator ephrin-A1, could act as an additional molecular switch controlling the effects of Slit2 on target endothelial cells.[44]

The effective inhibitory role of Slit2/Robo4 in the different angiogenesis steps of SSc-MVECs was further corroborated by targeting this axis through the blockade of autocrine Slit2 with a specific neutralising antibody or *ROBO4* gene silencing. In fact, when we interfered with Slit2/Robo4 signalling, SSc-MVECs exhibited a significant improvement in their ability to proliferate, migrate and form capillary-like structures in vitro. In endothelial cells, Slit2/Robo4 axis was found to prevent the activation of MAP kinases,[16] Arf small GTPases[21] or Src family kinase (SFK)[18] mediated by proangiogenic factors such as VEGF.[45] In this context, we observed that treatment of H-MVECs with Slit2 reduced p-Src to levels comparable with those of basal SSc-MVECs, suggesting that this secreted glycoprotein may suppress angiogenesis through the inhibition of SFK signalling pathways. On the other hand, interfering with Slit2/Robo4 axis effectively increased p-Src expression in SSc-MVECs, which further supports that Slit2/Robo4 antiangiogenic signalling is triggered in SSc microvascular endothelium.

The association of circulating Slit2 levels with peripheral microangiopathy in patients enrolled in the VEDOSS project[26] also deserves discussion. In fact, when we stratified those patients according to the NVC pattern, increased serum levels of Slit2 specifically correlated with the presence of microvascular derangement, as patients with normal NVC had Slit2 levels comparable with healthy controls. Thus, an increase in systemic Slit2 levels could reflect the presence of microvascular abnormalities since the very early phase of SSc. Of note, there were no significant differences in Slit2 levels between patients with VEDOSS and patients with SSc, strengthening the notion that patients with VEDOSS already present circulating biomarkers of defective angiogenesis and that the involvement of the microvascular system does occur in very early disease, even when only a few clinical signs and symptoms are present.[46]

In conclusion, our findings suggest that in SSc the Slit2/Robo4 antiangiogenic pathway is activated in dysfunctional endothelium and may contribute to peripheral microangiopathy since the very early phase of the disease. Prospective studies on larger cohorts of patients are warranted to decipher whether elevated circulating levels of Slit2 could even serve as a biomarker reflecting the shift from VEDOSS to definite SSc. Moreover, it could be of interest to investigate whether modulation of the Slit2/Robo4 axis might represent a new therapeutic strategy to achieve vascular repair and counteract the progression of peripheral microangiopathy in SSc. Further work is also necessary to

elucidate the mechanisms underlying Slit2/Robo4 overexpression in SSc, which might include either transcriptional or epigenetic regulation as reported for a plethora of factors dysregulated in this disorder.[47 48] Finally, though the present study was focused on the vascular spectrum of SSc, the upregulation of Slit2 and Robo4 in different skin cell types other than MVECs, such as keratinocytes and fibroblasts, raises the possibility that this pathway might participate in additional mechanisms relevant to disease pathogenesis.

Contributors Study conception and design: ER, MM, MM-C and SG. Acquisition of data: ER, MM, IR, BSF and SG. Interpretation of data: ER, MM, IR, LI-M and SG. Manuscript preparation: ER, MM, IR and MM-C.

Funding The authors have not declared a specific grant for this research from any funding agency in the public, commercial or not-for-profit sectors.

Competing interests None declared.

Patient consent Obtained.

Ethics approval The study was approved by the local institutional review board at the Azienda Ospedaliero-Universitaria Careggi (AOUC), Florence, Italy.

Provenance and peer review Not commissioned; externally peer reviewed.

REFERENCES

1 Van den Hoogen F, Khanna D, Fransen J, *et al*. Classification criteria for systemic sclerosis: an American College of Rheumatology/European League Against Rheumatism collaborative initiative. *Ann Rheum Dis* 2013;2013:1747–55.
2 Furue M, Mitoma C, Mitoma H, *et al*. Pathogenesis of systemic sclerosis—current concept and emerging treatments. *Immunol Res* 2017;65:790–7.
3 Varga J, Trojanowska M, Kuwana M. Pathogenesis of systemic sclerosis: recent insights of molecular and cellular mechanisms and therapeutic opportunities. *J Scleroderma Relat Disord* 2017;2:137–52.
4 Matucci-Cerinic M, Manetti M, Bruni C, *et al*. The "myth" of loss of angiogenesis in systemic sclerosis: a pivotal early pathogenetic process or just a late unavoidable event? *Arthritis Res Ther* 2017;19:162.
5 Altorok N, Wang Y, Kahaleh B. Endothelial dysfunction in systemic sclerosis. *Curr Opin Rheumatol* 2014;26:615–20.
6 Matucci-Cerinic M, Kahaleh B, Wigley FM. Review: evidence that systemic sclerosis is a vascular disease. *Arthritis Rheum* 2013;65:1953–62.
7 Kahaleh B, Matucci-Cerinic M. Raynaud's phenomenon and scleroderma. Dysregulated neuroendothelial control of vascular tone. *Arthritis Rheum* 1995;38:1–4.
8 Carmeliet P, Tessier-Lavigne M. Common mechanisms of nerve and blood vessel wiring. *Nature* 2005;436:193–200.
9 Adams RH, Eichmann A. Axon guidance molecules in vascular patterning. *Cold Spring Harb Perspect Biol* 2010;2:a001875.
10 Blockus H, Chédotal A. Slit-Robo signaling. *Development* 2016;143:3037–44.
11 Yadav SS, Narayan G. Role of ROBO4 signalling in developmental and pathological angiogenesis. *Biomed Res Int* 2014;2014:1–9.
12 Yuen DA, Robinson LA. Slit2-Robo signaling: a novel regulator of vascular injury. *Curr Opin Nephrol Hypertens* 2013;22:445–51.
13 Fujiwara M, Ghazizadeh M, Kawanami O. Potential role of the Slit/Robo signal pathway in angiogenesis. *Vasc Med* 2006;11:69–74.
14 Huminiecki L, Gorn M, Suchting S, *et al*. Magic roundabout is a new member of the roundabout receptor family that is endothelial specific and expressed at sites of active angiogenesis. *Genomics* 2002;79:547–52.
15 Wang B, Xiao Y, Ding BB, *et al*. Induction of tumor angiogenesis by slit-robo signaling and inhibition of cancer growth by blocking robo activity. *Cancer Cell* 2003;4:19–29.
16 Li S, Huang L, Sun Y, *et al*. Slit2 promotes angiogenic activity via the Robo1-VEGFR2-ERK1/2 pathway in both in vivo and in vitro studies. *Invest Ophthalmol Vis Sci* 2015;56:5210–7.
17 Rama N, Dubrac A, Mathivet T, *et al*. Slit2 signaling through Robo1 and Robo2 is required for retinal neovascularization. *Nat Med* 2015;21:483–91.
18 Jones CA, London NR, Chen H, *et al*. Robo4 stabilizes the vascular network by inhibiting pathologic angiogenesis and endothelial hyperpermeability. *Nat Med* 2008;14:448–53.
19 Marlow R, Binnewies M, Sorensen LK, *et al*. Vascular Robo4 restricts proangiogenic VEGF signaling in breast. *Proc Natl Acad Sci U S A* 2010;107:10520–5.
20 Park KW, Morrison CM, Sorensen LK, *et al*. Robo4 is a vascular-specific receptor that inhibits endothelial migration. *Dev Biol* 2003;261:251–67.
21 Jones CA, Nishiya N, London NR, *et al*. Slit2-Robo4 signalling promotes vascular stability by blocking Arf6 activity. *Nat Cell Biol* 2009;11:1325–31.
22 Seth P, Lin Y, Hanai J, *et al*. Magic roundabout, a tumor endothelial marker: expression and signaling. *Biochem Biophys Res Commun* 2005;332:533–41.
23 Koch AW, Mathivet T, Larrivée B, *et al*. Robo4 maintains vessel integrity and inhibits angiogenesis by interacting with UNC5B. *Dev Cell* 2011;20:33–46.
24 Romano E, Chora I, Manetti M, *et al*. Decreased expression of neuropilin-1 as a novel key factor contributing to peripheral microvasculopathy and defective angiogenesis in systemic sclerosis. *Ann Rheum Dis* 2016;75:1541–9.
25 Mazzotta C, Romano E, Bruni C, *et al*. Plexin-D1/Semaphorin 3E pathway may contribute to dysregulation of vascular tone control and defective angiogenesis in systemic sclerosis. *Arthritis Res Ther* 2015;17:221.
26 Avouac J, Fransen J, Walker UA, *et al*. Preliminary criteria for the very early diagnosis of systemic sclerosis: results of a Delphi Consensus Study from EULAR Scleroderma Trials and Research Group. *Ann Rheum Dis* 2011;70:476–81.
27 Ruaro B, Sulli A, Smith V, *et al*. Advances in nailfold capillaroscopic analysis in systemic sclerosis. *J Scleroderma Relat Disord* 2018;3:122–31.
28 Manetti M, Romano E, Rosa I, *et al*. Endothelial-to-mesenchymal transition contributes to endothelial dysfunction and dermal fibrosis in systemic sclerosis. *Ann Rheum Dis* 2017;76:924–34.
29 Romano E, Bellando-Randone S, Manetti M, *et al*. Bosentan blocks the antiangiogenic effects of sera from systemic sclerosis patients: an in vitro study. *Clin Exp Rheumatol* 2015;33:S148–52.
30 Borghini A, Manetti M, Nacci F, *et al*. Systemic sclerosis sera impair angiogenic performance of dermal microvascular endothelial cells: therapeutic implications of cyclophosphamide. *PLoS One* 2015;10:e0130166.
31 Manetti M, Guiducci S, Romano E, *et al*. Overexpression of VEGF165b, an inhibitory splice variant of vascular endothelial growth factor, leads to insufficient angiogenesis in patients with systemic sclerosis. *Circ Res* 2011;109:e14–e26.
32 D'Alessio S, Fibbi G, Cinelli M, *et al*. Matrix metalloproteinase 12-dependent cleavage of urokinase receptor in systemic sclerosis microvascular endothelial cells results in impaired angiogenesis. *Arthritis Rheum* 2004;50:3275–85.
33 Margheri F, Manetti M, Serratì S, *et al*. Domain 1 of the urokinase-type plasminogen activator receptor is required for its morphologic and functional, beta2 integrin-mediated connection with actin cytoskeleton in human microvascular endothelial cells: failure of association in systemic sclerosis endothelial cells. *Arthritis Rheum* 2006;54:3926–38.
34 Tsou PS, Rabquer BJ, Ohara RA, *et al*. Scleroderma dermal microvascular endothelial cells exhibit defective response to pro-angiogenic chemokines. *Rheumatology* 2016;55:745–54.
35 Mazzotta C, Manetti M, Rosa I, *et al*. Proangiogenic effects of soluble α-Klotho on systemic sclerosis dermal microvascular endothelial cells. *Arthritis Res Ther* 2017;19:27.
36 Kahaleh B, Guiducci S, Kuwana M. Recent updates in experimental protocols for endothelial cells. *J Scleroderma Relat Disord* 2016;1:257–65.
37 Giusti B, Margheri F, Rossi L, *et al*. Desmoglein-2-integrin Beta-8 interaction regulates actin assembly in endothelial cells: deregulation in systemic sclerosis. *PLoS One* 2013;8:e68117.
38 Manetti M, Guiducci S, Ibba-Manneschi L, *et al*. Mechanisms in the loss of capillaries in systemic sclerosis: angiogenesis versus vasculogenesis. *J Cell Mol Med* 2010;14:1241–54.
39 Chora I, Guiducci S, Manetti M, *et al*. Vascular biomarkers and correlation with peripheral vasculopathy in systemic sclerosis. *Autoimmun Rev* 2015;14:314–22.
40 Manetti M, Guiducci S, Matucci-Cerinic M. The crowded crossroad to angiogenesis in systemic sclerosis: where is the key to the problem? *Arthritis Res Ther* 2016;18:36.
41 Ribatti D, Crivellato E. "Sprouting angiogenesis", a reappraisal. *Dev Biol* 2012;372:157–65.
42 Yu J, Cao Q, Yu J, *et al*. The neuronal repellent SLIT2 is a target for repression by EZH2 in prostate cancer. *Oncogene* 2010;29:5370–80.
43 Li GJ, Yang Y, Yang GK, *et al*. Slit2 suppresses endothelial cell proliferation and migration by inhibiting the VEGF-Notch signaling pathway. *Mol Med Rep* 2017;15:1981–8.
44 Dunaway CM, Hwang Y, Lindsley CW, *et al*. Cooperative signaling between Slit2 and Ephrin-A1 regulates a balance between angiogenesis and angiostasis. *Mol Cell Biol* 2011;31:404–16.
45 Cross MJ, Dixelius J, Matsumoto T, *et al*. VEGF-receptor signal transduction. *Trends Biochem Sci* 2003;28:488–94.
46 Chora I, Romano E, Manetti M, *et al*. Evidence for a derangement of the microvascular system in patients with a very early diagnosis of systemic sclerosis. *J Rheumatol* 2017;44:1190–7.
47 Tsou PS, Sawalha AH. Unfolding the pathogenesis of scleroderma through genomics and epigenomics. *J Autoimmun* 2017;83:73–94.
48 Manetti M, Matucci-Cerinic M. The new frontier in systemic sclerosis: from epigenetics to new treatments. *Rheumatology* 2015;54:1757–8.

EXTENDED REPORT

Multi-OMICS analyses unveil *STAT1* as a potential modifier gene in mevalonate kinase deficiency

Raphael Carapito,[1,2,3,4,5] Christine Carapito,[3,6] Aurore Morlon,[7] Nicodème Paul,[1,2,3,4] Alvaro Sebastian Vaca Jacome,[6] Ghada Alsaleh,[1,3,4] Véronique Rolli,[1,2,3,4,5] Ouria Tahar,[1,2,3,4,5] Ismail Aouadi,[1,2,3,4,5] Magali Rompais,[6] François Delalande,[6] Angélique Pichot,[1,2,3,4] Philippe Georgel,[1,2,3,4] Laurent Messer,[8] Jean Sibilia,[1,3,4,9] Sarah Cianferani,[3,6] Alain Van Dorsselaer,[3,6] Seiamak Bahram[1,2,3,4,5]

Handling editor Josef S Smolen

► Additional material is published online only. To view please visit the journal online (http://dx.doi.org/10.1136/annrheumdis-2018-213524).

For numbered affiliations see end of article.

Correspondence to
Dr Raphael Carapito and Professor Seiamak Bahram, Laboratoire d'ImmunoRhumatologie Moléculaire, INSERM UMR_S1109, Plateforme GENOMAX, LabEx TRANSPLANTEX, Faculté de Médecine, University of Strasbourg, Strasbourg, France; carapito@unistra.fr, siamak@unistra.fr

RC and CC contributed equally.

Received 6 April 2018
Revised 14 June 2018
Accepted 30 June 2018
Published Online First 20 July 2018

To cite: Carapito R, Carapito C, Morlon A, *et al*. *Ann Rheum Dis* 2018;**77**:1675–1687.

ABSTRACT

Objectives The objective of the present study was to explain why two siblings carrying both the same homozygous pathogenic mutation for the autoinflammatory disease hyper IgD syndrome, show opposite phenotypes, that is, the first being asymptomatic, the second presenting all classical characteristics of the disease.

Methods Where single omics (mainly exome) analysis fails to identify culprit genes/mutations in human complex diseases, multiomics analyses may provide solutions, although this has been seldom used in a clinical setting. Here we combine exome, transcriptome and proteome analyses to decipher at a molecular level, the phenotypic differences between the two siblings.

Results This multiomics approach led to the identification of a single gene—*STAT1*—which harboured a rare missense variant and showed a significant overexpression of both mRNA and protein in the symptomatic versus the asymptomatic sister. This variant was shown to be of gain of function nature, involved in an increased activation of the Janus kinase/signal transducer and activator of transcription signalling (JAK/STAT) pathway, known to play a critical role in inflammatory diseases and for which specific biotherapies presently exist. Pathway analyses based on information from differentially expressed transcripts and proteins confirmed the central role of STAT1 in the proposed regulatory network leading to an increased inflammatory phenotype in the symptomatic sibling.

Conclusions This study demonstrates the power of a multiomics approach to uncover potential clinically actionable targets for a personalised therapy. In more general terms, we provide a proteogenomics analysis pipeline that takes advantage of subject-specific genomic and transcriptomic information to improve protein identification and hence advance individualised medicine.

INTRODUCTION

Mevalonate kinase (MVK) deficiency is a recessive autoinflammatory disease caused by mutations in the *MVK* gene. Its clinical picture includes recurring episodes of high fever and a variety of unspecific symptoms, for example, cephalalgia, joint and/or abdominal pain, diarrhoea, skin rash,[1 2] which can be regrouped in several syndromic entities including the severe form known as mevalonic aciduria and the milder phenotype known as hyperimmunoglobulinaemia D and periodic fever syndrome (HIDS), characterised predominantly by recurrent fever with inflammatory symptoms.

We recently reported two sisters (42 and 45 years of age) that despite being both homozygous for the p.V377I mutation in the *MVK* gene (which is found in 90% of patients with HIDS) did present radically opposite phenotypes, that is, one exhibited inflammatory symptoms while the other was disease-free.[3] Briefly, the one sister (subject S2) presented polyarthralgies involving fingers, wrists and ankles, central allodynia and hyperalgesia, small cervical infracentimetric painless lymphadenopathies, optic neuritis, frequent right upper abdominal pains, nausea, vomiting and disturbed night sleep. She presented no evidence for an autoimmune disease. Despite the absence of periodic fever episodes, known pathogenic *MVK* gene mutations were identified. The HIDS diagnosis was confirmed by an abnormal level of polyclonal IgD (690 UI/mL) and IgA (5.82 U/mL), a lowered MVK enzymatic activity in lymphocytes (0.3 μkat/kg prot; cf. 2.5<normal range <7.8 μkat/kg) and urinary mevalonic acid concentration twice above normal values (3.1 and 4.1 mmol/mol creatinine). In contrast, although she carried the same homozygous p.V377I mutation, a similar decrease in MVK enzyme activity (0.3 µkat/kg prot) and elevated serum levels of IgD (140 U/mL) and IgA (2.5 U/mL), the other sister (subject S1) had no history of disease or inflammatory signs.

The obvious hypothesis explaining this differential clinical symptomatology in this family being the existence of a modifier gene, we first turned to family exome sequencing and differential analyses between the two sisters in order to uncover such gene(s). Having failed to achieve this goal, we switched to multiomics analyses (for a review see Hasin *et al*[4]). Over the last few years, there has been indeed a massive expansion of large-scale genomics, transcriptomics and proteomics data that has facilitated the identification of potential markers for disease prognosis, diagnosis and treatment. Notwithstanding these developments, there has been nevertheless a lag in successfully implementing multiomics approaches to a single patient or family, with potential direct benefit to the patient. Here, through a multi(tri)omics analysis, we decipher at a molecular level, the phenotypic differences between patient S2 and her asymptomatic sister S1.

METHODS

Subjects and samples

Subjects reported in this study were members of a single non-consanguineous family of European descent (online supplementary figure S1). Patient S2 was diagnosed as Hyper IgD syndrome, whereas all other members of the family (parents, one sister and one brother) were healthy.[3] All participants gave their informed consent and the study was approved by Strasbourg University Hospitals institutional review board (immune-based diseases project; DC-2013–1911).

Cell culture

Peripheral blood mononuclear cells (PBMC) were isolated by density gradient centrifugation from blood samples of S1 and S2 using Ficoll-Paque. PBMC (10^6 cells) were seeded in 24-well plates in RPMI1640 supplemented with fetal calf serum (FCS), penicillin, streptomycin, amphotericin B (all from Invitrogen, Cergy-Pontoise, France) and stimulated with lipopolysaccharide (LPS) (1 µg/mL; from Salmonella *Abortus equi*; Sigma, Saint-Quentin-Fallavier, France) for 3 or 6 hours at 37°C in a humidified atmosphere containing 5% CO_2. The *STAT1* deficient-U3A cell line (ECACC reference 12021503) was used for recombinant expression of wild-type (wt) and mutated STAT1 proteins. U3A cells were cultivated in Dulbecco's Modified Eagle Medium (DMEM, ThermoFisher Scientific, Waltham, Massachusetts, USA) supplemented with 10% FCS, penicillin and streptomycin.

Exome sequencing

Whole exome sequencing was performed in both parents and the two sisters (S1 asymptomatic and S2 symptomatic). Genomic DNA was extracted and purified from peripheral blood using standard protocols. Exome capture was performed with the SureSelect 50 MB Target Enrichment System V.3 (Agilent Technologies, Santa Clare, California, USA) according to the manufacturer's protocol. Prepared libraries were subjected to 75 bp/35 bp paired-end sequencing on the SOLiD 5500 platform (ThermoFisher Scientific, Waltham, Massachusetts, USA). We obtained an average of 8.6 Gb of mappable sequence data per individual. Colour space reads were mapped to the hg19 reference genome with Lifescope software V.2.5.1 (ThermoFisher Scientific, Waltham, Massachusetts, USA). The mean coverage was 152-fold (median of 148-fold) and 84% of the target region was covered at a minimum of 10×. Single-nucleotide variants and small insertions and deletions were called using the GATK software[5] and algorithms of Lifescope with medium-stringency calling settings. Only variants called by both methods and covered by more than four variant reads were considered. Annotation was performed with the KGGSeq software package.[6]

RNAseq

Total RNA was extracted from 1×10^6 cells after 3 and 6 hours of culture using TRIzol reagent according to the manufacturer's instruction (Invitrogen, Cergy-Pontoise, France). Experiments were performed in duplicate for each condition. Purified RNA was checked for integrity (RIN>7) and quantified using a Pico Total RNA Bioanalyzer kit and Agilent 2100 BioAnalyzer (Agilent Technologies, Santa Clara, California, USA). Poly(A)+RNA was purified from 1500 ng of total RNA with a Micropoly(A) Purist kit (LifeTechnologies, Carlsbad, California, USA). Barcoded library construction was performed according to the SOLiD Total RNA-Seq Kit (ThermoFisher Scientific, Waltham, Massachusetts, USA) with 30 ng of poly(A)+RNA as input material. After quantification by Qbit (Life Technologies, Carlsbad, California, USA), libraries were pooled in equimolar amounts for template beads preparation using the SOLiD EZ-bead System (ThermoFisher Scientific, Waltham, Massachusetts, USA). Finally, the prepared beads were subjected to sequencing using the SOLiD 5500 sequencer (ThermoFisher Scientific, Waltham, Massachusetts, USA) with the paired-end 75bp/35 pb workflow.

After sequencing, the reads were aligned against the reference genome (hg19) using the Lifescope software V.2.5.1 (ThermoFisher Scientific, Waltham, Massachusetts, USA). The Bioconductor R package DESeq was used to compare the expression levels of the identified genes.[7] After normalisation and hypothesis testing, differentially expressed (DE) genes were selected based using a fold-change cut-off of minimum 1.5 and an adjusted p value of maximum 0.05.

Differential proteomic experiments

Detailed analytical procedures are described in online supplementary material. Briefly, proteins were extracted from 1×10^6 cells after 6 hours of culture with and without LPS activation. Experiments were performed in triplicate for each condition. One hundred µg proteins from each sample were separated on a 1D SDS-PAGE gel. Gel bands were systematically cut and proteins were *in-gel* trypsin digested. Differential analysis using a spectral counting approach was conducted on a NanoAcquity LC-system (Waters, Milford, Massachusetts, USA) coupled to a maXis 4G QToF mass spectrometer (Bruker Daltonics, Bremen, Germany). Liquid chromatography-mass spectrometry/mass spectrometry (LC-MS/MS) data were searched using a local Mascot server (Matrix Science, London, UK) against personalised databases for each subject containing all human entries extracted from the UniProtKB-SwissProt reference database (40 654 target entries with isoforms) and specific exome-derived variants (Personalised Database 1 for S1: 45 834 target entries, Personalised Database 1 for S2: 45 883 target entries). The generation of personalised protein databases is detailed in online supplementary material and in online supplementary figure S3.

Identification validation and spectral counting were performed with Scaffold software (Proteome Software, Portland, USA). Relative protein quantification and testing for differential protein expression were performed using the beta-binomial test implemented in R.[8] The acceptance criteria for statistically different protein abundance changes between two conditions were: a minimum of 4 summed spectral-counts for the three replicates in at least one of the conditions to be compared, a p value lower than 0.05 and a fold change higher than 1.5 (except when the summed spectral-count equals 0 in one of the conditions to be compared).

Proteomic experiments for deep proteome coverage and specific variants identification

Detailed analytical procedures are described in online supplementary material. Briefly, samples were prepared as described above but analysed on a more recent nanoLC-MS/MS coupling in order to increase depth of the proteome coverage. These experiments were conducted on a NanoAcquity LC-system (Waters, Milford, Massachusetts, USA) coupled to a TripleTOF 5600+mass spectrometer (Sciex, Framingham, USA). LC-MS/MS data were searched using Mascot against personalised databases containing specific sequence variants inferred for exome

sequencing on the one hand (personalised databases 1) and containing new splice variants inferred from RNAseq data on the other hand (personalised databases 2). For this purpose, we generated a list of genomic variants and splice junctions from exome and RNAseq datasets, respectively. Based on this list, a modified UniProtKB protein database was constructed containing the identified variant protein sequences in addition to all UniProtKB-SwissProt database entries, including presently known isoforms. Between the two search rounds, peak-list files were processed using an in-house developed software tool (Recover module of MSDA, https://msda.unistra.fr[9]) and identifications were validated using Proline software[10] (http://proline.profiproteomics.fr/). The overall identification pipeline is outlined in figure 1B. Sixty-nine identified single amino acid variants (SAAVs) were further validated by comparing their chromatographic and MS/MS fragmentation characteristics to heavy labelled synthetic peptides analysed and fragmented in identical conditions. All fragmentation spectra of light and heavy peptide pairs are provided in online supplementary figure S1.

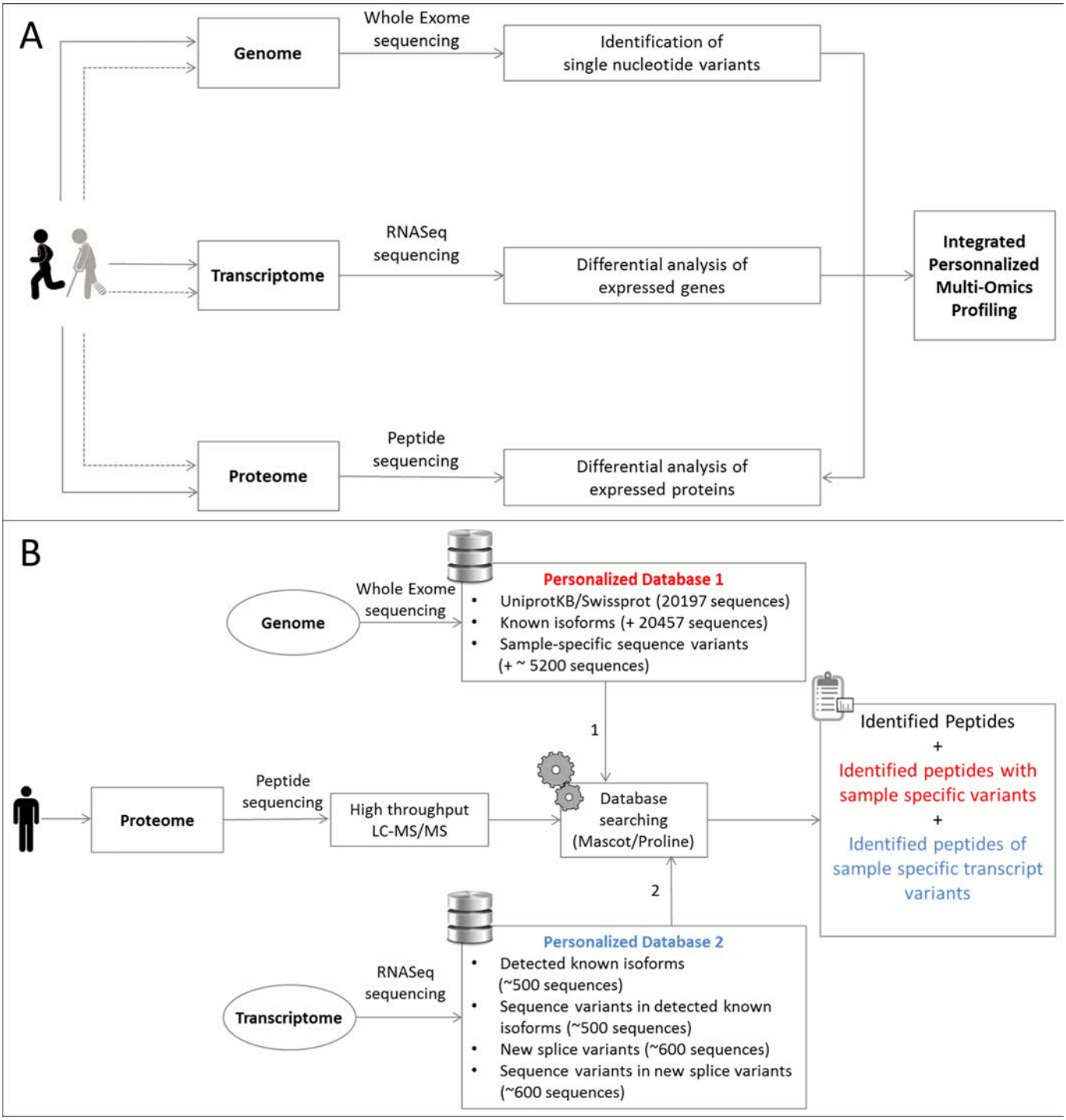

Figure 1 Experimental multiomics strategy. (A) Schematic view of the global strategy combining genomic, transcriptomic and proteomic data. (B) Detailed strategy of the interpretation of proteomic data making use of genomics (personalised database 1) and transcriptomics (personalised database 2) information.

Integrative omics data analyses

The first step of the integrative omics analysis was to assess the correlation of the proteomics and RNAseq datasets. For this purpose, we first applied the voom transformation to the RNAseq read counts in order to convert the counts to log-counts per million with associated precision weight.[11] Then the RNAseq data were analysed using limma method, which is a popular differential expression method developed for microarray data (continuous data), provided by the limma software package.[12] The same approach was used to analyse spectral count data from the proteomics dataset. The resulting datasets (RNAseq: n=24 364; proteins: n=736) were first filtered by removing rows with zero or very low counts. The filtered datasets (RNA-seq n=12 770; proteomic n=727) were then integrated using the multivariate co-inertia analysis (MCIA).[13 14] MCIA projects RNAseq and proteomic datasets, at the same time, into the same dimensional space to identify co-relationships between them. As this method requires identical number of replicates for both datasets, we generated an additional replicate for RNAseq using bootstrap method and validating beforehand that bootstrap did not cause any bias.[15]

The second analysis step consisted in combining S2-specific variants with DE genes in S2 vs S1 at both RNA and protein levels based on fold changes calculated from RNAseq and proteomic datasets, respectively (cf. RNAseq and proteomics sections of materials and methods). By doing so, we aimed at identifying genes that harboured a S2-specific variant and showed a differential expression level at both RNA and protein level as compared with S1.

Finally, identification of molecular network interactions and pathway analysis of DE genes at the RNA and protein levels was completed using the Ingenuity Pathway Analysis (Ingenuity Systems, www.ingenuity.com). The ingenuity knowledge base (genes only) with direct and indirect relationships was used and only molecules and/or relationships that had been experimentally observed in rat, mouse or human were considered.

Expression of recombinant STAT1 and IFN-ɣ stimulation

The human *STAT1* cDNA was PCR-amplified from HEK293 cells (ATCC CRL-1573) with the following forward and reverse primers respectively 5'-cgcaccggtatgtctcagtggtacgaacttcagca-3' and 5'-cgcttaattaacta tactgtgttcatcatactgtcgaattc-3'. It was then cloned into AgeI and PacI sites of pQCXIP (Clontech, Mountain View, California, USA). The mutated form (p.R241Q) was generated with the QuikChange Site-Directed Mutagenesis kit using the forward 5'-agtggagtggaagcagagacagagcg-3' and reverse 5'-cgctctgctgtctctgcttccactccact-3' primers, following manufacturer's recommendations (Stratagene, San Diego, California, USA). The pQCXIP plasmids harbouring the wt or the mutated *STAT1* were transiently transfected into the STAT1 deficient-U3A cell line with Lipofectamine 3000 according to manufacturer's instructions (Invitrogen, Carlsbad, California, USA). Two days after transfection, cells were stimulated with 2000 IU/mL of interferon-ɣ (IFN-ɣ) (RD Systems, Minneapolis, Minnesota, USA) during 30 min. After stimulation, proteins were extracted with NP-40 lysis buffer (150 mM sodium chloride, 50 mM Tris pH8, 1% NP-40) complemented with the cOmplete and phosSTOP protease and phosphatase inhibitor cocktail (Roche, Basel, Switzerland). Proteins were quantified using the Bradford assay according to manufacturer's instructions (Bio-Rad Laboratories, Hercules, California, USA).

Quantitative real-time PCR

The pQCXIP plasmids harbouring the wt or the mutated STAT1 forms were transiently transfected into the STAT1 deficient-U3A cell line with Lipofectamine 3000 according to manufacturer's instructions (Invitrogen, Carlsbad, California, USA). Two days after transfection, cells were stimulated with 1000 IU/mL of IFN-ɣ during 8 hours. Total RNA was extracted with TRIzol reagent (Invitrogen, Carlsbad, California, USA). Isolated RNA was reverse transcribed with iScript Reverse Transcription supermix (Bio-Rad Laboratories, Hercules, California, USA). PCR was performed with SSO advanced universal SYBRgreen supermix (Bio-Rad Laboratories, Hercules, California, USA) and run on a ABI7000 Real-Time PCR system (ThermoFisher Scientific, Waltham, Massachusetts, USA). PCR conditions were as follows: 10 min at 96°C followed by 45 cycles of 95°C for 10 s and 60°C for 30 s. Primers used were 5'-CTCTAAGTGGCA TTCAAGGAGTACCT-3' (forward) and 5'-TCTCAACACGTG GACAAAATTGGC-3' (reverse). The *GAPDH* gene was used as a normalising gene and was amplified with the forward primer 5'-GGTGAAGGTCGGAGTCAACGGA-3' and the reverse primer 5'-GAGGGATCTCGCTCCTGGAAGA-3'.

Luciferase reporter assay

*GAS (*Gamma interferon activation site) sequences were inserted into the multiple cloning site of the pMCS Tluc16 plasmid (ThermoFisher Scientific, Waltham, Massachusetts, USA). This reporter plasmid was co-transfected with the pQCXIP plasmids harbouring the wt or the mutated STAT1 or the mock vector into STAT1-deficient U3A cells. Transfections were done in 96-well plates using the Lipofectamine 3000 Reagent and following manufacturer's instruction (Invitrogen, Carlsbad, California, USA). Six hours after transfection, growth medium was replaced. One day after transfection, cells were stimulated with 1000 IU/mL of IFNɣ during 16 hours and subjected to luciferase assays with TurboLuc one-Step Glow Assay Kit (ThermoFisher Scientific, Waltham, Massachusetts, USA). Experiments were performed in triplicate and data are expressed as fold induction with respect to non-stimulated cells.

Quantification of proinflammatory cytokines

Cytokines were quantified in the supernatant of PBMCs after 6 hours of stimulation with LPS (1 µg/mL, *Salmonella abortus equi* LPS from Sigma). The cytokines IL-6, IL-1β, TNF-α were quantified by ELISA following the manufacturer's instruction (R&D Systems, Minneapolis, Minnesota, USA). The results are presented as mean values±SD in pg/mL. A two-tailed Mann-Whitney test was used to compare two independent groups using the GraphPad software (San Diego, California, USA).

RESULTS

Exomes

The exome of the asymptomatic subject S1, the symptomatic subject S2, their mother and father were sequenced (online supplementary figure S1). On average 49 420 SNPs (median of 49 351) and 1867 indels (median of 1869) were identified in each subject. For SNPs, we focused only on the average 8851 protein altering events (median of 8804), that is, missense, frameshift, splicing, stop loss and stop gain. In the case of indels, only frameshift, non-frameshift, stop loss, stop gain and splicing events were taken into account, which correspond to an average number of 182 (median of 183). To identify the candidate genes, the initial list of 8811 protein altering variants of the symptomatic subject S2 (proband) were filtered by

excluding variants shared with her asymptomatic sister S1. As both rare and common variants associated to the rare homozygous mutation p.V377I present in the two subjects could be associated with the phenotype, no filtering was performed using variant frequency databases. In addition, as it has been reported that homozygous p.V377I carriers could be milder or asymptomatic,[16] we focused only on S2-specific events that represented a total of 1135 variants in 876 different genes. The complete list of variants is available in the online supplementary table S1.

Proteomes

After extraction of PBMCs from whole blood and culture without (basal state) or with LPS (activated state) during 6 hours, proteins were isolated and analysed using bottom-up nanoLC-MS/MS-based proteomics workflows. In this proteome

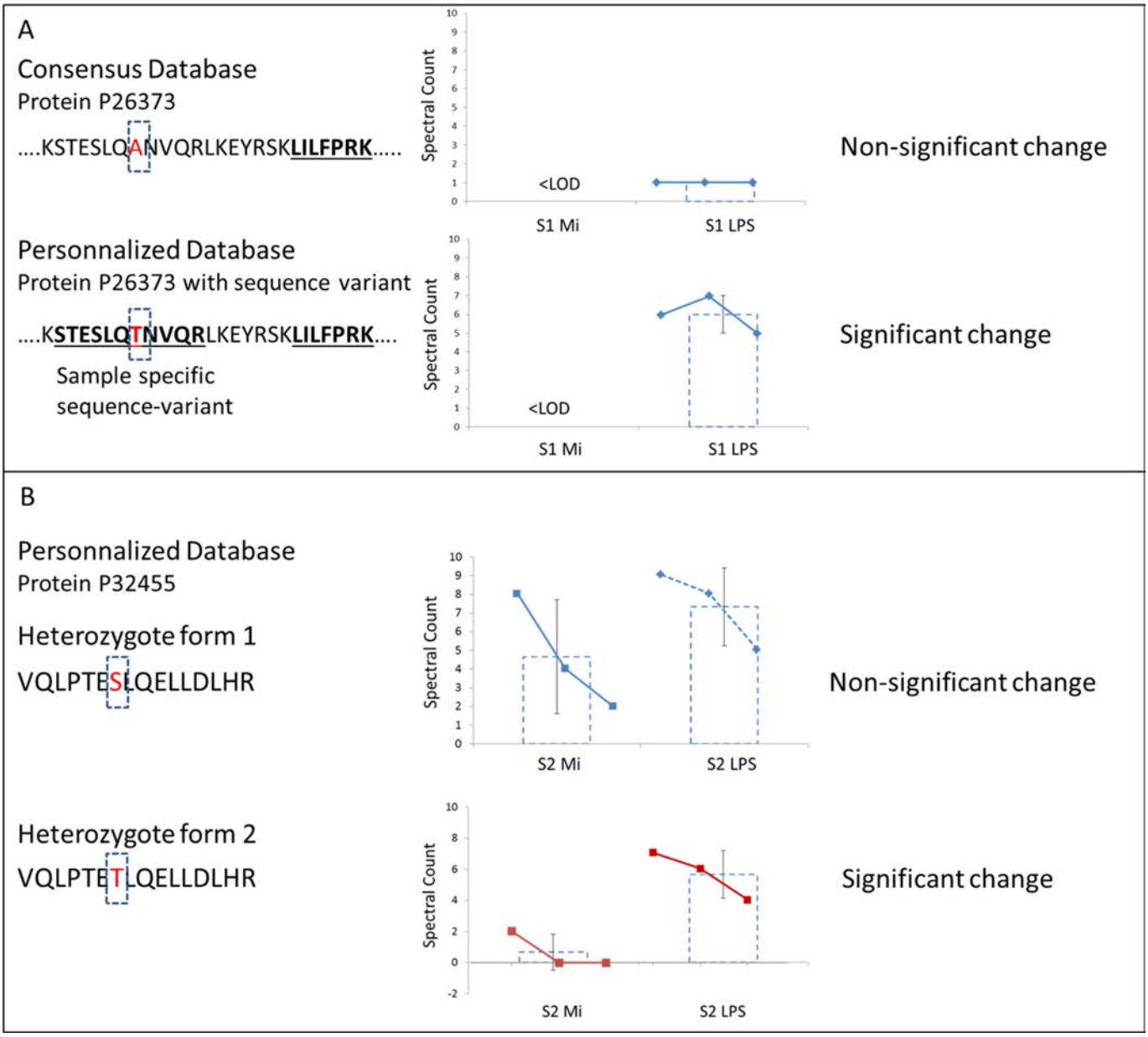

Figure 2 Benefits of using personalised databases for protein identification and quantification. (A) A sequence stretch of 60S ribosomal protein L13 (P26373) is given. Peptides identified in searches using the consensus database (UniProtKB-SwissProt) and the personalised databases (including subject-specific sequence variants) are underlined. When using the consensus database only a single peptide was identified and the spectral count values for protein P26373 show a non-significant change in abundance when comparing the basal to the activated state. However, when using the personalised database, an additional tryptic peptide including a subject-specific variant was identified (amino acid change from Alanine to Threonine at position 112). The relative quantification using spectral count is improved as the sequence coverage is greater and a significant overexpression of the protein could be detected. (B) In this example, two sequence variants of the Guanylate-binding protein 1 (P32455) are present in the personalised database 1 of S2. Both peptides, one with Threonine and one with Serine at position 349, were identified. This is the unambiguous proof that two heterozygote variants of the same gene are expressed. The spectral count-based relative quantification shows that one of the heterozygote forms is overexpressed when comparing the basal to the activated state. This example demonstrates that allele-specific quantification is possible at protein level.

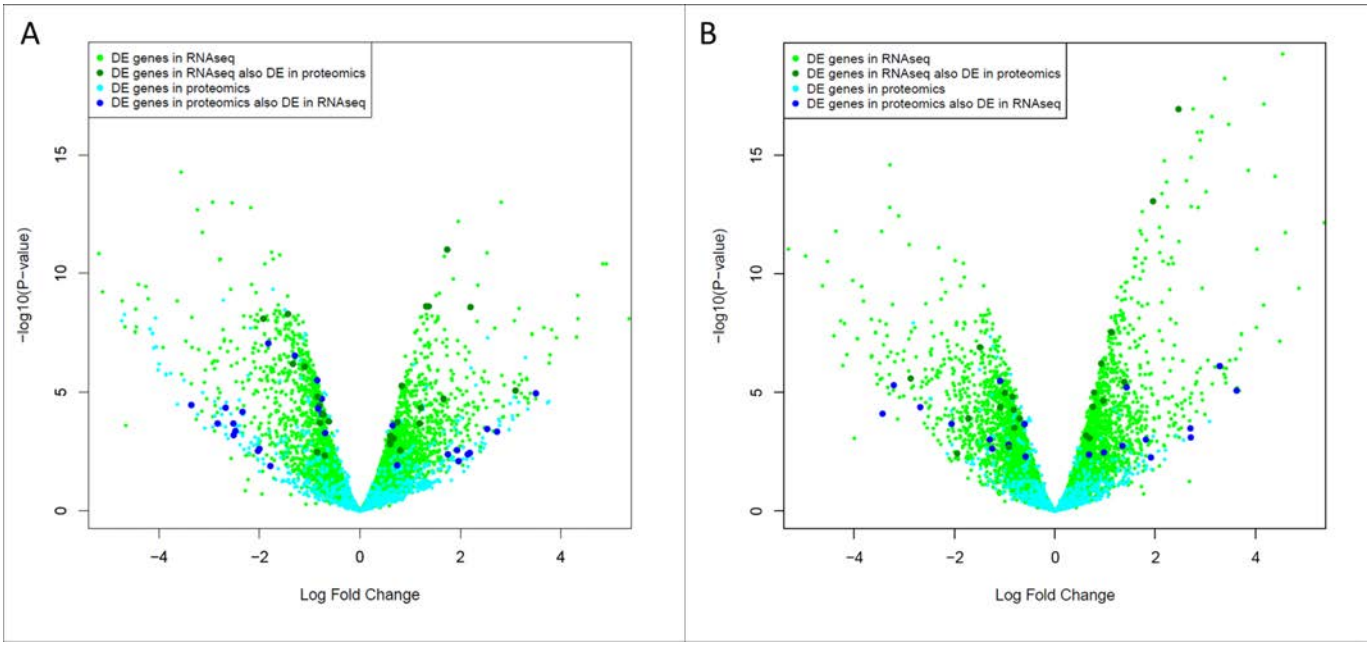

Figure 3 Volcano plots of DE genes in RNAseq and proteomics analyses. Statistical significance (−log10 p value) is plotted against log2 fold change for either basal (without LPS, Panel A) and activated (with LPS, Panel B) states. Data were selected at the cut-off values adjusted p<0.05 and fold change >1.5. For this analysis, RNAseq data at 3 and 6 hours were pooled. DE, differentially expressed; LPS, lipopolysaccharide.

analysis, we identified a total of 8335 distinct peptides among all samples, corresponding to 244 450 assigned MS/MS spectra in an assembly of 1428 unique protein groups with a false discovery rate below 1% at both peptide and protein levels (see online supplementary table S2). Protein abundances were estimated using a spectral count approach where the total number of MS/MS spectra acquired for the peptides of a given protein were used as a proxy for the protein quantities. Based on a minimal spectral count requirement of 4 (for the replicates in at least one of the conditions to be compared), 736 unique protein groups could be confidently quantified across samples. These quantitative results were aligned with those obtained at the transcriptome level using an RNAseq approach as described below (figure 1A, online supplementary table S2). Notably, in order to take advantage of the unique availability of multilevel omics data acquired on identical individuals/samples, the proteomics data interpretation strategy was adapted to use personalised protein databases including subject-specific information inferred from exome and transcriptome data. Therefore, for each subject, the human reference UniProtKB-SwissProt database was modified to take into account, on one hand, non-synonymous SNPs derived from exome sequencing (personalised databases 1) and on the other, the alternative transcripts uncovered from RNASeq experiments (personalised databases 2) (figure 1B, online supplementary material). Then, in order to further increase the depth of proteome coverage, improve overall numbers of identifications and leverage benefits of using personalised databases, all four samples were reinjected on a later generation nanoLC-MS/MS coupling, namely a TripleTOF 5600+QTOF instrument (Sciex). At the end, the complete dataset searched against the personalised databases enabled the unambiguous identification of 100 and 108 SAAVs for S1 and S2, respectively and two new splice variants common to S1 and S2 (online supplementary table S3). In order to further validate these SAAVs identifications, we synthesised a random selection of 69 SAAVs-containing peptides in heavy labelled form. These peptides were mixed and analysed using the same LC-MS/MS conditions as the samples. Both chromatographic and MS/MS fragmentation characteristics were compared and allowed ultimate validation of all SAAVs. Fragmentation spectra of light and heavy peptide pairs are provided in online supplementary figure S2. Finally, additional advantages of using personalised databases are illustrated in figure 2 where we show that using an incomplete consensus reference database can lead to errors in quantification (this has far ranging implications beyond the present manuscript). Indeed, in the example of figure 2A, reference database searches led to a non-significant change in abundance while the personalised database search enabled the identification of an additional SAAV peptide that allowed concluding for a significant overexpression. In figure 2B, we demonstrate that heterozygote variants of a given gene can be unequivocally identified and even individually quantified for allele-specific expression analysis.

Differentially expressed genes and proteins

DE genes were analysed at the RNA and protein levels. Figure 3 shows the statistical significance of differential transcript and protein levels by volcano plots along with respective fold changes. A total of 1661 transcripts and 190 proteins were DE in S2 vs S1 at the basal state (without LPS) using a cut-off value for adjusted p value of 0.05 and a minimum fold change of 1.5. Twenty-seven genes were shared by the protein and RNAseq datasets. In the activated state (with LPS), we identified 2502 and 69 genes that were DE in S2 vs S1 at the transcripts and protein levels, respectively. Twenty-one genes were common to both datasets. The complete lists of genes with significantly different expression levels at the RNA or protein levels are presented in online supplementary table S2.

Integrative analysis of RNAseq and proteome data

MCIA was applied to RNAseq and proteomic data to assess the correlation of the two datasets. Figure 4 shows the projection of samples onto the first two principal components (PCs) of MCIA. The coordinates of RNAseq and proteomic measurements for

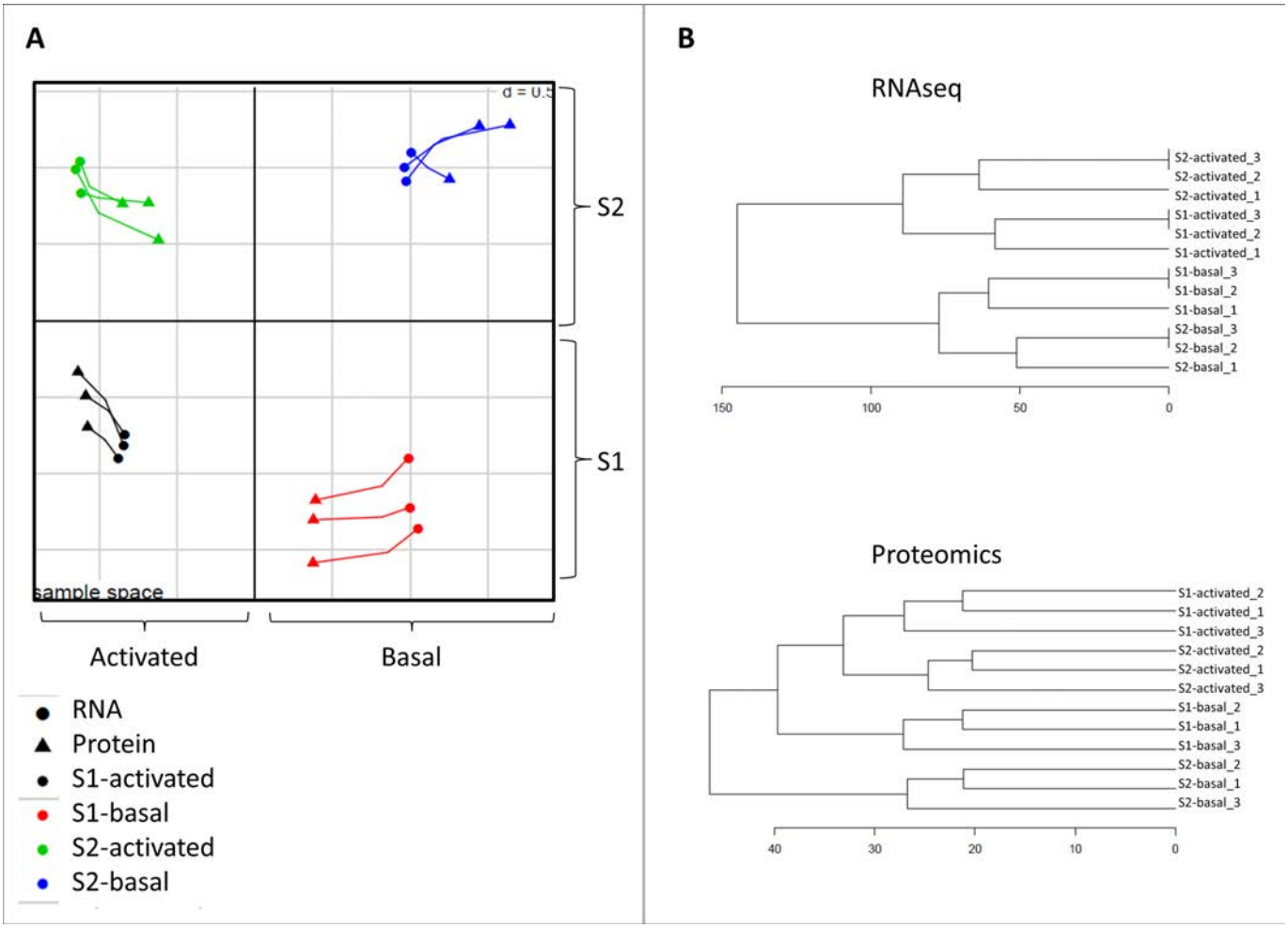

Figure 4 Integrative analysis of RNAseq and proteomics data. (A) MCIA of RNAseq and proteomic data. The projection of the samples on the first two PCs of MCIA is depicted. (B) Hierarchical clustering of RNA-seq and protein expression data. Dendrograms show the hierarchical clustering using Euclidean distance. MCIA, multiple co-inertia analysis; PCs, principal components.

each sample are linked by a line. The shorter the line, the higher is the level of consensus between the transcript and protein expression levels. The transcriptome and proteome profiles of the individual samples were projected close in space showing that the expression profiles of both techniques shared a high degree of concordance. The first axis of the MCIA (PC1; horizontal axis) separated the activated (negative on PC1) from the basal state (positive on PC1), suggesting that the transcriptome and proteome profiles are different in the two conditions. These results are consistent with independently performed hierarchical clustering analysis[17] (figure 4B).

Combined analysis of exome, RNAseq and proteome

Combining the lists of S2-specific non-synonymous variants, DE transcripts and proteins in S2 vs S1 led to the identification of a single gene—*STAT1*—harbouring a rare coding variant (minor allele frequency of 0.029% and 0% at heterozygous and homozygous states, respectively in GnomAD) and showing mRNA and protein abundances significantly more important in S2 than in S1 (figure 5). At basal state, mRNA and protein fold changes were 1.78 ($p=1.74\times10^{-4}$) and 11.32 ($p=2.22\times10^{-4}$), respectively. In the activated state, these values were 1.71 ($p=2.34\times10^{-4}$) for *STAT1* mRNA and 12.27 ($p=5.27\times10^{-4}$) for the protein. The variant (c.722G>A, rs146273341, NM_007315.3) is inherited from the father and causes an Arg to Gln modification (p.R241Q, NP_009330.1) in the coiled coil domain of the protein without predicted deleterious impacts on protein function (online supplementary table S4).

Activation of the interferon-ɣ/STAT1 pathway

Functional pathway analyses were performed on lists of DE genes in S2 vs S1 after activation with LPS. The top canonical pathways, upstream regulators and disease/biological functions are presented in table 1. Based on RNAseq data, the top canonical pathway identified was the interferon signalling pathway with 13 and 14 out of 36 genes of the pathway that were DE at the mRNA level, 3 and 6 hours post-LPS-activation, respectively. This pathway was associated with the activation of IFN-ɣ as the top upstream regulator. Protein level analyses that were restricted to intracellular protein revealed activation of pathways related to immune responses including granzyme A signalling or the antigen presenting pathway. Immune-mediated pathways were further confirmed by the identification of known disease pathways of immunological, inflammatory, antimicrobial, dermatological or connective/skeletal/muscular origin (table 1).

Figure 6A,B represents the molecules of the IFN-ɣ network and their interaction with STAT1, which is central in this pathway. Based on RNAseq data at 3 hour post-LPS-activation, 7 proteins of the IFN-ɣ pathway were found to be upregulated. To further validate the activation of the IFN-ɣ/STAT1 pathway,

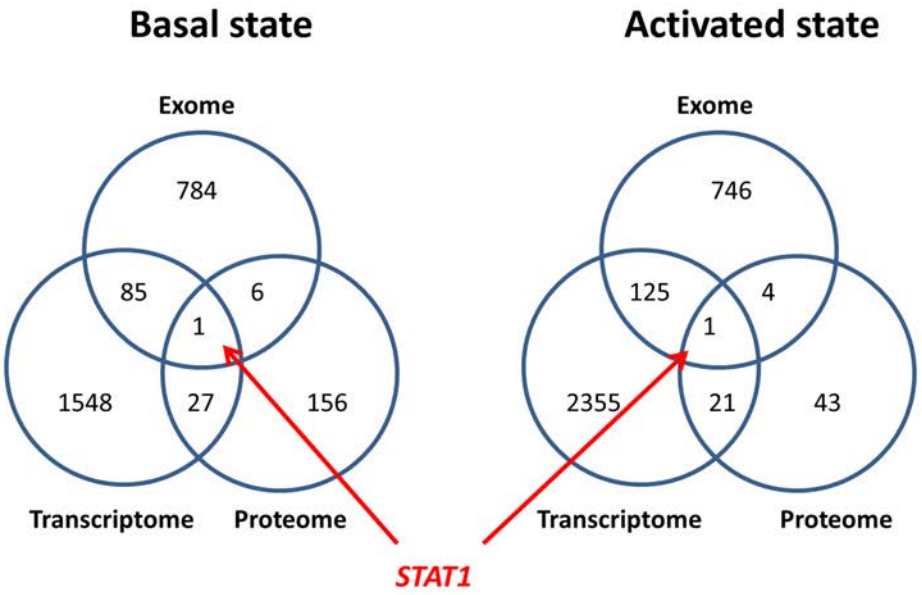

***STAT1* variant**

Nucleotide alteration [A]	chr2:191862645G>A
Exon	2
cDNA alteration [B]	cDNA.1110G>A
Coding sequence alteration	c.722G>A
Amino acid alteration [C]	p.R241Q
rs identification number	rs146273341

***STAT1* expression in basal state (S2>S1)[D]**

	Fold-change	p-value
mRNA	1.78	1.74×10^{-4}
Protein	11.32	2.22×10^{-4}

***STAT1* expression in activated state (S2>S1)[D]**

	Fold-change	p-value
mRNA	1.71	2.34×10^{-4}
Protein	12.27	5.27×10^{-4}

Figure 5 Combined analysis of exome, transcriptome and proteome datasets. The figure shows Venn diagrams of genes with S2-specific variants and genes that were upregulated in S2 at the mRNA (transcriptome) and protein (proteome) levels. The tables in the lower panel indicate the details of the *STAT1* variant and the differential expression values in RNAseq and proteomics datasets in both basal and activated states. [A]Positions refer to Hg19 (GRCh37). [B]Positions refer to GenBank transcript NM_007315.3. [C]Position refers to protein accession number NP_009330.1. [D]Increased expression in S2 versus S1.

we stimulated the STAT1 deficient U3A cell line transfected with the wild-type or mutated *STAT1* (c.722G>A, p.R241Q) gene with IFN-γ. On stimulation with IFN-γ, cells transfected with the R241Q allele responded two times more strongly than those transfected with the wild-type allele, as shown by measurement of the induction of GAS (γ-activated sequence)–dependent reporter gene transcription activity (figure 7A). Accordingly, the transcription of the CXCL10 target gene was enhanced (figure 7B).

Proinflammatory cytokine response of lipopolysaccharide (LPS)-stimulated peripheral blood mononuclear cells (PBMCs)

In order to assess the impact of the *STAT1* variant in presence or absence of the *MVK* variant at the homozygous state, the cytokine response of PBMCs isolated from different members of the family was evaluated (table 2). As expected, LPS-stimulated PBMCs from the symptomatic patient S2 released large amounts of TNF-α (10437±2804 pg/mL), IL-1β (5790±743 pg/mL) and IL-6 (24649±1408 pg/mL), while those of her asymptomatic sister S1 released lower quantities of those cytokines (4804±1251 pg/mL, 3868±709 pg/mL and 18316±1518 pg/mL for TNF-α, IL-1β and IL-6, respectively), at about the same level as those of the mother's (4804±1251 pg/mL, 3995±794 pg/mL and 14642±700 pg/mL for TNF-α, IL-1β and IL-6, respectively). Interestingly, the concentrations of cytokines produced by the PBMCs of the father, who also carries the *STAT1* variant but does not show any disease manifestation, were equivalent to those of the symptomatic patient S2 (8580±1073 pg/mL, 7388±831 pg/mL and 24727±479 pg/mL for TNF-α, IL-1β and IL-6, respectively; table 2).

DISCUSSION

Here we report a multiomics study in two siblings harbouring the same homozygous p.V377I pathogenic mutation in the *MVK*

Table 1 Pathway analysis of differentially expressed genes identified in the LPS-activated state using RNAseq and proteomics datasets

RNAseq data 3-hour post-LPS stimulation			RNAseq data 6-hour post-LPS stimulation			Proteomics data 6-hour post-LPS stimulation		
	P value	Overlap		P value	Overlap		P value	Overlap
Top canonical pathways								
Interferon signalling	9.47×10^{-14}	36.1%—13/36	Granulocyte adhesion and diapedesis	3.18×10^{-17}	18.2%—30/165	Granzyme A signalling	3.53×10^{-06}	23.5%—4/17
Crosstalk between dendritic cells and natural killer cells	2.29×10^{-10}	16.9%—15/89	Agranulocyte adhesion and diapedesis	1.11×10^{-14}	16.0%—28/175	Antigen presentation pathway	3.62×10^{-06}	13.5%—5/37
Granulocyte adhesion and diapedesis	8.07×10^{-10}	11.5%—19/165	Interferon signalling	1.15×10^{-13}	38.9%—14/36	Caveolar-mediated endocytosis signalling	6.12×10^{-06}	8.5%—6/71
T helper cell differentiation	8.75×10^{-10}	18.8%—13/69	Communication between innate and adaptive immune cells	2.58×10^{-12}	22.0%—18/82	Integrin signalling	8.89×10^{-06}	4.2%—9/212
Activation of IRF by cytosolic pattern recognition receptors	1.90×10^{-09}	20.0%—12/60	Altered T cell and B cell signalling in rheumatoid arthritis	3.42×10^{-11}	20.5%—17/83	Cdc42 signalling	1.91×10^{-05}	5.4%—7/129

	P value of overlap	Predicted activation		P value of overlap	Predicted activation		P value of overlap
Top upstream regulators							
IFNG	3.46×10^{-31}	Activated	IFNG	5.09×10^{-62}	Activated	EBI3	6.48×10^{-06}
TLR3	7.38×10^{-28}	Activated	IFNL1	1.33×10^{-60}	Activated	mir-122	9.91×10^{-06}
IFNA2	1.09×10^{-27}	Activated	PRL	1.51×10^{-58}	Activated	TGM2	2.75×10^{-05}
IL1RN	4.90×10^{-27}	Inhibited	MAPK1	1.86×10^{-45}	Inhibited	RFX5	4.28×10^{-05}
PRL	9.67×10^{-27}	Activated	IFNA2	2.07×10^{-45}	Activated	CEBPA	8.03×10^{-05}

	P value	Number of molecules		P value	Number of molecules		P value	Number of molecules
Top diseases and bio functions								
Antimicrobial response	1.33×10^{-16} –1.07×10^{-16}	35	Dermatological diseases and conditions	1.46×10^{-05}–1.75×10^{-32}	269	Dermatological diseases and conditions	1.88×10^{-02}–4.98×10^{-11}	37
Inflammatory response	2.88×10^{-04} –1.07×10^{-16}	131	Organismal injury and abnormalities	1.49×10^{-05}–1.75×10^{-32}	476	Immunological disease	1.37×10^{-02}–4.98×10^{-11}	43
Connective tissue disorders	1.49×10^{-04}–1.19×10^{-16}	79	Connective tissue disorders	2.68×10^{-06}–3.09×10^{-25}	110	Inflammatory disease	1.42×10^{-02}–4.98×10^{-11}	40
Inflammatory disease	1.99×10^{-04}–1.19×10^{-16}	113	Inflammatory disease	1.46×10^{-05}–3.09×10^{-25}	147	Organismal injury and abnormalities	1.90×10^{-02}–4.98×10^{-11}	121
Organismal injury and abnormalities	2.96×10^{-04}–1.19×10^{-16}	343	Skeletal and muscular disorders	1.44×10^{-05}–3.09×10^{-25}	143	Inflammatory response	1.57×10^{-02}–2.58×10^{-10}	50

IRF, interferon regulatory factor; LPS, lipopolysaccharide.

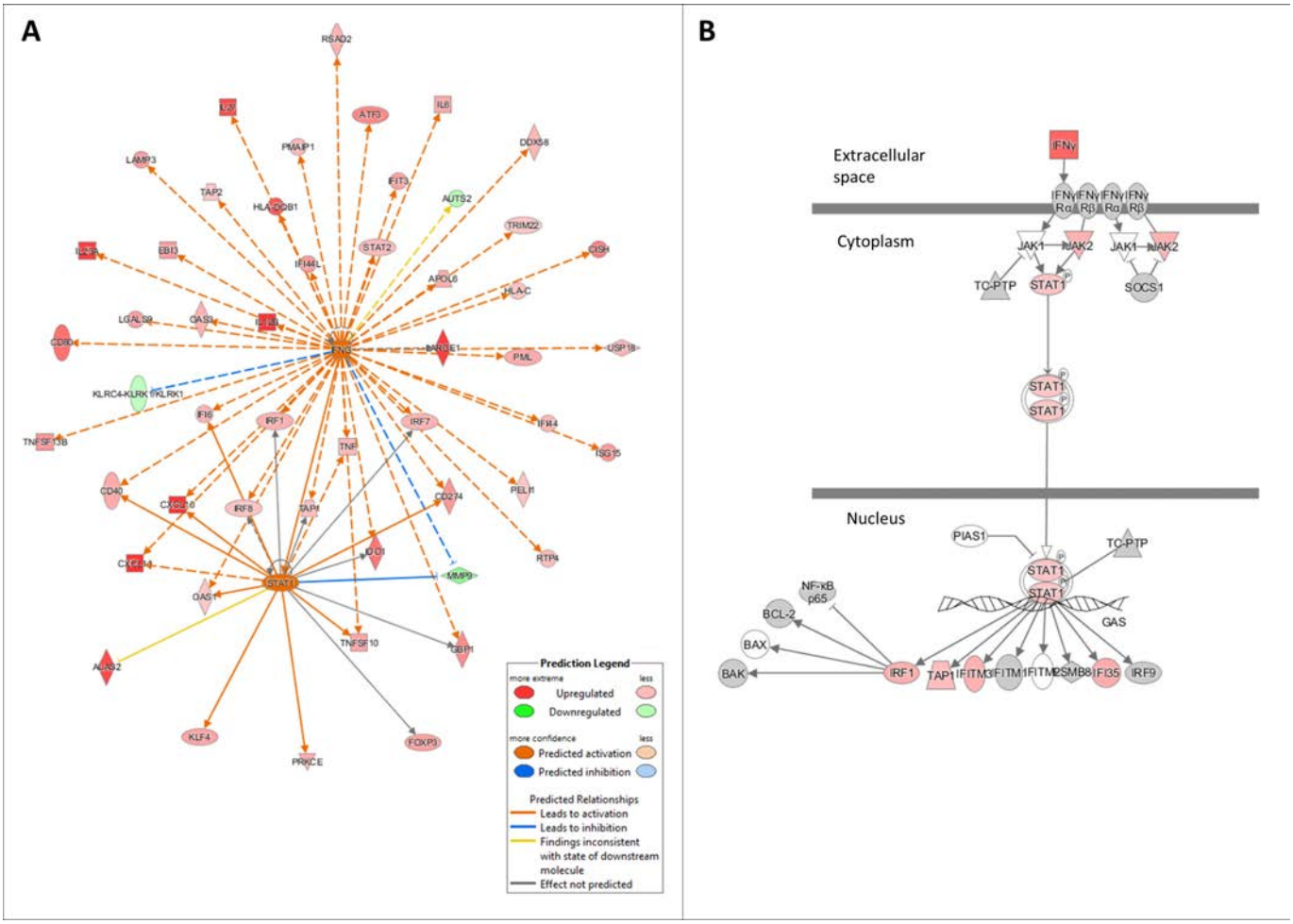

Figure 6 Activation of the interferon-γ/STAT1 pathway. (A) Functional network analysis by IPA using RNAseq data at 3 hour in the activated state. The genes involved in the top scoring pathway (ie, INFγ signalling) and their interaction with the STAT1 pathway are represented. (B) Canonical INFγ signalling pathway. The genes upregulated in the dataset are represented in red. IFN-γ, interferon-γ; IPA, ingenuity pathway analysis.

gene but presenting with opposite phenotypes (symptomatic in S2 vs asymptomatic in S1). By combining exome, transcriptome and proteome data, we uncovered the S2-specific variant p.R241Q in the *STAT1* gene which is central in the regulatory pathway of inflammation mediated by IFN-γ.[18] Differential expression and molecular pathway analyses at both mRNA and protein levels confirmed the key role of *STAT1* in the development of a higher level of IFN-γ mediated inflammation in S2. Finally, the *STAT1* pathway was experimentally shown to be more activated in the presence of the S2-specific *STAT1* variant p.R241Q.

The *STAT1* variant p.R241Q of patient S2 is inherited from her healthy father whose PBMCs' inflammatory response to LPS stimulation is equivalent to that of S2 (table 2). This result suggests that the presence of both the homozygous *MVK* p.V377I mutation and the heterozygous *STAT1* p.R241Q mutation is required to elicit clinical symptoms. The clinical symptoms of patient S2 could therefore be explained by a synergistic effect of *MVK* and *STAT1*.

STAT1 is a key component of the Janus kinase/signal transducer and activator of transcription signalling pathway (JAK/STAT). This pathway is a major signalling route for a wide range of cytokines and growth factors. Its activation stimulates broad cellular functions including cell proliferation, differentiation, migration and apoptosis, which are critical events in key processes such as haematopoiesis or immune response.[19 20] The JAK/STAT signalling is initiated on binding of cytokines to their cognate receptors. As a consequence, the receptors dimerise and phosphorylate JAKs, which in turn phosphorylate the STAT family members. These phosphorylated STATs then form parallel dimers and translocate to the nucleus where they act as transcription factors.[21] Dysregulation of JAK/STAT signalling is involved in a variety of conditions including hyper-IgE syndrome, haematological malignancies, diabetes or yet obesity.[22–24] When considering the transcription factor *STAT1* in particular, the activation of this gene has been observed in a number of inflammatory disorders such as liver inflammation, rheumatoid arthritis or yet cerebral ischaemia.[25–27] Based on these information, the involvement of STAT1 in the pathophysiology of the inflammatory phenotype observed in S2 is possible.

At the genetic level, inborn errors of this gene can be classified into four types[1]: (1) autosomal recessive complete *STAT1* deficiency, (2) autosomal recessive partial *STAT1* deficiency, (3) autosomal dominant STAT1 deficiency and (4) autosomal-dominant gain of *STAT1* activity.[28] The latter category is characterised by an increased activation of STAT1, which is known to be associated with a broad clinical spectrum including inherited infectious diseases (ie, the most common genetic cause of chronic mucocutaneous candidiasis), autoimmune/inflammatory features, carcinomas or yet aneurysms.[29–32] The functional translation of gain of function STAT1 variants is gain of phosphorylation by impairment of

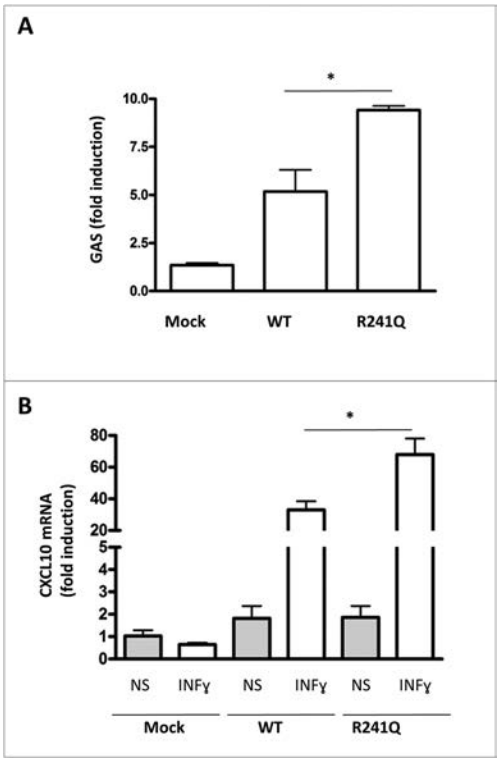

Figure 7 Functional characterisation of the gain-of-function variant R241Q U3A cells were transfected with a mock vector, a WT, or the mutant allele R241Q of STAT1. All experiments were performed at least three times independently. (A) Response to IFN-γ evaluated by luciferase activity of a reporter gene under the control of the GAS (Interferon-Gamma Activated Sequence) promoter. (B) Induction of CXCL10 after stimulation with IFN-γ measured by quantitative RT-PCR. IFN-γ, interferon-γ; WT, wild type.

nuclear dephosphorylation.[29] The heterozygous variant identified in S2 has several attributes to be a new gain of function variant[1]: it is located in the coiled coil domain of the protein, where the vast majority of variants described so far are dominant gain of function mutations[2 28] bioinformatics prediction tools classify the variant as non-deleterious for protein function (online supplementary table S4),[3] an important number of proteins of the STAT1 signalling pathway are upregulated in S2 vs S1,[4] in a cellular model, STAT1 with the p.R241Q variant showed a higher transcriptional activity compared with the wild type protein.

Given the important amount of data linking JAK/STAT signalling to health and disease, this pathway has become an important drug target. Inhibitors of JAKs have notably proven effective in the treatment of myeloproliferative diseases and rheumatoid arthritis.[33 34] STATs are also being investigated as targets using either oligonucleotide-based inhibitors[35] or inhibitory peptides and small interfering RNAs.[36] The results of the present study suggest that targeting the JAK/STAT pathway with approved JAK inhibitors such as tofacitinib or ruxolitinib could be a good therapeutic option to treat patient S2 who is currently under anti-IL1 (Anakinra 100 mg/day) without substantial amelioration.[37]

From a more general point of view, the unique availability of exome, transcriptome and proteome data for the two studied siblings allowed us to refine the common data interpretation strategy. Indeed, database search-driven algorithms used for proteomics data processing rely on exact matching between measured and theoretical sequences. Therefore, the use of personalised protein databases including subject-specific information derived from exome and RNASeq data allows improving proteomics data interpretation both qualitatively and quantitatively.[38] We could even perform allele-specific gene expression analysis up to the protein level. Finally, we were able to identify a significant number of SAAVs with regard to the achieved proteome coverage. Reverse benefits are also noteworthy as, for instance, the ability of RNASeq strategies to identify new splice variants and confirm their expression with proteomics thanks to personalised databases including them, will overall enable improving genome annotation.[39]

Our study has been focused on STAT1 as a unique potential trigger for increased inflammation in patient S2. Although we believe that it is a good candidate based on the results presented here, we cannot exclude other genes and mechanisms such as regulatory elements that could contribute to the observed phenotypic difference between the two siblings. Technically, quantitative data of the proteomics approach would have been more precise with the latest generation mass spectrometers that use an extracted ion chromatogram quantification strategy rather than a spectral count approach that is limited in dynamics and quantitative accuracy.[40] Globally, integration of multilevel datasets improves with the increase in depth of coverage of proteomics data.[41] As observed in other studies, we confirmed that mRNA and protein levels quite poorly correlate.[42–44] In this regard, performing a multilevel study provides a more precise view of the global genome expression profile. Finally, 20 years of technical progress has allowed access to multiomics characterisation at the level of a single patient and its potential to become an

Table 2 Clinical, mutational and inflammatory statuses of the family members

Subject	Clinical status (symptomatic)	*MVK* Homozygous p.V377I variant	*STAT1* Heterozygous p.R241Q variant	TNF-α (pg/mL)*	IL-1β (pg/mL)*	IL-6 (pg/mL)*
Mother	No	No	No	+ (4135±1838)	+ (3995±794)	+ (14642±700)
Subject S1†	No	Yes	No	+ (4804±1251)	+ (3868±709)	+ (18316±1518)
Father	No	No	Yes	++ (8580±1073)	++ (7388±831)	++ (24727±479)
Patient S2†	Yes	Yes	Yes	++ (10437±2804)	++ (5790±743)	++ (24649±1408)

*Peripheral blood mononuclear cells were stimulated with LPS (1 µg/mL) for 6 hours. Cytokine levels in the cell culture supernatant were quantified by ELISA. + and ++ represent the global estimate of concentrations. Values are the mean of at least three experiments±SD. + vs ++ conditions were statistically different for all three cytokines (Mann-Whitney U test $p<0.05$).
†Results from Messer *et al*.[3]
LPS, lipopolysaccharide.

efficient tool for personalised medicine is demonstrated here. However, to transform the proof-of-concept study to a routine application in clinics, a few challenging aspects still need to be improved, including delays in multilevel data generation and processing and the availability of more sophisticated data integration software solutions.

Author affiliations
[1]Laboratoire d'ImmunoRhumatologie Moléculaire, INSERM UMR_S1109, Plateforme GENOMAX, LabEx TRANSPLANTEX, Faculté de Médecine, Université de Strasbourg, Strasbourg, France
[2]Franco-Japanese Nextgen HLA laboratory, Laboratoire International Associé (LIA) INSERM, Nagano, Japan
[3]Fédération Hospitalo-Universitaire OMICARE, Université de Strasbourg, Strasbourg, France
[4]Fédération de Médecine Translationnelle de Strasbourg (FMTS), Université de Strasbourg, Strasbourg, France
[5]Laboratoire d'Immunologie, Plateau Technique de Biologie, Pôle de Biologie, Nouvel Hôpital Civil, Strasbourg, France
[6]Laboratoire de Spectrométrie de Masse BioOrganique, Université de Strasbourg, CNRS, IPHC, UMR 7178, Strasbourg, France
[7]Molecular Immunology Unit, BIOMICA SAS, Strasbourg, France
[8]Service de Rhumatologie, Hôpitaux Civils de Colmar, Colmar, France
[9]Service de Rhumatologie, Centre National de Référence pour les Maladies Autoimmunes Systémiques Rares, Hôpitaux Universitaires de Strasbourg, Strasbourg, France

Acknowledgements We would like to thank Drs Tom Chittenden (WuXiNextCODE, Cambridge, Massachusetts, USA), Sabina Pfister (Novartis, Basel, Switzerland), Amos Bairoch (University of Geneva Medical School, Geneva, Switzerland) and Fabien Campagne (Cornell University, New York City, New York, USA) for critical reading of this manuscript as well as Drs Hans R Waterham (University of Amsterdam, The Netherlands), Nora Benhabiles (CEA, France), Frédéric Bertrand (University of Strasbourg, France) and Myriam Maumy-Bertrand (University of Strasbourg, France) for helpful discussions as well as Dr Zehua Chen (WuXiNextCODE) for the nGOseq.R script. We thank Hilal Palabicak for technical assistance.

Contributors RC, CC and SB designed the study, analysed the data and wrote the manuscript. IA performed statistical analyses. NP analysed NGS data. ASVJ, MR and FD performed mass spectrometry experiments. AP was in charge of RNAseq and exome sequencing. AM, GA, VR and OT performed functional analysis. LM, JS, SC, PG and AVD interpreted data and discussed the results. All authors contributed to the writing and approved the final version of the manuscript.

Funding This work was supported by grants from the Agence Nationale de la Recherche (ANR) (ANR-11-LABX-0070_TRANSPLANTEX), the INSERM (UMR_S 1109) and the Institut Universitaire de France (IUF), all to SB; the French Proteomic Infrastructure (ProFI, ANR-10-INBS-08-03) to CC, SS and AvD; the European regional development fund (European Union) INTERREG V program (project n°3.2 TRIDIAG) to RC and SB; MSD Avenir grant to SB and JS.

Competing interests None declared.

Patient consent Obtained.

Ethics approval Strasbourg University Hospitals institutional review board (immune-based diseases project; DC-2013-1911).

Provenance and peer review Not commissioned; externally peer reviewed.

Data sharing statement The U3A cell line was purchased from ECACC (reference 12021503). The genomic data have been deposited in the NCBI Sequence Read Archive (accession number PRJNA434369). RNAseq data have been deposited in the EMBL-EBI ArrayExpress archive (accession number E-MTAB-6563). The mass spectrometry proteomics data have been deposited to the ProteomeXchange Consortium via the PRIDE partner repository with the dataset identifier PXD009063 and 10.6019/PXD009063.

REFERENCES

1 Haas D, Hoffmann GF. Mevalonate kinase deficiency and autoinflammatory disorders. *N Engl J Med* 2007;356:2671–3.
2 Haas D, Hoffmann GF. Mevalonate kinase deficiencies: from mevalonic aciduria to hyperimmunoglobulinemia D syndrome. *Orphanet J Rare Dis* 2006;1:13.
3 Messer L, Alsaleh G, Georgel P, *et al*. Homozygosity for the V377I mutation in mevalonate kinase causes distinct clinical phenotypes in two sibs with hyperimmunoglobulinaemia D and periodic fever syndrome (HIDS). *RMD Open* 2016;2:e000196.
4 Hasin Y, Seldin M, Lusis A. Multi-omics approaches to disease. *Genome Biol* 2017;18:83.
5 McKenna A, Hanna M, Banks E, *et al*. The genome analysis toolkit: a mapreduce framework for analyzing next-generation DNA sequencing data. *Genome Res* 2010;20:1297–303.
6 Li MX, Gui HS, Kwan JS, *et al*. A comprehensive framework for prioritizing variants in exome sequencing studies of Mendelian diseases. *Nucleic Acids Res* 2012;40:e53.
7 Anders S, Huber W. Differential expression analysis for sequence count data. *Genome Biol* 2010;11:R106.
8 Pham TV, Piersma SR, Warmoes M, *et al*. On the beta-binomial model for analysis of spectral count data in label-free tandem mass spectrometry-based proteomics. *Bioinformatics* 2010;26:363–9.
9 Carapito C, Burel A, Guterl P, *et al*. MSDA, a proteomics software suite for in-depth mass spectrometry data analysis using grid computing. *Proteomics* 2014;14:1014–9.
10 Carapito C, Lane L, Benama M, *et al*. Computational and mass-spectrometry-based workflow for the discovery and validation of missing human proteins: application to chromosomes 2 and 14. *J Proteome Res* 2015;14:3621–34.
11 Law CW, Chen Y, Shi W, *et al*. voom: Precision weights unlock linear model analysis tools for RNA-seq read counts. *Genome Biol* 2014;15:R29.
12 Smyth G. In: Dudoit S, Irizarry R, Huber W, eds. *Bioinformatics and computational biology solutions using R and bioconductor*. New York: Springer, 2005:397–420.
13 Meng C, Kuster B, Culhane AC, *et al*. A multivariate approach to the integration of multi-omics datasets. *BMC Bioinformatics* 2014;15:162.
14 Bady P, Dolédec S, Dumont B, *et al*. Multiple co-inertia analysis: a tool for assessing synchrony in the temporal variability of aquatic communities. *C R Biol* 2004;327:29–36.
15 Chernick MR, F RH. *Introduction biostatistics for the health sciences: modern applications including bootstrap. Wiley series in probability and statistics*. New York, United States: John Wiley and Sons Ltd, 2003:424.
16 Houten SM, van Woerden CS, Wijburg FA, *et al*. Carrier frequency of the V377I (1129G>A) MVK mutation, associated with Hyper-IgD and periodic fever syndrome, in the Netherlands. *Eur J Hum Genet* 2003;11:196–200.
17 Eisen MB, Spellman PT, Brown PO, *et al*. Cluster analysis and display of genome-wide expression patterns. *Proc Natl Acad Sci U S A* 1998;95:14863–8.
18 Rauch I, Müller M, Decker T. The regulation of inflammation by interferons and their STATs. *JAKSTAT* 2013;2:e23820.
19 Darnell JE, Kerr IM, Stark GR. Jak-STAT pathways and transcriptional activation in response to IFNs and other extracellular signaling proteins. *Science* 1994;264:1415–21.
20 Rawlings JS, Rosler KM, Harrison DA. The JAK/STAT signaling pathway. *J Cell Sci* 2004;117:1281–3.
21 Kiu H, Nicholson SE. Biology and significance of the JAK/STAT signalling pathways. *Growth Factors* 2012;30:88–106.
22 Minegishi Y, Karasuyama H. Defects in Jak-STAT-mediated cytokine signals cause hyper-IgE syndrome: lessons from a primary immunodeficiency. *Int Immunol* 2009;21:105–12.
23 Vainchenker W, Constantinescu SN. JAK/STAT signaling in hematological malignancies. *Oncogene* 2013;32:2601–13.
24 Gurzov EN, Stanley WJ, Pappas EG, *et al*. The JAK/STAT pathway in obesity and diabetes. *Febs J* 2016;283:3002–15.
25 Gao B. Cytokines, STATs and liver disease. *Cell Mol Immunol* 2005;2:92–100.
26 Kasperkovitz PV, Verbeet NL, Smeets TJ, *et al*. Activation of the STAT1 pathway in rheumatoid arthritis. *Ann Rheum Dis* 2004;63:233–9.
27 Takagi Y, Harada J, Chiarugi A, *et al*. STAT1 is activated in neurons after ischemia and contributes to ischemic brain injury. *J Cereb Blood Flow Metab* 2002;22:1311–8.
28 Boisson-Dupuis S, Kong XF, Okada S, *et al*. Inborn errors of human STAT1: allelic heterogeneity governs the diversity of immunological and infectious phenotypes. *Curr Opin Immunol* 2012;24:364–78.
29 Liu L, Okada S, Kong XF, *et al*. Gain-of-function human STAT1 mutations impair IL-17 immunity and underlie chronic mucocutaneous candidiasis. *J Exp Med* 2011;208:1635–48.
30 van de Veerdonk FL, Plantinga TS, Hoischen A, *et al*. STAT1 mutations in autosomal dominant chronic mucocutaneous candidiasis. *N Engl J Med* 2011;365:54–61.
31 Toubiana J, Okada S, Hiller J, *et al*. Heterozygous STAT1 gain-of-function mutations underlie an unexpectedly broad clinical phenotype. *Blood* 2016;127:3154–64.
32 Uzel G, Sampaio EP, Lawrence MG, *et al*. Dominant gain-of-function STAT1 mutations in FOXP3 wild-type immune dysregulation-polyendocrinopathy-enteropathy-X-linked-like syndrome. *J Allergy Clin Immunol* 2013;131:1611–23.

33 Hodge JA, Kawabata TT, Krishnaswami S, *et al*. The mechanism of action of tofacitinib - an oral Janus kinase inhibitor for the treatment of rheumatoid arthritis. *Clin Exp Rheumatol* 2016;34:318–28.
34 Sonbol MB, Firwana B, Zarzour A, *et al*. Comprehensive review of JAK inhibitors in myeloproliferative neoplasms. *Ther Adv Hematol* 2013;4:15–35.
35 Sen M, Grandis JR. Nucleic acid-based approaches to STAT inhibition. *JAKSTAT* 2012;1:285–91.
36 Miklossy G, Hilliard TS, Turkson J. Therapeutic modulators of STAT signalling for human diseases. *Nat Rev Drug Discov* 2013;12:611–29.
37 Aittomäki S, Pesu M. Therapeutic targeting of the Jak/STAT pathway. *Basic Clin Pharmacol Toxicol* 2014;114:18–23.
38 Nesvizhskii AI. Proteogenomics: concepts, applications and computational strategies. *Nat Methods* 2014;11:1114–25.
39 Marx H, Hahne H, Ulbrich SE, *et al*. Annotation of the Domestic Pig Genome by Quantitative Proteogenomics. *J Proteome Res* 2017;16:2887–98.
40 Ramus C, Hovasse A, Marcellin M, *et al*. Benchmarking quantitative label-free LC-MS data processing workflows using a complex spiked proteomic standard dataset. *J Proteomics* 2016;132:51–62.
41 Mitchell CJ, Getnet D, Kim MS, *et al*. A multi-omic analysis of human naïve CD4+ T cells. *BMC Syst Biol* 2015;9:75.
42 Zhang B, Wang J, Wang X, *et al*. Proteogenomic characterization of human colon and rectal cancer. *Nature* 2014;513:382–7.
43 Gry M, Rimini R, Strömberg S, *et al*. Correlations between RNA and protein expression profiles in 23 human cell lines. *BMC Genomics* 2009;10:365.
44 Edfors F, Danielsson F, Hallström BM, *et al*. Gene-specific correlation of RNA and protein levels in human cells and tissues. *Mol Syst Biol* 2016;12:883.

Three months of once-weekly isoniazid plus rifapentine (3HP) in treating latent tuberculosis infection is feasible in patients with rheumatoid arthritis

Tuberculosis (TB) remains a major public health issue: an estimated 10.4 million people developed TB disease and 1.4 million died from it in 2015.[1] TB risk was 2.28-fold greater in patients with rheumatoid arthritis (RA) compared with controls,[2] and even higher in those receiving biologic therapy.[3] Guidelines have recommended that latent TB infection (LTBI) screening should be performed and prophylactic therapy be initiated if LTBI exists.[4] Consequently, completion of LTBI treatment is essential for TB control in such patients.

The long therapeutic period and hepatotoxicity are barriers to completing 9-month daily isoniazid (9H) treatment,[5] the standard LTBI therapy. Recently, implementing 3-month once-weekly isoniazid plus rifapentine (3HP) by directly observed therapy effectively prevented TB and increased treatment adherence.[6] However, 3HP regimen has not been assessed for treating LTBI in RA.

Among 188 patients who fulfilled the 2010 RA classification criteria and were scheduled to receive biologics between January 2015 and December 2017, we consecutively enrolled 44 patients with LTBI (table 1), defined as QuantiFERON-TB Gold In-Tube positive result without TB disease (CE15286B). The participants underwent monthly follow-up monitoring of drug adherence and adverse events using common toxicity criteria.[7] The primary outcome was the treatment completion rates evaluated among 21 patients receiving 3HP and 23 receiving 9H, respectively, and the second outcome was the effective TB prevention or cost-effectiveness. Medication cost was the sum of cost of HP for 3 months or isoniazid for 9 months. The cost-effectiveness of one TB case avoided was also calculated.

Although not reaching statistical significance, a higher completion rate was observed in 3HP-treated patients compared with 9H

Table 1 Demographic data and characteristics of patients with RA who received the 3-month isoniazid/rifapentine (3HP) or 9-month isoniazid (9H) regimen

	3HP (n=21)	9H (n=23)
Mean age at study entry (years)	62.1±14.9	62.0±10.5
Female proportion	15 (71.4%)	15 (65.2%)
RF positivity at baseline	17 (81.0%)	16 (69.6%)
ACPA positivity at baseline	16 (76.2%)	14 (61.0%)
ESR (mm/first hour) at baseline	32.7±26.6	36.3±21.3
BCG vaccination	18 (85.7%)	19 (82.6%)
Daily steroid dose (mg) at baseline	5.8±2.3	6.0±1.8
Concomitant DMARDs at baseline		
Methotrexate	17 (81.0%)	19 (82.6%)
Sulfasalazine	16 (76.2%)	18 (78.3%)
Hydroxychloroquine	16 (76.2%)	16 (69.6%)
Biologics used after prophylactic Rx		
Adalimumab	9 (42.9%)	9 (39.2%)
Etanercept	3 (14.3%)	6 (26.1%)
Golimumab	3 (14.3%)	3 (13.0%)
Tocilizumab	3 (14.3%)	2 (8.7%)
Tofacitinib	3 (14.3%)	3 (13.0%)
Comorbidities		
Hypertension	7 (33.3%)	8 (34.8%)
Diabetes mellitus	2 (9.5%)	2 (8.7%)
Anaemia (<10.0 g/dL)	1 (4.8%)	2 (8.7%)

Values are mean±SD or the number (%) of patients.
ACPA, anti-cyclic citrullinated peptide antibodies; DMARD, disease-modifying antirheumatic drug; ESR, erythrocyte sedimentation rate; RA, rheumatoid arthritis; RF, rheumatoid factor.

Table 2 The treatment outcomes and adverse effects of therapy with 3-month isoniazid/rifapentine (3HP) or 9-month isoniazid (9H) in patients with rheumatoid arthritis

	3HP (n=21)	9H (n=23)
Treatment completion		
Completion	19 (90.5%)	18 (78.3%)
Non-completion	2 (9.5%)	5 (21.7%)
Reason for non-completion		
Adverse effects	2 (9.5%)	2 (8.7%)
Refusal of continuation	0 (0.0%)	2 (8.7%)
Lost follow-up	0 (0.0%)	1 (4.3%)
Adverse effects		
Flu-like symptoms*		
Grade 1 or 2	0 (0.0%)	0 (0.0%)
Grade 3	1 (4.8%)	0 (0.0%)
Grade 4	1 (4.8%)	0 (0.0%)
Cutaneous reaction†		
Grade 1 or 2	2 (9.5%)	1 (4.3%)
Grade 3	0 (0.0%)	0 (0.0%)
Grade 4	0 (0.0%)	0 (0.0%)
Gastrointestinal symptoms‡		
Grade 1 or 2	1 (4.8%)	0 (0.0%)
Grade 3	0 (0.0%)	0 (0.0%)
Grade 4	0 (0.0%)	0 (0.0%)
Hepatotoxicity§		
Grade 1 or 2	0 (0.0%)	2 (8.7%)
Grade 3	0 (0.0%)	0 (0.0%)
Grade 4	0 (0.0%)	0 (0.0%)
TB development		
Completion of LTBI Rx	0/19 (0.0%)	0/18 (0.0%)
Non-completion of LTBI Rx	0/2 (0.0%)	0/5 (0.0%)¶
Cost-effectiveness		
Medication costs for LTBI per patient	US$219.2	US$24.3
Labour costs for LTBI per patient**	US$42	US$693
Medication and labour cost per patient	US$261.2	US$717.3
Cases estimated to become active TB††	1	1
Cases actually become active TB	0	0
Cost for one TB case avoided	US$5485.2	US$16 497.9

*Presence of fever, chills, general malaise, muscle pain, palpitations (heart rate >100/min) or other flu-like symptoms.
†Presence of rashes, itching, urticaria, angioedema or even anaphylaxis that occurred within 24 hours of the medication used.
‡Presence of vomiting, diarrhoea or abdominal pain that occurred within 24 hours of the medication used.
§Presence of a threefold or more increase in alanine transaminase (ALT) that exceeded the upper limit of normal (ULM, 50 U/L) or increased bilirubin more than twofold of ULM.
¶Three patients who discontinued isoniazid therapy earlier did not receive biologic therapy.
**The labour costs were calculated according to Taiwanese Labor Law, minimum hourly wages US$3.5, and normally DOTS spend an hour for one patient.
††One TB case avoided when 20 LTBI cases treated.
DOTS, directly observed treatment short-court; LTBI, latent TB infection; TB, tuberculosis.

treatment group (90.5% vs 78.3%, (table 2)), similar to previous reports showing a high adherence to 3HP treatment.[6 8] Non-completion was observed in two (9.5%) of 3HP-treated patients because of severe flu-like symptoms: both patients were female and of age >60 years, consistent with previous studies showing that female gender and increased age were risk factors for flu-like symptoms in 3HP-treated subjects.[9] In contrast, five (21.7%) of 9H-treated patients failed to complete treatment due to liver dysfunction (n=2), refusal to receive long-term therapy (n=2) and lost follow-up (n=1).

None of 3HP-treated or 9H-treated patients developed TB at least 1 year after completion of LTBI treatment. Among patients without completion of treatment, two started with 3HP but then switched to 9H as described earlier, two started with 9H but switched to rifampin due to liver dysfunction, and the other three refused any LTBI or biologic therapy. Nevertheless, none of them developed TB during 2-year follow-up period. Similar to a previous report,[10] the cost-effectiveness ratio for 3HP was US$5485.2 per TB case avoided, compared with US$16 497.9 per TB case avoided for 9H in patients with RA receiving biologic therapy.

In conclusion, we demonstrated that implementing 3HP regimen is feasible for treating LTBI in patients with RA receiving biologic therapy. The administration of 3HP might be more favourable than 9H due to the higher treatment completion rate and better cost-effectiveness. However, severe flu-like symptoms may remain its major barrier, leading to early discontinuation of 3HP therapy.

Yi-Ming Chen,[1,2,3] Tsai-Ling Liao,[1,2] Hsin-Hua Chen,[1,2,3] Der-Yuan Chen[4,5,6]

[1]Department of Medical Research, Taichung Veterans General Hospital, Taichung, Taiwan
[2]Institute of Biomedical Science and Rong Hsing Research Center for Translational Medicine, National Chung Hsing University, Taichung, Taiwan
[3]Faculty of Medicine, National Yang Ming University, Taichung, Taiwan
[4]Department of Medicine, Rheumatology and Immunology Center, China Medical University Hospital, Taichung, Taiwan
[5]Department of Medical Research, Rheumatic Diseases Research Center, China Medical University Hospital, Taichung, Taiwan
[6]School of Medicine, China Medical University, Taichung, Taiwan

Correspondence to Professor Der-Yuan Chen, Department of Medicine, Rheumatology and Immunology Center, China Medical University Hospital, Taichung 40447, Taiwan; dychen1957@gmail.com

Handling editor Josef S Smolen

Acknowledgements We thank the Biostatistics Task Force of Taichung Veterans General Hospital.

Contributors YMC conceived and designed the study, acquired clinical data, conducted data analysis, and drafted and revised the manuscript. TLL and HHC conceived the study, acquired clinical data, conducted data analysis and drafted the manuscript. DYC generated the original hypothesis, conceived and designed the study, acquired clinical data, conducted data analysis, and drafted and revised the manuscript.

Funding This study was supported by a grant from the National Science Council, Taiwan (NSC-100-2321-B-075A-001) and a grant from Taichung Veterans General Hospital, Taiwan (TCVGH-993804C).

Competing interests None declared.

Patient consent Obtained.

Ethics approval The Ethics Committee of Clinical Research, Taichung Veterans General Hospital.

Provenance and peer review Not commissioned; externally peer reviewed.

Received 23 January 2018
Revised 22 March 2018
Accepted 2 April 2018
Published Online First 19 April 2018

Ann Rheum Dis 2018;**77**:1688–1689. doi:10.1136/annrheumdis-2018-213097

REFERENCES

1 WHO. Global tuberculosis report. 20th edition. 2016 http://www.who.int/tb/publications/global_report/en/
2 Liao TL, Lin CH, Shen GH, *et al*. Risk for mycobacterial disease among patients with rheumatoid arthritis, Taiwan, 2001-2011. *Emerg Infect Dis* 2015;21:1387–95.
3 Arkema EV, Jonsson J, Baecklund E, *et al*. Are patients with rheumatoid arthritis still at an increased risk of tuberculosis and what is the role of biological treatments? *Ann Rheum Dis* 2015;74:1212–7.
4 Carmona L, Gómez-Reino JJ, Rodríguez-Valverde V, *et al*. Effectiveness of recommendations to prevent reactivation of latent tuberculosis infection in patients treated with tumor necrosis factor antagonists. *Arthritis Rheum* 2005;52:1766–72.
5 Centers for Disease Control and Prevention. Targeted tuberculin testing and treatment of latent tuberculosis infection. *MMWR Morb Mortal Wkly Rep* 2000;49:1–54.
6 Sterling TR, Villarino ME, Borisov AS, *et al*. Three months of rifapentine and isoniazid for latent tuberculosis infection. *N Engl J Med* 2011;365:2155–66.
7 EORTC. Common toxicity criteria version 2.0. Bethesda MD: Cancer Therapy Evaluation Program, 1999. http://www.eortc.be/services/doc/ctc/ctcv20_4-30-992.pdf
8 Sandul AL, Nwana N, Holcombe JM, *et al*. High rate of treatment completion in program settings with 12-dose weekly isoniazid and rifapentine (3hp) for latent *Mycobacterium tuberculosis* infection. *Clin Infect Dis* 2017;65:1085–93.
9 Sterling TR, Moro RN, Borisov AS, *et al*. Flu-like and other systemic drug reactions among persons receiving weekly rifapentine plus isoniazid or daily isoniazid for treatment of latent tuberculosis infection in the PREVENT Tuberculosis Study. *Clin Infect Dis* 2015;61:527–35.
10 Huang YW, Yang SF, Yeh YP, *et al*. Impacts of 12-dose regimen for latent tuberculosis infection: treatment completion rate and cost-effectiveness in Taiwan. *Medicine* 2016;95:34.

To cite Chen Y-M, Liao T-L, Chen H-H, *et al*. *Ann Rheum Dis* 2018;**77**:1688–1689.

Quantitative imaging of inflammatory disease: are we missing a trick?

The role of conventional *qualitative* MRI is well established in the management of spondyloarthritis for assessment of inflammation and structural damage. The identification of a 'positive' MRI is now an important component of diagnostic pathways in spondyloarthritis.[1] The role of q*uantitative* MRI (QMRI) is less established but offers the potential for *direct measurement* of disease characteristics. This approach is yielding huge benefits in fields such as oncology and neurology, where quantifiable measurements can be used to identify, stage and monitor disease. Given the influence that radiological assessment of disease burden has on treatment decisions, we argue that a quantitative imaging approach should be rigorously explored as a tool for assessment of inflammation in musculoskeletal imaging.

Typically for QMRI, a model is fitted to a series of images to yield maps of a defined physical characteristic of the tissue. Assessment can then take the form of a measurement rather than image interpretation. With the correct methodology, this can reduce operator dependence and the potential for bias and imprecision. One methodological challenge is defining regions of interest. However, with the use of more sophisticated analyses, including machine learning techniques, there is potential to automate these processes, putting objective quantitative information, informing on tissue pathology, directly into the hands of the treating physician. These methods could increase the sensitivity of imaging for diagnosis and monitoring of disease activity, while analysis of large quantitative datasets using 'big data' approaches may help the understanding of disease phenotype.[2]

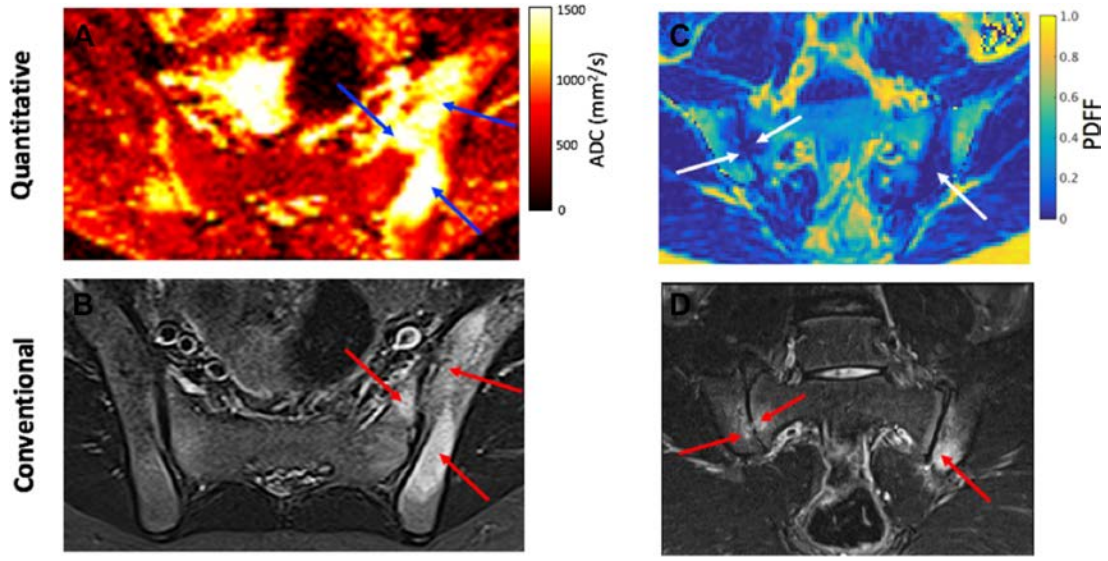

Figure 1 Examples of quantitative MRI. (A) ADC map showing increased ADC in areas of bone marrow oedema, corresponding to the increase in signal shown on the conventional MRI (short tau inversion recovery (STIR) image) (B). (C) FF map showing reduced FF in areas of oedema, corresponding to the areas of increased signal on the conventional STIR MRI (D). ADC, apparent diffusion coefficient; FF, fat fraction; PDFF, proton density fat fraction.

Recently, several groups have explored specific quantitative imaging biomarkers (QIBs) in spondyloarthritis, focusing on the sacroiliac joints, which are particularly difficult to assess clinically. Diffusion-weighted imaging has been used to generate *apparent diffusion coefficient (ADC)* maps (figure 1A), where the brightness of each pixel indicates the freedom with which water molecules diffuse[3 4] ADC is increased in areas of bone marrow oedema, likely due to increased water content and the size of the extracellular space in inflammatory exudates[3 4] and has been shown to be sensitive to treatment response with biologic therapy.[5] Similarly, measurement of fat fraction (FF; the proportion of the total MRI signal derived from fat) (figure 1B) can distinguish active inflammation (causing increased water content and a reduction in fat content) from chronic inflammation/damage (causing increased fat content known as fat metaplasia).[6] FF measurements in bone marrow are highly reproducible, and their accuracy can be readily assessed using specifically designed imaging phantoms.[6] Another parameter, R2*, can often be extracted from the same model used to calculate FF and is relatable to bone mineral density and therefore new bone formation.[5] Undoubtedly, new QIBs will continue to emerge, and the combination of appropriate QIBs (multiparametric assessment) is likely to facilitate understanding of the inflammatory process.

Despite the huge potential of QMRI, quantitative imaging research into inflammatory diseases is at an early stage. There are several issues that require addressing before these techniques can transition into clinical care, including standardisation of data acquisition and interpretation. Furthermore, QMRI techniques are subject to false-positive findings, similar to those in conventional imaging. Imaging methods in rheumatology are lagging behind those used in oncology and neurology, despite the dramatic advances made in the treatment of inflammatory diseases. If quantitative imaging is to be successful in this field, there will need to be a concerted effort to coordinate research into potential QIBs and to undertake prospective studies validating these biomarkers. We would urge the rheumatological community to engage with these techniques to drive them towards clinical implementation, aiming to improve management and to achieve a more tailored approach to therapy for patients with arthritis.

Margaret A Hall-Craggs,[1] Timothy P J Bray,[1] Alan P Bainbridge[2]

[1]Centre for Medical Imaging, University College London, London, UK
[2]Department of Medical Physics, University College Hospitals Trust, London, UK

Correspondence to Professor Margaret A Hall-Craggs, Centre for Medical Imaging, London W1W 7EJ, UK; hallcraggs@gmail.com, margaret.hall-craggs@nhs.net

Handling editor Josef S Smolen

Contributors All authors contributed to the intellectual ideas, preparation, writing and correction and final approval of the submitted letter.

Funding The authors have not declared a specific grant for this research from any funding agency in the public, commercial or not-for-profit sectors.

Competing interests None declared.

Patient consent Not required.

Provenance and peer review Not commissioned; externally peer reviewed.

To cite Hall-Craggs MA, Bray TPJ, Bainbridge AP. *Ann Rheum Dis* 2018;**77**:1689–1691.

Received 18 April 2018
Revised 23 May 2018
Accepted 5 June 2018
Published Online First 16 June 2018

Ann Rheum Dis 2018;**77**:1689–1691. doi:10.1136/annrheumdis-2018-213614

REFERENCES

1 Rudwaleit M, Jurik AG, Hermann KG, *et al*. Defining active sacroiliitis on magnetic resonance imaging (MRI) for classification of axial spondyloarthritis: a consensual approach by the ASAS/OMERACT MRI group. *Ann Rheum Dis* 2009;68:1520–7.
2 Andreu-Perez J, Poon CC, Merrifield RD, *et al*. Big data for health. *IEEE J Biomed Health Inform* 2015;19:1193–208.
3 Bozgeyik Z, Ozgocmen S, Kocakoc E. Role of diffusion-weighted MRI in the detection of early active sacroiliitis. *AJR Am J Roentgenol* 2008;191:980–6.
4 Vendhan K, Bray TJ, Atkinson D, *et al*. A diffusion-based quantification technique for assessment of sacroiliitis in adolescents with enthesitis-related arthritis. *Br J Radiol* 2016;89:20150775.
5 J P Bray T, Vendhan K, Ambrose N, *et al*. Diffusion-weighted imaging is a sensitive biomarker of response to biologic therapy in enthesitis-related arthritis. *Rheumatology* 2017;56:399–407.

6 Bray TJP, Bainbridge A, Punwani S, *et al*. Simultaneous Quantification of Bone Edema/Adiposity and Structure in Inflamed Bone Using Chemical Shift-Encoded MRI in Spondyloarthritis. *Magn Reson Med* 2018;79:1031–42.

Imputation-based analysis of *MICA* alleles in the susceptibility to ankylosing spondylitis

Ankylosing spondylitis (AS) susceptibility is strongly correlated with genetic variation within the major histocompatibility complex (MHC), and the class I *HLA-B*27* allele confers the major genetic risk factor to AS.[1] Furthermore, strong evidence for additional alleles in the MHC has been observed which affect susceptibility independently from the *HLA-B*27* allele, either by direct genotyping in candidate gene studies[2] or through large-scale imputation-driven association studies.[3 4] We have previously identified variants in both class I and II which affect susceptibility to AS through imputation of classical HLA alleles.[4]

The *MICA* gene is encoded 46 kbps from *HLA-B* and previous studies have reported genetic variants within this locus to affect susceptibility to AS and other inflammatory diseases.[5] In particular, in Annals of Rheumatic Diseases, Zhou *et al*[6] evaluated the association of *MICA* variants with susceptibility to AS in cohorts from North America and China. This study found that the allele *MICA*007:01* was strongly associated with risk of AS independently of *HLA-B*27*, with an association observed in the *HLA-B27*-negative cohort (US cohort OR=9.12, $p=4.28\times10^{-8}$; Chinese cohort OR=42.2, $p=9.35\times10^{-7}$). Weak protective associations with other *MICA* alleles were noted, likely because of the over-representation of the risk allele *MICA*007:01*.

Having previously observed extremely strong linkage disequilibrium (LD) between *HLA-B* and *MICA* single nucleotide polymorphisms (SNPs),[1] we sought to independently test this report. We performed imputation of alleles in the *MICA* gene using a large reference panel of 1046 psoriatic arthritis individuals of European ancestry[7] and assessed the evidence of association of *MICA* alleles controlling for susceptibility *HLA-B* alleles. We successfully imputed *HLA-B* and *MICA* alleles in 9429 AS cases and 13 459 controls of European ancestry from the IGAS cohort[3] genotyped using the Illumina Immunochip SNP microarray.[8] Within the *MICA* locus, we observed 14 distinct alleles where *MICA*008:01* was observed to be the most common with an allele frequency of 50%. We performed association analysis at *HLA-B* and *MICA* imputed alleles with logistic regression controlling for the *HLA-B*27* allele and 10 principal components from a genome-wide analysis to control for population structure.

In our study, we imputed the *MICA*007* allele with high confidence (imputation performed in batches, all $r^2>0.85$, mean $r^2=0.90$) and genotypes were confirmed by Sanger sequencing of exons 2, 3, 4 and 5 of the *MICA* gene with perfect accuracy in 7 *MICA*007* homozygote individuals and 5 non-carriers of the *MICA*007* allele. We observed no association with *MICA*007* after controlling for the effect of *HLA-B*27* ($p>0.05$). We also observed that the *HLA-B*27* and the *MICA*007* alleles are in high LD ($r^2=0.66$ in controls, $r^2=0.52$ in cases, $r^2=0.53$ in the reference imputation panel).

No association was observed between *MICA*007* and AS in either *HLA-B*27* negative subjects (1669 cases, 12 263 controls) (OR=1.32, p=0.07) or *HLA-B*27* positive subjects (7760 cases, 1196 controls) (OR=1.04, p=0.34), and our study had over 80% power to detect an association with *MICA*007* in both *HLA-B*27* negative and positive analyses given the study sample size and the effect size previously reported for *MICA*007* (OR=9). To assess whether heterogeneity of the different populations could have affected these findings, the analysis was repeated in the relatively homogenous UK population alone (n=4198 cases, 9611 controls). The findings were similar in *HLA-B*27* positive subjects (p=0.89) and in *HLA-B*27* negative subjects (p=0.53).

In this study, we found no evidence of association between the *MICA*007* allele and AS susceptibility in a large cohort of European ancestry. Given the sample size in *the HLA-B*27* negative cohort, we had 80% power to identify an independent effect of *MICA*007* with an effect size of at least 1.55. We identified strong LD between *HLA-B*27* and *MICA*007* potentially explaining previously reported associations with this allele.

Adrian Cortes,[1,2] Dafna Gladman,[3] Soumya Raychaudhuri,[4] Jing Cui,[4] Lawrie Wheeler,[5] Matthew A Brown,[5] International Genetics of Ankylosing Spondylitis Consortium (IGAS)

[1]Oxford Centre for Neuroinflammation, Nuffield Department of Clinical Neurosciences, Division of Clinical Neurology, John Radcliffe Hospital, University of Oxford, Oxford, UK
[2]Wellcome Trust Centre for Human Genetics, University of Oxford, Oxford, UK
[3]Toronto Western Hospital, University of Toronto, Toronto, Ontario, Canada
[4]Department of Medicine, Brigham and Women's Hospital, Boston, Massachusetts, USA
[5]Institute of Health and Biomedical Innovation, School of Biomedical Sciences, Queensland University of Technology (QUT) at Translational Research Institute, Brisbane, Queensland, Australia

Correspondence to Professor Matthew A Brown, Institute of Health and Biomedical Innovation, School of Biomedical Sciences, Queensland University of Technology (QUT) at Translational Research Institute, Brisbane, Queensland 4102, Australia; matt.brown@qut.edu.au

Handling editor Josef S Smolen

Acknowledgements We thank all participating subjects with ankylosing spondylitis and healthy individuals who provided the DNA and clinical information necessary for this study.

Collaborators International Genetics of Ankylosing Spondylitis (IGAS) Consortium: Paul Bowness, Paul Wordsworth: NIHR Oxford Musculoskeletal Biomedical Research Unit, Nuffield Orthopaedic Centre, Headington, Oxford, UK; Maxime Breban: INSERM UMR 1173, Université de Versailles Saint Quentin en Yvelines, Laboratoire d'excellence Inflamex, Saint-Quentn-En-Yvelines, France; Matthew Brown: School of Biomedical Sciences, Queensland University of Technology, Brisbane, Australia; Robert Colbert: National Institute of Arthritis and Musculoskeletal and Skin Diseases, NIH, Bethesda, Maryland, USA; Adrian Cortes: Nuffield Department of Clinical Neurosciences, University of Oxford, Oxford, UK; Bart Crusius: Department of Medical Microbiology and Infection Control, Laboratory of Immunogenetics, VU University Medical Center, Amsterdam, The Netherlands; Jing Cui, Soumya Raychaudhuri: Department of Medicine, Brigham and Women's Hospital, Boston, MA, USA; Dirk Elewaut: Department of Rheumatology, Gent University Hospital, Gent, Belgium; David Evans: University of Queensland Diamantina Institute, Princess Alexandra Hospital, Brisbane, Australia; Øystein Førre: Department of Rheumatology, Oslo University Hospital, and University of Oslo, Oslo, Norway; Dafna Gladman: Division of Rheumatology, University of Toronto, Toronto, Canada; Nigil Haroon, Robert Inman: Division of Rheumatology, Toronto Western Hospital, University of Toronto, Toronto, Canada; Benedicte Lie: Department of Medical Genetics, University of Oslo and Oslo University Hospital, Oslo, Norway; Carlos Lopez-Larrea: Department of Immunology, Hospital Universitario Central de Asturias, Oviedo, Spain; Walter Maksymowych: Department of Medicine, University of Alberta, Alberta, Canada; Javier Martin: Instituto de Parasitología y Biomedicina López-Neyra, Consejo Superior de Investigaciones-Científicas, Granada, Spain; Hans Nossent: School of Medicine, University of Western Australia, Perth, Australia Proton Rahman: Memorial University of Newfoundland, Newfoundland, Canada; John Reveille: Department of Rheumatology and Clinical Immunogenetics, University of Texas Health Science Center at Houston, Houston, Texas, USA; Fernando Santos: Chronic Diseases Research Centre (CEDOC), Faculdade de Ciências Médicas, Universidade Nova de Lisboa, Lisboa, Portugal; Simon Stebbings: Department of Medicine, Dunedin School of Medicine, University of Otago, Dunedin, New Zealand; Jaakko Tuomilehto: Department of Chronic Disease Prevention, National Institute for Health and Welfare, Helsinki, Finland; Rafael Valle-Oñate: Spondyloarthropaty Group-Division of Rheumatology, Hospital Militar Central/Universidad de La Sabana, Bogotá,

NA, Colombia; Irene van der Horst-Bruinsma: Department of Rheumatology, VU University Medical Centre, Amsterdam, Netherlands; Michael Weisman: Department of Medicine/Rheumatology, Cedars-Sinai Medical Center, Los Angeles, California, USA.

Contributors All authors contributed to the design and/or acquisition and analysis of data. All authors drafted or reviewed the manuscript critically and gave final approval for the version submitted. All authors agree to be accountable for all aspects of the submitted work.

Funding This research received no specific grant from any funding agency in the public, commercial or not-for-profit sectors.

Competing interests None declared.

Patient consent Not required.

Provenance and peer review Not commissioned; externally peer reviewed.

Data sharing statement Data will be made available on reasonable request.

To cite Cortes A, Gladman D, Raychaudhuri S, *et al*. *Ann Rheum Dis* 2018;**77**:1691–1692.

Received 13 March 2018
Accepted 16 April 2018
Published Online First 28 April 2018

Ann Rheum Dis 2018;**77**:1691–1692. doi:10.1136/annrheumdis-2018-213413

REFERENCES

1 Evans DM, Spencer CC, Pointon JJ, *et al*. Interaction between ERAP1 and HLA-B27 in ankylosing spondylitis implicates peptide handling in the mechanism for HLA-B27 in disease susceptibility. *Nat Genet* 2011;43:761–7.
2 Li Z, Brown MA. Progress of genome-wide association studies of ankylosing spondylitis. *Clin Transl Immunology* 2017;6:e163.
3 Cortes A, Hadler J, Pointon JP, *et al*. Identification of multiple risk variants for ankylosing spondylitis through high-density genotyping of immune-related loci. *Nat Genet* 2013;45:730–8.
4 Cortes A, Pulit SL, Leo PJ, *et al*. Major histocompatibility complex associations of ankylosing spondylitis are complex and involve further epistasis with ERAP1. *Nat Commun* 2015;6:7146.
5 Wang Q, Zhou X. Associations of MICA Polymorphisms with Inflammatory Rheumatic Diseases. *Open Rheumatol J* 2015;9:94–100.
6 Zhou X, Wang J, Zou H, *et al*. MICA, a gene contributing strong susceptibility to ankylosing spondylitis. *Ann Rheum Dis* 2014;73:1552–7.
7 Okada Y, Han B, Tsoi LC, *et al*. Fine mapping major histocompatibility complex associations in psoriasis and its clinical subtypes. *Am J Hum Genet* 2014;95:162–72.
8 Cortes A, Brown MA. Promise and pitfalls of the Immunochip. *Arthritis Res Ther* 2011;13:101.

Lymphocyte changes and vaccination response in a child exposed to belimumab during pregnancy

Apart from animal studies,[1] no human studies exist to document the transfer of belimumab (BEL) to the fetus and immunological alterations caused in the neonate.[2] We report the case of a mother treated with BEL for systemic lupus erythematosus (SLE) both before and during pregnancy and present the immunological changes observed in the child at birth and during 7 months of follow-up.

CASE REPORT

A 29-year-old woman with SLE from 2005 with arthritis and lupus skin disease. During her first pregnancy in 2005–2006, she had a severe flare of lupus with pericarditis and glomerulonephritis, hypertension and premature delivery at week 33. She recovered under therapy with prednisone, azathioprine (AZA; started after a normal thiopurine S-methyltransferase (TPMT) gen test) and hydroxychloroquine (HCQ), and experienced no relapse of lupus nephritis under continued triple therapy.

In 2013, she developed severe lupus skin disease that did not respond to AZA, HCQ and prednisone. AZA was discontinued and methotrexate (MTX) initiated, but despite increasing doses to 25 mg/week symptoms were not controlled. BEL (10 mg/kg/month) was started in April 2014 and symptoms improved. Prednisone dose and MTX dose could be reduced.

After achieving remission, the patient wanted a second child. Treatment options during pregnancy were discussed with her. MTX was withdrawn, therapy with AZA 75 mg × 2 restarted, HCQ 400 mg/day and BEL monthly continued during pregnancy to prevent lupus flares.

The patient got the last infusion of BEL at gestational week 26. She experienced no complications during pregnancy, had no lupus flare and delivered a healthy boy at week 40. Because of sustained remission, BEL was not restarted after delivery, but the patient continued her standard medication. The child was breast fed for 8 months, he developed normally and did not suffer any serious infection during the first year of life.

The child received one shot of rotavirus vaccination 6 weeks after birth. At 3 and 5 months of age, the child received diphtheria–tetanus–pertussis, haemophilus and pneumococcus vaccination with a high anti-pneumococcus titre at 7 months. The lymphocyte profile of mother and child and in three cord blood samples of term neonates is shown in table 1.

Our report is the first to show immunological changes in a newborn exposed to BEL in utero with marked B-cell depletion at birth, a finding similar to cynomolgus monkeys showing transplacental passage of BEL with decreased B-cell numbers in peripheral blood of mothers and infants with full recovery on cessation of exposure.[1] Despite having stored frozen serum samples, this indirect proof of transplacental passage could not be confirmed by measurement of BEL in serum due to unavailability of a laboratory test.

Compared with non-exposed neonates, the child had reduced T-cell subsets at birth though values still were well within adult reference values. Whether the lymphopenia resulted from maternal use of AZA or from the combination with BEL cannot be answered.

Treatment with BEL resulted in a significant reduction of B-cell numbers in the mother over the entire study period, even 10 months after discontinuation of BEL, whereas $CD3^+$, $CD4^+$ and $CD8^+$ T-cell numbers were in the normal range throughout. A striking finding were the low natural killer (NK) cell numbers throughout the observation period in the mother. It is not known whether BAFF inhibition influences proliferation of NK cells, resulting in reduced NK cell numbers. The child's B cells were in the normal range already 4 months after delivery despite continued full breast feeding. The vaccination response of the child was normal. Extended follow-up studies of children exposed prenatally to BEL are necessary to confirm the observed lymphocyte changes and to investigate their clinical relevance.

Helle Bitter,[1] Anne Noraas Bendvold,[2] Monika Elisabeth Østensen[1]

[1]Department of Rheumatology, Sørlandet Hospital, Kristiansand, Norway
[2]Rheumatology Specialists of Kristiansand, Kristiansand, Norway

Correspondence to Professor Monika Elisabeth Østensen, Department of Rheumatology, Sørlandet Hospital, Kristiansand 4615, Norway; monika.ostensen@gmail.com

Handling editor Josef S Smolen

Table 1 Lymphocyte profile of mother and child at birth, 4 and 7 months post partum and antibody titre after vaccination of the childs

	Mother			Child					
Lymphocyte subtypes	At birth	4 months post partum	7 months post partum	At birth	4 months post partum	7 months post partum	Cord blood 1	Cord blood 2	Cord blood 3
T-cells	µ/L	µ/L	µ/L	µ/L	µ/L	µ/L	µ/L	µ/L	µ/L
$CD3^+$ (ref. 800–2400)* (61.0%–81.0%)†	830	1630 (97.4%)†	1971 (97.6%)	1840	2937 (65.2%)	3289 (64.9%)	2427 (52.5%)	4493 (69.1%)	3593 (47.8%)
$CD8^+$ (ref. 200–1000)* (14.0%–40.0%)	358	613 (36.6%)	866 (42.9)	535	617 (13.7%)	822 (16.2%)	896 (19.4%)	1374 (21.1%)	1178 (15.7%)
$CD4^+$ (ref. 500–1400)* (33.0%–56.0%)	452	1015 (60.6%)	1140 (56.5%)	1292	2252 (50.0%)	2272 (44.8)	1530 (33.1%)	3152 (48.5%)	2385 (31.7%)
$CD16^+/CD56^+/CD3^-$ NK cells (ref. 100–400)* (6.3%–23.5%)	42	11	9 (0.5%)	752	372	274 (5.4%)	1401 (30.3%)	1252 (19.3%)	2354 (31.3)
B-cells	µ/L	µ/L	µ/L	µ/L	µ/L	µ/L	µ/L	µ/L	µ/L
$CD19^+$ (ref. 100–500)* (6.3%–17.0%)‡	4	5 (0.3%)	7 (0.4%)	14	1107 (24.6%)	1428 (28.2%)	593 (12.8%)	643 (9.9%)	1246 (16.6%)
Naive (82.1%–95.2%)‡	ND	ND	ND	ND	93.9%	90.4	ND	ND	ND
IgM memory (2.5%–8.7%)‡	ND	ND	ND	ND	4%	3.5%	ND	ND	ND
Switched (0.3%–9.0%)‡	ND	ND	ND	ND	1.3%	1.4%	ND	ND	ND
Transitorial (11.4%–38.4%)‡	ND	ND	ND	ND	0.2%	14.7%	ND	ND	ND
Plasmablasts (0.4%–3.3%)‡	ND	ND	ND	ND	0.1%	0.5%	ND	ND	ND
Antibody§ against pneumococcus						>30.0 U/mL (high)			

Three cord blood samples from term neonates not exposed to medications served as reference for lymphocyte subsets observed in the child exposed to belimumab. Subtype lymphocyte counts for T, B and NK cells were obtained by flow cytometry. The following B-cell subtypes were analysed: naive B-cells, memory B-cells and switched and transitorial B-cells.
*Adult reference values are given in parenthesis.
†Percentage of lymphocytes.
‡Percentage of $CD19^+$ B-cells.
§As a marker for the vaccination response antibodies to pneumococcus were measured.
ND, not done; NK, natural killer.

Contributors HB and ANB performed the clinical follow-up of the patient and her child. All authors were involved in the decision-making and the management during pregnancy and after delivery and have read and approved the manuscript.

Funding This research received no specific grant from any funding agency in the public, commercial or not-for-profit sectors.

Competing interests None declared.

Patient consent Obtained.

Provenance and peer review Not commissioned; externally peer reviewed.

To cite Bitter H, Bendvold AN, Østensen ME. *Ann Rheum Dis* 2018;**77**:1692–1693.

Received 12 January 2018
Revised 27 February 2018
Accepted 20 March 2018
Published Online First 28 March 2018

Ann Rheum Dis 2018;**77**:1692–1693. doi:10.1136/annrheumdis-2018-213004

REFERENCES

1 Auyeung-Kim DJ, Devalaraja MN, Migone TS, *et al*. Developmental and peri-postnatal study in cynomolgus monkeys with belimumab, a monoclonal antibody directed against B-lymphocyte stimulator. *Reprod Toxicol* 2009;28:443–55.

2 Glakso Smith Kline (GSK) group of companies. Cumulative pregnancy outcomes for belimumab from clinical trials, spontaneous reports, post-marketing surveillance reports, and the Belimumab Pregnancy Registry (BPR). 2016.

Anticardiolipin and anti-beta 2 glycoprotein-I antibodies disappearance in patients with systemic lupus erythematosus and antiphospholipid syndrome while on belimumab

The current management of antiphospholipid syndrome (APS) centres on attenuating the procoagulant state while balancing the haemorrhagic risks.[1] This approach relies mainly on a thromboprophylaxis strategy rather than targeting pathogenic antiphospholipid antibodies (aPL)-mediated pathways.

Herewith, we report the aPL disappearance in three patients with APS associated to systemic lupus erythematous (SLE) while on treatment with belimumab, potentially paving the way for development of new targeted therapies for APS. Belimumab is a monoclonal antibody that works by blocking the B-lymphocyte stimulator and avoiding B-cell activation.[2] It is the first biological drug approved for the treatment of autoantibody positive SLE

Table 1 Characteristics of the patients included in the study

	Sex	Age	Diagnosis	Associated autoimmune disease	aPL positivity	APS clinical events	Indication for starting belimumab	Concomitant immunomodulant treatment	Previous immunomodulant treatment
Patient #1	M	51	APS	SLE	LA, aCL IgG, anti-β2GPI IgG	Subpopliteal arterial thrombosis	Cutaneus* (face, upper trunk, arms) and articular involvement†	Low doses of steroids (5 mg/dL) and HCQ	IVIG, high doses of steroids
Patient #2	F	33	APS	SLE	aCL IgG, anti-β2GPI IgM	Three miscarriages <10th week of gestation	Haematological‡ and articular involvement†	Low doses of steroids (5 mg/dL) and HCQ	MMP, high doses of steroids, IVIG, AZA
Patient #3	M	39	APS	SLE	LA, aCL IgG	Three episodes of DVT, severe thrombocytopaenia	Haematological§ involvement	Low doses of steroids (5 mg/dL)	High doses of steroids, RTX and CYC

*Defined as annular scaly plaques, hypopigmentation; scaly erythematous patches, reticulate erythema.
†Defined as inflammatory arthritis involving more than three joints.
‡Defined as thrombocytopenia (<100.000 platelets × 10^9/L), leucopaenia (<2.500 white blood cells × 10^9/L) and anaemia (haemoglobin<9 g/dL).
§Defined as thrombocytopaenia (<50.000 platelets × 10^9/L) and leucopaenia (<3.000 white blood cells × 10^9/L.
aCL, anticardiolipin antibodies; aPL, antiphospholipid antibodies; APS, antiphospholipid syndrome; AZA, azathioprine; β2GPI, anti-β2 glycoprotein I antibodies; CYC, cyclophosphamide; DVT, deep vein thrombosis; HCQ, hydroxychloroquine; IVIG, intravenous immunoglobulin; LA, lupus anticoagulant; MMP, mycophenolate; RTX, rituximab; SLE, systemic lupus erythematosus.

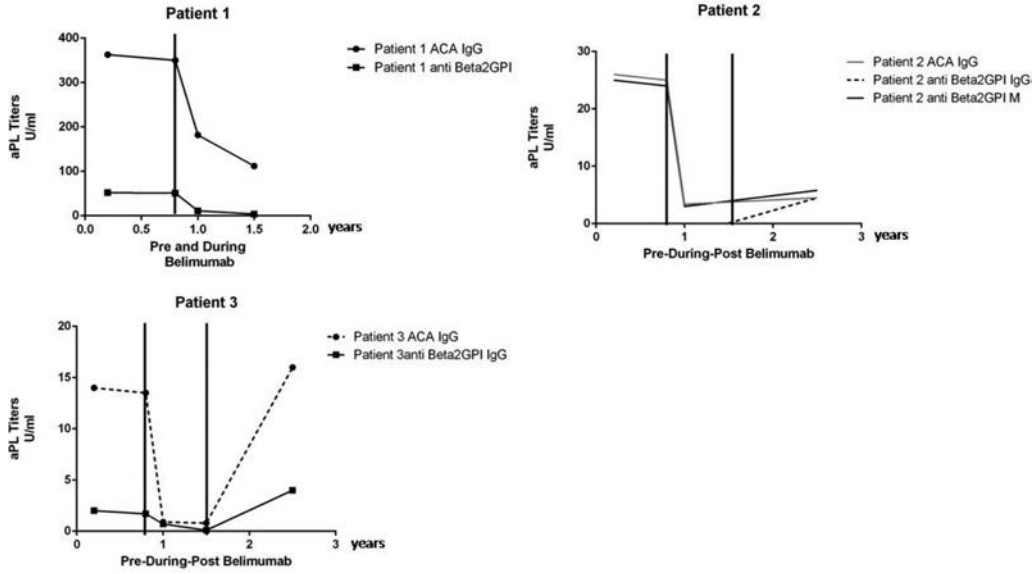

Figure 1 aPL titres of the three patients in relationship with belimumab therapy. aPL, antiphospholipid antibodies.

in active phase and it has shown its capability to reduce the antibodies levels, including anti-double stranded-DNA.[3] Intriguingly, in murine models of APS in the setting of SLE, belimumab proved its ability to stop disease progression and to reduce mortality rate.[4] However, its use in patients with APS needs further investigation.

After chart-reviewing all the aPL-positive patients with SLE treated in our centre with belimumab, investigating the changes in the aPL profile, we identified three patients with diagnosis of SLE[5] and APS (fulfilling Sydney classification criteria)[6] and persistent aPL positivity (confirmed in more than six occasions over the previous 5 years before starting belimumab) in whom we observed aPL disappearance. Clinical characteristics are detailed in table 1 and aPL testing methodology is detailed in online supplementary material S1. All patients received belimumab for active SLE (intravenous 10 mg/kg at 2-week intervals for the first three doses and at 4-week intervals thereafter). After 8 months since belimumab was started, Patient #1 became persistently negative for anti-β2-glycoprotein I antibodies (anti-β2GPI), while anticardiolipin antibodies (aCL) titre significantly decreased. While on treatment, anti-β2GPI and aCL levels both turned negative in Patient #2. Interestingly, after being on belimumab for 1 year, she planned a pregnancy and preferred to suspend the treatment, after 8 months since suspension, antiβ2GPI antibodies were detectable again. Patient #3 was persistently negative for aCL while being on belimumab (28 months). When he discontinued the therapy for lack of response, aCL antibodies returned positive after 2 months.

Figure 1 illustrates aPL titres of the three patients in relationship with belimumab therapy. Two patients (#1 and #3) persistently tested positive for lupus anticoagulant despite belimumab treatment. No patients experienced hypogammaglobulinaemia while on belimumab and IgG/IgM levels were constantly within normal range. Of note, none of the patients was started on a concomitant immunosuppressive treatment when belimumab was begun. However, a synergic role of hydroxychloroquine in the aCL and anti-β2GPI disappearance cannot be excluded.

Persistent aPL disappearance is a hot topic of discussion in the field of APS, but the clinical significance of sero-negativisation is still to be elucidated.[7 8] To the best of our knowledge, despite its limitations (eg, sample size and retrospective design), this pilot study is the first report of aPL negativisation after starting therapy with belimumab. Even more interesting, after stopping the treatment (mean time of 2 months), patients turned to be positive tested for IgG aPL again. The clinical relevance of these findings should be investigated in prospective multicentre studies, but if confirmed, they might modify the therapeutic management of patients with APS . Potentially, the current 'antithrombotic' approach to patients with APS will be at least combined in the future with an 'immunomodulatory' approach.

Savino Sciascia, Elena Rubini, Massimo Radin, Irene Cecchi, Daniela Rossi, Dario Roccatello

Center of Research of Immunopathology and Rare Diseases-Coordinating Center of Piemonte and Valle d'Aosta Network for Rare Diseases, Department of Clinical and Biological Sciences, S. Giovanni Bosco Hospital, University of Turin, Turin, Italy

Correspondence to Dr Savino Sciascia, Center of Research of Immunopathology and Rare Diseases-Coordinating Center of Piemonte and Valle d'Aosta Network for Rare Diseases, Department of Clinical and Biological Sciences, S. Giovanni Bosco Hospital, University of Turin, Turin 10154, Italy; savino.sciascia@unito.it

Handling editor Josef S Smolen

Contributors ER and SS designed the study, performed data analysis and drafted the manuscript. ER, IC, DR1, MR, DR2 and SS gave a substantial contribution to concept and study design and participated in the interpretation of data. All the authors gave the final approval of the version to be published.

Competing interests None declared.

Patient consent Not required.

Provenance and peer review Not commissioned; externally peer reviewed.

► Additional material is published online only. To view please visit the journal online (http://dx.doi.org/10.1136/annrheumdis-2018-213496).

SS and ER contributed equally.

To cite Sciascia S, Rubini E, Radin M, *et al*. *Ann Rheum Dis* 2018;**77**:1693–1695.

Received 29 March 2018
Revised 3 May 2018
Accepted 5 May 2018
Published Online First 18 May 2018

Ann Rheum Dis 2018;**77**:1693–1695. doi:10.1136/annrheumdis-2018-213496

REFERENCES

1 Khamashta MA, Cuadrado MJ, Mujic F, *et al*. The management of thrombosis in the antiphospholipid-antibody syndrome. *N Engl J Med* 1995;332:993–7.
2 Baker KP, Edwards BM, Main SH, *et al*. Generation and characterization of LymphoStat-B, a human monoclonal antibody that antagonizes the bioactivities of B lymphocyte stimulator. *Arthritis Rheum* 2003;48:3253–65.
3 Radin M, Cecchi I, Schreiber K, *et al*. Immunotherapies in phase II and III trials for the treatment of systemic lupus erythematosus. *Expert Opin Orphan Drugs* 2017;5:55–69.
4 Khattri S, Zandman-Goddard G, Peeva E. B-cell directed therapies in antiphospholipid antibody syndrome--new directions based on murine and human data. *Autoimmun Rev* 2012;11:717–22.
5 Hochberg MC. Updating the American College of Rheumatology revised criteria for the classification of systemic lupus erythematosus. *Arthritis Rheum* 1997;40:1725.
6 Miyakis S, Lockshin MD, Atsumi T, *et al*. International consensus statement on an update of the classification criteria for definite antiphospholipid syndrome (APS). *J Thromb Haemost* 2006;4:295–306.
7 Sciascia S, Coloma-Bazán E, Radin M, *et al*. Can we withdraw anticoagulation in patients with antiphospholipid syndrome after seroconvertion? *Autoimmun Rev* 2017;16:1109–14.
8 Radin M, Cecchi I, Pérez-Sánchez C. Antiphospholipid antibodies negativization: time for testing for non-criteria aPL? *Lupus* 2017;26:1457–8.

Platelet activation, as measured by plasma soluble glycoprotein VI, is not associated with disease activity or ischaemic events in giant cell arteritis

Giant cell arteritis (GCA) is associated with cranial ischaemic complications (CIC) including vision loss and stroke.[1] British Society of Rheumatology and European League against Rheumatism guidelines recommend platelet inhibition with aspirin for most patients with GCA; on the basis of two retrospective studies showing a reduction in CICs, these results were not replicated in two other retrospective studies.[2 3] There are no data from prospective or randomised controlled trials to support aspirin use in GCA.[4] The glycoprotein VI (GPVI) receptor is found exclusively on platelets and megakaryocytes.[5] GPVI is proteolytically cleaved following platelet activation and is detectable in plasma as soluble GPVI (sGPVI).[6] Elevated plasma sGPVI signifies platelet activation and an increased risk of cardiovascular events.[7] We have recently demonstrated enhanced platelet reactivity as measured by sGPVI in gout and rheumatoid arthritis, conditions associated with increased cardiovascular risk.[8 9] We hypothesised that GCA is associated with platelet hyper-reactivity, thereby supporting the rationale for aspirin use.

The aim of this study was to assess platelet reactivity, as measured by sGPVI, in patients with GCA, to compare these with healthy controls (HC) and patients with osteoarthritis (OA), and assess associations with clinical features and outcomes. Further information on inclusion criteria and definitions are shown in the online supplementary appendix. Following ethics approval and informed consent, blood samples were obtained and processed as double-spun platelet poor plasma. Demographic and clinical data were collected. sGPVI levels were measured using ELISA. Mann-Whitney U test was used to compare groups. Spearman's rank correlation coefficient was used to assess for associations between sGPVI levels and demographic and clinical markers.

A total of 146 patients were included: 70 with GCA, 53 HCs and 23 OA. Of the patients with GCA, 19 had active disease and 25 had CICs, 14 of which were permanent. Baseline characteristics are shown in table 1. There was no difference in sGPVI levels between GCA and HCs or OA, median (IQR) 2.32 ng/mL (1.60, 4.21) vs 2.19 ng/mL (1.72, 3.31) (p=0.76) and 2.73 ng/mL (2.17, 3.72) (p=0.38), figure 1. sGPVI levels were similar in patients with GCA with active and inactive diseases, median 2.31 ng/mL (1.86, 4.21) vs 2.33 ng/mL (1.57, 4.21) (p=0.93),

Table 1 Characteristics of 70 patients with GCA, 53 healthy controls and 23 patients with OA included in this study

	Active GCA	Inactive GCA	CIC	No CIC	HC	OA
Number	19	51	25	45	53	23
Age (years)	72 (65, 86)	68 (62, 79)	72 (66, 87)	68 (62, 79)	32 (25, 44)	68 (64, 75)
Female (%)	68	67	64	69	49	78
Biopsy positive (%)	53	43	72	33	0	0
ACR criteria (%)	79	88	96	84	0	0
ESR (mm/hour)	21 (15, 35)	10 (6, 15)	12 (8, 18)	12 (8, 21)	NA	NA
CRP (mg/L)	9 (4, 31)	4 (2, 8)	4 (2, 16)	4 (2, 9)	NA	NA
Fibrinogen	3.91 (3.14, 4.63)	3.32 (2.93, 3.79)	3.62 (2.67, 4.35)	3.32 (3.05, 3.85)	NA	NA
Aspirin use (%)	42	80	64	73	0	NA
BVAS	2 (0, 6)	0 (0, 0)	0 (0, 1)	0 (0, 0)	0 (0, 0)	0 (0, 0)
VDI	0 (0, 1)	0 (0, 2)	0 (0, 2)	0 (0, 1)	0 (0, 0)	0 (0, 0)
sGPVI (ng/mL)	2.31 (1.86, 4.21)	2.33 (1.57, 4.21)	2.04 (1.33, 4.21)	2.37 (1.88, 4.21)	2.19 (1.72, 3.31)	2.73 (2.17, 3.72)

Data are expressed as median (IQR) unless stated.
With VDI scoring damage must be present for 3 months or more to be scored.
ACR, American College of Rheumatology; BVAS, Birmingham Vasculitis Activity Score; CIC, cranial ischaemic complication; CRP, C-reactive protein; ESR, erythrocyte sedimentation rate; GCA, giant cell arteritis; HC, healthy control; NA, not applicable; OA, osteoarthritis; sGPVI, soluble glycoprotein VI; VDI, Vasculitis Damage Index.

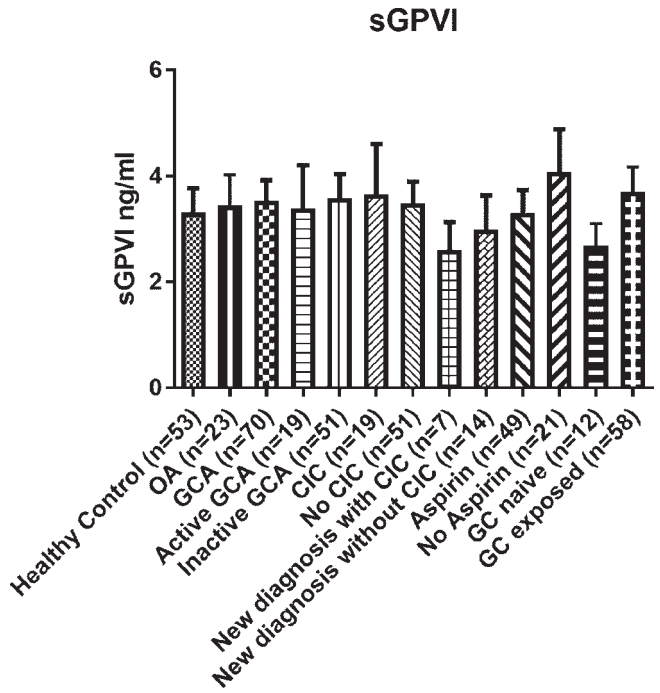

Figure 1 sGPVI levels in GCA. CIC, cranial ischaemic complication; GCA, giant cell arteritis; OA, osteoarthritis; sGPVI, soluble glycoprotein VI.

and those naïve to or receiving glucocorticoids, median 2.31 ng/mL (1.47, 3.99) vs 2.35 ng/mL (1.60, 4.37) (p=0.73). sGPVI levels were similar in patients with GCA with and without a history of CICs, median 2.04 ng/mL (1.33, 4.21) vs 2.37 ng/mL (1.88, 4.21) (p=0.85). sGPVI levels taken from patients at initial presentation with and without CICs were no different, median 2.31 ng/mL (1.33, 4.21) vs 2.27 ng/mL (1.72, 3.22) (p=0.91). Aspirin therapy did not significantly affect sGPVI levels, median 2.22 ng/mL (1.40, 4.20) vs 2.74 ng/mL (2.01, 4.64). There was no correlation between sGPVI levels and C-reactive protein (r=0.16), erythrocyte sedimentation rate (r=0.10) or prednisolone dose (r=−0.21).

Our work shows no evidence of increased platelet activation, as measured by sGPVI, in GCA. Analysis of other measures of platelet activation would strengthen our results. There was no association between platelet activation and disease activity or CICs; this contrasts with inflammatory diseases such as rheumatoid arthritis and gout where platelet activation is clearly demonstrable.[8 9]

Richard Conway,[1,2] Anne Madigan,[1] Niamh Redmond,[3] Laura Helbert,[1] Eamonn S Molloy,[4] Eimear Dunne,[5] Dermot Kenny,[5] Geraldine McCarthy[1]

[1]Department of Rheumatology, Mater Misericordiae University Hospital, Dublin Academic Medical Centre, Dublin, Ireland
[2]CARD Newman Research Fellow, University College Dublin, Dublin, Ireland
[3]Clinical Research Centre, Mater Misericordiae University Hospital, Dublin Academic Medical Centre, Dublin, Ireland
[4]Centre for Arthritis and Rheumatic Diseases, Dublin Academic Medical Centre, St Vincent's University Hospital, Dublin, Ireland
[5]Cardiovascular Biology and Clinical Research Centre, Royal College of Surgeons in Ireland, Dublin, Ireland

Correspondence to Dr Richard Conway, Department of Rheumatology, Mater Misericordiae University Hospital, Dublin Academic Medical Centre, Dublin D07 R2WY, Ireland; drrichardconway@gmail.com

Handling editor Josef S Smolen

Contributors RC, DK and GMC conceived the study. RC performed the data analysis. All authors critically appraised the manuscript and approved the final version.

Funding This research received no specific grant from any funding agency in the public, commercial or not-for-profit sectors.

Competing interests None declared.

Patient consent Obtained.

Ethics approval Mater Misericordiae University Hospital Ethics Committee.

Provenance and peer review Not commissioned; externally peer reviewed.

Data sharing statement Data used in this study are held in the Department of Rheumatology, Mater Misericordiae University Hospital, Dublin, Ireland, under the custody of GMC and can be made available on request.

► Additional material is published online only. To view please visit the journal online (http://dx.doi.org/10.1136/annrheumdis-2018-213487).

The results from this study were presented at the American College of Rheumatology Annual Meeting 2016 and have been published in abstract form: Conway R et al.[10]

To cite Conway R, Madigan A, Redmond N, *et al*. *Ann Rheum Dis* 2018;**77**:1695–1696.

Received 28 March 2018
Revised 23 April 2018
Accepted 24 April 2018
Published Online First 5 May 2018

Ann Rheum Dis 2018;**77**:1695–1696. doi:10.1136/annrheumdis-2018-213487

REFERENCES

1 Soriano A, Muratore F, Pipitone N, *et al*. Visual loss and other cranial ischaemic complications in giant cell arteritis. *Nat Rev Rheumatol* 2017;13:476–84.
2 Mukhtyar C, Guillevin L, Cid MC, *et al*. EULAR recommendations for the management of large vessel vasculitis. *Ann Rheum Dis* 2009;68:318–23.
3 Dasgupta B, Borg FA, Hassan N, *et al*. BSR and BHPR guidelines for the management of giant cell arteritis. *Rheumatology* 2010;49:1594–7.
4 Mollan SP, Sharrack N, Burdon MA, *et al*. Aspirin as adjunctive treatment for giant cell arteritis. *Cochrane Database Syst Rev* 2014;8:Cd010453.
5 Clemetson JM, Polgar J, Magnenat E, *et al*. The platelet collagen receptor glycoprotein VI is a member of the immunoglobulin superfamily closely related to FcalphaR and the natural killer receptors. *J Biol Chem* 1999;274:29019–24.
6 Al-Tamimi M, Mu FT, Moroi M, *et al*. Measuring soluble platelet glycoprotein VI in human plasma by ELISA. *Platelets* 2009;20:143–9.
7 Al-Tamimi M, Gardiner EE, Thom JY, *et al*. Soluble glycoprotein VI is raised in the plasma of patients with acute ischemic stroke. *Stroke* 2011;42:498–500.
8 Conway R, Murphy CL, Madigan A, *et al*. Increased platelet reactivity as measured by plasma glycoprotein VI in gout. *Platelets* 2017:1–6.
9 Stack JR, Madigan A, Helbert L, *et al*. Soluble glycoprotein VI, a specific marker of platelet activation is increased in the plasma of subjects with seropositive rheumatoid arthritis. *PLoS One* 2017;12:e0188027.
10 Conway R, Madigan A, Helbert L, *et al*. Platelet Activation, As Measured By Plasma Soluble Glycoprotein VI, Is Not Associated with Disease Activity or Ischaemic Events in Giant Cell Arteritis. *Arthritis Rheumatol* 2016;68(suppl 10):1196–997.

Large deletion in 6q associated to A20 haploinsufficiency and thoracoabdominal heterotaxy

Mutations in the *TNFAIP3* gene resulting in A20 haploinsufficiency (HA20) have been identified as a new cause of autoinflammation linked to uncontrolled nuclear factor kappa B (NF-κB) activation.[1] A recent report published in the *Annals of the Rheumatic Diseases* highlighted the main clinical manifestations of the 16 patients who presented with recurrent oral,

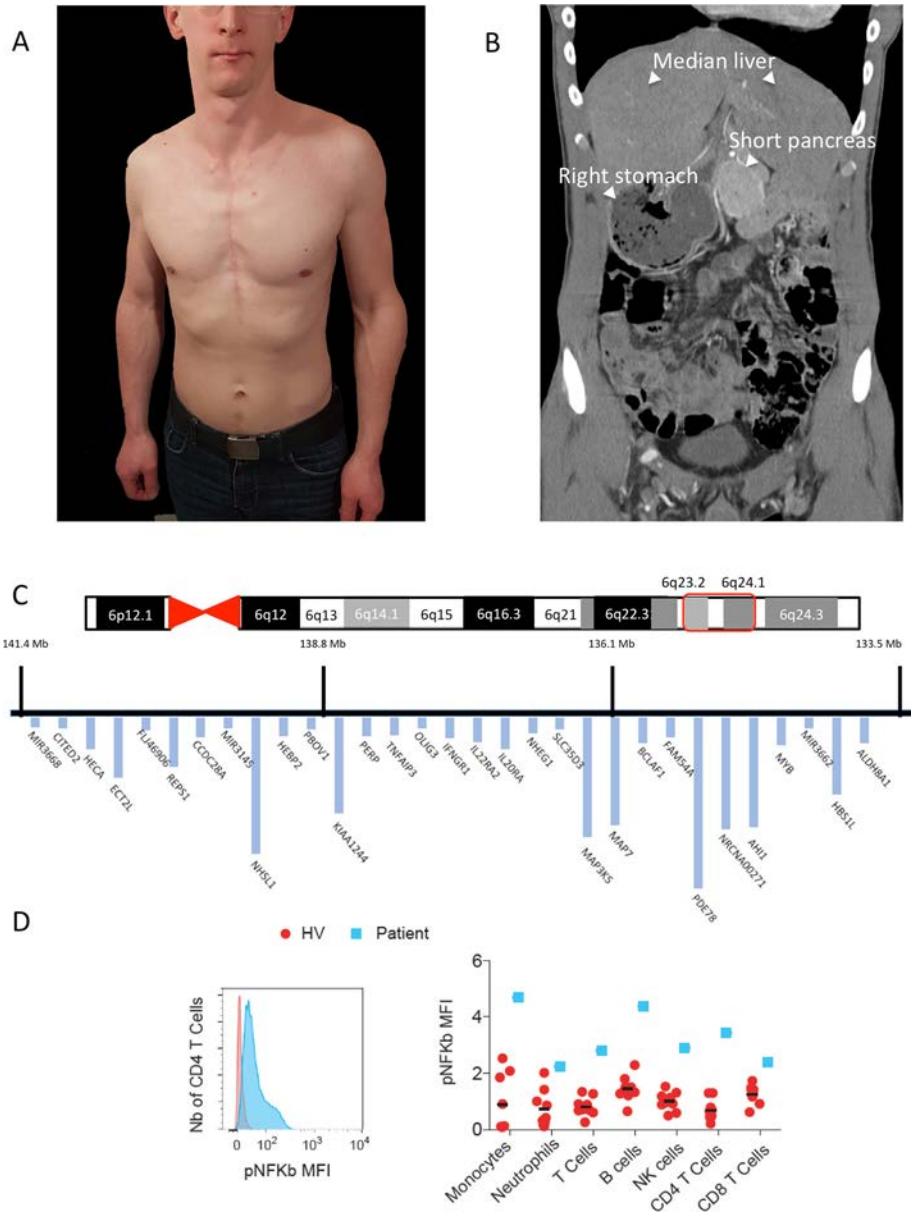

Figure 1 Clinical, radiological, genetic and immunological features of A20. (A) Large forehead with thin lips and prominent muscles. (B) Abdominal CT scan, coronal view, showing the viscera heterotaxy. (C) Large deletion in chromosome 6. (D) Phospho-NF-kB (pSer 529) in white blood cells of healthy volunteers (HV) and patients. MFI, mean fluorescence intensity; NK, natural killer; NF-kB, nuclear factor kappa B.

genital, gastrointestinal ulcerations and various inflammatory features (skin lesions, musculoskeletal disorders and recurrent fever) associated in some cases to autoimmunity mimicking a lupus.[2] Some of the patients also experienced recurrent infections. *TNFAIP3* anomalies included monoallelic nonsense and frameshift mutations.[1]

Here, we report that HA20 can be part of a more complex genetic syndrome. We describe the new case of a boy who presented with mild intellectual disability with normal MRI and dysmorphic features including short stature, large forehead, thin lips and visible muscles (figure 1A). Of note, he had a heterotaxis with a median liver, short pancreas, polysplenia and right stomach, and underwent cardiac surgery at birth for a complex heart malformation (figure 1B). At the age of 5, he presented a vasculitis with necrotising purpura, abdominal pain and arthralgia, consistent with the diagnosis of Henoch-Schönlein purpura. The symptoms were recurrent and the diagnosis of periarteritis nodosa was suspected. Later in life, at the age of 19, he presented an acute renal failure with macroscopic haematuria following a viral infection and was diagnosed for IgA nephropathy on kidney biopsy. Other autoimmune symptoms including haemolytic anaemia and thrombopaenia also occurred. Immunophenotyping revealed a global lymphopaenia (0.79 ×10 ^ 9/L) and hyper-IgE (756 kU/L).

A deletion in 22q11 was initially ruled out by a karyotype analysis. Targeted next-generation sequencing focusing on 55 genes revealed a complete heterozygous deletion of *TNFAIP3*. The comparative genomic hybridization (CGH) array detected a large deletion of 5.5 Mb in chromosome 6 (6q23.2q24.1) (figure 1C). This rearrangement comprised about 60 genes including *CITED2*, *IFNGR1* and *TNFAIP3*. The same deletion of 6q23.2q24.1 was already reported with mental retardation and dysmorphic features, but without inflammation or situs inversus.[3] A20 acts as a regulator of the NF-kB signalling cascade by its E3 ubiquitin ligase activity, preventing the degradation of inhibiting complex I-kappa-B kinase gamma IKKγ (also

known as NF-kB essential modulator/NEMO).[4] Accordingly the patient's white blood cells displayed spontaneous phosphorylation of the NF-kB p65 subunit (Serin529) in the absence of systemic inflammation (C reactive protein <5 mg/L) (figure 1D), which is consistent with a defective NF-kB signalling pathway regulation. Interestingly, *TNFAIP3* deletions were also associated with an NF-kB activation in lymphoma.[5] *CITED2* is a key transcriptional factor involved in cardiac development and acts as a regulator of laterality during embryogenesis in mice.[6] Missense mutations or small deletions were reported in association with congenital heart anomalies in human,[7] but abdominal laterality anomalies were not reported in human so far. In this report, the cardiac anomalies and abdominal viscera heterotaxy are probably secondary to the whole deletion of *CITED2*. *IFNGR1* encodes the ligand-binding chain of the interferon-γ receptor and heterozygous deletion may be associated to mycobacterial susceptibility,[8] although this patient did not present noticeable invasive or recurrent infections.

To conclude, autoinflammation and autoimmunity associated with thoracoabdominal heterotaxy are evocative of a large deletion in chromosome 6q comprising *CITED2* and *TNFAIP3*.

Sébastien Viel,[1,2,3,4,5,6] Elodie Cheyssac,[7] Rémi Pescarmona,[1,2,3,4,5,6] Laurie Besson,[1,2,3,4,5] Marianne Till,[8] Loïc Viremouneix,[9] Isabelle Touitou,[10] Guillaume Sarrabay,[10] Thierry Walzer,[1,2,3,4,5] Alexandre Belot[1,2,7,3,4,5]

[1]CIRI, Centre International de Recherche en Infectiologie - International Center for Infectiology Research, Lyon, France
[2]U1111, Inserm, Lyon, France
[3]Ecole Normale Supérieure de Lyon, Lyon, France
[4]Université Lyon 1, Lyon, France
[5]CNRS, UMR5308, Lyon, France
[6]Laboratoire d'Immunologie, Centre Hospitalier Lyon Sud, Hospices Civils de Lyon, Lyon, France
[7]Service de Néphrologie Rhumatologie Dermatologie Pédiatriques, Centre de référence RAISE, Hôpital Femme Mère Enfant, Hospices Civils de Lyon, Lyon, France
[8]Service de Cytogénétique, Groupe Hospitalier Est, Hospices Civils de Lyon, Lyon, France
[9]Service de Radiologie Pédiatrique, Hôpital Femme Mère Enfant, Hospices Civils de Lyon, Lyon, France
[10]Cellules souches, plasticité cellulaire, médecine régénératrice et immunothérapies, INSERM, Université de Montpellier, Département de génétique médicale, maladies rares et médecine personnalisée, CHU Montpellier, Montpellier, France

Correspondence to Dr Alexandre Belot, CIRI, Centre International de Recherche en Infectiologie - International Center for Infectiology Research, Lyon 69007, France; alexandre.belot@chu-lyon.fr

Handling editor Josef S Smolen

Acknowledgements We warmly thank the patient and his family.

Contributors SV wrote and revised the manuscript. EC draw the pictures and panel. LB, RP performed the immunological experiments and analysis. MT, IT, GS performed the genetic experiments (CGH array and exome sequencing) and analysis. LV performed CT scan and annotated panel B. TW supervised immunological work and reviewed the manuscript. AB is in charge of the patient and supervised the work. All authors critically reviewed the manuscript.

Funding This study is funded by Agence Nationale de la Recherche (grant number: ANR LUMUGENE 2014).

Competing interests None declared.

Patient consent Obtained.

Ethics approval Medical Ethics Committee of Sud Est III, Lyon, France.

Provenance and peer review Not commissioned; externally peer reviewed.

Data sharing statement No additional data available (raw data for genetic studies could be provided).

To cite Viel S, Cheyssac E, Pescarmona R, *et al*. *Ann Rheum Dis* 2018;**77**:1696–1698.

Received 26 February 2018
Revised 3 April 2018
Accepted 6 April 2018
Published Online First 20 April 2018

Ann Rheum Dis 2018;**77**:1696–1698. doi:10.1136/annrheumdis-2018-213300

REFERENCES

1 Zhou Q, Wang H, Schwartz DM, *et al*. Loss-of-function mutations in TNFAIP3 leading to A20 haploinsufficiency cause an early-onset autoinflammatory disease. *Nat Genet* 2016;48:67–73.
2 Aeschlimann FA, Batu ED, Canna SW, *et al*. A20 haploinsufficiency (HA20): clinical phenotypes and disease course of patients with a newly recognised NF-kB-mediated autoinflammatory disease. *Ann Rheum Dis* 2018:annrheumdis-2017-212403.
3 Dutrannoy V, Klopocki E, Wei R, *et al*. De novo 9 Mb deletion of 6q23.2q24.1 disrupting the gene EYA4 in a patient with sensorineural hearing loss, cardiac malformation, and mental retardation. *Eur J Med Genet* 2009;52:450–3.
4 Vereecke L, Beyaert R, van Loo G. The ubiquitin-editing enzyme A20 (TNFAIP3) is a central regulator of immunopathology. *Trends Immunol* 2009;30:383–91.
5 Jung H, Yoo HY, Lee SH, *et al*. The mutational landscape of ocular marginal zone lymphoma identifies frequent alterations in TNFAIP3 followed by mutations in TBL1XR1 and CREBBP. *Oncotarget* 2017;8:17038–49.
6 Lopes Floro K, Artap ST, Preis JI, *et al*. Loss of Cited2 causes congenital heart disease by perturbing left-right patterning of the body axis. *Hum Mol Genet* 2011;20:1097–110.
7 Liu Y, Wang F, Wu Y, *et al*. Variations of CITED2 are associated with congenital heart disease (CHD) in Chinese population. *PLoS One* 2014;9:e98157.
8 Jouanguy E, Lamhamedi-Cherradi S, Lammas D, *et al*. A human IFNGR1 small deletion hotspot associated with dominant susceptibility to mycobacterial infection. *Nat Genet* 1999;21:370–8.

Smoking paradox in the development of psoriatic arthritis among patients with psoriasis

We have read with great interest the article by Nguyen and colleagues[1] on the smoking paradox in the development of psoriatic arthritis (PsA) among patients with psoriasis. The authors present a large population-based study, in which they demonstrate that smoking is positively associated with PsA risk in the general population but negatively associated with PsA risk among patients with psoriasis, thereby suggesting that index event bias could result in the smoking paradox. The reasons for this smoking paradox are difficult to elucidate, but we agree with the authors' emphasis on the potential role of index event bias in the paradoxical finding that smoking appeared to be protective among patients with psoriasis. Index event bias is a consequence of selecting a study population on the basis of a prior event.[2] The possibility of index event bias should be considered in the causal interpretation of associations because it can conceal the effect of risk factors.[2] Group allocation based on an index event (psoriasis) affected by smoking can create a selection bias that might introduce a downward bias in the association between smoking and PsA, unless there is a thorough assessment for all shared risk factors.[3] In epidemiological studies, the difficultly in controlling for confounding variables and a high risk of bias are of constant concern.[4] As disease aetiology consists of both known and unknown risk factors, multivariable adjustment can only partially overcome this type of bias. However, the study by Nguyen and colleagues did not include sufficient adjustment for confounding factors. Although the study adjusted for age, alcohol, body mass index, sex and trauma, the confounding effect of additional unmeasured or unknown variables (eg, socioeconomic status, exercise, diet, drugs used, serum uric acid, etc) cannot be excluded. The index event bias will always be a concern because unmeasured or unknown risk factors are often operating to cause a disease. As a consequence, the association between smoking and PsA in patients with psoriasis might be biased. In addition, the results reported by Nguyen *et al* differ from those of another large cohort study,[5] which demonstrated an increased risk of PsA among psoriasis cases, wherein the risk was significant for those with higher cumulative measures of smoking. The study findings by Nguyen and colleagues might lead clinicians and the public to misunderstandings.[1] We believe that this negative association should not mislead readers that smoking could be beneficial in diminishing the risk of PsA in patients with psoriasis, as the smoking paradox is expected owing to index event bias, which should be more widely recognised. Further research is needed to clarify effect of smoking on the development of PsA among those with psoriasis.

Young Ho Lee, Gwan Gyu Song

Division of Rheumatology, Korea University Medical Center, Seoul, Republic of Korea

Correspondence to Professor Young Ho Lee, Division of Rheumatology, Korea University Medical Center, Seoul 136-705, Republic of Korea; lyhcgh@korea.ac.kr

Competing interests None declared.

Provenance and peer review Not commissioned; internally peer reviewed.

To cite Lee YH, Song GG. *Ann Rheum Dis* 2018;**77**:e75.

Received 28 November 2017
Accepted 29 November 2017
Published Online First 7 December 2017

Linked

► http://dx.doi.org/10.1136/annrheumdis-2017-212770

Ann Rheum Dis 2018;**77**:e75. doi:10.1136/annrheumdis-2017-212759

REFERENCES

1 Nguyen UDT, Zhang Y, Lu N, *et al*. Smoking paradox in the development of psoriatic arthritis among patients with psoriasis: a population-based study. *Ann Rheum Dis* 2017. doi:10.1136/annrheumdis-2017-211625. [Epub ahead of print 4 Nov 2017].
2 Smits LJ, van Kuijk SM, Leffers P, *et al*. Index event bias-a numerical example. *J Clin Epidemiol* 2013;66:192–6.
3 Dahabreh IJ, Kent DM. Index event bias as an explanation for the paradoxes of recurrence risk research. *JAMA* 2011;305:822–3.
4 Jepsen P, Johnsen SP, Gillman MW, *et al*. Interpretation of observational studies. *Heart* 2004;90:956–60.
5 Li W, Han J, Qureshi AA. Smoking and risk of incident psoriatic arthritis in US women. *Ann Rheum Dis* 2012;71:804–8.

Response to: 'Smoking paradox in the development of psoriatic arthritis among patients with psoriasis' by Lee and Song

We thank Lee and Song[1] for their interest in our extended report on the smoking paradox in the development of psoriatic arthritis among patients with psoriasis.[2] Please note that the point of our paper was indeed to demonstrate how the smoking paradox could be due to methodological issues (rather than some underlying biological phenomenon). Specifically, this includes (1) the misinterpretation of the direct effect as the total effect and (2) the presence of index event bias affecting the derived direct effect. While Lee and Song focused on the second point, it is our view that the former (ie, the methodological issue derived from the misinterpretation of different effects) is possibly the more fundamental flaw. Regardless, this leaves us wondering how our paper, which provided methodological (as opposed to biological) reasons for the smoking paradox, 'might lead clinicians and the public to misunderstandings'.

Uyen-Sa D T Nguyen,[1,2] Yuqing Zhang,[2,3] Hyon K Choi[4]

[1]Orthopedics and Physical Rehabilitation, University of Massachusetts Medical School, Worcester, Massachusetts, USA
[2]Medicine, Clin Epi Research and Training Unit, Boston University School of Medicine, Boston, Massachusetts, USA
[3]Division of Rheumatology, Allergy, and Immunology, Massachusetts General Hospital, Boston, Massachusetts, USA
[4]Department of Rheumatology, Harvard Medical School, Boston, Massachusetts, USA

Correspondence to Dr Uyen-Sa D T Nguyen, Orthopedics and Physical Rehabilitation, University of Massachusetts Medical School, 55 Lake Ave North, Worcester, MA 01655, USA; uyensa.nguyen@umassmed.edu

Handling editor Josef S Smolen

Contributors Drafting of authors' response letter, critical review and final approval: all authors.

Funding This study was funded by NIH-NIAMS, NIH K01AR064351, NIH R21AR068493 and Rheumatology Research Foundation Innovative Research Award.

Competing interests None declared.

Ethics approval IRB at the University of Massachusetts Medical School and Boston University School of Medicine.

Provenance and peer review Commissioned; internally peer reviewed.

To cite Nguyen U-SDT, Zhang Y, Choi HK. *Ann Rheum Dis* 2018;**77**:e76.

Received 5 January 2018
Accepted 7 January 2018
Published Online First 23 January 2018

► http://dx.doi.org/10.1136/annrheumdis-2017-212759

Ann Rheum Dis 2018;**77**:e76. doi:10.1136/annrheumdis-2017-212770

REFERENCES

1 Lee YH, Song GG. Smoking paradox in the development of psoriatic arthritis among patients with psoriasis. *Ann Rheum Dis* 2018;77:e75.
2 Nguyen UDT, Zhang Y, Lu N, *et al*. Smoking paradox in the development of psoriatic arthritis among patients with psoriasis: a population-based study. *Ann Rheum Dis* 2018;77:119–23.

2017 EULAR/ACR classification criteria for adult and juvenile idiopathic inflammatory myopathies and their major subgroups: little emphasis on autoantibodies, why?

The publication of the EULAR/ACR classification criteria for 'idiopathic inflammatory myopathy' group of disease would be considered a landmark work in this field.[1] The tremendous efforts of a large number of dedicated workers in the field of myositis from around the world coming together to produce this seminal document deserve high praise. The hope is that it will aid the drug trials on homogeneous subsets of this group of diseases yielding meaningful results. However, there is some concern for 'an outsider', a general rheumatologist like me, for not putting more emphasis on myositis-specific antibodies (MSAs). Most of the authors of this document have dedicated their careers to the discovery of MSAs. These are the same authors who have widely reported the clinical importance of the MSAs, their effect on the clinical features, clinical course as well as on the treatment response. Yet, they seem to have shied away from including MSAs in this classification (except anti-Jo1 antibody). It is from the publications of these reputed workers that we have learnt the importance of MSAs and how they define the clinical features, disease course and the response to treatment. Thus, we have learnt that there are mainly four subgroups that present as amyopathic dermatomyositis (ADM): those who are positive for anti-histidyl tRNA synthetase (anti-Jo-1), anti-non-Jo1, anti-melanoma differentiation-associated gene 5 (anti-MDA5) and anti-transcription intermediary factor-1 gamma (TIF-1γ) MSAs. Simply categorising a patient as 'ADM' and only testing for anti-Jo-1 autoantibody but not for anti-non-Jo-1, anti-MDA5 and TIF-1γ, might be problematic. The latter three categories are very different in their clinical involvements, response to treatment and outcomes. Any drug trial in this group of mixed patients would, therefore, fail to yield meaningful results. Similarly, we have learnt that there are four subgroups of patients who present with pathognomonic dermatomyositis rash and would get classified under 'DM'. Without screening for MSAs, one would not be able to distinguish between the four subgroups, namely, anti-nucleosome-remodelling deacetyalse complex (anti-Mi2) antibody, anti-small ubiquitin-like modifier activating enzyme (anti-SAE) antibody, anti-TIF-1γ antibody and anti-nuclear matrix protein 2 (NXP2) antibody syndromes. Many publications have shown that their clinical course and outcome with treatment are very different. Conducting drug trials in such a heterogeneous group would yield confusing results. A similar problem would arise in the group that would be classified as polymyositis. As we have learnt, if patients in this subgroup are screened for MSAs, the majority would be negative for autoantibodies. However, there would also be patients with anti-3-hydroxy-3-methylglutaryl-coenzyme A reductase (anti-HMGCoAR), anti-signal recognition particle (anti-SRP), anti-survival of motor neuron complex (anti-SMN) and anti-four-and-a-half LIM domain 1 (anti-FHL1) autoantibodies, each with different response to any form of treatment, that would muddle the results of any drug trial. Maybe it is rather naive for a 'general rheumatologist' to ask these questions. However, the response of the experts may help us understand this field better. As is mentioned in the document, this classification is 'provisional'. Maybe this international group of workers is already at an advanced stage of developing MSA-based/inclusive classification criteria for idiopathic inflammatory myopathies.

Anand N Malaviya[1,2]

[1]Department of Rheumatology, ISIC Superspeciality Hospital, New Delhi, Delhi, India
[2]A&R Clinic for Arthritis and Rheumatism, Vasant Kunj, New Delhi, Delhi, India

Correspondence to Professor Anand N Malaviya, Department of Rheumatology, ISIC Superspeciality Hospital, Vasant Kunj, NewDelhi 110070, India; anand_malaviya@yahoo.com

Competing interests None declared.

Provenance and peer review Not commissioned; internally peer reviewed.

To cite Malaviya AN. *Ann Rheum Dis* 2018;**77**:e77.

Received 15 November 2017
Accepted 16 November 2017
Published Online First 23 November 2017

Linked

► http://dx.doi.org/10.1136/annrheumdis-2017-212709

Ann Rheum Dis 2018;**77**:e77. doi:10.1136/annrheumdis-2017-212701

REFERENCE

1 Lundberg IE, Tjärnlund A, Bottai M, *et al*. 2017 European League Against Rheumatism/American College of Rheumatology classification criteria for adult and juvenile idiopathic inflammatory myopathies and their major subgroups. *Ann Rheum Dis* 2017;76:1955–64.

Response to: '2017 EULAR/ACR classification criteria for adult and juvenile idiopathic inflammatory myopathies and their major subgroups: little emphasis on autoantibodies, why?' by Malaviya

We are grateful for the insightful and highly relevant question raised by Dr Malaviya[1] concerning the 2017 European League Against Rheumatism/American College of Rheumatology classification criteria for adult and juvenile idiopathic inflammatory myopathies and their major subgroups. The question concerns autoantibodies, and in particular myositis-specific autoantibodies (MSAs), and why only the anti-Jo-1 autoantibody is included in the new classification criteria.

We understand the concern that was raised and we have discussed the limitation of having limited data on MSAs in our publication.[2] This letter gives us a possibility to expand on this limitation and include some more explanations. Our study was initiated more than 10 years ago, and during the last decade we have seen a great advancement in the knowledge of autoantibodies specific for and associated with idiopathic inflammatory myopathies (IIM). This includes identification of several new MSAs, as well as advancement in methods used to detect MSAs that have made it possible to test most of the MSAs in clinical practice by commercially available assays. Unfortunately, these assays were not available for most of the MSAs at the time of data collection for our project. Indeed, as pointed out by Dr Malaviya, an increasing knowledge has emerged concerning associations between presence of autoantibodies and clinical phenotype, disease progression and response to treatment, emphasising the importance of the MSAs in clinical practice and classification. The data on autoantibody profiles included in the data set of this study conducted at 47 clinics worldwide reflect the limited availabilities of detection methods for MSAs at the start of the study. Due to this we had data for only five MSAs included in the study. We found a strong association between all of them and cases being classified as IIM. However, only the anti-Jo-1 autoantibody reached sufficient number of observations (n=1062) in cases and comparators for valid inclusion in the classification criteria. In the manuscript we addressed the need for inclusion of more autoantibody data in a future update of the criteria.

It took many years to collect patient data for the myositis criteria project to include the number needed of cases and comparators cases, adults and children, representing different centres and different ethnicities. During these years we have seen scientific advances in myositis and development of several collaborative networks that will facilitate update of the criteria. One such international collaborative effort is the international, multidisciplinary myositis register, Euromyositis, currently including more than 4000 patients with IIM and involving 23 clinics worldwide. The steering committee of the Euromyositis register has long been working on standardisation of sample collection and assessment of autoantibodies for inclusion in the register. Data from this register can be one source for a future update of the classification criteria, but other cohorts are needed, including comparator cases where MSAs have been tested. The assessment of MSAs using validated methods will be of utmost importance for use in classification criteria development. We will then have the possibility to address the value of MSAs for classification of IIM, as well as to test association of certain autoantibodies with different clinical phenotypes, disease progression and response to treatment. This will enable us an even better subclassification of IIMs that will ultimately pave the way for clinical trials with relevant and homogeneous patient groups and hopefully development of improved treatment for these patients.

Dr Malaviya is correct that the classification criteria are provisional. As stated by the European League Against Rheumatism and the American College of Rheumatology, 'This signifies that the criteria set has been quantitatively validated using patient data, but it has not undergone full validation based on an independent dataset, using both cases and controls. This validation step is still needed before the criteria are fully validated'. Hence the term provisional refers to the need of validation of the criteria in an independent cohort including both cases and controls, but does not imply that the criteria items included are non-significant or not important. We welcome collaboration with experts who have access to such cohorts as a next step for an external validation of the new criteria.

We hope that we have addressed the concern raised by Dr Malaviya by this response and we welcome initiatives to perform external validation of the 'European League Against Rheumatism/American College of Rheumatology classification criteria for adult and juvenile idiopathic inflammatory myopathies and their major subgroups', as well as testing the whole panel of MSAs both for classification of IIM and for classification of subgroups of IIM. Only a systematic and harmonised collection of autoantibody data using validated antibody assays together with clinical data in a large international, multidisciplinary collaboration will make future revision of these novel classification criteria possible.

Ingrid E Lundberg, Anna Tjärnlund

Rheumatology Unit, Department of Medicine, Karolinska University Hospital, Karolinska Institutet, Stockholm, Sweden

Correspondence to Profossor Ingrid E Lundberg, Rheumatology Unit, Department of Medicine, Karolinska University Hospital, Karolinska Institutet, Solna, Stockholm S-171 76, Sweden; ingrid.lundberg@ki.se

Competing interests None declared.

Provenance and peer review Commissioned; internally peer reviewed.

To cite Lundberg IE, Tjärnlund A. *Ann Rheum Dis* 2018;**77**:e78.

Received 3 December 2017
Accepted 3 December 2017
Published Online First 15 December 2017

Linked

► http://dx.doi.org/10.1136/annrheumdis-2017-212701

Ann Rheum Dis 2018;**77**:e78. doi:10.1136/annrheumdis-2017-212709

REFERENCES

1 Malaviya AN. 2017 EULAR/ACR classification criteria for adult and juvenile idiopathic inflammatory myopathies and their major subgroups: little emphasis on autoantibodies, why? *Ann Rheum Dis* 2017. doi: 10.1136/annrheumdis-2017-212701. [E pub ahead of print 23 Nov 2017].
2 Lundberg IE, Tjärnlund A, Bottai M, *et al*. 2017 European league against rheumatism/American college of rheumatology classification criteria for adult and juvenile idiopathic inflammatory myopathies and their major subgroups. *Ann Rheum Dis* 2017;76:1955–64.

Cardiovascular effects of hydroxychloroquine: a systematic review and meta-analysis

I have read with interest the article by Mathieu and colleagues[1] regarding the cardiovascular effects of hydroxychloroquine (HCQ). This systematic review and meta-analysis demonstrates that HCQ treatment is associated with an improved cardiovascular risk profile. However, it has some methodological issues. First, although the authors searched conference abstracts, using the MEDLINE database alone may not be sufficient for a thorough literature search.[2] Identification of all relevant papers is a critical component in conducting a meta-analysis because its outcome depends on the studies included. Therefore, the search strategy has to be comprehensive, and a comprehensive search should include multiple databases, such as MEDLINE, EMBASE and Cochrane Controlled Trials Register.[3] Second, selection of an appropriate statistical model is important to ensure that the statistics have been estimated correctly.[4] I am unclear on how the authors chose among fixed-effects and random-effects models during the meta-analysis. The choice of the meta-analysis method should be explained, and a rationale for the choice of the statistical model should be stated.[5] Considering substantial and considerable between-study heterogeneity, the random-effects model would be a more appropriate choice. Third, a random-effects meta-analysis is used to incorporate heterogeneity among studies,[6] but is not a substitute for investigation of heterogeneity.[5] Heterogeneity should be explored by conducting subgroup analyses and/or meta-regression to determine the causes of heterogeneity among results of studies. I wonder whether age, sex, body mass index, drugs (eg, glucocorticoid or methotrexate) used and/or potential effect modifiers were matched or adjusted for. Thus, I believe that the findings of this study should be interpreted taking the aforementioned methodological concerns into consideration.

Young Ho Lee

Division of Rheumatology, Department of Internal Medicine, Korea University Anam Hospital, Korea University College of Medicine, Seoul, Korea

Correspondence to Professor Young Ho Lee, Division of Rheumatology, Department of Internal Medicine, Korea University Anam Hospital, Korea University College of Medicine, Seoul 136-705, Korea; lyhcgh@korea.ac.kr

Competing interests None declared.

Provenance and peer review Not commissioned; internally peer reviewed.

To cite Lee YH. *Ann Rheum Dis* 2018;**77**:e79.

Received 7 November 2017
Accepted 8 November 2017
Published Online First 16 November 2017

► http://dx.doi.org/10.1136/ annrheumdis-2017-212668

Ann Rheum Dis 2018;**77**:e79. doi:10.1136/annrheumdis-2017-212661

REFERENCES

1 Mathieu S, Pereira B, Tournadre A, *et al*. Cardiovascular effects of hydroxychloroquine: a systematic review and meta-analysis. *Ann Rheum Dis* 2018;77:e65.
2 Zheng MH, Zhang X, Ye Q, *et al*. Searching additional databases except PubMed are necessary for a systematic review. *Stroke* 2008;39:e139.
3 Relevo R. Chapter 4: effective search strategies for systematic reviews of medical tests. *J Gen Intern Med* 2012;27:28–32.
4 Borenstein M, Hedges LV, Higgins JP, *et al*. A basic introduction to fixed-effect and random-effects models for meta-analysis. *Res Synth Methods* 2010;1:97–111.
5 Collaboration C. *Cochrane handbook for systematic reviews of interventions 5.0. 0*: Cochrane Collaboration, 2008.
6 DerSimonian R, Laird N. Meta-analysis in clinical trials. *Control Clin Trials* 1986;7:177–88.

Cardiovascular effects of hydroxychloroquine: a systematic review and meta-analysis

With great interest, we have read Professor Lee's comments[1] concerning our letter 'Cardiovascular effects of hydroxychloroquine'.[2] We completely agree that the relevance of a meta-analysis depends on its completeness, optimally including all published articles and abstracts. Thus, our decision to only search the PubMed database could represent a methodological weakness. However, Rempenault *et al*[3] performed the same meta-analysis with searches of multiple databases (PubMed, EMBASE and Cochrane Library), and did not find additional references beyond what we retrieved. Thus, within the context of our study on the cardiovascular effects of hydroxychloroquine, the strategy of searching only PubMed was apparently sufficient to identify all articles of interest and to therefore limit the publication bias inherent to all meta-analyses.

Professor Lee further expresses some concerns regarding statistical considerations, particularly about the statistical models used to account for the heterogeneity. We completely agree with his perspective, and we affirm the appropriateness of the statistical models used in our work. All results described in our letter were obtained from random-effects models. It is true that random-effects and fixed-effects models give exactly the same results (standardised mean difference (SMD) and 95% CI) when I^2 equals 0, concerning the effects of 12 weeks of hydroxychloroquine (HCQ) treatment on lipid and glycaemic parameters (triglyceride, low-density lipoprotein cholesterol and high-density lipoprotein cholesterol). That is why we indicated that we assessed the effects of 12 weeks of HCQ treatment on the glycaemic and lipid profiles based on the estimation of paired SMD using fixed-effects or random-effects models. We agree that it would be helpful to explain the rationales behind the selection of meta-analysis method, and the choice of the statistical model. However, adherence to the Correspondence format precluded specification of all statistical choices regarding heterogeneity among studies, the usefulness of random-effects models and investigation of heterogeneity. Notably, the meta-regression analyses proposed by Professor Lee are quite difficult to perform due to the limited number of studies.

Sylvain Mathieu,[1] Bruno Pereira,[2] Anne Tournadre,[1] Martin Soubrier[1]

[1]Department of Rheumatology, Gabriel Montpied Teaching Hospital, Clermont University, Clermont-Ferrand, France
[2]Department of Clinical Research and Innovation, Gabriel Montpied Teaching Hospital, Clermont-Ferrand, France

Correspondence to Dr Sylvain Mathieu, Rheumatology Department, Gabriel Montpied Teaching Hospital, Clermont University, Clermont-Ferrand 63003, France; smathieu@chu-clermontferrand.fr

Handling editor Josef S Smolen

Contributors All authors: responsible for the study concept, design and drafting of the manuscript; equally contributed to the critical revision of the manuscript for important intellectual content.

Competing interests None declared.

Provenance and peer review Commissioned; internally peer reviewed.

To cite Mathieu S, Pereira B, Tournadre A, *et al*. *Ann Rheum Dis* 2018;**77**:e80.

Received 23 November 2017
Accepted 28 November 2017
Published Online First 7 December 2017

Linked

► http://dx.doi.org/10.1136/annrheumdis-2017-212661

Ann Rheum Dis 2018;**77**:e80. doi:10.1136/annrheumdis-2017-212668

REFERENCES

1 Lee YH. Cardiovascular effects of hydroxychloroquine: a systematic review and meta-analysis. *Ann Rheum Dis* 2018;77:e79.
2 Mathieu S, Pereira B, Tournadre A, *et al*. Cardiovascular effects of hydroxychloroquine: a systematic review and meta-analysis. *Ann Rheum Dis* 2018;77:e65.
3 Rempenault C, Combe B, Barnetche T, *et al*. Metabolic and cardiovascular benefits of hydroxychloroquine in patients with rheumatoid arthritis: a systematic review and meta-analysis. *Ann Rheum Dis* 2018;77:98–103.

Utility of PET/CT in the diagnosis of inflammatory rheumatic diseases: a systematic review and meta-analysis

In an article published in the *Annals of the Rheumatic Diseases*, Schönau *et al* suggested that positron emitted tomography (PET)/CT is useful in determining the cause of unexplained fever/inflammation.[1] In this letter, we wish to add further data to support the conclusions of this article. More and more, PET/CT is used to determine the cause of fever, systemic inflammation or atypical or resistant rheumatic disease. However, the utility of PET/CT in these diagnoses is not clear. Thus, we performed a meta-analysis to investigate the utility of PET/CT in the diagnosis of inflammatory rheumatic diseases.

We searched MEDLINE to identify all reports of interest published prior to June 2016 using the search terms: '(PET scan OR 18FDG PET OR positron emission tomography) AND (rheumatoid arthritis (RA) OR polymyalgia rheumatica (PMR) OR Horton OR giant cell arteritis (GCA) OR vasculitis OR spondylitis OR synovitis OR bursitis)'. We retrieved a total of 1110 articles. In addition, we searched for abstracts from the European League Against Rheumatism and American College of Rheumatology meetings between 2014 and 2016. The prevalence of high focal tracer uptakes according to localisation (articular, vascular, periarticular, interspinous) and the disease (RA, PMR, GCA, vasculitis, connective tissue disease or fever) was calculated using a meta-analysis of proportions (inverse of the variance method) using fixed or randomised models.

We included 90 references, including 22 abstracts, involving a total of 2300 patients having a PET/CT. The prevalence of PET/CT uptakes is summarised in table 1. Tracer uptake in the aortic wall was found in 22% of patients with GCA. The prevalence of aortic vasculitis in GCA varied from 3% to 18% in the literature. Even when the percentage of aortic wall tracer uptake was weak, PET/CT had a substantial sensitivity and specificity for the GCA diagnosis.[2]

Tracer uptake in the shoulders or hips was often reported in PMR, especially in periarticular sites.[3] As previously reported,[4] we found that interspinous tracer uptake was common in PMR, occurring in two-thirds of patients with PMR undergoing a PET/CT. However, this result is not very specific to PMR because one-third of patients with RA have also interspinous bursitis. Articular tracer uptake was also not very specific as it occurred in more than half of the studied patients, despite the rheumatic disease, except in vasculitis (23% (95% CI 13.4 to 33.2%)).

Our study results provide information that complements the conclusions of Schönau *et al*. We found that PET/CT is helpful in diagnostic research, but that the interpretation of tracer uptake at each site is not specific to a rheumatic disease. Rather, the overall assessment of PET/CT leads to the most probable diagnosis (rheumatic disease, infection, malignancy) along with good cooperation between clinicians and nuclear medicine specialists.

Lucie Descamps,[1] Louis Olagne,[2] Charles Merlin,[3] Florent Cachin,[3] Martin Soubrier,[1] Sylvain Mathieu[1]

[1]Rheumatology Department, Gabriel Montpied Teaching Hospital, Clermont University, Clermont-Ferrand, France
[2]Internal Medicine Department, Gabriel Montpied Teaching Hospital, Clermont University, Clermont-Ferrand, France
[3]Nuclear Medicine, Jean Perrin Comprehensive Cancer Center, Clermont-Ferrand, France

Correspondence to Sylvain Mathieu, Rheumatology Department, Gabriel Montpied Teaching Hospital, Clermont-Ferrand 63003, France; smathieu@chu-clermontferrand.fr

Contributors LD, MS and SM were responsible for the study concept and design and drafting the manuscript. LD, LO and SM were involved in the acquisition of data. LD, LO, MS and SM were responsible for the analysis and interpretation of data. LD and SM did the statistical analysis. SM had full access to all of the data in the study and takes responsibility for the integrity of the data and the accuracy of the data analysis and was involved in the supervision of the study. All the authors equally contributed to the critical revision of the manuscript for important intellectual content.

Competing interests None declared.

Provenance and peer review Not commissioned; internally peer reviewed.

Table 1 Prevalence of tracer uptakes in different sites according to the rheumatic disease or fever

Disease						
Tracer uptake site or interpretation	**GCA (n=14; n=259)**	**PMR (n=10; n=310)**	**RA (n=14; n=203)**	**Connective tissue disease (n=13; n=295)**	**Vasculitis (n=26; n=583)**	**Fever (n=8; n=451)**
Aortic wall	n=10; np=104; 0.22 (0.07 to 0.43)*	n=2; np=30; 0.37 (0.05 to 0.79)*		n=7; np=31; 0.10 (0.03–0.19)*	n=18; np=210; 0.59 (0.42 to 0.74)*	n=5; np=39; 0.17 (0.04 to 0.38)*
Other vascular	n=11; np=112; 0.06 (0.01 to 0.17)*	n=5; np=49; 0.30 (0.13 to 0.50)*		n=2; np=10; 0.27 (0.15 to 0.42)	n=17; np=178; 0.49 (0.33 to 0.61)*	n=6; np=48; 0.04 (0.01 to 0.13)*
Articular (shoulder or hip)		n=5; np=101; 0.76 (0.58 to 0.99)*	n=4; np=24; 0.66 (0.17 to 0.99)*			
Other articular	n=2; np=35; 0.72 (0.266 to 0.99)*	n=3; np=25; 0.54 (0.40 to 0.68)*	n=9; np=106; 0.78 (0.60 to 0.92)*	n=4; np=95; 0.70 (0.25 to 0.99)*	n=3; np=14; 0.23 (0.13 to 0.33)	
Periarticular (shoulder or hip)		n=5; np=94; 0.84 (0.63 to 0.97)*				
Interspinous		n=6; np=128; 0.67 (0.55 to 0.78)*	n=2; np=7; 0.34 (0.02 to 0.81)*			
Lymphadenopathy			n=2; np=19; 0.82 (0.32 to 0.99)*	n=7; np=93; 0.29 (0.17 to 0.42)*	n=3; np=9; 0.21 (0.06 to 0.42)*	
Malignancy						n=6; np=41; 0.10 (0.08 to 0.13)
Infection						n=7; np=74; 0.07 (0.03 to 0.14)*

Values in parentheses indicate 95% CI.
*Randomised effect.
GCA, giant cell arteritis; n, total number of patients; np, number of patients with tracer uptake; PMR, polymyalgia rheumatic; RA, rheumatoid arthritis.

To cite Descamps L, Olagne L, Merlin C, *et al*. *Ann Rheum Dis* 2018;**77**:e81.

Received 7 November 2017
Accepted 8 November 2017
Published Online First 16 November 2017

Ann Rheum Dis 2018;**77**:e81. doi:10.1136/annrheumdis-2017-212660

REFERENCES

1 Schönau V, Vogel K, Englbrecht M, *et al*. The value of ^{18}F-FDG-PET/CT in identifying the cause of fever of unknown origin (FUO) and inflammation of unknown origin (IUO): data from a prospective study. *Ann Rheum Dis* 2018;77:70–7.
2 Prieto-González S, Depetris M, García-Martínez A, *et al*. Positron emission tomography assessment of large vessel inflammation in patients with newly diagnosed, biopsy-proven giant cell arteritis: a prospective, case-control study. *Ann Rheum Dis* 2014;73:1388–92.
3 Sondag M, Guillot X, Verhoeven F, *et al*. Utility of 18F-fluoro-dexoxyglucose positron emission tomography for the diagnosis of polymyalgia rheumatica: a controlled study. *Rheumatology* 2016;55:1452–7.
4 Camellino D, Paparo F, Morbelli S, *et al*. Interspinous bursitis is common in polymyalgia rheumatica, but is not associated with spinal pain. *Arthritis Res Ther* 2014;16:492.

Is the PET/CT first choice for differential diagnosis of fever of FUO/IUO?

First, thanks for this interesting article that tries to answer a difficult clinical problem of patients with fever of unknown origin (FUO) and inflammation of unknown origin (IUO) who are discharged without diagnosis.[1]

This study is very important in creating a diagnostic algorithm for FUO and IUO. We wanted to address some of the important points for improving clinical implications. In the literature, different maximum standardized uptake values (SUV) (SUVMAX) levels were used as thresholds to detect or differentiate benign, malignant, infectious and inflammatory diseases with 18F-fluorodeoxyglucose positron emission tomography (18F-FDG-PET/CT).[2 3] In this study, we did not see any cut-off value for positive results. Which SUVMAX value was accepted as positive? Is there any specific cut-off value for differential diagnosis? In this study, 72 out of 240 PET/CT was positive even though that was not related to the diagnosis. Although PET/CT is very useful for differential diagnosis, some patients may have over diagnosis.

Another interesting point is the timing of 18F-FDG-PET/CT during glucocorticoid usage. Glucocorticoids even if withdrawn can effect SUVMAX values and the results of 18F-FDG-PET/CT.[4 5] In this study, it was mentioned that glucocorticoids were discontinued at the day of hospital administration, but we wonder about the time lag between the cessation of glucocorticoid therapy and 18F-FDG-PET/CT imaging.

Twelve out of 240 patients had defined diagnosis, although PET/CT results were negative. We wonder about the diagnosis of these patients. How did these patients get diagnosis? Can these patients under glucocorticoid therapy affect the PET/CT results?

Thank you again for such a great and useful work!

Berkan Armagan, Abdulsamet Erden, Ozlem Beydas, Alper Sari, Levent Kilic, Umut Kalyoncu

Department of Internal Medicine, Division of Rheumatology, Faculty of Medicine, Hacettepe University, Ankara, Turkey

Correspondence to Dr Berkan Armagan, Department of Internal Medicine, Division of Rheumatology, Faculty of Medicine, Hacettepe University, Ankara 06100, Turkey; berkanarmagan@gmail.com

Competing interests None declared.

Provenance and peer review Not commissioned; internally peer reviewed.

To cite Armagan B, Erden A, Beydas O, *et al*. *Ann Rheum Dis* 2018;**77**:e82.

Received 30 November 2017
Accepted 3 December 2017
Published Online First 13 December 2017

Linked

► http://dx.doi.org/10.1136/annrheumdis-2017-212785

Ann Rheum Dis 2018;**77**:e82. doi:10.1136/annrheumdis-2017-212771

REFERENCES

1 Schönau V, Vogel K, Englbrecht M, *et al*. The value of ^{18}F-FDG-PET/CT in identifying the cause of fever of unknown origin (FUO) and inflammation of unknown origin (IUO): data from a prospective study. *Ann Rheum Dis* 2018;77:70–7.
2 Parghane RV, Basu S. Dual-time point 18F-FDG-PET and PET/CT for differentiating benign from malignant musculoskeletal lesions: opportunities and limitations. *Semin Nucl Med* 2017;47:373–91.
3 Yamashita H, Kubota K, Takahashi Y, *et al*. Clinical value of 18 F-fluoro-dexoxyglucose positron emission tomography/computed tomography in patients with adult-onset Still's disease: a seven-case series and review of the literature. *Mod Rheumatol* 2014;24:645–50.
4 Yamashita H, Kubota K, Mimori A. Clinical value of whole-body PET/CT in patients with active rheumatic diseases. *Arthritis Res Ther* 2014;16:423.
5 Papathanasiou ND, Du Y, Menezes LJ, *et al*. 18F-Fludeoxyglucose PET/CT in the evaluation of large-vessel vasculitis: diagnostic performance and correlation with clinical and laboratory parameters. *Br J Radiol* 2012;85:188–94.

Response to: 'Is the PET/CT first choice for differential diagnosis of FUO/IUO?' by Armagan *et al*

We thank Dr Armagan and colleagues for their letter[1] regarding our article entitled, 'The value of 18F-FDG-PET/CT in identifying the cause of fever of unknown origin (FUO) and inflammation of unknown origin (IUO): data from a prospective study'.[2]

In their comment, Dr Armagan and colleagues ask whether a fixed cut-off level for the maximum standardised uptake value (SUVmax) in the 18F-fluorodeoxyglucose-positron emission tomography (FDG-PET) was used for data interpretation. We want to respond that, although SUVmax was documented in all patients, the use of a fixed SUVmax across the different diseases associated with fever (FUO)—and IUO—is not helpful.

They also raised the question about whether glucocorticoids were stopped before 18F-FDG-PET/CT scans. Especially high-dose glucocorticoids can influence imaging results due to induction of hyperglycaemia.[3] Glucocorticoids were taken by 59 patients at admission. These patients stopped glucocorticoids at admission on the average of 3.1 days before 18F-FDG-PET/CT scan was performed. The scans were helpful to find the underlying disease in 37 (62%) of these patients having received glucocorticoids.

We therefore think that previous use of glucocorticoids did not have a major influence on the scan results in our study. Importantly, only three patients, two of whom were diagnosed with large-vessel vasculitis and one with polymyalgia rheumatica, had received higher doses of glucocorticoids between 20 and 40 mg prednisolone daily. None of them were hyperglycaemic and 18F-FDG-PET/CT scan was considered helpful in ascertaining diagnosis also in these patients.

Furthermore, as mentioned in the study, false-negative results were rare in our study and only seen in 12 patients.[2] Among those with false-negative 18F-FDG-PET/CT scans were patients with Still's disease that fulfilled the Yamaguchi criteria, patients with polymyalgia rheumatica that fulfilled the Rice criteria and patients with isolated giant cell arteritis of the temporal artery.

Verena Schönau, Georg Schett

Department of Internal Medicine 3, Friedrich-Alexander-University Erlangen-Nuremberg, Universitatsklinikum Erlangen, Erlangen, Germany

Correspondence to Professor Georg Schett, Department of Internal Medicine 3, Rheumatology and Immunology, University Clinic of Erlangen-Nuremberg, Erlangen 91054, Germany; georg.schett@uk-erlangen.de

Handling editor Josef S Smolen

Contributors VS and GS wrote the letter.

Funding This research received no specific grant from any funding agency in the public, commercial or not-for-profit sectors.

Competing interests None declared.

Provenance and peer review Commissioned; internally peer reviewed.

To cite Schönau V, Schett G. *Ann Rheum Dis* 2018;**77**:e83.

Received 20 January 2018
Accepted 21 January 2018
Published Online First 2 February 2018

► http://dx.doi.org/10.1136/annrheumdis-2017-212771

Ann Rheum Dis 2018;**77**:e83. doi:10.1136/annrheumdis-2017-212785

REFERENCES

1 Armagan B, Erden A, Beydas O, *et al*. Is the PET/CT first choice for differential diagnosis of fever of FUO/IUO? *Ann Rheum Dis* 2018;77:e82.
2 Schönau V, Schett G. Response to: the value of 18(F)-FDG-PET/CT in identifying the cause of fever of unknown origin (FUO) and inflammation of unknown origin (IUO): data from a prospective study. *Ann Rheum Dis* 2018;77:e53.
3 Surasi DS, Bhambhvani P, Baldwin JA, *et al*. ^{18}F-FDG PET and PET/CT patient preparation: a review of the literature. *J Nucl Med Technol* 2014;42:5–13.